marine drugs

Special Issue Reprint

Marine Algae

Exploring Their Nutritional, Health, and Nutraceutical Potential

Edited by
Leonel Pereira and Ana Marta Gonçalves

mdpi.com/journal/marinedrugs

MDPI

Marine Algae: Exploring Their Nutritional, Health, and Nutraceutical Potential

Marine Algae: Exploring Their Nutritional, Health, and Nutraceutical Potential

Guest Editors

Leonel Pereira
Ana Marta Gonçalves

MDPI

Basel • Beijing • Wuhan • Barcelona • Belgrade • Novi Sad • Cluj • Manchester

Guest Editors

Leonel Pereira
Department of Life Sciences
University of Coimbra
Coimbra
Portugal

Ana Marta Gonçalves
Department of Life Sciences
University of Coimbra
Coimbra
Portugal

Editorial Office
MDPI AG
Grosspeteranlage 5
4052 Basel, Switzerland

This is a reprint of the Special Issue, published open access by the journal *Marine Drugs* (ISSN 1660-3397), freely accessible at: https://www.mdpi.com/journal/marinedrugs/special_issues/5AJ1B44W79.

For citation purposes, cite each article independently as indicated on the article page online and as indicated below:

Lastname, A.A.; Lastname, B.B. Article Title. *Journal Name* **Year**, *Volume Number*, Page Range.

ISBN 978-3-7258-4943-7 (Hbk)
ISBN 978-3-7258-4944-4 (PDF)
https://doi.org/10.3390/books978-3-7258-4944-4

Cover image courtesy of Leonel Pereira

Contents

About the Editors

Leonel Pereira

Leonel Pereira, University of Coimbra, Portugal, is a leading expert in marine biodiversity and biotechnology. He holds a PhD in Cellular Biology and an Aggregation in Biosciences, specializing in Biotechnology. His research focuses on marine macroalgae, bioactive compounds, and environmental assessment, with applications in nutraceuticals and sustainable development. He coordinates the Master's in Biodiversity and Plant Biotechnology and is an integrated researcher at the Centre for Functional Ecology. Leonel Pereira has authored over 20 books, 79 book chapters, and numerous scientific articles. He is the founder of MACOI—Portuguese Marine Algae Site, and serves on the editorial boards of Marine Drugs and Applied Sciences. Recognized among the top 2% of scientists worldwide (Stanford/Elsevier), he has received multiple awards, including the CHOICE Outstanding Academic Title for Edible Seaweeds of the World.

Ana Marta Gonçalves

Ana Marta Gonçalves, University of Coimbra, Portugal, is a specialist in aquatic ecology, ecotoxicology, and marine biotechnology. She holds a PhD in Biology with a focus on Ecology, completed in collaboration with Ghent University, Belgium. Her research explores biochemical pathways in aquatic ecosystems, trophic dynamics, and the valorization of marine resources for industrial applications, including food and nutraceuticals. Dr. Gonçalves has published over 110 ISI-indexed papers, 55 book chapters, and edited multiple thematic volumes. She serves on the editorial boards of Ecological Indicators, IJERPH, IEAM, and others. She is an active member of SETAC, AIL, and SIBECOL, and currently chairs the SETAC Europe Education Committee. Her work bridges science, education, and sustainability, with a strong commitment to interdisciplinary collaboration and public engagement.

Preface

Marine algae, often overlooked in the broader landscape of natural products, have emerged as a cornerstone of innovation in health sciences, nutrition, and sustainable biotechnology. This Reprint of Marine Drugs, titled "Marine Algae: Exploring Their Nutritional, Health, and Nutraceutical Potential", offers a comprehensive and multidisciplinary exploration of the vast biochemical and therapeutic promise held by macroalgae and microalgae.

Edited by Dr. Leonel Pereira and Dr. Ana Marta Gonçalves, this collection brings together pioneering research and critical reviews that underscore the growing relevance of marine algae in addressing some of the most pressing challenges in human health—particularly in the realm of chronic diseases and cancer. The issue spans a wide array of topics, including the following:

- Bioactive compounds such as polysaccharides, polyphenols, terpenoids, and pigments with antioxidant, anti-inflammatory, and anti-cancer properties.
- Functional nutrition and nutraceutical applications, highlighting algae's role in preventive health and dietary supplementation.
- Mechanistic insights into how algal compounds modulate cellular pathways, induce apoptosis, and inhibit tumor progression.
- In vitro and in vivo studies demonstrate the efficacy of algal extracts against various cancer models.
- Sustainability and ecological impact, emphasizing algae's role in environmental health and carbon sequestration.

The chapters within this Reprint reflect a paradigm shift: from viewing algae as mere aquatic flora to recognizing them as dynamic bio-factories capable of producing thousands of biologically active molecules. These compounds not only offer therapeutic potential but also align with the global movement toward natural, eco-friendly, and low-toxicity alternatives to synthetic drugs.

Importantly, the Reprint also addresses the challenges that remain—such as the standardization of extraction methods, understanding side effects, and translating preclinical findings into clinical applications. It calls for continued interdisciplinary collaboration among marine biologists, pharmacologists, nutritionists, and biotechnologists to unlock the full potential of these marine resources.

As the world turns increasingly toward nature for solutions to health and sustainability, marine algae stand out as one of the most promising candidates. We hope this Reprint inspires further research, innovation, and responsible utilization of marine algae in the service of human and planetary well-being.

Leonel Pereira and Ana Marta Gonçalves
Guest Editors

marine drugs

MDPI

Article

A Comparative Study of the Phytochemical Composition, Antioxidant Properties, and In Vitro Anti-Diabetic Efficacy of Different Extracts of *Caulerpa prolifera*

Safae Ouahabi [1,2], Nour Elhouda Daoudi [2,3], Mohamed Chebaibi [4,5], Ibrahim Mssillou [6], Ilyesse Rahhou [3], Mohamed Bnouham [2], Belkheir Hammouti [7], Marie-Laure Fauconnier [8], Alicia Ayerdi Gotor [9,*], Larbi Rhazi [10] and Mohammed Ramdani [11]

[1] Faculty of Medicine and Pharmacy of Oujda, Mohammed First University, 724, Oujda 60000, Morocco; ouahabi.safae@ump.ac.ma
[2] Laboratory of Bioresources, Biotechnology, Ethnopharmacology and Health, Faculty of Sciences, Mohammed First University, BP 717, Oujda 60000, Morocco; nourelhoudada95@gmail.com (N.E.D.); mbnouham@ump.ac.ma (M.B.)
[3] Higher Institute of Nursing Professions and Health Techniques, Oujda 60000, Morocco; ilyesse@hotmail.com
[4] Ministry of Health and Social Protection, Higher Institute of Nursing Professions and Health Techniques, Fez 30000, Morocco; mohamed.chebaibi@usmba.ac.ma
[5] Biomedical and Translational Research Laboratory, Faculty of Medicine and Pharmacy of Fez, Sidi Mohamed Ben Abdellah University, Fez 30000, Morocco
[6] National Agency of Medicinal and Aromatic Plants, BP 159, Principal, Taounate 34000, Morocco; mssillouibrahim@gmail.com
[7] Euromed Research Center, Euromed Polytechnic School, Euromed University of Fes (UEMF), Fes 30000, Morocco; hammoutib@gmail.com
[8] Laboratory of Chemistry of Natural Molecules, University of Liège, Gembloux Agro-Bio Tech. 2, Passage des Déportés, B-5030 Gembloux, Belgium; marie-laure.fauconnier@uliege.be
[9] Institut Polytechnique UniLaSalle, AGHYLE, UP 2018.C101, UniLaSalle, 19 rue Pierre Waguet, BP 30313, 60026 Beauvais, France
[10] Institut Polytechnique UniLaSalle, Université d'Artois, ULR 7519, 19 Rue Pierre Waguet, BP 30313, 60026 Beauvais, France; larbi.rhazi@unilasalle.fr
[11] Laboratory of Applied and Environmental Chemistry (LCAE), Faculty of Sciences, Mohammed First University, B.P. 717, Oujda 60000, Morocco; moharamdani2000@yahoo.fr
* Correspondence: alicia.ayerdi-gotor@unilasalle.fr; Tel.: +33-344062525

Abstract: The Moroccan coastline has been the focus of attention for researchers studying the national algal flora, with the aim of preserving these invaluable natural resources. Since the year 2000, these resources have stimulated great interest in the creation of new drugs, as well as their integration into food supplements and foods. Therefore, this study aims to explore the phytochemistry of a series of extracts derived from *Caulerpa prolifera*. To ensure better extraction of the various metabolites present, two extraction methods, namely maceration and the Soxhlet method, were employed using solvents of varying polarity (hexane, ethyl acetate, methanol, and water). The chemical composition of the extracts was analyzed using GC-MS for fatty acids and HPLC-DAD for phenolic compounds. Antioxidant activity was evaluated using DPPH and β-carotene bleaching assays, while antidiabetic potential was assessed by in vitro inhibition of α-amylase and α-glucosidase. In addition, Molecular docking models were employed to assess the interaction between the bioactive molecules and the human pancreatic α-amylase and α-glucosidase enzymes. Vanillin, p-coumaric acid, sinapic acid, 7,3′,4′-flavon-3-ol, and kaempferol were the most abundant phenolic compounds. Anti-diabetic and antioxidant effects were highly significant.

Keywords: *Caulerpa prolifera*; fatty acids; phenolic compounds; antioxidant activity; anti-diabetic properties; enzyme inhibition

1. Introduction

Morocco, an African nation renowned for its diverse ecosystems, boasts a dual maritime frontier bordering the Western Atlantic Ocean to the west and the Mediterranean Sea to the north. This extensive coastal expanse spans 3500 km [1]. Morocco undeniably boasts a diverse range of aquatic flora and fauna. This is evidenced by the extensive study conducted by Benhissoune et al. [2], who have identified an impressive 612 species of algae in Moroccan waters [3]. The Nador Lagoon, also known as Marchica, is situated in the northern region of the country and is considered to be one of the most important Mediterranean lagoons. It boasts a diverse array of 112 algae species, including 60 rhodophyceae, 31 chlorophyceae, 19 pheophyceae, and 2 phanerogam species. Despite the richness of these algae, their potential remains largely untapped due to limited research.

Caulerpa prolifera (Chlorophyta) is one of the most abundant algae in the lagoon [4]. This alga is characterized by the presence of an important extracellular polysaccharide called sulfated galacotans. Wang et al. [5], have classified this alga as the fourth producer of sulfated polysaccharides. The different species of *Caulerpa* are known to occupy various environmental niches that differ considerably in terms of temperature, light availability, water movement, depth, grazing pressure, and benthic substrate [6–10]. The invasive potential of this genus is attributed to intrinsic characteristics that promote its adaptation to diverse habitats. Features such as phenotypic plasticity, asexual reproduction, production of surface metabolites, and nutrient absorption by rhizoids contribute to the diversity of habitats suitable for this genus [6].

The green seaweed *Caulerpa* is widely cultured, especially in ponds, because of its rapid growth rate, high antioxidant activity, and nutritional value [11,12]. *Caulerpa* has an indeterminate prostrate axis, referred to as a stolon, which attaches to a substrate by filiform rhizoids. Upright fronds are the photosynthetic and reproductive units. Fragments of the stolon can regenerate a new thallus.

Caulerpa species are also rich in minerals, reaching up to 55% of their dry matter [13], notably iron, calcium, magnesium, and zinc [13,14]. They contain variable levels of carbohydrates, ranging from 3.6% to 83.2% of dry matter [13]. *Caulerpa* polysaccharides are complex in composition, with a wide variety of oses (galactose, glucose, arabinose, xylose, mannose, rhamnose and fucose) [15–18], but galactose is the most important component [19], and have interesting biological properties for medical and pharmaceutical applications, such as anticoagulant, anti-inflammatory, antioxidant, anti-diabetic, immunostimulant and antitumoral effects [5]. However, the protein content in edible *Caulerpa* is relatively low compared with other protein-rich plant sources. Lipids are present in small quantities [13], but seaweeds, including *Caulerpa*, are valued for their high content of long-chain polyunsaturated fatty acids and carotenoids [20].

Caulerpa species are rich in chlorophylls a and b, and also contain other pigments such as siphonaxanthin [14]. In addition, they provide significant amounts of vitamins C and E (up to 46.3 and 62.7% of the recommended daily allowance (RDA), respectively, per 100 g of *Caulerpa* consumed) [13], although their nutritional value is yet to be determined. It should be noted that the *Caulerpa* genus presents a wide chemical diversity, but it is important to be cautious due to its high toxicity [21].

Recent studies have also highlighted the pro-health properties of various *Caulerpa* species, including their antioxidant and antidiabetic potential due to their richness in bioactive compounds such as polyphenols, flavonoids, and sulfated polysaccharides. These

compounds are known to inhibit carbohydrate-hydrolyzing enzymes, including α-amylase and α-glucosidase, which are key targets in the management of type 2 diabetes. While species such as *Caulerpa racemosa* and *Caulerpa lentillifera* have shown promising antidiabetic activity [22,23], little is known about the antidiabetic potential of *Caulerpa prolifera*. Therefore, exploring this biological activity represents a relevant and novel aspect of its pharmacological profile.

The primary objective of this study was to conduct a comprehensive chromatographic analysis of the fatty acids and polyphenols present in *C. prolifera* extracts. Two distinct extraction methods were employed, utilizing solvents with varying polarities to facilitate a comparative assessment to optimize the recovery of bioactive compounds and better understand how the extraction method affects the biological properties of the resulting extracts. Furthermore, the research sought to evaluate the antioxidant properties of the extracts and their impact on pancreatic α-amylase and α-glucosidase activities. The outcomes of these analyses are intended to contribute to an enhanced understanding of the potential health benefits associated with *C. prolifera* extracts sourced from the Marchica lagoon, as well as their potential applications in the food and pharmaceutical sectors.

2. Results

2.1. Yields, Phenols, and Flavonoids Contents

In our recent study, we aimed to extract *C. prolifera* extracts using water, methanol, ethyl acetate, and hexane. The extraction yields ranged from 1.30% to 8.51%, and we found that the yield of extraction increases with the solvent's increasing polarity during the extraction process. Our findings also suggest that the extraction yield of organic solvents by the Soxhlet extraction method is higher than that of the maceration extraction method.

Table 1 also shows the total phenolic content of the extracts measured using the FC method. The results of the extracts were determined based on their equivalent to gallic acid (GAE). The highest TPC value is presented by the aqueous extract at 402.34 mg GAE/g and decreases in the following order: (179.88 mg GAE/g) EAcE (M) > (112.87 mg GAE/g) EAcE (S) > (99.47 mg GAE/g) ME (M) > (53.61 mg GAE/g) ME (S).

Table 1. Phenols and flavonoids contents of different extracts of *C. prolifera*.

Solvent	Extraction Methods	Yield (%)	Polyphenols (mg GAE/g)	Flavonoids (mg QE/g)
Hexane	M	1.30 ± 0.01	-	-
	S	2.23 ± 0.02	-	-
Ethyl acetate	M	4.46 ± 0.03	179.88 ± 0.03	154.64 ± 0.02
	S	6.81 ± 0.05	112.87 ± 0.07	40.35 ± 0.04
Methanol	M	7.12 ± 0.02	99.47 ± 0.06	22.93 ± 0.01
	S	8.41 ± 0.04	53.61 ± 0.02	16.70 ± 0.03
Water	M	8.51 ± 0.02	402.34 ± 0.08	196.65 ± 0.09

GAE: Gallic Acid Equivalent; QE: Quercetin Equivalent; M: Maceration; S: Soxhlet.

The TFC of the extracts is also reported in Table 1. It was observed that the effect of solvents on TFC is similar to that on TPC. The highest TFC was obtained in the aqueous extract, followed by the ethyl acetate extract and the methanol extract. A similar trend was observed in the amount of TPC. This correlation between TPC and TFC assay indicates that flavonoids are the dominating phenolic group in *C. prolifera*.

2.2. Fatty Acid Analysis

The present study aimed to investigate the fatty acid composition of hexanic and ethyl acetate extracts of *C. prolifera* using gas chromatography (GC) and mass spectroscopy (MS). The results are presented in Table 2. The hexane extracts were predominantly composed of saturated fatty acids, with a total saturated fatty acid (TUFA) composition of 70.71% and 69.3% for HE (S) and HE (M), respectively. In contrast, the ethyl acetate extracts were mainly composed of unsaturated fatty acids, with a total unsaturated fatty acid (TUFA) composition of 58.49% and 53.73% for EAcE (S) and EAcE (M), respectively. Among the saturated fatty acids (SFA), palmitic acid was found to be the most dominant in all extracts, with a percentage of 60.21%, 59.54%, 40.76%, and 39.31% for HE (S), HE (M), EAcE (S), and EAcE (M), respectively. Among the polyunsaturated fatty acids (PUFA), linoleic acid was the most dominant in all extracts, with approximately 15.62% and 12.25% for ethyl acetate extracts and hexane extracts, respectively. Lauric acid was present in a significant amount in EAcE (~12%) while a low percentage was observed in HE (~2%). Myristic acid, 7,10-Hexadecadienoic acid, and Linolenic acid were found in relatively smaller amounts in extracts, while Eicosenoic acid and Palmitoleic acid (C16:1) were detected in minor amounts.

Table 2. Fatty acid composition of hexane and ethyl acetate extracts from green algae *C. prolifera*.

Fatty Acids	RT (min)	HE (%)		EAcE (%)	
		M	S	M	S
Lauric acid (C1:0)	17.83	2.61 ± 0.03	2.31 ± 0.02	12.13 ± 0.04	12.45 ± 0.05
Eicosenoic acid (C20:1)	20.08	3.58 ± 0.02	3.20 ± 0.02	5.52 ± 0.03	nd
Myristic acid (C14:0)	20.39	7.15 ± 0.04	8.19 ± 0.04	2.29 ± 0.01	5.28 ± 0.02
7,10-Hexadecadienoic acid (C16:2)	21.17	7.09 ± 0.02	6.52 ± 0.03	9.32 ± 0.03	9.50 ± 0.04
Palmitoleic acid (C16:1)	23.11	1.19 ± 0.01	2.15 ± 0.02	6.35 ± 0.02	6.81 ± 0.03
Palmitic acid (C16:0)	23.31	59.54 ± 0.06	60.21 ± 0.05	39.31 ± 0.12	40.76 ± 0.08
Linoleic acid (C18:2)	25.03	12.25 ± 0.03	10.14 ± 0.03	15.62 ± 0.05	15.66 ± 0.04
Linolenic acid (C18:3)	25.09	6.59 ± 0.02	7.28 ± 0.03	9.46 ± 0.03	9.49 ± 0.03
SFA [a]		69.30	70.71	53.73	58.49
UFA [b]		30.70	29.29	46.27	41.46
UFA/SFA [c]		0.44	0.41	0.86	0.71

RT: Retention time; M: maceration; S: Soxhlet, HE: Hexane Extract; EAcE: Ethyl acetate Extract; nd: not detected; [a]: saturated fatty acids (SFA); [b]: unsaturated fatty acids (UFA); [c]: unsaturation ratio = UFA/SFA.

2.3. HPLC Analysis of C. prolifera Extracts

The present study aimed to investigate the chemical composition of ethyl acetate and methanol extracts of *Caulerpa prolifera* by employing HPLC-DAD analysis. The present methodology is characterized by its simplicity, ease of use, and high efficacy in the identification and quantification of major phenolic compounds in seaweed or aromatic plants. The obtained results were compared with the standards listed in Table 3, primarily based on retention time and ultraviolet spectrum.

The analysis revealed that *Caulerpa prolifera* extracts contain a diverse array of phenolic compounds, including nine phenolic acids and ten flavonoids. The extracts exhibited varying levels of abundance of the identified compounds. Sinapic acid was found to be the most abundant compound in EAcE (M) (18.54%), while Kaempferol (27%) and sinapic acid (21.28%) were the most prevalent compounds in EAcE (S). The most abundant compounds in ME (M) were 7,3,4-trihydroxy flavone (17.29%), Kaempferol (16.30%), and P-Coumaric acid (16.24%). Moreover, the extract ME (S) was found to contain a significant amount of flavonoids, primarily 7,3,4-flavon-3-ol (14.43%).

Table 3. Chemical composition of ethyl acetate and methanolic extracts from green algae *C. prolifera*.

N°	Compounds	RT (min)	EAcE (%)		ME (%)	
			M	S	M	S
1	Gallic acid	15.47	nd	0.99	nd	0.36
2	Catechin	18.68	1.23	0.87	1.94	0.90
3	4-hydroxy-benzoic acid	18.91	0.39	1.75	nd	0.87
4	Chlorogenic acid	19.15	0.63	1.50	2.55	0.77
5	Caffeic acid	19.45	0.47	2.22	0.91	0.74
6	Syringic acid	19.74	1.36	1.72	1.99	1.01
7	Vanillin	23.10	13.16	2.52	10.48	8.94
8	p-Coumaric acid	23.63	3.72	nd	16.24	12.84
9	Sinapic acid	24.09	18.54	21.28	7.27	6.82
10	7,3′,4′-flavon-3-ol	24.92	12.26	7.77	17.29	14.43
11	Rutin	25.16	3.27	6.03	nd	7.07
12	Salicylic acid	25.32	2.27	4.99	3.21	4.38
13	Quercetin	25.46	3.98	3.13	2.72	3.30
14	Cinnamic acid	25.48	5.98	6.05	6.85	11.13
15	Luteolin	25.64	2.86	3.52	1.67	nd
16	Apigenin	25.87	4.59	4.90	4.59	9.54
17	Kaempferol	26.10	6.03	27.00	16.30	2.99
18	Flavone	26.92	3.71	nd	nd	3.07
19	Flavonone	27.41	15.57	3.75	6.00	10.85

RT: Retention Time; M: maceration; S: Soxhlet; EAcE: Ethyl acetate Extract; ME: Methanolic Extract; nd: not detected.

2.4. Antioxidant Activity

The present study reports the results of the total antioxidant activity of the green seaweed *C. prolifera* using two popular assays. The results of this study are summarized in Table 4.

Table 4. IC_{50} values of *C. prolifera* extracts.

Extracts		IC_{50} (mg/mL)	
		DPPH	β-Carotene
EAcE	M	0.702 ± 0.311	0.01 ± 0.18
	S	0.767 ± 0.063	0.02 ± 0.25
ME	M	0.691 ± 0.041	0.29 ± 0.09
	S	0.723 ± 0.020	0.31 ± 0.31
AQE	M	0.091 ± 0.091	0.381 ± 0.11
Ascorbic Acid		0.06	-
BHA		-	0.02

EAcE: Ethyl Acetate extract; ME: Methanolic extract; AQE: Aqueous extract; M: Maceration; S: Soxhlet.

The findings of this study suggest that the aqueous extract displayed the highest level of antioxidant activity, with a recorded value of 0.091 mg/mL. In comparison, the reference antioxidant, ascorbic acid, had an IC_{50} value of 0.062 mg/mL. The ethyl acetate and methanolic extracts, however, demonstrated similar levels of antioxidant activity. With a value of approximately 0.7 mg/mL, regardless of the extraction method employed. It is important to note that factors such as the chemical composition of the extracts. Algae culture conditions and extraction methods used can influence the antioxidant efficacy.

The study also showed that the ethyl acetate extracts from *C. prolifera* demonstrated the highest antioxidant activity, using the β-carotene molecule bleaching method. The

recorded values for maceration and Soxhlet techniques were 0.01 mg/mL and 0.02 mg/mL, respectively. Besides, the ethyl acetate and methanol extracts manifested similar antioxidant activity, with an IC_{50} value of approximately 0.3 mg/mL. The bioactive compounds that effectively inhibited the degradation of beta-carotene were predominantly found in apolar or medium-polar extracts. Conversely, the majority of more polar extracts, including methanol and aqueous extracts, showed reduced antioxidant activity comparable to the activity of retinoic acid (RA).

2.5. In Vitro α-Amylase Inhibition

Figure 1 displays the impact of *Caulerpa prolifera* extracts on α-amylase inhibitory activity, with acarbose serving as the positive control. In vitro experiments were conducted to assess the influence of different concentrations of the extracts on α-amylase enzymatic activity. The findings indicate significant inhibition of α-amylase enzymatic activity across all tested concentrations for all extracts (Table 5). Notably, the concentration of 1.14 mg/mL demonstrated the most pronounced effect, showing inhibitory activities of 53.86 ± 0.46 for EACE (M), 60.76 ± 0.99 for EACE (S), 75.20 ± 0.58 for ME (M), 64.42 ± 4.99 for ME (S), and 67.81 ± 0.34 for AQE (M) (Figure 1A). Additionally, Figure 1B presents the IC_{50} values for each extract. The results indicate that EACE (M), EACE (S) exhibit similar inhibitory effects, albeit lower than acarbose ($p < 0.001$ for both extracts, compared to acarbose). However, ME (M), ME (S), and AQE (M) demonstrate a higher inhibitory effect compared to other extracts and exhibit a statistically similar effect to acarbose.

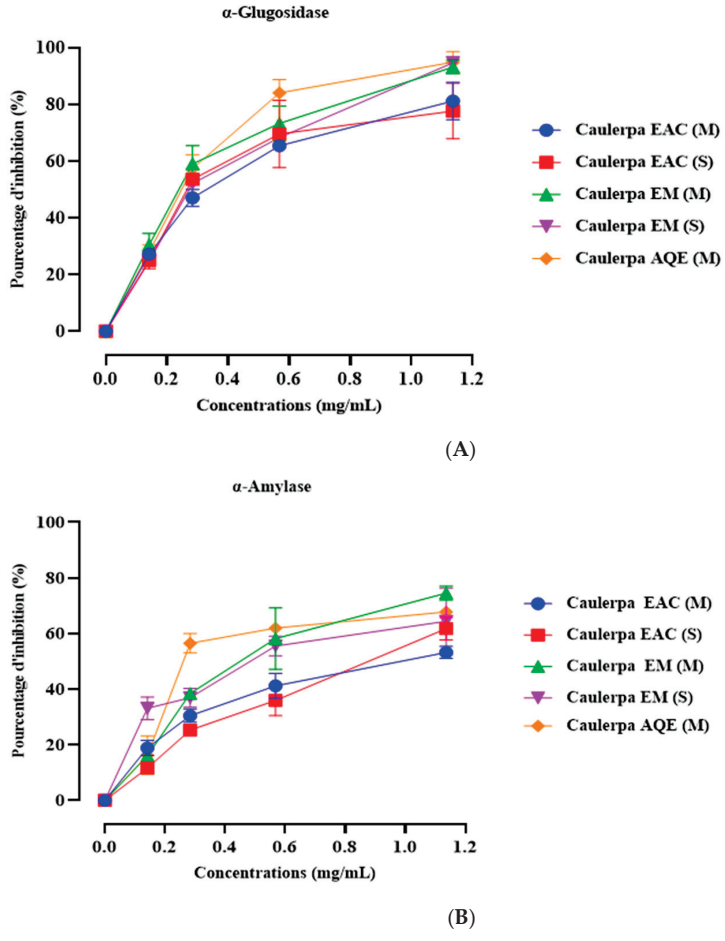

Figure 1. Inhibition percentage of *Caulerpa prolifera* extracts and acarbose against α-Glucosidase (**A**) and α-amylase (**B**) at different doses and their IC_{50} values. EAc: Ethyl Acetate; ME: Methanolic Extract.

Table 5. IC_{50} values of *C. prolifera* extracts and acarbose in α-amylase and α-glucosidase inhibition.

Inhibitors		IC_{50} (mg/mL)	
		α-Amylase	α-Glucosidase
Acarbose		0.35 ± 0.08	0.39 ± 0.04
EAcE	M	0.88 ± 0.08	0.48 ± 0.02
	S	0.83 ± 0.01	0.43 ± 0.07
ME	M	0.62 ± 0.11	0.35 ± 0.08
	S	0.63 ± 0.14	0.29 ± 0.05

EAcE: Ethyl Acetate extract; ME: Methanolic extract; AQE: Aqueous extract; M: Maceration; S: Soxhlet.

2.6. Molecular Modeling Studies

The inhibition of NADPH, a crucial cofactor in various enzymatic reactions contributing to cellular antioxidant defenses, plays a vital role in regulating cellular redox balance and antioxidant defense mechanisms [24].

Concerning the chemical compounds identified by HPLC in *Caulerpa prolifera* Extracts, Rutin, 7,3′,4′-flavon-3-ol, and Quercetin were the most active molecules against NADPH oxidase with glide gscore of −6,889, −6,803, and −6,587 kcal/mol (Table 6).

Table 6. Docking results in ligands in different receptors.

Compound Name		Glide Gscore (Kcal/mol)		
		NADPH Oxidase (PDB: 2CDU)	Alpha Amylase (PDB: 1B2Y)	Alpha Glucosidase (PDB: 5NN8)
Chemical compounds by HPLC analysis	4-hydroxybenzoic acid	−5.355	−5.016	−4.366
	7,3,4-flavon-3-ol	−6.803	−6.961	−5.558
	Apigenin	−6.405	−7.130	−5.202
	Caffeic acid	−5.484	−5.953	−4.237
	Catechin	−5.550	−6.283	−4.908
	Chlorogenic acid	−4.812	−6.254	−3.738
	Cinnamic acid	−4.637	−3.713	−3.353
	Flavone	−5.040	−5.175	−4.326
	Flavonone	−5.192	−5.389	−4.624
	Gallic acid	−5.878	−5.333	−4.32
	Kaempferol	−5.543	−6.617	−5.698
	Luteolin	−6.574	−6.807	−5.425
	p-Coumaric acid	−5.017	−5.742	−3.558
	Quercetin	−6.587	−6.817	−7.035
	Rutin	−6.889	−7.615	−5.237
	Salicylic acid	−5.469	−4.565	−3.911
	Sinapic acid	−5.299	−4.35	−3.543
	Syringic acid	−6.132	−5.973	−3.472
	Vanillin	−6.603	−6.012	−4.651
Fatty Acid by GC-MS	7,10-Hexadecadienoic acid	−1.001	-	-
	Eicosenoic acid	−3.048	−2.289	−2.008
	Lauric acid	-	-	-
	Linoleic acid	−0.817	-	-
	Linolenic acid	−0.546	-	−0.873
	Margaric acid	-	-	-
	Myristic acid	-	-	-
	Oleic acid	−0.665	-	-
	Palmitic acid	−0.006	-	-
	Palmitoleic acid	-	-	-
	Stearic acid	−0.552	-	-

In antidiabetic activity, molecular docking analysis revealed that Rutin, Apigenin, and 7,3′,4′-flavon-3-ol were the most active compounds against α-amylase, with glide gscores of −7.615, −7.13, and −6.96 kcal/mol, respectively. Similarly, Quercetin, Kaempferol, and 7,3′,4′-flavon-3-ol showed the strongest binding affinity toward α-glucosidase, with glide gscores of −7.035, −5.698, and −5.558 kcal/mol (Table 6). Among the fatty acids identified in *Caulerpa prolifera* extracts, Eicosenoic acid exhibited the most notable activity against NADPH oxidase, α-amylase, and α-glucosidase, with glide scores of −3.048, −2.289, and −2.008 kcal/mol, respectively. At the molecular interaction level, Rutin formed six hydrogen bonds within the active site of NADPH oxidase (PHE 245, THR 118, LYS 213, VAL 214, LYS 187, and ASP 179) and established a π-cation bond with LYS 187 (Figures 2A and 3A). Additionally, Rutin interacted with α-amylase via six hydrogen bonds (HIS 201, LYS 200, GLU 233, ASP 197, GLN 63, and TRP 59) (Figures 2B and 3B). In contrast, Quercetin formed four hydrogen bonds with ASP 518, ASP 616, and SER 676 in the α-glucosidase active site, along with two π–π stacking interactions with PHE 649 (Figures 2C and 3C).

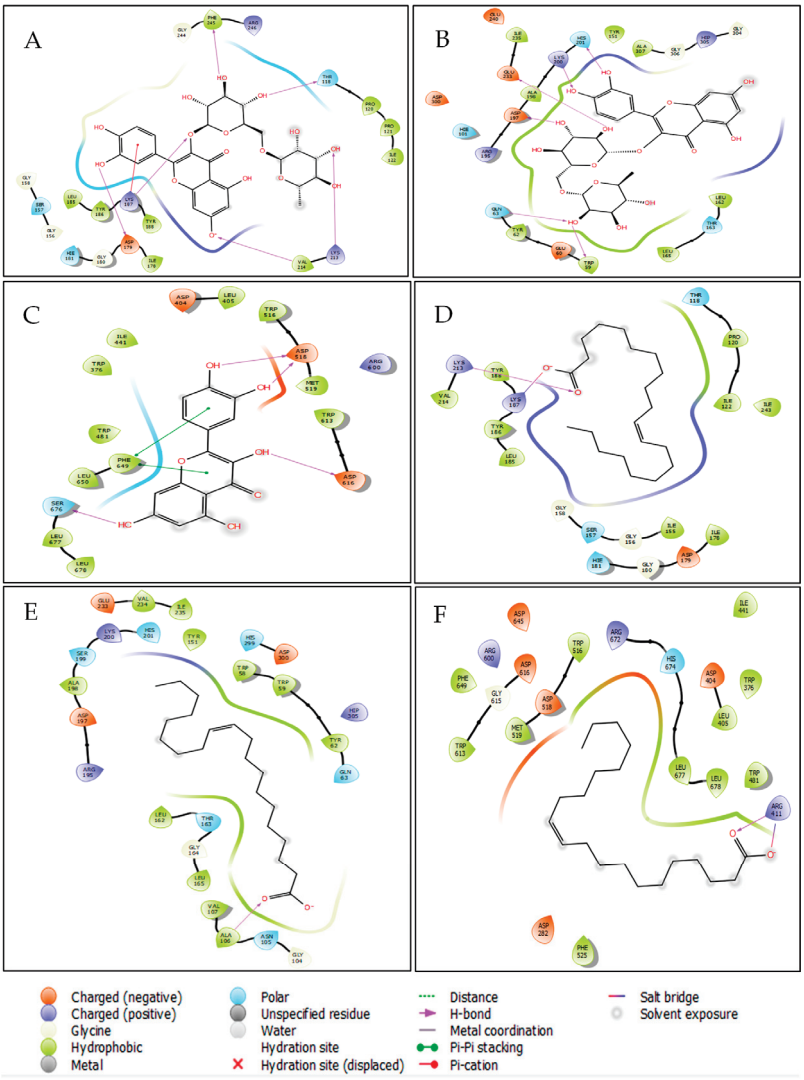

Figure 2. The 2D viewer of ligand interactions with the active site. (**A**,**B**): Rutin interactions with NADPHoxidase and alpha amylase active sites; (**C**): quercetin interactions with active site of alpha glucosidase; (**D**–**F**): Eicosenoic interactions with NADPHoxidase, alpha amylase, and alpha glucosidase active sites.

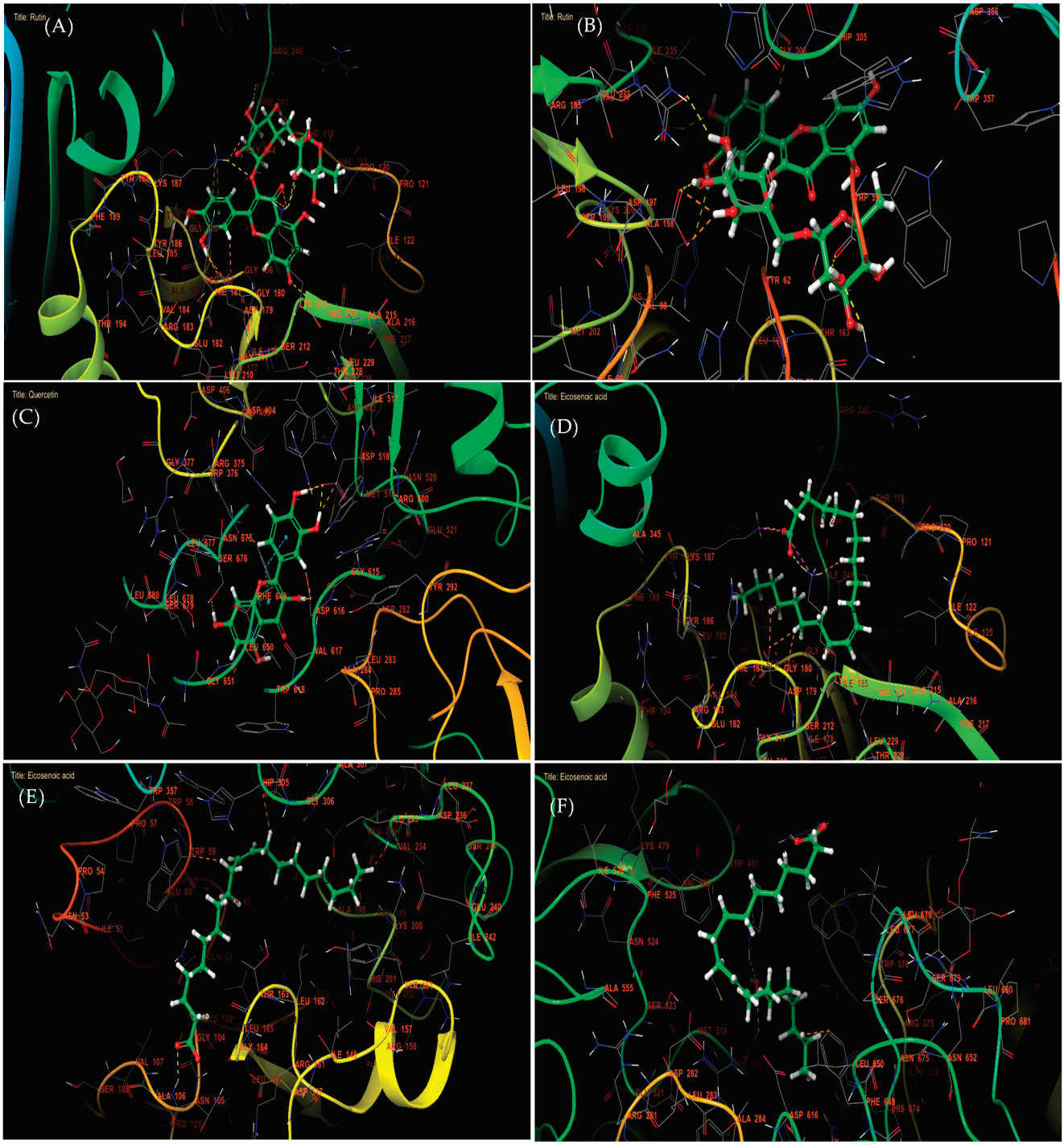

Figure 3. The 3D viewer of ligand interactions with the active site. (**A**,**B**): Rutin interactions with NADPHoxidase and alpha amylase active sites; (**C**): quercetin interactions with active site of alpha glucosidase; (**D**–**F**): Eicosenoic interactions with NADPHoxidase, alpha amylase, and alpha glucosidase active sites.

Moreover, in the active site of NADPH oxidase, Eicosenoic acid established one hydrogen bond with residue LYS 213 and one salt bridge with residue LYS 187 (Figures 2D and 3D). While in the active site of alpha amylase, the same molecule has established a single hydrogen bond with the residue (Figures 2E and 3E). This same molecule has established one hydrogen bond and one salt bridge with residue ARG 411 (Figures 2F and 3F).

3. Discussion

The process of obtaining phytochemicals from seaweed involves several crucial steps, including milling, grinding, homogenization, and extraction. Among these steps, extraction is considered the most vital for isolating and recovering phytochemicals from algae materials [25]. The efficiency of extraction is influenced by various factors, such as the chemical nature of phytochemicals, the extraction method used, sample particle size, the solvent chosen, and the presence of interfering substances [26,27]. The yield of extraction is dependent on the solvent's polarity, pH, temperature, extraction time, and the composition of the sample [28]. The phytochemical profile of Caulerpa species is highly responsive to environmental conditions and growing locations. In addition, abiotic factors such as salinity, nutrient levels, temperature, and light intensity have been shown to modulate both growth and the accumulation of bioactive compounds [29]. The result of our study suggests that *Caulerpa prolifera* extracts are a rich source of diverse and potent phenolic compounds that could be utilized in various applications.

Macroalgae are considerably different from terrestrial plants in their chemical composition, physiological features, and morphology [30]. They are highly valuable sources of protein, fiber, vitamins, polyunsaturated fatty acids, macro, and trace elements, as well as essential bioactive compounds [31]. The relative composition of saturated fatty acids (SFA), monounsaturated fatty acids (MUFA), and polyunsaturated fatty acids (PUFA) is subject to variation depending on a variety of factors such as the species, location of harvest, solvent, and extraction methodology employed.

The chemical composition of EAcE and HE was determined via gas chromatography coupled with mass spectrometry (GC-MS). It highlights the presence of palmitic acid, linoleic acid, and lauric acid as major compounds. Palmitic acid is a type of fatty acid that is abundantly found in various seaweeds, including *Caulerpa racemosa* [32], *Petalonia binghamiae* (formerly *Endarachne binghamiae*) (Phaeophyceae) [33], *Asparagopsis taxiformis* (formerly *Asparagopsis sandfordiana*) [34], and *Botryocladia leptopoda* (Rhodophyta). This fatty acid is the primary type found in all three groups of seaweeds, with green seaweeds generally exhibiting the largest amount of palmitic acid, followed by red seaweeds, while brown seaweeds possess the least amount. While some similarities exist in fatty acid composition with other green seaweeds, differences are also notable. Additionally, brown and red seaweed have a higher content of myristic and stearic acids compared to green seaweed. It is noteworthy that freshwater green algae usually lack fatty acids with more than 18 carbon atoms [35,36].

High-performance liquid chromatography (HPLC) analysis identified the principal phenolic compounds present in the ethyl acetate (EAcE) and methanolic (ME) extracts. The results indicated that *C. prolifera* extracts represent a rich source of flavonoids and polyphenolic compounds. Natural medicines are widely considered to be a safer option compared to synthetic drugs, owing to their ubiquity in the human diet and wider accessibility. Furthermore, natural drugs exhibit reduced side effects and possess the potential to target multiple signaling pathways associated with tumorigenesis. Given these advantages, natural product research is burgeoning to identify new anti-cancer, antidiabetic, and antioxidant compounds not only from terrestrial plants and microorganisms but also from marine organisms. Marine organisms offer a vast assortment of pharmaceutically significant natural products, which can be employed to treat different human diseases, particularly cancer. The molecular structures of marine bioactive compounds are unique and diverse, distinguishing them from their terrestrial counterparts. Presently, there are 14 marine-based drugs available in the market, with 9 of them being employed for cancer treatment.

Numerous experimental and epidemiological studies have suggested that dietary polyphenols are essential for providing protection against various degenerative diseases. These studies, including [37–39], have found that polyphenols have significant health benefits, mainly attributed to their potent antioxidant properties. However, to understand their health effects fully, it is crucial to enhance our understanding of their bioavailability. Although phenolic acids constitute the primary polyphenols consumed, their bioavailability has not received as much attention as that of flavonoids.

Flavonoids, a class of polyphenols ubiquitous in plants and present in our daily diets, possess a complex molecular structure that is intricately linked to various biological functions in the human body [40]. Furthermore, flavonoids are also found in algae [41] and can be enriched by various optimization techniques. In a recent study, the presence of flavonoids and other phenolic compounds was shown to confer antioxidant protection against lipid peroxidation in rat liver microsomes exposed to the oxidizing agent carbon tetrachloride [42,43]. Notably, the results of this investigation were comparable to those observed with the commercial antioxidants BHT and BHA.

The present study also reports the total antioxidant activity of the green seaweed *C. prolifera* using two popular assays. Namely, the DPPH free radical scavenging assay and the β-carotene bleaching assay. The study employed several solvents, including water, methanol, and ethyl acetate, to extract the seaweed's bioactive compounds. It is worth mentioning that the choice of solvents plays a vital role in extracting various chemical substances from the plant material, which consequently affects the antioxidant capacity. These findings are consistent with previous research [44]. The findings indicated that the aqueous extract, characterized by a high total phenolic content, exhibited strong antioxidant activity. These results provide valuable insights into the potential utilization of *C. prolifera* extracts as functional ingredients in the food and pharmaceutical industries.

The in vitro anti-diabetic activities of *C. prolifera* extracts were investigated through their potential to inhibit pancreatic enzyme activity. The inhibition of alpha-amylase and alpha-glucosidase is a key mechanism in the anti-diabetic activity [45]. Alpha-amylase is an enzyme found in saliva and the pancreas that breaks down polysaccharides (such as starch) into simple sugars. Inhibiting this enzyme slows down the breakdown of complex carbohydrates into simple sugars, thereby reducing the rise in blood glucose levels after meals. Therefore, alpha-amylase inhibitors can help control blood sugar levels in individuals with diabetes by delaying carbohydrate absorption.

Alpha-glucosidase is an enzyme located in the intestinal wall that breaks down complex sugars into simple sugars, facilitating their absorption into the bloodstream. Inhibiting this enzyme delays carbohydrate absorption and also helps reduce postprandial blood sugar spikes.

Diabetes mellitus is a metabolic endocrine disorder characterized by disruptions in the metabolism of carbohydrates, leading to persistent high levels of blood sugar [46]. This increase in blood glucose is a result of insufficient insulin secretion and/or inadequate responsiveness to this hormone [47]. Uncontrolled chronic hyperglycemia is linked to complications, notably impacting the eyes, kidneys, heart, nerves, and blood vessels [48]. Furthermore, it is established that oxidative stress plays a role in the onset of diabetes and the progression of its complications, particularly through the generation of free radicals [49,50]. Hence, the need for diabetes control. Several scientific studies have experimentally demonstrated the interest of natural resources in improving the metabolic dysregulation induced by diabetes mellitus, contributing notably to the maintenance of glycemic homeostasis [51]. Therefore, the aim of our work was to evaluate the effect of one of the marine green algae on

diabetes. To achieve this, we studied the impact of *Caulerpa prolifera* on digestive enzymes related to sugar catalysis, using in vitro experiments.

The main outcomes of the in vitro investigation regarding the inhibitory impact of α-amylase and α-glucosidase showed that each *Caulerpa prolifera* tested extract demonstrated notable inhibition of α-amylase enzymatic activity across all tested concentrations. Besides, IC_{50} values indicated comparable inhibitory effects among EACE (M) and EACE (S), all exhibiting lower activity compared to acarbose, a potent α-amylase and α-glucosidase inhibitor [52]. However, ME (M), ME (S), and AQE (M) exhibited higher inhibitory activity than the other extracts, showing a statistically similar effect to acarbose. This suggests that the extraction method of this algae has no influence on enzyme inhibition, as results remain consistent regardless of whether the extraction method used is Soxhlet or maceration. However, the type of extract (Ethyl Acetate, Methanolic Extract, or Aqueous Extract) significantly influences the results, indicating varied inhibitory effects. Our findings align with our previous research, indicating that the methanolic extract and aqueous extract obtained from maceration and Soxhlet possess the same effect and a potent effect than the Ethyl Acetate extract [53].

This consistency underscores the robustness of our results across different extraction methods and reinforces the notion that the choice of solvent significantly influences the inhibitory activity of the extracts. The biological activity of the identified compounds from *Caulerpa prolifera,* particularly their inhibitory effects on α-amylase and α-glucosidase, can be linked to their molecular structures. The results could be related to the presence of phenolic compounds, flavonoids, and tannins, with high concentrations in the methanolic extract [54,55]. According to [56], the methanolic extract of *Caulerpa prolifera* includes polyphenols in an amount of 66.61 ± 1.14 mg GAE/g DE. Furthermore, it includes tannins (19.06 ± 6.50 mg CE/g DE) and a higher flavonoid content (114.16 ± 0.91 mg QE/g DE). However, the specific phenolic compounds present in the methanolic extract of *Caulerpa prolifera* have not been discussed yet. According to [57] *Caleurpa* spp. have various flavonoids, such as kaempferol and quercetin. These flavonoids have been correlated with antioxidant activity, which may explain the beneficial effects of the extract on diabetes by its ability to inhibit α-amylase and α-glucosidase. These enzymes are involved in carbohydrate digestion, and their inhibition can help regulate blood glucose levels, which is beneficial for individuals with diabetes [58]. Additionally, *Caulerpa prolifera* contains fatty acids such as Tridecanoic acid, Tetradecanoic acid, hexadecanoic acid, cis-10-heptadecenoic acid, and sterols, including Stigmast-5-en-3-ol, (3.beta.)-, Stigmast-5-en-3-ol, oleate, Carvacrol, Phytol, Phytol acetate, and Squalene (all E) [56]. These compounds may also play a crucial role in anti-α-amylase and anti-α-glucosidase effects [59–61].

4. Materials and Methods

4.1. Chemicals and Reagents

Analytical-grade chemicals and reagents were procured from Merck (Darmstadt, Germany) and Carl Roth GmbH (Karlsruhe, Germany) to determine the total phenolic and flavonoid components. Methanol, ethyl acetate, and N-hexane were acquired from Merck (Darmstadt, Germany). α-amylase, α-glucosidase, β-carotene, 1,1-Diphenyl-2-picrylhydrazyl (DPPH•), acarbose, and 3,5-Dinitrosalicylic acid (DNSA) were obtained from Merck (Sigma-Aldrich, St. Louis, MO, USA). Phenolic standards, including ascorbic acid, kojic acid, gallic acid, apigenin, succinic acid, cholesterol, and tannic acid, were sourced from Merck and Carl Roth GmbH (Karlsruhe, Germany).

4.2. Plant Material and Extraction

In April 2021, the green algae species *C. prolifera* were harvested from the Nador lagoon located at 35°08′26.9″ N 2°29′09.6″ W in northern Morocco.

The collected seaweed sample was transported to the laboratory for further processing. *C. prolifera* was carefully cleaned and rinsed with distilled water before being exposed to light for 48 h. The dried sample was then placed in an oven at 35 °C for 24 h, as illustrated in Figure 4. The seaweed was then lyophilized and ground into a fine powder for extraction purposes. To extract the valuable components, we utilized maceration and Soxhlet techniques with four solvents: hexane, ethyl acetate, methanol, and distilled water [62–64]. The resulting extracts were then filtered using a glass filter crucible (50 mL, with Porosity 4, Isolab, Wertheim, Germany) and placed in flasks. The extracts were then dehydrated using a rotary evaporator (Laborota 4000, Heidolph Instruments, Schwabach, Germany). This thorough extraction process ensures that the resulting extracts are of the highest quality, making them ideal for further studies, and the extraction yield was calculated using the following Equation (1):

$$\text{Yield}(\%) = \frac{mass\ dried\ extract\ (g)}{mass\ dried\ matrix\ (g)} \times 100 \quad (1)$$

Figure 4. Powder of dried *C. prolifera*.

The recorded data is the median of three extraction replicates.

4.2.1. Maceration Extraction

To extract soluble compounds from a solid substance, maceration is the most common method, involving immersion in a cold liquid. In this case, extracts were prepared by stirring 100 g of macroalgae powder with 200 mL of solvent of increasing polarity (99% n-hexane for 2 h, ethyl acetate for 24 h, methanol for 24 h, and distilled water for 24 h) at room temperature.

4.2.2. Soxhlet Extraction

In order to extract active compounds from marine macroalgae, we utilized the alternative technique, namely the Soxhlet extraction method. This method involves employing a Soxhlet chamber, an extraction flask, and a condenser [47]. The process begins by placing 35 g of marine macroalgae powder into an extraction thimble, which is then combined with 300 mL of a selected solvent (such as hexane, ethyl acetate, or methanol) in the extraction flask. The duration of the Soxhlet extraction process is determined by the time it takes to extract all the soluble compounds with affinity for the solvent at a given temperature.

4.3. Phytochemical Compounds

4.3.1. Quantification of Total Phenolic Constituents

The study aimed to determine the total amount of polyphenols present in *C. prolifera* extracts. To achieve this, a modified Folin–Ciocalteu method was used. In this method, 200 µL of the extract solution with a concentration of 1 mg/mL was mixed with 1000 µL of Folin–Ciocalteu reagent dissolved in distilled water, followed by the addition of 800 µL of sodium carbonate (75 g/L). The resulting mixture was then incubated at room temperature for one hour in the dark. After incubation, absorbance readings were taken at 765 nm using a spectrophotometer, with ethanol serving as a control. To generate calibration curves, the concentration of gallic acid was altered (ranging from 0 to 0.1 mg/mL). All experiments were conducted in triplicate to obtain mean values and their corresponding standard deviations. The total amount of phenolic compounds was expressed in milligrams of gallic acid equivalents per gram of dry extract (mg GAE/g) [53].

4.3.2. Measurement of Total Flavonoid Content

200 µL of each *C. prolifera* extract, 1000 µL of distilled water, and 50 µL of $NaNO_2$ (5%) were combined. Subsequently, after a 6-min incubation period, 120 µL of $AlCl_3$ (10%) was introduced, followed by a further 5-min incubation period at room temperature in darkness. This was followed by the addition of 400 µL of 1 M NaOH and 230 µL of distilled water. The absorbance was then measured at 510 nm. To construct the calibration curve, various concentrations of quercetin solution (ranging from 0 to 0.1 mg/mL) were utilized as standards. Each measurement was conducted in triplicate to ensure result reproducibility [65].

4.4. Fatty Acid GC-MS Analysis of C. prolifera Extracts

In line with the methodology outlined in Loukili et al. [66], methyl esters of hexane fatty acids and ethyl acetate were extracted from *C. prolifera* with certain adaptations. The Shimadzu GC system (Kyoto, Japan) equipped with a BPX25 capillary column featuring a 5% diphenyl and 95% dimethylpolysiloxane phase (30 m × 0.25 mm × 0.25 µm) (Kyoto, Japan) coupled with a QP2010 MS was utilized for the characterization and identification of fatty acids. Helium gas (99.99%) served as the mobile phase with a flow rate set at 3 L/min. The temperature settings for the injection, ion source, and interface were maintained at 250 °C. The column oven temperature program began at 50 °C for 1 min, followed by a gradual increase to 250 °C at a rate of 10 °C/min, and held for 1 min. Sample components underwent ionization in Electron Ionization (EI) mode at 70 eV, scanning a mass range of 40 to 300 m/z. Each extract, in a volume of 1 µL, was injected in split mode, and triplicate analyses were conducted for each sample. Compound characterization relied on comparisons of retention times, mass spectra fragmentation patterns, and databases, including the National Institute of Standards and Technology's database (NIST). Data processing was conducted using LabSolutions (version 2.5, Shimadzu, Kyoto, Japan).

4.5. HPLC Analyses of C. prolifera Extracts

Identification of phenolic compounds within the ethyl acetate and methanolic extracts was accomplished utilizing High-Performance Liquid Chromatography (HPLC) employing an Agilent 1100 system (Agilent Technologies, Palo Alto, CA, USA) coupled with a diode array UV detector (Bruker, Berlin, Germany). Each extract (10 µL) underwent separation through a Zorbax XDB-C18 column (5 µm, 250 × 4.6 mm) connected to the Agilent 1100 system, preceded by a 4 × 3 mm C18 cartridge precolumn (Agilent Technologies). The elution gradient protocol employed was as follows: 0 to 5 min with 95% solvent A and

5% solvent B, 25 to 30 min with 65% solvent A and 35% solvent B, 35 to 40 min with 30% solvent A and 70% solvent B, and finally 40 to 45 min with 95% solvent A and 5% solvent B. Solvent A comprised water/methanol (9/1) with 0.1% phosphoric acid, while solvent B consisted of methanol with 0.1% phosphoric acid. The elution was carried out at a constant flow rate of 1 mL/min under a temperature of 40 °C. Spectrophotometric data were collected at wavelengths of 254 nm, 280 nm, 320 nm, 370 nm, and 510 nm. Compound identification was conducted by comparing their retention times and UV spectra with those of standard compounds.

4.6. Antioxidant Activity

4.6.1. Scavenging 2,2-Diphenyl-1-picrylhydrazyl Radical Test

The antioxidant activity of different extracts of *C. prolifera* was assessed using the 1,1-diphenyl-2-picrylhydrazyl (DPPH) radical bleaching method, following the protocol outlined by Brand-Williams et al., [67] with minor adjustments. The initial concentration of both the extracts and Ascorbic acid was maintained at 1 mg/mL. A solution comprising 0.8 mL of samples or standard (ascorbic acid) at varying concentrations (ranging from 0.02 to 0.32 mg/mL) and 2 mL of DPPH• solution (prepared by dissolving 2 mg of DPPH• in 200 mL of MeOH) was prepared and manually agitated. Following a 30-min incubation period in darkness at room temperature, the absorbance of the samples was measured using a UV/visible spectrophotometer at a wavelength of 517 nm, relative to the blank. Each analysis was conducted in triplicate.

The inhibitory activity of the DPPH radical by a sample was determined using the following Equation (2):

$$\text{Inhibition Percent} = \left[\frac{(Ab - As)}{Ab}\right] \times 100 \quad (2)$$

where *Ab*: Absorbance of the blank, *As*: Absorbance of a sample (or positive control).

The graph plotting inhibition percentage against extract concentration was used to calculate the IC_{50}.

4.6.2. β-Carotene Bleaching Assay

The antioxidant potential of *C. prolifera* extracts was assessed using the method described by Ref. [68]. This evaluation relied on the extracts' capacity to mitigate oxidative damage to β-carotene in an emulsion, employing the carotene bleaching assay. To prepare the emulsion, 2 mg of β-carotene was dissolved in 10 mL of chloroform, supplemented with 20 mg of linoleic acid and 200 mg of Tween 80 as an emulsifier. The chloroform was evaporated under vacuum at 40 °C, followed by the addition of 100 mL of distilled water while vigorously stirring the solution. Subsequently, 0.2 mL of the emulsion was dispensed into individual test tubes, along with either the extract or a reference antioxidant solution (BHA) at a concentration of 1 mg/mL. The absorbance was recorded at 470 nm using a 96-well microplate reader at t0 (immediately after emulsion addition) and after a 2-h incubation period.

The inhibition of the linoleate/β-carotene radical was determined using the following Equation (3):

$$\text{Bleaching inhibition } (\%) = 100 - \frac{initial\ (\beta - \text{carotene})(t0) - (\beta - \text{carotene})\ after\ 2h}{initial\ (\beta - \text{carotene})(t0)} \times 100 \quad (3)$$

4.7. In Vitro α-Amylase Inhibition

The inhibitory activity of various extracts of *C. prolifera* against α-amylase was assessed following the protocol outlined by Daoudi et al. [48]. A reaction mixture was prepared, comprising 0.2 mL of the sample or acarbose (utilized as a positive control at concentrations ranging from 2.27 to 0.14 mg/mL), 0.2 mL of phosphate buffer (pH 6.9), and 0.2 mL of enzyme solution (13 IU). This mixture was pre-incubated at 37 °C for 10 min before the addition of 0.2 mL of enzyme-substrate solution (1% starch dissolved in phosphate buffer). The reaction proceeded at 37 °C for 30 min. The enzymatic reaction was halted by adding 0.6 mL of DNSA reagent, followed by an incubation step at 100 °C for 8 min, followed by cooling in a cold-water bath. Absorbance was measured at 540 nm.

The inhibition percentage was calculated using the following Equation (4):

$$\text{Inhibition activity}(\%) = \frac{(\text{OD control 540 nm} - \text{OD control blank 540 nm}) - (\text{OD sample 540 nm} - \text{OD sample blank 540 nm})}{\text{OD control 540 nm} - \text{OD control blank 540 nm}} \times 10 \quad (4)$$

The IC_{50} of the various test was done graphically using the function:

$$\text{Inhibition percentage}(\%) = f(\log(\text{sample concentration})) \quad (5)$$

4.8. In Vitro α-Glucosidase Inhibition Assay

The effect of *C. prolifera* extracts on intestinal α-glucosidase activity was evaluated using a modified version of the protocol outlined by Hbika et al. [69]. A mixture was prepared by combining 100 mL of sucrose (50 mM), 1000 mL of phosphate buffer (50 mM, pH 7.5), and 100 mL of intestinal α-glucosidase enzyme solution (10 IU). This mixture was then supplemented with 10 mL of distilled water (as a control), acarbose (as the positive control), or *C. prolifera* extract solution at a concentration of 2.2 g/mL. Subsequently, the mixture was incubated for 25 min at 37 °C in a water bath. To terminate the enzymatic reaction and quantify the release of glucose, the mixture was heated at 100 °C for 5 min:

$$\text{Inhibition activity}(\%) = \frac{(\text{OD control 540 nm} - \text{OD control blank 540 nm}) - (\text{OD sample 540 nm} - \text{OD sample blank 540 nm})}{\text{OD control 540 nm} - \text{OD control blank 540 nm}} \times 10 \quad (6)$$

4.9. Theoretical Study

4.9.1. Ligands Preparation

To evaluate the antioxidant and antidiabetic activities of the compounds identified in *Caulerpa prolifera* extracts, a comprehensive molecular analysis was performed. All chemical compounds identified by HPLC Analysis or by GC/MS in *Caulerpa prolifera* extracts were downloaded from the PUBCHEM platform in .SDF format. Then, these molecules were prepared using the LigPrep subsystem in Maestro 11.5 from the Schrödinger suite (version 2018, Schrödinger). The minimization process employed the OPLS3 force field, and the generation of all possible ionic states was achieved at a target pH of 7.2 $\pm$ 2 using Epik. Additionally, for each ligand, plausible stereo isomers and lower-energy ring conformations were generated [70].

4.9.2. Receptor Preparation

The structure of human NADPH oxidase (PDB ID: 2CDU) [71], and the alpha amylase (PDB ID: 1B2Y) [38] and alpha glucosidase (PDB ID: 5NN8) [53] were downloaded from the PDB data bank. The protein preparation wizard of the Schrödinger suite was utilized to process the receptor, involving tasks such as assigning bond orders, adding hydrogen, filling empty side chains and loops with PRIME, and ultimately removing all water from the crystal structures. Following the optimization of these crystal structures, a restrained minimization with a root mean square deviation (RMSD) of 0.3 Å was performed using the OPLS3 force field [72].

4.9.3. Grid Generation and Molecular Docking

The minimized protein structures were then utilized to generate grids through the "Receptor Grid Generation" panel. For each protein, a grid was established with default parameters, including a Van Der Waals scaling factor of 1.00 and a charging cut-off value of 0.25, in accordance with the OPLS3 force field. A cubic receptor grid box with dimensions of 20 Å × 20 Å × 20 Å was centered on the selected co-crystallized ligand. The molecular docking assay utilized the Standard Precision (SP) scoring method of Glide, integrated into the Schrödinger suite-Maestro version 12.5 [73].

5. Conclusions

Macroalgae are a highly promising resource for the future due to their high nutritional value and versatile applications in various fields such as food, energy, medicine, cosmetics, and biotechnology. To explore the potential of macroalgae, a study was conducted to analyze seven extracts of *Caulerpa prolifera* and to determine their nutritional properties. The results revealed that the methanolic and ethyl acetate extracts contained a significant amount of Sinapic acid, Kaempferol, 7,3,4-trihydroxy flavone, and P-Coumaric acid. The hexanic and ethyl acetate extracts were rich in Palmitic acid and linoleic acid, which are the main fatty acids detected. The ethyl acetate extracts demonstrated strong antioxidant activity by the beta-carotene bleaching method, while the aqueous extract of *C. prolifera* exhibited remarkable antioxidant properties against the DPPH method. The aqueous extract also demonstrated a strong capacity to inhibit pancreatic α-amylase and intestinal α-glucosidase enzymes involved in sugar degradation, which can be attributed to the high content of polyphenols and flavonoids. The findings of this study hold significant importance in the development of commercial products based on cultivated marine macroalgae and can provide a novel solution for the sustainable production of biomass.

Author Contributions: Conceptualization, S.O.; methodology, N.E.D., M.C., M.R., I.R. and M.B.; software, M.C. and I.M.; validation, L.R. and M.-L.F.; formal analysis, S.O.; investigation, S.O. and N.E.D.; data curation, M.C. and I.M.; writing—original draft preparation, S.O.; writing—review and editing, S.O., L.R., A.A.G. and M.-L.F.; visualization, L.R., A.A.G. and M.-L.F.; supervision, M.R. and B.H.; project administration, M.R. All authors have read and agreed to the published version of the manuscript.

Funding: This research received no external funding.

Institutional Review Board Statement: Not applicable.

Data Availability Statement: Data are available upon request to the authors.

Acknowledgments: The authors thank the Faculty of Science Oujda of the Chemical Department for their help with local physical measurements. Great thanks are addressed to Danny and Thomas for their help. Support was also provided by the Laboratory of Chemistry of Natural Molecules, Gembloux AgroBio Tech, University of Liege, Belgium.

Conflicts of Interest: The authors report no commercial or proprietary interest in any product or concept discussed in this article.

References

1. Snoussi, M.; Ouchani, T.; Khouakhi, A.; Niang-Diop, I. Impacts of Sea-Level Rise on the Moroccan Coastal Zone: Quantifying Coastal Erosion and Flooding in the Tangier Bay. *Geomorphology* **2009**, *107*, 32–40. [CrossRef]
2. Benhissoune, S.; Boudouresque, C.; Verlaque, M. A CheckList of Marine Seaweeds of the Mediterranean and Atlantic Coasts of Morocco. I. Chlorophyceae Wille s. l. *Bot. Mar.* **2001**, *44*, 171–182. [CrossRef]

3. Benhissoune, S.; Boudouresque, C.; Perret-Boudouresque, M.; Verlaque, M. A Checklist of the Seaweeds of the Mediterranean and Atlantic Coasts of Morocco. III. Rhodophyceae (Excluding Ceramiales). *Bot. Mar.* **2002**, *45*, 391–412. [CrossRef]
4. Elasri, O.; Ramdani, M.; Latrach, L.; Benyounes, H.; Mohamed elamin, A.; Mohammed, R. Comparison of Energy Recovery after Anaerobic Digestion of Three Marchica Lagoon Algae (*Caulerpa prolifera*, *Colpomenia sinuosa*, *Gracilaria bursa-pastoris*). *Sustain. Mater. Technol.* **2017**, *11*, 47–52.
5. Wang, L.; Wang, X.; Wu, H.; Liu, R. Overview on Biological Activities and Molecular Characteristics of Sulfated Polysaccharides from Marine Green Algae in Recent Years. *Mar. Drugs* **2014**, *12*, 4984–5020. [CrossRef]
6. Crockett, P.F.; Keough, M.J. Ecological Niches of Three Abundant Caulerpa Species in Port Phillip Bay, Southeast Australia. *Aquat. Bot.* **2014**, *119*, 120–131. [CrossRef]
7. de Senerpont Domis, L.; Famà, P.; Bartlett, A.; Prud'homme van Reine, W.; Espinosa, C.; Trono, J. Gavino Defining Taxon Boundaries in Members of the Morphologically and Genetically Plastic Genus Caulerpa (Caulerpales, Chlorophyta). *J. Phycol.* **2003**, *39*, 1019–1037. [CrossRef]
8. Fernández-García, C.; Cortés, J.; Alvarado, J.J.; Nivia-Ruiz, J. Physical Factors Contributing to the Benthic Dominance of the Alga *Caulerpa sertularioides* (Caulerpaceae, Chlorophyta) in the Upwelling Bahía Culebra, North Pacific of Costa Rica. *Rev. Biol. Trop.* **2015**, *60*, 93. [CrossRef]
9. Gacia, E.; Rodríguez-Prieto, C.; Delgado, O.; Ballesteros, E. Seasonal Light and Temperature Responses of Caulerpa Taxifolia from the Northwestern Mediterranean. *Aquat. Bot.* **1996**, *53*, 215–225. [CrossRef]
10. Ohba, H.; Nashima, H.; Enomoto, S. Culture Studies on *Caulerpa* (Caulerpales, Chlorophyceae) III. Reproduction, Development and Morphological Variation of Laboratory-Cultured, *C. racemosa* Var. *peltata*. *Bot. Mag.* **1992**, *105*, 589–600. [CrossRef]
11. Kumari, P.; Kumar, M.; Gupta, V.; Reddy, C.R.K.; Jha, B. Tropical Marine Macroalgae as Potential Sources of Nutritionally Important PUFAs. *Food Chem.* **2010**, *120*, 749–757. [CrossRef]
12. Nagappan, T.; Vairappan, C.S. Nutritional and Bioactive Properties of Three Edible Species of Green Algae, Genus Caulerpa (Caulerpaceae). *J. Appl. Phycol.* **2014**, *26*, 1019–1027. [CrossRef]
13. de Gaillande, C.; Payri, C.; Remoissenet, G.; Zubia, M. Caulerpa Consumption, Nutritional Value and Farming in the Indo-Pacific Region. *J. Appl. Phycol.* **2017**, *29*, 2249–2266. [CrossRef]
14. Paul, N.A.; Neveux, N.; Magnusson, M.; de Nys, R. Comparative Production and Nutritional Value of "Sea Grapes"—The Tropical Green Seaweeds *Caulerpa lentillifera* and *C. racemosa*. *J. Appl. Phycol.* **2014**, *26*, 1833–1844. [CrossRef]
15. Ghosh, P.; Adhikari, U.; Ghosal, P.K.; Pujol, C.A.; Carlucci, M.J.; Damonte, E.B.; Ray, B. In Vitro Anti-Herpetic Activity of Sulfated Polysaccharide Fractions from Caulerpa Racemosa. *Phytochemistry* **2004**, *65*, 3151–3157. [CrossRef]
16. Hayakawa, Y.; Hayashi, T.; Lee, J.-B.; Srisomporn, P.; Maeda, M.; Ozawa, T.; Sakuragawa, N. Inhibition of Thrombin by Sulfated Polysaccharides Isolated from Green Algae. *Biochim. Biophys. Acta (BBA)-Protein Struct. Mol. Enzymol.* **2000**, *1543*, 86–94. [CrossRef]
17. Ji, H.; Shao, H.; Zhang, C.; Hong, P.; Xiong, H. Separation of the Polysaccharides in *Caulerpa racemosa* and Their Chemical Composition and Antitumor Activity. *J. Appl. Polym. Sci.* **2008**, *110*, 1435–1440. [CrossRef]
18. Maeda, R.; Ida, T.; Ihara, H.; Sakamoto, T. Immunostimulatory Activity of Polysaccharides Isolated from *Caulerpa lentillifera* on Macrophage Cells. *Biosci. Biotechnol. Biochem.* **2012**, *76*, 501–505. [CrossRef]
19. Rodrigues, J.A.G.; Neto, É.M.; Teixeira, L.A.C.; de Paula, R.C.M.; Mourão, P.A.d.S.; Benevides, N.M.B. Structural Features and Inactivation of Coagulation Proteases of a Sulfated Polysaccharidic Fraction from *Caulerpa cupressoides* Var. *Lycopodium* (Caulerpaceae, Chlorophyta). *Acta Sci. Technol.* **2013**, *35*, 611–619. [CrossRef]
20. Holdt, S.L.; Kraan, S. Bioactive Compounds in Seaweed: Functional Food Applications and Legislation. *J. Appl. Phycol.* **2011**, *23*, 543–597. [CrossRef]
21. Doty, M.S.; Aguilar-Santos, G. Caulerpicin, a Toxic Constituent of Caulerpa. *Nature* **1966**, *211*, 990. [CrossRef] [PubMed]
22. Mandlik, R.V.; Naik, S.R.; Zine, S.; Ved, H.; Doshi, G. Antidiabetic Activity of Caulerpa Racemosa: Role of Proinflammatory Mediators, Oxidative Stress, and Other Biomarkers. *Planta Medica Int. Open* **2022**, *9*, e60–e71. [CrossRef]
23. Fajriah, S.; Rizki, I.F.; Sinurat, E. Characterization and Analysis of the Antidiabetic Activities of Sulphated Polysaccharide Extract from *Caulerpa lentillifera*. *Pharmacia* **2021**, *68*, 869–875. [CrossRef]
24. Bradshaw, P.C. Cytoplasmic and Mitochondrial NADPH-Coupled Redox Systems in the Regulation of Aging. *Nutrients* **2019**, *11*, 504. [CrossRef]
25. Bitwell, C.; Indra, S.S.; Luke, C.; Kakoma, M.K. A Review of Modern and Conventional Extraction Techniques and Their Applications for Extracting Phytochemicals from Plants. *Sci. Afr.* **2023**, *19*, e01585. [CrossRef]
26. Alara, O.R.; Abdurahman, N.H.; Ukaegbu, C.I. Extraction of Phenolic Compounds: A Review. *Curr. Res. Food Sci.* **2021**, *4*, 200–214. [CrossRef]

27. Do, Q.D.; Angkawijaya, A.E.; Tran-Nguyen, P.L.; Huynh, L.H.; Soetaredjo, F.E.; Ismadji, S.; Ju, Y.-H. Effect of Extraction Solvent on Total Phenol Content, Total Flavonoid Content, and Antioxidant Activity of *Limnophila aromatica*. *J. Food Drug Anal.* **2014**, *22*, 296–302. [CrossRef]
28. Dhanani, T.; Shah, S.; Gajbhiye, N.A.; Kumar, S. Effect of Extraction Methods on Yield, Phytochemical Constituents and Antioxidant Activity of *Withania somnifera*. *Arab. J. Chem.* **2017**, *10*, S1193–S1199. [CrossRef]
29. Guo, H.; Yao, J.; Sun, Z.; Duan, D. Effects of Salinity and Nutrients on the Growth and Chlorophyll Fluorescence of *Caulerpa lentillifera*. *Chin. J. Ocean. Limnol.* **2015**, *33*, 410–418. [CrossRef]
30. Jung, K.A.; Lim, S.-R.; Kim, Y.; Park, J.M. Potentials of Macroalgae as Feedstocks for Biorefinery. *Bioresour. Technol.* **2013**, *135*, 182–190. [CrossRef]
31. Ortiz, J.; Romero, N.; Robert, P.; Araya, J.; Lopez-Hernández, J.; Bozzo, C.; Navarrete, E.; Osorio, A.; Rios, A. Dietary Fiber, Amino Acid, Fatty Acid and Tocopherol Contents of the Edible Seaweeds Ulva Lactuca and *Durvillaea antarctica*. *Food Chem.* **2006**, *99*, 98–104. [CrossRef]
32. Qudus, B.; Aroyehun, A.; Abdul Razak, S.; Palaniveloo, K.; Nagappan, T.; Suraiza Nabila Rahmah, N.; Wee Jin, G.; Chellappan, D.K.; Chellian, J.; Kunnath, A.P. Bioprospecting Cultivated Tropical Green Algae, Caulerpa Racemosa (Forsskal) J. Agardh: A Perspective on Nutritional Properties, Antioxidative Capacity and Anti-Diabetic Potential. *Foods* **2020**, *9*, 1313. [CrossRef] [PubMed]
33. Bano, S.; Perveen, S.; Ahmad, V.U.; Bano, N.; Shameel, M. Chemical Constituents of *Endarachne binghamiae* (Scytosiphonales, Phaeophyta) from the Karachi Coast. *Bot. Mar.* **1987**, *30*, 371–372. [CrossRef]
34. Bano, S.; Hayee, A.; Ahmad, V.U.; Shaikh, W.; Usmanghani, K.; Shameel, M. Marine Natural Products. Part VII. Steroids from a Red Alga *Asparagopsis sandfordiana*. *Pol. J. Chem.* **1988**, *62*, 905–906.
35. Gunstone, F.D. Fatty Acids and Glycerides. *Nat. Prod. Rep.* **1987**, *4*, 95. [CrossRef]
36. Wood, B.J.B. Fatty Acids and Lipids in Algae. In *Microbial Lipids*; Academic Press: New York, NY, USA, 1988; pp. 807–867.
37. Hertog, M.G.L.; Feskens, E.J.M.; Kromhout, D.; Hertog, M.G.L.; Hollman, P.C.H.; Hertog, M.G.L.; Katan, M.B. Dietary Antioxidant Flavonoids and Risk of Coronary Heart Disease: The Zutphen Elderly Study. *Lancet* **1993**, *342*, 1007–1011. [CrossRef]
38. Manach, C.; Mazur, A.; Scalbert, A. Polyphenols and Prevention of Cardiovascular Diseases. *Curr. Opin. Lipidol.* **2005**, *16*, 77–84. [CrossRef]
39. van Dam, R.M.; Hu, F.B. Coffee Consumption and Risk of Type 2 Diabetes: A Systematic Review. *JAMA* **2005**, *294*, 97. [CrossRef]
40. Panche, A.N.; Diwan, A.D.; Chandra, S.R. Flavonoids: An Overview. *J. Nutr. Sci.* **2016**, *5*, e47. [CrossRef]
41. Ferdous, U.T.; Balia Yusof, Z.N. Insight into Potential Anticancer Activity of Algal Flavonoids: Current Status and Challenges. *Molecules* **2021**, *26*, 6844. [CrossRef]
42. Duthie, G.; Morrice, P. Antioxidant Capacity of Flavonoids in Hepatic Microsomes Is Not Reflected by Antioxidant Effects In Vivo. *Oxidative Med. Cell. Longev.* **2012**, *2012*, 1–6. [CrossRef] [PubMed]
43. Tungmunnithum, D.; Thongboonyou, A.; Pholboon, A.; Yangsabai, A. Flavonoids and Other Phenolic Compounds from Medicinal Plants for Pharmaceutical and Medical Aspects: An Overview. *Medicines* **2018**, *5*, 93. [CrossRef] [PubMed]
44. Fernández-Agulló, A.; Pereira, E.; Freire, M.S.; Valentão, P.; Andrade, P.B.; González-Álvarez, J.; Pereira, J.A. Influence of Solvent on the Antioxidant and Antimicrobial Properties of Walnut (*Juglans regia* L.) Green Husk Extracts. *Ind. Crops Prod.* **2013**, *42*, 126–132. [CrossRef]
45. Tundis, R.; Loizzo, M.R.; Menichini, F. Natural Products as α-Amylase and α-Glucosidase Inhibitors and Their Hypoglycaemic Potential in the Treatment of Diabetes: An Update. *Mini Rev. Med. Chem.* **2010**, *10*, 315–331. [CrossRef]
46. Hameed, I.; Masoodi, S.R.; Mir, S.A.; Nabi, M.; Ghazanfar, K.; Ganai, B.A. Type 2 Diabetes Mellitus: From a Metabolic Disorder to an Inflammatory Condition. *World J. Diabetes* **2015**, *6*, 598. [CrossRef]
47. Arayne, M.; Sultana, N.; Mirza, A.; MH, Z.; Siddiqui, F. In Vitro Hypoglycemic Activity of Methanolic Extracts of Some Indigenous Plants. *Pak. J. Pharm. Sci.* **2007**, *20*, 268–273.
48. Daoudi, N.E.; Bouziane, O.; Bouhrim, M.; Bnouham, M. Natural Aldose Reductase Inhibitors for Treatment and Prevention of Diabetic Cataract: A Review. *Herba Pol.* **2022**, *68*, 35–58. [CrossRef]
49. Baynes, J.W.; Thorpe, S.R. Role of Oxidative Stress in Diabetic Complications: A New Perspective on an Old Paradigm. *Diabetes* **1999**, *48*, 1–9. [CrossRef]
50. Dalli, M.; Daoudi, N.E.; Abrigach, F.; Azizi, S.; Bnouham, M.; Kim, B.; Gseyra, N. In Vitro α-Amylase and Hemoglobin Glycation Inhibitory Potential of Nigella Sativa Essential Oil, and Molecular Docking Studies of Its Principal Components. *Front. Pharmacol.* **2022**, *13*, 1036129. [CrossRef]
51. Nainu, F.; Frediansyah, A.; Mamada, S.S.; Permana, A.D.; Salampe, M.; Chandran, D.; Emran, T.B.; Simal-Gandara, J. Natural Products Targeting Inflammation-Related Metabolic Disorders: A Comprehensive Review. *Heliyon* **2023**, *9*, e16919. [CrossRef]

52. Oboh, G.; Ogunsuyi, O.B.; Ogunbadejo, M.D.; Adefegha, S.A. Influence of Gallic Acid on α-Amylase and α-Glucosidase Inhibitory Properties of Acarbose. *J. Food Drug Anal.* **2016**, *24*, 627–634. [CrossRef] [PubMed]
53. Ouahabi, S.; Loukili, E.H.; Daoudi, N.E.; Chebaibi, M.; Ramdani, M.; Rahhou, I.; Bnouham, M.; Fauconnier, M.-L.; Hammouti, B.; Rhazi, L.; et al. Study of the Phytochemical Composition, Antioxidant Properties, and In Vitro Anti-Diabetic Efficacy of Gracilaria Bursa-Pastoris Extracts. *Mar. Drugs* **2023**, *21*, 372. [CrossRef] [PubMed]
54. Hayat, J.; Akodad, M.; Moumen, A.; Baghour, M.; Skalli, A.; Ezrari, S.; Belmalha, S. Phytochemical Screening, Polyphenols, Flavonoids and Tannin Content, Antioxidant Activities and FTIR Characterization of *Marrubium vulgare* L. from 2 Different Localities of Northeast of Morocco. *Heliyon* **2020**, *6*, e05609. [CrossRef] [PubMed]
55. Muniyandi, K.; George, E.; Sathyanarayanan, S.; George, B.P.; Abrahamse, H.; Thamburaj, S.; Thangaraj, P. Phenolics, Tannins, Flavonoids and Anthocyanins Contents Influenced Antioxidant and Anticancer Activities of Rubus Fruits from Western Ghats, India. *Food Sci. Hum. Wellness* **2019**, *8*, 73–81. [CrossRef]
56. Belkacemi, L.; Belalia, M.; Djendara, A.; Bouhadda, Y. Antioxidant and Antibacterial Activities and Identification of Bioactive Compounds of Various Extracts of Caulerpa Racemosa from Algerian Coast. *Asian Pac. J. Trop. Biomed.* **2020**, *10*, 87. [CrossRef]
57. Cotas, J.; Leandro, A.; Monteiro, P.; Pacheco, D.; Figueirinha, A.; Gonçalves, A.M.M.; da Silva, G.J.; Pereira, L. Seaweed Phenolics: From Extraction to Applications. *Mar. Drugs* **2020**, *18*, 384. [CrossRef]
58. Daoudi, N.E.; Bouhrim, M.; Ouassou, H.; Legssyer, A.; Mekhfi, H.; Ziyyat, A.; Aziz, M.; Bnouham, M. Inhibitory Effect of Roasted/ Unroasted Argania Spinosa Seeds Oil on α- Glucosidase, α-Amylase and Intestinal Glucose Absorption Activities. *S. Afr. J. Bot.* **2020**, *135*, 413–420. [CrossRef]
59. Lakshmanasenthil, S.; Vinoth Kumar, T.; Geetharamani, D.; Shanthi Priya, S. α-Amylase and α-Glucosidase InhibitoryActivity of Tetradecanoic Acid (TDA) from *Sargassum wightii* with Relevance to Type 2 Diabetes Mellitus. *J. Biol. Act. Prod. Nat.* **2018**, *8*, 180–191. [CrossRef]
60. Salazar, M.O.; Osella, M.I.; Arcusin, D.E.J.; Lescano, L.E.; Furlan, R.L.E. New α-Glucosidase Inhibitors from a Chemically Engineered Essential Oil of *Origanum vulgare* L. *Ind. Crops Prod.* **2020**, *156*, 112855. [CrossRef]
61. Wuttke, A.; Idevall-Hagren, O.; Tengholm, A. P2Y $_1$ Receptor-dependent Diacylglycerol Signaling Microdomains in β Cells Promote Insulin Secretion. *FASEB J.* **2013**, *27*, 1610–1620. [CrossRef]
62. Stalikas, C.D. Extraction, Separation, and Detection Methods for Phenolic Acids and Flavonoids. *J. Sep. Sci.* **2007**, *30*, 3268–3295. [CrossRef] [PubMed]
63. Azwanida, N. A Review on the Extraction Methods Use in Medicinal Plants, Principle, Strength and Limitation. *Med. Aromat. Plants* **2015**, *4*, 196. [CrossRef]
64. Dai, J.; Mumper, R.J. Plant Phenolics: Extraction, Analysis and Their Antioxidant and Anticancer Properties. *Molecules* **2010**, *15*, 7313–7352. [CrossRef] [PubMed]
65. Taibi, M.; Loukili, E.H.; Elbouzidi, A.; Baraich, A.; Haddou, M.; Bellaouchi, R.; Saalaoui, E.; Asehraou, A.; Addi, M.; Bourhia, M.; et al. Exploring the Pharmacological Potential of the Chemically Characterized Essential Oil from *Clinopodium nepeta* Subsp. Ascendens: A Combined In Vitro and In Silico Analysis. *Moroc. J. Chem.* **2024**, *12*, 997–1021. [CrossRef]
66. Loukili, E.H.; Abrigach, F.; Bouhrim, M.; Bnouham, M.; Fauconnier, M.; Ramdani, M. Chemical Composition and Physicochemical Analysis of *Opuntia dillenii* Extracts Grown in Morocco. *J. Chem.* **2021**, *2021*, 8858929. [CrossRef]
67. Brand-Williams, W.; Cuvelier, M.E.; Berset, C. Use of a Free Radical Method to Evaluate Antioxidant Activity. *LWT-Food Sci. Technol.* **1995**, *28*, 25–30. [CrossRef]
68. Bekkouch, O.; Harnafi, M.; Touiss, I.; Khatib, S.; Harnafi, H.; Alem, C.; Amrani, S. In Vitro Antioxidant and In Vivo Lipid-Lowering Properties of *Zingiber officinale* Crude Aqueous Extract and Methanolic Fraction: A Follow-Up Study. *Evid.-Based Complement. Altern. Med.* **2019**, *2019*, 9734390. [CrossRef]
69. Hbika, A.; Daoudi, N.E.; Bouyanzer, A.; Bouhrim, M.; Mohti, H.; Loukili, E.H.; Mechchate, H.; Al-Salahi, R.; Nasr, F.A.; Bnouham, M.; et al. Artemisia Absinthium L. Aqueous and Ethyl Acetate Extracts: Antioxidant Effect and Potential Activity In Vitro and In Vivo against Pancreatic α-Amylase and Intestinal α-Glucosidase. *Pharmaceutics* **2022**, *14*, 481. [CrossRef]
70. Lafraxo, S.; El Moussaoui, A.; A Bin Jardan, Y.; El Barnossi, A.; Chebaibi, M.; Baammi, S.; Ait Akka, A.; Chebbac, K.; Akhazzane, M.; Chelouati, T.; et al. GC-MS Profiling, In Vitro Antioxidant, Antimicrobial, and In Silico NADPH Oxidase Inhibition Studies of Essential Oil of *Juniperus thurifera* Bark. *Evid.-Based Complement. Altern. Med.* **2022**, *2022*, 6305672. [CrossRef]
71. Herrera-Calderon, O.; Chacaltana-Ramos, L.J.; Huayanca-Gutiérrez, I.C.; Algarni, M.A.; Alqarni, M.; Batiha, G.E.-S. Chemical Constituents, In Vitro Antioxidant Activity and In Silico Study on NADPH Oxidase of *Allium sativum* L. (Garlic) Essential Oil. *Antioxidants* **2021**, *10*, 1844. [CrossRef]
72. El Abdali, Y.; Mahraz, A.M.; Beniaich, G.; Mssillou, I.; Chebaibi, M.; Bin Jardan, Y.A.; Lahkimi, A.; Nafidi, H.-A.; Aboul-Soud, M.A.M.; Bourhia, M.; et al. Essential Oils of *Origanum compactum* Benth: Chemical Characterization, in Vitro, in Silico, Antioxidant, and Antibacterial Activities. *Open Chem.* **2023**, *21*, 20220282. [CrossRef]

73. Amrati, F.E.-Z.; Elmadbouh, O.H.M.; Chebaibi, M.; Soufi, B.; Conte, R.; Slighoua, M.; Saleh, A.; Al Kamaly, O.; Drioiche, A.; Zair, T.; et al. Evaluation of the Toxicity of *Caralluma europaea* (*C.E*) Extracts and Their Effects on Apoptosis and Chemoresistance in Pancreatic Cancer Cells. *J. Biomol. Struct. Dyn.* **2023**, *41*, 8517–8534. [CrossRef]

marine drugs

MDPI

Article

Exploration of Bioactive Compounds, Antioxidant and Antibacterial Properties, and Their Potential Efficacy Against HT29 Cell Lines in *Dictyota bartayresiana*

Durairaj Swarna Bharathi [1,*], Andiyappan Boopathy Raja [1], Suganthi Nachimuthu [2], S. Thangavel [3], Karthik Kannan [4], Sengottaiyan Shanmugan [5] and Vinaya Tari [6,*]

[1] PG and Research Department of Zoology, Nehru Memorial College, Affiliated to Bharathidasan University, Puthanampatti 621004, Tamil Nadu, India; boopathyraja07@gmail.com
[2] PG and Research Department of Physics, Government Arts College (Autonomous), Affiliated to Bharathidasan University, Karur 639005, Tamil Nadu, India; suganthiphyupm@gmail.com
[3] Department of Physics, C.S.I. Bishop Solomon Doraisawmy College of Arts and Science, Karur 639001, Tamil Nadu, India; suhithangam@gmail.com
[4] Department of Mechanical Engineering, Advanced Institute of Manufacturing with High-Tech Innovations, National Chung Cheng University, Chia-Yi 621301, Taiwan; karthikkannanphotochem@gmail.com
[5] Research Centre for Solar Energy, Integrated Research and Discovery, Department of Physics, Koneru Lakshmaiah Education Foundation, Green Fields, Vaddeswaram, Guntur 522502, Andhra Pradesh, India; shanmugan@kluniversity.in
[6] Department of Biology, Faculty of Science and Technology, Universitas Airlangga, Surabaya 60115, East Java, Indonesia
* Correspondence: swarnaraj93@gmail.com (D.S.B.); drvinaya89@outlook.com (V.T.)

Abstract: This study investigates the rare seaweed alga *Dictyota bartayresiana* lamour for biological activity. Antioxidant and antibacterial activities were examined. An MTT assay was carried out to examine cytotoxicity activity against colon cancer cells. The HPTLC analysis was performed for four different extracts, which exhibited clear flavonoid band formation at 254 nm and 366 nm with varied ranges of R_f values: methanolic extract (R_f 0.87), acetone extract (R_f 0.82), and benzene (R_f 0.83). Methanolic Extract Fraction One (MEF1) has a distinct band formation at 366 nm, it is shown to have the highest inhibition (6.20 ± 0.53 mm) against *Escherichia coli*, and the MTT assay reveals that the aqueous extract of *Dictyota bartayresiana* extract has an IC_{50} value of 300 µg/mL. It is divulged that methanolic extract shows the highest phytochemical compound level among the four extracts of *Dictyota bartayresiana*. A GC/MS analysis was employed to investigate the flavonoid profile of the crude seaweed extract. Although LC/MS is typically preferred for flavonoid analysis due to thermal sensitivity, GC/MS was used in this study owing to time constraints, with optimized conditions to reduce thermal degradation. The GC-MS analysis identified Quinoline and other flavonoids, suggesting potential bioactivity. The cytotoxicity activity of MEF1 shows that the development of a promising drug may be evaluated from a seaweed source. The present study provides excellent insight with the first report of the biologically active compound of *Dictyota bartayresiana*.

Keywords: *Dictyota barteyresiana*; HP-TLC analysis; GC-MS; antioxidant activity; antibacterial activity; HT 29 cancer cells

1. Introduction

Seaweed is a valuable source from the marine environment and can survive with plenty of struggles. According to Darwin's postulation, the "Ability of fitness of organism progressively increased by adapting themselves for their corresponding environment with natural support" [1]. This competence may be biotic, or abiotic factors may encourage the development of physical or chemical changes in populations. External forces stimulate secondary metabolite production, which is tightly enveloped with the organism's evolution and defense against predators, which mainly involves the eradication of specific organisms such as fungi, bacteria, viruses, inflammatory substances, free radicals, etc. The secondary metabolites have strengthened species in various ways [2–4]. Ancestors knew that algae were used as a food supplement, and recent research has found that algae contain phytochemical compounds that can help to treat various diseases [5,6].

Seaweed possesses anticoagulant properties, preventing excessive blood clotting [7]. It produces a wide range of chemically active compounds in its environment, which show antibacterial, antifungal, antimacrofouling, and other pharmacological properties [8]. Compounds, like chlorophyll-a, fucoxanthin, and phenols, and flavonoids assist seaweeds in scavenging free radicals capably, suppress oxidation enzymes, and provide other favorable bioactive properties. Seaweeds containing both water and lipid-soluble vitamins, including thiamine and riboflavin, β-carotene, and tocopherols, which may lower the risk of heart disease, thrombosis, and atherosclerosis, neutralize free radicals and suppress the extent of oxidative deterioration [9]. The reactive oxygen species (ROS) formed in human tissues can promote extensive oxidative damage that leads to age-related degenerative processes, cancer, and a wide range of other human diseases [10]. An enormous variety of fibers is present in seaweed, especially fucose, mannose, galactose, and uronic acids, which depend on the seaweed group [11]. Seaweed fiber contains structural polysaccharides in brown seaweed (alginate and fucoidan), red seaweed (carageenan, agar, and porphyrin), and green seaweed (ulvan). A previous investigation reported that polysaccharides and oligosaccharides extracted from seaweeds may improve intestinal function, prevent pathogen adhesion and avoidance, and potentially cure inflammatory bowel disease. Anticoagulant, antitumor, and antihyperlipidemic effects are also exhibited in certain seaweed polysaccharides [12].

Seaweeds' composition includes steroids, phenols, tannins, saponins, flavonoids, terpenoids, and glycosides, which have been extensively studied and used in therapeutic applications. Tannins have been found to exhibit antimicrobial properties, as they can bind to adhesins and are involved in enzyme inhibition, substrate deprivation, and membrane disruption [13]. Saponins have such specific biological activities as anticancer, anti-inflammatory, antimicrobial, and antioxidant properties [14]. Saponins also have the property of precipitating and coagulating red blood cells [15]. Flavonoids are hydroxylated phenolic constituents that are known for their response to antioxidant activity [16]. Steroids play a vital role in antimicrobial, anticancer, antiarthritic, antiasthma, and anti-inflammatory properties [17]. Terpenoids extensively show their cytotoxicity against a variety of cancer cells and cancer prophylaxis; on the other hand, glycosides can be used as food additives and bio-preservatives [18,19].

Seaweed prevents the growth of microorganisms that commonly cause diseases such as diarrhea, skin infections, infection in the internal organs, bloodstream infections, bone and joint infections, pneumonia, etc., in human beings and acts as an antimicrobial component [20,21]. It also cures the inflammation and rupturing of intestinal endothelial cells and acts as an anti-ulcer drug. It acts as an anti-inflammatory substance by repairing and treating tissue injuries [22]. Seaweed helps with its radiological activities in treating dreadful diseases like cancer, so it can be termed an anticancer agent [23]. It is used as

an antiviral agent for humans infected with viruses [24,25]. In addition, it helps in the scavenging of free radicals, which can be proven by in vitro studies, and it also acts as an antioxidant agent [26].

Seaweed has been broadly categorized as Chlorophyta, Phaeophyceae, and Rhodophyta based on its nutrient content and chemical composition [27]. Taxonomical studies have revealed that seaweeds deviate from terrestrial plants by their absence of vascular tissue, roots, shoots, and flowers. The chlorophyta community is commonly found in nature. There are more than 7000 species present in a range of ecological systems like freshwater, marine, and terrestrial habitats [28]. Among the three phyla, only two phyla are considered to have predominant levels of applications in industry as well as in food consumption, Phaeophyceae and Rhodophyta. Phaeophyceae, unlike Chlorophyta, dominate marine environments, and less than 1% of them reside in freshwater ecosystems. They contain chloroplasts, which are surrounded by four membranes of three thylakoid stacks and a polysaccharide membrane. The polysaccharide membrane acts as a potential outer covering that elicits the biological activities of organisms and protects them from external environmental struggles [29]. Rhodophyta differ from other phyla by three important characteristics: thylakoids without stacks, external endoplasmic reticulum unseen in chloroplasts, and absence of flagella, but they possess two major accessory pigments, known as phycoerythrin and phycocyanin. Of these phyla, dominant in marine environments, only 3% (5000 species) thrive in freshwater habitats [30].

They largely consist of minerals, minor levels of carbohydrates, proteins, carotenoids, vitamins, and essential fatty acids; other than agar-agar, alginate and carrageenan can also be extracted from seaweed. In coastal areas, people are consuming seaweed as an important dietary source because of its potential nutritional content and its delicious nature, especially in Asian countries, which largely export seaweed to various countries for medicinal purposes and foodstuffs. Medicinal fields have utilized seaweed as a valuable component [31]. This paper describes *Dictyota bartayresiana*, which belongs to the brown algae family, and the external structure indicates that homogenized segments are less than four breadth long, but internodes are longer; the upper sinuses are broad and the sinuses are usually narrower.

This study gives a new insight into a few reports about *Dictyota bartayresiana* on its total bioactive contents and biological activities with mass spectroscopic analysis. To supplement the current investigation with a new potential source of cytotoxicity properties, the antibacterial properties and the antioxidant activities of extracts against a range of radicals (ABTS, nitric oxide, and hydrogen peroxide radicals) were examined, as well as their phytochemical contents (total protein, total flavonoid, total tannin, total carbohydrate, total ash, and total fat), and a GC-MS analysis was performed.

2. Results and Discussion

2.1. Phytochemicals Screening

The phytochemical screening was performed through various tests for the occurrence of resins, glycosides, saponins, steroids, tannins, terpenoids, flavonoids, phenols, alkaloids, and carbohydrates, as well as the absence of notable compound gums, as illustrated in Table 1 [32,33].

Table 1. Phytochemical screening of *Dictyota bartayresiana*.

S. No.	Tests	Experimental Conditions	Results
1	Test for alkaloids (Wagner's test)	Seaweed extract added with 2 mL of Wagner's reagent	Reddish brown precipitates appeared
2	Test for glycosides (Fehling's test)	25 mL of dilute H_2SO_4 was added to 5 mL of seaweed extract and boiled, cooled, and neutralized with 10% sodium hydroxide, and then 5 mL of Fehling solution A and B were added	Red precipitate appeared
3	Test for phenolic compounds (ferric chloride test)	Seaweed extract was dissolved in 5 mL of distilled water. A few drops of neutral 5% ferric chloride solution were added	Dark green color appeared
4	Test for steroids and Terpenoids (Salkowski's test)	Seaweed extracts were treated with chloroform and filtered. The filtrates were treated with a few drops of concentrated H_2SO_4, shaken gently, and allowed to stand.	Golden yellow color indicates the presence.
5	Test for carbohydrates (Benedict's test)	0.5 mL of filtrate, 0.5 mL of Benedict's reagent were added. The mixture was kept in a boiling water bath for 2 min.	Reddish brown color appeared.
6	Test for resins	Solubility test: seaweed extract was dissolved in different solvents	The extract dissolves completely, which indicates the presence of resins
7	Test for saponin	Foam test: 5 mL of seaweed extract in a test tube. Shake vigorously for 30 s and let it stand for 10 min	Persistent foam for 10 min indicates the presence of saponins
8	Test for tannin	In total, 3 g of a seaweed powdered sample was boiled in 50 mL distilled water for 3 min on a hot plate. The mixture was filtered, a portion of the filtrate was diluted with sterile distilled water in a ratio of 1:4, and three drops of 10% ferric chloride solution were also added.	The appearance of a blue color indicates the presence of tannins
9	Test for flavonoids	Ferric chloride test: 2 mL of extract added with a few drops of $FeCl_3$ solution	Formation of blackish green color indicates the presence of flavonoid

2.2. Quantitative Analysis (Determination of Compounds)

The dried *Dictyota bartayresiana* was estimated to contain a quantity of phytochemical compounds, such as flavonoids and tannins. The flavonoids showed 0.92%, and the tannins showed 0.09%. The primary compounds of ash, fat, and carbohydrates were also estimated; the total for ash was 37.4% higher than the protein, which contained 20.8%, the carbohydrates exhibited 8.43%, and the fat contained 2.25% (Table 2).

Table 2. Test results of phytochemical estimation.

S. No.	Parameters	Results
1	Protein	20.8% *w*/*w*
2	Flavonoids	0.92% *w*/*w*
3	Tannins	0.09% *w*/*w*
4	Total Ash	37.4% *w*/*w*
5	Total fat	2.25% *w*/*w*
6	Carbohydrates	8.43% *w*/*w*

2.3. Thin-Layer Chromatography

TLC is the confirmation analysis for identifying the phytochemical compound in the extracts by forming unique bands in the TLC plate. There were four alcoholic extracts

examined under a constant mobile phase, but the methanolic extract showed a dark yellow–brown band formation and appeared dark on green fluorescence UV light at 254 nm, rather than ethanol, acetone, and benzene. Among these, methanolic extracts were taken into consideration for the following analysis. The R_f value indicated the presence of a flavonoid compound in the methanolic extracts of *Dictyota bartayresiana*.

2.4. Column Chromatography

The current analysis was started to find out the presence of flavonoid compounds in the selected seaweed, which was confirmed by column chromatography. Using column chromatography, a flavonoid was specifically purified from seaweed. The purified form of the flavonoid was confirmed once again by a preliminary analysis, i.e., phytochemical screening.

2.5. GC-MS Evaluation

The bioactive compounds present in two different fractions of the methanolic extracts and crude extracts, which were obtained from the *D. bartayresiana* seaweed, are shown in Tables S1–S3. Their identification and characterization were based on their elution order in a TLC scanner. The acquisition time, molecular formula, and biological activities are represented in the table. The chromatogram peaks were unified and related through the database of spectra of recognized components (Wily-275) stored in the GC–MS library. The described presentations of the GC–MS investigation of the extracts are listed in Tables S1–S3 (given in the Supplementary Information), and the peak variation of the *D. barteyresiana* crude extract is displayed in Figure 1. It is concluded that the presence of Hexadecane, Quinoline, and 1,2-dihydro-2,2,4-trimethyl compounds has received great attention due to the significant biological activity noted in previous reports [34–36], such as antimicrobial and cytotoxicity activity.

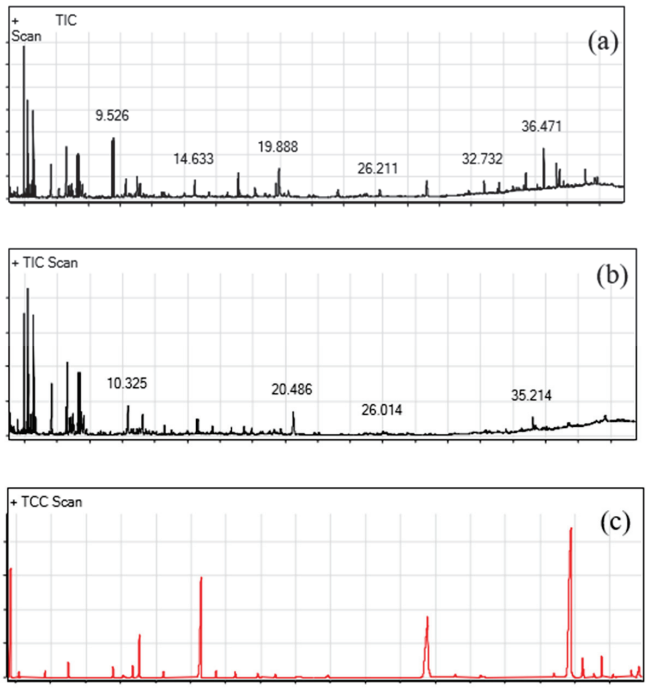

Figure 1. GC-MS interpretation. (**a**) GC-MS analysis of peak variation for *D. bartayresiana* crude extract. (**b**) GC-MS analysis of peak variation for *D. bartayresiana* extract fraction I. (**c**) GC-MS analysis of peak variation for *D. bartayresiana* extract fraction 2.

While LC/MS is commonly used for flavonoid analysis due to the prevention of thermal degradation of flavonoids, GC/MS was employed in this study due to time and equipment availability. The temperature program and analysis duration were optimized to minimize thermal decomposition, and compound identification was supported by comparison with authentic standards and NIST library spectra.

2.6. HP-TLC Profile

High-performance thin-layer chromatography (HP-TLC) was used for identifying phytochemical compounds in seaweed extractions with highly qualified photographic figures, which are responsible for improving the medicinal value of seaweed. The identification of the bioactive compounds can be carried out from selected seaweed, extracted by using four different solvents, and their Rf values can be compared with known standards. The flavonoid compound appeared in the light red and dark red fluorescent bands at 366 nm in the extractions of ethanol, methanol, acetone, and benzene, whereas at 254 nm, the compound appeared in the slight brown band and dark brown bands in each extraction. The R_f values are given below 1.00, 0.57, 0.01, 0.13, 0.53, 0.61, 0.65, −0.01, 0.68, 0.78, and 0.74. From these Rf values, those of 0.13 and 0.61 represent the presence of myricetin and galangin, respectively, based on the standard R_f value (Figure 2 and Table 3). The presence of flavonoid compounds in Figure 2a was measured at 254 nm, which depicts the light band lane when compared to 366 nm. Among four different extracts, from right to left, ethanol, methanol, acetone, and benzene, the methanol showed a dark lane and point. Myricetin is a common plant-derived flavonoid and is well recognized for its nutraceutical value. It is one of the key ingredients in various foods and beverages. The compound exhibits a wide range of activities, which include strong anti-oxidant, cytotoxicity, antidiabetic, and anti-inflammatory activities. Previous studies have reported that galangin and myricetin inhibited cell growth in several cancer cells, such as hepatoma, pancreatic, esophageal, melanoma, gastric, and colon carcinoma cells [37].

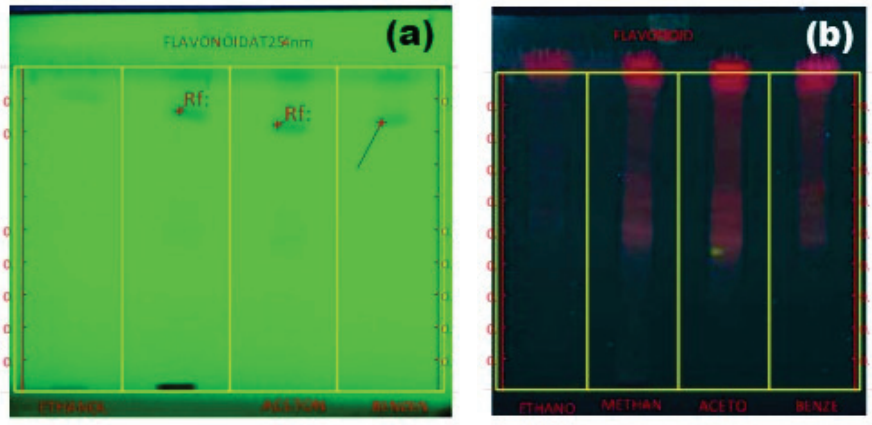

Figure 2. (**a**,**b**) HP-TLC results for *Dictyota bartayresiana* extract at two different nanometers.

Table 3. High-performance thin-layer chromatography wavelengths of various extracts.

S. No.	Position	Volume	Vial	Sample ID	Active
>1	15.0 mm	5.0 µL	1	ETHANOL	Yes
>2	38.3 mm	5.0 µL	2	METHANOL	Yes
>3	61.6 mm	5.0 µL	3	ACETONE	Yes
>4	84.9 mm	5.0 µL	4	BENZENE	Yes

Figure 3 reveals the antioxidant activities of the free radical scavenging capacity of synthesized samples in different dosages in addition to standard drugs.

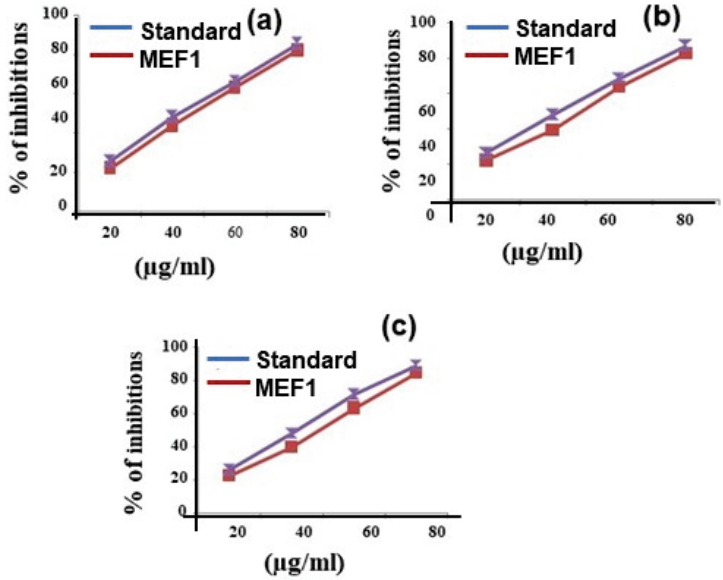

Figure 3. Antioxidant activity of Methanolic Extract Fraction One for (**a**) nitric oxide, (**b**) hydrogen peroxide, and (**c**) ABTS radical scavenging assay.

The antioxidant parameters were as follows: nitric oxide scavenging activity, hydrogen peroxide decomposition assay, and ABTS assay. These values are duly obtained from the half inhibition rate of the IC_{50} values (Table 4). In the hydrogen peroxide decomposition activity, the ability of the extract to decompose hydrogen peroxide was assessed, which may involve both the direct action of antioxidant compounds and the possible influence of trace metals present in the extract through the Fenton reaction. The presence of metals can catalyze the degradation of hydrogen peroxide and, therefore, the effect observed may not solely be due to the compounds in the extract. To accurately evaluate the contribution of the compounds, future experiments could include the use of chelating agents to minimize the influence of metal ions.

Table 4. Antioxidant parameters of Methanolic Extract Fraction One tested by nitric oxide, hydrogen peroxide, and ABTS radical scavenging assay.

Samples	% of Inhibitions				IC_{50} Value (µg/mL)
	20 (µg/mL)	40 (µg/mL)	60 (µg/mL)	80 (µg/mL)	
Methanolic Extract Fraction One (NOS)	22.38 ± 1.56	39.52 ± 2.76	63.81 ± 4.46	82.85 ± 5.79	47.91
Ascorbic acid (Std)	26.66 ± 1.86	48.09 ± 3.36	68.57 ± 4.79	87.14 ± 6.09	42.45
Methanolic Extract Fraction One (HPS)	22.50 ± 1.57	39.64 ± 2.77	63.21 ± 4.42	84.64 ± 5.92	47.61
Ascorbic acid (Std)	25.71 ± 1.79	47.85 ± 3.34	71.42 ± 4.99	88.92 ± 6.22	42.04
Methanolic Extract Fraction One (ABTS)	22.22 ± 1.55	44.22 ± 3.09	63.55 ± 4.44	82.44 ± 5.77	46.89
Ascorbic acid (Std)	25.77 ± 1.80	48.44 ± 3.39	66.66 ± 4.66	85.77 ± 6.01	43.28

Values mentioned as mean ± SD for triplicates.

The scavenging activities fluctuated according to the concentration used in the analysis; 80 (µg/mL) exhibited the best inhibition percentage, which decreased following dosages of 60 (µg/mL), 40 (µg/mL), and 20 (µg/mL). All the parameters merely had similar inhibition values (µg/mL); the NOS, HPS, and ABTS assay IC_{50} values were 47.91, 47.61, and 46.89, respectively.

The MEF1 of *Dictyota bartayresiana* was tested for cytotoxicity activity in the colon cancer cell line HT 29. The samples were analyzed for anti-carcinogenic action in different concentrations of 50, 100, 150, 200, and 250 µg/mL. The sample showed concentration-dependent cytotoxicity activity of the HT29 colon cancer cell line. It showed an inhibition concentration in terms of an IC_{50} value of 300 µg/mL. The seaweed extract can slow down the growth of HT29 cell lines as small as 50 µg/mL, which is depicted in Table 5 and Figure 4. *Dictyota bartayresiana* has cytotoxicity properties against colon cancer cells because of the existence of beneficial bioactive compounds. Molecular docking studies of *Dictyota bartayresiana* have proven their capacity to invade colon cancer cells and provide potential support for current research.

Table 5. Cell viability results of colon cancer HT-29 by untreated, treated with *Dictyota bartayresiana* Methanolic Extract Fraction One (MEF1), and standard drug.

S. No	Treatment	Conc (µg/mL)	Absorbance 570 nm
1.	HT-29 by untreated cells	-	0.517 ± 0.05
2.	DBE treated	50	0.495 ± 0.03
3.		100	0.431 ± 0.02 *
4.		150	0.401 ± 0.03 *
5.		200	0.367 ± 0.02 **
6.		250	0.301 ± 0.02 **
7.	5-Fluoro uracil treated	50	0.118 ± 0.01 ***

Values are mean ± SEM stated as (n = 3); * $p < 0.05$; ** $p < 0.01$; *** $p < 0.001$; statistical significance tested for HT-29 untreated cells. Methanolic Extract Fraction One: IC_{50} value of the extract is 300 µg/mL.

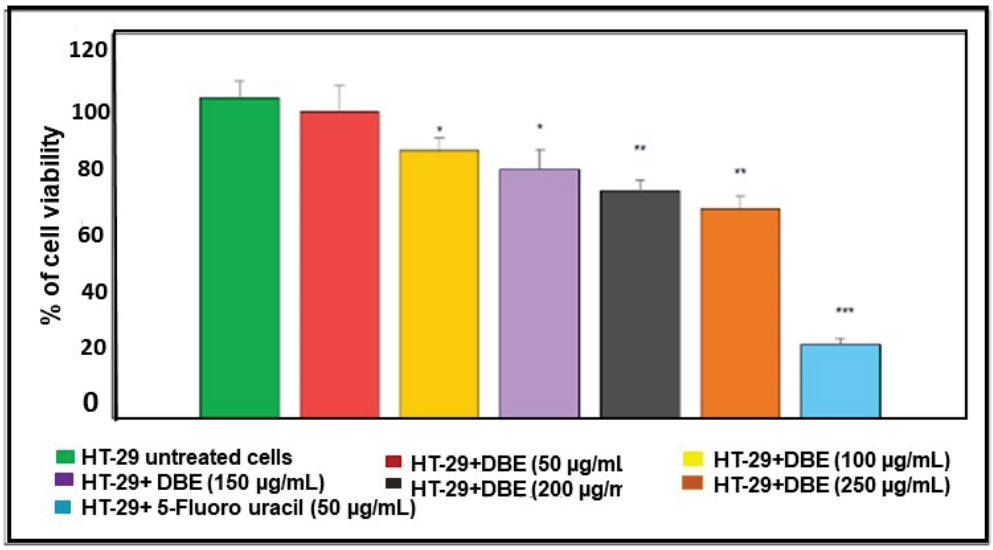

Figure 4. HT-29 cell viability percentage in the treated and untreated groups. Values are stated as Mean ± SEM (n = 3); * $p < 0.05$; ** $p < 0.01$; *** $p < 0.001$; statistical significance as evaluated with HT-29 untreated.

The MEF1 extract has proven its biological activities through the following assays: nitric oxide scavenging assay, hydrogen peroxide ABTS assay, MTT assay, and well diffusion assay. Among all these assays, the MTT assay shows significant value against colon cancer cell lines. The presence of flavonoids and other phytochemical compounds in the MEFI extract may be the major reason for its cytotoxicity.

Many reports support the significant anticancer action of phytochemical compounds [38,39]. The flavonoid could interfere with cancer cell line arrest of the cancer cycle at the G_2 phase, which promotes DNA damage. It can inhibit thymidine kinase, which is responsible for further growth of the cell. The tumor suppression gene plays a vital role in the prevention of cancer; when it is activated by a stimulus, cell growth can be stopped. Flavonoids can activate the tumor suppressor gene to reduce the further development of cancer cells. Apoptosis (or) cell death is natural when cells decide to die by themselves. This process could be a targeted step for all kinds of anticancer drugs. Flavonoids can provoke the apoptosis mechanism and allow cancer cells to die, and cease further development [40–46]. The standard anticancer drug, 5-fluorouracil, also involves the above events. Fortunately, flavonoids of phytochemical compounds have been studied in cancer research [47]. Numerous mechanisms still need to be investigated further. Oncogenesis is a broad spectrum when it deals with phytochemical compounds and could be a side-effect-free, easily available, large-scale production in the future.

The current investigation suggests that among eighteen bacteria, six bacteria have shown the best effects, as presented in Figure 5. The MEF1 antibacterial activity was examined against *Escherichia coli*, *Vibrio cholerae*, *Pseudomonas aeruginosa*, *Bacillus subtilis*, *Klebsiella pneumonia*, and *Staphylococcus aureus* (Table 6). The concentration of the sample is directly proportional to the inhibition percentage. The maximum action of *Escherichia coli* (6.20 ± 0.53 mm) was detected in a 4% dilution of MEF1. The minimum activity (0.60 ± 0.04) for *Vibrio cholerae* was obtained in a 1% dilution of MEF1, and it has possible activity in every concentration, and adjacent to the standard dose, as shown in Figure 5.

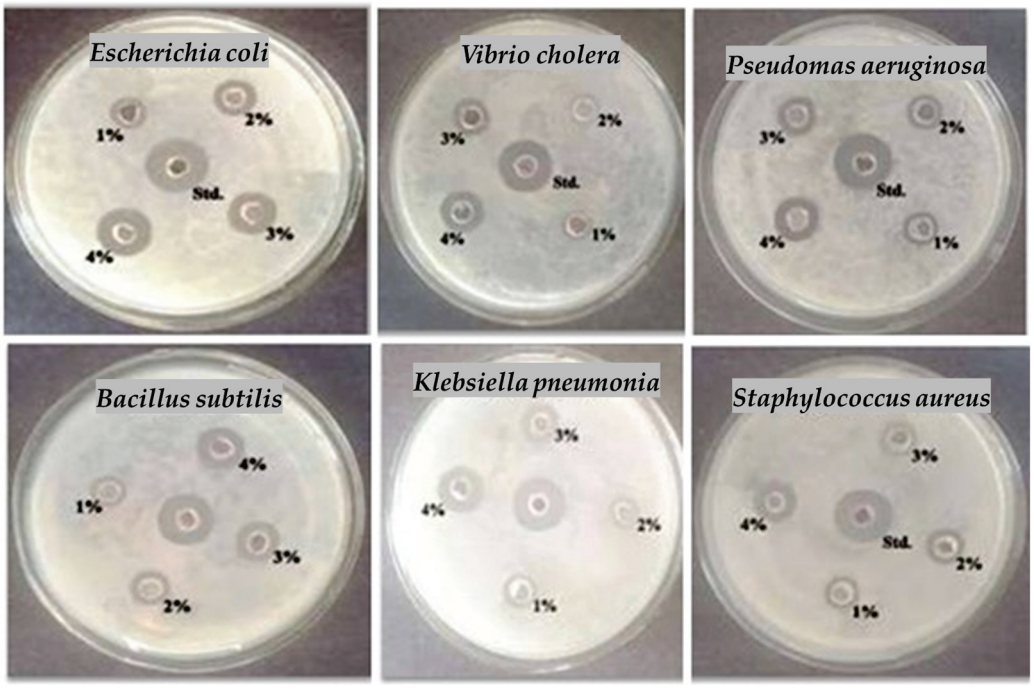

Figure 5. Antibacterial activities of the methanolic extract of fraction 1 for Gram-positive and Gram-negative bacteria.

Herbal medicines are commonly used as drugs for many lifesaving treatments, especially in the Siddha and Ayurvedic methods of medicine. Ancestors knew plenty of terrestrial plants and explained their morphological, anatomical, as well as medicinal value. Their editions were helpful for upcoming generations, but their knowledge of marine organisms had few countable records due to their marine origin, and they were focused only on their visible nature and failed to make observations about the behind-the-scenes of the marine world. Currently, researchers are curious about marine organisms that can survive in several problematic environments with the help of secondary metabolites. They have discovered that a bioactive compound may be easily extracted from marine algae. In the current investigation, we evaluated the bioactive compounds in the *Dictyota bartayresiana* marine alga by the GC-MS method.

Table 6. Antibacterial activity of Methanolic Extract Fraction One for Gram-positive and Gram-negative bacteria.

Tested Bacteria	Dose (50 µL) Sample				Std. (30 µL)
	1%	2%	3%	4%	
Escherichia coli	2.00 ± 0.14	3.10 ± 0.21	4.60 ± 0.32	6.20 ± 0.43	7.60 ± 0.53
Vibrio cholera	0.60 ± 0.04	1.80 ± 0.12	2.90 ± 0.20	4.10 ± 0.28	6.40 ± 0.44
Pseudomas aeruginosa	1.00 ± 0.07	2.20 ± 0.15	3.60 ± 0.25	5.00 ± 0.35	6.70 ± 0.46
Bacillus subtilis	1.50 ± 0.10	2.60 ± 0.18	3.90 ± 0.27	5.10 ± 0.35	6.90 ± 0.48
Klebsiella pneumonia	0.80 ± 0.05	2.10 ± 0.14	3.20 ± 0.22	4.50 ± 0.31	6.60 ± 0.46
Staphylococcus aureus	1.70 ± 0.11	2.80 ± 0.19	4.20 ± 0.29	5.50 ± 0.38	7.40 ± 0.51

The primary constituents were estimated in seaweed extract according to the standard methods, and the highest content of the sample was ash (37.4%), followed by protein (20.8%), carbohydrate (8.43%), and total fat (2.25%). Tables 1 and 2 of the quantitative analysis of the phytochemical compounds results is considered as supporting evidence for the flavonoid group (0.92%) in the extract, rather than tannins (0.09%).

The crude extract contains Dihydroxyphenyl ($C_{10}H_{12}O$), Methoxyacetopheone ($C_9H_{10}O_2$), Naphthalene ($C_{10}H_8$), Desmethyl selegiline ($C_{12}H_{15}N$), Zingerone ($C_{11}H_{14}O_3$), Quinoline ($C_{12}H_{15}N$), Methyl palmitate ($C_{17}H_{34}O_2$), Behenic acid ($C_{22}H_{44}O_2$), and Hexadecane ($C_{16}H_{34}$). Every compound shows a pharmacological function of its own. For instance, the Dihydroxyphenyl compound, otherwise known as coniferyl alcohol, exhibits good antidiabetic activity, and this compound is present in the queen bee and important constituents of the pheromone group, which involves the retinue pathway. Methoxyacetopheone acts as a food additive in the USA [48], Zingerone and Quinoline are considered as a novel drug that promotes antioxidant and antibacterial activity [34], and Desmethyl selegeline is a potential compound in opposition to N-methyl-D-aspartate-induced rat retinal damage [35]. Hexadecane is a potential antifungal agent whose activity is elicited due to its volatile constituents [36].

Fraction 1 contains Fisetin ($C_8H_{24}O_4Si_4$), Zingiberene ($C_{15}H_{24}$), Dihydromyristicin ($C_{11}H_{14}O_3$), Hexadecane ($C_{16}H_{34}$), Diethylhexylphthalate ($C_{24}H_{38}O_4$), and Hexadecane ($C_{16}H_{34}$) components. Fisetin has potential anticancer activity against cancer cells, especially in ovarian cancer [49]. Myristicin is a successful inhibitor of B[a]P-induced tumor formation. This type of disease is commonly exposed to the environment by polycyclic aromatic hydrocarbon [50], which is a breakdown product of Dihydromyristicin. Acinetobacter in bacterial strains could make use of Hexadecane and phenolics considered as

carbon and energy sources for their growth [51]. DHP's actions are different from species to species, and these actions suppress the growth of tumor cells in rats, promote hepatocyte growth regulation, and induce DNA synthesis [52].

Fraction 2 contains a few phytochemical compounds, such as Isopropenylphenol ($C_9H_{10}O$), Quinoline, 1,2-dihydro-2,2,4-trimethyl-($C_{12}H_{15}N$), Naphthalene ($C_{10}H_8$), n-Tridecan-1-ol ($C_{13}H_{28}O$), and n-pentadecanol ($C_{15}H_{32}O$). Quinoline is an essential constituent, which has an electron-donating amino group that promotes the free radical scavenger action of components, and a vital oil of n-pentadecanol has the property of acting against bacterial pathogens [53].

There is no available research on the total flavonoid, tannin, total ash, carbohydrate, protein, and total fat content in *D. bartayresiana.* Commonly, the antioxidant action of plants may be directly contributed by phenolic compounds. Tannins and flavonoids are well-known medicinal agents that possess antioxidant and anti-inflammatory properties [54–56]. The high-performance thin-layer chromatography technique was performed for obtaining the best photographic figures for analyzing the flavonoid wavelengths of various extracts, and the application positions changed depending on the solvents (Table 3). In previous work, we carried out molecular docking to analyze the binding properties of the mediator called 3HNG with Hexadecane, hexadecanoic acid methyl ester, and Quinoline,1,2-dihydro-2,2,4-trimethyl) reported from *Dictyota bartayresiana*, and 5-β fluorouracil used as a standard. The wet analysis carried out by us showed the best result with 3HNG and proved the presence of an anti-colon cancer property. Among the various compounds, hexadecanoic acid methyl ester and Quinoline, 1,2-dihydro-2,2,4-trimethyl) had higher binding energy than the standard. The present study may strongly conclude that the seaweed extract displays cytotoxicity against colon cancer cells [47].

3. Methodology

3.1. Preparation of Extract and Identification

The seaweed was collected from the Mandabam area in November 2018, and authenticated by the Botanical Survey of India (BSI), Coimbatore, India. A voucher sample has been placed in the herbarium of BSI. Reg no: BSI/SRC/5/23/2019/Tech/3070). Seaweeds that had been shade-dried were ground into powder and dissolved in acetone, methanol, ethanol, and benzene (10 g of plant sample in 100 mL solvent). For 6 to 8 h, the solvent extracts were put through the Soxhlet apparatus [57], depending on the phytochemical split-up.

3.2. Screening of Phytochemical Compounds

The phytochemical compounds were screened out through standard procedures, which indicate the presence or absence of bioactive compounds in a crude extract. Figure 6 shows the schematic presentation of the detection of compounds from *Dictyota bartayresiana* extract.

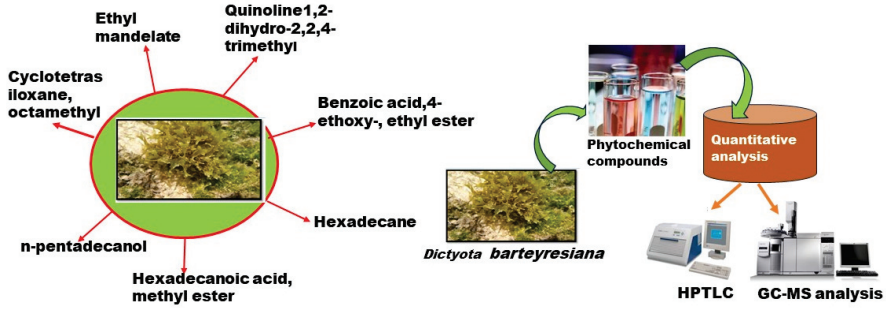

Figure 6. Detection of valuable compounds from *Dictyota bartayresiana* extract.

3.3. Quantitative Analysis

3.3.1. Estimation of Protein

Seaweed powder (100 mg) was homogenized with 3 mL of 10% trichloroacetic acid. The samples were centrifuged at 10,000 rpm. Supernatants were removed. In total, 3 mL of 1 N sodium hydroxide (NaOH) pellets were added to each sample, and samples were allowed to cool for seven minutes in a water bath. The samples were again centrifuged for 5 to 10 min at 5000 rpm. After centrifugation, 5 mL of reagent having 0.5 mL of supernatant was mixed with 100 parts of a 2% sodium carbonate mixture and one part of a 2% sodium potassium tartrate mixture. The supernatant was kept for 10–15 min. Finally, the supernatant was added to 5 mL of Folin–Ciocalteu's phenol reagent and left undisturbed for half an hour to examine the progress of color, and the absorbance was also measured at 700 nm [58].

3.3.2. Estimation of Flavonoids

Total flavonoid contents were estimated by using the aluminum chloride approach, in which quercetin was used as a standard. The seaweed excerpt was adjoined with distilled water and 5% $NaNO_2$ was added drop by drop. This sample was kept at 25 °C for 5 min, and then $AlCl_3$ was added. These mixture reagents were kept to cool for 5 min, with 0.2 mL of 1 mM NaOH added. Finally, 1 mL of water was added to the reaction mixture. The absorbance was measured at 510 nm [59].

3.3.3. Estimation of Tannins

The seaweed crude extract was diluted using 50 mL of water and maintained in a water bath through continuous stirring for 30 min. The supernatants were transferred into a volumetric flask, and the extraction process was overfed until the mixture became colorless. The resulting solution was cooled and then mixed with 25 mL indigo sulphonic acid solution. The resulting content was titrated by 0.1 M potassium permanganate solution with continuous stirring until the development of a yellow color. Each 1 mL of 0.1 M aqueous potassium permanganate is comparable to 0.004157 g of tannins. The total tannin content was determined depending on the titration value [58].

3.3.4. Estimation of Total Ash

A total of 3 g of seaweed powder was taken in a silica crucible. It was incinerated quietly at first and the temperature was slowly raised to 475 °C ± 25 °C until a carbon-free state was cooled and weighed. The extract's burned mass, including boiling water, the insoluble residuum was gathered over ashless filter paper, and the remains were burned and filtered until the ash was white or close; the filtrate was then added, dried to dryness, and then ignited and evaporated to dry out and the whole sample was heated to a temperature of 475 °C ± 25 °C.

The percentage of total ash is calculated as follows:

$$\%\ \text{of total ash}\left(\frac{\%\text{w}}{\text{w}}\right) = \frac{\text{Weight of ash(g)} \times 100}{\text{weight of the sample (g)}} \quad (1)$$

3.3.5. Estimation of Total Fat

A total of 3 g of seaweed powder was taken into the Soxhlet Apparatus. The Soxhlet apparatus condenser and solvent flask were connected. The solvent was added in the required volume, and the boiling point varied between 40 and 60 °C. The extract was continuously monitored until the colorless solvent was obtained, which took 16 h. The

thimble was removed, and the solvent was evaporated and weighed [58]. The flask was cooled and weighed ('b',g).

$$\%\ \text{Fat Content}\left(\frac{\%w}{w}\right) = \frac{(b-a)(g)\times 100}{\text{Weight of the sample}(g)} \quad (2)$$

3.3.6. Estimation of Total Carbohydrates

A total of 100 mg seaweed powder was added, with 5 mL of 2.5 N HCl taken in a hot tube, kept in water for 3 h, and then cooled to the optimum temperature. A neutralization state was obtained by adding sodium carbonate to the reaction mixture. The resulting mixtures were centrifuged, and the supernatant was collected. Glucose standard mixtures were arranged into 0, 0.2, 0.4, 0.6, 0.8, and 1 mL of the running standard. In total, 4 mL of anthrone reagent was added to the sample solution. The volume was made up of 5 mL of each tube. The sample solution was kept in a hot water bath for 8 min. Absorbance was examined at 630 nm [60].

$$\%\ \text{Total Carbohydrates} = \frac{\text{Sample absorbance}}{\text{Standard absorbance}} \times \frac{\text{Standard weigth}}{\text{Standard dilution}} \times \frac{\text{Sample dilution}\times 100}{\text{Sample weight}} \quad (3)$$

3.4. Thin-Layer Chromatography

TLC was used to analyze the bioactive compounds in the extracts with the help of R_f values. In this technique, silica gel precoated plates were used, and a ratio of ethyl acetate (100): formic acid (11): glacial acetic acid (11): water (26) of the mobile phase solvent system was utilized for determining the phytochemical compound. The extracts were placed on a silica plate in a drop-by-drop manner, which took place above the mobile phase system. Every bioactive compound has a particular polarity [57,61,62]. After a few minutes, active compounds were separated according to polarity. The plates were kept for air drying and sprayed with an iodine vapor background to examine the flavonoid compound [63].

R_f value can be expressed by

$$R_f = \frac{\text{Distance moved by solute}}{\text{Distance moved by solvant}} \quad (4)$$

3.5. Refinement of Active Compounds

The chromatography technique was used to separate the desired compound from the bulk of the compound in the extract. Based on the standard procedure, silica gel was used as a static phase along with a chloroform (5): ethyl acetate (4): formic acid (1) solvent system, followed by chloroform (15): methanol (1) as nonpolar solvents, which helped to separate the flavonoid compound into individual fractions. From this, column value −30 cm in analytical scale, standard phase–silica gel, mobile phase—ethyl acetate: formic acid: glacial acetic acid: water. The continuous separation was performed using the appropriate solvent system in different ratios. There were twelve different fractions obtained from this analysis. After confirmation by TLC, two fractions were subjected to Gas–Mass Spectroscopy [64].

3.6. Gas Chromatography–Mass Spectroscopy

GC–MS investigation was performed using an Agilent Technologies system following previously reported methods [57,61,62], with the TNTH_SCAN_45Min_300 °C.M method and an autosampler. Gas chromatography was carried out using a fused silica capillary column (30 m × 0.25 mm i.d., 0.25 μm film thickness). Helium gas was used as the carrier at a flow rate of 1.51 mL/min for 1 min. The mass spectrometer operated in electron impact

(EI) mode at 70 eV, scanning a mass range of m/z 91–283. The split ratio was set to 1:10, with an injection volume of 1 µL. The column temperature program ensured a total run time of 37 min.

Compound identification in the crude seaweed extract was carried out based on peak evaluation, retention time comparison with authentic standards, and matching of the acquired mass spectra with those in the NIST mass spectral library [65]. Selected compounds were verified by injecting commercially available standard substances under identical GC–MS conditions to confirm both retention time and fragmentation patterns. This dual approach enhanced the reliability of compound identification and ensured accurate characterization of the extract components.

3.7. Preparative HPTLC

Preparative HPTLC was performed on silica gel 60F 254 by using a CAMAG TLC Scanner (CAMAG, Muttenz, Switzerland) with the development of a twin trough chamber of about 20 × 10 cm. The plant material was dissolved in the following solvents: ethanol, acetone, benzene, and methanol. Temperatures were maintained at 60 °C, and the mobile phase was prepared by chloroform (8.5): methanol (1): formic acid (0.5). The different solvent extractions were taken to compare bioactivity among them to find out the best solvent for further analyses. The extracts were subjected to the mobile phase solvent, which showed 4 different tracks, with an application position of 8.0 mm. Bioactive compounds were formed as a band with the help of an inert gas. The developed bands were allowed to dry, and photography was performed using TLC Scanner with Win CATS Planner software (1.4.10). UV light facilitated the visualization from two different wavelengths under 254 nm and 366 nm, respectively.

3.8. Preparation of Sample

The samples were taken in various concentrations to investigate in vitro antioxidant activity [66], which followed 20, 40, 60, and 80 µg/mL.

3.8.1. Nitric Oxide Scavenging Activity Analysis

Nitric oxide radical scavenging activity was estimated, consistent with the previous method [67].

Procedure

According to the Griess-Ilosvay reaction, the formation of sodium nitroprusside in an aqueous mixture happens by the liberation of nitrite ions. The sample of 0.5 mL was taken in a prepared reaction mixture of 0.5 mL phosphate buffered saline and 2 mL of 10 mM sodium nitroprusside at a mixture of concentrations, and the sample solution was set aside at 25 °C for 150 min. Subsequently, a 0.5 mL sample mixture was added to the 1 mL sulfanilic acid at room temperature for 5 min. Later, 1 mL of naphthyl ethylenediamine dihydrochloride was poured at room temperature, proceeding for 30 min. Absorbance was measured at 540 nm by a spectrophotometer. The nitric oxide inhibition action was resolved through the following calculation:

$$\% \text{ Inhibition} = \frac{(A_0 - A_1)}{A_0 \times 100} \quad (5)$$

where A_0—absorbance of the control, blank, without sample, and A_1—absorbance for the tested sample.

3.8.2. Hydrogen Peroxide Decomposition Activity

The hydrogen peroxide decomposition activity of the sample was determined using the standard technique [68]. A total of 1 mL of extract was added in different doses of 1 mL of 0.1 mM H_2O_2, which was followed by adding 3% ammonium molybdate in the range of two drops, 7.0 mL of 1.8 M potassium iodide, and 10 mL of 2 M sulfuric acid. The reaction mixtures were titrated with 5.09 mM sodium thiosulfate, awaiting the fading of the yellow color. The percentage inhibition of hydrogen peroxide was computed as

$$\% \text{ Inhibition} = \frac{(V_0 - V_1)}{V_0 \times 100} \quad (6)$$

Titrated solution: sodium thiosulfate (NaS_2O_3) used for controlling the sample and solution volume represented as V_0 in the presence of hydrogen peroxide (without sample), the volume of sodium thiosulfate solution represented as V_1.

3.8.3. ABTS Scavenging Assay

The prepared sample was determined for antioxidant effect employing ABTS decolorization assay from the previous method [69].

The ABTS radical cation formation was performed through the reaction of ABTS solution (7 mM) with 2.45 mM $K_2S_2O_8$ (potassium persulfate). The sample solutions were undisturbed for 12 to 16 h in the dark at room temperature, which yielded the formation of ($ABTS^{\bullet+}$) radicals, as well as the appearance of dark color. The 1 mL ABTS reagent was dropped in different dilutions of the sample. After 6 min, the calorimetric absorbance was determined near 734 nm, which was evaluated with L ascorbic acid standard solution. Blank was utilized in each assay. The above antioxidant parameters were performed by triplicate, and the percentage inhibition was calculated via the following method:

$$\text{Inhibition } (\%) = \frac{(\text{Control} - \text{Test})}{\text{Control}} \quad (7)$$

3.9. Antibacterial Activities

Nutrient agar was added to the flask, accompanied by distilled water, which was also heated. The boiling agents are directly dispensed into a culture dish before the formation of the solidification process [70–72]. The diverse bacterial strains are injected into the culture vessels. For example, the following strains are injected into the culture plate: *Klebsiella pneumoniae*, *Escherichia coli*, *Enterobacter faecalis*, and *Flavobacterium* sp. *Klebsiella oxytoca*, *Proteus mirabilis*, *Providentiarettigeri*, *Salmonella typhi*, *Salmonella paratyphi*, *Serratia marcescens*, *Shigella flexineri*, *Shigella sonnei*, *Staphylococcus aureus*, *Methicillin-resistant S. aureus*, *Staphylococcus epidermidis*, *Vibrio cholera*, and *pseudomonas aeruginosa*. The agar dish was kept in an incubator at 37 °C. Chloramphenicol (30 µL) was used as a standard drug and positive control. The methanolic extract fraction was taken as a sample. Labeling of concentration facilitated obtaining the apparent results. The inhibition zone was assessed after 24 h. The antibacterial activity was achieved by a well-cut drug diffusion assay [70].

3.10. Cytotoxicity Study by MTT Assay

Human colon cancer cell adenocarcinoma (HT-29 cell line) was accessed from the National Centre for Cell Sciences (NCCS), Pune, India. To evaluate the cytotoxicity result of the methanolic fraction of the one extract of *Dictyota bartayresiana*, MTT assay was used. The colorimetric assessment was performed in 96-well plates. The whole experimentation was performed in sterilized states, and the sub-culturing technique was implemented

according to the typical methods. The cell viability percentage was the result of the test drugs' effect on cell growth inhibition, which was compared with the standard drug 5-fluorouracil (50 μg/mL). The experimental condition of 5-fluorouracil was considered a positive control.

3.11. Statistical Study

All test samples were studied for three individual factors. The quantity of the sample is mandatory to determine the free radical scavenging concentration through 50%, IC_{50}, and was graphically further defined by linear regression method through MS Windows GraphPad Instat (version 3) software. Outcomes were extracted graphically/by mean ± standard deviation.

4. Conclusions

The above findings confirm the presence of several bioactive compounds in the extract. Among the identified constituents from *Dictyota bartayresiana* Fraction 1, long-chain fatty alcohols such as n-pentadecanol and n-nonadecanol, as well as isoflavones, were detected. These compounds are known for their notable antibacterial, antioxidant, and cytotoxic activities. Although these fatty alcohols are not classified as flavonoids, they may still play a significant role in the biological activity of the seaweed extract. This study offers valuable insight into the chemical profile of the extract and supports its potential for further pharmacological investigation.

The antioxidant activity of MEF1 (NOS) was demonstrated by its ability to scavenge free radicals, with an IC_{50} value of 47.91 μg/mL. The GC–MS analysis confirmed the presence of compounds such as Hexadecane, Quinoline, and 1,2-dihydro-2,2,4-trimethyl derivatives, which exhibited significant antibacterial and antioxidant properties.

Supplementary Materials: The following supporting information can be downloaded at: https://www.mdpi.com/article/10.3390/md23060224/s1, Table S1. Qualitative compound reported in crude extract; Table S2. Qualitative compounds reported in DBE Fraction 1; Table S3. Qualitative compound reported in DBE Fraction 2. Ref. [73] is cited in the Supplementary Materials.

Author Contributions: D.S.B.: Methodology, Formal Analysis, Visualization, Writing—Original Draft. A.B.R.: Conceptualization, Methodology, Supervision, Writing—Review and Editing. S.N.: Visualization, Investigation, Writing—Review and Editing. S.T.: Visualization, Investigation. K.K.: Visualization, Investigation, Writing—Review and Editing. S.S.: Visualization, Investigation, Writing—Review and Editing; V.T.: Conceptualization, Methodology, Writing—Review and Editing. All authors have read and agreed to the published version of the manuscript.

Funding: This research received no external funding.

Institutional Review Board Statement: Not applicable.

Informed Consent Statement: Not applicable.

Data Availability Statement: Data are contained within the article.

Conflicts of Interest: The authors declare no conflicts of interest.

References

1. Shanahan, T. *The Evolution of Darwinism: Selection, Adaptation and Progress in Evolutinary Biology*; Cambridge University Press: Cambridge, UK, 2004.
2. Generalić Mekinić, I.; Skroza, D.; Šimat, V.; Hamed, I.; Čagalj, M.; Popović Perković, Z. Phenolic content of brown algae (*Pheophyceae*) species: Extraction, identification, and quantification. *Biomolecules* **2019**, *9*, 244. [CrossRef] [PubMed]

3. Bhatla, S.C.; Lal, M.A. Secondary Metabolites. In *Plant Physiology, Development and Metabolism*; Springer Nature: Singapore, 2023; pp. 765–808. [CrossRef]
4. Rocha, D.H.A.; Seca, A.M.L.; Pinto, D.C.G.A. Seaweed Secondary Metabolites In Vitro and In Vivo Anticancer Activity. *Mar. Drugs* **2018**, *16*, 410. [CrossRef]
5. Durairaj, S.B.; Andiyappan, B.R. Screening of phytochemicals, antibacterial, antioxidant and anti-inflammatory activity of *Dictyota barteyresiana* seaweed extracts. *Asian J. Biol. Life Sci.* **2020**, *9*, 20–26. [CrossRef]
6. Chellamanimegalai, P.; Deshmukhe, G.; Balange, A.K.; Layana, P. Unveiling the nutritional and antioxidant properties of brown algae resources (*Dictyota* J.V. Lamouroux) from the Bay of Bengal and Arabian Sea, Indian coast. *Heliyon* **2025**, *11*, e40693. [CrossRef]
7. Wijesinghe, W.A.J.P.; Athukorala, Y.; Jeon, Y.J. Effect of anticoagulative sulfated polysaccharide purified from enzyme-assistant extract of a brown seaweed Ecklonia cava on Wistar rats. *Carbohydr. Polym.* **2011**, *86*, 917–921. [CrossRef]
8. Imran, M.; Iqbal, A.; Badshah, S.L.; Sher, A.A.; Ullah, H.; Ayaz, M.; Mosa, O.F.; Mostafa, N.M.; Daglia, M. Chemical and Nutritional Profiling of the Seaweed *Dictyota dichotoma* and Evaluation of Its Antioxidant, Antimicrobial and Hypoglycemic Potentials. *Mar. Drugs* **2023**, *21*, 273. [CrossRef] [PubMed]
9. Miyashita, K. Marine antioxidants: Polyphenols and carotenoids from algae. In *Antioxidants and Functional Components in Aquatic Foods*; Kristinsson, H.G., Ed.; Wiley-Blackwell: Oxford, UK, 2014; pp. 233–249. [CrossRef]
10. Rengasamy, K.R.R.; Amoo, S.O.; Aremu, A.O.; Stirk, W.A.; Gruz, J.; Šubrtová, M.; Doležal, K.; Van Staden, J. Phenolic profiles, antioxidant capacity, and acetylcholinesterase inhibitory activity of eight south African seaweeds. *J. Appl. Phycol.* **2015**, *27*, 1599–1605. [CrossRef]
11. Nunes, N.; Ferraz, S.; Valente, S.; Barreto, M.C.; Pinheiro de Carvalho, M.A. Biochemical composition, nutritional value, and antioxidant properties of seven seaweed species from the Madeira Archipelago. *J. Appl. Phycol.* **2017**, *29*, 2427–2437. [CrossRef]
12. Dierick, N.; Ovyn, A.; De Smet, S. In vitro assessment of the effect of intact marine brown macro-algae *Ascophyllum nodosum* on the gut flora of piglets. *Livest. Sci.* **2010**, *133*, 154–156. [CrossRef]
13. Lopez-Santamarina, A.; Miranda, J.M.; Mondragon, A.D.C.; Lamas, A.; Cardelle-Cobas, A.; Franco, C.M.; Cepeda, A. Potential Use of Marine Seaweeds as Prebiotics: A Review. *Molecules* **2020**, *25*, 1004. [CrossRef]
14. Mehdinezhad, N.; Ghannadi, A.; Yegdaneh, A. Phytochemical and biological evaluation of some *Sargassum* species from Persian Gulf. *Res. Pharm. Sci.* **2016**, *11*, 243–249. [PubMed]
15. Guo, J.; Sun, W.; Kim, J.P.; Lu, X.; Li, Q.; Lin, M.; Mrowczynski, O.; Rizk, E.B.; Cheng, J.; Qian, G.; et al. Development of tannin-inspired antimicrobial bioadhesives. *Acta Biomater.* **2018**, *72*, 35–44. [CrossRef] [PubMed]
16. Sidana, J.; Singh, B.; Sharma, O.P. Saponins of Agave: Chemistry and bioactivity. *Phytochemistry* **2016**, *130*, 22–46. [CrossRef]
17. Sytar, O.; Hemmerich, I.; Zivcak, M.; Rauh, C.; Brestic, M. Comparative analysis of bioactive phenolic compounds composition from 26 medicinal plants. *Saudi J. Biol. Sci.* **2018**, *25*, 631–641. [CrossRef] [PubMed]
18. O' Connor, J.; Meaney, S.; Williams, G.A.; Hayes, M. Extraction of Protein from Four Different Seaweeds Using Three Different Physical Pre-Treatment Strategies. *Molecules* **2020**, *25*, 2005. [CrossRef] [PubMed]
19. Circuncisão, A.R.; Catarino, M.D.; Cardoso, S.M.; Silva, A.M.S. Minerals from Macroalgae Origin: Health Benefits and Risks for Consumers. *Mar. Drugs* **2018**, *16*, 400. [CrossRef]
20. Bharathi, D.S.; Boopathyraja, A.; Nachimuthu, S.; Kannan, K. Green Synthesis, Characterization and antibacterial activity of SiO_2–ZnO nanocomposite by *Dictyota bartayresiana* extract and its cytotoxic effect on HT29 Cell Line. *J. Clust. Sci.* **2022**, *33*, 2499–2515. [CrossRef]
21. Hejna, M.; Dell'anno, M.; Liu, Y.; Rossi, L.; Aksmann, A.; Pogorzelski, G.; Jóźwik, A. Assessment of the antibacterial and antioxidant activities of seaweed-derived extracts. *Sci. Rep.* **2024**, *14*, 21044. [CrossRef]
22. Kazlowska, K.; Hsu, T.; Hou, C.C.; Yang, W.C.; Tsai, G.J. Anti-inflammatory properties of phenolic compounds and crude extract from *Porphyra dentate*. *J. Ethnopharmacol.* **2010**, *128*, 123–130. [CrossRef]
23. Namvar, F.; Tahir, P.M.; Mohamad, R.; Mahdavi, M.; Abedi, P.; Najafi, T.F.; Rahman, H.S.; Jawaid, M. Biomedical Properties of Edible Seaweed in Cancer Therapy and Chemoprevention Trials: A Review. *Nat. Prod. Commun.* **2013**, *8*, 1811–1820. [CrossRef]
24. Pravin, R.; Dong, C.-D.; Praveenkumar, R.; Patel, A.K.; Pandey, A.; Baskar, G. Technoeconomic Assessment and Optimization of Algal Oil Extraction from Marine Macroalgae *Dictyota bartayresiana* Biomass. *Algal Res.* **2023**, *76*, 103319. [CrossRef]
25. Bouraï, L.; Logez, M.; Laplace-Treyture, C.; Argillier, C. How Do Eutrophication and Temperature Interact to Shape the Community Structures of Phytoplankton and Fish in Lakes? *Water* **2020**, *12*, 779. [CrossRef]
26. Cox, S.; Abu-Ghannam, N.; Gupta, S. An assessment of the antioxidant and antimicrobial activity of six species of edible Irish seaweeds. *Int. Food Res. J.* **2010**, *17*, 205–220.

27. Ravichandran, P.; Rajendran, N.; Al-Ghanim, K.A.; Govindarajan, M.; Gurunathan, B. Investigations on evaluation of marine macroalgae *Dictyota bartayresiana* oil for industrial scale production of biodiesel through technoeconomic analysis. *Bioresour. Technol.* **2023**, *374*, 128769. [CrossRef]
28. Nagarajan, S.; Mathaiyan, M. Emerging novel anti-HIV biomolecules from marine Algae: An overview. *J. Appl. Pharm. Sci.* **2015**, *5*, 153–158. [CrossRef]
29. Aravind, S.; Barik, D.; Ragupathi, P.; Vignesh, G. Investigation on algae oil extraction from algae Spirogyra by Soxhlet extraction method. *Mater. Today Proc.* **2021**, *43*, 308–313. [CrossRef]
30. Ghasemi, Y.; Rasoul-Amini, S.; Morowvat, M.H. *Algae for the Production of SCP*; Nova Science Publishers Inc.: Hauppauge, NY, USA, 2011; pp. 163–184.
31. Rajendrasozhan, S.; Moll, H.E.; Snoussi, M.; Romeilah, R.M.; Shalaby, E.A.; Younes, K.M.; El-Beltagi, H.S. Phytochemical Screening and Antimicrobial Activity of Various Extracts of Aerial Parts of *Rhanterium epapposum*. *Processes* **2021**, *9*, 1351. [CrossRef]
32. Harborne, J.B. *Phytochemical Methods: A Guide to Modern Techniques of Plant Analysis*; Chapman and Hall Ltd.: London, UK, 1973; pp. 49–188.
33. Ghosal, M.; Mandal, P. Phytochemical screening and antioxidant activities of two selected 'BIHI' fruits used as vegetables in Darjeeling Himalaya. *Int. J. Pharm. Pharm. Sci.* **2012**, *4*, 567–574.
34. Manjunatha, J.R.; Bettadaiah, B.K.; Negi, P.S.; Srinivas, P. Synthesis of quinoline derivatives of tetrahydrocurcumin and zingerone and evaluation of their antioxidant and antibacterial attributes. *Food Chem.* **2013**, *136*, 650–658. [CrossRef]
35. Takahata, K.; Katsuki, H.; Kobayashi, Y.; Muraoka, S.; Yoneda, F.; Kume, T.; Kashii, S.; Honda, Y.; Akaike, A. Protective effects of selegiline and desmethylselegiline against N-methyl-D-aspartate-induced rat retinal damage. *Eur. J. Pharmacol.* **2003**, *458*, 81–89. [CrossRef]
36. Gehrke, I.T.; Neto, A.T.; Pedroso, M.; Mostardeiro, C.P.; Da Cruz, I.B.; Silva, U.F.; Ilha, V.; Dalcol, I.I.; Morel, A.F. Antimicrobial activity of *Schinus lentiscifolius* (Anacardiaceae). *J. Ethnopharmacol.* **2013**, *148*, 486–491. [CrossRef] [PubMed]
37. Huang, H.; Chen, A.Y.; Rojanasakul, Y.; Ye, X.; Rankin, G.O.; Chen, Y.C. Dietary compounds galangin and myricetin suppress ovarian cancer cell angiogenesis. *J. Funct. Foods* **2015**, *15*, 464–475. [CrossRef] [PubMed] [PubMed Central]
38. Johnson, I.T. Phytochemicals and cancer. *Proc. Nutr. Soc.* **2007**, *66*, 207–215. [CrossRef] [PubMed]
39. Gaige, S.; Djelloul, M.; Tardivel, C.; Airault, C.; Felix, B.; Jean, A. Modification of energy balance induced by the food contaminant T-2 toxin: A multimodal gut-to-brain connection. *Brain Behav. Immun.* **2014**, *37*, 54–72. [CrossRef]
40. Rodriguez-Garcia, C.; Sanchez-Quesada, C. Dietary Flavonoids as Cancer Chemopreventive Agents: An Updated Review of Human Studies. *Antioxidants* **2019**, *8*, 137. [CrossRef]
41. Yahfoufi, N.; Alsadi, N.; Jambi, M.; Matar, C. The Immunomodulatory and Anti-Inflammatory Role of Polyphenols. *Nutrients* **2018**, *10*, 1618. [CrossRef]
42. Abotaleb, M.; Samuel, S.M.; Varghese, E.; Varghese, S.; Kubatka, P.; Liskova, A.; Busselberg, D. Flavonoids in Cancer and Apoptosis. *Cancers* **2018**, *11*, 28. [CrossRef]
43. Chirumbolo, S.; Bjorklund, G.; Lysiuk, R.; Vella, A.; Lenchyk, L.; Upyr, T. Targeting Cancer with Phytochemicals via Their Fine Tuning of the Cell Survival Signaling Pathways. *Int. J. Mol. Sci.* **2018**, *19*, 3568. [CrossRef]
44. Perez-Vizcaino, F.; Fraga, C.G. Research trends in flavonoids and health. *Arch. Biochem. Biophys.* **2018**, *646*, 107–112. [CrossRef]
45. Gorlach, S.; Fichna, J.; Lewandowska, U. Polyphenols as mitochondria-targeted anticancer drugs. *Cancer Lett.* **2015**, *366*, 141–149. [CrossRef]
46. Moraes, V.R.d.S.; Tomazela, D.M.; Ferracin, R.J.; Garcia, C.F.; Sannomiya, M.; Soriano, M.d.P.C.; Silva, M.F.d.G.F.d.; Vieira, P.C.; Fernandes, J.B.; Filho, E.R.; et al. Enzymatic inhibition studies of selected flavonoids and chemosystematic significance of polymethoxylated flavonoids and quinoline alkaloids in Neoraputia (Rutaceae). *J. Braz. Chem. Soc.* **2003**, *14*, 380–387. [CrossRef]
47. Bharathi, D.S.; Boopathy Raja, A. In Silico Studies On Colon Cancer Against Hexadecane, Hexadecanoic Acid Methyl Ester and Quinoline, 1, 2-Dihydro-2, 2, 4-Trimethyl Compounds from Brown Seaweed. *Int. J. Res. Pharm. Sci.* **2020**, *11*, 1927–1935. [CrossRef]
48. Keeling, C.I.; Slessor, K.N.; Higo, H.A.; Winston, M.L. New components of the honey bee (*Apis mellifera* L.) queen retinue pheromone. *Proc. Natl. Acad. Sci. USA* **2003**, *100*, 4486–4491. [CrossRef]
49. Xiao, X.; Zou, J.; Fang, Y.; Meng, Y.; Xiao, C.; Fu, J.; Liu, S.; Bai, P.; Yao, Y. Fisetin and polymeric micelles encapsulating fisetin exhibit potent cytotoxic effects towards ovarian cancer cells. *BMC Complement. Altern. Med.* **2018**, *18*, 91. [CrossRef]
50. Zheng, G.Q.; Kenney, P.M.; Zhang, J.; Lam, L.K. Inhibition of benzo[a]pyrene-induced tumorigenesis by myristicin, a volatile aroma constituent of parsley leaf oil. *Carcinogenesis* **1992**, *13*, 1921–1923. [CrossRef]
51. Sun, J.-Q.; Xu, L.; Tang, Y.-Q.; Chen, F.-M.; Wu, X.-L. Simultaneous degradation of phenol and n-hexadecane by Acinetobacter strains. *Bioresour. Technol.* **2012**, *123*, 664–668. [CrossRef]

52. Ito, Y.; Kamijima, M.; Nakajima, T. Di (2-ethylhexyl) phthalate-induced toxicity and peroxisome proliferator-activated receptor alpha: A review. *Environ. Health Prev. Med.* **2019**, *24*, 47. [CrossRef] [PubMed]
53. Zhang, L.L.; Lin, Y.M. Tannins from Canarium album with potent antioxidant activity. *J. Zhejiang Univ. Sci. B* **2008**, *9*, 407–415. [CrossRef]
54. Fawole, O.A.; Amoo, S.O.; Ndhala, A.R.; Light, M.E.; Finnie, J.F.; Van Staden, J. Anti-inflammatory, ant cholinesterase, antioxidant and phytochemical properties of medicinal plant used for pain-related ailments in South Africa. *J. Ethnopharmacol.* **2010**, *127*, 235–241. [CrossRef]
55. Lin, Y.; Shi, R.; Wang, X.; Shen, H.M. Luteolin, a flavonoid with potential for cancer prevention therapy. *Curr. Cancer Drug Targets* **2008**, *8*, 634–646. [CrossRef]
56. Amaral, S.; Mira, L.; Nogueira, J.; da Silva, A.P.; Florêncio, M.H. Plant extracts with anti-inflammatory properties approach for characterization of their bioactive compounds and establishment of structure- antioxidant activity relationships. *Bioorg. Med. Chem.* **2009**, *17*, 1876–1883. [CrossRef]
57. Rajauria, G.; Abu-Ghannam, N. Isolation and Partial Characterization of Bioactive Fucoxanthin from *Himanthalia elongata* Brown Seaweed: A TLC-Based Approach. *Int. J. Anal. Chem.* **2013**, *2013*, 802573. [CrossRef]
58. Joshi, V.K.; Joshi, A.; Dhiman, K.S. *The Ayurvedic Pharmacopoeia of India*; Part-II, Vol-I (Formulations); Ministry of Health and Family Welfare: New Delhi, India, 2007; Volume 239, p. 147.
59. Al-Khayri, J.M.; Sahana, G.R.; Nagella, P.; Joseph, B.V.; Alessa, F.M.; Al-Mssallem, M.Q. Flavonoids as potential anti-inflammatory molecules: A review. *Molecules* **2022**, *27*, 2901. [CrossRef] [PubMed]
60. Sadasivam, S. *A Textbook of Biochemical Methods*; New Age International: New Delhi, India, 2005; pp. 8–9.
61. Yalçın, M.; Turgut, N.; Gökbulut, C.; Mermer, S.; Sofuoğlu, S.C.; Tari, V.; Turgut, C. Removal of pesticide residues from apple and tomato cuticle. *Environ. Sci. Pollut. Res.* **2022**, *30*, 15821–15829. [CrossRef] [PubMed]
62. Özşirvan, G.; Yalçın, M.; Turgut, N.; Tari, V.; Turgut, C. Insights into the uptake, translocation, and accumulation dynamics of cyantraniliprole and thiamethoxam seed coating pesticides in maize plants. *Environ. Sci. Pollut. Res.* **2024**, *31*, 44900–44907. [CrossRef]
63. Balamurugan, V.; Fatima, S.; Velurajan, S.A. guide to phytochemical analysis. *Int. J. Adv. Res. Innov. Ideas Educ.* **2019**, *5*, 236–245.
64. Wagner, E.H. Organizing care for patients with chronic illness revisited. *Milbank Q.* **2019**, *97*, 659. [CrossRef]
65. Musharraf, S.G.; Ahmed, M.A.; Zehra, N.; Kabir, N.; Choudhary, M.I.; Rahman, A.-U. Biodiesel production from microalgal isolates of southern Pakistan and quantification of FAMEs by GC-MS/MS analysis. *Chem. Cent. J.* **2012**, *6*, 149. [CrossRef]
66. Wahyuni, D.K.; Nuha, G.A.; Atere, T.G.; Kharisma, V.D.; Tari, V.S.; Rahmawati, C.T.; Murtadlo, A.A.A.; Syukriya, A.J.; Wacharasindu, S.; Prasongsuk, S.; et al. Antimicrobial potentials of *Pandanus amaryllifolius* Roxb.: Phytochemical profiling, antioxidant, and molecular docking studies. *PLoS ONE* **2024**, *19*, e030534. [CrossRef]
67. Badami, S.; Moorkoth, S.; Rai, S.R.; Kannan, E.; Bhojraj, S. Antioxidant activity of *Caesalpinia sappan* heartwood. *Biol. Pharm. Bull.* **2003**, *26*, 1534–1537. [CrossRef]
68. Valcárcel, M. *Principles of Analytical Chemistry: A Textbook*; Springer Science & Business Media: Berlin, Germany, 2012.
69. Re, R.; Pellegrini, N.; Proteggente, A.; Pannala, A.; Yang, M.; Rice-Evans, C. Antioxidant activity applying an improved ABTS radical cation decolorization assay. *Free Radic. Biol. Med.* **1999**, *26*, 1231–1237. [CrossRef] [PubMed]
70. Gupta, V.; Chandra, N.; Tari, V.; Kannan, K. A Sustainable Approach for the Green synthesis of Silver Nanoparticles Using *Brassica oleracea* sub sp. *botrytis (L.) leaves and its Antibacterial Activity. Phys. Chem. Solids* **2024**, *25*, 303–310. [CrossRef]
71. Umesha, S.; Singh, P.K.; Singh, R.P. Microbial Biotechnology and Sustainable Agriculture. In *Biotechnology for Sustainable Agriculture: Emerging Approaches and Strategies*; Singh, R.L., Mondal, S., Eds.; Woodhead Publishing: Sawston, UK, 2018; pp. 185–205. [CrossRef]
72. Li, Y.; Sun, S.; Pu, X.; Yang, Y.; Zhu, F.; Zhang, S.; Xu, N. Evaluation of Antimicrobial Activities of Seaweed Resources from Zhejiang Coast, China. *Sustainability* **2018**, *10*, 2158. [CrossRef]
73. Chandrasekaran, M.; Senthilkumar, A.; Venkatesalu, V. Antibacterial and antifungal efficacy of fatty acid methyl esters from leaves of *Sesuvium portulacastrum* L. *Eur. Rev. Med. Pharmacol. Sci.* **2011**, *15*, 775–780.

marine drugs

MDPI

Article

Metabolite Profiling and Antioxidant Activities in Seagrass Biomass

Pilar Garcia-Jimenez [1,*], Milagros Rico [2], Diana del Rosario-Santana [1], Vicent Arbona [3], Marina Carrasco-Acosta [1] and David Osca [1]

[1] Department of Biology, Faculty of Marine Sciences, Instituto Universitario de Investigación en Estudios Ambientales y Recursos Naturales IUNAT, Universidad de Las Palmas de Gran Canaria, 35017 Las Palmas, Spain; diana.delrosario@ulpgc.es (D.d.R.-S.); marina.carrasco@ulpgc.es (M.C.-A.); david.osca@ulpgc.es (D.O.)
[2] Department of Chemistry, Instituto Universitario de Oceanografía y Cambio Global-IOCAG, Universidad de Las Palmas de Gran Canaria, 35017 Las Palmas, Spain; milagros.ricosantos@ulpgc.es
[3] Departament de Biologia, Bioquímica i Ciències Naturals, Universitat Jaume I, 12071 Castelló de la Plana, Spain; arbona@uji.es
* Correspondence: pilar.garcia@ulpgc.es

Abstract: In this work, metabolite profiling of seeds and antioxidant analysis of fragments of two marine seagrasses, *Posidonia oceanica* and *Cymodocea nodosa,* were carried out to identify metabolite signature involved in seed viability and to evaluate the potential of fragments as a source of bioactive compounds. Using HILIC/QTOF-MS, UHPLC-MS and spectrophotometric analysis, seed metabolites and polyphenols and antioxidant activities, such as those of radical scavenging (RSA), reduction (FRAP, CUPRAC) and complexation (CCA), of rhizome fragments were evaluated. Metabolite comparison between seeds revealed differences across development stages (germinated and non-germinated) and seed types (dormant and non-dormant), providing insights into metabolic activity potentially associated with germination processes and seed viability. Furthermore, polyphenol analysis showed the highest content of caffeic acid in mature leaves (17.00 ± 0.02 μg g^{-1} dw for *P. oceanica* and 98.00 ± 0.03 μg g^{-1} dw for *C. nodosa*). Total phenolic content was correlated with flavonoids and with reduction and complexation activities. The combination of radical scavenging activity and $t_{1/2}$ was higher in *P. oceanica* than *C. nodosa* and also surpassed the commercial synthetic antioxidant BHA. We conclude *P. oceanica* and *C. nodosa* exhibit distinct seed metabolite profiles related to germination and type of seeds, and that fragments are rich in antioxidants, with potential as sustainable sources of bioactive compounds.

Keywords: antioxidants; *Cymodocea nodosa*; metabolites; *Posidonia oceanica*; ramets; seeds

1. Introduction

Metabolomic approaches have been proposed for the detection and characterisation of compounds involved in crucial plant physiological processes, including seed behaviour during germination [1–4]. In particular, the identification of specialised metabolites offers insights into potential biomarkers and their associated bioactivities while also revealing how environmental conditions affect plant metabolic dynamics [5–7]. Among the main classes of plant metabolites, lipids—including isoprenoids and steroids—serve structural and signalling roles, although several functions remain to be clarified [8]. Phenolic compounds, including flavonoids, lignans and phenolic acids [9,10], are also widely recognised for

their physiological significance in plants, particularly in oxidative stress protection [11,12], growth and reproduction [13]. In general, flavonoids are widely distributed in plants and include compounds such as chalcones and (iso) flavones. Lignans are represented by secoisolariciresinol diglucosides, while phenolic acids can be categorised into a general group known as organoheterocyclic compounds, which includes hydroxybenzoic acids, acetophenones, phenylacetic acids and hydroxycinnamic acids.

In contrast to terrestrial plants, seagrasses have been less explored in terms of secondary metabolites. Nonetheless, secondary metabolites, such as zosteric acid and caffeic acid, have been discovered [14–16], highlighting the potential of these marine species as valuable biochemical resources. In terms of seed analysis, seagrass seeds can exhibit different behavioural and physiological states, outlining stages of dormancy and non-dormancy. *Posidonia oceanica* seeds are in a non-dormant state and can be transported away from the plant mother and germinate in the meantime [17], whereas *Cymodocea nodosa* seeds are in a dormant state and settle close to the mother plant [18]. This difference enables investigation of the metabolic profiles associated with dormancy and viability as disruption of seed dormancy is followed by seed germination [19–21]. Furthermore, rhizome fragments allow the assessment of biochemical resources which could be relevant for potential biotechnological exploitation.

As *P. oceanica*, an endemic species in the Mediterranean Sea, and *C. nodosa*, widely distributed in the Canary Islands (Spain), are protected species and ecosystems, seeds and ramets (i.e., fragments containing rhizome, roots and leaves) washed up on the coast can be exploited due to inconvenience of obtaining a sustainable supply of biomass from meadows for large scale production of such compounds. This biomass can be predictably found throughout the year depending on certain atmospheric and oceanographic conditions [22,23]. Under these expected conditions, biomass washed ashore from seagrass meadows can be an alternative to study target metabolites as well as its contribution to the characterisation of biocompounds and assessment of antioxidant activities. This study focuses on (i) the identification of potential metabolites through HILIC/QTOF-MS in two developmental stages of seeds (germinated and non-germinated) of both *P. oceanica* and *C. nodosa* to unveil potential metabolites associated with germination processes and (ii) the assessment of phenolic compounds and antioxidant capacities of seagrass fragments to be used as a sustainable source of natural antioxidants. These findings contribute to the valorisation of seagrass residues, demonstrating their potential as valuable sources of bioactive compounds.

2. Results

2.1. Global Analysis of Seed Metabolites

Principal Component Analysis (PCA), a multivariate statistical technique, is applied to metabolite datasets to uncover patterns by identifying directions of greatest variance. Data are then transformed into new variables called principal components that summarise variation. To continue, components are ranked according to the amount of variance they capture, helping to reveal metabolic differences between two seed types (*Cymodocea* and *Posidonia*) and their developmental stages (germinated and non-germinated seeds) under both positive and negative ionisation modes. Thus, the results of the PCA reveal that the first two principal components (PC1 and PC2) explain most of the variance in the data: 85% and 10%, respectively, in negative mode and 84% and 12% in positive mode (Figure 1). The analysis shows that all samples representing two different marine plants and two seed development stages are grouped into two clusters corresponding to *C. nodosa* and *P. oceanica* (Figure 1A,B). These findings indicate significant metabolic differences between

the two marine plants. Furthermore, differences between germinated and non-germinated seeds of *P. oceanica* were also observed (Figure 1A,B)

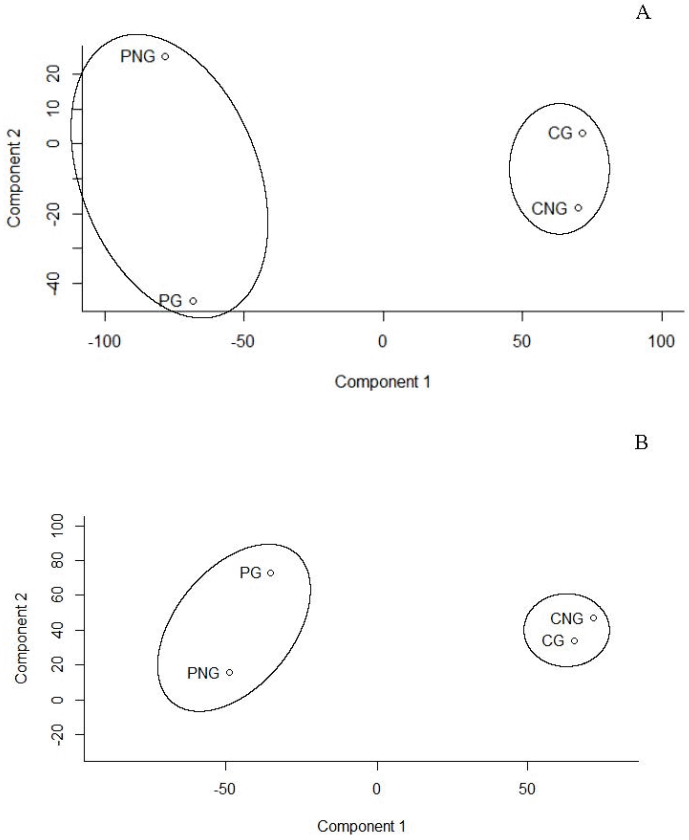

Figure 1. Principal component analysis (PCA) for metabolites of *Posidonia oceanica* (P) and *Cymodocea nodosa* (C) for germinated (G) and non-germinated (NG) seeds according to (**A**) positive and (**B**) negative modes. Points in PCA are the result of analysis performed by compilation of metabolites from negative and positive mode analysis with pooled seeds for each stage. This means non-germinated (PNG) and germinate (PG) seeds of *P. oceanica* and non-germinated (CNG) and germinate (CG) seeds of *C. nodosa.* Note that four points in the PCA are the result of analysis performed by compilation of metabolites from negative and positive mode analysis with pooled seeds for each stage.

2.2. Metabolites in Seeds of Seagrasses

Metabolite data using the estimated compound mass [M] (considering all features as $[M + H]^+$ or $[M - H]^-$) allowed the detection of 1964 peaks of known and unknown metabolites (Tables S1 and S2). Metabolites were mainly classified into phenolic compounds (flavonoids), organoheterocyclic compounds, carboxylic acids and derivatives involved in cellular responses towards tricarboxylic acid cycle (TCA cycle) and lipids. For facilitating analysis, lipids were further subdivided into glycerolipids, fatty acyls and steroids for both seagrasses. Analysis of the filtered data using default ppm of 0–10 ppm mass error and values of germinated/non-germinated ratios for each compound (average value of all $\geq$1 ratio) resulted in significant changes in the metabolite profiles of both seagrasses and seed stages (Figure 2).

Under constrictions, the metabolite profile of seeds of *P. nodosa* and *C. nodosa* has provided a chemical fingerprint of how metabolites changed with seed maturation, i.e., germinated/non-germinated ratio. Thus, most of the metabolites identified in *P. oceanica* were reported 3- and 4-fold higher in germinated seeds (Figure 2A), whereas non-significative changes were observed between two development stages of seeds of *C. nodosa*,

with the exception of some lipid compounds (Figure 2B). Furthermore, the metabolite profile is dominated by the presence of fatty acyls in *C. nodosa* with 54% of the total metabolites, and flavonoids (31%) and glycerolipids (23%) in *P. oceanica* (Figure 3).

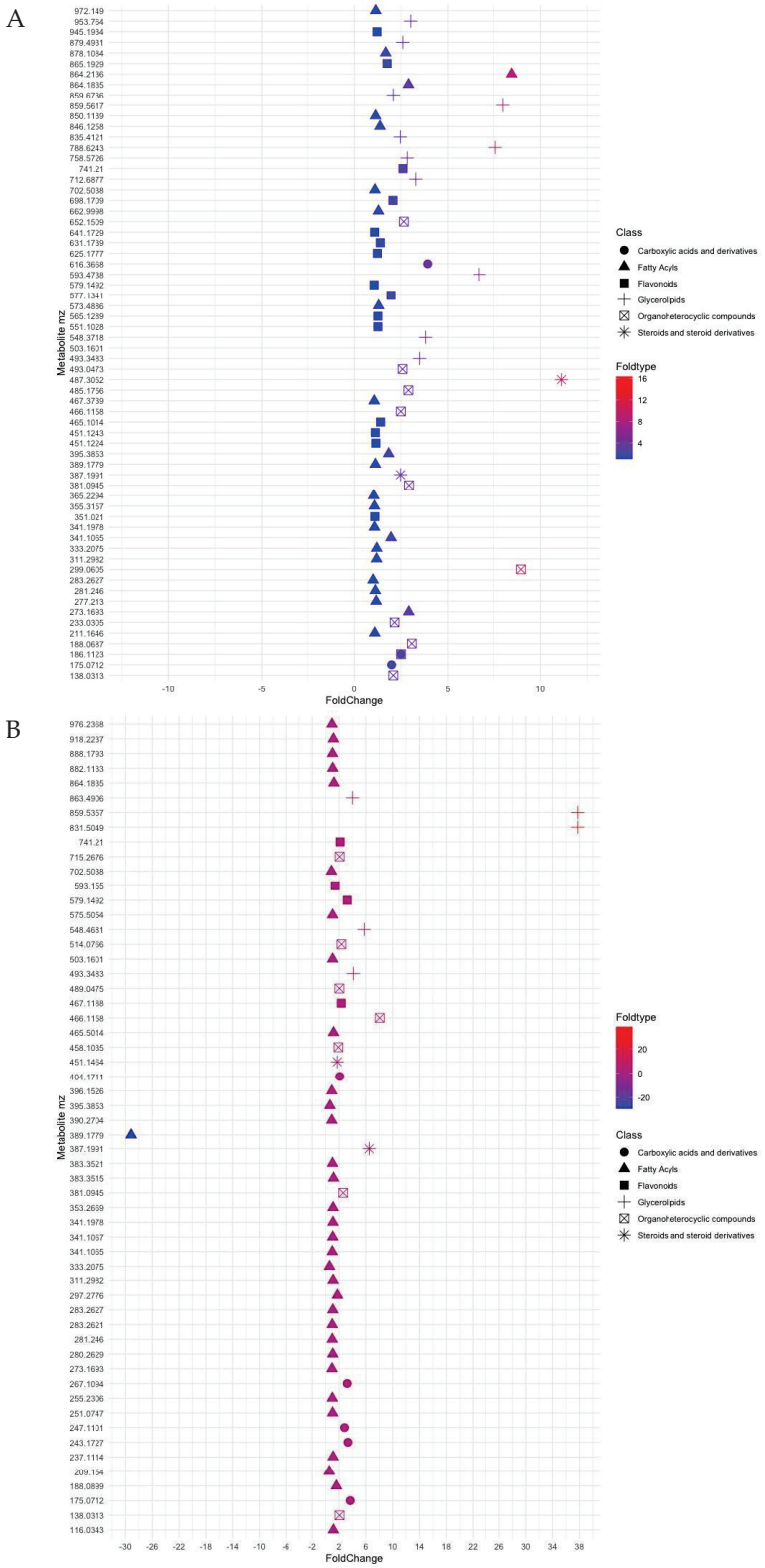

Figure 2. Plot showing log2 fold change values (x-axis) for ratios m/z of metabolites of (**A**) *Posidonia oceanica* and (**B**) *Cymodocea nodosa*, classified according to six groups, namely derivatives from tricarboxylic acid cycle, fatty acyls, flavonoids, glycerolipids, organoheterocyclic compounds and steroids.

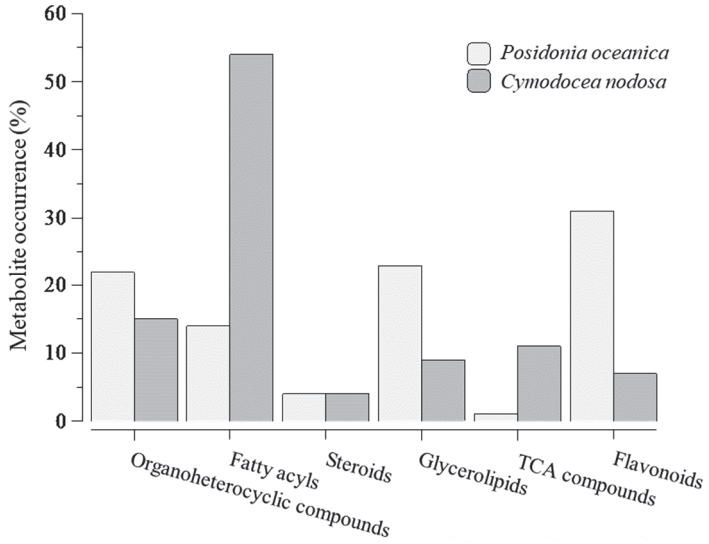

Figure 3. Distribution of metabolites by categories, namely organoheterocyclic compounds, fatty acyls, steroids, glycerolipids, compounds from tricarboxylic acid cycle and flavonoids, after analysis according to ratios over average value of all ≥1-ratios and metabolites selection constrained to a default 0–10 ppm mass error. 100% for *Posidonia oceanica* = 51 metabolites and for *Cymodocea nodosa* = 54 metabolites.

Exploration of metabolites of *C. nodosa* through ratio assessment (Table S3) showed that glycerophospholipids (PG) were well-represented in germinated seeds (m/z 831.5049; ratio 37) of *C. nodosa* and, to a lesser extent, by ceramides, phosphatidylcholines (PC) and phosphatidylinositols (PI) with ratios ranging from 4- (m/z 863.4906) to 5.7-fold times (m/z 548.4681). In *P. oceanica*, the presence of glycerophospholipids was also reported abundantly in germinated seeds with ratios ranging between 6.7 (m/z 593.4738) and 7.99 (m/z 859.5617). Alterations in the ratios of seeds of *C. nodosa* for 29 compounds, recognised after the restrictive selection into the fatty acyls category, ranged from 1.0 to 1.6 (m/z 188.0899). In *P. oceanica,* the ratios reached values of 16 for a fatty acyl glycoside of mannotriose (m/z 503.1601; ppm, 3) in germinated seeds.

Regarding steroid-type compounds, it is highlighted a compound such as spironolactone (m/z 387.1991; ratio 6.5) in germinated seeds and isohydroxymethasone with m/z 389.1779 (ratio −29) for non-germinated seeds of *C. nodosa*. In *P. oceanica*, the occurrence of triterpenoid named Antcin k (m/z 487.3052; ppm, 3) was reported with a ratio 12-fold higher in germinated seeds compared with those non-germinated. Moreover, the organoheterocyclic category is mainly characterised by several types of molecules, such as pyrrolidines, indoles and benzopyrans. Benzopyrans (m/z 381.0945) of the mollicellin type were determined in germinated seeds of both seagrasses with similar ratios (2.6–2.9). In *P. oceanica*, a compound of m/z 299.0605 (ppm 4) was identified as a pyrrolidine with a ratio of 8.9-higher in germinated seeds. Apart from these types of molecules in *C. nodosa*, this category also included a molecule with a m/z 466.1158 (ppm 10) identified like thienodiazepines with a ratio 8-fold higher in germinated seeds.

Flavonoids have been identified in germinated seeds of *C. nodosa*, two and three times higher than in non-germinated seeds and in forms of quadrangularin and catechins, respectively. In the case of *Posidonia*, from 15 compounds constrained by ppm value and ratio, it is relevant the presence of anthocyanins such as cyanidin and pelargonidin derivatives (2 times higher in germinated seeds). Metabolites activated as carboxylic acids and derivatives were also encountered in similar proportions in both seeds of *C. nodosa* and *P. oceanica* (range of 2–3).

2.3. Marine Plant Fragment Metabolites: Assessing Antioxidant Activity in Marine Plants Washed Up Coast

Polyphenols such as caffeic and coumaric acids are detected three times higher in the whole plant of *C. nodosa* compared with those of *P. oceanica*. Moreover, the highest contents of caffeic acid are quantified in mature leaves of *C. nodosa* (Table 1), while high concentrations are also reported in rhizomes and roots (Table 1). Otherwise, coumaric acid is significantly reported in the whole plant of *P. oceanica* and *C. nodosa* (Table 1) in contrast to ferulic acid, which is only detected in leaves. Gallic acid (GA) is undetected in either marine plant.

Table 1. Phenolic content (μg g^{-1} dw) quantified by UPLC-MS in seagrass sections from *Posidonia oceanica* and *Cymodocea nodosa*.

	Phenolic Compounds					
	CA	**CAA**	**COU**	**FA**	**SYR**	**Sum**
			Posidonia oceanica			
Mature leaves	n.d.	17.00 ± 0.02 ° *	0.12 ± 0.01	0.11 ± 0.01 ° *	$0.03 \pm 2 \times 10^{-3}$ *	$17.27 \pm 9 \times 10^{-4}$ ° *
Young leaves	n.d.	1.53 ± 0.02 *	$0.26 \pm 9 \times 10^{-4}$ *	n.d.	n.d.	1.80 ± 0.01
Sheaths	n.d.	0.12 ± 0.01 *	0.11 ± 0.01 *	n.d.	$0.028 \pm 2 \times 10^{-3}$ *	0.25 ± 0.02 *
Rhizomes	$0.010 \pm 1 \times 10^{-3}$	0.17 ± 0.01 *	$0.02. \pm 0.002$ *	n.d.	$0.05 \pm 4 \times 10^{-3}$	0.35 ± 0.02 *
Roots	n.d.	0.28 ± 0.02 *	0.07 ± 0.01 *	n.d.	$0.03 \pm 1 \times 10^{-3}$	0.39 ± 0.02 *
Whole plant	$0.097 \pm 9 \times 10^{-3}$	$0.01 \pm 9 \times 10^{-4}$ *	0.43 ± 0.04 ° *	n.d.	$0.07 \pm 3 \times 10^{-3}$	0.62 ± 0.02 *
			Cymodocea nodosa			
Mature leaves	n.d.	98.00 ± 0.03 °	0.14 ± 0.01	n.d.	n.d.	98.14 ± 0.02
Young leaves	0.48 ± 0.01	0.26 ± 0.01	0.50 ± 0.02	0.30 ± 0.01 ° *	$0.04 \pm 9.8 \times 10^{-4}$ *	1.58 ± 0.01 °
Sheaths	$0.07 \pm 8.6 \times 10^{-4}$	0.22 ± 0.01	0.36 ± 0.02	$0.08 \pm 7 \times 10^{-3}$ *	n.d.	0.73 ± 0.03
Rhizomes	n.d.	0.69 ± 0.02	0.43 ± 0.02	n.d.	$0.06 \pm 3 \times 10^{-3}$	1.17 ± 0.06
Roots	n.d.	0.54 ± 0.03	0.25 ± 0.01	n.d.	0.03 ± 0.001	0.82 ± 0.07
Whole plant	n.d.	$0.04 \pm 1 \times 10^{-3}$	1.44 ± 0.02 °	n.d.	$0.06 \pm 2 \times 10^{-3}$ °	1.54 ± 0.21

* Significant differences ($p \leq 0.01$) between *Posidonia* and *Cymodocea*; ° Significant differences ($p \leq 0.01$) within plant. Data are a result of pooled samples for each part of plant; $n = 2$ independent measurements (mean ± standard deviation (SD)). CA, cinnamic acid; CAA, caffeic acid; COU, *p*-coumaric acid; FA, ferulic acid; SYR, syringic acid; sum means total contents of phenols in each corresponding plant fraction. n.d., non-determined.

The total carbohydrate content is mainly supported by rhizomes with significant differences within other plant parts (262.50 ± 0.10 mg glucose equivalent g^{-1} dw for *P. oceanica* and 526.00 ± 1.00 mg glucose equivalent g^{-1} dw for *C. nodosa*; Table 2). Total phenolic compounds and flavonoids show significant differences in the roots and rhizomes of *P. oceanica* compared with *C. nodosa* (Table 2).

Table 2. Total carbohydrates (mg glucose equivalent g^{-1} dw) and total phenolic (mg gallic acid equivalent g^{-1} dw) and flavonoid contents (mg quercetin equivalent g^{-1} dw) of different seagrass sections (mature and young leaves, sheaths, rhizomes and roots and whole plant) from *Posidonia oceanica* and *Cymodocea nodosa*.

Seagrass Part	***Posidonia oceanica***			***Cymodocea nodosa***		
	TCH	**TPC**	**FLAV**	**TCH**	**TPC**	**FLAV**
Mature leaves	26.97 ± 0.09	10.76 ± 0.12	7.10 ± 0.50	44.10 ± 0.10	7.04 ± 0.20	3.38 ± 0.01
Young leaves	9.73 ± 0.07 *	7.80 ± 0.36	2.50 ± 0.40	44.40 ± 0.20	12.77 ± 0.40	7.40 ± 0.60
Sheaths	212.30 ± 0.08 *	17.82 ± 0.26	9.10 ± 0.40	111.90 ± 0.40	14.00 ± 0.06	6.50 ± 0.60
Rhizomes	262.50 ± 0.10 ° *	51.57 ± 0.92 *	42.00 ± 1.00 ° *	526.00 ± 1.00	20.70 ± 0.18	13.00 ± 1.00
Roots	60.70 ± 0.30 *	32.70 ± 1.27 *	30.00 ± 1.00 *	283.00 ± 1.00	18.21 ± 0.44	13.00 ± 1.00
Whole plant	118.10 ± 0.20 *	14.00 ± 0.21	8.20 ± 0.50	137.00 ± 00	13.65 ± 0.06	8.80 ± 0.30

* Significant differences ($p \leq 0.01$) between *Posidonia oceanica* and *Cymodocea nodosa*; ° significant differences ($p \leq 0.01$) within plant parts. Data are mean ± standard deviation (SD) from three measurements with two independent replicates each. TCH, total carbohydrates; TPC, total phenolic content; FLAV, flavonoids.

The scavenging activities of seagrasses are higher than that of the synthetic antioxidant food additive BHA (64.4%, $t_{1/2}$ 405 s; Table 3). The inhibition percentage ranged from 80.2% to 87.3%, with the lowest $t_{1/2}$ reported in rhizomes (87.3%, 33 s) and roots (87.0%, 38 s) for *P. oceanica*, whereas DPPH inhibition activity for *C. nodosa* corresponded to 73.70% and $t_{1/2}$ 239 s for rhizomes and 85.2% and $t_{1/2}$ 131 s for roots (Table 3).

Table 3. Radical scavenging activities (RSA, inhibition %) and $t_{1/2}$ (s) for extracts from plant sections of *Posidonia oceanica* and *Cymodocea nodosa* and for synthetic compound BHA.

Seagrass Part	*Posidonia oceanica*		*Cymodocea nodosa*	
	RSA	$t_{1/2}$	RSA	$t_{1/2}$
Mature leaves	80.20 ± 0.50	107.00 ± 6.00	65.00 ± 1.00	309.00 ± 2.00
Young leaves	45.10 ± 0.30	923.00 ± 53.00	70.80 ± 0.60	249.00 ± 4.00
Sheaths	84.10 ± 0.30	80.00 ± 4.00	84.30 ± 0.10	138.00 ± 4.00
Rhizomes	87.30 ± 00	33.00 ± 00	73.70 ± 0.90	239.00 ± 19.00
Roots	87.00 ± 0.03	38.00 ± 00	85.20 ± 0.20	131.00
Whole plant	85.90 ± 0.64	61.00 ± 6.00	73.00 ± 5.00	267.00 ± 2.00
BHA (0.5 mg mL^{-1})	64.40 ± 1.50	405.00 ± 6.00		

Data are mean ± standard deviation (SD) from three measurements with two independent replicates each. BHA, butylated hydroxyanisole.

Activities of reduction of Fe^{3+} and Cu^{2+} (i.e., FRAP, CUPRAC) and of Cu^{2+}-chelating (CCA) are higher in rhizomes of both seagrasses compared with leaves, sheaths, roots and whole plant (Table 4). Otherwise, the lowest activities for FRAP, CUPRAC and CCA correspond to young leaves of *P. oceanica* (Table 4).

Table 4. Antioxidant activities, namely FRAP (μmol of reduced Fe (III) g^{-1} dw), CUPRAC (μmol equivalent of Trolox g^{-1} dw) and CCA (inhibition percentage of PV–Cu^{2+} complex formation) of extracts derived from *Posidonia oceanica* and *Cymodocea nodosa* sections.

Seagrass Part	*Posidonia oceanica*			*Cymodocea nodosa*		
	FRAP	**CUPRAC**	**CCA**	**FRAP**	**CUPRAC**	**CCA**
Mature leaves	40.30 ± 0.50	45.00 ± 2.00	70.89 ± 8 × 10^{-3}	45.70 ± 0.40	51.90 ± 0.60	51.50 ± 0.40
Young leaves	26.40 ± 8 × 10^{-3}	35.20 ± 0.40	66.30 ± 0.60	37.60 ± 0.40	37.80 ± 0.40	51.30 ± 0.60
Sheaths	173.00 ± 1.00 *	144.90 ± 0.10 *	83.50 ± 0.40 *	40.22 ± 0.02	42.00 ± 1.00	62.40 ± 0.90
Rhizomes	234.20 ± 0.62 °	199.00 ± 1.00 °	87.10 ± 0.30 °	222.90 ± 0.40 °	181.00 ± 2.00 °	93.60 ± 0.20
Roots	121.00 ± 0.60	116.00 ± 5.00	44.00 ± 0.90 *	150.00 ± 0.10	133.40 ± 0.30	90.40 ± 0.30
Whole plant	79.70 ± 0.05	96.00 ± 1.00	79.80 ± 0.80	39.90 ± 0.10	50.70 ± 0. 60	69.00 ± 0.10

* Significant differences ($p \leq 0.01$) between *Posidonia oceanica* and *Cymodocea nodosa*; ° significant differences ($p \leq 0.01$) within plant parts. Data are mean ± standard deviation (SD) from three measurements with two independent replicates each.

Statistical analysis in Table 5 indicates significant correlations between TPC and flavonoids for *P. oceanica* (R^2 = 0.988, $p < 0.001$) and *C. nodosa* (R^2 =0.963, $p < 0.01$). Positive correlations are also reported between total carbohydrates and FRAP activity (R^2 = 0.936, $p < 0.006$) for *P. oceanica,* and with R^2 0.969 ($p < 0.001$) for *C. nodosa*. Likewise, total carbohydrates and CRUPAC are correlated for *P. oceanica* (R^2 = 0.935, $p < 0.006$) and for *C. nodosa* (R^2 0.965 with $p < 0.002$). Additionally, TCH and TPC correlate with CCA ($p < 0.009$ and $p < 0.014$ respectively) for *C. nodosa.* No correlations for RSA are encountered.

Table 5. Statistical relationship between the data of carbohydrate, polyphenol and flavonoid contents and antioxidant activities of *Posidonia oceanica* and *Cymodocea nodosa* through the Pearson correlation test.

Assay	Correlation Coefficients	*Posidonia oceanica*			*Cymodocea nodosa*		
		TCH	**TPC**	**FLAV**	**TCH**	**TPC**	**FLAV**
TCH	Pearson's R	1.0		0.569	1.0		0.863 *
	p-value	-		0.238	-		0.027
TPC	Pearson's R	0.678	1.0	0.988 ***	0.863 *	1.0	0.963 **
	p-value	0.139		<0.001	0.027		0.002
RSA	Pearson's R	0.563	0.527	0.527	0.266	0.602	0.488
	p-value	0.245	0.283	0.279	0.610	0.103	0.327
FRAP	Pearson's R	0.936 **	0.854 *	0.779	0.969 **	0.814 *	0.841 *
	p-value	0.006	0.030	0.068	0.001	0.049	0.036
CUPRAC	Pearson's R	0.935 **	0.865 *	0.794	0.965 **	0.805	0.847 *
	p-value	0.006	0.026	0.059	0.002	0.054	0.033
CCA	Pearson's R	0.690	0.099	−0.042	0.921 **	0.902 *	0.936 **
	p-value	0.130	0.852	0.936	0.009	0.014	0.006

* $p < 0.05$, ** $p < 0.01$, *** $p < 0.001$; TCH, total carbohydrates; TPC, total phenolic content; FLAV, flavonoids; RSA, radical scavenging activity; FRAP, Ferric Reducing Antioxidant Power; CUPRAC, cupric ion reducing capacities; CCA, Cu^{2+}-chelating activity.

3. Discussion

3.1. Metabolites in Seeds of Seagrasses

Seed metabolite profiles of two seagrasses exhibited different patterns, which can be explained by the distinctive reproductive strategies and seedling establishment of *P. oceanica* and *C. nodosa* plants (Figure 1). Seed differences can be attributed to the buoyant fruits of *P. oceanica*, which are transported away from the mother plant, allowing for the released seeds to trigger germination in the meantime [17,18,24]. In contrast, *Cymodocea* seeds sink, settle in the soil and continue to initiate germination.

Metabolite analysis in seeds indicated that a phospholipid pool (i.e., phosphatidylinositol, phosphatidylcholines and sphingolipids) may reflect lipid trafficking, which can act in the biogenesis of organelle membranes, signalling processes and the mobilisation of storage lipids required for seed germination in both seagrasses. These results correlate with the observation that *P. oceanica* seeds display high metabolic activity to supply carbon, nitrogen and phosphorus during early seedling growth [24,25]. In terrestrial plants, lipids have played a primary role in the initial stages of seed germination, as they provide the sugars and energy necessary for growth and development [26–28].

Notably, changes in the glycerophospholipid pool have also been associated with phosphate release in phosphorus-deficient terrestrial plants [29]. In *C. nodosa*, a high ratio (ratio 37.746; Table S3) for glycerophospholipid compounds suggests that changes in the phospholipid pool support the release of inorganic phosphorus in germinated seeds. The viability of ramets (fragments of rhizome, roots and leaves) in *C. nodosa* is known to be linked to the presence of phosphorus in the soil, as phosphorus is the main nutrient required to fulfil growth requirements [30]. This aspect warrants further study due to its significance for seed propagation and in vitro culture of this seagrass. Furthermore, the identification of a higher number of metabolites involved in the TCA cycle in *C. nodosa* compared with those in *P. oceanica* may suggest that mechanisms to mobilise carbon and nitrogen differ between the two marine plants. This indicates a mobilisation of TCA compounds in dormant seeds of *C. nodosa*, which do not float and germinate upon falling to the ground, in contrast to the mobilisation of fatty acyls in non-dormant seeds of *P. oceanica* that germinate before settling.

Otherwise, in terrestrial plants, the contribution of fatty acyls to ecological mechanisms, such as signals for growth and interaction with microorganisms, has been reported [31]. During seed germination and development, the degradation of hydroxy fatty acids is associated with variations in seed size and seedling growth [8,32]. Importantly, hydroxy fatty acids are known within the category of signalling molecules for associations between plants and fungal populations [33]. These relationships between microorganisms and seeds suggest that a higher number of acyl metabolites in *C. nodosa* seeds could be associated with their dormant nature.

Hydroxytetracosanoic acid, the most abundant long-chain fatty acid in *C. nodosa* seeds, has been described for its neuroprotective properties and as a functional ingredient in food and cosmetic products [34]. Additionally, lipids interact with flavonoids to maintain reactive species homeostasis as germination and development of seeds bring more oxidised acyl and fewer unsaturated chains from lipids. Therefore, positive ratios between germinated and non-germinated seeds would be indicative of protection against damage caused by ageing tissues as seed development progresses.

In relation to steroids, the presence of a compound similar to methasone in non-germinated seeds (ratio −29; Table S2) of *C. nodosa* is significant, as it has been described as an anti-inflammatory and anti-cancer glucocorticoid [35]. To date, this compound has not been documented in plant metabolism, but results indicate that this metabolite might affect seed dormancy, as it appeared in non-germinated seeds. Hence, further studies on the synthesis pathway of this steroid are required, as control of its biosynthesis may be critical to the success of seed germination.

Another steroid metabolite in the seagrass *C. nodosa*, such as spironolactone (Table S3), is a recognised inhibitor of the action of the plant growth regulator brassinosteroids in plants. The presence of spironolactone causes retardation of the growth of the embryogenic axis in Arabidopsis [36]. If, as occurs in terrestrial plants, the presence of this metabolite retards hypocotyl growth in *C. nodosa*, it would suggest that seed germination could fail, indicating seed non-viability. These results suggest that steroids control hypocotyl growth at all stages of seed development (germinated and non-germinated) in *C. nodosa*. Conversely, steroids in *P. oceanica* are represented by triterpenoids, which are recognised as secondary plant metabolites with beneficial roles in plant defence against various stress types. Again, the buoyant nature of *P. oceanica* fruits and non-dormant seeds allows for the inference that metabolites can be used as distinctive markers of developing seeds compared to those of *C. nodosa* seeds.

Moreover, organoheterocyclic compounds, represented by a benzopyran structural motif and pyrrolidines, are biologically active and naturally occurring compounds reported in both seagrasses. The benzopyran core offers potential for the design of new drug-like molecules with therapeutic applications [37,38], and particularly mollicellin (Table S3), a metabolite naturally produced by plant endophytes, has been described for resistance under adverse conditions [37]. Meanwhile, indole-based compounds have demonstrated appropriate functions as defence and resistance promoters, as well as regulators of maturation and germination of seeds [39]. Pyrrolidines attract interest in in vitro cultures as they are degradation products of the catabolism of the polyamines spermidine and spermine. Polyamines have engaged effects during the growth and development of *C. nodosa*, being reported in the apical section of the rhizome and described as an anti-senescence-inducing factor [40]. Furthermore, metabolite analysis revealed the occurrence of molecules such as benzodiazepines, which modulate the synthesis of γ-aminobutyric acid (GABA), and in turn, GABA is synthesized through the polyamine metabolic pathway. GABA accumulation works in synergy for plant growth and development and plant stress tolerance [41].

All in all, metabolite analysis has unveiled a compound profile for two types of seeds (dormant vs. non-dormant) according to developmental stage (germinated vs. non-germinated). Although we cannot disentangle certain information, such as the age of seeds, burial or buoyant time and water content, among other factors, glycerophospholipids seem to support seed germination through their mobilisation and degradation in *P. oceanica*. Contrastingly, in *C. nodosa*, mobilisation seems to occur through the TCA cycle as dormant seeds need to ensure germination at the optimal time. Steroids report a differential role according to whether seeds have or not dormancy. In the case of dormant seeds such as *Cymodocea*, metabolites seem to be responsible for delaying germination by controlling brassinosteroid biosynthesis and polyamine pathways. Otherwise in non-dormant seeds, they synthetised steroids to act in defence against stresses, as occurred to *Posidonia*.

3.2. Marine Plant Metabolites: Assessing Antioxidant Activity in Marine Plants Washed up Coast

There is considerable evidence with respect to the importance of phenolic compounds in scavenging free radicals and preventing oxidative damage caused by different stresses [42,43]. In the present work, mature leaves of seagrasses showed the highest total content of identified polyphenols mainly due to caffeic acid reported in both plants (17.00 ± 0.02 and 98.00 ± 0.03 μg g^{-1} dw; Table 1). This could be explained as caffeic acid favours lignin synthesis that, in turn, deals with the cell wall thickness and deceleration of cell wall expansion in mature leaves [43–45]. In addition, caffeic tartrates have been reported as the most abundant compounds in leaves of *P. oceanica* compared with the low levels of ferulic and coumaric tartrates [46]. In young leaves of *C. nodosa*, ferulic acid can be correlated to mechanical strength as FA-mediated cross-linking between polysaccharides. Low levels of FA and cinnamic acid (Table 1) may also be associated with changes in the lignin monomer composition, as can be exemplified with FA, which results from the methylation of caffeic acid [47]. In this sense, Leri et al. [42] determined 1.79% of ferulic acid from the total of polyphenols analysed in *P. oceanica*.

Notwithstanding, RSA was higher in marine plants than in that of the commercial synthetic antioxidant BHA (64.4%) despite being used at twice the legally permitted concentration (Table 3). Moreover, RSA is intricately linked to short $t_{1/2,}$ which refers to the time required to reduce the initial concentration of DPPH radical by 50%. The combination of RSA and $t_{1/2}$ revealed that reasonable scavenging activity was reported in *P. oceanica* compared with *C. nodosa*, which required longer times to scavenge radicals (Table 3). Taking into consideration our results on TPC, flavonoids (Table 2) and RSA (Table 3), these would indicate that rhizomes and roots from seagrasses washed up on the coast can be used as priming to analyse new potential polyphenols as high TPC and flavonoids are associated with rhizomes and roots of both seagrasses (Tables 2–5). Notably, TPC in *P. oceanica* ranged from 7.80 ± 0.36 to 51.57 ± 0.92 mg GA equivalent g^{-1} dw, and from 7.04 ± 0.20 to 20.70 ± 0.18 mg GA equivalent g^{-1} dw in *C. nodosa* extracts. While flavonoids in *P. oceanica* reached levels of 30.00 ± 1.00 and 42.00 ± 1.00 mg quercetin equivalent g^{-1} dw in roots and rhizomes, respectively, and ca. 13.00 ± 1.00 mg quercetin equivalent g^{-1} dw in *C. nodosa* in both roots and rhizomes (Table 2). In naturally collected seagrass species, TPC ranged from 0.29 to 14.24 mg GA equivalent g^{-1} dw and flavonoid content fluctuated from 0.091 to 24.5 mg quercetin equivalent g^{-1} dw for *Oceana serrulata* (formerly *Cymodocea serrulata*) [11,48,49].

Similarly, the total carbohydrate contents of seagrasses (118.10 ± 0.20 and 137.00 ± 00 mg glucose g^{-1} dw in *P. oceanica* and *C. nodosa*, respectively; Table 2) were comparable to those of naturally collected seagrasses (130 mg glucose g^{-1} dw for *C. nodosa* [50]). Considering plant parts, carbohydrate contents were significant in roots, sheaths and rhizomes

(Table 2), consistent with the results reported by Kim et al. [51], with leaves showing the lowest contents, in agreement with data obtained by El Din and El-Sheri [52] (28.98 and 47.22 mg g^{-1} dw for *Posidonia* and *Cymodocea,* respectively).

No correlation was found between TPC and RSA (Table 5) in either of the seagrasses. This suggests the presence of other types of metabolites responsible for this antioxidant activity. However, TPC correlates with FRAP and CCA in *C. nodosa*; specifically, flavonoids correlate with the reducing and chelating activities, indicating that these compounds, along with TCH, are the main contributors to these activities, as they show the same correlations. In fact, two new prenylated flavonoids, along with others identified as catechins, have been detected in the rhizomes of *C. nodosa* [53].

Furthermore, reducing activities (FRAP and CRUPAC) correlate with TPC and TCH in *P. oceanica*, but not with flavonoids, indicating that other types of polyphenols may be responsible for this activity. In fact, chicoric and caftaric acids, which have shown high reducing capacity [54], have been identified as the most abundant phenolic compounds in *P. oceanica* [46]. The lack of correlation for radical scavenging activity can be explained by the different chemical reactions and kinetics associated with these reactions.

Despite previous reports showing that polysaccharides of seagrasses exhibit free radical scavenging activity, the biological activities of carbohydrates depend on multiple structural features, with the most important being the presence of protein moieties and covalently linked phenolic compounds. These features allow carbohydrates to exhibit RSA and metal-reducing ability, which polysaccharides devoid of phenolic and protein groups do not exhibit [55,56]. This could explain the significant correlations found between TCH and TPC and between TCH and flavonoids in *C. nodosa* (Table 5). Overall, it is assumed that *Posidonia* and *Cymodocea* are structurally different plants as changes in lignin monomer (e.g., carbohydrates and phenolic compounds and different flavonoids; Tables 1, 2 and 5) and in both antioxidant activities of reduction and complexation (Tables 3–5) were obtained. Our results reinforce the idea that seagrasses washed up on the coast can be exploited, as they are potential sources of natural antioxidants with important applications for the pharmaceutical and food industries [51,57–60]. Chelation of redox-active metals can prevent their participation in the formation of Reactive Oxygen Species (ROS) and the subsequent oxidative damage that would lead to certain diseases [61–64].

4. Materials and Methods

4.1. Sampling of Seeds and Fragments Washed up on Coast

Posidonia oceanica fragments and seeds were collected at 38°38.137′ N; 0°4.267′ E (Alicante, Spain) and *C. nodosa* at 27°45.208′ N; 15°40.255′ W in Gran Canaria (Canary Islands, Spain) when winter storms dragged fragments from natural meadows, i.e., 3–4 collections by season. After collection, samples were immediately stored in portable fridges at 4 °C until arrival at the laboratory. In the case of *P. oceanica*, samples were mailed to the Gran Canaria laboratory in crystal blue pearls hydrated with seawater (water crystal pearls, Amazon.co.uk [65]). To continue, sand and salt were removed by rinsing with distilled water, and samples were sorted into different parts, namely rhizome, roots, mature and young leaves, sheaths and ramets (henceforth whole plant; Figure 4).

Freeze-dried fragments (ca. 30 g for each part of the plant) were separately milled and kept in darkness at −20 °C before analysis. Pooled samples from different collections allow averaging out individual variations and minimizing the impact of fluctuations in concentrations as normalization through pooled samples maintains overall metabolite balance.

Regarding seeds and due to seed scarcity, seeds of *P. oceanica* and *C. nodosa* were both sorted into two groups, such as germinated and non-germinated seeds, for metabolomic

analysis. Germinated seeds were assumed according to a morphological criterium based on the presence of a small sprout of 0.2–0.5 cm in length for *P. oceanica* and on detachment of the dorsal ridge of the *C. nodosa* seeds (Figure 5; [20]). All seeds were surface-sterilized, weighed and freeze-dried.

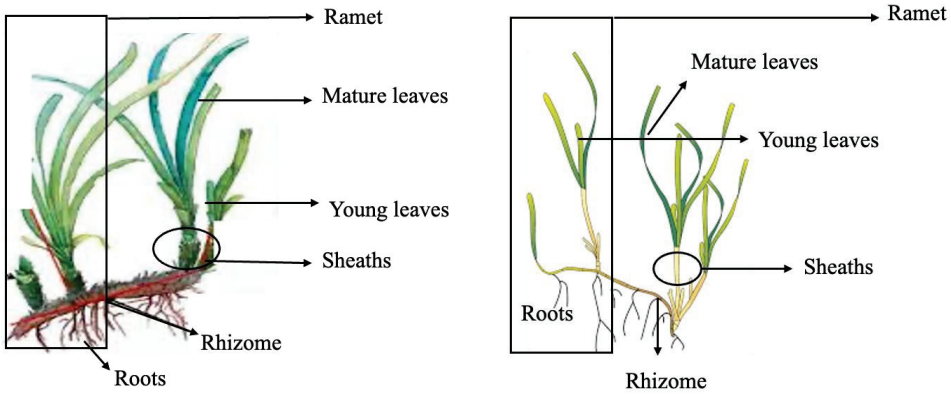

Figure 4. Schematic of *Posidonia oceanica* and *Cymodocea nodosa* showing parts of an individual ramet and each part of the plant.

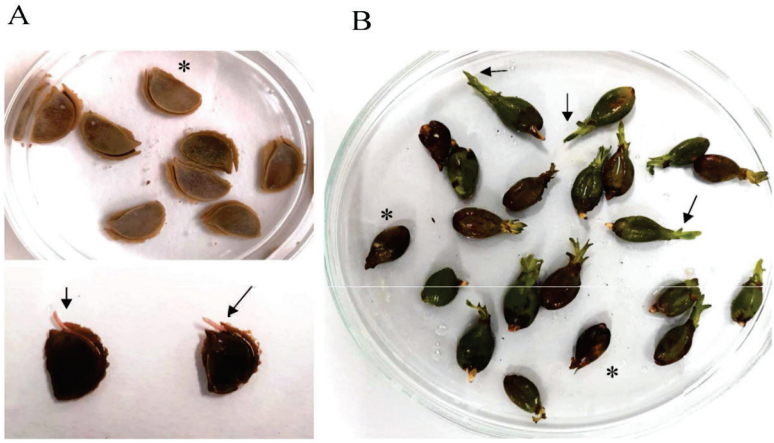

Figure 5. Seeds of (**A**) *Cymodocea nodosa* and (**B**) *Posidonia oceanica*. Asterisk shows non-germinated seeds, and arrows indicate small sprout for *P. oceanica* and detachment of the dorsal ridge of the *C. nodosa* seeds.

4.2. Hydrophilic Interaction Liquid Chromatography (HILIC) Coupled to Hybrid Quadrupole-Time of Flight Mass Spectrometry (QTOF-MS)-Based Metabolomic Analysis of Seeds of Two Seagrasses

Metabolomic analysis, following Gika et al. [66], was carried out with germinated and non-germinated seeds of *P. oceanica* and *C. nodosa*. Seeds (ca. 15–20 for stage) were homogenised to generate 15 mg of pooled sample, and then 300 µL methanol solution (80%) spiked with kinetin at 2 mg L^{-1} final concentration was added. The mixture was then placed in an ultrasound bath for 10 min at room temperature. To continue, the sample was centrifuged at 10,000 rpm for 10 min at 4 °C. For analysis, the supernatant was diluted 1:4 with pure acetonitrile (LCMS grade) and then filtered through PTFE filters (0.2 µm pore size). Metabolite profiling was performed using hydrophilic interaction liquid chromatography (HILIC) coupled to hybrid quadrupole-time of flight mass spectrometry (QTOF-MS). HILIC separation was performed on a 2.1 mm × 150 mm ACQUITY UPLC 1.7 µm BEH amide column (Ethylene Bridged Hybrid; Waters Corp. Ltd., Milford, MA, USA) using two-step gradients over the course of 30 min at 300 µL min^{-1}. The gradient started with a 4 min isocratic step at 100% A (acetonitrile: water, 95:5 (*v*/*v*), 0.1% ammonium

formate), then rising to 28% B (acetonitrile: water, 2:98 (v/v), 0.2% ammonium formate) over the next 21 min and finally to 60% B over 5 min. The injection volume was 5 µL, and the column temperature was maintained at 40 °C. A mass spectrometer is calibrated on a daily basis by infusing an aqueous solution of HCOOLi, which is acquired within the 50–1000 mass range with a resolution of 6500, rendering a residual of 0.0007 arbitrary mass units. Variations in retention time range between 0.54–1.2 s. Accurate mass value is ensured by co-infusion of a lockmass reference compound leukine enkephalin, which ensures that any mass value drift caused by environmental changes will be compensated automatically. Hence, reproducibility and correlation efficiency in each batch run is assumed.

4.3. Processing and Analysis of Metabolomic Data of Seagrass Seeds

Raw data were processed, and metabolites were identified through a comparison of experimental mass spectra with entries in public databases (Massbank, HMDB; [67,68]), involving manual searches for metabolites and leveraging the Galaxy platform. The relative amount of each metabolite was comparatively quantified and normalised with internal standards, such as kinetin, and with a precise weight of each pooled sample. Then, data of the relative amount of each compound were transformed to log2. For a global analysis of seed metabolites, principal component analysis (PCA) was implemented using R package version 4.2.1 (http://www.r-project.org/ (accessed on 1 November 2024)). Also, R statistical language was used for data plotting for heat maps and for plotting log2 fold-change values (x-axis).

To study variations of metabolites among two stages of development, namely germinated and non-germinated for each one of seagrasses, data of the normalised amount of each compound were transformed to log2, and then ratios of germinated/non-germinated for each compound of the same ratio m/z were calculated. For analysis, metabolites were selected constrained to a default 0–10 ppm mass error (mass accuracy; [69]). As a ratio of one means equal or similar proportion between germinated and non-germinated seeds, metabolites with a ratio with values below one are assumed to be part of non-germinated seed metabolism. Similarly, ratio values of each of the different metabolites were constrained to ratios over 1, and once obtained, another selection was carried out with ratios over the average value of all $\geq$1 ratio. These metabolites are significantly assigned to germinated-seed metabolism.

4.4. Marine Plant Fragment Metabolites: Assessing of Antioxidant Activity

The identification and quantification of six selected polyphenols was carried out by UHPLC-MS: GA, *p*-coumaric acid (COU), ferulic acid (FA), syringic acid (SYR), cinnamic acid (CA) and caffeic acid (CAA). For it, freeze-dried each fragment type (pooled 100 mg) was resuspended in 1 mL methanol–water (1:1) mixture, sonicated for 15 min and centrifuged. The supernatant was then filtered through a 0.21 µm nylon filter. Analyses were performed on a Thermo Orbitrap Q exactive focus mass spectrometer coupled to a Thermo Vanquish UHPLC system (Thermo Fisher Sci., Waltham, MA, USA). Measurements were performed by electrospray ionization in positive or negative mode, as required by each analyte. A chromatography column Acentis Express C-18 of 2.7 µm pore size 2.1 × 100 mm was used and eluted with water with 0.1% formic acid (solution A) and methanol (solution B) at a flow rate of 0.4 mL min^{-1}. The chromatographic conditions were programmed as follows: 95% solution A and 5% solution B for 5 min. Then, a course of 2.5 min run was at 100% solution B and continued with 95% solution A and 5% solution B until 12 min. External calibration was performed for each of the compounds. The correlation coefficients were not less than 0.9995. Reproducibility was assessed using five determinations at 0.5 ng g^{-1}

and expressed as relative standard deviation (RSD), which ranged from 0.9 to 6.5%. The limits of detection (LOD) and the limits of quantification (LOQ) were calculated assuming a minimum detectable signal-to-noise level of 3 and 10, respectively. LOD were found to be in the range of 0.05–0.01 ng g^{-1}, and the LOQ were observed in the range of 0.1–0.03 ng g^{-1}. The recoveries were found in the range of 80–110%. Standard and sample chromatograms are deposited as Supplementary Material (Table S4). To assure determination, a default 5 ppm mass error was set. All samples were assayed with two independent replicates for each fragment type. Results were reported as mean ± standard deviation (SD).

Also, each freeze-dried plant fragment (ca. 100 mg pooled each; Figure 4) was suspended in 1.5 mL of Milli-Q water, sonicated for 30 min, stirred for 30 min and centrifuged at 7000 rpm for 15 min. The supernatant was then withdrawn, and the pellet was extracted with 1.5 mL of water for 30 min and centrifuged as indicated above. Supernatants were collected and reserved at 4 °C for determining total carbohydrates and reducing antioxidant power (FRAP and CUPRAC) and Cu (II) chelating (CCA) activities. Extraction of freeze-dried plant-sorted material (ca. 100 mg each) was also carried out with 1.5 mL of methanol for phenolic contents, flavonoids and RSA activity following the same procedure described below.

The total carbohydrate content (TCH) was determined using the colorimetric method described by Brooks et al. [70] with modifications. Each aqueous extract (100 μL) was diluted with water (900 μL) and mixed with 2 mL of freshly prepared anthrone reagent (1.0 mM in 96% sulphuric acid). Then, the mixture was heated at 100 °C in a water bath for 10 min. To follow, samples were cooled in an ice bath, and the absorbance (Abs) was recorded at 620 nm on a Shimadzu UV-1800 spectrophotometer (Shimadzu Co., Kioto, Japan).

Carbohydrate content was calculated from a standard calibration curve in a concentration range from 50 to 500 μg mL^{-1} and expressed as grams equivalent of glucose per 100 g of corresponding plant fragment (% of dry biomass). All samples were assayed in triplicate with two independent replicates for each fragment type. Results were reported as mean ± standard deviation (SD).

The total phenolic content (TPC) was determined according to the Folin–Ciocalteu assay [71]. Each sample (50 μL) was mixed with 4.2 mL of distilled water, 250 μL of Folin–Ciocalteu's reagent and 0.5 mL of sodium carbonate (20%), and the mixture was allowed to stand for 1 h in the darkness at room temperature. The Abs was measured at 765 nm using a Shimadzu 1800 UV–Vis spectrophotometer (Shimadzu Co., Kioto, Japan). The TPC was calculated from a standard calibration curve of GA in methanol (ranging from 0.10 to 1.06 mg mL^{-1}), and the results were expressed as mg of GA equivalents per gram of dry plant section powder (means ± standard deviation of three measurements with two independent replicates for each fragment type).

Total flavonoid content was quantified by an aluminium chloride colorimetric assay according to Li et al. [72] with modifications. Quercetin was used as a standard to prepare the calibration curve. A hundred μL of sample or standard solution was mixed with 400 μL of 60% ethanol and 30 μL of 5% $NaNO_2$ for 6 min. Then, 15 μL of 10% $AlCl_3$ was added, and the mixture was allowed to react for another 6 min. The reaction was stopped by adding 400 μL of 4% NaOH and 100 μL of ethanol. The Abs was measured after 15 min at 510 nm. Total flavonoid content was expressed as mg quercetin equivalents per gram dry weight (mean ± standard deviation of three measurements with two independent replicates for each fragment type) and was calculated from a calibration curve.

To determine radical scavenging activity (RSA), each sample (30 μL of methanolic extract) was added to 1 mL of 2,2-diphenyl-1-picrylhydrazyl (free radical DPPH) solution

(0.078 mM) and left for 10 min [73]. Then, Abs was measured at 515 nm, and the ability of the plant extracts to inhibit DPPH radical was expressed as inhibition percentage and calculated as follows: RSA = 100 × (1 − (Abs in the presence of sample/Abs in the absence of sample)). The capacity to scavenge DPPH radical was referenced with that of butylated hydroxyanisole (BHA) at 500 mgL^{-1}. BHA is a food additive with known antioxidant activity, whose use is permitted at a maximum level of 200 mgL^{-1} [74]. The time required to reduce the initial DPPH radical concentration by 50% ($t_{1/2}$) was also calculated. Measurements were assayed in triplicate with two independent replicates for each fragment type, and data were expressed as the mean ± standard deviation (SD).

Ferric Reducing Antioxidant Power (FRAP) procedure was followed according to [73] with modifications. The FRAP reagent was freshly prepared by mixing 25 mL of acetate buffer solution 0.3 M (pH 3.6), 2.5 mL of 2,3,5-triphenyltetrazolium chloride (TPTZ, 10 mM) in HCl (40 mM) and 2.5 mL of $FeCl_3 \cdot 6H_2O$ solution (20 mM). Each aqueous sample (50 µL) was mixed with 1.5 mL FRAP reagent and warmed at 37 °C for 10 min and later cooled in an ice bath. Absorbance was recorded at 593 nm. Results were expressed as µmol of reduced Fe^{3+} and calculated from a calibration curve designed by adding the FRAP reagent to a range of Fe^{2+} solutions (iron (II) sulphate heptahydrate) of known concentrations in the range from 0.58–4.64 mM. All samples were assayed in triplicate with two independent replicates for each fragment type. Results were reported as mean ± standard deviation (SD).

The cupric ion reducing capacities (CUPRAC) were determined using a solution at a ratio of 1:1 $CuSO_4 \cdot 5H_2O$ (10 mM)/neocuproine ethanolic solution (7.5 mM) in ammonium acetate buffer (1 M; [73]). A total of 570 µL of the solution was added water (1.08 mL) plus 50 µL of each plant section extract, and then mixed for 20 min. Absorbance against a blank reagent was recorded at 450 nm. A standard curve was prepared with Trolox (TR) solutions in the range of concentrations from 0.044 to 1.22 mM. The results were expressed as µmol equivalent of TR per gram of dry biomass. The estimation was carried out in triplicate with two independent replicates, and the results were averaged as mean ± standard deviation (SD).

The Cu^{2+}-chelating activity (CCA) was quantified according to Saiga et al. [75] with modifications. Extract of each sample (0.25 mL) was mixed with 1 mL sodium acetate buffer (50 mM and pH 6.0) and 50 µL of $CuSO_4$ (5 mM) for 30 min at room temperature. Then pyrocatechol violet (PV; 50 µL, 4 mM) was added, and the sample was left for 30 min. After that, absorbance was recorded at 632 nm. Distilled water was used as a control. The results were expressed as the inhibition percentage of PV–Cu^{2+} complex formation and calculated according to the equation: $(1 - Abs_1/Abs_0) \times 100$, where Abs_0 was the absorbance of the control, and Abs_1 was the absorbance of each of the extracts. All samples were assayed in triplicate with two independent replicates for each fragment type. Results were reported as mean ± standard deviation (SD).

4.5. Chemicals

Methanol (HPLC gradient grade), $FeCl_3 \cdot 6H_2O$ and $FeSO_4 \cdot 7H_2O$ were purchased from Scharlab (Barcelona, Spain). Butylated hydroxyanisole (BHA) (analysis quality), D-glucose and aluminium chloride were supplied by Panreac (Barcelona, Spain). Ammonium acetate, sodium nitrite, epicatechin, anthrone, pyrocatechol violet (PV), Folin–Ciocalteu reagent, 1,1-diphenyl-2-picrylhydrazyl (DPPH), $CuSO_4 \cdot 5H_2O$, 2,4,6-tri(2-pyridyl)-triazine (TPTZ), 2,9-dimethyl-1,10-phenanthroline (neocuproine), 6-hydroxy-2,5,7,8-tetramethyl-chroman-2-carboxylic acid (Trolox TR), copper(II) chloride and 96% ethanol of analytical quality were provided by Sigma–Aldrich Chemie (Steinheim, Germany). Sulfuric acid (97%) was

provided by Honeywell (Charlotte, NC, USA). Ultrapure water was obtained from a Milli-Q system from Millipore (Bedford, MA, USA).

4.6. Data Analysis

Statistical comparisons of concentrations were performed using R software version 4.5.0 (https://www.r-project.org; accessed on 17 November 2023). A one-way ANOVA followed by the post hoc tests Tukey HSD and Dunnett T3 was used to detect significant differences ($p \leq 0.01$) between plants and within corresponding sections. The statistical relationship between phenolic compound, carbohydrate and flavonoid contents and antioxidant activities was analysed through Pearson's correlation test (tests were accepted as statistically significant with p-values < 0.05).

5. Conclusions

In conclusion, seagrasses *P. oceanica* and *C. nodosa* are rich sources of metabolites and antioxidant activities, with the possibility of benefiting from the different sections washed ashore. Seeds accumulate metabolites with different functionality depending on seed dormancy. These are involved in inorganic nutrient mobilization, defence and germination control. Also, the antioxidant capacities of the different plant fragments and their relationship with flavonoids and total carbohydrates are relevant. It is worth mentioning the extension of the study to new polyphenols and the investigation of the economic values of the wasted washed-up biomass of these two species. This study also opens a framework to analyse new metabolites responsible for the antioxidant activity in seagrasses.

Supplementary Materials: The following supporting information can be downloaded at: https://www.mdpi.com/article/10.3390/md23050193/s1, Table S1. Metabolite data using the estimated compound mass [M] in modeposirtive $[M + H]^+$; Table S2. Metabolite data using the estimated compound mass [M] in mode negative $[M - H]^-$; Table S3. Metabolite data using the estimated compound mass [M] in mode postive $[M + H]^+$ and negative $[M - H]^-$ categorised in glycerolipids, OrganHeterocyclics, Fatty acyls (LIPIDS), flavonoids, steroids, compounds involved in activation processes; Table S4. Chromatogram for standard of each polyphenol analised through UHPLC-MS.

Author Contributions: Conceptualization, P.G.-J.; Methodology, M.R. and P.G.-J.; Validation, M.R. and P.G.-J.; Formal Analysis, D.d.R.-S., V.A. and M.R.; Investigation, M.R. and P.G.-J.; Collecting and processing samples: M.C.-A. and D.O.; Writing–Original Draft Preparation, P.G.-J. and M.R.; Writing–Review & Editing, P.G.-J. and M.R.; Supervision, P.G.-J.; Funding Acquisition, P.G.-J. All authors have read and agreed to the published version of the manuscript.

Funding: This work was financed by the Ministerio de Ciencia e Innovacion of Spain (TED2021-129249B-I00); AEI/10.13039/501100011033/Union Europea Next Generation EU/PRTR), and collaboration agreement between Transformación Agraria, S.A., S.M.E., M.P. and the Universidad de Las Palmas de Gran Canaria (Convenio CC21/57). D.O. was financed through the Maria Zambrano program (ULPGC, Ministerio de Universidades (Orden UNI/501/2021) and Funding Next Generation EU). M.C.-A. was financed by the Catalina Ruiz Programme-ULPGC contract, co-funded by the European Social Fund and the Gobierno de Canarias-Consejería de Universidades, Ciencia e Innovación y Cultura.

Institutional Review Board Statement: Not applicable.

Data Availability Statement: All data have been supplied in the results and Supplementary Material of this paper.

Acknowledgments: Fellowships from the Maria Zambrano program to D.O. and from Catalina Ruiz to M.C.-A. are acknowledged. Also, D.d.R.-S. would also like to thank the Universidad de Las Palmas de Gran Canaria for its funding.

Conflicts of Interest: The authors declare that they have no conflicts of interest related to the present investigation.

References

1. Moreno-Curtidor, C.; Annunziata, M.G.; Gupta, S.; Apelt, F.; Richard, S.I.; Kragler, F.; Mueller-Roeber, B.; Olas, J.J. Physiological profiling of embryos and dormant seeds in two Arabidopsis accessions reveals a metabolic switch in carbon reserve accumulation. *Front. Plant Sci.* **2020**, *11*, 588433. [CrossRef]
2. Liu, C.; Du, B.; Hao, F.; Lei, H.; Wan, Q.; He, G.; Wang, Y.; Tang, H. Dynamic metabolic responses of brown planthoppers towards susceptible and resistant rice plants. *Plant Biotechnol. J.* **2017**, *15*, 1346–1357. [CrossRef] [PubMed]
3. Liu, J.; Hasanuzzaman, M.; Wen, H.; Zhang, J.; Peng, T.; Sun, H.; Zhao, Q. High temperature and drought stress cause abscisic acid and reactive oxygen species accumulation and suppress seed germination growth in rice. *Protoplasma* **2019**, *256*, 1217–1227. [CrossRef]
4. Graeber, K.A.I.; Nakabayashi, K.; Miatton, E.; Leubner-Metzger, G.E.R.H.A.R.D.; Soppe, W.J. Molecular mechanisms of seed dormancy. *Plant Cell Environ.* **2012**, *35*, 1769–1786. [CrossRef] [PubMed]
5. Danaraj, J.; Mariasingarayan, Y.; Ayyappan, S. Comparative metabolomics analysis of wild and suspension cultured cells (SCC) of seagrass *Halodule pinifolia* (Miki) Hartog of Cymodoceaceae family. *Aquat. Bot.* **2020**, *167*, 103278. [CrossRef]
6. Guerriero, G.; Berni, R.; Muñoz-Sanchez, J.A.; Apone, F.; Abdel-Salam, E.M.; Qahtan, A.A.; Alatar, A.A.; Cantini, C.; Cai, G.; Hausman, J.-F.; et al. Production of plant secondary metabolites: Examples, tips and suggestions for biotechnologists. *Genes* **2018**, *9*, 309. [CrossRef] [PubMed]
7. Maciel, E.; Leal, M.C.; Lillebø, A.I.; Domingues, P.; Domingues, M.R.; Calado, R. Bioprospecting of marine macrophytes using MS-based lipidomics as a new approach. *Mar. Drugs* **2016**, *14*, 49. [CrossRef]
8. Qian, W.; Zhu, Y.; Chen, Q.; Wang, S.; Chen, L.; Liu, T.; Tang, H.; Yao, H. Comprehensive metabolomic and lipidomic alterations in response to heat stress during seed germination and seedling growth of Arabidopsis. *Front. Plant Sci.* **2023**, *14*, 1132881. [CrossRef]
9. Alu'datt, M.H.; Rababah, T.; Alhamad, M.N.; Al-Mahasneh, M.A.; Almajwal, A.; Gammoh, S.; Ereifej, K.; Johargy, A.; Alli, I. A review of phenolic compounds in oil-bearing plants: Distribution, identification and occurrence of phenolic compounds. *Food Chem.* **2017**, *218*, 99–106. [CrossRef]
10. Xu, C.-C.; Wang, B.; Pu, Y.-Q.; Tao, J.-S.; Zhang, T. Advances in extraction and analysis of phenolic compounds from plant materials. *Chin. J. Nat. Med.* **2017**, *15*, 721–731. [CrossRef]
11. Baby, L.; Sankar, T.V.; Chandramohanakumar, N. Changes in phenolic compounds in seagrasses against changes in the ecosystem. *J. Pharmacog. Phytochem.* **2017**, *6*, 742–747.
12. Quideau, S.; Deffieux, D.; Douat-Casassus, C.; Pouységu, L. Plant polyphenols: Chemical properties, biological activities, and synthesis. *Angew. Chem. Int. Ed.* **2011**, *50*, 586–621. [CrossRef]
13. Sansone, C.; Brunet, C. Promises and challenges of microalgal antioxidant production. *Antioxidants* **2019**, *8*, 199. [CrossRef]
14. Benito-González, I.; López-Rubio, A.; Martínez-Abad, A.; Ballester, A.R.; Falcó, I.; González-Candelas, L.; Sánchez, G.; Lozano-Sánchez, J.; Borrás-Linares, I.; Segura-Carretero, A.; et al. In-Depth Characterization of Bioactive Extracts from Posidonia oceanica Waste Biomass. *Mar. Drugs* **2019**, *17*, 409. [CrossRef] [PubMed]
15. Achamlale, S.; Rezzonico, B.; Dubois, M.G. Evaluation of Zostera detritus as a potential new source of zosteric acid. *J. Appl. Phycol.* **2009**, *21*, 347–352. [CrossRef]
16. Ravn, H.; Pedersen, M.F.; Borum, J.; Andary, C.; Anthoni, U.; Christophen, C.; Nielsen, P.H. Seasonal variation and distribution of two phenolic compounds, rosmarinic acid and caffeic acid, in leaves and roots-rhizomes of eelgrass (*Zostera marina* L). *Ophelia* **1994**, *40*, 51–61. [CrossRef]
17. Kuo, J.; den Hartog, C.d. Seagrass morphology, anatomy, and ultrastructure. In *Seagrasses: Biology, Ecology and Conservation*; Springer: Dordrecht, The Netherlands, 2006; pp. 51–87. [CrossRef]
18. Buia, M.C.; Mazzella, L. Reproductive phenology of the Mediterranean seagrasses *Posidonia oceanica* (L.) Delile, Cymodocea nodosa (Ucria) Aschers., and Zostera noltii Hornem. *Aquat. Bot.* **1991**, *40*, 343–362. [CrossRef]
19. Zarranz, M.E.; González-Henríquez, N.; García-Jimenez, P.; Robaina, R.R. Restoration of *Cymodocea nodosa* (Uchria) Ascherson seagrass meadows through seed propagation: Seed storage and influences of plant hormones and mineral nutrients on seedling growth in vitro. *Bot. Mar.* **2010**, *53*, 439–448. [CrossRef]

20. Zarranz, M.E.; Garcia-Jimenez, P.; Robaina, R.R. Endogenous polyamine content and photosynthetic performance under hypo-osmotic conditions reveal *Cymodocea nodosa* as an obligate halophyte. *Aquat. Biol.* **2012**, *17*, 7–17. [CrossRef]
21. Weatherall, E.J.; Jackson, E.L.; Hendry, R.A.; Campbell, M.L. Quantifying the dispersal potential of seagrass vegetative fragments: A comparison of multiple subtropical species. *Estuar. Coast. Shelf Sci.* **2016**, *169*, 207–215. [CrossRef]
22. Portillo-Hahnefeld, E. *Arribazones de Algas y Plantas Marinas en Gran Canaria. Características, Gestión y Posibles Usos*; Instituto Tecnológico de Canarias: Las Palmas, Spain, 2008; p. 90. ISBN 978-84-691-5105-1.
23. Caye, G.; Meinesz, A. Observations sur la floraison et la fructification de Posidonia oceanica dans la Baie de Villefranche et en Corse du Sud. In *International Workshop on Posidonia Oceanica Beds*; GIS Posidonie: Marseille, France, 1984.
24. Celdrán, D.; Marín, A. Photosynthetic activity of the non-dormant Posidonia oceanica seed. *Mar. Biol.* **2011**, *158*, 853–858. [CrossRef]
25. Celdrán, D.; Marín, A. Seed photosynthesis enhances *Posidonia oceanica* seedling growth. *Ecosphere* **2013**, *4*, 1–11. [CrossRef]
26. Dolui, A.K.; Latha, M.; Vijayaraj, P. OsPLB gene expressed during seed germination encodes a phospholipase in rice. *3 Biotech* **2020**, *10*, 30. [CrossRef] [PubMed]
27. Lin, Y.X.; Xin, X.; Yin, G.K.; He, J.J.; Zhou, Y.C.; Chen, J.Y.; Lu, X.X. Membrane phospholipids remodeling upon imbibition in Brassica napus L. seeds. *Biochem. Biophys. Res. Commun.* **2019**, *515*, 289–295. [CrossRef] [PubMed]
28. Gupta, A.; Bhatla, S.C. Preferential phospholipase A2 activity on the oil bodies in cotyledons during seed germination in *Helianthus annuus* L.; cv. Morden. *Plant Sci.* **2007**, *172*, 535–543. [CrossRef]
29. Michaud, M.; Prinz, W.A.; Jouhet, J. Glycerolipid synthesis and lipid trafficking in plant mitochondria. *FEBS J.* **2017**, *284*, 376–390. [CrossRef]
30. Garcia-Jimenez, P.; Navarro, E.P.; Santana, C.H.; Luque, A.; Robaina, R.R. Anatomical and nutritional requirements for induction and sustained growth in vitro of *Cymodocea nodosa* (Ucria) Ascherson. *Aquat. Bot.* **2006**, *84*, 79–84. [CrossRef]
31. de Carvalho, C.C.; Caramujo, M.J. The various roles of fatty acids. *Molecules* **2018**, *23*, 2583. [CrossRef]
32. Quettier, A.L.; Eastmond, P.J. Storage oil hydrolysis during early seedling growth. *Plant Physiol. Biochem.* **2009**, *47*, 485–490. [CrossRef]
33. Nagahashi, G.; Douds, D.D., Jr. Partial separation of root exudate components and their effects upon the growth of germinated spores of AM fungi. *Mycol. Res.* **2000**, *104*, 1453–1464. [CrossRef]
34. Bhalla, T.C.; Kumar, V.; Bhatia, S.K. Hydroxy acids: Production and applications. In *Advances in Industrial Biotechnology*; Singh, R.S., Pandey, A., Larroche, C., Eds.; IK International Publishing House Pvt. Itd.: Delhi, India, 2014; pp. 56–76.
35. Motafeghi, F.; Mortazavi, P.; Ghassemi-Barghi, N.; Zahedi, M.; Shokrzadeh, M. Dexamethasone as an anti-cancer or hepatotoxic. *Toxicol. Mech. Methods* **2023**, *33*, 161–171. [CrossRef] [PubMed]
36. Asami, T.; Oh, K.; Jikumaru, Y.; Shimada, Y.; Kaneko, I.; Nakano, T.; Takatsuto, S.; Fujioka, S.; Yoshida, S. A mammalian steroid action inhibitor spironolactone retards plant growth by inhibition of brassinosteroid action and induces light-induced gene expression in the dark. *J. Steroid Biochem. Mol. Biol.* **2004**, *91*, 41–47. [CrossRef]
37. Simelane, S.B.; Moshapo, P.T.; Masuka, R.W. Benzopyran-Core as an Antimycobacterial Agent. *Org. Med. Chem. Int. J.* **2020**, *10*, 56–72. [CrossRef]
38. Gomtsyan, A. Heterocycles in drugs and drug discovery. *Chem. Heterocycl. Compd.* **2020**, *48*, 7–10. [CrossRef]
39. Sun, L.; Gong, M.; Lv, X.; Huang, Z.; Gu, Y.; Li, J.; Du, G.; Liu, L. Current advance in biological production of short-chain organic acid. *Appl. Microbiol. Biotechnol.* **2020**, *104*, 9109–9124. [CrossRef] [PubMed]
40. Marián, F.D.; Garcia-Jimenez, P.; Robaina, R.R. Polyamine levels in the seagrass *Cymodocea nodosa*. *Aquat. Bot.* **2000**, *68*, 179–184. [CrossRef]
41. Li, L.; Dou, N.; Zhang, H.; Wu, C. The versatile GABA in plants. *Plant Signal. Behav.* **2021**, *16*, 1862565. [CrossRef]
42. Leri, M.; Ramazzotti, M.; Vasarri, M.; Peri, S.; Barletta, E.; Pretti, C.; Degl'Innocenti, D. Bioactive compounds from *Posidonia oceanica* (L.) delile impair malignant cell migration through autophagy modulation. *Mar. Drugs* **2018**, *16*, 137. [CrossRef]
43. Haznedaroglu, M.Z.; Zeybek, U. HPLC Determination of Chicoric Acid in Leaves of *Posidonia oceanica*. *Pharm. Biol.* **2007**, *45*, 745–748. [CrossRef]
44. Klap, V.A.; Hemminga, M.A.; Boon, J.J. Retention of lignin in seagrasses: Angiosperms that returned to the sea. *Mar. Ecol. Prog. Ser.* **2000**, *194*, 1–11. [CrossRef]
45. Riaz, U.; Kharal, M.A.; Murtaza, G.; uz Zaman, Q.; Javaid, S.; Malik, H.A.; Humera Aziz, H.A.; Zafar Abbas, Z.A. Prospective roles and mechanisms of caffeic acid in counter plant stress: A mini review. *Pak. J. Agric. Res.* **2019**, *32*, 8. [CrossRef]
46. Grignon-Dubois, M.; Rezzonico, B. Phenolic fingerprint of the seagrass *Posidonia oceanica* from four locations in the Mediterranean Sea: First evidence for the large predominance of chicoric acid. *Bot. Mar.* **2015**, *58*, 379–391. [CrossRef]
47. Salvador, V.H.; Lima, R.B.; dos Santos, W.D.; Soares, A.R.; Böhm, P.A.F.; Marchiosi, R.; Ferrarese Mde, L.; Ferrarese-Filho, O. Cinnamic acid increases lignin production and inhibits soybean root growth. *PLoS ONE* **2013**, *8*, e69105. [CrossRef] [PubMed]

48. Kannan, R.; Arumugam, R.; Iyapparaj, P.; Thangaradjou, T.; Anantharaman, P. In vitro antibacterial, cytotoxicity and haemolytic activities and phytochemical analysis of seagrasses from the Gulf of Mannar, South India. *Food Chem.* **2013**, *136*, 1484–1489. [CrossRef]
49. Athiperumalsami, T.; Rajeswari, V.D.; Poorna, S.H.; Kumar, V.; Jesudass, L.L. Antioxidant activity of seagrasses and seaweeds. *Bot. Mar.* **2010**, *53*, 251–257. [CrossRef]
50. Abdel Hady, H.H.; Daboor, S.M.; Ghonemy, A.E. Nutritive and antimicrobial profiles of some seagrasses from Bardawil Lake, Egypt. *Egypt. J. Aquat. Res.* **2007**, *33*, 103–110.
51. Kim, D.H.; Mahomoodally, M.F.; Sadeer, N.B.; Seok, P.G.; Zengin, G.; Palaniveloo, K.; Khalil, A.A.; Rauf, A.; Rengasamy, K.R. Nutritional and bioactive potential of seagrasses: A review. *S. Afr. J. Bot.* **2021**, *137*, 216–227. [CrossRef]
52. El Din, N.G.S.; El-Sherif, Z.M. Nutritional value of Cymodocea nodosa and *Posidonia oceanica* along the western Egyptian Mediterranean coast. *Egypt. J. Aquat. Res.* **2013**, *39*, 153–165. [CrossRef]
53. Smadi, A.; Ciavatta, M.L.; Bitam, F.; Carbone, M.; Villani, G.; Gavagnin, M. Prenylated flavonoids and phenolic compounds from the rhizomes of marine phanerogam *Cymodocea nodosa*. *Planta Med.* **2018**, *84*, 704–709. [CrossRef]
54. Liu, Q.; Liu, F.; Zhang, L.; Niu, Y.; Liu, Z.; Liu, X. Comparison of chicoric acid, and its metabolites caffeic acid and caftaric acid: In vitro protection of biological macromolecules and inflammatory responses in BV2 microglial cells. *Food Sci. Hum. Wellness* **2017**, *6*, 155–166. [CrossRef]
55. Fernandes, P.A.R.; Coimbra, M.A. The antioxidant activity of polysaccharides: A structure-function relationship overview. *Carbohydr. Polym.* **2023**, *314*, 120965. [CrossRef] [PubMed]
56. He, J.; Xu, Y.; Chen, H.; Sun, P. Extraction, structural characterization, and potential antioxidant activity of the polysaccharides from four seaweeds. *Int. J. Mol. Sci.* **2016**, *17*, 1988. [CrossRef]
57. Gokce, G.; Haznedaroglu, M.Z. Evaluation of antidiabetic, antioxidant and vasoprotective effects of *Posidonia oceanica* extract. *J. Ethnopharmacol.* **2008**, *115*, 122–130. [CrossRef] [PubMed]
58. Kolsi, R.B.A.; Gargouri, B.; Sassi, S.; Frikha, D.; Lassoued, S.; Belghith, K. In vitro biological properties and health benefits of a novel sulfated polysaccharide isolated from *Cymodocea nodosa*. *Lipids Health Dis.* **2017**, *16*, 252. [CrossRef] [PubMed]
59. Kontiza, I.; Stavri, M.; Zloh, M.; Vagias, C.; Gibbons, S.; Roussis, V. New metabolites with antibacterial activity from the marine angiosperm *Cymodocea nodosa*. *Tetrahedron* **2008**, *64*, 1696–1702. [CrossRef]
60. Vasarri, M.; Leri, M.; Barletta, E.; Ramazzotti, M.; Marzocchini, R.; Degl'Innocenti, D. Anti-inflammatory properties of the marine plant *Posidonia oceanica* (L.) Delile. *J. Ethnopharmacol.* **2020**, *247*, 112252. [CrossRef]
61. Liu, J.; Yang, S.; Li, X.; Yan, Q.; Martin, J.T. Reaney, Zhengqiang Jiang Alginate Oligosaccharides: Production, Biological Activities, and Potential Applications. *Compr. Rev. Food Sci. Food Saf.* **2019**, *18*, 1659–2067. [CrossRef]
62. Shon, M.-Y.; Kim, T.-H.; Sung, N.-J. Antioxidants and free radical scavenging activity of *Phellinus baumii* (Phellinus of Hymenochaetaceae) extracts. *Food Chem.* **2003**, *82*, 593–597. [CrossRef]
63. Tian, H.; Liu, H.; Song, W.; Zhu, L.; Zhang, T.; Li, R.; Yin, X. Structure, antioxidant and immunostimulatory activities of the polysaccharides from *Sargassum carpophyllum*. *Algal Res.* **2020**, *49*, 101853. [CrossRef]
64. Wu, S.; Li, F.; Jia, S.; Ren, H.; Gong, G.; Wang, Y.; Lv, Z.; Liu, Y. Drying effects on the antioxidant properties of polysaccharides obtained from Agaricus blazei Murrill. *Carbohydr. Polym.* **2014**, *103*, 414–417. [CrossRef]
65. Carrasco-Acosta, M.; Garcia-Jimenez, P. Maintaining and storing encapsulated cells for propagation of *Posidonia oceanica* (L.) Delile. *Aquat. Biol.* **2021**, *30*, 47–57. [CrossRef]
66. Gika, H.G.; Theodoridis, G.A.; Earll, M.; Wilson, I.D. A QC approach to the determination of day-to-day reproducibility and robustness of LC–MS methods for global metabolite profiling in metabonomics/metabolomics. *Bioanalysis* **2012**, *4*, 2239–2247. [CrossRef]
67. Wishart, D.S.; Feunang, Y.D.; Marcu, A.; Guo, A.C.; Liang, K. HMDB 4.0—The Human Metabolome Database for 2018. *Nucleic Acids Res.* **2018**, *46*, D608–D617. [CrossRef]
68. Wishart, D.S.; Jewison, T.; Guo, A.C.; Wilson, M.; Knox, C.; Liu, Y.; Djoumbou, Y.; Mandal, R.; Aziat, F.; Dong, E.; et al. HMDB 3.0—The Human Metabolome Database in 2013. *Nucleic Acids Res.* **2013**, *41*, D801–D807. [CrossRef]
69. López-Hidalgo, C.; Lamelas, L.; Cañal, M.J.; Valledor, L.; Meijón, M. Untargeted metabolomics revealed essential biochemical rearrangements towards combined heat and drought stress acclimatization in Pinus pinaster. *Environ. Exp. Bot.* **2023**, *208*, 105261. [CrossRef]
70. Brooks, J.R.; Griffin, V.K.; Kattan, M.W. A Modified Method for Total Carbohydrate Analysis of Glucose Syrups, Maltodextrins, and Other Starch Hydrolysis Products. *Cereal Chem.* **1986**, *63*, 465–466.
71. Julkunen-Tiitto, R. Phenolic constituents in the leaves of northern willows: Methods for the analysis of certain phenolics. *J. Agric. Food Chem.* **1985**, *330*, 213–217. [CrossRef]

72. Li, J.-E.; Fan, S.-T.; Qiu, Z.-H.; Li, C.; Nie, S.-P. Total flavonoids content, antioxidant and antimicrobial activities of extracts from *Mosla chinensis* Maxim. cv. Jiangxiangru. *LWT–Food Sci. Technol.* **2015**, *64*, 1022–1027. [CrossRef]
73. Sethi, S.; Joshi, A.; Arora, B.; Bhowmik, A.; Sharma, R.R.; Kumar, P. Significance of FRAP, DPPH, and CUPRAC assays for antioxidant activity determination in apple fruit extracts. *Eur. Food Res. Technol.* **2020**, *246*, 591–598. [CrossRef]
74. Pop, A.; Kiss, B.; Loghin, F. Endocrine Disrupting Effects of Butylated Hydroxyanisole (BHA–E320). *Clujul Med.* **2013**, *86*, 16–20.
75. Saiga, A.; Tanabe, S.; Nishimura, T. Antioxidant activity of peptides obtained from porcine myofibrillar proteins by protease treatment. *J. Agric. Food Chem.* **2003**, *51*, 3661–3667. [CrossRef] [PubMed]

marine drugs

MDPI

Article

The Role of Brown Algae as a Capping Agent in the Synthesis of ZnO Nanoparticles to Enhance the Antibacterial Activities of Cotton Fabrics

Eli Rohaeti [1,*], Helmiyati [2], Rasamimanana Joronavalona [3], Paulina Taba [4], Dewi Sondari [5] and Azlan Kamari [6]

[1] Department of Chemistry Education, Faculty of Mathematics and Natural Science, Universitas Negeri Yogyakarta, Yogyakarta 55281, Indonesia
[2] Department of Chemistry, Faculty of Mathematics and Natural Science, Universitas Indonesia, Depok 16424, Indonesia; helmiyati@sci.ui.ac.id
[3] Department of Organic Chemistry, University of Antananarivo, VS 21 GAI Ankatso, Antananarivo 101, Madagascar; joronavalonachemist@gmail.com
[4] Department of Chemistry, University of Hasanudin, Makasar 90245, Indonesia; paulinataba@unhas.ac.id
[5] The National Research and Innovation Agency, Jakarta Pusat 10340, Indonesia; sondaridewi@gmail.com
[6] Department of Chemistry, Universiti Pendidikan Sultan Idris, Tanjong Malim 35900, Malaysia; azlan.kamari@fsmt.upsi.edu.my
* Correspondence: eli_rohaeti@uny.ac.id

Abstract: Research was conducted on the role of brown algae as a capping agent in the synthesis of ZnO nanoparticles, the characteristics of ZnO nanoparticles, and the effect of the addition of ZnO nanoparticles and/or silane compounds on antibacterial and antifungal activities. The synthesis of ZnO nanoparticles involved green synthesis, and then nanoparticles were characterized using UV/VIS/NIR, ATR-FTIR, XRD, PSA, and SEM-EDS, followed by the in situ deposition of ZnO nanoparticles on cotton fabrics and the addition of silane compounds. The characterization of modified and unmodified cotton fabrics and antibacterial and antifungal activity tests were carried out using the disc diffusion method through measurements of the diameter of the inhibition zone against *Pseudomonas aeruginosa*, *Staphylococcus epidermidis*, and *Malassezia furfur*. The characterization of ZnO nanoparticles showed absorption at a wavelength of 357 nm; the number of waves was 450 cm^{-1}; the diffraction peak occurred at an angle of 36.14°; the crystal size was 15.35 nm; there was a heterogeneous particle distribution; the particle size was in the ranges of 1.74–706 nm (PSA) and 45–297 nm (SEM); and an irregular particle shape was noted. The results showed that the best antibacterial and antifungal activity was obtained in cotton + HDTMS + ZnO nanoparticles (K8) and cotton + ZnO nanoparticles+HDTMS/MTMS (K4).

Keywords: brown algae extract; cotton fabric; green synthesis; silane compounds; ZnO nanoparticles

1. Introduction

Cotton, spandex, polyester, and nylon are a few textile materials that can be made into goods with antibacterial and antifouling qualities [1]. Cotton is one of the natural fibers derived from plants; its main constituent is cellulose and it is used as a raw material for the textile industry. Cotton fabric has the property of easily absorbing water molecules (hygroscopic) and is biodegradable [2]. The hygroscopic properties of cotton fabric can

facilitate the absorption of sweat, meaning that cotton fabric easily becomes dirty and overrun by microorganisms. Therefore, cotton fabrics can be modified to increase their resistance to microorganism and antifouling attacks by using zinc oxide (ZnO) nanoparticles and silane compounds.

ZnO nanoparticles have the ability to inhibit microbial activity by damaging cell membranes and producing ROS (Reactive Oxygen Species), which results in oxidative stress in microbes [3,4]. The antimicrobial properties of ZnO nanoparticles can protect cotton fabrics from the growth of microorganisms that can reduce the quality of the fabric, cause the colors to fade, etc. In addition to their antimicrobial properties, ZnO nanoparticles have several advantages, namely being biocompatible and photocatalytic and inhibiting UV rays. ZnO nanoparticles have a white color that does not change the appearance of the fabric, and they are cheaper to produce compared to other nanoparticles, such as silver nanoparticles. ZnO nanoparticles can be produced using two approaches to nanoparticle synthesis, namely top-down (physics) and bottom-up (chemical) approaches.

The top-down approach is carried out by breaking down large particles into small particles of a nanometer size through methods such as the laser beam irradiation method [5] and ball milling [6]. The bottom-up approach involves chemical reactions in which atoms form larger particles of nanometer size. The bottom-up approach can be achieved in several ways, such as coprecipitation, sol–gel, and chemical reduction methods. However, both approaches have weaknesses. The top-down method requires considerable energy use and has high costs. Meanwhile, the bottom-up approach uses several chemical reducing materials that are toxic and also requires considerable costs [7]. Therefore, a method of synthesizing ZnO nanoparticles was developed that is low cost and environmentally friendly, using a bottom-up approach, namely green synthesis.

The green synthesis of ZnO nanoparticles can be carried out with the help of ultrasonication [8] and microwave [9], utilizing secondary metabolite compounds from plant extracts as bio-reductors. The use of microwave and ultrasound can significantly reduce the time needed to synthesize nanoparticles, help control the particle size of nanoparticles, reduce the cost of nanoparticle synthesis by reducing the time and energy used, and also reduce the environmental impact by reducing the use of chemicals and energy. The ZnO nanoparticles in this study are the result of their preparation using brown algae (*Padina* sp.) which is derived from natural materials that are environmentally friendly. The carbohydrate content and secondary metabolite compounds of *Padina* sp., which occur in the form of flavonoids, tannins, saponins, alkaloids, and other metabolites, have -OH functional groups as bio-reducers and capping agents that can prevent particle agglomeration during the synthesis of ZnO nanoparticles [10,11].

ZnO nanoparticles that have antimicrobial properties can be deposited into cotton fabrics in situ (one step) and ex situ (two step). ZnO nanoparticles in the textile industry are generally processed using the ex situ method, in which the synthesis of ZnO nanoparticles is carried out first and then the ZnO nanoparticles are characterized and deposited onto the fabric. This method has the advantage of allowing for large-scale production; in addition, the morphology, size, and distribution of the produced ZnO nanoparticles can be controlled. However, the disadvantage of this method is that it is a complicated and inefficient process. In contrast, in situ methods can produce ZnO nanoparticles that have an uncontrollable morphology, size, and distribution. This method has high efficiency because the creation of ZnO nanoparticles occurs directly on the surface of the fabric. The stronger bond between the fabric fibers and the ZnO nanoparticles provides the fabric with resistance to different washing frequencies [12]. Therefore, this study uses an in situ method for the deposition of ZnO nanoparticles on cotton fabrics.

The cotton fabrics on which ZnO nanoparticles were deposited were characterized using UV/VIS/NIR, ATR-FTIR, XRD, and SEM-EDS instruments. The ZnO nanoparticles that were synthesized independently were characterized using UV/VIS/NIR, ATR-FTIR, XRD, PSA, and SEM-EDS instruments.

The functionalization of antifouling properties in cotton fabrics can be obtained through the addition of silane compounds that cause increased hydrophobicity. Octtiltrietoxilane (OTES), hexadecyltrimethoxylan (HDTMS), and methyltrimethoxylane (MTMS) compounds [13–15] show potential in the modification of textile fabrics. The silane compounds applied to cotton fabrics are HDTMS, MTMS, and HDTMS/MTMS composites. The analysis of antimicrobial properties was determined with the disc diffusion method using *Staphylococcus epidermidis* as a Gram-positive bacterium, *Pseudomonas aeruginosa* as a Gram-negative bacteriaum, and the fungus *Malassezia furfur*.

2. Results and Discussions

2.1. Green Synthesis of ZnO Nanoparticles with Brown Algae (Padina sp.)

The green synthesis process in this study used a ratio of the volume of brown algae: early precursor ($Zn(NO_3)_2$) of 0.01 M:NaOH 0.1 M, respectively, which is 1:20:5; the ratio was an optimum comparison of the experimental results. The synthesis process began with the addition of algae extract and an initial precursor ($Zn(NO_3)_2$) of 0.01 M to produce a slightly cloudy brown solution caused by brown algae extract. Synthesis reactions require heating treatment and controlled time for the reaction to be stable. The green synthesis process can be reviewed before and after the addition of NaOH by marking the presence of white deposits of ZnO nanoparticles. Then, pH measurements can be taken on *Padina* sp., solution ($Zn(NO_3)_2$) 0.01 M, and brown algae extract + solution ($Zn(NO_3)_2$) 0.01 M (before adding NaOH) and after adding NaOH. The pH values obtained consecutively were 7.58, 5.35, 6.33, and 10.69 (around 10–11). The addition of NaOH can cause an increase in pH, which has a role as a settling agent in the deposition reaction of Zn^{2+} ions in the initial precursor ($Zn(NO_3)_2$) to $Zn(OH)_2$ and then to ZnO nanoparticles.

The green synthesis process of ZnO nanoparticles involves the use of natural material extracts, namely *Padina* sp. as a bio reducer and capping agent, with the possibility of a reaction to reduce Zn^{2+} ions to Zn+ to Zn^0 and then nucleation, growth, and autooxidation into ZnO nanoparticles [16]. The green synthesis process that occurred in this study began with the interaction of biomolecular compounds of brown algae extract with Zn^{2+} ions from the initial precursor ($Zn(NO_3)_2$). After the addition of NaOH, a deposition reaction occurs, which is characterized by the formation of metal hydroxides and biomolecular compounds that play a role in binding to the Zn^{2+} ion cluster, which causes the particle surface to be enveloped by negative ions, which results in a repulsive force between similar charges so as to prevent particle aggregation [17,18]. *Padina* sp. is a type of seaweed used in the synthesis of ZnO nanoparticles for several reasons: *Padina* sp. is an abundant and easily obtained biomass, so it can be used as a source of raw material for the synthesis of ZnO nanoparticles. *Padina* sp. contains active compounds such as alginic acid, fucoidan, and other compounds that can function as reducing agents and stabilizers in the synthesis of ZnO nanoparticles. *Padina* sp. is a biocompatible biomass, so it can be used in biomedical and environmental applications. *Padina* sp. extract can function as a reducing agent to convert Zn^{2+} ions into ZnO nanoparticles. *Padina* sp. extract can also function as a stabilizer to prevent the aggregation of ZnO nanoparticles. The use of *Padina* sp. in the synthesis of ZnO nanoparticles is environmentally friendly because it does not involve the use of hazardous chemicals and can reduce waste. Thus, *Padina* sp. can be used as an environmentally friendly and biocompatible alternative for the synthesis of ZnO nanoparticles.

The Zn^{2+} ion reacts with the hydroxide ions from NaOH to form a milky white suspension mixture. White deposits can be obtained and separated due to the properties of ZnO nanoparticles that are insoluble in water. However, when in the suspension mixture, the compound formed is $Zn(OH)_2$. Meanwhile, the excess OH^- ions will react with $Zn(OH)_2$ to form a $[Zn(OH)_4]^{2-}$ complex. For the H_2O molecules present in the mixture and the energy obtained when the solution is stirred using a magnetic stirrer, the $[Zn(OH)_4]^{2-}$ complex is dissociated again to form Zn^{2+} and OH^- ions, which further form solids (powders) of ZnO nanoparticles during the heating process (drying), marked by the release of water vapor [19]. Furthermore, the calcination process of ZnO nanoparticles can improve the crystallinity [20]. The green synthesis process can be reviewed in the reaction scheme shown in Figure 1 [10,17,19,21]. However, the literature shows that a biological pathway for the synthesis of zinc oxide nanoparticles using *Pseudomonas aeruginosa* rhamnolipids has already been reported [22].

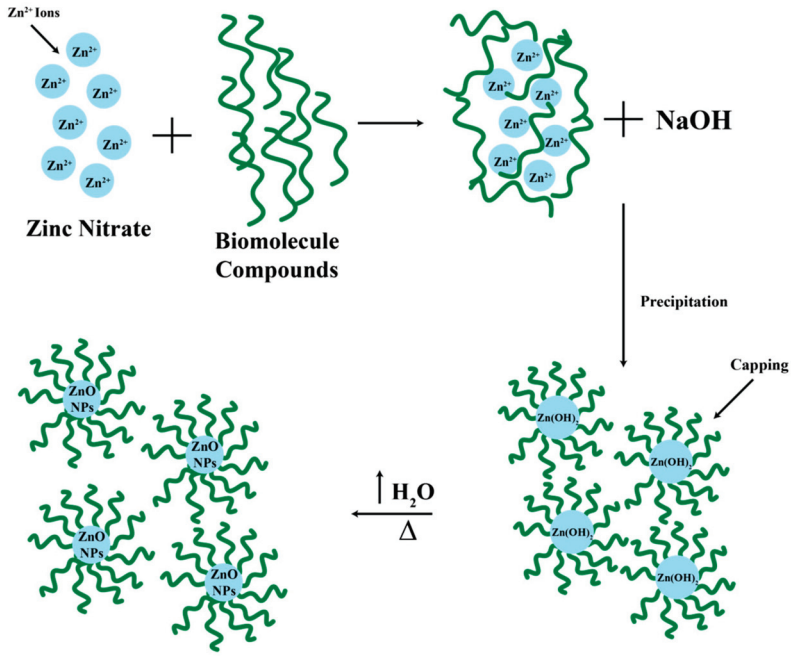

Figure 1. Green synthesis reaction scheme of ZnO nanoparticles.

2.2. Modification of Cotton Fabric with ZnO Nanoparticles and Silane Compounds

The curing process was carried out on cotton fabrics that were modified with ZnO nanoparticles to bind the material or ZnO nanoparticles to the surface of the fabric to make it stronger and more durable [23]. The results of the modification of ZnO nanoparticles and/or silane compounds did not show a significant qualitative difference because the color of the white cotton fabric was the same as the color of the ZnO nanoparticle deposits and silane compounds, which had clear visuals. After modification, the modified cotton fabric was characterized and tested for contact angle, mechanical properties, and antimicrobial activity.

2.3. Analysis of ZnO Nanoparticle Function Cluster and Cotton Fabric With and Without Modification

Based on the results of UV/VIS/NIR tests in the wavelength range of 200–800 nm, the spectra of ZnO nanoparticles, cotton fabrics, and cotton fabrics + ZnO nanoparticles showed absorption peaks at wavelengths of 327 nm and 357 nm, respectively, showing no absorption peaks, and 329 nm. The peak absorption of ZnO nanoparticles is in the

wavelength range of 300–380 nm [10,22]. The peak absorption results have different values in the research that has been carried out, namely 320 nm [24], 327 nm [25], 355 nm [26], 357 nm [27], and 365 nm [8].

The peak uptake of ZnO nanoparticles varies due to the influence of diverse particle sizes. Particles that are not necessarily uniform certainly have absorption peaks at different wavelengths. The decreasing particle size causes a decrease in absorption and a blue shift (a shift in wavelength from long to short). In addition, there is a decrease in the UV A/UV B ratio and the effect of quantum size on absorbance with changes in particle size [28].

The difference in absorption peaks in cotton fabrics and cotton fabrics deposited with ZnO nanoparticles is found at the wavelength of 329 nm, which is estimated to be the wavelength of ZnO nanoparticles. The presence of absorption peaks at these wavelengths indicates that ZnO nanoparticles have been deposited on the cotton fabrics. The value of one of the peaks of absorption of ZnO nanoparticles (327 nm) is different from that of the ZnO nanoparticles deposited in cotton fabrics (329 nm) due to the presence of cotton fabrics, which can cause the signal captured by the detector to be less noisy, although the difference is not too significant.

Tests that were carried out with the ATR-FTIR spectrophotometer instrument produced spectral data that show the interpretation of the functional cluster. The ATR-FTIR K0 spectra show the peak absorption position at 3323, 3257, 2884, 1637, 1425, 1363, 1312, 1015, and 898 cm^{-1}. Meanwhile, the ATR-FTIR K1 spectra in Figure 2 show the peak absorption positions of 3323, 3250, 2886, 1636, 1423, 1382, 1312, 1021, 900, and 452 cm^{-1}. Wide absorption bands in regions 3323, 3257, and 3250 cm^{-1} with an area range of 3500–3200 cm^{-1} indicate the presence of vibration stretching of the O-H group from cellulose (cotton) [29].

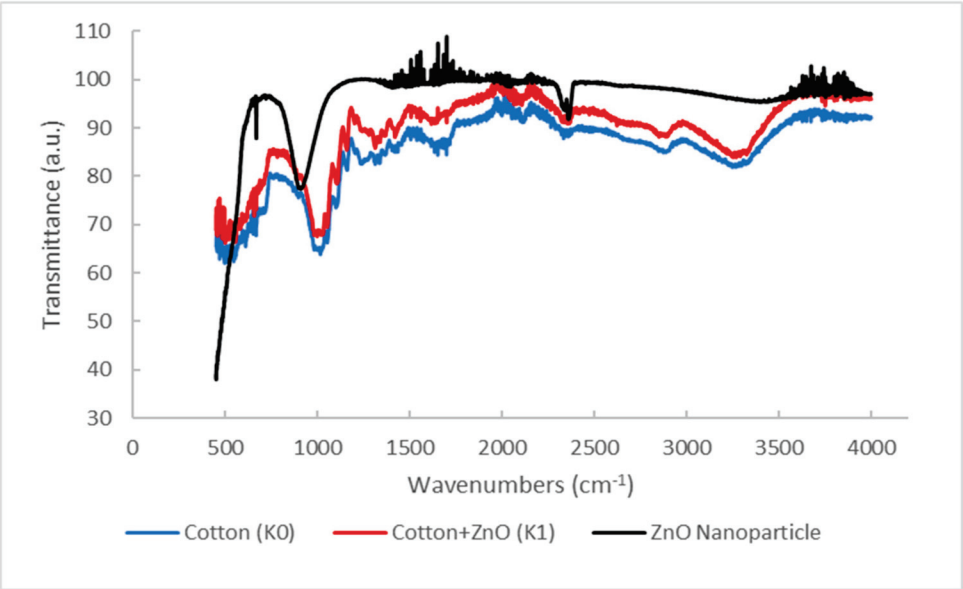

Figure 2. Comparison of the FTIR spectra of K0, K1, and ZnO nanoparticles.

The absorption band positions in the 2884 and 2886 cm^{-1} regions showed the presence of vibration stretching of the C-H group derived from polysaccharides in cellulose and brown algae extract compounds used as capping agents in the process of depositing ZnO nanoparticles in situ [30]. The absorption bands in the region of 1637 and 1636 cm^{-1} are characterized as water molecules found in the cotton fabric (cellulose). Small absorption bands in the 1425 and 1423 cm^{-1} regions indicate the presence of the CH_2 symmetric bend-

ing of cellulose. The position of the absorption peak in the regions (1353 and 1382 cm^{-1}) and 1312 cm^{-1} respectively shows the presence of bending vibration of the C-H and C-O groups. Wide absorption peaks in the 1015 and 1021 cm^{-1} regions showed a vibration relationship between C-O and O-H stretching in polysaccharides from cellulose. In addition, the peak of uptake in the regions of 898 and 900 cm^{-1} is characterized as a β-glycosidic relationship with monosaccharides [31].

The ATR-FTIR spectra show the peak absorption positions of 2362, 2338, 908, 669, and 450 cm^{-1}. The peak of absorption in the region of 2362 cm^{-1} indicates the presence of a C=O functional group [32]. The position of the absorption band in the area of 2338 cm^{-1} indicates the vibration of the stretching of the Amina group (C=N) [33]. In addition, the absorption band in the area of 908 cm^{-1} shows the presence of C-H out-of-plane bending [34]. The band of absorption in the region of 669 cm^{-1} is characterized as a Zn-OH functional group [35]. The position of the absorption band in the region of 450 cm^{-1} is characterized as a Zn-O functional group that enters the wave number range of the Zn-O functional group, which is 650–400 cm^{-1} [33,36].

The K0 and K1 spectra have almost the same spectrum, but in K1, there is a differentiating absorption peak at 452 cm^{-1}, which is characterized as the Zn-O functional group. This value indicates that the deposition of ZnO nanoparticles on cotton fabrics has been successfully carried out. The comparison of the spectral range of K0, K1, and ZnO nanoparticles can be seen in Figure 2.

The ZnO nanoparticles formed have a $Zn(OH)_2$ component with the identification of the Zn-OH functional group, which indicates that the drying process needs to be studied further so as to produce ZnO nanoparticles that are close to high purity. The peak of uptake found in the spectrum of ZnO nanoparticles indicates the presence of an analyzed organic functional group. This is in accordance with the role of biomolecular compounds contained in brown algae extract as a capping agent. The biomolecular compounds that can be predicted, namely alkaloids, are indicated by the identification of C=O, C-H, and C=N functional groups. Biomolecular compounds that play a definite role in green synthesis need to be further studied using compound elucidation methods, such as GC-MS, 13C-NMR, and 1H-NMR analysis.

2.4. Analysis of the Diffraction Patterns and Crystal Size of ZnO Nanoparticles

Tests that were carried out with XRD spectrometer instruments produced diffraction pattern data so that the crystal size could be clearly determined. The test was carried out on ZnO nanoparticles and cotton fabrics deposited with ZnO (K1) nanoparticles using an angle range of 2θ in the range of 3–90° and 4–80°, respectively. The results of XRD analysis were processed using the X'pert HighScore Plus program to match with the XRD database, namely the Crystallography Open Database (COD), and the OriginLab version 2023b program to determine the FWHM value that can be used in determining crystal size with the Debye–Scherrer equation shown in Equation (1) [9]. The diffraction pattern of ZnO nanoparticles and cotton fabrics deposited with ZnO (K1) nanoparticles can be reviewed in Figures 3 and 4.

$$\boldsymbol{D = \frac{k\lambda}{\beta cos\theta}} \quad (1)$$

With:
D = Crystal size (nm)
k = Form factor constant (0.91 for hexagonal shapes)
λ = Wavelength (Cu-Kα1 = 0.15406 nm)
β = FWHM (*Full Width at Half Maximum*) (radian)

θ = X-ray diffraction angle (radian)

Based on Figure 3, the diffraction pattern of ZnO nanoparticles that has been confirmed with COD data 96-900-4180 shows matched peaks at 2θ = 31.63°; 34.3°; 36.14°; 47.42°; 56.52°; 62.76°; 66.28°; 67.87°; 68,92°; 72,54°; 76,84°; and 89.47°, with Miller index values (h k l) of (1 0 0), (0 0 2), (1 0 1), (1 0 2), (1 0 2), (1 1 0), (1 0 3), (2 0 0), (1 1 2), (2 0 1), (0 0 4), (2 0 2), and (2 0 3), respectively. Based on matching with the COD database, the crystal structure of ZnO nanoparticles from green synthesis using *Padina* sp. forms the hexagonal crystal structure of wurtzite (zincite). In addition, the crystal size of the ZnO nanoparticles from the Debye–Scherrer equation is 15.35 nm at the peak position of the crystal with a Miller index value (1 0 1). The resulting peaks have values that do not differ significantly from the COD database. Some unmatched peaks indicate the presence of impurities from compounds derived from the algae extract of *Padina* sp., meaning that there can be a decrease in the crystallinity of ZnO nanoparticles. This can occur due to the influence of temperature during the calcination process. Successive increases or decreases in calcination temperature can increase or decrease the crystallinity and crystal size of ZnO nanoparticles [37].

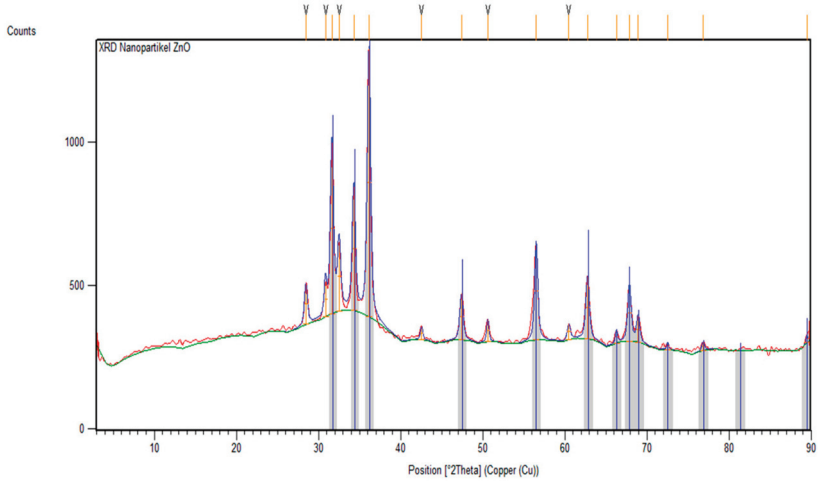

Figure 3. XRD diffractogram of ZnO nanoparticles compared with the COD Database 96-900-4180.

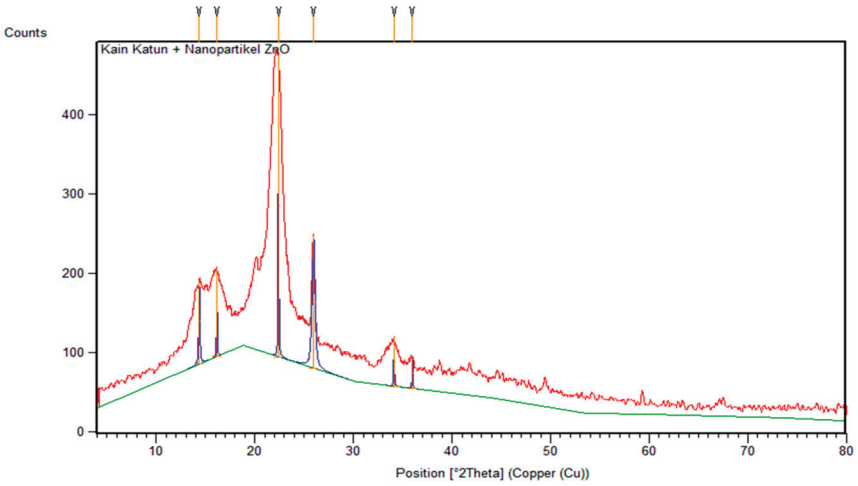

Figure 4. XRD diffractogram of cotton fabric-deposited nanoparticles ZnO (K1).

Meanwhile, the diffraction pattern of cotton fabric deposited with ZnO nanoparticles, shown in Figure 4, shows peaks at 2θ = 14.37°; 16.15°; 22.40°; 25.96°; and 34.11°, identified as crystalline cellulose. The peaks cannot be identified with the COD database due to

the number of phases being more than one. In addition, the ZnO nanoparticles in cotton fabrics are shown at a peak of 35.98°. The peaks are not crystalline (amorphous) and shift somewhat because the identified phases are not dominant compared to the peaks that show crystalline cellulose. The crystal size of ZnO nanoparticles in cotton fabrics can be determined using the Debye–Scherrer equation assuming the phase in which crystals are formed so that a crystal size of 20.43 nm is obtained.

2.5. Results of Particle Size and Distribution Analysis of ZnO Nanoparticles

Analysis of particle size and distribution using the Particle Size Analyzer (PSA) instrument was carried out. The analysis began with the dispersion of ZnO nanoparticles with a concentration of 0.1% (b/v) using ethanol and then sonication for 30 min. The results of the PSA data of ZnO nanoparticles are reviewed in Table 1.

Table 1. Polydispersity index and particle size of ZnO nanoparticles.

Polydispersity Index	Particle Size (nm)	Vol%
0.537	1.74	1.4
	24.54	3.3
	164	20.5
	706	66
	3.860	4.1
	5.710	4.7

Based on Table 1, PSA data were obtained, which include a PDI (Polydispersity Index) of 0.537, a nanoscale particle size in the range of 1.74–706 nm, and a microscale particle size in the range of 3860–5710 nm. The polydispersity index value is in the range of 0–1, which indicates the particle size distribution. A PDI value close to zero indicates a homogeneous particle distribution, while a polydispersity index value of >0.5 indicates that the particles have a high level of heterogeneity [38]. The results of the PSA data showed that the particles were still not homogeneously distributed, which could be reviewed at a PDI value of >0.5, and the size of the ZnO particles was in the nano- and micro-regions. The dominant particle size is on the nanoscale (1–1000 nm) with a total percentage of 91.2%. However, the ZnO particles that are still present at the microscale (3860 and 5710 nm) have a percentage of 4.1 and 4.7%, indicating that the particles formed are agglomerating. This is suspected to be due to the effectiveness of *Padina* sp. as the amount of capping agent is still low. Conversely, a strong capping agent role can limit the growth of ZnO clusters and prevent aggregations from being large. The formation of nanoparticles can be affected by the pH of the reaction solution, the concentration of seaweed, the concentration of metal salts (precursors), the time and temperature of the reaction, and the temperature and time of drying and calcining [37,39].

The difference occurred between the results of particle measurements using PSA instruments and crystal measurements using the Debye–Scherrer equation. This is because the Debye–Scherrer equation used is an estimate of the size of the crystal material and not the size of the particle. One particle is made up of a number of tiny crystals. A particle that is nanometer in size by having one crystal in one particle indicates that the crystal size is equal to the particle size [39]. On the other hand, the results of measuring ZnO particles using *Padina* sp. extract in this study with the PSA instrument showed particles that were nanometers and micrometers in size, so the crystals obtained became heterogeneous and did not necessarily indicate the particle size.

2.6. Analysis of yjr Morphology, Particle Form, and Elemental Composition of ZnO Nanoparticles

The results obtained were in the form of SEM images that could inform on the shape and morphology of the surface of ZnO nanoparticles, cotton fabrics (K0), cotton fabrics deposited with ZnO nanoparticles (K1), and cotton fabrics deposited with ZnO nanoparticles and silane compounds (HDTMS/MTMS) (K4). In addition, the elemental composition of each sample tested was determined using EDS analysis. Testing was carried out with several SEM instruments (Thermo Fisher Scientific Axia ChemiSEM, Phenom Pro X G6, and JEOL JSM-6510LA) and FESEM (JEOL JSM-IT700HR) with coating using a sputter coater that uses conductive target materials such as Au and Au/Pd to increase the conductivity of the sample in minimizing the electron charging effect, which can have an impact on the quality of SEM image resolution. The results of SEM and EDS images of ZnO, K0, K1, and K4 nanoparticles with varying magnifications can be reviewed in Figures 5–8.

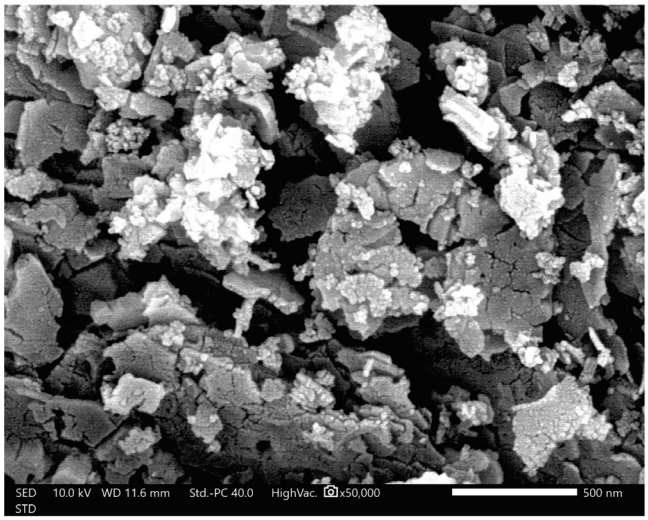

Figure 5. SEM image of ZnO nanoparticles with JEOL JSM-6510LA. Magnification: 50,000×.

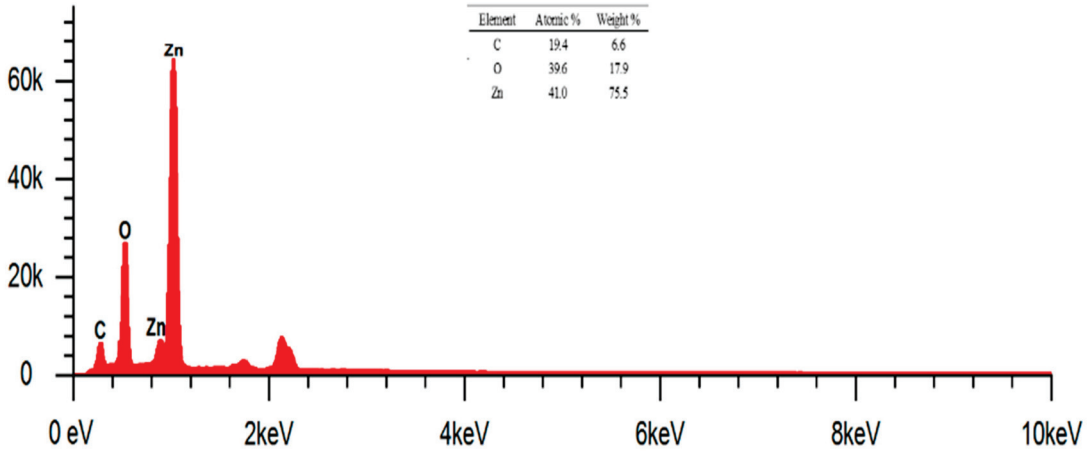

Figure 6. EDS results of ZnO nanoparticles.

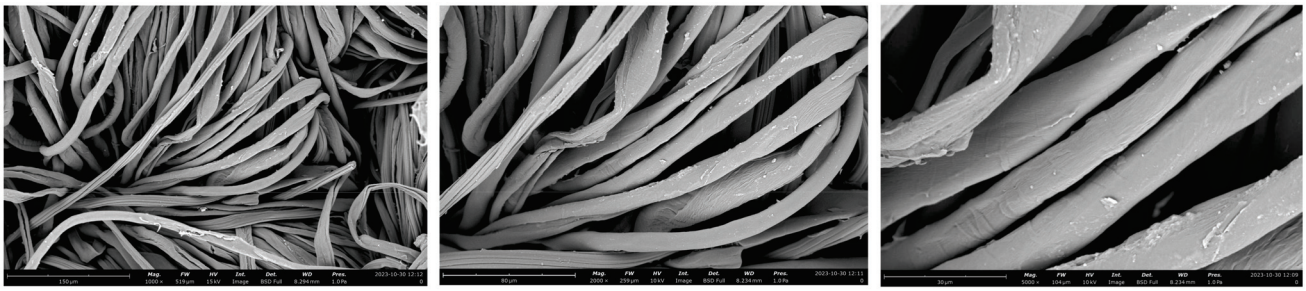

(**a**) (**b**) (**c**)

Figure 7. SEM image of cotton fabric with Phenom Pro X G6. Magnification: (**a**) 1000×; (**b**) 2000×; (**c**) 5000×.

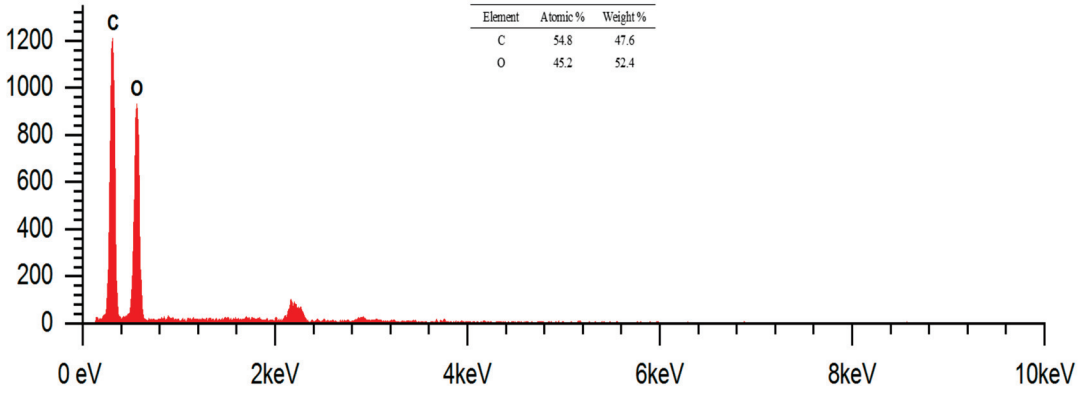

Element	Atomic %	Weight %
C	54.8	47.6
O	45.2	52.4

Figure 8. EDS region results for cotton fabric. Magnification: 5000×.

SEM image results with a magnification of 50,000× using JEOL JSM-6510LA at an accelerating voltage (AV) of 10 kV are shown in Figure 5.

Particle measurements using SEM can be performed directly using the tool or image processing software such as ImageJ. Particle measurement with a magnification of 50,000×, as shown in Figure 5, yields a particle size in the range of 45–297 nm. Meanwhile, at smaller magnifications such as 10,000× and 20,000×, particles with varying sizes from the nanometer and micrometer scales show an uneven distribution of particles. In addition, the 50,000× magnification shown in Figure 5 shows a heterogeneous particle distribution. This is due to the ZnO particles that have undergone agglomeration events, meaning that the results of particle size and distribution analysis using SEM are in accordance with the PSA results.

Analysis of particle shape can be observed at high magnifications such as 100,000× and 200,000× showing irregularly shaped particles such as rod-like and leaf-like particles. The irregular shape of the particles can be caused by several factors such as precursor concentration, pH conditions, heating temperature during the reaction, stirring speed, reaction time, and other factors. Therefore, it is necessary to further study the factors that affect the irregularity of particle shape.

Figure 6 shows the EDS results of ZnO nanoparticles at a magnification of 20,000×. The EDS results for ZnO nanoparticles can be analyzed qualitatively in the presence of several identified elements, namely C, O, and Zn. The mass percentage (%) of the identified elements was 6.6, 17.9, and 75.5, respectively. Meanwhile, the known atomic percentages (%) were 19.4, 39.6, and 41, respectively. The presence of element C in ZnO nanoparticles indicates that there is still a capping agent derived from biomolecular compounds.

2.7. SEM Images and Composition of Cotton Fabrics (K0)

Morphological analysis of cotton fabrics was performed using SEM Phenom Pro X G6 with magnifications of 1000×, 2000×, and 5000×, which can be seen in Figure 7. The shape of the cotton fabric observed in the SEM images is in accordance with the theory, namely, cotton fibers in the form of ribbons or tubes that collapse and twist. The surface of the raw cotton fiber has a clean area and very few contaminants can be observed. This was confirmed using the EDS analysis, with it only containing elements C and O derived from the constituent of cotton fabrics, namely cellulose. The results of the EDS analysis can be reviewed in Figure 8, which shows the mass and atomic percentage. The mass percentage (%) identified was 47.6 and 52.4, respectively. Meanwhile, the atomic percentage (%) was 54.8 and 45.2, respectively.

2.8. SEM Images and Composition of Cotton Fabrics After Modification with ZnO (K1) Nanoparticles

The morphological analysis of cotton fabrics deposited with ZnO nanoparticles using Axia ChemiSEM at magnifications of 1000× can be seen in Figure 9. The surface of cotton fabrics that have been deposited with ZnO nanoparticles looks rougher than cotton fabrics without modification. The presence of ZnO nanoparticles deposited on cotton fabrics can be confirmed by the EDS results and those shown in Figure 9.

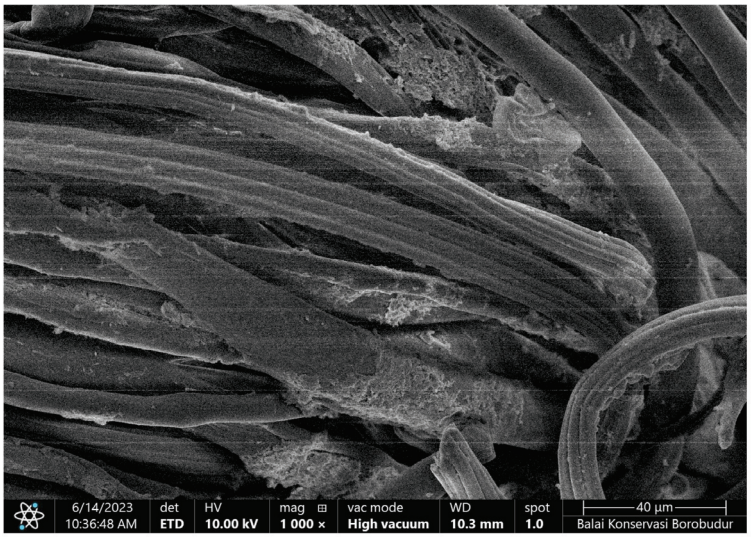

Figure 9. SEM image of cotton fabric + ZnO nanoparticles (K1) with Axia ChemiSEM. Magnification: 1000×.

The results of EDS analysis (Figure 10) at a magnification of 1000× showed the presence of elements C, O, and Zn. The identified mass percentages (%) were 23.7, 41.3, and 35, respectively. Meanwhile, the atomic percentages (%) were 38.8, 50.7, and 10.5, respectively. The presence of the Zn element indicates that the deposition of ZnO nanoparticles on cotton fabrics using the in situ method has been successfully carried out. Element C in K1 shows the presence of cellulose as a constituent of cotton fabrics and biomolecular compounds that act as capping agents in in situ deposits of ZnO nanoparticles. Based on the mass percentage from smallest to largest, namely, elements C, Zn, and O, respectively, the sum of the mass percentage of the element Zn is smaller than O because the Zn of the deposited ZnO nanoparticles is unevenly deposited and is less dominant than cotton fabrics composed of elements C and O.

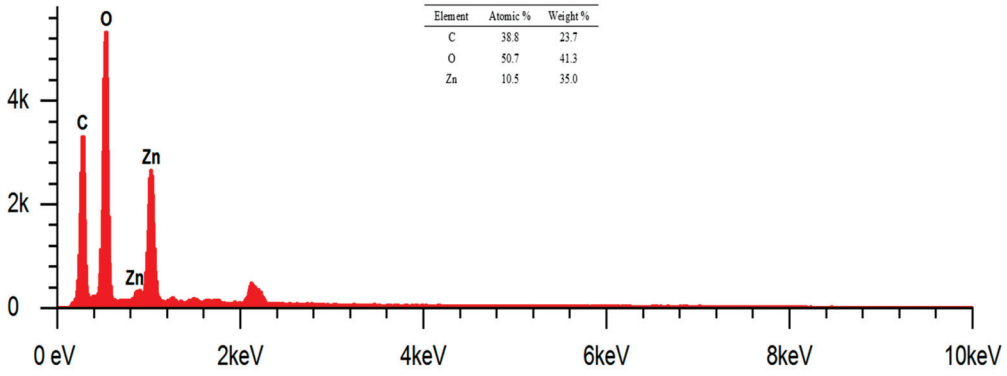

Figure 10. EDS results of cotton fabric + nanoparticles ZnO (K1). Magnification: 1000×.

2.9. SEM Images and Composition of Modified Cotton Fabrics with ZnO Nanoparticles and HDTMS/MTMS

Morphological analysis of cotton fabrics deposited with ZnO nanoparticles and silane compounds (HDTMS/MTMS) (K4) using Axia ChemiSEM at a magnification of 1000× can be seen in Figure 11.

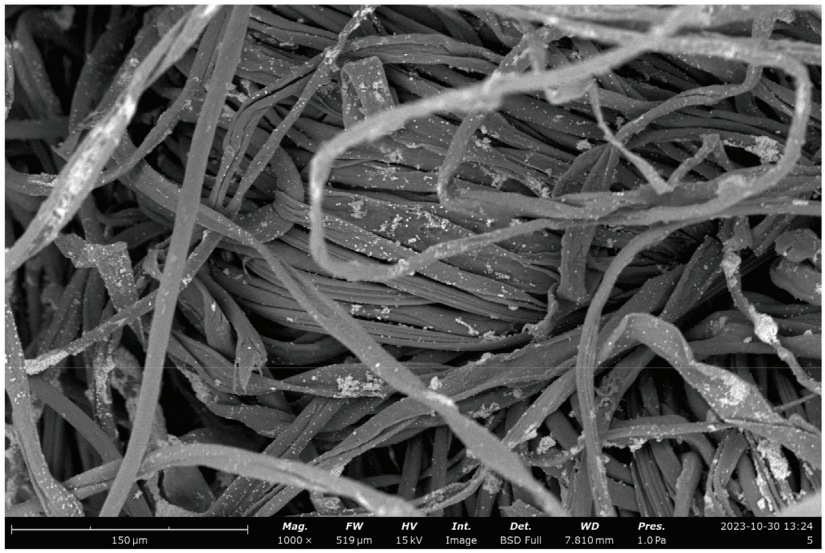

Figure 11. SEM image of cotton fabric + nanoparticles ZnO + HDTMS/MTMS (K4) with Phenom ProX G6. Magnification: 1000×.

Based on the SEM image in Figure 11, the surface of K4 is characterized by the presence of ZnO nanoparticles that have an uneven distribution but that are more homogeneous or uniform with particles in the form of micro-nanoflowers. This can be seen in the SEM images with a magnification of 17,500×.

ZnO deposited on cotton fabric has a smaller number of agglomerated particles compared to K1. The growth of ZnO clusters in K4 is easier to control than in K1 due to the addition of silane compounds as coupling agents by increasing the adhesion force and interface interaction of ZnO nanoparticles or matrix polymers such as cotton fabrics. Coupling agents have the ability to balance the hydrophilic and hydrophobic properties of a polymer or membrane material, thereby increasing the hydrophobic properties of the material. Increased hydrophobic properties can reduce the water absorption in ZnO nanoparticles so that agglomeration events in ZnO nanoparticles can be minimized [40].

ZnO particles in the form of micro-nanoflowers can be measured with the help of ImageJ software at a magnification of 17,500×. Particle sizes are obtained in the range of

224–1688 nm. Higher magnification can make it easier to measure ZnO nanoparticles, but the resolution of the SEM image is reduced, meaning that the resulting image becomes more opaque. In addition, the nanoparticles of ZnO and silane compounds (HDTMS/MTMS) deposited on cotton fabrics can be confirmed by the results of EDS analysis at the magnification of 17,500×, as shown in Figure 12.

The EDS results at 17,500× magnification using AV of 15 kV showed the presence of elements C, O, Zn, Si, and Au. The mass percentage (%) identified were 61.7, 32.9, 4.5, 0.7, and 0.2, respectively. Meanwhile, the atomic percentages (%) were 45.9, 32.5, 18, 1.2, and 2.4, respectively. The presence of the element Zn indicates that the deposition of ZnO nanoparticles on cotton fabrics has been successfully carried out. Element C in K1 shows the presence of cellulose as the dominant constituent of cotton fabrics and biomolecular compounds that act as capping agents in ZnO nanoparticle deposits. In addition, the element Si shows the presence of silane compounds as a coupling agent that can increase the hydrophobicity of cotton fabrics. Meanwhile, the analyzed Au element comes from the Au target material in increasing the conductivity of cotton fabric samples. The peaks of Zn and Au in the energy range of 8–10 keV respectively show the X-ray characteristics at Kα and Lα energies. This is due to the use of AV of 15 kV so that the peaks can be analyzed.

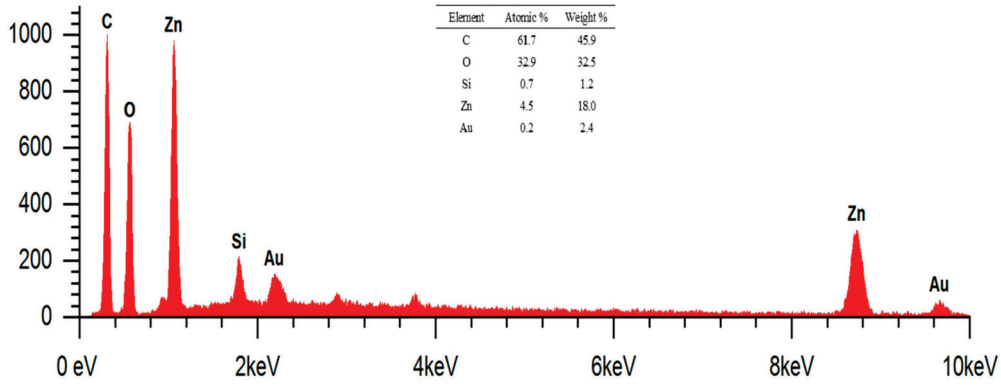

Figure 12. EDS results for spot cotton fabric + nanoparticles ZnO + HDTMS/MTMS (K4). Magnification: 17,500×.

2.10. Antibacterial Activity of Cotton Fabric With and Without Modification

Antibacterial activity can be seen from the clear zone that forms or what is known as the inhibition zone around the cotton fabric sample. The formed resistance zone can be measured to find out the magnitude of the diameter through three sides, namely horizontally, vertically, and diagonally. The effectiveness of antibacterial activity can be observed through the formation of inhibitory zones. Bacterial growth inhibitory responses are classified into four groups, namely weak (≤5 mm in diameter), medium (5–10 mm in diameter), strong (10–20 mm in diameter), and very strong (≥20 mm in diameter) [41].

Antibacterial testing was carried out on cotton fabrics without modification as well as after modification (K0–K10). In addition, tests were also carried out on ZnO nanoparticles dispersed in aquabidest with a concentration of 1000 ppm (Z). The use of a positive control (K+) such as ciprofloxacin results in an inhibitory zone with a large diameter against Gram-positive (*Staphylococcus epidermidis*) and Gram-negative (*Pseudomonas aeruginosa*) test bacteria [42]. Meanwhile, the negative control (K−) used is aquabidest. Positive and negative controls were used as a comparison of sample test results. Antibacterial testing was carried out for 48 h with the measurement time being every 3 h.

2.11. Measurement of the Inhibition Zone Against Pseudomonas aeruginosa

Antibacterial testing on modified cotton fabrics was carried out by measuring the inhibition zone against *Pseudomonas aeruginosa*. The results of the sample inhibition zone measurements compared to the positive and negative controls can be reviewed in Figure 13.

Based on Figure 13 showing the results for the antibacterial test samples, the results are almost the same, so some samples look like they overlap, except for samples K8 and Z, which showed maximum values at the 42nd hour of 3.93 mm and 2.79 mm, respectively. Based on the graph, the formation of a large inhibition zone diameter in the test sample tends to be at the 42nd hour. After the 42nd hour, the test sample experienced resistance to the test bacteria, indicated by the instability events up and down the diameter of the inhibition zone of the test sample. However, before the 42nd hour, the test sample also had values that tended to go up and down. This can be caused by the medium used, the environmental conditions during testing such as temperature and humidity, the stability of antibacterial substances, the condition of cotton fabric samples, the incubation time, metabolic activity, and the number of bacteria.

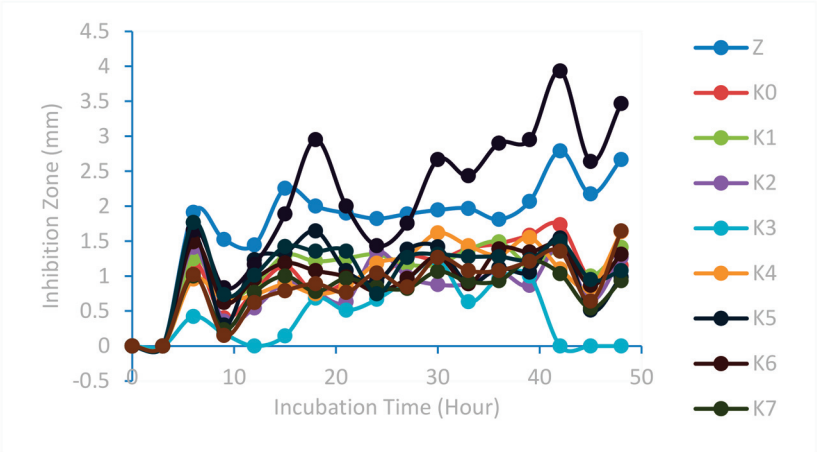

Figure 13. Graph of the relationship between bacterial inhibition zone diameter and incubation time against *Pseudomonas aeruginosa*.

The K8 modified cotton fabric sample type has the highest value when compared to the other modifications and the one without modification (K0). This shows that the K8 sample type has the highest antibacterial activity against the bacterium *Pseudomonas aeruginosa*. HDTMS-modified ZnO nanoparticles provide a larger surface area for bacterial interaction. In addition, the hydrophobicity of HDTMS helps maintain the stability of ZnO nanoparticles, ensuring prolonged antibacterial activity [43–45]. Meanwhile, ZnO nanoparticles have the second-highest antibacterial activity. The incubation time from the 0th hour to the 9th hour does not show an inhibition zone, so it begins with the 9th hour. In addition, the best incubation time is at the 42nd hour as evidenced by the results of measuring the diameter of the maximum inhibition zone.

2.12. Measurement of Inhibition Zones Against Staphylococcus epidermidis

Measurements of the inhibitory zone on modified cotton fabrics against *Staphylococcus epidermidis* can be reviewed in Figure 14. In addition, measurements were also taken on unmodified cotton fabrics (K0), ZnO nanoparticles (Z), and positive (K+) and negative (K−) controls.

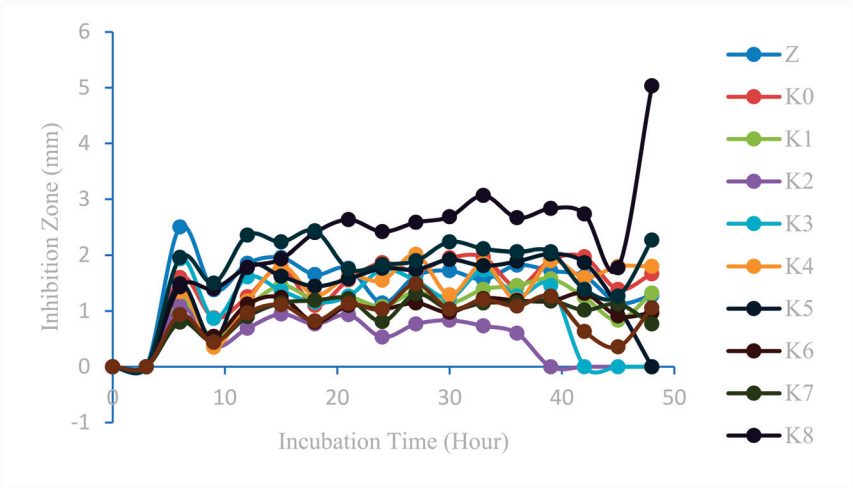

Figure 14. Graph of the relationship between inhibition zone diameter and incubation time against *Staphylococcus epidermidis*.

Inhibition zone measurements were also taken three times per sample and Figure 14 shows that one of the samples has a large inhibition zone. The results of measuring the diameter of the inhibitory zone of *Staphylococcus epidermidis* in Z, K0–K10, and K+ samples are presented. In addition, K− was also measured, but an inhibition zone was not formed.

Based on the results of the ANOVA test, a post hoc ANOVA follow-up test was then carried out, namely, the Tukey HSD (Honestly Significant Difference), test to determine the variation in sample type and the best incubation time in the antibacterial test against *Staphylococcus epidermidis.* Based on the results of the Tukey HSD antibacterial test against *Staphylococcus epidermidis* bacteria, it was shown that the K8 modified cotton fabric sample type had the highest value when compared to the other modifications and that without modification (K0). This shows that the K8 sample type has the highest antibacterial activity against *Staphylococcus epidermidis*. HDTMS and ZnO nanoparticles have a synergistic effect. HDTMS and ZnO nanoparticles can synergistically enhance the formation of ROS, thereby enhancing antibacterial efficacy. HDTMS-modified ZnO nanoparticles provide a larger surface area for bacterial interaction. In addition, the hydrophobicity of HDTMS helps maintain the stability of ZnO nanoparticles, ensuring prolonged antibacterial activity [44–46]. Meanwhile, the K9 sample type showed almost the same results as K8 so it did not differ significantly. ZnO nanoparticles had the third-highest value, which proves the existence of antibacterial activity against *Staphylococcus epidermidis*. In addition, based on the results of the Tukey HSD test, the best incubation time was at the 48th hour followed by the results of measuring the maximum diameter of the inhibition zone. The incubation time of the 6th, 15th, 30th, 27th, 33rd, 39th, and 42nd hours showed results close to the 48th hour, resulting in almost the same antibacterial activity.

2.13. Antifungal Activity of Cotton Fabric With and Without Modification

Measurement of antifungal activity inhibition zones that have similarities with the working principle of antibacterial activity measurement. Antifungal testing was carried out on cotton fabrics without modification as well as after modification (K0–K10). In addition, tests were also carried out on ZnO nanoparticles dispersed in aqua bidest with a concentration of 1000 ppm (Z). The use of a positive control (K+) such as ketoconazole results in an inhibitory zone with a large diameter against the fungus *Malassezia furfur* [46]. Meanwhile, the negative control (K−) used was aquabidest. Positive and negative controls are used as a comparison of sample test results. Antifungal testing was carried out for

48 h with a measurement time of every 6 h. The measurement of the inhibition zone for antifungal activity can be reviewed in Figure 15.

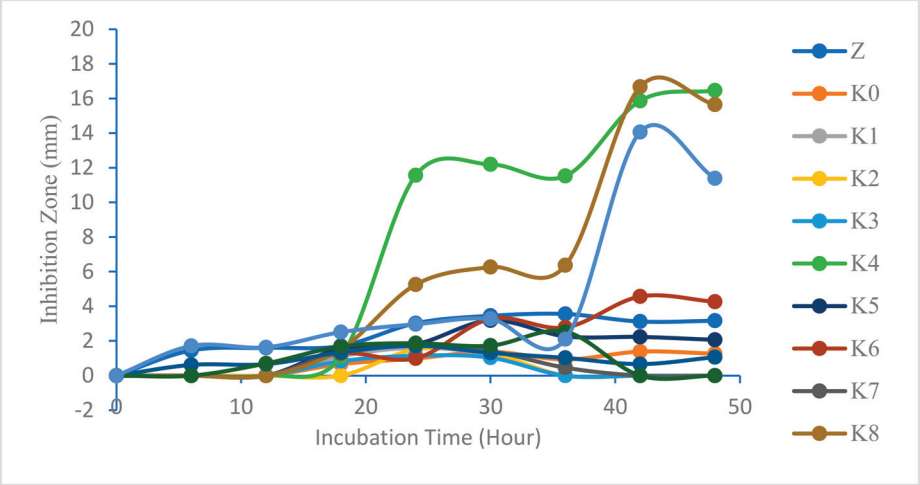

Figure 15. Relationship between the diameter of the inhibition zone and incubation time against *Malassezia furfur*.

Based on Figure 15, the antifungal test samples showed almost the same results, so some samples showed overlapping and stagnant increases, except for samples K4 and K8, which showed maximum values of 16.47 mm and 16.78 mm at the 42nd and 48th hours, respectively. The stagnant state can be affected by the medium used, the environmental conditions during testing such as temperature and humidity, the stability of antifungal substances, the condition of cotton fabric samples, the incubation time, metabolic activity, and the number of fungi.

The positive control (K+) can be included in the graph because the value of the inhibition zone formed does not show much difference from the K4 and K8 samples. The maximum resistance zone that can be formed at K+ is 14.07 mm at the 42nd hour measurement. The value of the maximum inhibition zone of the positive control is smaller than that of the test sample due to the improper quality, particle size, and concentration of K+, so it is necessary to further study the particle size and the minimum inhibition concentration of the positive control. The decrease in the value of the inhibition zone occurs at the 48th hour, which indicates that the medium has the potential to rise or decrease after 48 h, so the antifungal measurement is better than 48 h in order to find out the best inhibition zone.

Based on the results of the Tukey HSD antifungal test against *Malassezia furfur* fungus, they show that the K4 modified cotton fabric sample type has the highest value when compared to other modifications and that without modification (K0). This shows that the K4 sample type has the highest antifungal activity against *Malassezia furfur*. Meanwhile, K4 is the type of sample that has the second-largest inhibition zone value, showing almost the same results statistically as K8, so it does not differ significantly. The Tukey HSD test was then carried out to determine the variation in incubation time, showing the best incubation time, which was at the 42nd hour followed by the 48th hour. This is in accordance with the results of the measurement of the diameter of the maximum resistance zone that occurred in K4 and K8, respectively. Simplification of the Tukey HSD antifungal test against *Malassezia furfur* fungus on sample type variations can be reviewed in Table 2.

Table 2. Simplification of the Tukey HSD test results for *Malassezia furfur* on sample types.

Sample Type	Average Diameter of the Resistance Zone (mm) ± SD
	Malassezia furfur
ZnO NPs	2.64 ± 0.887^{a}
K0	1.10 ± 0.287^{a}
K1	1.31 ± 0.255^{a}
K2	1.39 ± 0.177^{a}
K3	1.00 ± 0.160^{a}
K4	11.45 ± 5.529^{c}
K5	2.19 ± 0.558^{a}
K6	2.86 ± 1.486^{ab}
K7	1.22 ± 0.539^{a}
K8	8.62 ± 6.109^{bc}
K9	1.05 ± 0.395^{a}
K10	1.70 ± 0.656^{a}
K+	4.96 ± 4.883^{ab}
K−	0 ± 0

Description: The average value of the diameter of the inhibition zone followed by different superscript letters shows significantly different results (significant), while the same superscript letters show significantly different results (insignificant) with a significance level of 95%.

The fungal growth inhibitory response of Z, K+, and K0–K10 samples, except K4 and K8, was classified in the weak group. Meanwhile, the K4 and K8 samples could be classified into the strong and medium groups, respectively, because the cotton cloth had been modified with ZnO nanoparticles and/or silane compounds that provided interactions between compounds in terms of antifungal activity in the fungus *Malassezia furfur*. Therefore, further research is needed on the effects of the interaction between ZnO nanoparticles and/or silane compounds on antifungal activity in the *Malassezia furfur* fungus. ZnO nanoparticles, HDTMS, and MTMS synergistically enhance ROS formation in cotton composites, attacking *Malassezia furfur*. Silane composites enhance the dispersion of ZnO nanoparticles [47]. HDTMS and MTMS can maintain the stability of ZnO nanoparticles. Thus, ZnO nanoparticles, HDTMS, and MTMS composites can cause long-lasting antifungal activity in cotton fabrics.

Mechanism of antibacterial and antifungal properties [44–47] include the following: 1. Surface area: Smaller NPs (10–100 nm) have larger surface areas, increasing interactions with microorganisms; 2. Reactive Oxygen Species: NPs generate ROS, damaging microbial cell membranes and DNA; 3. Cell membrane disruption: NPs interact with bacterial cell membranes, causing structural changes and leakage; 4. DNA binding: NPs bind to microbial DNA, inhibiting replication; and 5. Protein denaturation: NPs disrupt essential protein functions.

However, the size, distribution, and shape of nanoparticles can affect antibacterial activities. Smaller NPs (<10 nm) can enhance penetration into microbial cells, increasing antibacterial efficacy. Larger NPs (10–100 nm) can cause a greater surface area, improving ROS generation and cell membrane disruption. Optimal size (20–50 nm) can balance penetration, ROS generation, and surface area for maximum antibacterial activity [44–46]. Nanoparticle distribution affects antibacterial activities. Uniform distribution can ensure consistent antibacterial activity across fabric surfaces. Aggregation can reduce efficacy due to decreased surface area and ROS generation. Cluster formation can enhance antibacterial activity through localized ROS generation [44–47]. Nanoparticle shape can cause antibacterial activities. Spherical NPs are the optimal shape for ROS generation and cell membrane disruption. Rod-shaped

NPs can increase surface area, improving antibacterial activity. Triangular/Hexagonal NPs can enhance ROS generation due to increased surface roughness [44–46].

3. Materials and Methods

The instruments used in this study were a UV/VIS/NIR spectrophotometer (Shimadzu UV-3600 Plus, Shimadzu Corporation, Kyoto, Japan), an ATR-FTIR spectrophotometer (Shimadzu IRSpirit QATR-S, Shimadzu Corporation, Kyoto, Japan), an XRD spectrometer (Rigaku MiniFlex 600 and Shimadzu LabX XRD-6000, Rigaku Corporation, The Woodlands, TX, USA), a PSA (Microtrac Nanotrac Wave II, Shimadzu, Kyoto, Japan), an SEM-EDS (Axia ChemiSEM, Phenom Pro X G6, Thermo Fisher Scientific, Waltham, MA, USA, and JEOL JSM-6510LA, Jeol Ltd., Tokyo, Japan), a FESEM (JEOL JSM-IT700HR, Phenom Scientific, Eindhoven, The Netherlands), a sputter coater (cressington Sputter Coater 108auto/SE (Cressington Scientific Instruments Ltd., Watford, UK), Quorum SC7620 (Quorum Technologies Ltd., Lewes, UK), JEOL JEC-3000FC and Smart Coater DII-29030SCTR from Jeol USA Headquarters and Technology Center, New England, ME, USA), an ultrasonic cleaner (GT Sonic, Guangdong GT Ultrasonic Limited Company, Shenzhen, China), laminar air flow (LAF, Thermo Fisher Scientific, Waltham, USA), glassware, a micropipette, a magnetic stirrer, a blender, an 80-mesh test sieve, an oven, a muffle furnace, centrifuges, vacuum filters, pH meters, refrigerators, shakers, analytical scales, HDPE plastic bottles, thermometers, statives, clamps, hair dryers, cooler boxes, a digital capillary, hole punches, autoclaves, incubators, Petri dishes, an Ose wire, and a drigalski.

The materials were cotton fabric and brown algae (*Padina* sp.) taken from Drini Beach, Gunung Kidul, Special Region of Yogyakarta, Indonesia. The brown color of the algae is caused by the pigment fucoxanthin, which belongs to the xanthophyll group and is more dominant than other pigments such as chlorophyll. $Zn(NO_3)_2{\cdot}6H_2O$ was purchased from Sigma Aldrich (MilliporeSigma, Darmstadt, Germany, Methyltrimethoxylane (MTMS > 98% from Sigma Aldrich, MilliporeSigma, Darmstadt, Germany), hexadecyltrimethoxyxylane (HDTMS > 85% from Sigma Aldrich, MilliporeSigma, Darmstadt, Germany), ethanol 96% (Merck Millipore, MilliporeSigma, Darmstadt, Germany), NaOH, aquabidest, acetone, *Staphylococcus epidermidis* (FNCC 0048 strain), *Pseudomonas aeruginosa* (FNCC 0063 strain), *Malassezia furfur*, Nutrient Agar (NA) (Oxoid, Thermo Fisher Scientific, Shrewsbury, UK), Nutrient Broth (NB) (Merck Millipore, MilliporeSigma, Darmstadt, Germany), Potato Dextrose Agar (PDA) (Oxoid, Thermo Fisher Scientific, Shrewsbury, UK), and Whatmann filter paper no. 41 were used in this study.

3.1. Extraction of Brown Algae (Padina sp.)

The brown algae was washed using running water and then dried in an oven for 24 h at 50 °C until it had a water content of around 5%, and then it was cooled for 30 min at room temperature. After that, the dried brown algae was ground into powder form, so that it had a long shelf life and to make extraction easier. A total of 1.5 g of *Padina* sp. powder with a size of 100 mesh was dissolved in 150 mL of distilled water and heated at 100 °C for 25 min, with occasional stirring so that the solution was not saturated. After it was heated, the mixture was cooled and centrifuged for 30 min at a speed of 5000 rpm until the supernatant and pellet were produced. The separated supernatant in the form of brown algae extract was filtered using Whatman filter paper no. 41 with the help of a filter vacuum so that the extract results obtained were more optimal. The resulting filtrate extracted was put into an HDPE plastic bottle and stored in a refrigerator with a temperature of 4 °C.

3.2. Preparation of 0.1 M NaOH Solution

A 0.1 M NaOH solution was prepared by dissolving 1 g of solid NaOH in a 250 mL distilled water and homogenizing it.

3.3. Green Synthesis of ZnO Nanoparticles

Green synthesis begins by mixing 25 mL of brown algae extract (with aquabidest solvent) and 500 mL of 0.01 M zinc nitrate solution ($Zn(NO_3)_2$). The mixture was then stirred and heated at 80 °C for 5 min and then cooled at room temperature for 30 min. Then, 125 mL of NaOH solution was added slowly until the pH of the mixture was around 10–11, before it was placed in a refrigerator for 24 h at 4 °C. After that, the mixture was centrifuged at a speed of 5000 rpm for 30 min until the supernatant and pellets were produced. The pellets were separately washed 3 times to minimize dirt aquabidest. The pellets were dried in an oven at 100 °C for 6 h, and then we continued with the calcination process using a muffle furnace at a temperature of 400 °C for 4 h until the pellets became ZnO nanoparticles powder.

3.4. ZnO Nanoparticle Characterization

ZnO nanoparticle characterization tests were carried out using UV/VIS/NIR, ATR-FTIR, XRD, PSA, and SEM-EDS instruments.

In Situ Deposition of ZnO Nanoparticles onto Cotton Fabric (K0) was cut to a size 15 × 15 cm. It was then washed using acetone solution with soaking for 30 min and then soaked using distilled water for 30 min. Next, the cloth was dried using a hair dryer. Cotton cloth (K0) or modified cotton cloth (K5, K6, and K7) was placed in a beaker containing 5 mL of brown algae extract (Padina sp.) and 100 mL of 0.01 M zinc nitrate ($Zn(NO_3)_2$) solution. It was then stirred and heated at 80 °C for 5 min and then cooled at room temperature for 30 min. We then added 25 mL of NaOH solution slowly until the pH of the mixture was around 10–11. The mixture was transferred to a 250 mL Erlenmeyer flask and then shaken with a shaker for 24 h. The fabric that had been deposited with ZnO nanoparticles in situ was dried in an oven for 30 min at a temperature of 100 °C and then cured for 5 min at a temperature of 140 °C to obtain cotton fabric that had been deposited with ZnO nanoparticles (K1 or K8, K9, and K10).

3.5. Modification of Cotton Fabric with Silane Compound

Surface modification of unmodified cotton fabric (K0) or modified cotton fabric (K1) with silane compounds was carried out by immersing the fabric in an Erlenmeyer flask containing 300 mL of HDTMS in a solution of 20 mL and 10 mL of ethanol and aquabidest, respectively, for 4 h. Next, the fabric was removed and dried in an oven at 100 °C for 30 min to obtain samples K2 or K5.

Surface modification of unmodified cotton fabric (K0) or modified cotton fabric (K1) with silane compounds was carried out by immersing the fabric in an Erlenmeyer flask containing 300 µL of MTMS in a solution of 20 mL and 10 mL of ethanol and aquabidest, respectively, for 4 h. Next, the fabric was removed and dried in an oven at 100 °C for 30 min to obtain samples K3 or K6.

Surface modification to cotton fabric (K0) or modified cotton fabric with silane compounds (K1) was carried out by immersing the fabric in an Erlenmeyer flask containing a mixture of 100 µL and 150 µL of HDTMS and MTMS in 20 mL ethanol and in 10 mL distilled water, respectively, for 1.5 h. Next, the fabric was removed and dried in an oven at 100 °C for 30 min to obtain samples K4 or K7.

3.6. Antimicrobial Activity Assay of Cotton Fabric

The antimicrobial activity test began with the process of sterilizing the equipment and media using an autoclave. The media were made from nutrient agar (NA) for bacteria and potato dextrose agar (PDA) for fungi. Next, the bacteria *Pseudomonas aeruginosa* and *Staphylococcus epidermidis* and the fungus *Malassezia furfur* were placed in one cycle of nutrient broth and then incubated with a shaker incubator at a speed of 124 rpm for 24 h. Then, the sterilized NA or PDA was put into a Petri dish, about $\frac{1}{2}$ of the Petri dish covered by it, and then left for 24 h until the media became solid.

The solid media were inoculated with the bacteria or fungus using a micropipette and leveled using a drigalski. After that, antimicrobial activity testing was carried out using the disc diffusion method by analyzing the inhibition zone formed around the paper disc or disc sample which is marked by the width of the clear zone. This test was carried out using a paper disc and a sample shaped like a disc with a diameter of 6 mm. Bacterial inhibition zones were measured using digital calipers every 3 h, while for the fungus, this took place every 6 h. The formation of a clear zone indicates antimicrobial activity capabilities.

4. Conclusions

The success of ZnO nanoparticle synthesis using *Padina* sp. as a capping agent is indicated by the absorption at a wavelength of 357 nm; the Zn-O functional group in the wave number region of 450 cm^{-1}; the peak of diffraction being at an angle of 36.14° with a Miller index of (1 0 1), indicating a crystal size of 15.35 nm; the heterogeneous and uneven particle distribution; the particle size in the range of 1.74–706 nm (PSA) and 45–297 nm (SEM); and the irregular particle shapes such as rod-like and leaf-like. There was a significant difference in antibacterial activity between modified and unmodified cotton fabrics against *Pseudomonas aeruginosa* and *Staphylococcus epidermidis*. Cotton fabrics with the addition of HDTMS compounds and modification of ZnO (K8) nanoparticles showed the best results in inhibiting bacterial growth with the best time variation of each bacterium at the 42nd and 48th hours, respectively. There was a significant difference in antifungal activity between modified and unmodified cotton fabrics against *Malassezia furfur.* Cotton fabrics with ZnO nanoparticle modification and the addition of HDTMS and MTMS composites (K4) showed the best results in inhibiting fungal growth with the best time variation at 42 h.

Author Contributions: E.R. proposed the concept. R.J. performed the experiments. E.R., H., P.T. and A.K. wrote the manuscript. D.S. conducted the characterization. All authors participated in data analysis and manuscript discussion. All authors have read and agreed to the published version of the manuscript.

Funding: This research was funded by Indonesia Collaboration Research (Riset Kolaborasi Indonesia/RKI) with no. Contract T/18.1.1/UN34.9/PT.01.03/2024 and Professor Assignment Research with no. Contract T/15.5.140 /UN/34.9/PT.01.03/2024.

Institutional Review Board Statement: Not applicable.

Data Availability Statement: The data presented in this study are available on request from the corresponding author.

Acknowledgments: This research was conducted with the support of several parties. Therefore, the authors would like to express their gratitude to Yogyakarta State University for the Indonesia Collaboration Research funding with no. Contract T/18.1.1/UN34.9/PT.01.03/2024.

Conflicts of Interest: The authors declare no conflicts of interest.

References

1. Purnaningrum, R. *Sudut Kontak dan Aktivitas Antibakteri Kain Nylon 6,6 Dengan Modifikasi Penambahan Nanopartikel Perak dan Senyawa Silan*; Universitas Negeri Yogyakarta: Sleman, Indonesia, 2017.
2. Haryono, A.; Harmami, S.B. Aplikasi Nanopartikel Perak pada Serat Katun Sebagai Produk Jadi Tekstil Antimikroba. *J. Kim. Indones.* **2010**, *5*, 1–6.
3. Sabir, S.; Arshad, M.; Chaudhari, S.K. Zinc Oxide Nanoparticles for Revolutionizing Agriculture: Synthesis and Applications. *Sci. World J.* **2014**, *2014*, 925494. [CrossRef] [PubMed]
4. Sun, Q.; Li, J.; Le, T. Zinc Oxide Nanoparticle as a Novel Class of Antifungal Agents: Current Advances and Future Perspectives. *J. Agric. Food Chem.* **2018**, *66*, 11209–11220. [CrossRef]
5. Al-Nassar, S.I.; Hussein, F.I.; Adel, K.M. The Effect of Laser Pulse Energy on ZnO Nanoparticles Formation by Liquid Phase Pulsed Laser Ablation. *J. Mater. Res. Technol.* **2019**, *8*, 4026–4031. [CrossRef]
6. Wirunchit, S.; Gansa, P.; Koetniyom, W. Synthesis of ZnO Nanoparticles by Ball-Milling Process for Biological Applications. *Mater. Today Proc.* **2021**, *47*, 3554–3559. [CrossRef]
7. Ramadhani, Z.F. *Modifikasi Kulit Kambing Pikel Dengan Nanopartikel Perak Hasil Preparasi Menggunakan Tumbuhan Alga Merah (Gracilaria sp.) dan Biodegradasinya*; Universitas Negeri Yogyakarta: Sleman, Indonesia, 2021.
8. Bayrami, A.; Alioghli, S.; Pouran, S.R.; Habibi-Yangjeh, A.; Khataee, A.; Ramesh, S. A Facile Ultrasonic-Aided Biosynthesis of ZnO Nanoparticles Using *Vaccinium arctostaphylos* L. Leaf Extract and Its Antidiabetic, Antibacterial, and Oxidative Activity Evaluation. *Ultrason. Sonochemistry* **2019**, *55*, 57–66. [CrossRef]
9. Sari, R.N.; Irianto, H.E.; Ayudiarti, D.L. Using Oven Microwave for Synthesis ZnO Nps Using *Sargassum* sp. and *Padina* sp. Extract. *J. Pengolah. Has. Perikan. Indones.* **2019**, *22*, 375–390. [CrossRef]
10. Barzinjy, A.A.; Azeez, H.H. Green Synthesis and Characterization of Zinc Oxide Nanoparticles Using Eucalyptus globulus Labill. Leaf Extract and Zinc Nitrate Hexahydrate Salt. *SN Appl. Sci.* **2020**, *2*, 991. [CrossRef]
11. Nurrahman, N.W.D.; Sudjarwo, G.W.; Putra, O.N. Skrining Fitokimia Metabolit Sekunder Alga Cokelat (*Padina australis*) dari Kepulauan Poteran Madura. *J. Pharm. Care Anwar Med. (J-PhAM)* **2020**, *2*, 60–69. [CrossRef]
12. d'Água, R.B.; Branquinho, R.; Duarte, M.P.; Maurício, E.; Fernando, A.L.; Martins, R.; Fortunato, E. Efficient Coverage of ZnO Nanoparticles on Cotton Fibres for Antibacterial Finishing Using a Rapid and Low Cost In Situ Synthesis. *New J. Chem.* **2018**, *42*, 1052–1060.
13. Ou, J.; Wang, F.; Li, W.; Yan, M.; Amirfazli, A. Methyltrimethoxysilane as a Multipurpose Chemical for Durable Superhydrophobic Cotton Fabric. *Prog. Org. Coat.* **2020**, *146*, 105700. [CrossRef]
14. Zhang, J.; Raza, S.; Wang, P.; Wen, H.; Zhu, Z.; Huang, W.; Mohamed, I.M.A.; Liu, C. Polymer Brush-Grafted ZnO-Modified Cotton for Efficient Oil/Water Separation with Abrasion/Acid/Alkali Resistance and Temperature "Switch" Property. *J. Colloid Interface Sci.* **2020**, *580*, 822–833. [CrossRef] [PubMed]
15. Wenten, I.G.; Himma, N.; Anisah, S.; Prasetya, N. *Membran Superhidrofobik Pembuatan, Karakterisasi, dan Aplikasi*; Departemen Teknik Kimia ITB: Bandung, Indonesia, 2015.
16. Mohammadi, C.; Mahmud, S.; Abdullah, S.M.; Mirzaei, Y. Green Synthesis of ZnO Nanoparticles Using the Aqueous Extract of Euphorbia petiolata and Study of Its Stability and Antibacterial Properties. *Moroc. J. Chem.* **2017**, *5*, 476–484.
17. Yunita, Y.; Nurlina, N.; Syahbanu, I. Sintesis Nanopartikel Zink Oksida (ZnO) dengan Penambahan Ekstrak Klorofil Sebagai Sumber Capping Agent. *Positron* **2020**, *10*, 123–130. [CrossRef]
18. Javed, R.; Zia, M.; Naz, S.; Aisida, S.O.; Ain, N.U.; Ao, Q. Role of Capping Agents in the Application of Nanoparticles in Biomedicine and Environmental Remediation: Recent Trends and Future Prospects. *J. Nanobiotechnol.* **2020**, *18*, 172. [CrossRef]
19. Sari, R.N.; Saridewi, N.; Shofwatunnisa. *Biosintesis dan Karakterisasi Nanopartikel ZnO dengan Ekstrak Rumput Laut Hijau Caulerpa sp.*; Fakultas Sains dan Teknologi UIN Syarif Hidayatullah Jakarta: South Tangerang, Indonesia, 2017.
20. Supin, K.K.; PM, P.N.; Vasundhara, M. Enhanced Photocatalytic Activity in ZnO Nanoparticles Developed Using Novel Lepidagathis ananthapuramensis Leaf Extract. *RSC Adv.* **2023**, *13*, 1497–1515.
21. Barzinjy, A.A. Characterization of ZnO Nanoparticles Prepared from Green Synthesis Using Euphorbia petiolata Leaves. *Eurasian J. Sci. Eng.* **2019**, *4*, 74–83.
22. Singh, B.N.; Rawat, A.K.S.; Khan, W.; Naqvi, A.H.; Singh, B.R. Biosynthesis of Stable Antioxidant ZnO Nanoparticles by Pseudomonas aeruginosa Rhamnolipids. *PLoS ONE* **2014**, *9*, e106937. [CrossRef]
23. Verbič, A.; Šala, M.; Jerman, I.; Gorjanc, M. Novel Green In Situ Synthesis of ZnO Nanoparticles on Cotton using Pomegranate Peel Extract. *Materials* **2021**, *14*, 4472. [CrossRef]
24. Jayachandran, A.; Aswathy, T.R.; Nair, A.S. Green Synthesis and Characterization of Zinc Oxide Nanoparticles Using Cayratia pedata Leaf Extract. *Biochem. Biophys. Rep.* **2021**, *26*, 100995. [CrossRef]
25. Nagajyothi, P.C.; An, T.N.M.; Sreekanth, T.V.M.; Lee, J.; Lee, D.J.; Lee, K.D. Green Route Biosynthesis: Characterization and Catalytic Activity of ZnO Nanoparticles. *Mater. Lett.* **2013**, *108*, 160–163. [CrossRef]

26. Talam, S.; Karumuri, S.R.; Gunnam, N. Synthesis, Characterization, and Spectroscopic Properties of ZnO Nanoparticles. *Int. Sch. Res. Not.* **2012**, *2012*, 372505. [CrossRef]
27. Shamhari, N.M.; Wee, B.S.; Chin, S.F.; Kok, K.Y. Synthesis and Characterization of Zinc Oxide Nanoparticles with Small Particle Size Distribution. *Acta Chim. Slov.* **2018**, *65*, 578–585. [CrossRef] [PubMed]
28. Goh, E.G.; Xu, X.; McCormick, P.G. Effect of Particle Size on the UV Absorbance of Zinc Oxide Nanoparticles. *Scr. Mater.* **2014**, *78*, 49–52. [CrossRef]
29. Kannan, P.; Banat, F. Investigating the Residual Characteristics of Dryer Lint for Developing Resource Recovery Strategies. *SN Appl. Sci.* **2020**, *2*, 1929. [CrossRef]
30. Hospodarova, V.; Singovszka, E.; Stevulova, N. Characterization of Cellulosic Fibers by FTIR Spectroscopy for Their Further Implementation to Building Materials. *Am. J. Anal. Chem.* **2018**, *9*, 303–310. [CrossRef]
31. Portella, E.H.; Romanzini, D.; Angrizani, C.C.; Amico, S.C.; Zattera, A.J. Influence of Stacking Sequence on the Mechanical and Dynamic Mechanical Properties of Cotton/Glass fiber Reinforced Polyester Composites. *Mater. Res.* **2016**, *19*, 542–547. [CrossRef]
32. Kalimuthu, R.; Meenachi Sellan, K.; Antony, D.; Rajaprakasam, S.; Chokkalingam, V.; Chidambaram, P.; Kanagarajan, S. Nanopriming Action of Microwave-Assisted Biofunctionalized ZnO Nanoparticles to Enhance the Growth under Moisture Stress in Vigna radiata. *ACS Omega* **2023**, *8*, 28143–28155. [CrossRef]
33. Mohamed, H.E.A.; Afridi, S.; Khalil, A.T.; Zia, D.; Shinwari, Z.K.; Dhlamini, M.S.; Maaza, M. Structural, Morphological and Biological Features of ZnO Nanoparticles Using *Hyphaene thebaica* (L.) Mart. Fruits. *J. Inorg. Organomet. Polym. Mater.* **2020**, *30*, 3241–3254. [CrossRef]
34. Delcourt, N.; Rébufa, C.; Dupuy, N.; Boukhdoud, N.; Brunel, C.; Abadie, J.; Giffard, I.; Farnet-Da Silva, A.M. Infrared Spectroscopy as a Useful Tool to Predict Land Use Depending on Mediterranean Contrasted Climate Conditions: A Case Study on Soils from Olive-Orchards and Forests. *Sci. Total Environ.* **2019**, *686*, 179–190. [CrossRef]
35. Abd-Elkader, O.H.; Deraz, N.M.; Aleya, L. Rapid Bio-Assisted Synthesis and Magnetic Behavior of Zinc Oxide/Carbon Nanoparticles. *Crystals* **2023**, *13*, 1081. [CrossRef]
36. Sangeetha, G.; Rajeshwari, S.; Venckatesh, R. Green Synthesis of Zinc Oxide Nanoparticles by aloe barbadensis miller Leaf Extract: Structure and Optical Properties. *Mater. Res. Bull.* **2011**, *46*, 2560–2566. [CrossRef]
37. Baharudin, K.B.; Abdullah, N.; Derawi, D. Effect of Calcination Temperature on the Physicochemical Properties of Zinc Oxide Nanoparticles Synthesized by Coprecipitation. *Mater. Res. Express* **2018**, *5*, 125018. [CrossRef]
38. Taurina, W.; Sari, R.; Hafinur, U.C.; Isnindar, S.W. Optimasi Kecepatan dan Lama Pengadukan Terhadap Ukuran Nanopartikel Kitosan-Ekstrak Etanol 70% Kulit Jeruk Siam (*Citrus nobilis* L. var Microcarpa). *Tradit. Med. J.* **2017**, *22*, 16–20. [CrossRef]
39. Sari, R.N.; Chasanah, E.; Nurhayati, N. Nanopartikel Seng Oksida (ZnO) dari Biosintesis Ekstrak Rumput Laut Coklat *Sargassum* sp. dan *Padina* sp. *J. Pascapanen Dan Bioteknol. Kelaut. Dan Perikan.* **2018**, *13*, 41–60. [CrossRef]
40. Batu, M.S. *Pengaruh Penambahan Asam Sulfosuksinat Terhadap Sifat dan Kinerja Membran Komposit Kitosan-Montmorillonit Termodifikasi Silan untuk Aplikasi DMFC*; Institut Teknologi Sepuluh Nopember: Surabaya, Indonesia, 2016.
41. Mahmudah, F.L.; Atun, S. Uji Aktivitas Antibakteri dari Ekstrak Etanol Temukunci (Boesenbergia pandurata) Terhadap Bakteri Streptococcus mutans. *J. Penelit. Saintek* **2017**, *22*, 59–66. [CrossRef]
42. Masadeh, M.M.; Alzoubi, K.H.; Al-Azzam, S.I.; Al-Buhairan, A.M. Possible Involvement of ROS Generation in Vorinostat Pretreatment Induced Enhancement of the Antibacterial Activity of Ciprofloxacin. *Clin. Pharmacol. Adv. Appl.* **2017**, *9*, 119–124. [CrossRef]
43. Paralikar, P. Fabrication of Ketoconazole Nanoparticles and Their Activity Against Malassezia furfur. *Nusant. Biosci.* **2015**, *7*, 43–47. [CrossRef]
44. Singh, P.; Ali, S.W.; Kale, R.D. Antimicrobial Nanomaterials as Advanced Coatings for Self-sanitizing of Textile Clothing and Personal Protective Equipment. *ACS Omega* **2023**, *8*, 8159–8171. [CrossRef]
45. Cheon, J.Y.; Kim, S.J.; Rhee, Y.H.; Kwon, O.H.; Park, W.H. Shape-dependent Antimicrobial Activities of Silver Nanoparticles. *Int. J. Nanomed.* **2019**, *23*, 2773–2780. [CrossRef]
46. Suddhasattya, D.; Dibya, L.M.; Noota, D.; Vasudha, B.; Anshuman, M.; Deepankar, R.; Sriparni, D.; Arijit, M.; Sourav, R.; Rajarshee, S. A Critical Review on Zinc Oxide Nanoparticles: Synthesis, Properties and Biomedical Applications. *Intell. Pharm.* **2024**, *8*, 1–18. [CrossRef]
47. Débora, A.S.; Aimée, G.J.; Pollyana, T.; Albuquerque, W.; Ricardo, B.; Luan, N.; Luciano, C.A.; Guerra, Y.; Josy, A.O.; Padrón-Hernández, E.; et al. Synergistic Effects of Al3+/La3+ co-doped ZnO Photocatalysts for Enhanced Removal of Remazol Red Dye and Diclofenac in Aqueous Solutions. *Colloids Surf. A Physicochem. Eng. Asp.* **2025**, *709*, 136130. [CrossRef]

marine drugs

MDPI

Article

Antimicrobial Activities of Polysaccharide-Rich Extracts from the Irish Seaweed *Alaria esculenta*, Generated Using Green and Conventional Extraction Technologies, Against Foodborne Pathogens

Ailbhe McGurrin [1,2], Rahel Suchintita Das [1,2], Arturo B. Soro [3,4], Julie Maguire [5], Noelia Flórez Fernández [6], Herminia Dominguez [6], Maria Dolores Torres [6], Brijesh K. Tiwari [2] and Marco Garcia-Vaquero [1,*]

[1] Section of Food and Nutrition, School of Agriculture and Food Science, University College Dublin, Belfield, D04 V1W8 Dublin, Ireland; ailbhe.mcgurrin@ucdconnect.ie (A.M.); rahel.suchintitadas@ucdconnect.ie (R.S.D.)
[2] TEAGASC, Food Research Centre, Ashtown, D15 DY05 Dublin, Ireland; brijesh.tiwari@teagasc.ie
[3] Departament de Nutrició, Ciències de l'Alimentació i Gastronomia, Facultat de Farmàcia i Ciències de l'Alimentació, Campus de l'Alimentació de Torribera, University of Barcelona, 08921 Barcelona, Spain; arturoblazquezsoro@ub.edu
[4] Institut de Recerca en Nutrició i Seguretat Alimentària (INSA·UB), University of Barcelona, 08921 Barcelona, Spain
[5] Bantry Marine Research Station Ltd., Gearhies, Bantry, P75 AX07 Co. Cork, Ireland; jmaguire@bmrs.ie
[6] Grupo de Biomasa y Desarrollo Sostenible, Departamento de Ingeniería Química, Facultad de Ciencias, Universidade de Vigo, 32004 Ourense, Spain; noelia.florez@uvigo.gal (N.F.F.); herminia@uvigo.gal (H.D.); matorres@uvigo.gal (M.D.T.)
* Correspondence: marco.garciavaquero@ucd.ie; Tel.: +353-(01)-716-2513

Abstract: A rise in antimicrobial resistance coupled with consumer preferences towards natural preservatives has resulted in increased research towards investigating antimicrobial compounds from natural sources such as macroalgae (seaweeds), which contain antioxidant, antimicrobial, and anticancer compounds. This study investigates the antimicrobial activity of compounds produced by the Irish seaweed *Alaria esculenta* against *Escherichia coli* and *Listeria innocua*, bacterial species which are relevant for food safety. Microwave-assisted extraction (MAE), ultrasound-assisted extraction (UAE), ultrasound–microwave-assisted extraction (UMAE), and conventional extraction technologies (maceration) were applied to generate extracts from *A. esculenta*, followed by their preliminary chemical composition (total phenolic content, total protein content, total soluble sugars) and antimicrobial activity (with minimum inhibitory concentration determined by broth microdilution methods), examining also the molecular weight distribution (via high performance size exclusion chromatography) and oligosaccharide fraction composition (via high-performance liquid chromatography) of the polysaccharides, as they were the predominant compounds in these extracts, aiming to elucidate structure–function relationships. The chemical composition of the extracts demonstrated that they were high in total soluble sugars, with the highest total sugars being seen from the extract prepared with UAE, having 32.68 mg glucose equivalents/100 mg dried extract. Extracts had antimicrobial activity against *E. coli* and featured minimum inhibitory concentration (MIC) values of 6.25 mg/mL (in the case of the extract prepared with UAE) and 12.5 mg/mL (in the case of the extracts prepared with MAE, UMAE, and conventional maceration). No antimicrobial activity was seen by any extracts against *L. innocua*. An analysis of molar mass distribution of *A. esculenta* extracts showed high heterogeneity, with high-molecular-weight areas possibly indicating the presence of fucoidan. The FTIR spectra also indicated the presence of fucoidan as well

as alginate, both of which are commonly found in brown seaweeds. These results indicate the potential of antimicrobials from seaweeds extracted using green technologies.

Keywords: bioactive; antimicrobial; *Alaria esculenta*; polysaccharide; green chemistry; bio-preservative; seaweed

1. Introduction

Antimicrobial resistance is becoming an increasingly concerning issue for human health.The World Health Organisation declared antimicrobial resistance one of the top ten global public health threats, and the landmark 2014 report by economist Jim O'Neill predicts that by 2050 over 10 million global deaths each year will be a result of infection from antimicrobial-resistant microorganisms [1,2]. Moreover, there is a global paucity of new conventional antibiotics in the pipeline which has caused a shift in research towards antibiotics from alternative sources. In recent years, antimicrobial compounds from natural sources, such as those from terrestrial plants and marine organisms, have gained the attention of the research community as a potential resource to obtain novel antimicrobials from relatively unexplored forms of biomass. These novel antimicrobials may be able to act in concert with conventional antibiotics or act as a replacement for antibiotics if their own antimicrobial activity is robust enough.

Macroalgae (seaweeds) have emerged as one such biomass with reported antimicrobial activities [3–5]. The marine environment can often pose extreme conditions, including large variations in abiotic factors such as pH, UV irradiation, and oxygen availability, and biotic factors, such as microbial competitors, and pathogens [6]. Macroalgae produce a wide variety of secondary metabolites, such as polysaccharides, phenolic compounds, lipids, and terpenoids, which act as defence mechanisms against these harsh environmental factors [7,8]. Many of these secondary metabolites from macroalgae have been recently investigated as bioactive compounds or compounds that can be beneficial to human health. Multiple biological activities have been reported from compounds isolated from macroalgae including antioxidant, anti-inflammatory, antimicrobial, anticancer, and anti-hypertensive [3,9,10]. In an ecological context, antimicrobial compounds produced by macroalgae contribute towards their defence against biofouling organisms and pathogens. These antimicrobial compounds may also be useful for pharmaceutical and biotechnological applications. Antimicrobial activities of polysaccharides from macroalgae have been increasingly reported in recent years. Fucoidan and laminarin from brown macroalgae have been described as carbohydrates with strong antimicrobial activity against a wide variety of bacteria [11–13].

Concurrent with the rise in searching for novel antimicrobials from natural sources is the rise in consumer demand for food preservatives derived from natural origins. Ensuring food products do not become contaminated by microorganisms is a cornerstone of food preservative treatments, with the most common foodborne pathogens being represented by *Escherichia coli* and *Listeria* spp. amongst others. Conventionally, food preservatives comprise chemically synthesised agents, including nitrates/nitrites and the antioxidants BHA and BHT [14]. In recent years, consumer preferences have moved away from chemically derived food preservatives; nitrates/nitrites have been linked with carcinogenic properties [15], and, with the increasing number of climate crises, more consumers have shown a preference for agriculture and food processing which does not rely on chemically synthesised compounds. Natural antimicrobial compounds from terrestrial plants, such

as herbs, spices, Cruciferae and hops, have already been investigated as potential bio-preservatives, that is, food preservatives derived from natural origin [3,16]. Thus, bioactive compounds from macroalgae with antimicrobial properties could pose a potential solution to the dual global challenges of lack of novel antimicrobials in the pipeline, and shift in consumer preferences towards bio-preservatives.

Research on bioactive compounds from natural sources has increasingly shifted towards sustainable methods of extracting these compounds from inside the biomass to be studied. Conventional extraction methods often involve temperatures >100 °C, environmentally damaging solvents, and long extraction times [9,17]. Next-generation extraction technologies such as ultrasound-assisted extraction (UAE) [18], microwave-assisted extraction (MAE) [19], and supercritical fluid extraction (SFE) [20] have the ability to preserve the extraction efficiency of bioactive compounds while utilising greener solvents, lower temperatures, and reduced extraction times [5,21,22]. Different extraction technologies can influence the nature and activity of bioactive compounds isolated from seaweeds; Dang, Bowyer [23] reported that MAE resulted in higher phenolic content extractions than UAE, while Garcia-Vaquero, Ravindran [22] reported enhanced phytochemical extraction due to UAE over MAE. Depending on the particular classes of chemical compounds extracted by different technologies (phenolic compounds, polysaccharides, lipids), the associated bioactivities of these compounds will also differ.

Alaria esculenta (winged kelp) is an edible brown macroalgae found in temperate waters of the North Atlantic Ocean, including in Ireland, Scotland, and Greenland [24]. High in minerals and vitamins, is it commercially available as a food product or used in animal feed. Bioactive properties, such as antioxidant- and Cu^{2+}-chelating activities, have been previously reported from this species [24–26], as well as high contents of polyunsaturated fatty acids (PUFAs), which are beneficial for cardiovascular health [27]. While there are emerging studies analysing the antimicrobial activities of extracts of *A. esculenta* [24,28], to the best of the authors' knowledge, its antibacterial activity against the food safety pathogen *E. coli* has not yet been reported.

This study assesses the antimicrobial activity against *E. coli* and *Listeria innocua* of polysaccharide-rich extracts from the Irish brown macroalga *A. esculenta* achieved by green extraction technologies and procedures, by MAE, UAE, and a combination of ultrasound–microwave-assisted extraction (UMAE), and conventional extraction technologies, such as maceration. The molecular weight distribution and oligosaccharide fraction composition of the extracts were also determined, aiming to elucidate the structure–function relationships of these bioactives.

2. Results

2.1. Chemical Composition

The chemical composition of the *A. esculenta* extracts selected for this study were determined in a previous study [29] and are summarised in Figure 1. The extracts selected had high levels of total soluble sugars (TSS), with UAE having the highest TSS levels. In contrast, all the extracts had, in general, low levels of TPC and total proteins ranging between 1.27 and 1.65 mg gallic acid equivalents/100 mg dried extract and between 3.15 and 9.93 mg bovine serum albumin equivalents/100 mg dried extract, respectively.

2.2. Antimicrobial Analyses

2.2.1. Minimum Inhibitory Concentration (MIC) Assay

The results of the MIC assays are depicted in Figure 2. In the case of *E. coli*, the extract prepared with MAE inhibited bacterial growth at concentrations $\geq$ 12.5 mg/mL (MIC), the

extract prepared with UAE had a MIC of 6.25 mg/mL, the extract prepared with UMAE had a MIC of 12.5 mg/mL, and the extract prepared using conventional maceration had an MIC of 12.5 mg/mL. Extracts of *A. esculenta* did not show any antimicrobial activity towards *L. innocua*, even at the highest concentrations tested (25 mg/mL).

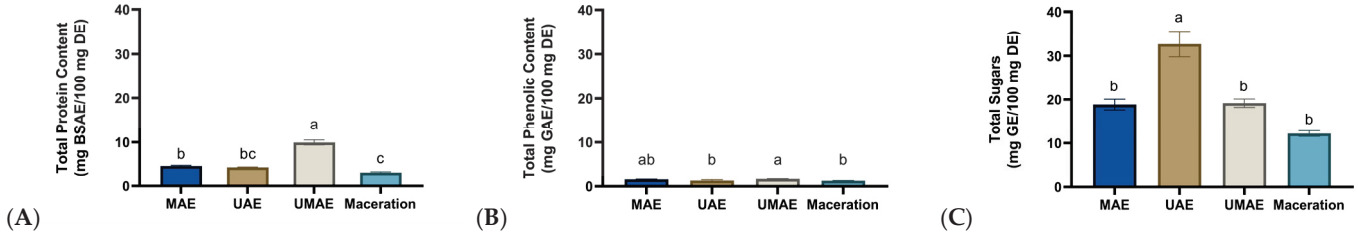

Figure 1. Summary of the (**A**) total protein content, (**B**) total phenolic content, and (**C**) total sugar content of extracts of *A. esculenta* prepared by either microwave-assisted extraction (MAE), ultrasound-assisted extraction (UAE), ultrasound–microwave-assisted extraction (UMAE), or maceration, as reported by [29]. Results are expressed as the average ± standard error of the mean (SEM) with n = 6. Different letters on bars indicate a significant difference ($p < 0.05$) between means. Abbreviations within the figure are as follows: BSAEs (bovine serum albumin equivalents), GAEs (gallic acid equivalents), GEs (glucose equivalents), and DEs (dried extract).

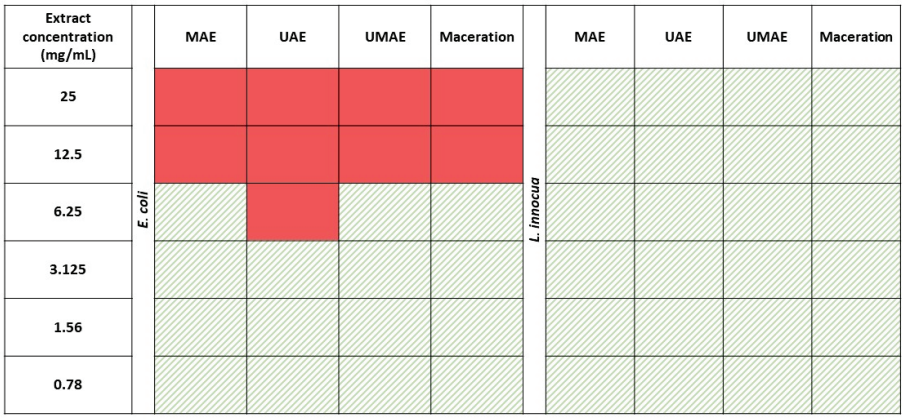

Figure 2. Antimicrobial activity of extracts of *A. esculenta* at concentrations of 0.78–25 mg/mL prepared via either ultrasound-assisted extraction (UAE), microwave-assisted extraction (MAE), a combination of ultrasound–microwave-assisted extraction (UMAE), or maceration extracts against *E. coli* and *L. innocua*. A solid-red colour indicates inhibition of bacterial growth, while green patterned cells indicate bacterial growth.

2.2.2. Bacterial Growth Curves

After initial MIC determination, extracts of *A. esculenta* prepared with either MAE, UAE, UMAE, or maceration were incubated with *E. coli* for 24 h and the optical density was measured every 30 min. The results of this growth curve were subjected to Gompertz modelling, which is detailed in Figure 3. Extrapolation of Gompertz modelling yielded the growth parameter rate (μ_{max}) and lag (λ), as summarised in Table 1. The optical density of *E. coli* alone, with no inhibitory compounds, was recorded as a control. In the presence of extracts of *A. esculenta* at their MIC prepared via either UAE, MAE, UMAE, or maceration, the rate of microbial growth (μ_{max}) did not decrease in comparison with the control. It was observed that the rate of growth of *E. coli* increased significantly in the presence of *A. esculenta*. In contrast, regarding the lag phase (λ) for *E. coli*, it was observed that the addition of the *A. esculenta* extract prepared with MAE extended the length of the lag phase significantly in comparison with the control, where the lag phase of *E. coli* was extended to

5.73 h. The addition of *A. esculenta* that was prepared via UAE, UMAE, and by maceration did not have a significant effect on the lag phase of *E. coli* growth.

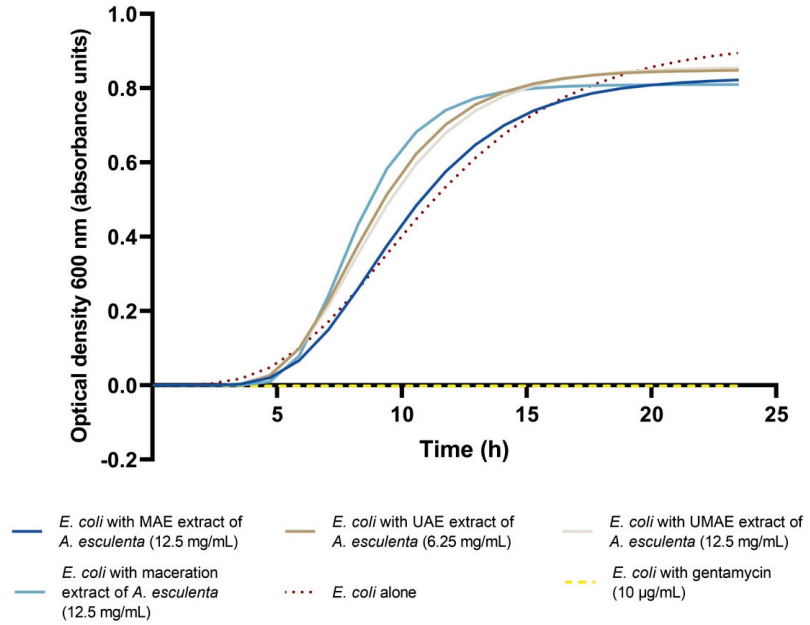

Figure 3. Gompertz modelling of *E. coli* incubated with *A. esculenta* extracts prepared via either microwave-assisted extraction (MAE), ultrasound-assisted extraction (UAE), a combination of ultrasound–microwave-assisted extraction (UMAE), or maceration extraction over 24 h (each line portrays a representative sample). All extracts were applied at their MIC, determined above. A control of *E. coli* incubated with an antibiotic (gentamycin at 10 µg/mL) was also included.

Table 1. Microbial growth parameters (rate (μ_{max}) and lag (λ)) of *E. coli* DSM1103 incubated with extracts of *A. esculenta* extracted with either microwave-assisted extraction (MAE), ultrasound-assisted extraction (UAE), ultrasound–microwave-assisted extraction (UMAE), and maceration. Rate (μ_{max}) and lag (λ), as well as the coefficient of determination (R^2), were extrapolated from Gompertz modelling. Results of μ_{max} and λ are expressed as average ± standard deviation (n = 4). Each extract was applied at its MIC (12.5 mg/mL for MAE, 6.25 mg/mL for UAE, 12.5 mg/mL for both UMAE and maceration extract). Different letters indicate a significant difference ($p < 0.05$) between means. Abbreviations in the table are as follows: optical density at 600 nm measured every 30 min ($OD_{600\ nm}$ 0.5 h^{-1}), (h) hours.

Sample	Rate μ_{max} ($OD_{600\ nm}$ 0.5 h^{-1})	Lag λ (h)	R^2
E. coli DSM1103 alone	0.08 ± 0.003 ^{c}	5.01 ± 0.16 ^{a}	0.98
E. coli + MAE extract	0.12 ± 0.010 ^{b}	5.73 ± 0.17 ^{b}	0.99
E. coli + UAE extract	0.12 ± 0.012 ^{b}	5.15 ± 0.22 ^{a}	0.99
E. coli + UMAE extract	0.12 ± 0.008 ^{b}	5.34 ± 0.04 ^{a}	0.99
E. coli + Maceration extract	0.15 ± 0.011 ^{a}	5.28 ± 0.24 ^{a}	0.99

2.3. Polysaccharide Analyses

2.3.1. Molecular Weight Distribution

The molecular weight profile of extracts of *A. esculenta* is depicted in Figure 4. Two well-defined areas were observed that were associated with low molecular weights (for polymer size < 10 kDa) and medium molecular weights (for polymers between 10 and 10,000 kDa) [30]. Peaks with retention times longer than 45 min were found in the extract achieved by maceration, eluted after the standard dextran of 1000 Da, indicating the

presence of compounds with smaller molecular weights. All samples exhibited peaks above 50 kDa, with higher intensities being found for extracts prepared by UMAE and maceration.

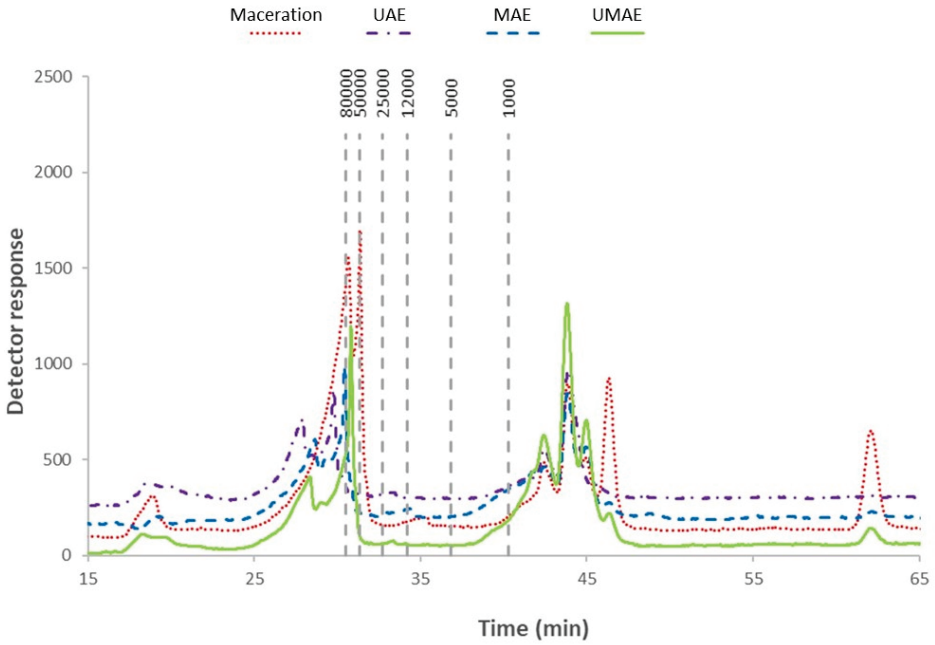

Figure 4. Molecular weight distribution profile of extracts of *A. esculenta* prepared with either microwave-assisted extraction (MAE), ultrasound-assisted extraction (UAE), ultrasound–microwave-assisted extraction (UMAE), or maceration. Marks within the figure represent molecular weight (80,000–1000) in Daltons of the dextran standard.

2.3.2. FTIR

The FTIR spectra of the extracts are exhibited in Figure 5, where the wave number region studied was from 1800 cm^{-1} to 600 cm^{-1}.

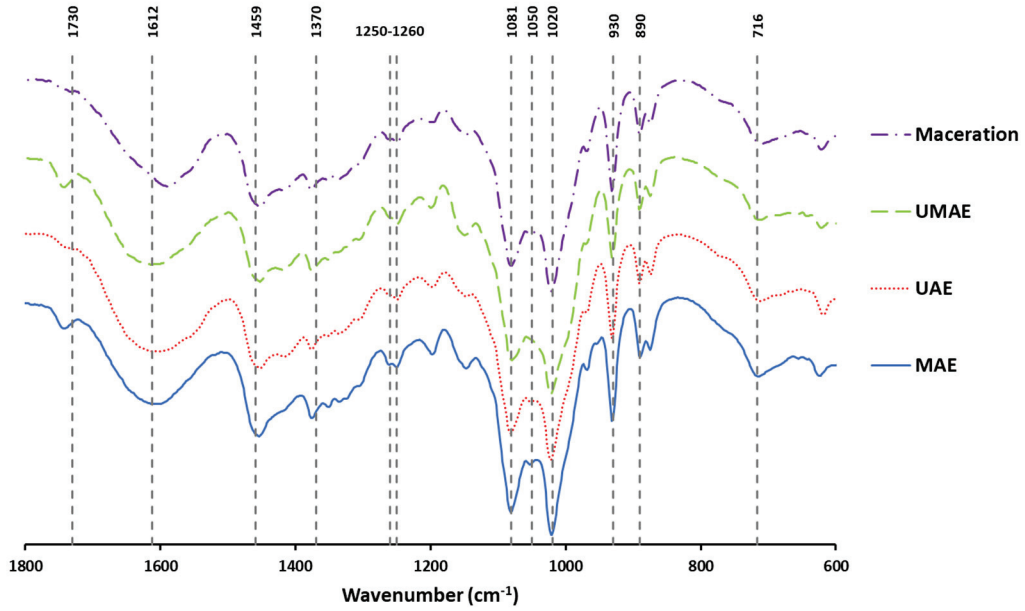

Figure 5. FTIR spectra of extracts obtained from *A. esculenta* using either microwave-assisted extraction (MAE), ultrasound-assisted extraction (UAE), ultrasound–microwave-assisted extraction (UMAE), or maceration.

2.3.3. Oligosaccharide Composition

After hydrolysis, the oligosaccharide composition of extracts from *A. esculenta* were analysed and summarised in Table 2. The extract prepared with UMAE had the largest amounts of oligosaccharides (≈50%), followed by the maceration extract (46%).

Table 2. Monosaccharide composition (g oligosaccharide/100 g dried extract) of extracts generated by either microwave-assisted extraction (MAE), ultrasound-assisted extraction (UAE), ultrasound–microwave-assisted extraction (UMAE), and maceration from the brown seaweed *A. esculenta*. Results are expressed as the average ± standard deviation (n = 3). Different letters indicate a significant difference ($p < 0.05$) between means. The retention time (RT) of compounds was as follows: glucuronic acid (RT 8.29 min), glucose (RT 9.42 min), galactose (RT 10.11 min), rhamnose (RT 10.63 min), and fucose (RT 11.617 min).

Hydrolysed Extract	Glucuronic Acid	Glucose	Galactose	Rhamnose	Fucose
MAE extract	2.25 ± 0.15 ^{a}	15.73 ± 1.05 ^{c}	2.31 ± 0.38 ^{b}	3.66 ± 0.37 ^{c}	0.52 ± 0.10 ^{c}
UAE extract	3.77 ± 0.35 ^{b}	11.07 ± 0.57 ^{d}	1.90 ± 0.25 ^{b}	4.99 ± 0.37 ^{c}	1.28 ± 0.20 ^{b}
UMAE extract	2.38 ± 0.11 ^{a}	33.27 ± 0.67 ^{a}	3.91 ± 0.45 ^{a}	7.18 ± 0.80 ^{b}	2.60 ± 0.04 ^{a}
Maceration extract	4.48 ± 0.44 ^{b}	20.28 ± 0.10 ^{b}	3.94 ± 0.22 ^{a}	12.89 ± 0.48 ^{a}	0.66 ± 0.17 ^{c}

2.4. Pearson's Correlation Matrix and Principal Component Analysis (PCA)

A correlation matrix (Figure 6) was carried out to examine the relationship between oligosaccharide fractions present in extracts of *A. esculenta* and the effects of *A. esculenta* extracts on microbial growth parameters. The increased microbial growth rate (μ_{max}) was correlated with the presence of rhamnose and glucuronic acid ($p < 0.05$). Increased microbial lag time (λ) was associated with glucuronic acid ($p < 0.05$).

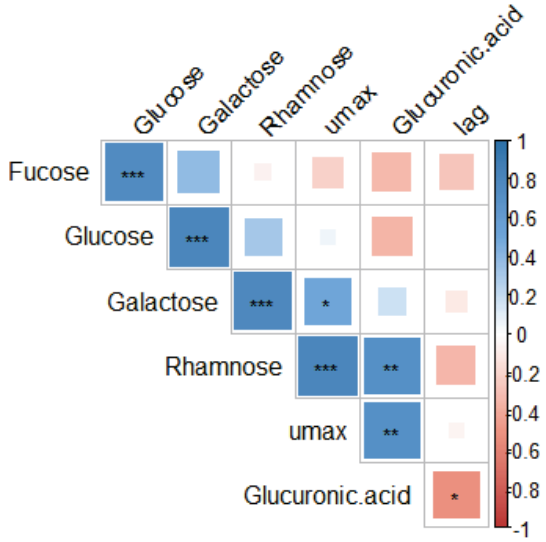

Figure 6. Correlation matrix of the parameters of microbial growth (rate (μ_{max}) and lag (λ)) and the oligosaccharide fraction composition of extracts of *A. esculenta*. Abbreviations in the figure are as follows: μ_{max} (rate), λ (lag). The statistical significance of the correlations is indicated in the figure as * $p < 0.05$, ** $p < 0.01$, *** $p < 0.001$.

A Principal Component Analysis (PCA) (Figure 7) was performed to analyse the similarities and differences between the oligosaccharide fraction composition of *A. esculenta* extracts with respect to the growth parameter rate (μ_{max}) and lag (λ) that were determined in the antimicrobial analysis in this study. Together, the two PCs (principal components)

obtained here explain 77.69% of the cumulative variation in the data, with PC1 accounting for 42.76% of the data variation and PC2 accounting for 34.93%.

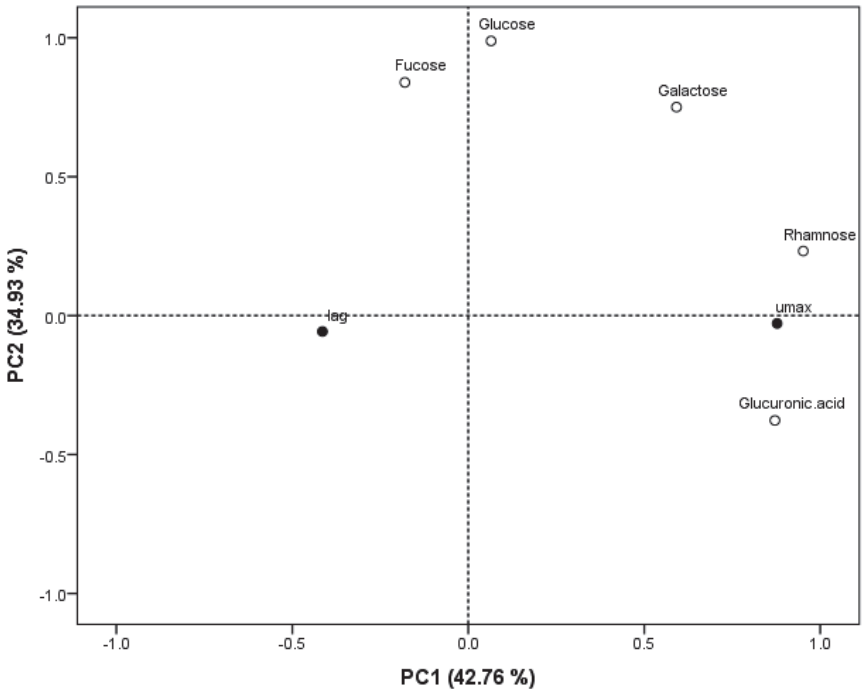

Figure 7. Principal Component Analysis (PCA) scatter plot representing the scores for parameters of microbial growth (rate (μ_{max}) and lag (λ)) and oligosaccharide fraction composition of extracts of *A. esculenta*. Abbreviations in the figure are as follows: μ_{max} (rate), λ (lag).

3. Discussion

3.1. Chemical Composition

In this study, treatment with UAE extracted significantly more TSS than either MAE or UMAE. Macroalgal polysaccharides are often contained within the biomass cell wall, having a structural function, and thus, these compounds can be difficult to extract from the biomass [31]. The application of UAE on the biomass results in a variety of physical and chemical phenomena, including shear forces and cavitation, resulting in compression, rarefaction, and acoustic streaming [18]. Previous work reported an enhanced phytochemical extraction due to UAE over MAE [22], which may be the case here. Interestingly, Schiener, Black [32] reported similar comparative chemical composition results from brown macroalgae, including *A. esculenta*, whereby the extracts with the highest content of polysaccharides, such as laminarin and mannitol, were the lowest in polyphenols (as well as the lowest in protein, ash, and moisture). The authors suggested that this result could be used to guide extraction of brown macroalgae to target extraction of certain chemical compounds.

The antimicrobial activity of macroalgal polysaccharides has been reported previously [11,13,33], particularly from sulfated polysaccharides, such as fucoidan, galactan, and ulvan, and non-sulfated polysaccharides, such as laminarin [34]. The antimicrobial mechanism of action of polysaccharides has been linked to interactions with the bacterial cell wall, resulting in membrane leakage, as well as interactions of negatively charged sulfated polysaccharides with surrounding cationic nutrients in the bacterial medium [33]. However, the antimicrobial activity of these polysaccharides can be influenced by the relative proportion of different polysaccharides within polysaccharide-rich extracts [33,35], as well as differences in the structure of these compounds, including molecular weight

and monosaccharide composition [36,37]. A wide variety of factors can influence the abundance of macroalgal polysaccharides, their chemical structure, and, thus, their biological properties, including seasonal and environmental conditions affecting the biomass (for example, [32] reported higher levels of laminarin in the autumn and lower levels in the winter) as well as the extraction technology and conditions used to generate polysaccharide-rich ingredients (i.e., parameters such as temperature, pH, pressure, extraction time, extraction solvent) [38,39].

3.2. Antimicrobial Analyses

Few studies focus on the biological activities of polysaccharides or polysaccharide-rich extracts from *A. esculenta*, with the majority of studies being focused mainly on alginates and cellulose for industrial applications [40,41] and fucoidan and laminarin. Birgersson, Oftebro [42] sequentially extracted fucoidan and laminarin from *A. esculenta*, but the biological activities of these compounds were not analysed in this study. Similarly, Rhein-Knudsen, Reyes-Weiss, and Horn [43] extracted high-purity fucoidans from *A. esculenta*, but their biological activities were not analysed. Zhu, Healy [28] did characterise the biological activity of laminarin extracted from *A. esculenta* using hydrodynamic cavitation and reported antioxidant, anti-inflammatory, and antimicrobial activity against *Bacillus subtilis*. In the present study, *A. esculenta* extracts contained a greater quantity of TSS than any other chemical components analysed, and thus the authors suggest that the antimicrobial activity of these extracts is related to their polysaccharide-rich nature. It should be noted that crude extracts contain complex mixes of various chemical compounds and small molecules [44,45]. For the scope of this study, only the polysaccharide content of the extracts was further explored. The extent to which other chemical components within the extracts interact with each other to form synergistic/antagonistic antimicrobial activities is unknown. The extract of *A. esculenta* prepared with UAE had the strongest antimicrobial activity against *E. coli* with the lowest numerical MIC of the extracts tested. This extract also had the highest level of TSSs, and it was significantly greater than the other extracts. Thus, the enhanced antimicrobial effect from this extract could be attributed to the abundance of total sugars present in this extract. Antimicrobial activity from extracts of macroalgae have been reported on in numerous studies [46–48]. Polysaccharides have been identified as one of the main classes of bioactive compounds within macroalgae that possess antimicrobial activity [11,13], with the main studies being represented by sulfated polysaccharides [49]. The degree of antimicrobial activity of isolated polysaccharides or polysaccharide-rich extracts from macroalgae can vary greatly depending on the species of microorganism targeted and the methods implemented [50].

The antimicrobial activity of *A. esculenta* (crude extracts or isolated compounds) remains understudied. Most studies investigating biological activity from *A. esculenta* extracts have focused on antioxidant [24], ACE-inhibiting, and Fe^{2+} or Cu^{2+} activity [27]. Sapatinha, Oliveira [24] tested crude extracts from four seaweed species, including *A. esculenta*, for antimicrobial activity against *Citrobacter freundii*, *Enterococcus faecalis*, *E. coli*, *L. monocytogenes*, *Pseudomonas aeruginosa*, *Salmonella* Typhimurium, and *Staphylococcus aureus*. No antimicrobial activity was reported from *A. esculenta* extracts nor the other seaweed species tested. Zhu, Healy [28] reported antimicrobial activity from laminarin extracted from *A. esculenta*, where laminarin reduced the rate of growth of *B. subtilis*. This study also tested the activity of the laminarin against *E. coli* and *Saccharomyces cerevisiae* and found no antimicrobial activity. Thus, as far as the authors are aware, the present study is the first report of antimicrobial activity by polysaccharides from *A. esculenta* against the important food pathogen *E. coli*.

The current study reports MIC values of 6–12.5 mg/mL from this polysaccharide-rich extract of *A. esculenta*, which is in a similar order of magnitude to MIC values reported in certain other studies. Rajauria, Jaiswal [51] reported an MIC of 60 mg/mL from a crude extract of *Himanthalia elongata* against a range of bacteria. Otero, Quintana [52] observed an IC_{50} of 2.24 mg/mL against *E. coli*, and Liu, Liu [33] reported an MIC of 6 mg/mL against *E. coli* from a depolymerised fucoidan fraction. Other studies showed more potent antimicrobial activity from macroalgal extracts: Nshimiyumukiza, Kang [53] reported an MIC of 256 μg/mL from an extract of the brown seaweed *Ecklonia cava*, Martins, Nedel [10] reported an MIC of 500 μg/mL against *E. faecalis* from an extract of *Cystosphaera jacquinotii*, and Palanisamy, Vinosha [13] studied a crude fucoidan fraction which had an MIC of 200 μg/mL against *E. coli*. Generally, large variations can be seen in the results of the antimicrobial activity of macroalgal extracts, with certain studies reporting extensive antimicrobial activity against multiple microorganisms [37,54] while others report antimicrobial activity towards some microorganisms but not others [55]. The extent of antimicrobial activity from macroalgal polysaccharides, and macroalgal extracts in general, is influenced by a variety of factors, such as chemical structures and conformation, molecular weight, charge density, and sulphate content in the case of sulphated polysaccharides [4]. While certain studies have reported broad spectrum antimicrobial activity from macroalgal extracts and macroalgal polysaccharides [56], others have shown targeted effects on either Gram-negative or Gram-positive bacteria. The current study observed antimicrobial activity against the Gram-negative *E. coli* only, with no activity against the Gram-positive *Listeria innocua*. Amorim, Rodrigues [57] also reported antimicrobial activity from macroalgal polysaccharides against *E. coli* but not against certain Gram-positive bacteria tested (*B. subtilis*, *S. aureus*). However, this study also reported no antimicrobial activity against other Gram-negative bacteria, including *P. aeruginosa*. Interestingly, Yamashita, Yoshiko, and Shimizu [58] reported antimicrobial activity from macroalgal carrageenan against *E. coli* and other Gram-negative and Gram-positive bacteria but not *Listeria* spp. Other studies found no antimicrobial effects on Gram-negative bacteria by macroalgal extracts [12]. Overall, the results of this study indicate promising antimicrobial activity for the brown seaweed *A. esculenta* against *E. coli*, a relevant pathogen for food safety.

As was observed in the bacterial growth curves in this study, previous studies also observed an increase in microbial biomass after the addition of antimicrobial extracts of a natural origin. Carneiro, Dos Santos [59] studied the antimicrobial activity of casbane diterpene (CD) isolated from a plant extract and reported an increase in *P. aeruginosa* biomass upon addition of the CD at sub-inhibitory levels. The authors suggested that this may be due to an increased production of exopolysaccharides by *P. aeruginosa* as a response to treatment of CD. Cabral, Mondala [37] reported a similar result with increased microbial biomass after treatment with a fucoidan-rich extract from *Fucus vesiculosus*. Furthermore, Jun, Jung [12] investigated the antimicrobial activity of sulphated polysaccharides from macroalgae and reported that fucoidan isolated from *F. vesiculosus did* not possess a direct killing effect for microbial cells. Rather, the authors reported an indirect antimicrobial effect which they suggest was caused by the ability of fucoidan to trap nutrients in the medium. Future research should explore microbe–antimicrobial agent interactions at a molecular level to better understand mechanisms of action beyond direct killing effects. The extension of the lag phase of *E. coli* by extracts of *A. esculenta* indicates the bacteriostatic nature of these extracts and opens avenues of further development of these extracts in the food industry as food preservatives, a household cleaning agent, or as a pharmaceutical antibacterial agent.

3.3. Polysaccharide Analysis

In the molecular weight distribution profile of *A. esculenta* extracts, a low-molecular-weight area (<10 kDa) and a medium-molecular-weight area (between 10 and 10,000 kDa) were defined. Gómez-Ordóñez, Jiménez-Escrig, and Rupérez [60] also reported the high heterogeneity of the molecular weight of polysaccharides present in the brown seaweed *Saccharina latissima.* High performance size exclusion chromatography (HPSEC) yielded four defined peaks associated with 5.7–5.8 kDa (which the authors tentatively identified as laminarin), 23–27 kDa, 338–351 kDa, and 2111–2190 kDa. The authors attributed the heterogeneity of polysaccharides in *S. latissima* to the complex polysaccharide composition of brown macroalgae as well as the extraction process and time of collection. The differences in molecular weight profiles observed here could be due to the different extraction technologies applied. For example, the lower-molecular-weight peaks observed in the maceration extract could represent heat-sensitive compounds which were degraded in the other treatments where either ultrasound and/or microwaves were applied. Tsubaki, Oono [61] reported that conditions of microwave extraction can impact polysaccharide molecular weight and viscosity in *Ulva* spp., while Rodriguez-Jasso, Mussatto [62] noted that fucoidan yields from *F. vesiculosus* were improved by increasing pressure within the microwave extraction system. Laminarin has a low molecular weight of around 4–5 kDa [63], which may be representative of the low-molecular-weight band observed in this study. The medium-molecular-weight band (between 10 and 10,000 kDa) may be representative of fucoidans, as this group of compounds are often characterised by high molecular weights reaching 950 kDa [64] but which can span a variety of molecular weights depending on specific extraction conditions [65]. Fucoidans belong to the family fucose-rich sulphated polysaccharides, compounds of heterogenous polymeric structure of sulphated fucose or other monosaccharides [66]. Among other bioactivities (antioxidant, anticancer) [65,67], the antimicrobial activity of fucoidans has been reported [12,68,69]. Palanisamy, Vinosha [13] reported the antibacterial activity of a fucoidan fraction isolated from *Sargassum polycystum* against *E. coli*, with an MIC of 200 mg/mL. The same study also reported antibacterial activity against *P. aeruginosa*, *Streptococcus mutans*, and *S. aureus.* Liu, Liu [33] reported the antibacterial activity of fucoidan against *E. coli*, where a depolymerised fucoidan isolated from *Saccharina japonica* (formerly *Laminaria japonica*) inhibited *E. coli* and *S. aureus*. This study by Liu, Liu [33] reported stronger antibacterial activity against a Gram-negative organism (*E. coli*) than a Gram-positive organism (*S. aureus*), similar to what is being reported here in this study, where antibacterial activity is observed against *E. coli* but not *L. innocua*. Cabral, Mondala [37] observed antibacterial activity against *E. coli* from a fucoidan-rich extract from the brown seaweed *F. vesiculosus*, as well as antibacterial activity against pathogens related to food safety such as *B. subtilis*, *P. aeruginosa*, and *L. innocua*.

In the FTIR spectra, the band obtained at 716 cm^{-1} was associated with C-O-C bending vibrations and glycosidic linkages, and the peak obtained at 890 cm^{-1} was assigned to anomeric C-H of β-galactopyranosyl residues [70]. The peak obtained at 930 cm^{-1} was reported as uronic acid residues (C-O stretching vibration) [71]. The bands observed at 1020 and 1081 cm^{-1} can be related to stretching vibrations of the pyranose ring (C-O and C-C), and a slight peak at 1050 cm^{-1} (observed in the extract prepared with MAE and maceration extracts) was attributed to a stretching vibration of C-O-C [72]. The bands observed at 1250 cm^{-1} and 1260 cm^{-1} can be attributed to the presence of asymmetric O=S=O stretching vibrations of a sulphate group and to the stretching vibration of the S-O of sulphate, respectively [73], that are indicative of the presence of fucoidan [74]. The peak observed at 1370 cm^{-1} is related to the -C-O=S stretching vibration and to the -C-O-S group [74]. The bands at 1459 and 1612 cm^{-1} could be associated with carboxyl groups [75]. The small

signal obtained at 1730 cm^{-1} is characteristic of alginate and is associated with carboxylic acid in ester form (C=O) [71]. Fucoidan and alginate are some of the most common polysaccharides reported from brown macroalgae [74], with a variety of bioactivities being associated with these compounds (antioxidant, anti-inflammatory, antimicrobial).

An oligosaccharide composition analysis showed that the extract prepared with UMAE had the largest amounts of oligosaccharide followed by the maceration extract. A similar value of the total quantity of these compounds was also achieved by Cebrián-Lloret, Metz [76]. In both cases, glucose was the main saccharide (highest for the extract prepared with UMAE), and similar values were obtained using acidic extraction [77]. This behaviour is associated with the extraction process [78,79]. Brown macroalgae, such as *A. esculenta*, have been reported to have glucose as the main oligomer, with the major reported saccharides being laminarin and fucoidan [80,81].

3.4. Pearson's Correlation Matrix and Principal Component Analysis (PCA)

A correlation matrix was carried out to examine the relationship between oligosaccharide fractions present in extracts of *A. esculenta* and the effects of *A. esculenta* extracts on microbial growth parameters. Increased microbial growth rate (μ_{max}) was correlated with the presence of rhamnose and glucuronic acid ($p < 0.05$). Increased microbial lag time (λ) was associated with glucuronic acid ($p < 0.05$), which may be related to the antimicrobial effect of these extracts on *E. coli.* Glucuronic acid is one of the main components of ulvans, polysaccharides from green seaweeds which have reported antimicrobial activity [82–84].

Principal Component Analysis (PCA) was performed to analyse the similarities and differences between the oligosaccharide fraction composition of *A. esculenta* extracts with respect to the growth parameter rate (μ_{max}) and lag (λ), that were determined in the antimicrobial analysis in this study. PC1 appears to cluster the microbial growth rate (μ_{max}) with the presence of the oligosaccharide fractions glucuronic acid, rhamnose, galactose, and glucose, while the microbial lag (λ) appears to be clustered with the presence of fucose. PC2 further explains the variation in data by appearing to relate fucose, glucose, galactose and rhamnose to each other, while μ_{max} and λ appear to be related with the presence of glucuronic acid. A correlation of lag (λ) with fucose indicates that the presence of fucose may be related to increased lag times of microbial growth, and thus fucose may be representative of the antimicrobial effects of *A. esculenta* extracts against *E. coli.* This is supported by numerous reports of the antimicrobial activity observed from fucose-containing polysaccharides from macroalgae, or fucoidans, in macroalgae [4,21,33]. Future studies should aim to further purify extracts of *A. esculenta* that show antimicrobial activity to further elucidate the bioactivities of this species.

4. Materials and Methods

4.1. Extract Preparation and Chemical Composition

Extracts explored in this study were generated in a previous study [29]. Fresh *A. esculenta* was supplied by Dúlra Ltd. and harvested from Blacksod Bay, Mayo, Ireland, in April 2021. Extracts of *A. esculenta* were prepared using MAE, UAE, or UMAE using an IDCO E200 extractor (IDCO SAS, Marseille, France) (Figure 8 below) of 1.25 L capacity, which allows for UAE, MAE, or simultaneous UMAE. Fresh seaweed samples were extracted using distilled water at a seaweed–solvent ratio 1:10 w/v and extracted by multiple sessions of MAE, UAE, UMAE, and maceration using multiple conditions. The mixtures were filtered and the extracts were freeze-dried and stored in vacuum-packed containers at -20 °C for further analyses. Following the determination of their chemical composition through total soluble sugars [85], total phenolic content [86], and total protein [87], the

extracts achieved by UAE (200 W ultrasound power for 20 min), MAE (1340 W microwave power for 20 min), UMAE (200 W ultrasound power and 1340 W microwave power for 20 min), and control (maceration for 20 min) were selected for this antimicrobial study on the basis of their high content in polysaccharides (chemical composition results above in Figure 1).

Figure 8. E200 Ultrasound–Microwave extractor (IDCO, Marseille, France).

4.2. Antimicrobial Analyses

4.2.1. Microorganisms

The antimicrobial activity of *A. esculenta* extracts was tested using *E. coli* DSM1103 and *L. innocua* NCTC 11288. These two bacterial species were selected to model the pathogenic bacteria (*E. coli* and *L. monocytogenes*) due to their biological similarity [88,89]. Bacterial strains were obtained from Teagasc National Food Research Centre (Dublin, Ireland) and were maintained at −80 °C in 25% glycerol. Each bacterial strain was streaked onto Tryptone Soy Agar (TSA, Oxoid, Basingstoke, UK) and incubated at 37 °C for 24 h in aerobic conditions. Then, a single colony was used to inoculate 10 mL Tryptone Soy Broth (TSB, Oxoid, UK), which was incubated at 37 °C for 20 h in aerobic conditions.

4.2.2. Minimum Inhibitory Concentration (MIC) Assay

The minimum inhibitory concentrations of the extracts of *A. esculenta* were determined according to an established protocol [90]. Assays were performed in 96-well microtitre plates. Briefly, bacteria were grown to a mid-exponential phase in overnight cultures, diluted in Maximum Recovery Diluent (MRD, Oxoid, UK) and 50 µL used to inoculate microtitre plates. The concentration of bacteria used was confirmed by enumerating serial dilutions of bacteria which were plated on TSA and incubated at 37 °C for 24 h in aerobic conditions. Extracts of *A. esculenta* were diluted in sterile water, and 50 µL were added to

the microtitre plate wells to achieve the following concentrations of extract to be tested: 25, 12.5, 6.25, 3.12, 1.56, and 0.78 mg/mL. An amount of 100 µL Muller-Hinton Broth (MHB, Oxoid, UK) was added to all wells. Wells containing MHB alone, bacteria incubated with MHB only, and bacteria incubated with gentamycin (10 µg/mL) were included as controls. The microtitre plates were covered and incubated at 37 °C for 24 h. Then, 40 µL of iodonitrotetrazolium chloride (INT, Sigma-Aldrich, St. Louis, MO, USA) at 0.2 mg/mL was added to each well as an indicator of microbial growth [91], which turns a pink colour in the presence of microbial growth. The MIC was determined as the lowest concentration of each extract where no pink colour was observed after incubation of 2 h with INT dye. All measurements were carried out in triplicate on independent days with at least three replicates per experiment.

4.2.3. Bacterial Growth Curve Analysis

The antimicrobial effects of extracts of *A. esculenta* over time were analysed via a bacterial growth curve analysis using 96-well microtiter plates. Briefly, 50 µL extracts of *A. esculenta* at their MIC were incubated with 50 µL of either *E. coli* or *L. innocua* which was grown to a mid-exponential phase, as above. An amount of 100 µL MHB were added to each well. Wells containing MHB alone, bacteria incubated with MHB only, and bacteria incubated with gentamycin (10 µg/mL) were included as controls. Microtitre plates were covered and incubated at 37 °C for 24 h in a plate reader (Tecan, Männedorf, Switzerland), with optical density (OD) measurements at 600 nm being conducted every 30 min. All measurements were performed in triplicate on independent days with at least three replicates per experiment.

4.3. Characterisation of Polysaccharides

4.3.1. Molar Mass Distribution

The profile associated with the molar mass distribution of the samples was estimated by High Performance Size Exclusion Chromatography (SEC) using two columns in series: TSKGel G3000PW$_{XL}$ and TSKGel G2500PW$_{XL}$ (300 × 7.8 mm) with a pre-guard column PWX-guard (40 × 6 mm) (Tosoh Bioscience, Griesheim, Germany) performed in a 1100 series Hewlett-Packard chromatograph (Agilent, Waldbronn, Germany). Samples were previously dialysed using membrane tubing (MWCO 0.5 kDa, SpectrumLabs, San Francisco, CA, USA). The detector used was a refractive index, and the mobile phase was Milli-Q water at 0.4 mL/min at 70 °C. The standards used were dextrans from 1000 to 80,000 g/mol (Honeywell Fluka, Charlotte, NC, USA).

4.3.2. Fourier-Transform Infrared Spectroscopy (FTIR)

The characteristic bands associated with different groups were determined by FTIR. The lyophilised extracts were blended with KBr and dried for 30 min using an infrared lamp. The measurements were performed on a Bruker IFS 28 Equinox (Billerica, MA, USA), and the software for data acquisition was OPUS-2.52. The range of the spectra was from 400 to 2000 cm^{-1} (25 scans/min).

4.3.3. Oligosaccharide Contents

The extracts were dissolved in Milli-Q water, hydrolysed (4% sulfuric acid, 121 °C, 20 min), and dialysed (membrane tubing MWCO 0.5 kDa, SpectrumLabs, San Francisco, CA, USA). Monosaccharide contents were determined by high-performance liquid chromatography (HPLC) using a 1100 series Hewlett-Packard chromatograph (Agilent, Waldbronn, Germany) equipped with a refractive index detector and a Aminex HPX-87H column with

pre-guard (300 × 7.8 mm, BioRad, Hercules, CA, USA). The separation of the monosaccharides was performed at 60 °C using sulfuric acid (0.003 M) as a mobile phase at 0.6 mL/min. The quantification was expressed as oligossacharide.

4.4. Statistical Analyses

For biochemical characterisation and MIC data, statistical analysis was carried out in SPSS version 23.0. Differences in biochemical composition and microbial growth were analysed by ANOVA with Tukey HSD post hoc tests. Growth parameters from bacterial growth curve analysis were determined using DMFit Excel software (version 3.5, ComBase, Wyndmoor, PA, USA). Optical density and incubation time were plotted on DMFit and fitted to the Gompertz model [92], where the goodness of fit was determined by a coefficient of regression (R^2). The primary growth parameters, rate (μmax) (optical density/30 min interval), and lag (λ) (h) were determined from extrapolation of the model. The correlations between the growth and composition parameters were analysed in R [93] version 4.3.2 (accessed on 4 April 2024), while "ggplot2" and "corrplot" were used to generate the Pearson's correlation matrix [94] and "cor.mtest" was used to include the *p*-values within the matrix. The variance within the full data set was explored by a principal component analysis (PCA) using Varimax rotation with Kaiser normalisation to extract the eigenvalues values of the components using SPSS version 23.0.

5. Conclusions

Extracts of *A. esculenta*, a brown macroalgae common in the North Atlantic, have been shown in this study to possess antimicrobial activity against *E. coli*, one of the most common pathogens relevant for food safety. The authors suggest that the observed antimicrobial activity is due to the quantity of polysaccharides in the extracts, which are known to contribute to the antimicrobial activity of seaweeds. The strongest antimicrobial activity from these extracts was observed from the extract prepared using UAE with an MIC of 6.25 mg/mL. No antimicrobial activity was seen against *L. innocua*. Further polysaccharide analyses of these extracts indicated the presence of fucoidan and laminarin, some of the most widely reported polysaccharides present in brown macroalgae with associated bioactivities. Future research should focus on further fractionation of these extracts to elucidate antimicrobial compounds and further examination of these extracts in an applied setting relevant for food safety. For example, these extracts may be investigated for use as an antimicrobial agent incorporated in the formulation of food products, during the food washing process, or as part of active food packaging (for example incorporated into compostable plastic wrap). In conclusion, this study indicates the potential for extracts of the brown seaweed *A. esculenta* to be used as an antimicrobial agent in food safety settings.

Author Contributions: A.M.: Methodology, Formal analysis, Investigation, Writing—Original Draft, Writing—Review and Editing, Visualisation, Project administration, Funding acquisition. R.S.D.: Methodology, Investigation, Writing—Review and Editing. A.B.S.: Methodology, Writing—Review and Editing. J.M.: Supervision, Writing—Review and Editing, Funding acquisition. N.F.F.: Investigation, Writing—Review and Editing. H.D.: Investigation, Writing—Review and Editing. M.D.T.: Investigation, Writing—Review and Editing. B.K.T.: Conceptualisation, Methodology, Resources, Supervision, Project administration, Funding acquisition. M.G.-V.: Conceptualisation, Methodology, Formal analysis, Writing—Review and Editing, Visualisation, Supervision, Project administration, Funding acquisition. All authors have read and agreed to the published version of the manuscript.

Funding: Ailbhe McGurrin acknowledges funding by Irish Research Council Enterprise Partnership Scheme Postgraduate Scholarship (code: EPSPG/2021/154). The authors acknowledge the funding received from the project AMBROSIA funded by the Department of Agriculture Food and the Marine

(DAFM) under the umbrella of the European Joint Programming Initiative "A Healthy Diet for a Healthy Life" (JPI-HDHL) and of the ERA-NET Cofund ERA HDHL (GA No 696295 of the EU Horizon 2020 Research and Innovation Programme); and IMPRESS project co-funded by the European Union (GA No. 101084437). Authors acknowledge Consellería de Cultura, Educación e Universidade da Xunta de Galicia (GRC-ED431C 2022/08) and measurements performed at the services of analysis of Universidade de Vigo (CACTI). Noelia Flórez-Fernández acknowledges to the Xunta de Galicia for her postdoctoral grant (ED481D-2022/018). María Dolores Torres thanks the Ministry of Science, Innovation and Universities (Spain) for her postdoctoral grant (RYC2018-024454-I).

Institutional Review Board Statement: Not applicable.

Data Availability Statement: Data will be made available upon request.

Acknowledgments: The authors would like to thank Des Walsh for the cultivation of bacterial strains used in this study.

Conflicts of Interest: Ailbhe McGurrin is pursuing her Ph.D. in collaboration with Bantry Marine Research Station Ltd., which owns and operates seaweed cultivation sites in Co. Cork, Ireland. Julie Maguire is the Research Director at Bantry Marine Research station Ltd. As far as the authors are aware no conflict of interest has arisen throughout this research study. Bantry Marine Research station Ltd. has no role in the study design, collection, analysis, interpretation of data, the writing of this article or the decision to submit it for publication.

References

1. O'Neill, J. Antimicrobial resistance: Tackling a crisis for the health and wealth of nations. *Rev. Antimicrob. Resist.* **2014**, 5–6.
2. Kumar, S. Antimicrobial resistance: A top ten global public health threat. *EClinicalMedicine* **2021**, *41*, 101221.
3. Cabral, E.M.; Oliveira, M.; Mondala, J.R.M.; Curtin, J.; Tiwari, B.K.; Garcia-Vaquero, M. Antimicrobials from seaweeds for food applications. *Mar. Drugs* **2021**, *19*, 221. [CrossRef] [PubMed]
4. Perez, M.J.; Falque, E.; Dominguez, H. Antimicrobial action of compounds from marine seaweed. *Mar. Drugs* **2016**, *14*, 52. [CrossRef] [PubMed]
5. Silva, A.; Silva, S.A.; Carpena, M.; Garcia-Oliveira, P.; Gullon, P.; Barroso, M.F.; Prieto, M.A.; Simal-Gandara, J. Macroalgae as a Source of Valuable Antimicrobial Compounds: Extraction and Applications. *Antibiotics* **2020**, *9*, 642. [CrossRef]
6. Kurhekar, J.V. Antimicrobial lead compounds from marine plants. In *Phytochemicals as Lead Compounds for New Drug Discovery*; Elsevier: Amsterdam, The Netherlands, 2020; pp. 257–274. [CrossRef]
7. Mateos, R.; Perez-Correa, J.R.; Dominguez, H. Bioactive properties of marine phenolics. *Mar. Drugs* **2020**, *18*, 501. [CrossRef] [PubMed]
8. Morais, M.F.d.J.R.; Rui Manuel Santos Costa De, M.; Alcina Maria Miranda Bernardo, d. Bioactivity and Applications of Sulphated Polysaccharides from Marine Microalgae. *Mar. Drugs* **2013**, *11*, 233–252. [CrossRef] [PubMed]
9. Getachew, A.T.; Jacobsen, C.; Holdt, S.L. Emerging Technologies for the Extraction of Marine Phenolics: Opportunities and Challenges. *Mar. Drugs* **2020**, *18*, 389. [CrossRef] [PubMed]
10. Martins, R.M.; Nedel, F.; Guimaraes, V.B.S.; da Silva, A.F.; Colepicolo, P.; de Pereira, C.M.P.; Lund, R.G. Macroalgae Extracts From Antarctica Have Antimicrobial and Anticancer Potential. *Front. Microbiol.* **2018**, *9*, 412. [CrossRef]
11. Kadam, S.U.; O'Donnell, C.P.; Rai, D.K.; Hossain, M.B.; Burgess, C.M.; Walsh, D.; Tiwari, B.K. Laminarin from Irish Brown Seaweeds *Ascophyllum nodosum* and *Laminaria hyperborea*: Ultrasound Assisted Extraction, Characterization and Bioactivity. *Mar. Drugs* **2015**, *13*, 4270–4280. [CrossRef]
12. Kim, J.-Y.J.; Min-Jeong, J.; In-Hak, J.; Koji, Y.; Yuji, K.; Byoung, M. Antimicrobial and Antibiofilm Activities of Sulfated Polysaccharides from Marine Algae against Dental Plaque Bacteria. *Mar. Drugs* **2018**, *16*, 301. [CrossRef]
13. Palanisamy, S.; Vinosha, M.; Rajasekar, P.; Anjali, R.; Sathiyaraj, G.; Marudhupandi, T.; Selvam, S.; Prabhu, N.M.; You, S. Antibacterial efficacy of a fucoidan fraction (Fu-F2) extracted from *Sargassum polycystum*. *Int. J. Biol. Macromol.* **2019**, *125*, 485–495. [CrossRef] [PubMed]
14. Jiang, Z.; Chen, Y.; Yao, F.; Chen, W.; Zhong, S.; Zheng, F.; Shi, G. Antioxidant, antibacterial and antischistosomal activities of extracts from *Grateloupia livida* (Harv). Yamada. *PLoS ONE* **2013**, *8*, e80413. [CrossRef] [PubMed]
15. Felter, S.P.; Zhang, X.; Thompson, C. Butylated Hydroxyanisole: Carcinogenic food additive to be avoided or harmless antioxidant important to protect food supply? *Regul. Toxicol. Pharmacol.* **2021**, *121*, 104887. [CrossRef]

16. Arulkumar, A.; Satheeshkumar, K.; Paramasivam, S.; Rameshthangam, P.; Miranda, J.M. Chemical biopreservative effects of red seaweed on the shelf life of black tiger shrimp (*Penaeus monodon*). *Foods* **2020**, *9*, 634. [CrossRef] [PubMed]
17. Cikos, A.M.; Jokic, S.; Subaric, D.; Jerkovic, I. Overview on the Application of Modern Methods for the Extraction of Bioactive Compounds from Marine Macroalgae. *Mar. Drugs* **2018**, *16*, 348. [CrossRef] [PubMed]
18. Tiwari, B.K. Ultrasound: A clean, green extraction technology. *TrAC Trends Anal. Chem.* **2015**, *71*, 100–109. [CrossRef]
19. Kadam, S.U.; Tiwari, B.K.; O'Donnell, C.P. Application of novel extraction technologies for bioactives from marine algae. *J. Agric. Food Chem.* **2013**, *61*, 4667–4675. [CrossRef] [PubMed]
20. Esquivel-Hernandez, D.A.; Lopez, V.H.; Rodriguez-Rodriguez, J.; Aleman-Nava, G.S.; Cuellar-Bermudez, S.P.; Rostro-Alanis, M.; Parra-Saldivar, R. Supercritical Carbon Dioxide and Microwave-Assisted Extraction of Functional Lipophilic Compounds from *Arthrospira platensis*. *Int. J. Mol. Sci.* **2016**, *17*, 658. [CrossRef] [PubMed]
21. Alboofetileh, M.; Rezaei, M.; Tabarsa, M.; Ritta, M.; Donalisio, M.; Mariatti, F.; You, S.; Lembo, D.; Cravotto, G. Effect of different non-conventional extraction methods on the antibacterial and antiviral activity of fucoidans extracted from *Nizamuddinia zanardinii*. *Int. J. Biol. Macromol.* **2019**, *124*, 131–137. [CrossRef]
22. Garcia-Vaquero, M.; Ravindran, R.; Walsh, O.; O'Doherty, J.; Jaiswal, A.K.; Tiwari, B.K.; Rajauria, G. Evaluation of ultrasound, microwave, ultrasound–microwave, hydrothermal and high pressure assisted extraction technologies for the recovery of phytochemicals and antioxidants from brown macroalgae. *Mar. Drugs* **2021**, *19*, 309. [CrossRef] [PubMed]
23. Dang, T.T.; Bowyer, M.C.; Van Altena, I.A.; Scarlett, C.J. Comparison of chemical profile and antioxidant properties of the brown algae. *Int. J. Food Sci. Technol.* **2017**, *53*, 174–181. [CrossRef]
24. Sapatinha, M.; Oliveira, A.; Costa, S.; Pedro, S.; Gonçalves, A.; Mendes, R.; Bandarra, N.M.; Pires, C. Red and brown seaweeds extracts: A source of biologically active compounds. *Food Chem.* **2022**, *393*, 133453. [CrossRef] [PubMed]
25. Afonso, C.; Matos, J.; Guarda, I.; Gomes-Bispo, A.; Gomes, R.; Cardoso, C.; Gueifão, S.; Delgado, I.; Coelho, I.; Castanheira, I.; et al. Bioactive and nutritional potential of *Alaria esculenta* and *Saccharina latissima*. *J. Appl. Phycol.* **2021**, *33*, 501–513. [CrossRef]
26. Einarsdóttir, R.; Þórarinsdóttir, K.A.; Aðalbjörnsson, B.V.; Guðmundsson, M.; Marteinsdóttir, G.; Kristbergsson, K. Extraction of bioactive compounds from *Alaria esculenta* with pulsed electric field. *J. Appl. Phycol.* **2022**, *34*, 1–12. [CrossRef]
27. Blanco, S.; Sapatinha, M.; Mackey, M.; Maguire, J.; Paolacci, S.; Gonçalves, S.; Lourenço, H.M.; Mendes, R.; Bandarra, N.M.; Pires, C. Effect of Deployment and Harvest Date on Growth and High-Value Compounds of Farmed *Alaria esculenta*. *Mar. Drugs* **2023**, *21*, 305. [CrossRef]
28. Zhu, X.; Healy, L.; Das, R.S.; Bhavya, M.; Karuppusamy, S.; Sun, D.-W.; O'Donnell, C.; Tiwari, B.K. Novel biorefinery process for extraction of laminarin, alginate and protein from brown seaweed using hydrodynamic cavitation. *Algal Res.* **2023**, *74*, 103243. [CrossRef]
29. Das, R.S.; Tiwari, B.K.; Selli, S.; Kelebek, H.; Garcia-Vaquero, M. Exploring pilot scale ultrasound microwave assisted extraction of organic acids and phytochemicals from brown seaweed *Alaria esculenta*. *Algal Res.* **2025**, *86*, 103896. [CrossRef]
30. Van Weelden, G.; Bobiński, M.; Okła, K.; Van Weelden, W.J.; Romano, A.; Pijnenborg, J.M. Fucoidan structure and activity in relation to anti-cancer mechanisms. *Mar. Drugs* **2019**, *17*, 32. [CrossRef]
31. Jönsson, M.; Allahgholi, L.; Sardari, R.R.; Hreggviðsson, G.O.; Nordberg Karlsson, E. Extraction and modification of macroalgal polysaccharides for current and next-generation applications. *Molecules* **2020**, *25*, 930. [CrossRef] [PubMed]
32. Schiener, P.; Black, K.D.; Stanley, M.S.; Green, D.H. The seasonal variation in the chemical composition of the kelp species *Laminaria digitata*, *Laminaria hyperborea*, *Saccharina latissima* and *Alaria esculenta*. *J. Appl. Phycol.* **2015**, *27*, 363–373. [CrossRef]
33. Liu, M.; Liu, Y.; Cao, M.J.; Liu, G.M.; Chen, Q.; Sun, L.; Chen, Q. Antibacterial activity and mechanisms of depolymerized fucoidans isolated from *Laminaria japonica*. *Carbohydr. Polym.* **2017**, *172*, 294–305. [CrossRef] [PubMed]
34. Lutay, N.; Nilsson, I.; Wadström, T.; Ljungh, Å. Effect of Heparin, Fucoidan and Other Polysaccharides on Adhesion of Enterohepatic Helicobacter Species to Murine Macrophages. *Appl. Biochem. Biotechnol.* **2010**, *164*, 1–9. [CrossRef]
35. Ale, M.T.; Mikkelsen, J.D.; Meyer, A.S. Important determinants for fucoidan bioactivity: A critical review of structure-function relations and extraction methods for fucose-containing sulfated polysaccharides from brown seaweeds. *Mar. Drugs* **2011**, *9*, 2106–2130. [CrossRef] [PubMed]
36. Bilan, M.I.; Grachev, A.A.; Shashkov, A.S.; Nifantiev, N.E.; Usov, A.I. Structure of a fucoidan from the brown seaweed *Fucus serratus* L. *Carbohydr. Res.* **2006**, *341*, 238–245. [CrossRef] [PubMed]
37. Cabral, E.M.; Mondala, J.R.M.; Oliveira, M.; Przyborska, J.; Fitzpatrick, S.; Rai, D.K.; Sivagnanam, S.P.; Garcia-Vaquero, M.; O'Shea, D.; Devereux, M.; et al. Influence of molecular weight fractionation on the antimicrobial and anticancer properties of a fucoidan rich-extract from the macroalgae *Fucus vesiculosus*. *Int. J. Biol. Macromol.* **2021**, *186*, 994–1002. [CrossRef] [PubMed]
38. Garcia-Vaquero, M.; Rajauria, G.; O'Doherty, J.V.; Sweeney, T. Polysaccharides from macroalgae: Recent advances, innovative technologies and challenges in extraction and purification. *Food Res. Int.* **2017**, *99*, 1011–1020. [CrossRef]

39. Otero, P.; Carpena, M.; Garcia-Oliveira, P.; Echave, J.; Soria-Lopez, A.; García-Pérez, P.; Fraga-Corral, M.; Cao, H.; Nie, S.; Xiao, J. Seaweed polysaccharides: Emerging extraction technologies, chemical modifications and bioactive properties. *Crit. Rev. Food Sci. Nutr.* **2023**, *63*, 1901–1929. [CrossRef] [PubMed]
40. Nøkling-Eide, K.; Tan, F.; Wang, S.; Zhou, Q.; Gravdahl, M.; Langeng, A.-M.; Bulone, V.; Aachmann, F.L.; Sletta, H.; Arlov, Ø. Acid preservation of cultivated brown algae *Saccharina latissima* and *Alaria esculenta* and characterization of extracted alginate and cellulose. *Algal Res.* **2023**, *71*, 103057. [CrossRef]
41. Nøkling-Eide, K.; Langeng, A.-M.; Åslund, A.; Aachmann, F.L.; Sletta, H.; Arlov, Ø. An assessment of physical and chemical conditions in alginate extraction from two cultivated brown algal species in Norway: Alaria esculenta and Saccharina latissima. *Algal Res.* **2023**, *69*, 102951. [CrossRef]
42. Birgersson, P.S.; Oftebro, M.; Strand, W.I.; Aarstad, O.A.; Sætrom, G.I.; Sletta, H.; Arlov, Ø.; Aachmann, F.L. Sequential extraction and fractionation of four polysaccharides from cultivated brown algae *Saccharina latissima* and *Alaria esculenta*. *Algal Res.* **2023**, *69*, 102928. [CrossRef]
43. Rhein-Knudsen, N.; Reyes-Weiss, D.; Horn, S.J. Extraction of high purity fucoidans from brown seaweeds using cellulases and alginate lyases. *Int. J. Biol. Macromol.* **2023**, *229*, 199–209. [CrossRef]
44. Khallil, A.; Daghman, I. Antifungal Potential in Crude Extracts of Five Selected Brown Seaweeds Collected from the Western Libya Coast. *J. Micro. Creat.* **2015**, *1*, 103.
45. Riyanti; Marner, M.; Hartwig, C.; Patras, M.A.; Wodi, S.I.M.; Rieuwpassa, F.J.; Ijong, F.G.; Balansa, W.; Schaberle, T.F. Sustainable Low-Volume Analysis of Environmental Samples by Semi-Automated Prioritization of Extracts for Natural Product Research (SeaPEPR). *Mar. Drugs* **2020**, *18*, 649. [CrossRef] [PubMed]
46. Martelli, F.; Cirlini, M.; Lazzi, C.; Neviani, E.; Bernini, V. Edible Seaweeds and Spirulina Extracts for Food Application: In Vitro and In Situ Evaluation of Antimicrobial Activity towards Foodborne Pathogenic Bacteria. *Foods* **2020**, *9*, 1442. [CrossRef] [PubMed]
47. Martelli, F.; Favari, C.; Mena, P.; Guazzetti, S.; Ricci, A.; Del Rio, D.; Lazzi, C.; Neviani, E.; Bernini, V. Antimicrobial and Fermentation Potential of *Himanthalia elongata* in Food Applications. *Microorganisms* **2020**, *8*, 248. [CrossRef] [PubMed]
48. Pina-Perez, M.C.; Rivas, A.; Martinez, A.; Rodrigo, D. Antimicrobial potential of macro and microalgae against pathogenic and spoilage microorganisms in food. *Food Chem* **2017**, *235*, 34–44. [CrossRef] [PubMed]
49. Silva, A.; Silva, S.A.; Lourenco-Lopes, C.; Jimenez-Lopez, C.; Carpena, M.; Gullon, P.; Fraga-Corral, M.; Domingues, V.F.; Barroso, M.F.; Simal-Gandara, J.; et al. Antibacterial Use of Macroalgae Compounds against Foodborne Pathogens. *Antibiotics* **2020**, *9*, 712. [CrossRef]
50. Balouiri, M.; Sadiki, M.; Ibnsouda, S.K. Methods for in vitro evaluating antimicrobial activity: A review. *J. Pharm. Anal.* **2016**, *6*, 71–79. [CrossRef]
51. Rajauria, G.; Jaiswal, A.K.; Abu-Gannam, N.; Gupta, S. Antimicrobial, Antioxidant and Free Radical-Scavenging Capacity of Brown Seaweed *Himanthalia elongata* from Western Coast of Ireland. *J. Food Biochem.* **2013**, *37*, 322–335. [CrossRef]
52. Otero, P.; Quintana, S.E.; Reglero, G.; Fornari, T.; Garcia-Risco, M.R. Pressurized Liquid Extraction (PLE) as an Innovative Green Technology for the Effective Enrichment of Galician Algae Extracts with High Quality Fatty Acids and Antimicrobial and Antioxidant Properties. *Mar. Drugs* **2018**, *16*, 156. [CrossRef] [PubMed]
53. Nshimiyumukiza, O.; Kang, S.-K.; Kim, H.-J.; Lee, E.-H.; Han, H.-N.; Kim, Y.; Kim, D.-H.; Kim, J.-H.; Eom, S.-H.; Kim, Y.-M. Synergistic Antibacterial Activity *of Ecklonia cava* (*Phaeophyceae: Laminariales*) against *Listeria monocytogenes* (*Bacillales*: *Listeriaceae*). *Fish. Aquat. Sci.* **2015**, *18*, 1–6. [CrossRef]
54. Gupta, S.; Cox, S.; Rajauria, G.; Jaiswal, A.K.; Abu-Ghannam, N. Growth Inhibition of Common Food Spoilage and Pathogenic Microorganisms in the Presence of Brown Seaweed Extracts. *Food Bioprocess Technol.* **2011**, *5*, 1907–1916. [CrossRef]
55. Čmiková, N.; Galovičová, L.; Miškeje, M.; Borotová, P.; Kluz, M.; Kačániová, M. Determination of antioxidant, antimicrobial activity, heavy metals and elements content of seaweed extracts. *Plants* **2022**, *11*, 1493. [CrossRef] [PubMed]
56. Vijayabaskar, P.; Vaseela, N.; Thirumaran, G. Potential antibacterial and antioxidant properties of a sulfated polysaccharide from the brown marine algae *Sargassum swartzii*. *Chin. J. Nat. Med.* **2012**, *10*, 421–428. [CrossRef]
57. Amorim, R.d.N.d.S.; Rodrigues, J.A.G.; Holanda, M.L.; Quinderé, A.L.G.; Paula, R.C.M.d.; Melo, V.M.M.; Benevides, N.M.B. Antimicrobial effect of a crude sulfated polysaccharide from the red seaweed *Gracilaria ornata*. *Braz. Arch. Biol. Technol.* **2012**, *55*, 171–181. [CrossRef]
58. Yamashita, S.; Yoshiko, S.-K.; Shimizu, M. In vitro bacteriostatic effects of dietary polysaccharides. *Food Sci. Technol. Res.* **2001**, *7*, 262–264. [CrossRef]
59. Carneiro, V.A.; Dos Santos, H.S.; Arruda, F.V.S.; Bandeira, P.N.; Albuquerque, M.R.J.R.; Pereira, M.O.; Henriques, M.; Cavada, B.S.; Teixeira, E.H. Casbane diterpene as a promising natural antimicrobial agent against biofilm-associated infections. *Molecules* **2010**, *16*, 190–201. [CrossRef]

60. Gómez-Ordóñez, E.; Jiménez-Escrig, A.; Rupérez, P. Molecular weight distribution of polysaccharides from edible seaweeds by high-performance size-exclusion chromatography (HPSEC). *Talanta* **2012**, *93*, 153–159. [CrossRef]
61. Tsubaki, S.; Oono, K.; Hiraoka, M.; Onda, A.; Mitani, T. Microwave-assisted hydrothermal extraction of sulfated polysaccharides from *Ulva* spp. and *Monostroma latissimum*. *Food Chem.* **2016**, *210*, 311–316. [CrossRef]
62. Rodriguez-Jasso, R.M.; Mussatto, S.I.; Pastrana, L.; Aguilar, C.N.; Teixeira, J.A. Microwave-assisted extraction of sulfated polysaccharides (fucoidan) from brown seaweed. *Carbohydr. Polym.* **2011**, *86*, 1137–1144. [CrossRef]
63. Zargarzadeh, M.; Amaral, A.J.; Custódio, C.A.; Mano, J.F. Biomedical applications of laminarin. *Carbohydr. Polym.* **2020**, *232*, 115774. [CrossRef]
64. Zayed, A.; El-Aasr, M.; Ibrahim, A.-R.S.; Ulber, R. Fucoidan characterization: Determination of purity and physicochemical and chemical properties. *Mar. Drugs* **2020**, *18*, 571. [CrossRef] [PubMed]
65. Tsai, H.-L.; Tai, C.-J.; Huang, C.-W.; Chang, F.-R.; Wang, J.-Y. Efficacy of low-molecular-weight fucoidan as a supplemental therapy in metastatic colorectal cancer patients: A double-blind randomized controlled trial. *Mar. Drugs* **2017**, *15*, 122. [CrossRef] [PubMed]
66. Vandanjon, L.; Burlot, A.-S.; Zamanileha, E.F.; Douzenel, P.; Ravelonandro, P.H.; Bourgougnon, N.; Bedoux, G. The Use of FTIR Spectroscopy as a Tool for the Seasonal Variation Analysis and for the Quality Control of Polysaccharides from Seaweeds. *Mar. Drugs* **2023**, *21*, 482. [CrossRef]
67. Wang, L.; Jayawardena, T.U.; Yang, H.-W.; Lee, H.G.; Kang, M.-C.; Sanjeewa, K.A.; Oh, J.Y.; Jeon, Y.-J. Isolation, characterization, and antioxidant activity evaluation of a fucoidan from an enzymatic digest of the edible seaweed, *Hizikia fusiforme*. *Antioxidants* **2020**, *9*, 363. [CrossRef] [PubMed]
68. Marudhupandi, T.; Kumar, T.T.A. Antibacterial effect of fucoidan from *Sargassum wightii* against the chosen human bacterial pathogens. *Int. Curr. Pharm. J.* **2013**, *2*, 156–158. [CrossRef]
69. Poveda-Castillo, G.; Rodrigo, D.; Martínez, A.; Pina-Pérez, M. Bioactivity of Fucoidan as an Antimicrobial Agent in a New Functional Beverage. *Beverages* **2018**, *4*, 64. [CrossRef]
70. Abeytunga, D.; Fernando, I.; Sanjeewa, K.; Samarakoon, K.W.; Lee, W.W.; Kim, H.-S.; Kim, E.-A.; Gunasekara, U.; Nanayakkara, C.; de Silva, E. FTIR characterization and antioxidant activity of water soluble crude polysaccharides of Sri Lankan marine algae. *Algae* **2017**, *32*, 75–86.
71. Belattmania, Z.; Kaidi, S.; El Atouani, S.; Katif, C.; Bentiss, F.; Jama, C.; Reani, A.; Sabour, B.; Vasconcelos, V. Isolation and FTIR-ATR and 1H NMR characterization of alginates from the main alginophyte species of the atlantic coast of Morocco. *Molecules* **2020**, *25*, 4335. [CrossRef] [PubMed]
72. Lin, P.; Chen, S.; Liao, M.; Wang, W. Physicochemical characterization of fucoidans from *Sargassum henslowianum C. Agardh* and their antithrombotic activity in vitro. *Mar. Drugs* **2022**, *20*, 300. [CrossRef] [PubMed]
73. Saravana, P.S.; Tilahun, A.; Gerenew, C.; Tri, V.D.; Kim, N.H.; Kim, G.-D.; Woo, H.-C.; Chun, B.-S. Subcritical water extraction of fucoidan from *Saccharina japonica*: Optimization, characterization and biological studies. *J. Appl. Phycol.* **2018**, *30*, 579–590. [CrossRef]
74. Sharma, P.P.; Baskaran, V. Polysaccharide (laminaran and fucoidan), fucoxanthin and lipids as functional components from brown algae (*Padina tetrastromatica*) modulates adipogenesis and thermogenesis in diet-induced obesity in C57BL6 mice. *Algal Res.* **2021**, *54*, 102187. [CrossRef]
75. Arunkumar, K.; Raj, R.; Raja, R.; Carvalho, I.S. Brown seaweeds as a source of anti-hyaluronidase compounds. *S. Afr. J. Bot.* **2021**, *139*, 470–477. [CrossRef]
76. Cebrián-Lloret, V.; Metz, M.; Martínez-Abad, A.; Knutsen, S.H.; Ballance, S.; López-Rubio, A.; Martínez-Sanz, M. Valorization of alginate-extracted seaweed biomass for the development of cellulose-based packaging films. *Algal Res.* **2022**, *61*, 102576. [CrossRef]
77. Skriptsova, A.V.; Miroshnikova, N.V. Laboratory experiment to determine the potential of two macroalgae from the Russian Far-East as biofilters for integrated multi-trophic aquaculture (IMTA). *Bioresour. Technol.* **2011**, *102*, 3149–3154. [CrossRef]
78. Zayed, A.; Ulber, R. Fucoidan production: Approval key challenges and opportunities. *Carbohydr. Polym.* **2019**, *211*, 289–297. [CrossRef]
79. Dobrinčić, A.; Balbino, S.; Zorić, Z.; Pedisić, S.; Bursać Kovačević, D.; Elez Garofulić, I.; Dragović-Uzelac, V. Advanced technologies for the extraction of marine brown algal polysaccharides. *Mar. Drugs* **2020**, *18*, 168. [CrossRef] [PubMed]
80. Bilan, M.; Klochkova, N.; Shashkov, A.; Usov, A. Polysaccharides of Algae 71*. Polysaccharides of the Pacific brown alga *Alaria marginata*. *Russ. Chem. Bull.* **2018**, *67*, 137–143. [CrossRef]
81. Malyarenko, O.S.; Malyarenko, T.V.; Usoltseva, R.V.; Surits, V.V.; Kicha, A.A.; Ivanchina, N.V.; Ermakova, S.P. Combined anticancer effect of sulfated laminaran from the brown alga *Alaria angusta* and polyhydroxysteroid glycosides from the starfish *Protoreaster lincki* on 3D colorectal carcinoma HCT 116 cell line. *Mar. Drugs* **2021**, *19*, 540. [CrossRef]

82. Ibrahim, M.I.; Amer, M.S.; Ibrahim, H.A.; Zaghloul, E.H. Considerable production of ulvan from *Ulva lactuca* with special emphasis on its antimicrobial and anti-fouling properties. *Appl. Biochem. Biotechnol.* **2022**, *194*, 3097–3118. [CrossRef]
83. Tran, T.T.V.; Truong, H.B.; Tran, N.H.V.; Quach, T.M.T.; Nguyen, T.N.; Bui, M.L.; Yuguchi, Y.; Thanh, T.T.T. Structure, conformation in aqueous solution and antimicrobial activity of ulvan extracted from green seaweed *Ulva reticulata*. *Nat. Prod. Res.* **2018**, *32*, 2291–2296. [CrossRef] [PubMed]
84. Berri, M.; Slugocki, C.; Olivier, M.; Helloin, E.; Jacques, I.; Salmon, H.; Demais, H.; Le Goff, M.; Collen, P.N. Marine-sulfated polysaccharides extract of *Ulva armoricana* green algae exhibits an antimicrobial activity and stimulates cytokine expression by intestinal epithelial cells. *J. Appl. Phycol.* **2016**, *28*, 2999–3008. [CrossRef]
85. Masuko, T.; Minami, A.; Iwasaki, N.; Majima, T.; Nishimura, S.-I.; Lee, Y.C. Carbohydrate analysis by a phenol–sulfuric acid method in microplate format. *Anal. Biochem.* **2005**, *339*, 69–72. [CrossRef]
86. Ainsworth, E.A.; Gillespie, K.M. Estimation of total phenolic content and other oxidation substrates in plant tissues using Folin–Ciocalteu reagent. *Nat. Protoc.* **2007**, *2*, 875–877. [CrossRef] [PubMed]
87. Smith, P.e.; Krohn, R.I.; Hermanson, G.; Mallia, A.; Gartner, F.; Provenzano, M.; Fujimoto, E.; Goeke, N.; Olson, B.; Klenk, D. Measurement of protein using bicinchoninic acid. *Anal. Biochem.* **1985**, *150*, 76–85. [CrossRef]
88. Gleeson, E.; O'beirne, D. Effects of process severity on survival and growth of *Escherichia coli* and *Listeria innocua* on minimally processed vegetables. *Food Control* **2005**, *16*, 677–685. [CrossRef]
89. Thielmann, J.; Muranyi, P.; Kazman, P. Screening essential oils for their antimicrobial activities against the foodborne pathogenic bacteria *Escherichia coli* and *Staphylococcus aureus*. *Heliyon* **2019**, *5*. [CrossRef] [PubMed]
90. Clinical Laboratory Standards Institute. *M100Ed33 | Performance Standards for Antimicrobial Susceptibility Testing*, 33rd ed.; Published by Clinical Laboratory Standards Institute (CLSI): Malvern, PA, USA, 2023.
91. Eloff, J.N. A sensitive and quick microplate method to determine the minimal inhibitory concentration of plant extracts for bacteria. *Planta Medica* **1998**, *64*, 711–713. [CrossRef]
92. Baranyi, J.; Roberts, T.A. A dynamic approach to predicting bacterial growth in food. *Int. J. Food Microbiol.* **1994**, *23*, 277–294. [CrossRef] [PubMed]
93. 4.3.2, R.V. Available online: https://www.r-project.org/ (accessed on 4 April 2024).
94. Friendly, M. Corrgrams: Exploratory displays for correlation matrices. *Am. Stat.* **2002**, *56*, 316–324. [CrossRef]

marine drugs

MDPI

Article

Extraction Optimization of Polysaccharides from Wet Red Microalga *Porphyridium purpureum* Using Response Surface Methodology

Yi Chen [1,2], Qianmei Li [2], Bingqi Xu [1], Wenzhou Xiang [1], Aifen Li [2,*] and Tao Li [1,*]

[1] CAS Key Laboratory of Tropical Marine Bio-Resources and Ecology, Guangdong Key Laboratory of Marine Materia Medica, South China Sea Institute of Oceanology, Chinese Academy of Sciences, Guangzhou 510301, China; chenyi2021301@163.com (Y.C.); xubingqi24@mails.ucas.ac.cn (B.X.); xwz@scsio.ac.cn (W.X.)

[2] Institute of Hydrobiology, Jinan University, Guangzhou 510632, China; lqm8523@stu2021.jnu.edu.cn

* Correspondence: tiger@jnu.edu.cn (A.L.); taoli@scsio.ac.cn (T.L.)

Abstract: *Porphyridium* is a unicellular marine microalga that is rich in polysaccharides and has excellent biological activities. Optimizing the extraction of polysaccharides can significantly improve the value of *Porphyridium* biomass. In the present study, response surface methodology was employed to optimize the extraction conditions of polysaccharides, including extraction time, extraction temperature, and biomass-to-water ratio. Furthermore, microwave-assisted extraction was used to improve the yield of polysaccharides further. The results showed that increasing the extraction temperature and extraction time could enhance the yield of polysaccharides. The multiple regression analysis of RSM indicated that the model could be employed to optimize the extraction of polysaccharides. The optimal extraction time, extraction temperature, and biomass-to-water ratio were 45 min, 87 °C, and 1:63 g mL^{-1}, respectively. Under these optimal conditions, the maximum yield of polysaccharides was 23.66% DW, which well matched the predicted yield. The results indicated that the extraction temperature was the most significant condition affecting the yield of polysaccharides. The microwave-assisted extraction could further improve the yield of polysaccharides to 25.48% DW. In conclusion, hot water with microwave-assisted extraction was effective for polysaccharide extraction in *P. purpureum*.

Keywords: *Porphyridium*; intracellular polysaccharides; wet biomass; response surface methodology; microwave-assisted extraction

1. Introduction

Microalga polysaccharides have excellent antioxidant, immunomodulatory, antiviral, hypoglycemic, and hypolipidemic activities [1,2]. For example, the polysaccharides of the red macroalga *Pyropia yezoensis* have the potential to scavenge hydrogen peroxide and alkyl radicals [3]. The polysaccharides from the microalga *Limnospira platensis* (formerly *Spirulina platensis*) were demonstrated to inhibit the replication of the herpes simplex virus 1, mumps virus, and influenza A virus [4].

Porphyridium purpureum is a unicellular marine red microalga that can synthesize a variety of high-value bioactive products, including intracellular polysaccharides, exopolysaccharides, polyunsaturated fatty acids, and B-phycoerythrin [5]. The exopolysaccharides of *P. purpureum* have become a research hotspot in recent years. The exopolysaccharides of *P. purpureum* have potential applications in functional foods, pharmaceuticals, and skin care cosmetics [6] due to their antioxidant [7], antiviral [8,9], and immunomodulatory activities [10,11]. However, to date, the large-scale production of exopolysaccharides has not been achieved because of the low yield and difficulty in harvesting (the high viscosity of exopolysaccharides makes it difficult to separate from the cells). The content of

intracellular polysaccharides of *P. purpureum* can reach 15−52% DW (dry weight) [12], and it consists of glucuronic acid and several neutral monosaccharides (xylose, galactose, and glucose) [13]. The yield of intracellular polysaccharides of *P. purpureum* is 2.19 g L^{-1}, which is much higher than the yield of exopolysaccharides (0.34 g L^{-1}) [12]. Moreover, the composition of intracellular polysaccharides is similar to that of exopolysaccharides [14], and these polysaccharides may also have bioactivities and applications similar to those of exopolysaccharides. However, there are few studies on the extraction of intracellular polysaccharides of *P. purpureum*.

Conventional extraction methods for polysaccharides include hot water extraction, acid extraction, and alkali extraction [15]. Recently, several novel methods for polysaccharide extraction, such as microwave-assisted, ultrasound-assisted, enzyme-assisted, and pressurized liquid extraction, have been used to improve extraction efficiency and reduce energy consumption [16–19]. For conventional extraction methods for polysaccharides, temperature, time, and biomass-to-water ratio have great effects on the extraction efficiency. The extraction yield of alginate from *Sargassum binderi* is affected by temperature. The maximum yield of alginate is 27% DW at 90 °C [17]. Response surface methodology (RSM) is an ideal approach to avoid the interaction of a single extraction condition [20]. By RSM, the optimal extraction conditions for *Fucus vesiculosus* polysaccharides are 120 psi for the pressure, 1 min for the extraction time, and 1:25 g mL^{-1} for the biomass-to-water ratio [21]. Similarly, the optimal extraction conditions for the polysaccharides of *Isocrysis galbana* (Haptophyta) are 3.6 h for the extraction time, 67 °C for the extraction temperature, and 1:9 g mL^{-1} for the biomass-to-water ratio [22].

Water as an extractant can preserve the structural information of polysaccharides and reduce the damage to their activity. Microwave-assisted extraction (MAE) directly generates heat through ion conduction and dipole rotation [16], which has been widely used to improve the extraction efficiency of natural products. In the present study, the extraction method of *P. purpureum* polysaccharides is investigated by RSM and MAE. The results will provide an optimal strategy to obtain high-efficiency polysaccharide extraction from *P. purpureum*.

2. Results

2.1. Effects of Temperature, Time, and Biomass-to-Water Ratio on the Extraction Yield of Polysaccharides

The extraction yields of polysaccharides under different extraction temperatures (50 °C, 60 °C, 70 °C, 80 °C, and 90 °C) are shown in Figure 1a. Within the temperature range of 50−80 °C, there was a positive correlation between the extraction temperature and the yield of polysaccharides. However, there were no significant differences in the yield as the extraction temperature exceeded 80 °C. The maximum yield was 22.96% DW, which was obtained at 90 °C. Based on these results, the optimal extraction temperature was 80 °C.

The extraction yields of polysaccharides under different extraction times (15 min, 30 min, 45 min, 60 min, and 75 min) are shown in Figure 1b. The extraction yield of polysaccharides increased as the time increased from 15 to 45 min, but there were no significant differences in the yield when the extraction time was beyond 45 min. The maximum yield (22.62% DW) was obtained at 75 min. This result indicated that the polysaccharides were mainly released at the initial stage of extraction. Thus, the optimal extraction time was 45 min.

The extraction yields of polysaccharides under different biomass-to-water ratios (1:20, 1:40, 1:60, 1:80, and 1:100 g mL^{-1}) are shown in Figure 1c. The yield increased rapidly when the biomass-to-water ratio ranged from 1:20 to 1:60 g mL^{-1}; the maximum yield (24.08% DW) was obtained at 1:60 g mL^{-1}. However, when the biomass-to-water ratio ranged from 1:60 to 1:100 g mL^{-1}, the yield of polysaccharides decreased from 24.08% DW to 22.67% DW. Therefore, the optimal biomass-to-water ratio was 1:60 g mL^{-1}.

Based on the results of the single-factor experiment, the optimal extraction conditions were an 80 °C extraction temperature, a 45 min extraction time, and a 1:60 g mL^{-1}1 biomass-to-water ratio.

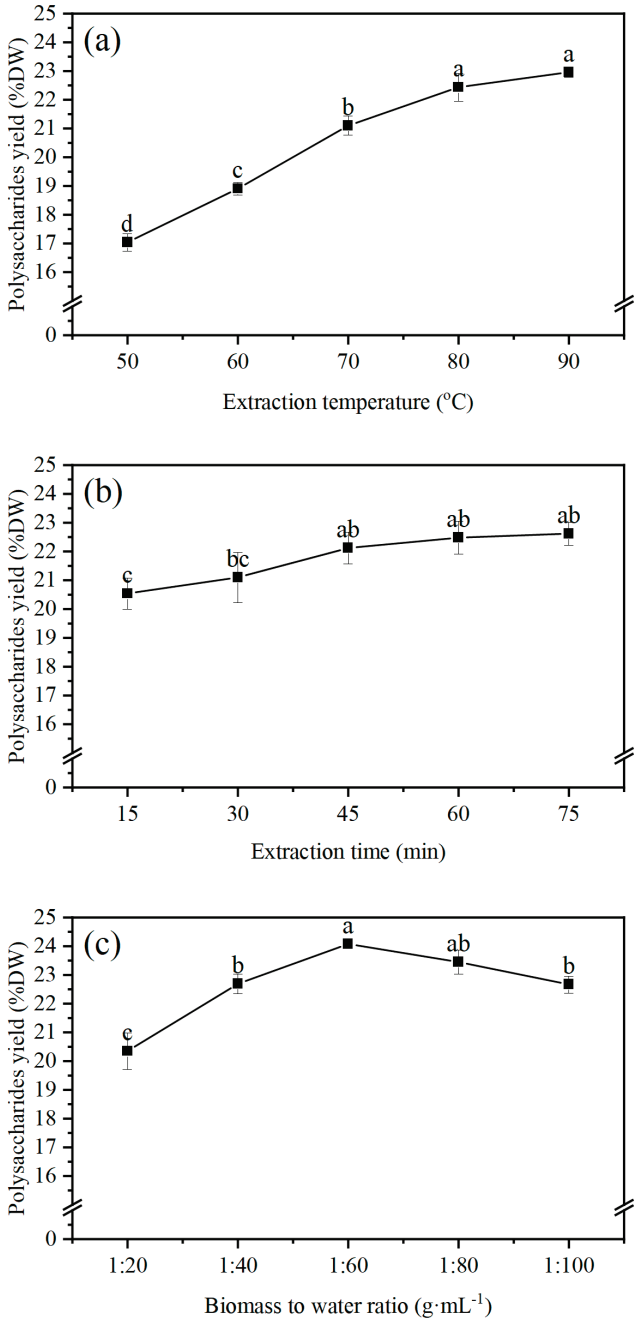

Figure 1. The effects of extraction temperature, extraction time, and biomass-to-water ratio on the yield of polysaccharides: (**a**) extraction temperature (the extraction time and biomass-to-water ratio were fixed at 60 min and 1:50 g mL^{-1}); (**b**) extraction time (the extraction temperature and biomass-to-water ratio were fixed at 80 °C and 1:50 g mL^{-1}); (**c**) biomass-to-water ratio (the extraction temperature and extraction time were fixed at 80 °C and 60 min). Each mean value represents the mean value of three biological replicates and three technical replicates, $n = 6$. The error bars represent the standard deviations of those means, and different letters indicate significant differences among the treatments at the $p = 0.05$ level.

2.2. Statistical Analysis and Model Fitting Based on RSM

The interaction effects of temperature, time, and biomass-to-water ratio on the extraction yield of polysaccharides were investigated by using multiple regression analysis. There was a total of 17 groups (Table 1). The extraction yields of polysaccharides were analyzed by using the Box–Behnken Design (BBD) method. Based on the results of the multiple regression analysis, the predicted extraction yield could be fitted into the following second-order polynomial equation:

$$Y = 23.27 + 0.42 \times A + 1.23 \times B + 0.83 \times C - 0.11 \times A \times B + 0.17 \times A \times C - 0.16 \times B \times C - 1.84 \times A^2 - 0.97 \times B^2 - 1.30 \times C^2, \quad (1)$$

where Y is the extraction yield of polysaccharides, and A, B, and C are the extraction time, the extraction temperature, and the biomass-to-water ratio, respectively.

Table 1. The response surface design and extraction yield of polysaccharides.

Run	(A) Extraction Time (min)	(B) Extraction Temperature (°C)	(C) Biomass to Water Ratio (g mL^{-1})	Extraction Yield (%DW)
1	45	90	40	21.69
2	60	70	60	19.96
3	30	90	60	21.15
4	45	80	60	23.64
5	60	80	40	19.56
6	45	70	40	18.55
7	45	80	60	23.15
8	30	80	80	20.35
9	60	90	60	21.84
10	30	70	60	18.84
11	45	80	60	23.11
12	60	80	80	21.45
13	45	70	80	20.60
14	45	80	60	23.52
15	45	90	80	23.12
16	45	80	60	22.88
17	30	80	40	19.12

The analysis of variance (ANOVA) was used to analyze the significance and suitability of the model. As shown in Table 2, the F-value of this model was 53.58 ($p < 0.05$), implying that the model was used to predict the yield of polysaccharides. The lack of fit was insignificant ($p > 0.05$), confirming the validity of the model. The determination coefficient (R^2) was 0.9857, indicating that only 1.43% of the total variation could not be explained by the model. The 0.9673 adjusted R^2 showed that the model was highly significant. At the same time, the coefficient of the variation (C.V.% = 1.47%) further proved the good reliability and precision of the model. The adeq. precision was 17.222, which was higher than the critical value of 4, indicating the accuracy of the model. The regression model indicated that this model was adequate to predict the yield of polysaccharides in the present study.

The regression coefficients of the equation are listed in Table 2. The linear coefficients (A, B, and C) and quadratic coefficients (A2, B2, and C2) had remarkable influences on the polysaccharide yield ($p < 0.05$). The cross-product coefficients (AB, AC, and BC) had no significant influence on the yield of polysaccharides ($p > 0.05$). By analyzing the linear and quadratic coefficients, it could be concluded that the order of extraction conditions influencing the polysaccharide yield, from strong to weak, was extraction temperature, biomass-to-water ratio, and extraction time.

Table 2. The ANOVA of the experimental results of the RSM-BBD.

Source	Sum of Squares	df	Mean Square	*F*-Value	*p*-Value
Model	47.28	9	5.25	53.58	<0.0001 **
A	1.4	1	1.4	14.31	0.0069 **
B	12.13	1	12.13	123.68	<0.0001 **
C	5.45	1	5.45	55.53	0.0001 **
AB	0.046	1	0.046	0.47	0.5144
AC	0.11	1	0.11	1.11	0.3270
BC	0.096	1	0.096	0.98	0.3552
A^2	14.27	1	14.27	145.57	<0.0001 **
B^2	3.97	1	3.97	40.5	0.0004 **
C^2	7.1	1	7.1	72.43	<0.0001 **
Residual	0.69	7	0.098		
Lack of fit	0.3	3	0.098	1.01	0.4764
Pure error	0.39	4	0.098		
Cor total	47.97	16			
R^2	0.9857		C.V.%	1.47	
R^2_{Adj}	0.9673		Adeq. precision	19.028	

** highly significant ($p < 0.01$).

2.3. Interaction Among Extraction Conditions

Figure 2a shows the interaction effect between the extraction time and the extraction temperature on the yield when the biomass-to-water ratio was fixed at 1:60 g mL^{-1}. The 3D plot was steep and the 2D plot was elliptical. The plots indicated that the optimal polysaccharide yield could be obtained when the extraction temperature was in the range of 78 °C–90 °C and the extraction time was in the range of 37–56 min. The extraction temperature showed a synergistic effect on polysaccharide yield when coupled with the extraction time.

Figure 2b shows the interaction effect between the extraction time and the biomass-to-water ratio on the yield when the extraction temperature was fixed at 80 °C. The yield increased quickly to the maximum value as the biomass-to-water ratio ranged from 1:55 to 1:78 g mL^{-1} and as the extraction time ranged from 40 to 54 min. The interaction of the extraction time and the biomass-to-water ratio showed a positive synergistic effect on the yield of polysaccharides.

Figure 2c illustrates the interaction effect between the extraction temperature and the biomass-to-water ratio on the yield when the extraction time was fixed at 45 min. The yield of polysaccharides increased rapidly with the increase in the extraction temperature and the biomass-to-water ratio. The maximum yield was obtained when the extraction temperature ranged from 77 °C to 90 °C and when the biomass-to-water ratio ranged from 1:50 to 1:81 g mL^{-1}. The extraction temperature showed a synergistic effect on the yield of polysaccharides when coupled with the biomass-to-water ratio.

By using the software of Design-Expert 8.0.6, the quadratic polynomial equation was solved. The optimal extraction conditions by RSM were that the extraction time was 44.81 min, the extraction temperature was 86.75 °C and the biomass-to-water ratio was 1:62.55 g mL^{-1}. The predicted polysaccharide yield under the condition was 23.71% DW. To validate the accuracy of the predicted result, a new experimental group was set up. The extraction conditions were as follows: extraction time of 45 min, extraction temperature of 87 °C, and biomass-to-water ratio of 1:63 g mL^{-1}. Under these conditions, the extraction yield of polysaccharides reached 23.66% DW. There were no significant differences between the predicted yield and the experimental yield ($p > 0.05$), indicating that the model equation was reliable and accurate.

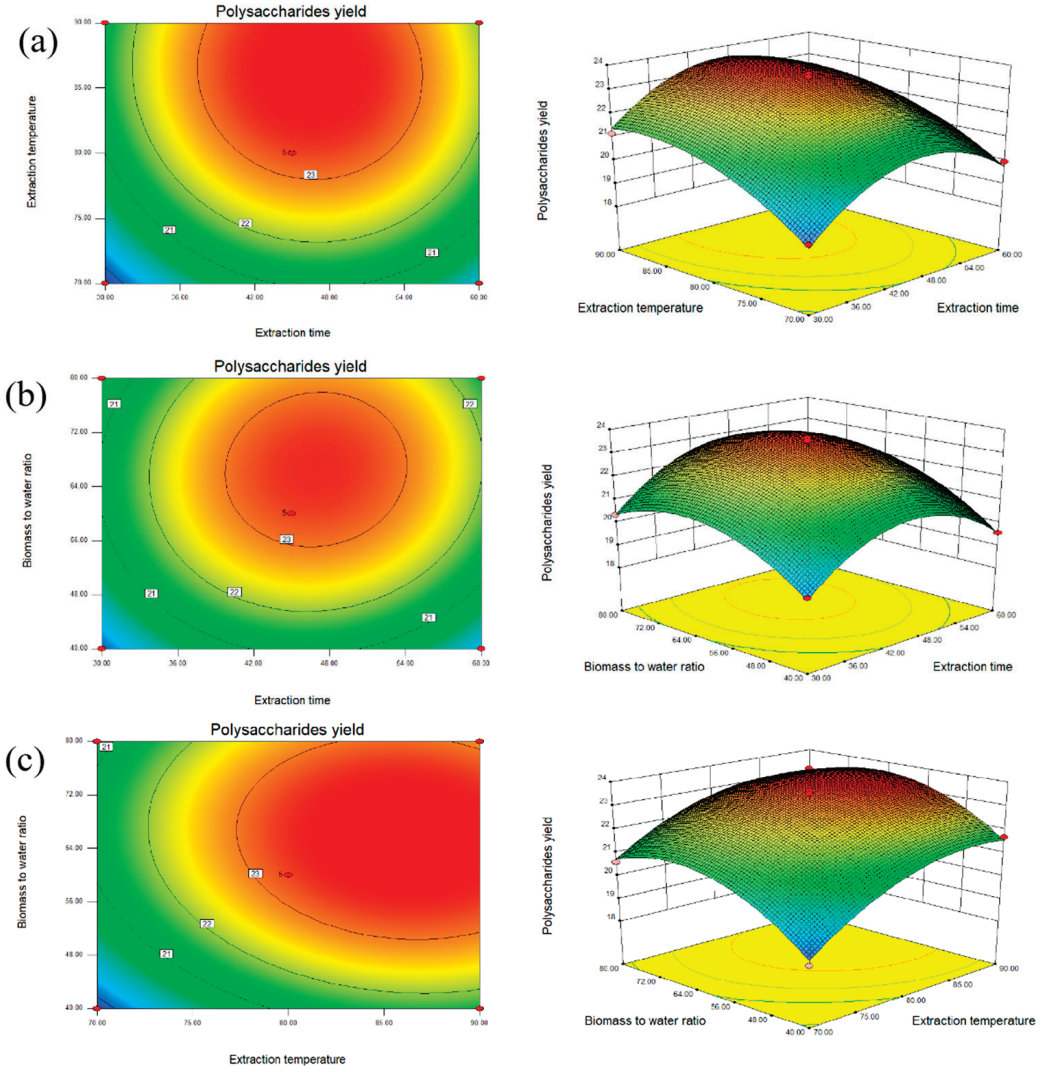

Figure 2. The contour plots and response surface plots of the effects of the extraction temperature, extraction time, and biomass-to-water ratio on the polysaccharide yield: (**a**) the contour plot and response surface plot of the effects of the extraction time, extraction temperature, and their interaction on the extraction yield; (**b**) the contour plot and response surface plot of the effects of the extraction time, biomass-to-water ratio, and their interaction on the extraction yield; and (**c**) the contour plot and response surface plot of the effects of the extraction temperature, biomass-to-water ratio, and their reciprocal interaction on the extraction yield.

2.4. Effect of Microwave-Assisted Extraction on the Yield of Polysaccharides

As shown in Figure 3, the extraction yield of polysaccharides showed an increasing trend as the extraction time ranged from 1 to 5 min by using microwave-assisted extraction. The yield of polysaccharides increased from 13.63% DW to 25.41% DW when the extraction time increased from 1 to 3 min. There was no significant difference in the yield of polysaccharides at 3−5 min ($p > 0.05$). The maximum yield of polysaccharides was 25.48% DW at 5 min. At the same time, the extraction efficiency of polysaccharides reached 96.66%. Moreover, the yield of polysaccharides obtained by microwave-assisted extraction was 7.69% higher than the yield of polysaccharides obtained by RSM extraction (23.66% DW).

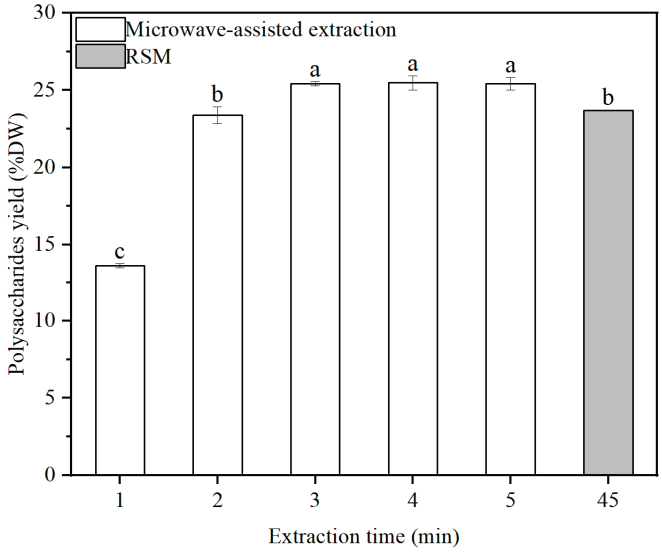

Figure 3. The yields of polysaccharides obtained by microwave-assisted extraction and response surface methodology. The error bars represent standard deviations from three independent samples. The different letters (a–c) indicate significant differences among the treatments at the $p = 0.05$ level.

3. Discussion

The polysaccharides of *P. purpureum* are widely available with the potential for application in medicines, foods, and cosmetics [5]. The content of polysaccharides of *P. purpureum* can reach 52% DW [12]. In our previous study, the extraction yield and extraction efficiency of polysaccharides were found to be 22.43% DW and 85.12% by hot water extraction with an extraction time of 240 min (unpublished). It is necessary to find an efficient extraction method to improve the yield of polysaccharides.

Increasing the extraction temperature can enhance the solubility of polysaccharides and promote the release of polysaccharides into the water [23]. The present study showed that the yield of polysaccharides increased from 17.04% DW to 22.96% DW as the extraction temperature increased from 50 °C to 90 °C (Figure 1a). Similarly, the polysaccharide yield of *Ulva intestinalis* (Chlorophyta) increased from 2.7% DW to 8.0% DW as the temperature increased from 30 °C to 90 °C [24]. The polysaccharide yield of *Isocrysis galbana* increased significantly with the increase in temperature [22]. The reason might be that the high temperature improved the solubility and diffusion rate of polysaccharides [25]. The polysaccharides extraction at room temperature is more favorable for large-scale industrial production as it can significantly reduce energy consumption. The enzyme-assisted extraction of polysaccharides is often carried out at room temperature. The high-efficiency commercial enzyme is essential for enzyme-assisted extraction. If the activity of the existing commercial enzyme is low, the time-consuming screening and modification of the enzyme will have to be conducted. In contrast, the heating method in the present study is commonly used for polysaccharide extraction. In addition, the cells of *P. purpureum* are encapsulated by a thick gelatinous layer, which limits the release of intracellular polysaccharides [5]. High-temperature extraction can effectively destroy the gelatinous layer to accelerate the release of polysaccharides.

Extraction time is also an important factor that affects extraction efficiency. In this study, the yield of polysaccharides showed an increasing trend with the extraction time increased from 15 min to 45 min (Figure 1b). This finding indicated that the polysaccharides were mainly released during the initial stage of extraction. In addition, there was no significant difference in the yield of polysaccharides after 45 min, probably because the temporal requirement for the polysaccharides to be released into the solvent was met at this time. The maximum yield of polysaccharides reached 22.62% DW, and the extraction time was 3−5 times shorter than that of the hot water extraction method we used before. The

yield of polysaccharides of *Chlorella* sp. increased rapidly as the extraction time increased within 3 h [26]. The polysaccharide yield of *L. platensis* increased from 8.2% DW to 12.2% DW as the extraction time increased from 5 to 35 min [27].

The concentration difference between the inside and outside of the cell increases the diffusion of polysaccharides [28]. The present study showed that the polysaccharide yield of *P. purpureum* enhanced rapidly with the increase in the biomass-to-water ratio (Figure 1c). The highest yield (24.08% DW) was obtained at 1:60 g mL^{-1}. This was consistent with the results of Song et al. [26], who reported that the polysaccharide yield of *Chlorella* sp. increased from 3.57% to 7.38% as the ratio increased from 1:10 to 1:40 mg mL^{-1}. The maximum yield (3.05% DW) of *Dictyopteris divaricata* was obtained at 1:110 g mL^{-1} [29]. The reason might be that the low concentration of polysaccharides had a low viscosity in the solution, thus improving the solubilization and diffusion of polysaccharides [30]. However, as the biomass-to-water ratio increased from 1:60−1:100 g mL^{-1}, the yield of polysaccharides showed a decreasing trend. It could be inferred that the high biomass-to-water ratio extended the diffusion distance, resulting in a decrease in the polysaccharide yield. Similar results were obtained by Rahimi et al.; the polysaccharide yield of *Ulva intestinali* (Chlorophyta) showed a decreasing trend when the biomass-to-water ratio exceeded 1:60 g mL^{-1} [24]. Moreover, the polysaccharide yield of *Dictyosphaerium* sp. showed an upward trend as the ratio increased and the maximum polysaccharide yield was 6.82% DW. However, when the biomass-to-water ratio exceeded 1:25 g mL^{-1}, the yield showed a decreasing trend [31]. Therefore, to obtain a high polysaccharide yield, it is essential to determine the optimal range of biomass-to-water ratios.

The use of an ethanol/water solvent mixture is common in food extraction. However, the ethanol/water solvent mixture is not suitable for extracting polysaccharides. In order to improve the extraction yield of polysaccharides from *P. purpureum*, we used the ethanol/water solvent mixture to extract polysaccharides. The results showed that the extraction yield of polysaccharides did not significantly increase. Unfortunately, using this solvent mixture as an extractant changed the color of polysaccharides to dark green, which could reduce the quality of polysaccharides. The reason for this phenomenon might be that the ethanol/water solvent mixture could extract a small amount of chlorophyll and carotenoids, which are lipid-soluble compounds. Furthermore, considering the large-scale production of polysaccharides, the application of ethanol will increase the safety level and the costs of the enterprise. In our study, the in-situ structural information of polysaccharides can be preserved by using water as an extractant. Additionally, polysaccharides are insoluble in ethanol, and ethanol is commonly used to harvest polysaccharides from extracts.

RSM is an effective method to reduce the costs, energy, and time in the process of extraction [20]. It is widely used in optimizing the extraction conditions, such as polysaccharides, vitamin E, anthocyanins, and phycobiliprotein [31–33]. In the present study, the optimal extraction conditions for the polysaccharides of *P. purpureum* by RSM were an extraction time of 45 min, extraction temperature of 87 °C, and biomass-to-water ratio of 1:63 g mL^{-1}. In addition, the extraction yield of polysaccharides (23.66% DW) using RSM was significantly higher than the yield using hot water extraction (22.43% DW). Moreover, the extraction time was 4 times shorter compared to the hot water extraction methodused in our previous study. By RSM, the optimum extraction conditions for the polysaccharides of *Dictyopteris divaricata* were determined to be a biomass-to-water ratio of 1:110 g mL^{-1}, an extraction time of 6 h, and an extraction temperature of 100 °C [29]. Similarly, the optimal extraction conditions for the polysaccharides of *Caulerpa lentillifera* were a biomass-to-water ratio of 1:10 g mL^{-1}, an extraction temperature of 90 °C, and an extraction time of 45 min [23]. The polysaccharide yield (9.29% DW) of *Rhodosorus* sp. was markedly higher than that by hot water extraction, with an extraction yield of 3.13% DW [34]. Therefore, RSM is usually used to identify the optimum extraction conditions. The main advantage of RSM is the reduced number of experimental groups needed to

evaluate multiple extraction conditions and their interactions [20]. RSM is more efficient and easier to use to arrange experiments.

MAE can improve the extraction yield of polysaccharides while reducing the solvent and energy consumption levels [16]. In the present study, the polysaccharide yield increased obviously at 1−3 min. Heat is generated directly into the cell matrix by the permeation of electromagnetic energy, leading to the acceleration of polysaccharide transfer [35]. The results showed that the yield of polysaccharides by microwave-assisted extraction had no significant differences after 3 min, and the maximum yield (25.48% DW) was higher than that resulting from hot water extraction (22.43% DW) in our previous study. Similarly, the extraction yield of polysaccharides from *Ulva meridionalis* using MAE was 40.40% DW, which was 21.7% greater than that of the conventional method [16]. In addition, the yield of fucoidan extracted from *Fucus vesiculosus* by MAE increased 17-fold compared to the conventional method [21]. The reason might be that the energy absorption led to the redistribution of energy between the molecules, which caused penetration of the solvent into the substrate.

The physical and chemical properties of polysaccharides are crucial for commercial applications. Polysaccharides obtained by different extraction methods may have different physical properties and activities. For example, different extraction temperatures lead to different monosaccharide compositions of the macroalga *Ascophyllum nodosum*. Glucuronic acid is the major component of polysaccharides extracted at a temperature of 150 °C, while fucose is the major component of polysaccharides extracted at 90 °C [16]. Based on the research purposes of different products in the future, our study will be conducted on the effects of extraction conditions on the physical properties and activities of the polysaccharides, such as antioxidant activity for functional foods and moisturizing activity for cosmetics. This is also a complex and systematic study.

In the present study, the extraction material was wet biomass. The drying of wet biomass usually consumes a large amount of energy, which accounts for 40% of the costs. The results of this study showed that polysaccharides could be directly extracted from wet biomass. Moreover, the extraction efficiency was more than 90%, providing a reference solution for the commercial application of *P. purpureum* in the future. Even though microwave-assisted extraction further improved the yield of polysaccharides and reduced the extraction time, it required additional consumption costs and corresponding equipment [36]. Its application in marine polysaccharide extraction has so far been limited to laboratory research since few studies on an industrial scale have been reported. If MAE is used to promote the large-scale industrial production of polysaccharides, it is necessary to find a balance between polysaccharide value and consumption. In addition, the development of the standard extraction method is crucial to protect the structural integrity and bioactivities of polysaccharides [37]. However, the excessive extraction temperature and microwave power might cause the degradation of polysaccharides themselves and damage their structures [2]. Therefore, it is important to develop a simple and reliable structural characterization for polysaccharides, which will contribute to a better understanding of the structure–bioactivity relationship in polysaccharides.

4. Materials and Methods

4.1. Microorganisms and Culture Conditions

P. purpureum FACHB 806 was purchased from the Freshwater Algae Culture Collection of the Institute of Hydrobiology in China. *P. purpureum* FACHB 806 were cultured in the modified ASW medium [12]. Illumination was provided by T8 fluorescent lamps (Philips; Suzhou, China) at 300 μmol photons m^{-2} s^{-1}. The photoperiod was 24 h: 0 h (light: dark). The culture temperature was 25 ± 1 °C. CO_2-enriched compressed air (1% CO_2, v:v) was continuously bubbled into the photobioreactor to provide a carbon source. After 10 days of cultivation, the culture was centrifuged at 8000 rpm for 10 min and washed with deionized water three times. The wet biomass was collected and stored at −20 °C.

4.2. Determination of the Content of Polysaccharides and Moisture of Wet Biomass

Moisture content of wet biomass: Wet biomass (100 mg) was added to pre-weighed filters. The filters were dried at 80 °C to a constant weight and re-weighed.

$$W = (m_2 - m_1)/100 \times 100\%, \quad (2)$$

where W is the moisture content of wet biomass, m_1 (mg) is the weight of the pre-weighed filter, and m_2 (mg) is the weight of the filter with dry biomass. The moisture content of the wet biomass used in this study was determined to be 90%.

Polysaccharide content: The wet biomass was freeze-dried using an FD-1-50 freeze dryer (Boyikang, Beijing, China). The freeze-dried biomass was used to measure the polysaccharide content. The freeze-dried biomass (m_1) was hydrolyzed with 1.0 N H_2SO_4 at 80 °C for 1 h. The supernatant was collected by centrifugation at 8000 rpm for 5 min, and this process was repeated three times. The concentration of polysaccharides in the supernatant was determined according to the phenol–sulfuric acid method [38]. The polysaccharide content was estimated using the following equation:

$$\text{Polysaccharide concentration (\% DW)} = C \times V/m_1 \times 100\%, \quad (3)$$

where C (mg mL^{-1}) is the concentration of polysaccharides, V (mL) is the total volume of the supernatants, and m_1 (mg) is the weight of the freeze-dried biomass.

4.3. Single-Factor Experiment

Wet biomass (100 mg) was added to a glass centrifuge tube. The single extraction condition included the extraction temperature (50 °C, 60 °C, 70 °C, 80 °C, and 90 °C), the biomass-to-water ratio (1:20, 1:40, 1:60, 1:80, and 1:100 g mL^{-1}) and the extraction time (15 min, 30 min, 45 min, 60 min, and 75 min). The extracts were collected by centrifugation at 4000 rpm for 5 min, and the supernatants were combined; this process was repeated three times. The polysaccharide content was determined according to the phenol–sulfuric acid method [38]. The polysaccharide yield was estimated using the following equations:

$$\text{Polysaccharide yield (\% DW)} = C \times V/100 \times (1 - W) \times 100\% \quad (4)$$

where C (mg mL^{-1}) is the concentration of polysaccharides, V (mL) is the total volume of the supernatants, and W (%) is the moisture content of wet biomass.

4.4. RSM Experiment

Wet biomass (100 mg) was added to a glass centrifuge tube. Based on the results of the single-factor experiment, the Box–Behnken Design (BBD) was used to set the extraction conditions of the RSM experiment. The factors and levels are shown in Table 3. After the extraction process was completed, the extracts were collected by centrifugation at 4000 rpm for 5 min, and the supernatants were combined; this process was repeated three times. The polysaccharide content was determined according to the phenol–sulfuric acid method [38]. The extraction yield of polysaccharides was used as the dependent variable. The whole RSM experiment contains 17 experimental groups (Table 1). The interactions among the extraction conditions and their corresponding optimum levels were expressed by a second-order polynomial equation. The calculation method of polysaccharide yield refers to 4.3.

Table 3. The independent variables and levels of the response surface method.

Independent Variables	Factor Levels		
	−1	**0**	**1**
A (Extraction time, min)	30	45	60
B (Extraction temperature, °C)	70	80	90
C (Biomass-to-water ratio, g mL^{-1})	40	60	80

4.5. Microwave-Assisted Extraction

Wet biomass (100 mg) was added to a glass centrifuge tube. The microwave power was 210 W using the M1-L213B microwave (Guangdong Midea Electric Appliances Co., Ltd., Foshan, China). The different extraction times (1−5 min) were set to evaluate the yield of polysaccharides. After the extraction was completed, the extracts were collected by centrifugation at 4000 rpm for 5 min, and the supernatants were combined. This process was repeated three times. The polysaccharide contents of different extraction methods were determined according to the phenol–sulfuric acid method [38]. The calculation method of the polysaccharide yield refers to Section 4.3.

4.6. Statistical Analysis

All the treatments had three independent biological replicates and three technical replicates. Multiple regression analysis of RSM was carried out using Design-Expert Software (8.0.6). One-way analysis of variance (ANOVA) was performed to determine the significant differences between the target datasets using SPSS version 18.0 software (SPSS, Chicago, IL, USA). Differences between sample means were analyzed using the least significant difference method (significance level, $p < 0.05$).

5. Conclusions

In summary, the results showed that the increasing extraction temperature and extraction time could enhance the yield of polysaccharides. The optimal extraction method by RSM was an effective method to obtain polysaccharides from *P. purpureum*. This method required shorter extraction times and reduced costs compared to the hot water extraction method. The optimal extraction conditions were an extraction time of 45 min, extraction temperature of 87 °C, and biomass-to-water ratio of 1:63 g mL^{-1}. Under these conditions, the maximum polysaccharide yield was 23.66% DW, which well matched the predicted yield. Microwave-assisted extraction could further improve the yield of polysaccharides (25.48% DW). Therefore, it was essential to determine the optimal range of the extraction conditions to improve the yield of polysaccharides.

Author Contributions: Conceptualization, Y.C. and Q.L.; methodology, T.L.; formal analysis, Y.C. and Q.L.; investigation, Y.C., Q.L., B.X. and T.L.; data curation, Y.C. and T.L.; writing—original draft preparation, Y.C. and Q.L.; writing—review and editing, Y.C., Q.L., B.X., T.L., W.X. and A.L.; project administration, T.L.; funding acquisition, T.L. and A.L. All authors have read and agreed to the published version of the manuscript.

Funding: This research was funded by the Marine Economic Development Project, grant number GDNRC [2023] 38, and the Guangdong Basic and Applied Basic Research Foundation, grant numbers 2024A1515010754.

Institutional Review Board Statement: Not applicable.

Data Availability Statement: The data presented in this study are available from the corresponding author upon request.

Conflicts of Interest: The authors declare that they have no competing interests.

References

1. Kumar, D.; Kaštánek, P.; Adhikary, S.P. Exopolysaccharides from Cyanobacteria and Microalgae and their Commercial Application. *Curr. Sci.* **2018**, *115*, 234–241. [CrossRef]
2. Xu, S.Y.; Huang, X.; Cheong, K.L. Recent Advances in Marine Algae Polysaccharides: Isolation, Structure, and Activities. *Mar. Drugs* **2017**, *15*, 388. [CrossRef] [PubMed]
3. Lee, J.H.; Kim, H.H.; Ko, J.Y.; Jang, J.H.; Kim, G.H.; Lee, J.S.; Nah, J.W.; Jeon, Y.J. Rapid Preparation of Functional Polysaccharides from *Pyropia yezoensis* by Microwave-assistant Rapid Enzyme Digest System. *Carbohydr. Polym.* **2016**, *153*, 512–517. [CrossRef]
4. Hayashi, T.; Hayashi, K.; Maeda, M.; Kojima, I. Calcium Spirulan, An Inhibitor of Enveloped Virus Replication, from A Blue-green Alga *Spirulina platensis*. *J. Nat. Prod.* **1996**, *59*, 83–87. [CrossRef]
5. Li, S.; Ji, L.; Shi, Q.; Wu, H.; Fan, J. Advances in the Production of Bioactive Substances from Marine Unicellular Microalgae *Porphyridium* spp. *Bioresour. Technol.* **2019**, *292*, 122048. [CrossRef]

6. Fernando, S.; Kim, K.N.; Kim, D.; You, J.J. Algal Polysaccharides: Potential Bioactive Substances for Cosmeceutical Applications. *Crit. Rev. Biotechnol.* **2018**, *39*, 99–113. [CrossRef]
7. Sun, L.; Wang, C.; Shi, Q.; Ma, C. Preparation of Different Molecular Weight Polysaccharides from *Porphyridium cruentum* and their Antioxidant Activities. *Int. J. Biol. Macromol.* **2009**, *45*, 42–47. [CrossRef]
8. Huheihel, M.; Ishanu, V.; Tal, J.; Arad, S. Activity of *Porphyridium* sp. Polysaccharide against Herpes Simplex Viruses in Vitro and in Vivo. *J. Biochem. Biophys. Methods* **2002**, *48*, 189–200. [CrossRef]
9. Levy-Ontman, O.; Huleihel, M.; Hamias, R.; Wolak, T.; Paran, E. An Anti-inflammatory Effect of Red Microalga Polysaccharides in Coronary Artery Endothelial Cells. *Atherosclerosis* **2017**, *264*, 11–18. [CrossRef]
10. Ben, H.H.; Farhat, A.; Akermi, S.; Khemakhem, B.; Ben, H.Y.; Michaud, P.; Fendri, I.; Abdelkafi, S. In Silico Evidence of Antiviral Activity against SARS-CoV-2 main Protease of Oligosaccharides from *Porphyridium* sp. *Sci. Total Environ.* **2022**, *836*, 155580.
11. Sun, L.; Wang, L.; Zhou, Y. Immunomodulation and Antitumor Activities of Different-molecular-weight Polysaccharides from *Porphyridium cruentum*. *Carbohyd. Polym.* **2012**, *87*, 1206–1210. [CrossRef]
12. Li, T.; Xu, J.; Wu, H.; Jiang, P.; Chen, Z.; Xiang, W. Growth and Biochemical Composition of *Porphyridium purpureum* SCS-02 under Different Nitrogen Concentrations. *Mar. Drugs* **2019**, *17*, 124. [CrossRef] [PubMed]
13. Bayu, A.; Noerdjito, D.R.; Rahmawati, S.I.; Putra, M.Y.; Karnjanakom, S. Biological and Technical Aspects on Valorization of Red Microalgae Genera *Porphyridium*. *Biomass Convers. Biorefinery* **2022**, *13*, 12395–12411. [CrossRef]
14. Li, T.; Xu, J.; Wang, W.; Chen, Z.; Li, C.; Wu, H.; Wu, H.; Xiang, W. A Novel Three-step Extraction Strategy for High-value Products from Red Algae *Porphyridium purpureum*. *Foods* **2021**, *10*, 2164. [CrossRef]
15. Maliki, I.M.; Misson, M.; Teoh, P.L.; Rodrigues, K.F.; Yong, W.T.L. Production of Lectins from Marine Algae: Current Status, Challenges, and Opportunities for Non-destructive extraction. *Mar. Drugs* **2022**, *20*, 102. [CrossRef]
16. Yuan, Y.; Macquarrie, D. Microwave Assisted Extraction of Sulfated Polysaccharides (Fucoidan) from *Ascophyllum nodosum* and its Antioxidant Activity. *Carbohydr. Polym.* **2015**, *129*, 101–107. [CrossRef]
17. Youssouf, L.; Lallemand, L.; Giraud, P.; Soulé, F.; Bhaw-Luximon, A.; Meilhac, O.; D'Hellencourt, C.; Jhurry, D.; Couprie, J. Ultrasound-assisted Extraction and Structural Characterization by NMR of Alginates and Carrageenans from Seaweeds. *Carbohydr. Polym.* **2017**, *166*, 55–63. [CrossRef]
18. Wijesinghe, W.A.J.P.; Jeon, Y.J. Enzyme-assistant Extraction (EAE) of Bioactive Components: A Useful Approach for Recovery of Industrially Important Metabolites from Seaweeds: A Review. *Fitoterapia* **2012**, *83*, 6–12. [CrossRef]
19. Alboofetileh, M.; Rezaei, M.; Tabarsa, M.; Ritta, M.; Donalisio, M.; Mariatti, F.; You, S.; Lembo, D.; Cravotto, G. Effect of Different Non-conventional Extraction Methods on the Antibacterial and Antiviral Activity of Fucoidans Extracted from *Nizamuddinia zanardinii*. *Int. J. Biol. Macromol.* **2019**, *124*, 131–137. [CrossRef]
20. Bezerra, M.A.; Santelli, R.E.; Oliveira, E.P.; Villar, L.S.; Escaleira, L.A. Response Surface Methodology (RSM) as a Tool for Optimization in Analytical Chemistry. *Talanta* **2008**, *76*, 965–977. [CrossRef]
21. Rodriguez-Jasso, R.M.; Mussatto, S.I.; Pastrana, L.; Aguilar, C.N.; Teixeira, J.A. Microwave-assisted Extraction of Sulfated Polysaccharides (Fucoidan) from Brown Seaweed. *Carbohydr. Polym.* **2011**, *86*, 1137–1144. [CrossRef]
22. Balavigneswaran, C.K.; Sujin Jeba Kumar, T.; Moses Packiaraj, R.; Veeraraj, A.; Prakash, S. Anti-oxidant Activity of Polysaccharides Extracted from *Isocrysis galbana* using RSM Optimized Conditions. *Int. J. Biol. Macromol.* **2013**, *60*, 100–108. [CrossRef] [PubMed]
23. Tesvichian, S.; Sangtanoo, P.; Srimongkol, P.; Saisavoey, T.; Buakeaw, A.; Puthong, S.; Thitiprasert, S.; Mekboonsonglarp, W.; Liangsakul, J.; Sopon, A.; et al. Sulfated Polysaccharides from *Caulerpa lentillifera*: Optimizing the Process of Extraction, Structural Characteristics, Antioxidant Capabilities, and Anti-glycation Properties. *Heliyon* **2024**, *10*, e24444. [CrossRef] [PubMed]
24. Rahimi, F.; Tabarsa, M.; Rezaei, M. Ulvan from Green Algae *Ulva intestinalis*: Optimization of Ultrasound-assisted Extraction and Antioxidant Activity. *J. Appl. Phycol.* **2016**, *28*, 2979–2990. [CrossRef]
25. Birgersson, P.S.; Oftebro, M.; Strand, W.I.; Aarstad, O.A.; Sætrom, G.I.; Sletta, H.; Arlov, Ø.; Aachmann, F.L. Sequential Extraction and Fractionation of Four Polysaccharides from Cultivated Brown Algae *Saccharina latissima* and *Alaria esculenta*. *Algal Res.* **2023**, *69*, 102928. [CrossRef]
26. Song, H.; He, M.; Gu, C.; Wei, D.; Liang, Y.; Yan, J.; Wang, C. Extraction Optimization, Purification, Antioxidant Activity, and Preliminary Structural Characterization of Crude Polysaccharide from An Arctic *Chlorella* sp. *Polymers* **2018**, *10*, 292. [CrossRef]
27. Kurd, F.; Samavati, V. Water Soluble Polysaccharides from *Spirulina platensis*: Extraction and in Vitro Anti-cancer Activity. *Int. J. Biol. Macromol.* **2015**, *74*, 498–506. [CrossRef]
28. Zhu, C.P.; Zhai, X.C.; Li, L.Q.; Wu, X.X.; Li, B. Response Surface Optimization of Ultrasound-assisted Polysaccharides Extraction from Pomegranate Peel. *Food Chem.* **2015**, *177*, 139–146. [CrossRef]
29. Cui, Y.; Liu, X.; Li, S.; Hao, L.; Du, J.; Gao, D.; Kang, Q.; Lu, J. Extraction, Characterization and Biological Activity of Sulfated Polysaccharides from Seaweed *Dictyopteris divaricata*. *Int. J. Biol. Macromol.* **2018**, *117*, 256–263. [CrossRef]
30. Xu, Y.; Zhang, L.; Bailina, Y.; Ge, Z.; Ding, T.; Ye, X.; Liu, D. Effects of Ultrasound and/or Heating on the Extraction of Pectin from Grapefruit Peel. *J. Food Eng.* **2014**, *126*, 72–81. [CrossRef]
31. Chen, C.; Zhao, Z.; Ma, S.; Rasool, M.A.; Wang, L.; Zhang, J. Optimization of Ultrasonic-assisted Extraction, Refinement and Characterization of Water-soluble Polysaccharide from *Dictyosphaerium* sp. and Evaluation of Antioxidant Activity in Vitro. *J. Food Meas. Charact.* **2020**, *14*, 963–977. [CrossRef]
32. Ge, Y.; Ni, Y.; Yan, H.; Chen, Y.; Cai, T. Optimization of the Supercritical Fluid Extraction of Natural Vitamin E from Wheat Germ Using Response Surface Methodology. *J. Food Sci.* **2002**, *67*, 239–243. [CrossRef]

33. Pereira, T.; Barroso, S.; Mendes, S.; Amaral, R.A.; Dias, J.R.; Baptista, T.; Saraiva, J.A.; Alves, N.M.; Gil, M.M. Optimization of Phycobiliprotein Pigments Extraction from Red Algae *Gracilaria gracilis* for Substitution of Synthetic Food Colorants. *Food Chem.* **2020**, *321*, 126688. [CrossRef] [PubMed]
34. Wang, N.; Dai, L.; Chen, Z.; Li, T.; Wu, J.; Wu, H.; Wu, H.; Xiang, W. Extraction Optimization, Physicochemical Characterization, and Antioxidant Activity of Polysaccharides from *Rhodosorus* sp. SCSIO-45730. *J. Appl. Phycol.* **2022**, *34*, 285–299. [CrossRef] [PubMed]
35. Torabi, P.; Hamdami, N.; Keramat, J. Optimization and Kinetics of Microwave-assisted Extraction of Sulfated Fucose-rich Polysaccharides from *Nizamuddinia zanardinii*. *Biomass Convers. Biorefinery* **2022**, *14*, 14707–14723. [CrossRef]
36. Dobrinčić, A.; Balbino, S.; Zorić, Z.; Pedisić, S.; Bursać Kovačević, D.; Elez Garofulić, I.; Dragović-Uzelac, V. Advanced Technologies for the Extraction of Marine Brown Algal Polysaccharides. *Mar. Drugs* **2020**, *18*, 168. [CrossRef]
37. Kadam, S.U.; Tiwari, B.K.; O'Donnell, C.P. Application of Novel Extraction Technologies for Bioactives from Marine Algae. *J. Agric. Food Chem.* **2013**, *61*, 4667–4675. [CrossRef]
38. Dubois, M.; Gilles, K.A.; Hamilton, J.K.; Rebers, P.A.; Smith, F. Colorimetric Method for Determination of Sugars and Related Substances. *Anal. Chem.* **1956**, *28*, 350–356. [CrossRef]

marine drugs

MDPI

Article

Advanced Extraction Techniques and Physicochemical Properties of Carrageenan from a Novel *Kappaphycus alvarezii* Cultivar

Madalena Mendes [1], João Cotas [1], Irene B. Gutiérrez [2], Ana M. M. Gonçalves [1,3], Alan T. Critchley [4], Lourie Ann R. Hinaloc [5,6], Michael Y. Roleda [5,6] and Leonel Pereira [1,*]

1 CFE—Centre for Functional Ecology: Science for People & Planet, Marine Resources, Conservation and Technology—Marine Algae Lab, Department of Life Sciences, University of Coimbra, 3000-456 Coimbra, Portugal; 2018283963@student.uc.pt (M.M.); jcotas@uc.pt (J.C.); amgoncalves@uc.pt (A.M.M.G.)
2 Marine and Environmental Sciences Centre (MARE), Department of Life Sciences, University of Coimbra, 3000-456 Coimbra, Portugal; ibgutierrez@uc.pt
3 Department of Biology and CESAM, University of Aveiro, 3810-193 Aveiro, Portugal
4 Verschuren Centre for Sustainability in Energy and Environment, Sydney, NC B1M 1A2, Canada; alan.critchley2016@gmail.com
5 The Marine Science Institute, College of Science, University of the Philippines Diliman (UP-MSI), Quezon City 1101, Philippines; lrhinaloc@msi.upd.edu.ph (L.A.R.H.); myroleda@up.edu.ph (M.Y.R.)
6 Bolinao Marine Laboratory, University of the Philippines Diliman (UP-MSI), Luciente I, Bolinao 2406, Philippines
* Correspondence: leonel.pereira@uc.pt

Abstract: Carrageenans are valuable marine polysaccharides derived from specific species of red seaweed (Rhodophyta) widely used as thickening and stabilizing agents across various industries. *Kappaphycus alvarezii*, predominantly cultivated in tropical countries, is the primary source of kappa-carrageenan. Traditional industrial extraction methods involve alkaline treatment for up to three hours followed by heating, which is inefficient and generates substantial waste. Thus, developing improved extraction techniques would be helpful for enhancing efficiency and reducing environmental impacts, solvent costs, energy consumption, and the required processing time. In this study, we explored innovative extraction methods, such as ultrasound-assisted extraction (UAE) and supercritical water extraction (SFE), together with other extraction methods to produce kappa-carrageenan from a new strain of *K. alvarezii* from the Philippines. FTIR-ATR spectroscopy was employed to characterize the structure of the different carrageenan fractions. We also examined the physicochemical properties of isolated phycocolloids, including viscosity, and the content of fatty acids, proteins, and carbohydrates. For refined carrageenan (RC), both the traditional extraction method and the UAE method used 1 M NaOH. Additionally, UAE (8% KOH) was employed to produce semi-refined carrageenan (SRC). UAE (8% KOH) produced a high yield of carrageenan, in half the extraction time (extraction yield: 76.70 ± 1.44), and improved carrageenan viscosity (658.7 cP), making this technique highly promising for industrial scaling up. On the other hand, SFE also yielded a significant amount of carrageenan, but the resulting product had the lowest viscosity and an acidic pH, posing safety concerns as classified by the EFSA's re-evaluation of carrageenan as a food additive.

Keywords: marine polysaccharides; kappa-carrageenan; alkaline treatment; ultrasound-assisted extraction; supercritical fluid extraction; semi-refined carrageenan (SRC); food safety

1. Introduction

Traditional methods for extracting polysaccharides from seaweed are labor-intensive and require substantial quantities of chemicals, water, and energy. Hot water extraction (HWE) is one of the most commonly used techniques, but it demands extended extraction

times at high temperatures and yields low returns, including low selectivity and extraction efficiency. This method typically produces "native" (i.e., non-modified) polysaccharides [1].

Green industries are emerging to contribute to the reduction in carbon footprints and the consequent climate change impacts by scaling down industrial chemical usage and processing time while enhancing the quality and quantity of extracted seaweed polysaccharides. This creates a beneficial scenario both environmentally and economically. Some of these innovative industrial testing techniques include the following: microwave-assisted extraction (MAE); enzymatic-assisted extraction (EAE); ultrasound-assisted extraction (UAE), which operates at lower temperatures and yields higher outputs [2]; and green solvent extraction methods like subcritical water extraction (SWE) and ionic liquid extraction. Other advanced methods include supercritical fluid extraction (SFE) [3], reactive extrusion, and photo-bleaching.

Seaweeds from the family Solieriaceae (Gigartinales, Rhodophyta), specifically from the genera *Kappaphycus* and *Eucheuma*, are collectively known as eucheumatoids. Eucheumatoids do not produce pure forms of κ- or ι-carrageenans but instead generate a variety of hybrid structures. These macroalgae produce various types of carrageenans, primarily kappa and iota. The domestication of these seaweeds began in the 1960s when harvesting wild populations could no longer meet the increasing global demand for carrageenans. Carrageenans are polysaccharides composed of D-galactose and 3,6-anhydro-D-galactose sulfate. Their chemical structure is heterogeneous and classified based on the number and position of sulfate esters and the location of the 3,6-anhydro-bridge in (1→4)-linked galactopyranose molecules. The industrially significant types extracted from various eucheumatoids are kappa (κ)-, iota (ι)-, and lambda (λ)-carrageenans [4]. Kappa-carrageenan features a sulfate group on the O-4 position of every third galactosyl unit in its repeating dimer. Its structure consists of a right-handed double helix formed by parallel chains [4]. To chemically stabilize carrageenan, there is a need for the alkali modification of carrageenan in industrial extraction to enhance polysaccharide extraction yield, boost gel strength, and increase the product's reactivity with proteins [5].

Carrageenans can be classified based on their production method into refined carrageenan (RC) and semi-refined carrageenan (SRC). RC, recognized as food-grade carrageenan, is labeled with the EU additive number E407, whereas SRC is E407a [5]. The European Food Safety Authority (EFSA) considers both refined carrageenan (RC) and semi-refined carrageenan (SRC) to be safe, with no evidence of adverse effects in humans, when consumed in the amounts necessary to achieve the desired food texture [6]. According to the Commission Regulation (EU), the purity criteria for refined carrageenan (RC) and semi-refined carrageenan (SRC) include parameters such as appearance, viscosity, sulfate content, ash content, pH, moisture, solubility, heavy metals/metalloids (arsenic, lead, mercury, and cadmium), and molecular weight. Carrageenans are defined as having an average molecular weight ranging from 200 to 800 kDa [7]. Carrageenan preparations exhibit high polydispersity, with a small fraction of lower-molecular-weight polymeric chains (20–50 kDa) naturally present in all samples [6]. However, under conditions of extensive hydrolysis, at low pH (<1.3) and high temperatures (>80 °C) for extended periods, a non-naturally occurring fraction of degraded carrageenan can form. This degraded fraction has a weight average molecular weight of 10–20 kDa and lacks texturizing properties; it has also been called poligeenan [6]. Studies conducted in rodents have shown that consuming high amounts of poligeenan is associated with the development of ulcerative colitis [8]. Therefore, the number of low-molecular-weight polysaccharide chains in food-grade carrageenan is regulated. Although there is currently no validated testing method for quantifying this low-molecular-weight fraction in carrageenan samples, viscosity measurements can differentiate between carrageenans and poligeenans. A viscosity of 5 mPa·s (for a 1.5% solution at 75 °C) corresponds to a sample with a molecular weight of approximately 100–150 kDa [7].

In the production of RC, polysaccharides are dissolved in hot alkaline solutions, such as sodium hydroxide (NaOH), at temperatures between 95 and 110 °C. Insoluble

compounds are then removed through filtration. The solution is concentrated, and carrageenan is purified by precipitating it with alcohol, a method used for purifying all types of carrageenan [9]. Following this step, the biomass is dried and then ground into a powder.

In RC production, the hydrocolloid is extracted from the seaweed matrix. In contrast, SRC processing involves treating seaweed thalli (dried seaweed) with aqueous potassium hydroxide (KOH) at 75–80 °C for 2 h to dissolve and remove soluble compounds other than carrageenans, such as salts, soluble sugars, and proteins [10]. The hydroxide in the reagent interacts with the seaweed polymers, reducing the sulfate content in carrageenan while increasing the amount of 3,6-anhydrogalactose. The potassium component of the reagent reacts with carrageenan to form a gel, which prevents it from dissolving in the hot solution. Soluble carbohydrates, proteins, fats, and salts are removed when the solution is drained, and the residue is rinsed multiple times. This washing step is designed to remove the processing alkali and any other water-soluble compounds. The alkali-treated seaweed (ATC) is then dried, cut, and ground into a powder, known as SRC or seaweed flour [10].

RC, often referred to as raw carrageenan [5], is known for its higher quality and clear appearance, making it suitable for a wide range of applications. However, SRC production is more economical than RC extraction as it avoids the costs associated with carrageenan precipitation and solvent recovery. Although SRC is generally of lower quality and less suitable for human food applications, it is increasingly used as a cost-effective extender in food products such as processed meat. SRC is primarily employed in pet food production due to its slightly cloudy and colored appearance and may have a higher bacterial count, which is nullified during meat processing [11].

Kappaphycus alvarezii is a commercially valuable red macroalga highly sought after for its cell wall polysaccharide, κ-carrageenan [12]. Once harvested, these seaweeds yield a relatively high polysaccharide content, e.g., approximately 40–60% on a dry weight basis [5]. *K. alvarezii* is preferred by industrial processors for producing both SRC and RC.

Ironically, even after nearly six decades, the sex and ploidy of commercially cultivated *Kappaphycus* species remain entirely understudied. Furthermore, potential differences in growth rates, biochemistry, and rheological properties between vegetative and reproductive thalli and amongst different life history stages (i.e., male and female haploid gametophytes and diploid tetrasporophytes) are rarely considered, despite their possible significant economic impacts. For example, in other commercially important taxa, such as *Gelidiella acerosa*, agar yield and quality vary between vegetative and reproductive fronds [13]. In *Chondrus crispus*, the carrageenan composition varies significantly between life stages: the diploid tetrasporophyte primarily produces lambda-carrageenan, while the haploid gametophyte mainly produces kappa- and iota-carrageenans [4].

Carrageenans have been extracted on an industrial scale primarily from farmed, highly selected tropical eucheumatoids using a conventional method. This process involves exposing seaweed biomass to high temperatures for up to 3 h in an alkaline environment. This traditional method could be improved by employing novel technologies that offer higher extraction yields, better properties, reduced extraction time, and lower production costs.

In this study, native (NE), conventional (CE), and advanced extraction technologies, e.g., ultrasound-assisted extraction (UAE) and supercritical fluid extraction (SFE), were tested to quantify their effects on the yield and properties of extracted carrageenan—a regulated food additive product [2]. Aqueous UAE methods have previously shown that an increased extraction yield in the red alga *Hypnea musciformis* caused the disruption of cell walls, decreased particle size, and increased the mass transfer of cell contents [14]. In the SFE method, temperature and pressure were co-applied to quickly permeate into seaweed thalli in order to produce pure extracts. The efficiency of SFE, on the other hand, is dependent on the water content of the starting seaweed material, as well as the ratio of solvent, the flow rate, temperature, pressure, and the biomass particle size [3]. SFE has several benefits, including the use of environmentally friendly solvents (i.e., water), speedy extraction, and high-quality outputs [1]. However, the above studies lack product quality assurance which substantiate and guarantee the applications of the various extracts as

human food additives. It is essential that such products produced using novel or advanced green technology must achieve certification.

Thus, the main objective of this study was to evaluate various extraction methods on the yield and properties of extracted carrageenans from a designated novel, haploid, female gametophyte of the *Kappaphycus alvarezii* strain G-N7. [15]. The comparisons will allow us to understand whether green technologies promote and maintain the expected properties and retain the necessary qualities of the certified food additive

Carrageenan quality was measured using FTIR-ATR, coupled with viscosity and proximate chemistry (e.g., proteins, fatty acids, uronic acids, and carbohydrates) analyses. The goal was to determine which extraction method produced the best carrageenan yield and properties and which might be adapted for industrial-scale carrageenan production based on the Codex Alimentarius and EFSA regulations. Therefore, this study can provide insights to optimize production costs and recommend sustainable and environmentally friendly alternatives with enhanced efficiencies, as compared to traditional industrial methods.

2. Materials and Methods

2.1. Seaweed Cultivation and Harvest

The novel cultivar G-N7 is a haploid female gametophyte clonally propagated in an outdoor hatchery located in Bolinao, Pangasinan, Philippines. The specific life history phase, sex, and ploidy of G-N7 were established from the progeny of a wild, fertile diploid tetrasporophyte, known as KaTR-N, which was collected from Guiuan, Samar, Philippines [15]. Based on the cox2-3 spacer sequence, this strain belongs to KALV-3, a predominantly wild haplotype from the collection site. It is genetically distinct from the commercially cultivated haplotype 3, known commercially as the "Tambalang" strain, which is the cultivar mostly farmed for carrageenan processing [16] (Figure 1).

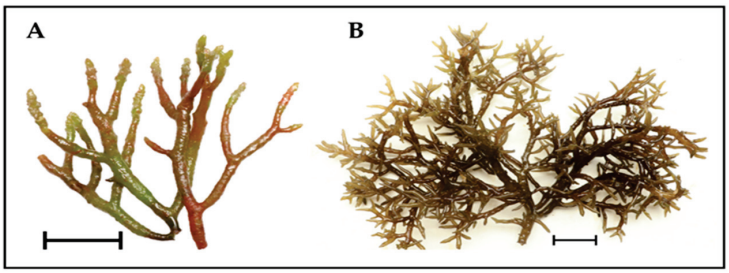

Figure 1. *Kappaphycus alvarezii* cultivars. (**A**) Novel haploid female gametophyte G-N7 strain. (**B**) Commercially cultivated "Tambalang" strain. Scale bar = 5 cm.

G-N7 was clonally propagated using branch cuttings in an aquarium (58 × 30 × 40 cm) supplied with air and flow-through, nutrient-replete, sand-filtered seawater pumped from a depth of approximately 12–15 m in the Guiguiwanen Channel, near the land-based hatchery. The outdoor hatchery, covered by translucent roofing, received semi-natural solar radiation, with an average noontime surface irradiance of 506 µmol photons m^{-2} s^{-1}, measured using a cosine sensor coupled to a LI-COR light meter (LI-14000, LiCOR, Lincoln, NE, USA). The mean daytime water temperature was 31.7 °C, measured using HOBO data loggers (UA-002-64, HOBO, Onset Computer Corporation, Bourne, MA, USA) [17]. The average daily growth rate (DGR) in the nursery was approximately 2% per day. Biomass was harvested every 45–50 days or when the aquarium was filled with biomass. Harvested samples were sun-dried to an approximate 10% moisture content and packed in airtight plastic bags until transport for further chemical analyses.

2.2. Sample Preparation

The sun-dried, or commercially known as raw dried seaweed (RDS), biomass of the G-N7 *K. alvarezii* cultivar was, on receipt in the Portuguese laboratories, washed with

distilled water to remove excess salt. The washed biomass (318 g) was dried in a forced air oven (Raypa DAF-135, R. Espinar S.L., Barcelona, Spain) at 60 °C for 48 h until its moisture content was <2%.

2.3. Carrageenan Extraction and Recovery

Carrageenan extraction was performed in triplicate using 1 g RDS per replicate. The extraction methods used were native or conventional, or ultrasound-assisted extraction (UAE) or supercritical fluid extraction (SFE) was applied, as described below. After extraction, processing for refined carrageenan (RC) and SRC adopted the following general protocols for precipitation, drying, and grinding for further analyses. Briefly, the carrageenan extract was precipitated by adding twice its volume of 96% ethanol and stirred. The precipitate was collected and drained using a cloth filter (mesh 60). This was washed and stored in 96% ethanol, at 4 °C for 48 h. Samples were then placed into Petri dishes and dried in a forced air oven (Raypa DAF-135, R. Espinar S.L., Barcelona, Spain) at 60 °C for 48 h, as described and determined by Pereira et al. [4,9]. Finally, dried carrageenan was weighed to determine the extraction yield (% of dry weight) and milled into powder (particle size < 0.05 cm) with a commercial grinder (TitanMill 300 DuoClean, Cecotec, Valencia, Spain) for further analyses.

2.4. Native Extraction (NE)

"Native" phycocolloid was extracted by placing 1 g of dry seaweed biomass (n = 3) in distilled water (100 mL), pH 7, at 100 °C for 3 h [4]. The solution was hot-filtered under vacuum through a cloth filter supported in a Buchner funnel, followed by a Gooch 2 silica funnel filtration. The extract was evaporated (rotary evaporator: 2600000, Witeg, Germany) under vacuum to one-third of the initial volume. This was followed by ethanol precipitation, drying, and grinding protocols to obtain carrageenan powder for further chemical analyses, as described below.

2.5. Carrageenan Extraction via Refined and Semi-Refined Processes

In conventional (CE) and ultrasound-assisted (UAE) carrageenan extractions, (1) refined and (2) semi-refined processes were performed to obtain refined carrageenan (RC) and semi-refined carrageenan (SRC), respectively.

(1) Refining process—The solution was hot-filtered under vacuum through a cloth filter supported in a Buchner funnel. After this, the extract was filtered under vacuum with a Gooch 2 silica funnel. The extract was evaporated under vacuum to one-third of the initial volume (50 mL). Carrageenan was precipitated by adding twice its volume of 96% ethanol (100 mL). Due to gelling, after precipitation, carrageenan was collected through a filtration cloth. After this, the carrageenan fiber retained in the cloth was washed and stored with 96% ethanol for 48 h at 4 °C. Drying was conducted at 60 °C for 48 h, and fibers were milled into powder (particle size < 0.05 cm) using a commercial grinder (TitanMill 300 DuoClean, Cecotec, Valencia, Spain). This process was repeated three times to obtain triplicate replicates.

(2) Semi-refining process—The solution was hot-filtered under vacuum through a cloth filter supported in a Buchner funnel. The residue, retained in the cloth, was rinsed several times to remove the alkali and anything else that might dissolve in the water during the rinsing process. The alkali-treated seaweed was washed with 96% ethanol for 48 h at 4 °C. Drying, and grinding protocols were performed. The process was repeated three times to obtain triplicate replicates.

2.5.1. Conventional Extraction (CE)

2.5.1.1. RC Obtention

Dry seaweed biomass (1 g, n = 3) was placed in a solution (150 mL) of NaOH (1 M) at 90–100 °C for 3 h, which was stirred every 15 min, according to the method described by Pereira and Van De Velde [18] (Figure 2).

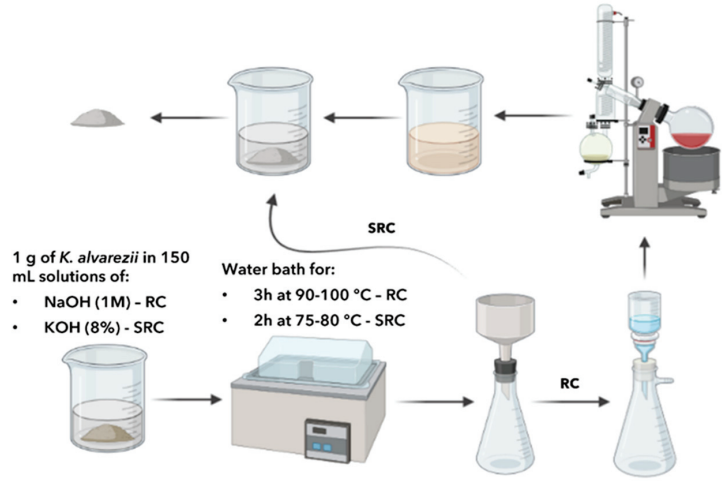

Figure 2. Workflow of conventional extraction method performed for carrageenan extraction (RC: refined extraction; SRC: semi-refined extraction).

2.5.1.2. SRC Sample Production

Dry seaweed biomass (1 g, $n = 3$) was placed in a solution (150 mL) of KOH (8%) at 75–80 °C for 2 h, which was stirred every 15 min, as shown in Figure 2.

2.5.2. Ultrasound-Assisted Extraction (UAE) Method

Extraction conditions were based on the previous method of Youssouf et al. [19] with modifications. Briefly, water was added to a heated pulsed ultrasound bath (120 W) (ultrasonic cleaner ULTR-3L2-001, IBX instruments, Barcelona, Spain) until the extraction beaker was in full contact with the external medium. After, temperature and time were set, before putting the extraction beaker (with seaweed and extraction solvent (NaOH or KOH)) in the ultrasound unit. After, the conventional pulsed ultrasound technique was applied to the extraction beaker with the following modified methodology (Sections 2.5.2.1 and 2.5.2.2).

2.5.2.1. RC Sample Production

Dry seaweed biomass (1 g; $n = 3$) was placed in a solution (150 mL) of NaOH (1 M) and subject to a heated pulsed ultrasound bath (120 W) (ultrasonic cleaner ULTR-3L2-001, IBX instruments, Barcelona, Spain) at 70 °C for 60 min (Figure 3).

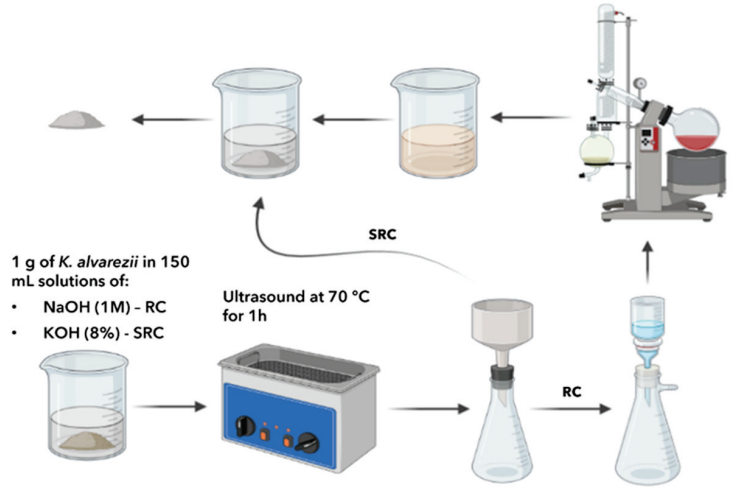

Figure 3. Workflow of ultrasound-assisted extraction method performed for carrageenan extraction (RC: refined extraction; SRC: semi-refined extraction).

2.5.2.2. SRC Sample Production

Dry seaweed biomass (1 g; n = 3) was placed in a solution (150 mL) of KOH (8%) and subjected to ultrasound at different temperatures (45 °C and 70 °C) for 60 min (Figure 3).

2.5.3. Supercritical Water Extraction (SFE)

Supercritical water extraction was performed by placing forced air-dried seaweed (1 g, n = 3) and 100 mL distilled water into an electric pressure cooker (Aigostar 300008IAU, Aigostar, Madrid, Spain) at a temperature of 115 °C with an air pressure of 80 KPa for 2 h. The solution was hot-filtered under vacuum through a cloth filter supported in a Buchner funnel. Alcohol precipitation, drying, and grinding protocols were performed to obtain powdered RC for further analyses.

2.6. Analyses of Extracted Carrageenans

2.6.1. Yield

The formula used to determine the carrageenan yield of each extraction is as follows:

$$Yield = \frac{We}{Wds} \times 100$$

where *We* is the extracted carrageenan weight (g), and *Wds* is the dried seaweed weight (g) used for extraction.

2.6.2. Fatty Acid Content

Carrageenan obtained from each extraction method was processed to obtain lipid extracts. Lipid extraction was performed in triplicate following the technique described by Gonçalves et al. [20]. Samples were incubated with methanol for the methylation of lipids. Then, n-hexane was added, and the samples were centrifuged to extract fatty acid methyl esters (FAMEs). The internal standard nonadecanoic acid C19 was added to each sample to quantify the fatty acid (FA) content and stored at −80 °C. FAME separation was carried out through gas chromatography-mass spectrometry (GC-MS) equipped with a 0.32 mm internal diameter, 0.25 µm film thickness, and 30 m long TR-FFAP column. The sample (1.00 µL) was injected into spitless mode. The initial column temperature was programmed at 80 °C and held for 3 min; the first ramp (20 °C min^{-1}) increased the temperature to 160 °C. The second ramp (2 °C min^{-1}) reached up to 190 °C, and the last ramp (5 °C min^{-1}) reached a final temperature of 220 °C that was held for 10 min, as described by Gonçalves et al. [20]. Helium was used as the carrier gas, at a flow rate of 1.4 mL min^{-1}. The identification of each peak was performed by comparing the retention time and mass spectrum of each FAME to those of the Supelco®37 component FAME mix (Sigma-Aldrich, Steinheim, Germany). The integration of the FAME peaks were carried out using the equipment's software. The quantification of the FAMEs was performed as previously described in Gonçalves et al. [20].

2.6.3. Carbohydrate and Uronic Acid Content

Carrageenan obtained from each triple replicated extraction method underwent hydrolysis in triplicate according to Selvendran et al. [21] to extract neutral sugars and uronic acids. These sugars were then reduced and acetylated as described by Coimbra et al. [22] to produce alditol acetates, which were subsequently analyzed by gas chromatography. The analysis was performed using a Thermo Scientific Trace 1310 chromatograph (Waltham, MA, USA) equipped with a flame ionization detector (GC-FID). A TG-WAXMS A GC column (30 m length, 0.32 mm i.d., 0.25 µm film thickness) was employed. The initial temperature of the oven was set at 180 °C and maintained for 1 min, then increased at a rate of 15 °C/min to 220 °C, held for 5 min, followed by a final ramp of 1 °C/min to reach 230 °C, where it was held for another 5 min. Helium served as the carrier gas at a flow rate of 1.7 mL/min. Peaks were identified by their retention times and quantified by comparison with standards. Uronic acids were measured using the Blumenkrantz and Asboe-Hansen

method [23] with a Biochrom EZ Read 2000 Microplate reader (Biochrom Ltd., Cambridge, UK) at an absorbance wavelength of 520 nm. Galacturonic acid (Merck KGaA, Darmstadt, Germany) was used for the calibration curve, and 3-phenylphenol was the colorimetric reagent. The results are presented as the percentage of the dried polymer biomass.

2.6.4. Protein Content

Carrageenan solutions (1% m/v) (n = 3) were prepared from powder obtained from the different extraction methods applied by dissolving the polysaccharide in distilled water. Protein content was measured after Bradford [24], based on spectrophotometry, adapted to the microplate. Samples were analyzed at 595 nm using a Biochrom EZ Read 2000 Microplate reader (Biochrom Ltd., Cambridge, UK). Protein concentration was calculated by comparison using bovine serum albumin (Merck KGaA, Darmstadt, Germany) as a standard.

2.6.5. Viscosity, pH, EC, and TDS

Carrageenan solutions (1% m/v; n = 1 from each extraction method) were prepared by dissolving the powdered polysaccharide in distilled water using a heating plate and magnetic stirring. Then, the solutions were cooled until reaching room temperature, and viscosity measurement was carried out using spindles SP2 and SP3 in an IKA Rotavisc Viscometer (KA-Werke GmbH & Co. KG, 79219 Staufen, Germany), with a speed of 100 rpm for 1 min. A pH/Conductivity/TDS meter (Combo HI98129, HANNA instruments, Smithfield, RI, USA) was used to measure the pH and TDS values of the carrageenan solutions. Commercial standards of kappa- and iota-carrageenans were obtained from Thermo Fisher Scientific (Waltham, MA, USA).

2.6.6. Spectrophotometric Profiles of Carrageenan Solutions

Carrageenan solutions (1% m/v; n = 1) prepared for the viscosity analyses were diluted with distilled water (1:2), and UV-VIS absorption spectra were measured in the range of 200–800 nm using a UV-3100PC, UV/VIS Scanning Spectrophotometer (VWR® Radnor, PA, USA) with 1 cm quartz cuvettes.

Attenuated total reflectance (ATR) Fourier transform infrared (FT-IR) spectroscopy was employed to characterize the structure of dried extracted carrageenans. The IR spectra (24 scans) were obtained at room temperature (referenced against air) in the wave number range of 400–4000 cm^{-1} (resolution of 4 cm^{-1}) using a Bruker Alpha II (Bruker, Ettlingen, Germany). Spectra were analyzed with OPUS 7.2 software (Bruker, Ettlingen, Germany). Commercial standards of kappa- and iota-carrageenans were obtained from Thermo Fisher Scientific (Waltham, MA, USA). The ratios between the 805 and 845 cm^{-1} absorption bands in the spectra were calculated [4] and used to determine the degree of iota/kappa hybridization [4].

2.7. Statistical Analyses

All experiments and subsequent analyses were performed in triplicate, and data are presented as the means ± standard deviations. An analysis of variance (ANOVA) was performed, and comparisons of means were conducted using different multiple comparison tests using the Sigmaplot program (version 14.0, SigmaPlot, D-40212 Düsseldorf, Germany). Values were considered to differ significantly if the p value was <0.05.

For the exploratory analysis, a multi-linear regression (singular value decomposition) was used to estimate the relationship between each sample and the standard commercial kappa-carrageenan and iota-carrageenan using the Spectragryph program (Spectragryph, 87561 Oberstdorf, Germany) [25] in the spectral range of 400–4000 cm^{-1}.

3. Results

3.1. Extraction Yield and Biochemical Composition

The mean yield of carrageenans obtained using different protocols ranged from 33.73 ± 10.52 to 77.33% of the initial dry weight of the sample (detailed in Table 1). The highest mean yield (i.e., 77.3 ± 2.5%) was achieved using the alkali (KOH)-treated conventional method, while the lowest yield (33.73 ± 10.52%) came from the alkali (NaOH)-treated UAE method. Despite the 44% difference between the minimum and maximum mean yields, the variations among the different extraction protocols were not statistically significant, though they could have economic implications.

Table 1. Carrageenan extraction methods versus yield, protein content, uronic acid content, and the relative and total composition of fatty acids and monosaccharides (wt%) present in carrageenan extracted using different methods. Data are given as the mean ± SDs. Values with the same letter are not significantly different ($p > 0.05$).

		Extraction Method						
Parameters		**NE**	**SFE**	**CE (NaOH)**	**CE (KOH)**	**UAE (NaOH)**	**UAE (KOH45)**	**UAE (KOH)**
Extraction yield (%)		45.47 ± 1.92 ^{a}	53.40 ± 1.80 ^{a}	35.67 ± 1.89 ^{a}	77.33 ± 2.49 ^{a}	33.73 ± 10.52 ^{a}	63.20 ± 3.23 ^{a}	76.70 ± 1.44 ^{a}
Protein (%)		0.00 ± 0.01 ^{b}	0.01 ± 0.01 ^{a,b}	0.02 ± 0.01 ^{a,b}	0.01 ± 0.01 ^{a,b}	0.04 ± 0.02 ^{a}	0.02 ± 0.01 ^{a,b}	0.01 ± 0.01 ^{a,b}
Uronic acids (%)		13.59 ± 1.97 ^{a}	13.52 ± 1.37 ^{a}	13.95 ± 1.05 ^{a}	9.43 ± 2.78 ^{a,b}	6.43 ± 0.11 ^{b}	8.95 ± 0.23 ^{a,b}	10.06 ± 1.28 ^{a,b}
Fatty acids (%)	C16:0	0.02 ± 0.01 ^{a}	0.01 ± 0.00 ^{a}	0.02 ± 0.01 ^{a}	0.05 ± 0.02 ^{a}	0.01 ± 0.00 ^{a}	0.07 ± 0.02 ^{a}	0.07 ± 0.00 ^{a}
	C18:0	0.01 ± 0.01 ^{a}	0.01 ± 0.00 ^{a}	0.02 ± 0.00 ^{a}	0.01 ± 0.00 ^{a}	0.01 ± 0.00 ^{a}	0.01 ± 0.00 ^{a}	0.01 ± 0.00 ^{a}
	C18:1	nd	nd	0.01 ± 0.01 ^{a}	0.01 ± 0.00 ^{a}	nd	0.01 ± 0.00 ^{a}	nd
	Σ	0.03	0.03	0.05	0.07	0.03	0.09	0.08
Monosaccharides (%)	Galactose	6.98 ± 0.23 ^{a,b}	7.28 ± 0.29 ^{a,b}	7.87 ± 0.36 ^{a}	5.23 ± 0.30 ^{c}	6.45 ± 0.37 ^{b}	5.06 ± 0.05 ^{c}	6.29 ± 0.34 ^{b}
	Glucose	nd	nd	nd	1.92 ± 0.08	0.04 ± 0.06	1.87 ± 0.19	2.20 ± 0.03
	Fucose	0.21 ± 0.03 ^{b,c}	0.15 ± 0.02 ^{c}	0.36 ± 0.09 ^{b,c}	0.68 ± 0.02 ^{a}	0.31 ± 0.12 ^{b,c}	0.44 ± 0.11 ^{a,b}	0.34 ± 0.11 ^{b,c}
	Arabinose	nd	nd	nd	0.03 ± 0.01 ^{a}	nd	0.06 ± 0.02 ^{a}	0.08 ± 0.00 ^{a}
	Xylose	0.10 ± 0.00 ^{b,c}	0.05 ± 0.03 ^{c}	0.24 ± 0.03 ^{a}	0.32 ± 0.02 ^{a}	0.23 ± 0.08 ^{a}	0.19 ± 0.02 ^{a,b}	0.05 ± 0.03 ^{c}
	Σ	7.29	7.49	8.48	10.10	7.06	9.49	11.16

nd—non-detectable, value below the detection limit.

In general, the yield under an alkaline (KOH) environment was higher for both the conventional (CE; 90 °C, 2 h) and ultrasound-assisted (UAE; 120 W, 1 h) extraction methods. UAE (120 W, 1 h) revealed values close to the conventional carrageenan yield in a shorter time.

The protein content (Table 1) in all treatments showed very low values, with UAE (NaOH) exhibiting the highest content (0.04 ± 0.02%), which is very important for analyzing extraction quality and obtaining the approval of carrageenan as a human food additive ingredient.

Uronic acid content analysis (Table 1) revealed significant differences amongst the extraction methods. The NE, SFE, and CE (NaOH) methods showed a notably higher mean uronic acid content (i.e., 13.59 ± 1.97, 13.52 ± 1.37, and 13.95 ± 1.05% of DW, respectively), as compared to the others. In contrast, the UAE (NaOH) method resulted in the lowest uronic acid content.

A higher total content of FAMEs was observed in KOH alkali-treated RC (Table 1). FAME analysis identified two saturated fatty acids (SFAs) (palmitic acid [C16:0] and stearic acid [C18:0]) and one monounsaturated fatty acid (MUFA) (oleic acid [C18:1]). While palmitic acid (C16:0) values did not show statistically significant differences, all KOH alkali treatments exhibited higher mean values. Stearic acid (C18:0) values were very similar across extraction methods, and oleic acid (C18:1) was detected only in the conventional extraction method [CE (NaOH) and CE (KOH)] and UAE (KOH45).

The total monosaccharide content (Table 1) was higher for the alkali treatments performed with KOH [CE (KOH), UAE (KOH45), and UAE (KOH)]. Carbohydrate analysis

identified four different monosaccharides in addition to galactose: glucose, fucose, arabinose, and xylose. Galactose was the most abundant residue in all treatments. Glucose had the second highest value, detected in all KOH alkali extractions [CE (KOH), UAE (KOH45), and UAE (KOH)] and in very low amounts in UAE (NaOH.

3.2. Viscosity, pH, EC, and TDS

The physicochemical parameters measured are summarized in Table 2. All 1% solutions of carrageenan extracts obtained through alkali (UAE KOH) treatment exhibited non-dissolvable particles and had a yellowish appearance, except for the commercial samples, which were clear. Solutions made with commercial iota- and kappa-carrageenan had the lowest EC and TDS values. Carrageenan extracted using the alkali (UAE; KOH; 70 °C) method had the highest viscosity at 658.7 cP. The pH of all samples from different extraction methods was alkaline, except for SFE, which had a slightly acidic pH (6.79), and NE, which had a neutral pH (7.34). The EC and TDS of alkaline (UAE; NaOH)-treated extracts were higher compared to the others, with values in a similar range.

Table 2. Physicochemical parameters of the *Kappaphycus alvarezii* haploid strain solution (1%): viscosity, pH, electrical conductivity (EC), and total dissolved solids (TDS).

Extraction Method	Viscosity (cP)	pH	EC (µS cm^{-1})	TDS (ppm)
NE	16.8	7.34	2373	1158
SFE	7.8	6.79	2323	1170
CE (NaOH)	15.9	10.25	3156	1604
CE (KOH)	50.87	10.85	2733	1366
UAE (NaOH)	8.1	10.70	>3999	>2000
UAE (KOH45)	183.6	10.89	2817	1439
UAE (KOH)	658.7	9.30	2492	1286
Iota standard (i)	134.7	9.69	2019	1012
Kappa standard (k)	79.2	8.66	1891	949

3.3. UV-VIS Absorption Spectra of Carrageenan Solutions

The carrageenans obtained through the different methods differed in their spectral profiles, suggesting that the composition and the UV absorbance potential varied depending on the extraction method (Figure 4).

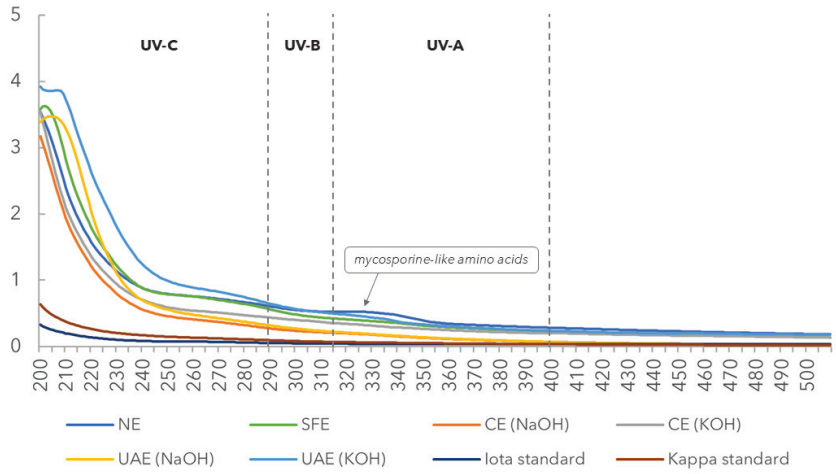

Figure 4. UV absorption spectra (λ = 200–600 nm) of carrageenan solutions extracted by native extraction (NE), conventional extraction (CE: NaOH and CE: KOH), ultrasound-assisted extraction (UAE: NaOH, 120 W, 70 °C, 1 h; UAE: KOH, 120 W, 45 °C, 1 h; UAE: KOH, 120 W, 70 °C, 1 h), and supercritical water extraction (SFE). UV-C range: 100–290 nm; UV-B range: 290–315 nm; and UVA range: 315–400 nm.

Only the native (NE) carrageenan solution absorbed part of UV-A radiation (320–400 nm), exhibiting a peak at 321 nm.

The SFE, UAE (NaOH), UAE (KOH), UAE (NaOH), and UAE (KOH45) extracts showed peaks at 202, 204, 206, and 206 nm, respectively.

No pigments were detected in the carrageenan solutions.

3.4. FTIR-ATR Analysis

The FTIR-ATR spectra of commercial iota-carrageenan and kappa-carrageenan (Figures 5a and 5b, respectively) were used as baselines for a comparison with the spectral profiles of carrageenans extracted using different methods (Figure 5c–i). The FTIR-ATR band assignments, letter code nomenclature, and band identification of the extracted carrageenans are detailed in Table 3.

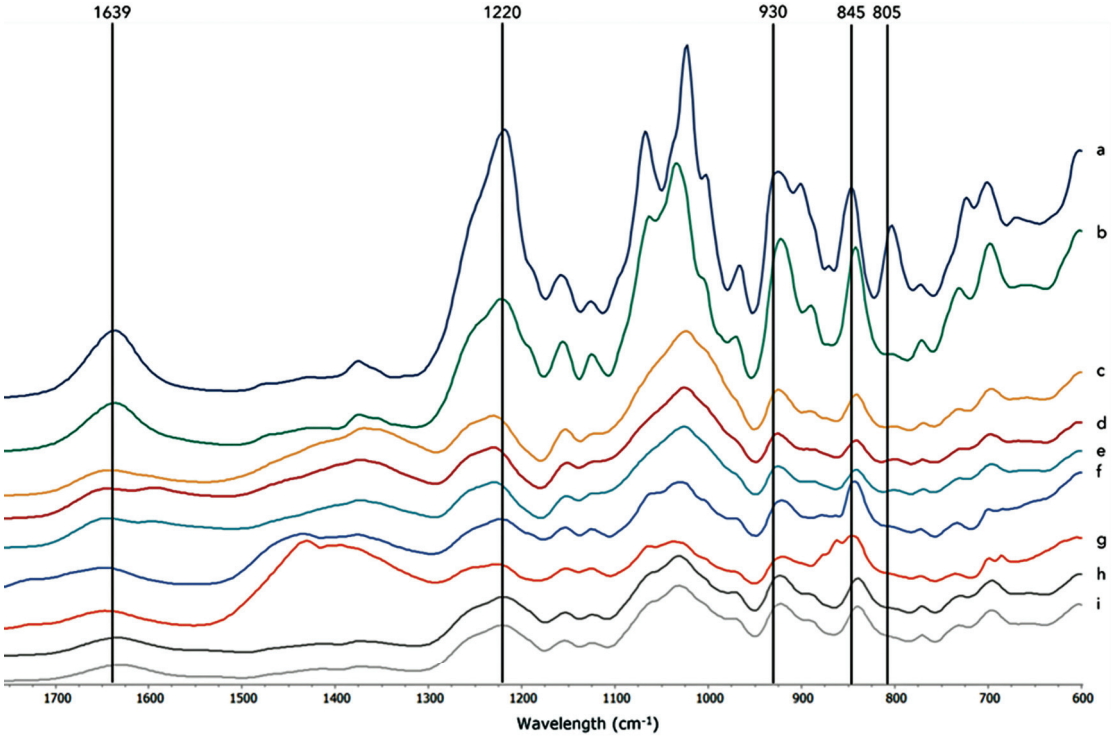

Figure 5. FTIR-ATR spectra of carrageenan standards: (**a**) iota-carrageenan and (**b**) kappa-carrageenan from Thermo Scientific and carrageenans from the novel strain of *Kappaphycus alvarezii* obtained through the various extraction techniques: (**c**) conventional extraction (KOH); (**d**) ultrasound-assisted extraction (UAE) (KOH 45); (**e**) ultrasound-assisted extraction (KOH); (**f**) conventional extraction (NaOH); (**g**) ultrasound-assisted extraction (NaOH); (**h**) native extraction; and (**i**) supercritical water extraction.

The broad band around 1220 cm^{-1} (between 1210 and 1260 cm^{-1}) is characteristic of sulfate esters in general and serves as a good indicator of total sulfates (sulfate esters) in sulfated polysaccharides [9]. This band is strong in the carrageenan standards, as shown in the spectra (Figure 5a,b) [26]. Several vibrational bands are characteristic of carrageenans. The absorption band at 930 cm^{-1} indicated the presence of 3,6-anhydrogalactose (DA), which is seen in the spectra of kappa- and iota-carrageenans. Additionally, the band at 845 cm^{-1} is related to the presence of D-galactose-4-sulfate (G4S), characteristic of kappa-, mu-, iota-, and nu-carrageenans. Conversely, the band at 805 cm^{-1}, associated with the sulfate ester at position 2 of anhydrous-D-galactose (DA2S) residues, is only observed in the spectra of iota-carrageenan.

The weak bands in the 770 cm^{-1} region are related, according to Matsuhiro [27], to the skeleton bending of pyranose present in the carrageenan structure. Additionally, the band

at 1150 cm^{-1} may be assigned to the C-O and C-C stretching vibrations of the pyranose ring common to all polysaccharides [18].

Table 3. FTIR band assignment (wave number cm^{-1}), letter code nomenclature, and band identification of carrageenans obtained through various methods.

Wave Number (cm^{-1})	Bound	Letter Code	Iota (ι)	Kappa (κ)	NE	SFE	CE (NaOH)	CE (KOH)	UAE (NaOH)	UAE (KOH45)	UAE (KOH)
1210–1260	Sulfate ester (S=O)	S	1219	1222	1220	1221	1223	1231	1227	1231	1230
928–933, 1070 (shoulder)	3,6-anhydro-D-galactose	DA	925.2 (1067)	922.3 (1063)	923.1	923	921.5	924.6	920.9 (1063)	925.7	925.1
970–975	Galactose	G/D	967	971.3	972.8	972.8	-	-	-	-	-
890–900	β-D-galactose-de-sulfated	G/D	902.1	889.9	-	-	-	890.9	-	-	888.5
840–850	D-galactose-4-sulfate	G4S	846.4	842.2	839.7	839.7	842.4	841.5	846.2	841.6	841.4
830	D-galactose-2-sulfate	G2S	-	-	-	-	-	-	-	-	-
820, 825 (shoulder)	D-galactose-2,6-disulphate	D2S, D6S	-	-	-	-	-	-	-	-	-
810–820, 867 (shoulder)	D-galactose-6-sulfate	G/D6S	-	-	-	-	-	-	-	-	-
800–805, 905 (shoulder)	3,6-anhydro-D-galactose-2-sulfate	DA2S	803.4	-	-	-	-	800.2	-	800.7	800.9

- not detected.

Going further on the spectra, the band at 1639 cm^{-1} is known to be an indicator of amide I, the presence of H_2O, or proteins CO-NH/amide II from proteins [28].

The FTIR-ATR spectra of extracted carrageenans from the novel haploid *K. alvarezii* strain using various methods present absorption bands at the 930 cm^{-1} region and at the 845 cm^{-1} region, which were both considered typical and revealed the presence of kappa-carrageenan.

Conventionally extracted [CE (NaOH)] carrageenan (Figure 5f) showed a slightly higher shoulder at 930 cm^{-1} in the spectra and a decrease in the ratio 805/845, as compared to native carrageenans, was verified, meaning that there was a decrease in the iota fraction relative to the kappa fraction (Table 4).

Table 4. Iota/kappa ratios of carrageenans extracted by various methods and each commercial sample.

	Iota (ι)	Kappa (κ)	NE	SFE	CE (NaOH)	CE (KOH)	UAE (NaOH)	UAE (KOH45)	UAE (KOH)
iota/kappa ratio	0.82	0.51	0.68	0.66	0.65	0.73	0.65	0.79	0.78

The FTIR-ATR spectra of conventionally extracted [CE (KOH)] carrageenans (Figure 5c) were different from those of CE (NaOH), showing a slightly more visible band in the 805 cm^{-1} region (DA2S). An increase in the iota/kappa ratio was verified in comparison to native carrageenan and overall alkali extracted (NaOH) carrageenans, which corresponded to an increase in the iota fraction relative to the kappa fraction.

Ultrasound-assisted extracted refined carrageenans [UAE (NaOH)] (Figure 5g) were similar to those conventionally extracted [CE (NaOH)], and although the peak at 845 cm^{-1} was less sharp, the ratio 805/845 remained the same (Table 4).

Ultrasound-assisted extracted semi-refined carrageenans [UAE (KOH)] and UAE (KOH45) (Figures 5e and 5d, respectively) revealed very similar spectra, with UAE (KOH) presenting a slightly higher peak in the 845 cm^{-1} region, which was visible in the lower iota/kappa ration in comparison to UAE (KOH45) (Table 4).

Bands at the 970–975 cm^{-1} regions were related to galactose (G) and were present in all samples, with CE(NaOH), NE, and SFE (Figure 5f, Figure 5h, and Figure 5i, respectively) showing more absorption in comparison to other samples.

Comparing the ratio of iota/kappa (Table 4) of each extraction method, with the iota-(0.82) and kappa-carrageenan (0.51) commercial samples, values ranged from 0.65 to 0.79.

Table 5 presents the absolute spectral similarities between carrageenans extracted from the various methods and each commercial sample. Commercial kappa-carrageenan samples revealed higher absolute spectral similarity than iota-carrageenan in all carrageenan samples obtained through the different extraction methods. However, iota-carrageenan still showed relatively high values. Carrageenan extracted through CE (KOH) showed the highest mean value of 64.66%.

Table 5. Absolute spectral similarity between carrageenans extracted from various methods and each commercial sample.

	Similarity (%)						
	NE	**SFE**	**CE (NaOH)**	**CE (KOH)**	**UAE (NaOH)**	**UAE (KOH45)**	**UAE (KOH)**
Iota (ι)	33.59	32.17	47.39	53.83	38.82	43.18	41.55
Kappa (κ)	40.10	38.35	56.83	64.66	46.92	51.98	49.93

4. Discussion

The yield of native carrageenan obtained was slightly higher compared to that in most published studies using different cultivars (Table 6). The content and quality of polysaccharides in seaweeds can vary significantly with the season and are influenced by various biotic and abiotic factors [29,30]. Although there are many reports on carrageenan yields from *K. alvarezii*, making quantitative and qualitative comparisons is challenging due to variations in extraction methods and the strains or cultivars of the species. When comparable extraction conditions are used, the observed higher yield may be attributed to the higher carrageenan content of the specific strain. The lack of statistically significant differences demonstrates that the seaweed biomass had high heterogeneity, due to the mean range from 34 to 77, although the methods demonstrated significant carrageenan extraction power (Table 6) when compared to other studies, as presented in Table 6.

Table 6. Extraction yield mean (%) of carrageenan extracted from *Kappaphycus alvarezii* of different localities using different methods.

Extraction Conditions	**Yield Mean (%)**	**Locality**	**Reference**
Aqueous (Native)	40–50	Cam Ranh Bay, Vietnam	[31]
Aqueous (SFE)	71	Wagina, Solomon Islands	[11]
Alkali (NaOH)	48	Palk Bay, India	[32]
Alkali (KOH)	52	Palk Bay, India	[32]
Alkali (4% KOH)	53.2	Philippines (commercial sample)	[33]
Alkali (6% KOH)	54.6	Philippines (commercial sample)	[33]
Alkali (8% KOH)	53.7	Philippines (commercial sample)	[33]
Aqueous UAE	50-55	BIS Algoculture (Madagascar)	[19]
Various (7 methods)	34–77	Philippines (novel variant)	This study, Table 1

The CE (NaOH) method presented close but lower values (35.67 ± 1.89% dw of carrageenan extracted) than previously reported (48%), while CE (KOH) had higher values (77.33 ± 2.49% dw of carrageenan extracted). It is important to note that this higher yield measured in the CE (KOH) treatment could be because residual cellulose from the cell walls remained in the carrageenan fibers after washing, which only eliminates residual minerals, proteins, and lipids. SRC production consists of a method where carrageenan is never extracted from seaweed, but non-polysaccharide compounds are cleaned from seaweed. Thus, other polysaccharides (such as cellulose) are present in SRC.

According to a study conducted by Rafiquzzaman et al. [14] on carrageenan extracted from *Hypnea musciformis*, the yield was higher using the aqueous UAE (500 W, 20 min) method, as compared to the conventional aqueous extraction method (native extraction). The present work compared conventional methods with ultrasound-assisted extraction, CE (NaOH) (35.67 ± 1.89% dw of carrageenan extracted) vs. UAE (NaOH) (33.73 ± 10.52% dw of carrageenan extracted), and CE (KOH) (77.33 ± 2.49% dw of carrageenan extracted) vs. UAE (KOH) (76.70 ± 1.44% dw of carrageenan extracted). The ultrasound-assisted method gave slightly lower extraction yields than conventional extraction. However, these were performed in a shorter time (i.e., one-third of the time in NaOH solution and half of KOH) and at a lower temperature. Such results can be attributed to the effective disruption of cell walls, reduction in particle size, and increased mass transfer of cell contents [32]. Looking at the two performed ultrasound-assisted extraction methods using KOH, UAE (KOH45) (63.20 ± 3.23), the yield was lower than UAE (KOH) (76.70 ± 1.44). Conversely, it operated at almost half of the extraction temperature (45 °C). A less abrupt reduction in the yield may be due to a lower level of possible degradation of the polysaccharide due to temperature.

The mean SFE carrageenan value (53.40 ± 1.80% dw of carrageenan extracted) was lower than that reported by Gereniu et al. [12] but still higher than CE (NaOH) and UAE (NaOH).

The biochemical analyses performed on the extracted carrageenans provided information on both composition and quality. There are several studies on the biochemical composition of the dried biomass of different *K. alvarezii* strains. However, there are very few studies on the polysaccharide of this species, specifically the FAME content. The FAME composition and content of carrageenans extracted by the different methods in this study were used to understand to what extent the extraction method was able to remove these compounds. A total of three fatty acids were detected: two saturated fatty acids (SFAs) and one monounsaturated fatty acid (MUFA). These results, as expected, were lower than those reported for the raw biomass of *K. alvarezii* in previous studies but present the same proportions as previous results [12,34], with saturated fatty acids (SFAs) presenting higher contents, especially palmitic acid (C16:0) and stearic acid (C18:0), followed by monounsaturated fatty acid (MUFA) oleic acid (C18:1). From all extraction methods, the CE (NaOH) extract produced the highest fatty acid content, followed by that of UAE (KOH), UAE (KOH45), and NE. These values were even lower, if before extraction, the ground dry material was pre-treated with a mixture of solvents (such as acetone and methanol). In the present work, this was not applied, and the values are still acceptable for human food approval.

The present work reports on the carbohydrate composition of carrageenans from a novel *Kappaphycus alvarezii* strain (G-N7). The obtained results were compared to those of previous studies, such as Rhein-Knudsen et al. [35], which evaluated the monosaccharide composition of native and alkali-extracted carrageenan of *K. alvarezii* from Nha Trang, Vietnam, by HPAEC-PAD analysis. The values obtained in their study presented high contents of galactose (68–70% carrageenan dw) and a low content of glucose (3–6% carrageenan dw), and other monosaccharides were detected at vestigial contents (2% carrageenan dw), namely, fucose, xylose, and mannose. In another study conducted by Meinita et al. [36], the total carbohydrate content of raw seaweed *K. alvarezii* was obtained from various places in Indonesia, and the mean values were even higher, ranging from 35 to 78%, by weight.

These variations seem to be related to the type of extraction method performed, geographic origin, strain/cultivar, and harvest time [30].

No previous studies determined the uronic acid content in carrageenan extracted from *K. alvarezii*, but in comparison to analyses performed on the dried seaweed biomass of other red seaweed species, namely *Asparagospis armata*, *Calliblepharis jubata*, *Chondracanthus teedei* var. *lusitanicus*, and *Grateloupia turuturu*, the values reported were very low [37]. For the presence of uronic acids, in FTIR-ATR-obtained spectra, a clear peak around 1700 cm^{-1} would be expected, but this was not the case. Nevertheless, this did not necessarily mean that the colorimetric reaction was not effective. Depending on the seaweed, the carboxyl groups of uronic acids can react with carbohydrates (which can reduce sulfate esters in polysaccharides), as previously reported in the red seaweed *Hypnea musciformis* [38] and described in pattern detection [39].

In general, the alkali extractions performed with KOH showed lower values of galactose, possibly due to the benefit to 3,6-anhydrogalactose. This corresponded to the conversion of the 4-linked galactose-6-sulfate in native samples to anhydro-galactose in the alkali-extracted carrageenans. Thus, the biological precursors mu- and nu-carrageenan were converted into the kappa- and iota-carrageenan forms, respectively [4].

The protein content of all samples presented very low values, similar to commercial carrageenans [40], meeting the Food and Agriculture Organization of the United Nations (FAO) quality criteria, which require values lower than 2%.

Regarding the measured physicochemical parameters, in addition to protein content, carrageenan pH and viscosity were also monitored and regulated parameters used to assess the quality of commercially produced polysaccharides, and the value must be greater than 5 cP to meet FAO quality criteria. The results from the present work showed that, relative to pH criteria, the extracted carrageenan from the NE, SFE, and alkali (NaOH) methods were not suitable for food applications due to having a pH < 8 and thus cannot be adopted for an industrial-scale extraction process as the resulting product does not conform with the food additive regulations.

The viscosity varied greatly (from 7.8 to 658.7 cP). This could be due to the different independent variables, e.g., (1) extraction time, (2) alkali treatment, (3) type of alkali (NaOH or KOH), (4) extraction method (NE, UAE, or SFE), and (5) temperature.

SFE showed the lowest viscosity value (7.8 cP), possibly due to irregularities in the chain, as reported by BeMiller [41], caused by the high temperature and pressure, causing carrageenan to lose its properties. Higher viscosity values are usually attributed to carrageenans obtained by extraction methods using an alkali solution of KOH. Bono et al. [42] investigated the influence of process conditions on the viscosity of conventional alkali KOH-extracted carrageenan from *K. alvarezii* and determined the optimal conditions to be 80 °C for 30 min and a 10% *w*/*w* KOH solution, which resulted in a gel viscosity of 1291.84 cP. In the present work, UAE (KOH) revealed the highest value of viscosity (658.7 cP at 1%). Comparing UAE (KOH) with UAE (KOH45), these higher values might be due to temperature, since it is the only parameter varying between them. The high viscosity value can also mean that higher sulfate levels are present. According to Bono et al. [42], the viscosity of carrageenans can be influenced by the levels of, and directly proportional to, sulfate. A higher sulfate content resulted in a higher viscosity, this being due to the ability of the sulfate group to exert a repulsion force between negative charges along the polymer chain, and as a result, the molecular chain stiffens, and hence, the viscosity increases [43]. The neutral-pH and low-viscosity carrageenan obtained using SFE suggest that it has limited applications for the food industry, due to not complying with the carrageenan safety and quality control check (human food-approved carrageenan needs to have a pH above 8 and a, at least, viscosity above 10 cP). However, this neutral and low-viscosity carrageenan can be useful for exploring its biostimulant properties in agriculture.

No studies regarding EC and TDS values from carrageenan solutions of *K. alvarezii* were found. Nevertheless, in comparison to the commercial carrageenans used as standards, all values were higher, especially in UAE (NaOH), CE (NaOH), CE (KOH), and UAE

(KOH45), possibly indicating high levels of charged ions and substances not soluble or precipitated.

Among the UV-VIS spectra of different carrageenan solutions, only the native extracted carrageenan samples absorbed part of the UV-A radiation (320–400 nm). As previously reported, red seaweeds accumulate photoprotective compounds with ultraviolet radiation absorption capabilities, such as mycosporine-like amino acids (MAAs), which absorb in this specific UV region [44]. The UV absorption spectrum with prominent peaks between 320 and 340 nm is in accordance with the presence of MAAs absorbing in this range [44]. This finding revealed a possible application of the novel strain of *K. alvarezii* in para-pharmaceutical and cosmetic industries for UV protection. The NE, CE (KOH), UAE (KOH; 45 °C), and UAE (NaOH) extracts showed a peak between 200 and 270 nm, which corresponds to polysaccharides bound covalently with aromatic compounds [45]. Additionally, these results were partially correlated with the protein content. The lack of pigment detected in the UV-VIS spectra supported the purity of the extracted carrageenans and reinforced that a de-pigmentation step in the extraction processes of this seaweed strain was not required.

The FTIR-ATR spectra of extracted carrageenan from the *K. alvarezii* (G-N7) strain using various methods revealed the presence of kappa- and iota-carrageenans, especially in alkali-extracted CE (NaOH) and UAE (NaOH) (Figure 5h, Figure 5i, Figure 5f, and Figure 5g, respectively), indicating that the novel strain presents a hybrid kappa/iota-carrageenan, as verified in previous studies in several other *K. alvarezii* strains [18]. This is easily understood, especially in the iota/kappa ratio (Table 5), with CE (NaOH) and UAE (NaOH) presenting a lower value (0.65), meaning a lower content in iota-carrageenan, while UAE (KOH45) presented the highest ratio (0.79), and there was a higher content in iota-carrageenan. Bands in the 970–975 cm^{-1} region were identified as galactose (G), especially in CE (NaOH), NE, and SFE (Figure 5f, Figure 5h, and Figure 5i, respectively), and showed more absorption in comparison to the rest of the samples, which corroborated the results obtained in its quantification.

Similarity values provided valuable insights regarding carrageenan composition. Nonetheless, it is important to consider that similarity is relative in all spectra. The fact that sample G-N7 contained hybrid carrageenan is highlighted, and from the higher values of the kappa fraction, we could conclude that there was a higher content; however, the similarity regarding all spectra could be due to other less determinant peaks, and iota-carrageenan still showed relatively high values. This study demonstrated that KOH extraction can reduce processing time and enhance industrial efficiency, and although KOH extraction is a semi-refined extraction method, it demonstrated good quality when compared to the standards set by the carrageenan regulatory body. The carrageenan viscosity properties (although measured only once here) can be very important for carrageenan applications in various types of drug delivery and tissue engineering. This study demonstrated that some extraction techniques altered not only the purity but also the physicochemical properties of extracted colloids. Therefore, the properties could perhaps be more easily altered during extraction. This would be conducted as opposed to chemical modifications after extraction but before integration in pharmaceutical, drug, and medical applications.

5. Conclusions

This study is the first to evaluate the potential of the novel haploid *Kappaphycus alvarezii* G-N7 strain as a new seedstock for commercial cultivation and biomass yield for carrageenan production. Carrageenans extracted using conventional, UAE, and SFE methods were subjected to comprehensive physico-biochemical analyses, with values compared to benchmark, commercial samples of standard-grade kappa- and iota-carrageenans. UAE (KOH) extracts demonstrated a similar yield to those obtained from the conventional method but required less than half the extraction time and produced improved carrageenan viscosity. The extraction method (UAE (KOH)) presented here can reduce

carrageenan extraction costs with an enhanced control of the chemical characterization of the polymer produced.

This study found kappa- and iota-carrageenans with comparable iota/kappa ratios and protein yields, particularly in alkali-extracted CE (NaOH) and UAE (NaOH). The samples yielded less carrageenan (CE (NaOH) (35.67 $\pm$ 1.89)) than UAE (NaOH) (33.73 $\pm$ 10.52). However, UAE (NaOH) showed variances in viscosity and conductivity (when compared to the other extraction methods), which might be troublesome in the food business, due to carrageenan physiochemical safety check regulations. Thus, UAE (NAOH) carrageenan can have different behavior and chemical hazards from carrageenan approved as a human food additive. This question can be answered by employing an osmosis procedure to lower the ion concentration in carrageenan. Thus, these novel methods which are not currently used by the phycocolloid industry need more research before being applied at the industrial scale, due to strict regulations required for carrageenan as a *(human) food additive ingredient.

The FTIR-ATR spectra of the extracted carrageenans matched the commercial benchmark samples of both standard-grade iota- and kappa-carrageenans, although the manufacturing method was not specified by the supplier (Thermo Scientific).

Consequently, the clonally propagated novel strain of *Kappaphycus alvarezii* represents a promising raw material for future commercial carrageenan production for the food industry as an additive, with potential pharmacological and cosmetic applications.

In the future, there is a need to conduct more extensive chemical and physicochemical studies (with more replications), applying different techniques, such as HPLC, NIR, and XRF to analyze molecular weight, mineral content, and other compounds in the carrageenan extracted.

Author Contributions: Conceptualization, M.M., J.C., L.P., M.Y.R., A.M.M.G., and A.T.C.; Methodology, M.M., J.C., L.P., M.Y.R., A.M.M.G., and A.T.C.; Seaweed cultivation, M.Y.R. and L.A.R.H.; Seaweed extraction, M.M.; Chemical characterization, M.M., J.C., and L.P.; Biochemical characterization, M.M., I.B.G., and A.M.M.G.; Data curation; M.M., J.C., L.P., I.B.G., A.M.M.G., M.Y.R., and L.A.R.H.; Formal analysis, M.M., J.C., and I.B.G.; Validation, L.P., A.M.M.G., M.Y.R., and A.T.C.; Writing—original draft preparation, M.M.; Draft revision, J.C., L.P., I.B.G., A.M.M.G., M.Y.R., and A.T.C.; Funding acquisition, L.P., A.M.M.G., and M.Y.R.; Writing—review and editing, M.M., J.C., L.P., I.B.G., A.M.M.G., M.Y.R., and L.A.R.H.; Supervision, L.P., A.M.M.G., M.Y.R., and A.T.C. All authors have read and agreed to the published version of the manuscript.

Funding: The authors thank Foundation for Science and Technology (FCT) for their support by providing institutional funding to the Centre for Functional Ecology—Science for People and the Planet (CFE; UIDB/04004/2020; https://doi.org/10.54499/UIDB/04004/2020), financed by FCT/MCTES through national funds (PIDDAC), Associate Laboratory TERRA (LA/P/0092/2020; https://doi.org/10.54499/LA/P/0092/2020). UIDP/50017/2020+UIDB/50017/2020 (by FCT/MTCES) granted to CESAM—Centre for Environmental and Marine Studies. A.M.M.G. acknowledges University of Coimbra for the contract IT057-18-7253. M.Y.R. acknowledges the Philippines' Department of Science and Technology (DOST) Balik Scientist Program (BSP) fellowship. The eucheumatoid seaweed research program of the Algal Ecophysiology (AlgaE) Laboratory led by M.Y.R. received funding from the UPMSI inhouse research grant, Safe Seaweed Coalition funded project "SecureFuture" (LS249100), Sea6 Energy Pvt. Ltd., and the CHED-LAKAS funded project "Phytochemical Characterization of Macroalgae for Food and High Value Products (PhycoPRO)". M.Y.R. is also supported by the DOST-PCAARRD-funded PLOIDY Program: Ploidy-dependent physiological and chemical traits of *Kappaphycus* cultivars covering Project 1: Prevalence and ploidy-dependent physiological responses in farmed cultivars and novel strains of *Kappaphycus* spp.

Institutional Review Board Statement: Not applicable.

Data Availability Statement: Data can be made available by the author on request.

Acknowledgments: This is contribution no. 1595 from the University of the Philippines–Marine Science Institute (UPMSI). We thank the Bolinao Marine Laboratory (BML) of UPMSI for providing a venue to produce cultivated eucheumatoid biomass in the land-based hatchery facility. We thank

Guillermo Valenzuela and Jerry Arboleda for maintaining the cultures. This work was also supported by FCT-Fundação para a Ciência e Tecnologia, I.P., in the framework of the Project UIDB/04004/2020 and DOI identifier 10.54499/UIDB/04004/2020 (https://doi.org/10.54499/UIDB/04004/2020 accessed on 30 July 2024).

Conflicts of Interest: The authors declare no conflicts of interest.

References

1. Abdul Khalil, H.P.S.; Lai, T.K.; Tye, Y.Y.; Rizal, S.; Chong, E.W.N.; Yap, S.W.; Hamzah, A.A.; Nurul Fazita, M.R.; Paridah, M.T. A Review of Extractions of Seaweed Hydrocolloids: Properties and Applications. *Express Polym. Lett.* **2018**, *12*, 296–317. [CrossRef]
2. Shen, L.; Pang, S.; Zhong, M.; Sun, Y.; Qayum, A.; Liu, Y.; Rashid, A.; Xu, B.; Liang, Q.; Ma, H.; et al. A Comprehensive Review of Ultrasonic Assisted Extraction (UAE) for Bioactive Components: Principles, Advantages, Equipment, and Combined Technologies. *Ultrason. Sonochem.* **2023**, *101*, 106646. [CrossRef] [PubMed]
3. Dulanlebit, Y.H.; Hernani, H. Overview of Extraction Methods for Extracting Seaweed and Its Applications. *J. Penelit. Pendidik. IPA* **2023**, *9*, 817–824. [CrossRef]
4. Pereira, L.; Mesquita, J.F. Population Studies and Carrageenan Properties of *Chondracanthus Teedei* var. *Lusitanicus* (Gigartinaceae, Rhodophyta). *J. Appl. Phycol.* **2004**, *16*, 369–383. [CrossRef]
5. Rupert, R.; Rodrigues, K.F.; Thien, V.Y.; Yong, W.T.L. Carrageenan from *Kappaphycus alvarezii* (Rhodophyta, Solieriaceae): Metabolism, Structure, Production, and Application. *Front. Plant Sci.* **2022**, *13*, 859635. [CrossRef]
6. Weiner, M.L. Parameters and Pitfalls to Consider in the Conduct of Food Additive Research, Carrageenan as a Case Study. *Food Chem. Toxicol.* **2016**, *87*, 31–44. [CrossRef]
7. Younes, M.; Aggett, P.; Aguilar, F.; Crebelli, R.; Filipič, M.; Frutos, M.J.; Galtier, P.; Gott, D.; Gundert-Remy, U.; Kuhnle, G.G.; et al. Re-Evaluation of Carrageenan (E 407) and Processed *Eucheuma* Seaweed (E 407a) as Food Additives. *EFSA J.* **2018**, *16*, e05238. [CrossRef]
8. Benard, C.; Cultrone, A.; Michel, C.; Rosales, C.; Segain, J.-P.; Lahaye, M.; Galmiche, J.-P.; Cherbut, C.; Blottière, H.M. Degraded Carrageenan Causing Colitis in Rats Induces TNF Secretion and ICAM-1 Upregulation in Monocytes through NF-KB Activation. *PLoS ONE* **2010**, *5*, e8666. [CrossRef]
9. Pereira, L.; Sousa, A.; Coelho, H.; Amado, A.M.; Ribeiro-Claro, P.J.A. Use of FTIR, FT-Raman and 13C-NMR Spectroscopy for Identification of Some Seaweed Phycocolloids. *Biomol. Eng.* **2003**, *20*, 223–228. [CrossRef]
10. Heriyanto, H.; Kustiningsih, I.; Sari, D.K. The Effect of Temperature and Time of Extraction on the Quality of Semi Refined Carrageenan (SRC). *MATEC Web. Conf.* **2018**, *154*, 01034. [CrossRef]
11. Rhein-Knudsen, N.; Ale, M.; Meyer, A. Seaweed Hydrocolloid Production: An Update on Enzyme Assisted Extraction and Modification Technologies. *Mar. Drugs* **2015**, *13*, 3340–3359. [CrossRef] [PubMed]
12. Gereniu, C.R.N.; Saravana, P.S.; Getachew, A.T.; Chun, B.S. Characteristics of Functional Materials Recovered from Solomon Islands Red Seaweed (*Kappaphycus alvarezii*) Using Pressurized Hot Water Extraction. *J. Appl. Phycol.* **2017**, *29*, 1609–1621. [CrossRef]
13. Roleda, M.Y.; Ganzon-Fortes, E.T.; Montaño, N.E. Agar from Vegetative and Tetrasporic *Gelidiella acerosa* (Gelidiales, Rhodophyta). *Bot. Mar.* **1997**, *40*, 501–506. [CrossRef]
14. Rafiquzzaman, S.M.; Ahmed, R.; Lee, J.M.; Noh, G.; Jo, G.A.; Kong, I.S. Improved Methods for Isolation of Carrageenan from *Hypnea musciformis* and Its Antioxidant Activity. *J. Appl. Phycol.* **2016**, *28*, 1265–1274. [CrossRef]
15. Hinaloc, L.A.R.; Roleda, M.Y. Phenotypic Diversity, Growth and Sexual Differentiation in the Progeny of Wild *Kappaphycus alvarezii* (Gigartinales, Florideophyceae). *Phycologia* **2021**, *60*, 547–557. [CrossRef]
16. Roleda, M.Y.; Aguinaldo, Z.-Z.A.; Crisostomo, B.A.; Hinaloc, L.A.R.; Projimo, V.Z.; Dumilag, R.V.; Lluisma, A.O.; Roleda, M.Y.; Aguinaldo, Z.-Z.A.; Crisostomo, B.A.; et al. Discovery of Novel Haplotypes from Wild Populations of *Kappaphycus* (Gigartinales, Rhodophyta) in the Philippines. *Algae* **2021**, *36*, 1–12. [CrossRef]
17. Narvarte, B.C.V.; Hinaloc, L.A.R.; Genovia, T.G.T.; Gonzaga, S.M.C.; Tabonda-Nabor, A.M.; Roleda, M.Y. Physiological and Biochemical Characterization of New Wild Strains of *Kappaphycus alvarezii* (Gigartinales, Rhodophyta) Cultivated under Land-Based Hatchery Conditions. *Aquat. Bot.* **2022**, *183*, 103567. [CrossRef]
18. Pereira, L.; Van De Velde, F. Portuguese Carrageenophytes: Carrageenan Composition and Geographic Distribution of Eight Species (Gigartinales, Rhodophyta). *Carbohydr. Polym.* **2011**, *84*, 614–623. [CrossRef]
19. Youssouf, L.; Lallemand, L.; Giraud, P.; Soulé, F.; Bhaw-Luximon, A.; Meilhac, O.; D'Hellencourt, C.L.; Jhurry, D.; Couprie, J. Ultrasound-Assisted Extraction and Structural Characterization by NMR of Alginates and Carrageenans from Seaweeds. *Carbohydr. Polym.* **2017**, *166*, 55–63. [CrossRef]
20. Gonçalves, A.M.M.; Pardal, M.A.; Marques, S.C.; Mendes, S.; Fernández-Gómez, M.J.; Galindo-Villardón, M.P.; Azeiteiro, U.M. Responses of Copepoda Life-History Stages to Climatic Variability in a Southern-European Temperate Estuary. *Zool. Stud.* **2012**, *51*, 321–335.
21. Selvendran, R.R.; March, J.F.; Ring, S.G. Determination of Aldoses and Uronic Acid Content of Vegetable Fiber. *Anal. Biochem.* **1979**, *96*, 282–292. [CrossRef] [PubMed]

22. Coimbra, M.A.; Waldron, K.W.; Selvendran, R.R. Isolation and Characterisation of Cell Wall Polymers from Olive Pulp (*Olea europaea* L.). *Carbohydr. Res.* **1994**, *252*, 245–262. [CrossRef]
23. Blumenkrantz, N.; Asboe-Hansen, G. New Method for Quantitative Determination of Uronic Acids. *Anal. Biochem.* **1973**, *54*, 484–489. [CrossRef] [PubMed]
24. Bradford, M.M. A Rapid and Sensitive Method for the Quantitation of Microgram Quantities of Protein Utilizing the Principle of Protein-Dye Binding. *Anal. Biochem.* **1976**, *72*, 248–254. [CrossRef] [PubMed]
25. Menges, F. Spectragryph—Optical Spectroscopy Software. 2024.
26. Gómez-Ordóñez, E.; Rupérez, P. FTIR-ATR Spectroscopy as a Tool for Polysaccharide Identification in Edible Brown and Red Seaweeds. *Food Hydrocoll.* **2011**, *25*, 1514–1520. [CrossRef]
27. Matsuhiro, B. Vibrational Spectroscopy of Seaweed Galactans. *Hydrobiologia* **1996**, *326–327*, 481–489. [CrossRef]
28. Marques, J.F.; Leonel, P. A revision on the red alga *Dilsea carnosa*. In *Carrageenans: Sources and Extraction Methods, Molecular Structure, Bioactive Properties and Health Effects*; Nova Science Publishers: Hauppauge, NY, USA, 2016.
29. Hung, L.D.; Hori, K.; Nang, H.Q.; Kha, T.; Hoa, L.T. Seasonal Changes in Growth Rate, Carrageenan Yield and Lectin Content in the Red Alga *Kappaphycus alvarezii* Cultivated in Camranh Bay, Vietnam. *J. Appl. Phycol.* **2009**, *21*, 265–272. [CrossRef]
30. Véliz, K.; Chandía, N.; Rivadeneira, M.; Thiel, M. Seasonal Variation of Carrageenans from *Chondracanthus chamissoi* with a Review of Variation in the Carrageenan Contents Produced by Gigartinales. *J. Appl. Phycol.* **2017**, *29*, 3139–3150. [CrossRef]
31. Bui, V.T.N.T.; Nguyen, B.T.; Renou, F.; Nicolai, T. Structure and Rheological Properties of Carrageenans Extracted from Different Red Algae Species Cultivated in Cam Ranh Bay, Vietnam. *J. Appl. Phycol.* **2019**, *31*, 1947–1953. [CrossRef]
32. Mishra, P.C.; Jayasankar, R.; Seema, C. Yield and Quality of Carrageenan from *Kappaphycus alvarezii* Subjected to Different Physical and Chemical Treatments. *Seaweed Res. Utiln.* **2006**, *28*, 113–117.
33. Ohno, M.; Nang, H.Q.; Hirase, S. Cultivation and carrageenan yield and quality of *Kappaphycus alvarezii* in the waters of Vietnam. *J. Appl. Phycol.* **1996**, *8*, 431–437. [CrossRef]
34. Illijas, M.I.; Kim, G.-W.; Honda, M.; Itabashi, Y. Characteristics of Fatty Acids from the Red Alga *Kappaphycus alvarezii* (Doty) Doty (Rhodophyta, Solieriaceae). *Algal Res.* **2023**, *71*, 103005. [CrossRef]
35. Rhein-Knudsen, N.; Ale, M.T.; Ajalloueian, F.; Yu, L.; Meyer, A.S. Rheological Properties of Agar and Carrageenan from Ghanaian Red Seaweeds. *Food Hydrocoll.* **2017**, *63*, 50–58. [CrossRef]
36. Meinita, M.D.N.; Kang, J.-Y.; Jeong, G.-T.; Koo, H.M.; Park, S.M.; Hong, Y.-K. Bioethanol Production from the Acid Hydrolysate of the Carrageenophyte *Kappaphycus alvarezii* (Cottonii). *J. Appl. Phycol.* **2012**, *24*, 857–862. [CrossRef]
37. Pacheco, D.; Cotas, J.; Rocha, C.P.; Araújo, G.S.; Figueirinha, A.; Gonçalves, A.M.M.; Bahcevandziev, K.; Pereira, L. Seaweeds' Carbohydrate Polymers as Plant Growth Promoters. *Carbohydr. Polym. Technol. Appl.* **2021**, *2*, 100097. [CrossRef]
38. Arman, M.; Qader, S.A.U. Structural Analysis of Kappa-Carrageenan Isolated from *Hypnea musciformis* (Red Algae) and Evaluation as an Elicitor of Plant Defense Mechanism. *Carbohydr. Polym.* **2012**, *88*, 1264–1271. [CrossRef]
39. Raman, M.; Doble, M. κ-Carrageenan from marine red algae, *Kappaphycus alvarezii*—A functional food to prevent colon carcinogenesis. *J. Funct. Foods* **2015**, *15*, 354–364. [CrossRef]
40. Chan, S.W.; Mirhosseini, H.; Taip, F.S.; Ling, T.C.; Tan, C.P. Comparative study on the physicochemical properties of κ-carrageenan extracted from *Kappaphycus alvarezii* (doty) doty ex Silva in Tawau, Sabah, Malaysia and commercial κ-carrageenans. *Food Hydrocoll.* **2013**, *30*, 581–588. [CrossRef]
41. BeMiller, J.N. *Carbohydrate Chemistry for Food Scientists*; Elsevier: Amsterdam, The Netherlands, 2019; ISBN 9780128120699.
42. Bono, A.; Anisuzzaman, S.M.; Ding, O.W. Effect of Process Conditions on the Gel Viscosity and Gel Strength of Semi-Refined Carrageenan (SRC) Produced from Seaweed (*Kappaphycus alvarezii*). *J. King Saud Univ. Eng. Sci.* **2014**, *26*, 3–9. [CrossRef]
43. Montoro, M.A.; Francisca, F.M. Effect of Ion Type and Concentration on Rheological Properties of Natural Sodium Bentonite Dispersions at Low Shear Rates. *Appl. Clay Sci.* **2019**, *178*, 105132. [CrossRef]
44. Orfanoudaki, M.; Hartmann, A.; Karsten, U.; Ganzera, M. Chemical Profiling of Mycosporine-like Amino Acids in Twenty-Three Red Algal Species. *J. Phycol.* **2019**, *55*, 393–403. [CrossRef] [PubMed]
45. Jesumani, V.; Du, H.; Pei, P.; Aslam, M.; Huang, N. Comparative study on skin protection activity of polyphenol-rich extract and polysaccharide-rich extract from *Sargassum vachellianum*. *PLoS ONE* **2020**, *15*, e0227308. [CrossRef] [PubMed]

marine drugs

MDPI

Review

Bioactive Compounds of Marine Algae and Their Potential Health and Nutraceutical Applications: A Review

Emin Cadar [1,†], Antoanela Popescu [1,†], Ana-Maria-Laura Dragan [2,*,†], Ana-Maria Pesterau [2], Carolina Pascale [2], Valentina Anuta [3], Irina Prasacu [3], Bruno Stefan Velescu [3], Cezar Laurentiu Tomescu [4,5], Claudia Florina Bogdan-Andreescu [6], Rodica Sirbu [2,*,†] and Ana-Maria Ionescu [4,7]

[1] Faculty of Pharmacy, "Ovidius" University of Constanta, Capitan Aviator Al. Serbanescu Street, No. 6, Campus, Corp C, 900470 Constanta, Romania; emin.cadar@gmail.com (E.C.); antoniapopescu2002@yahoo.co.uk (A.P.)
[2] Organizing Institution for Doctoral University Studies of "Carol Davila", University of Medicine and Pharmacy of Bucharest, Dionisie Lupu Street, No. 37, Sector 2, 020021 Bucharest, Romania; ana-maria.pesterau@drd.umfcd.ro (A.-M.P.); carolina.pascale@drd.umfcd.ro (C.P.)
[3] Faculty of Pharmacy, "Carol Davila" University of Medicine and Pharmacy of Bucharest, Traian Vuia Street, No. 6, Sector 2, 020021 Bucharest, Romania; valentina.anuta@umfcd.ro (V.A.); irina.prasacu@umfcd.ro (I.P.); bruno_velescu@yahoo.co.uk (B.S.V.)
[4] Faculty of Medicine, "Ovidius" University of Constanta, University Alley, No. 1, Campus, Corp B, 900470 Constanta, Romania; tomescu.cezar.laurentiu@gmail.com (C.L.T.); anaiulius@yahoo.com (A.-M.I.)
[5] "Sf. Ap. Andrei" County Clinical Emergency Hospital, Tomis Bvd., No. 145, 900591 Constanta, Romania
[6] Faculty of Dental Medicine, Department of Speciality Disciplines, "Titu Maiorescu" University, 031593 Bucharest, Romania; claudia.andreescu@prof.utm.ro
[7] Clinical Hospital C F Constanta, 1 Mai Bvd., No. 3–5, 900123 Constanta, Romania
* Correspondence: ana-maria-laura.dragan@drd.umfcd.ro (A.-M.-L.D.); sirbu_27@yahoo.com (R.S.)
† These authors contributed equally to this work.

Abstract: Currently, marine algae are still an under-exploited natural bioresource of bioactive compounds. Seaweeds represent a sustainable source for obtaining bioactive compounds that can be useful for the fabrication of new active products with biomedical benefits and applications as biomedicinals and nutraceuticals. The objective of this review is to highlight scientific papers that identify biocompounds from marine macroalgae and emphasize their benefits. The method used was data analysis to systematize information to identify biocompounds and their various benefits in pharmaceuticals, cosmetics, and nutraceuticals. The research results demonstrate the multiple uses of seaweeds. As pharmaceuticals, seaweeds are rich sources of bioactive compounds like polysaccharides, protein compounds, pigments, and polyphenols, which have demonstrated various pharmacological activities such as antioxidant, antibacterial, anti-inflammatory, antiviral, anticoagulant, and potentially anticarcinogenic effects. Seaweed has gained recognition as a functional food and offers a unique set of compounds that promote body health, including vitamins, minerals, and antioxidants. In conclusion, the importance of this review is to expand the possibilities for utilizing natural resources by broadening the areas of research for human health and marine nutraceuticals.

Keywords: seaweeds; nutritional composition; antioxidant properties; anti-inflammatory effects; anti-cancer potential; functional foods; dietary supplements; nutraceuticals

1. Introduction

Maintaining health is humanity's most important concern. The aquatic environment is one of the abundant sources of bioactive substances that are proven to be good for

human health. The biodiversity of the marine ecosystem provides a large reservoir of novel bioactive nutrients for both marine organisms and humans [1]. In this regard, seaweeds represent one of the potential sources of marine bioactive compounds [1,2]. Seaweeds, as aquatic plants, are eukaryotic, photosynthetic organisms found in both marine and freshwater [3]. Seaweeds have been consumed as food since prehistoric times in the Chinese, Japanese, and Korean diets, with written evidence attesting to their use. Although the consumption of seaweeds by humans dates back to ancient times, the study of bioactive compounds started to develop significantly in recent decades, as shown by Cadar et al. (2019) [4]. In Europe, seaweed consumption has increased with people's interest in the use of natural marine products and functional foods as shown by Ferrara et al. (2020) and Ferdouse et al. (2018) [5,6]. The use of macroalgae as food and feed has been addressed by Embling et al. (2022) and Cherry et al. (2019) [7,8]. Cadar et al. (2019) showed that seaweeds can be utilized for their ability to accumulate heavy metals which are considered as pollutants to the marine environment [9]. Seaweeds can also be used as an ingredient in combination with other marine-derived materials to obtain preparations usable in the treatment of some dermal diseases as shown by Cherim et. al. (2019) and Sirbu et al. (2019) [10,11]. The biggest use of macroalgae is as food for humans and animals. Araújo et al. (2021) indicated that although algae production from the marine environment accounts for 68% of the total, in Europe, algae culture (32% of the total) has started to expand [12]. Cai et al. (2021) analyzed the Global Status of Algae Production in FAO from 1990 to 2019 and showed that the world production of brown and red algae from aquaculture has increased, but the cultivation of green algae has decreased by about half [13]. Worldwide, according to the global trade statistics reported to FAO on world seaweed production, Asia contributed 97.38%, the two Americas (North and South) 1.36%, Europe 0.8%, followed by Africa 0.41% and Oceania 0.05% [13,14]. The development of macroalgae aquaculture has evolved by optimizing culture systems for several algal species. Seaweed can be a source of secondary metabolites that have multiple beneficial health effects for different diseases, as reported by André et al. (2021) [15]. Ouyang et al. (2021) reported that algal polysaccharides as nutraceuticals present an important potential for combating cancer [16]. Activities of marine algae in anti-HPV and anti-cervical cancer are studied by Moga et al. (2021) [17]. The properties of the fucoidan extracted from brown seaweeds, such as anti-inflammatory, immunomodulatory, antitumoral, anticoagulant, neuroprotective antioxidant, and cardioprotective, were studied by Saeed et al. (2021) [18]. Lomartire et al. (2021) presented the biocompounds of macroalgae with a polysaccharide structure and their applications for medical benefits [19]. In recent years, the demand for nutritious and nourishing food products has been steadily increasing. According to the FAO analysis from 2022, this global growth for healthy food is accounted for by the development of the aquaculture sector, which grew worldwide in 2019 by approximately 30% compared to the previous period [20]. Marine macroalgae constitute a rich resource of bioactive compounds such as polysaccharides, polyphenols, minerals, vitamins, carotenoids, fibers, proteins, amino acids, and polyunsaturated fatty acids, which are important for health as medicines or nutraceutical compounds, as shown by Park et al. (2023), Beaumont et al. (2021), Caf et al. (2019), and [21–23].

Seaweed industrialization has progressed significantly, with applications extending beyond traditional food consumption into high-value sectors such as cosmetics, biomedicine, and biofuels. Innovations in farming techniques, including large-scale mariculture and controlled bioreactor systems, have increased production efficiency and sustainability. Advances in biotechnology, including genetic modification and optimized extraction methods, further contribute to maximizing the potential of compounds derived from seaweed. De-

spite these advances, challenges such as environmental issues and resource management remain areas of active research. In addition to industrial progress, political support and areas of legislative regulation play a crucial role in shaping the future of seaweed utilization. Governments around the world are implementing policies to promote sustainable aquaculture, stimulate research, and regulate the marketing of algae products. The European Union, for example, has introduced directives to encourage sustainable seaweed farming, while the United States and Asian countries have included seaweed in their blue economy strategies.

These policy-driven initiatives help to bridge the gap between scientific discoveries and commercial applications, ensuring that seaweed remains a viable resource for future innovation.

The aim of our study is to analyze the data on biocompounds with significant biological activity that have pharmaceutical, biomedical, and nutraceutical benefits. Methods of the extraction and the structures of active biocompounds such as polysaccharides, terpenoid compounds, proteins, saturated and unsaturated fatty acids, and polyphenolic and flavonoid compounds and data on pigments, vitamins, and minerals existing in marine macroalgae are described. The biomedical and nutraceutical applications due to these biocompounds are systematized. The biomedical and nutraceutical benefits are presented based on the biological activities of secondary metabolites in macroalgae.

2. Methodology

The research methodology involved the systematic collection and analysis of literature data from 2017 to 2024. The methodology for selecting the reviewed papers followed a systematic approach to ensure the inclusion of high-quality and relevant studies on bioactive compounds from marine algae. The selection process involved a structured literature search using multiple scientific databases, including ScienceDirect, SCOPUS, Google Scholar, and Web of Science. The search strategy was designed to retrieve the most relevant articles by using a combination of carefully selected keywords and Boolean operators. Keywords included the following: “algal bioactive principles”, “marine macroalgae”, “algae primary and secondary metabolites”, “algal pharmaceuticals”, “seaweed-based medicines”, “seaweed health benefits”, “anti-inflammatory potential”, “antioxidant properties”, “pharmaceutical compounds from marine algae”, “biomedical applications”, “marine-derived drugs”, “seaweed supplements”, “nutraceutical compounds from marine algae”, “seaweed skincare”, and “algal cosmeceuticals”. These keywords were applied in different combinations to maximize the retrieval of relevant literature.

For inclusion, the studies had to meet specific criteria: (1) published between 2017 and 2024 to ensure up-to-date information, (2) peer-reviewed articles focusing on bioactive compounds from marine macroalgae and their biomedical, pharmaceutical, and nutraceutical applications, (3) studies providing detailed information on the extraction, characterization, and functional properties of these compounds, and (4) research presenting experimental or clinical evidence on the efficacy and safety of bioactive compounds derived from marine algae.

Exclusion criteria were also applied to eliminate irrelevant or low-quality studies. Articles were excluded if they (1) focused primarily on freshwater algae rather than marine macroalgae, (2) lacked experimental data and were purely theoretical or speculative, (3) were duplicate studies or conference abstracts without full research findings, (4) did not provide substantial information on bioactive compound applications, and (5) were published in predatory or non-peer-reviewed journals.

The final selection of studies was conducted by screening titles and abstracts for relevance, followed by a full-text review of shortlisted papers. Any discrepancies in selection were resolved through discussion among the researchers to ensure objectivity and comprehensiveness in the review. This rigorous methodology ensured a high-quality synthesis of relevant literature on the bioactive potential of marine algae.

3. Chemical Bioactive Compounds from Macroalgae

3.1. Biodiversity of Algae

Macroalgae are classified into three main taxa: Chlorophyta (green algae), Rhodophyta (red algae), and Phaeophyceae (brown algae), based on factors such as photosynthetic pigment type, cell wall composition, flagella type, and storage compounds as shown by Zhong et al. (2020), Pereira (2021), and Cadar et al. (2019) [24–26]. In marine environments, the presence of seaweeds significantly influences aquatic ecosystems, with various factors affecting their biochemical composition. Macroalgae are commonly found in abundance on rocky coastal shores, and some species form extensive underwater forests, known as algae forests, which can cover over 50 m^2 as shown by Pereira (2021) and Gaspar et al. (2020) [25,27]. According to Veluchamy, C. et al. (2020) and Kennedy, J. (2019), approximately 7000 species of red algae, distinguished by their bright coloration due to phycoerythrin pigment, and 4000 species of green algae, which owe their color to chlorophyll pigments, have been identified so far [28,29]. Green algae inhabit marine and freshwater environments as well as wet soils [30,31]. Sirbu et al. (2019) and Tanna et al. (2021) showed that *Ulva lactuca* (Chlorophyta) is commonly found in coastal marine waters and tidal pools [31,32]. Tanna et al. (2021) showed that red algae, which are typically multicellular and have a reddish hue, thrive at greater depths than green and brown algae because they efficiently absorb blue light [32]. Hakim et al. showed that brown algae are abundant on rocky shores in temperate regions [33]. Seaweeds endure harsh environmental conditions influenced by various external factors, including climatic fluctuations, seasonal and temperature changes, geographic location, mineral concentration, pH levels, light availability, and contaminants in the aquatic environment. These factors can significantly impact their biochemical composition. Badar et al. (2021) noted that macroalgae can thrive in challenging conditions with high heavy metal concentrations and can be utilized as a source of energy, biochemical components, and food [34]. Their ability to adapt to diverse marine environments accounts for the wide variability in their secondary metabolites and biochemical composition.

3.2. Seaweed Cultivation and Harvesting

With the rising global demand for natural food, mariculture has become essential for sustainably supplying functional foods and medical products derived from marine resources. Algae farming is now practiced in over 30 countries, utilizing cold, tropical, and temperate waters for food, pharmaceuticals, and biofuel production. According to Buschmann et al. (2019), annual seaweed harvests exceed 2 million tons in countries such as China, Japan, South Korea, Indonesia, and France [35]. In South American countries such as Chile, algae are harvested for their medicinal benefits, thus Cochayuyo (*Durvillaea incurvata*) (Phaeophyceae) extracts have been tested for potential uses as an antioxidant-active ingredient as reported by Pacheco et al. (2023) and for the potential to fight age-related diseases as reported by Muñoz-Molina, et al. (2024) [36,37]. Macroalgae cultivation has become increasingly profitable, as it requires no freshwater and can be sustained year-round in both coastal and offshore areas through various methods. Kumar et al. (2021) noted that cultivation techniques depend on location and seaweed species [38]. Globally, species

such as *Gracilaria* sp., *Eucheuma* sp., *Laminaria* sp., *Kappaphycus* sp., *Gelidium* sp., *Pyropia* sp., *Undaria* sp., *Saccharina* sp., *Sargassum* sp., and *Ulva* sp. are widely farmed [38]. Suthar et al. (2019) emphasized that achieving high algal biomass requires careful monitoring of environmental factors, including temperature, light, salinity, nutrient availability, water movement, cultivation depth, herbivorous fish, and epiphytes in the marine ecosystem [39]. Different methods are used for seaweed cultivation depending on the location and species. Techniques such as rope, raft, tubular net, and photo-bioreactor systems have been developed for certain species of *Ulva* sp. Hwang et al. (2020) reviewed macroalgae cultivation and harvesting methods used in South Korea [40]. The challenges of genetic degradation, poor environmental adaptation, and increased disease incidence have led to the preference for farm-based seaweed cultivation, which ensures higher-quality yields.

Obando et al. (2022) demonstrated that optimizing macroalgae cultivation for growth control, development, and secondary metabolite production requires more advanced techniques. These include selecting competent cells for growth induction using chemical regulators in the culture medium, as well as incorporating carbon and nitrogen sources to support the growth of protoplast and algal cell cultures. Such approaches are essential for enhancing macroalgae cultivation to meet various objectives [41].

3.3. Biochemical Composition of Algae

The nutritional composition of seaweeds includes bioactive compounds with significant medical, nutraceutical, and food-related benefits. Selecting the appropriate algae for study is crucial to ensuring that the biomass is clean and sourced from designated areas, preventing contamination that could compromise its quality, whether obtained from natural environments or aquaculture systems. The biochemical composition of algae is influenced by various factors, including biotic factors, such as symbiotic relationships with other organisms, and abiotic factors, such as temperature, light, carbon source, and nutrient availability as shown by Regal et al. (2020), Olsson et al. (2020), and Alvarez-Gomez (2019) [42–44]. Another key challenge is the collection of algal biomass, as the lack of standardized collection methods can impact the entire extraction process. Several factors affect the composition of the algal extract and the bioactivity of its compounds, including biomass drying methods, extraction techniques, solvent type and ratio, working temperature, and extraction duration as shown by Sobuj et al. (2021), Mansur et al. (2020), Uribe et al. (2019), and Getachew et al. (2022) [45–48].

3.3.1. The Extraction Methods of Biocompounds from Seaweeds

The process of extracting biocompounds from seaweed involves multiple stages of physicochemical analysis, including pre-treatment, extraction, and purification. Figure 1 presents the pre-treatment processes, followed by the isolation and identification of bioactive compounds from macroalgae harvested from the Black Sea, as outlined by Cadar et al. (2023) [49]. The extraction of bioactive compounds from algae can be performed using classical methods, such as Conventional Chemical Extraction, which requires further purification and separation through chromatographic and spectrophotometric techniques (e.g., UV-VIS) or coupled methods like GC-MS to ensure extract purity.

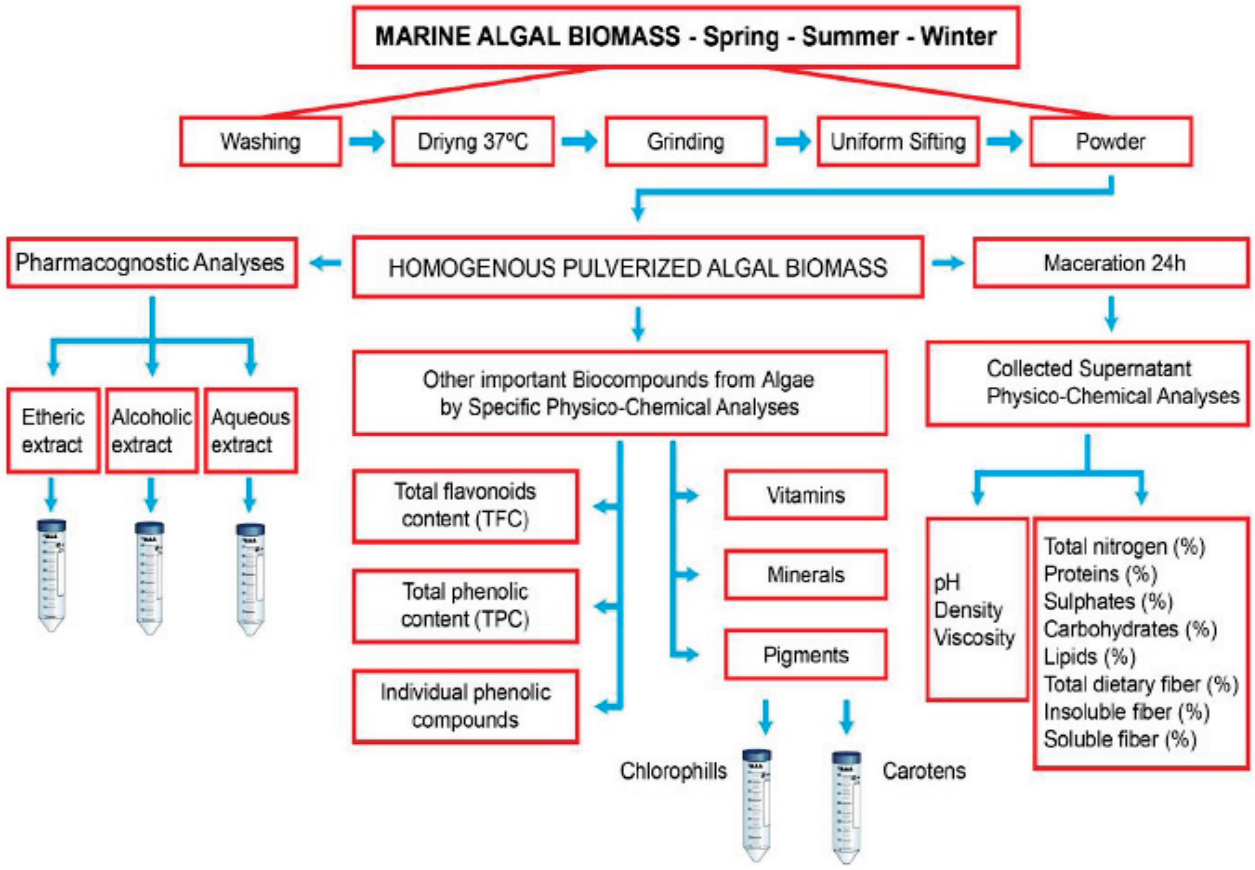

Figure 1. The scheme of the processes in physicochemical analysis of seaweed biocompounds.

Conventional Solvent Extraction (CSE) encompasses techniques such as Soxhlet extraction, solid–liquid extraction (SLE), and liquid–liquid extraction (LLE). Additionally, water-based extraction methods (boiling, autoclaving, and halogenation) and acid or alkaline hydrolysis are commonly employed. Several modern alternatives to Conventional Chemical Extraction have been proposed by Amlani et al. (2022), and Jönsson et al. (2020). These include microwave-assisted extraction (MAE), enzyme-assisted extraction (EAE), supercritical fluid extraction (SFE), ultrasound-assisted extraction (UAE), and pressurized solvent extraction (PSE), which offer improved efficiency for isolating bioactive compounds [50,51]. It is necessary to perform the validation of the extraction and purification methods by using statistical validation methods with the establishment of validation parameters for each method as done by Sirbu et al. (2019) [52]. Figure 2 illustrates the various extraction methods along with their respective advantages and disadvantages for obtaining algal extracts.

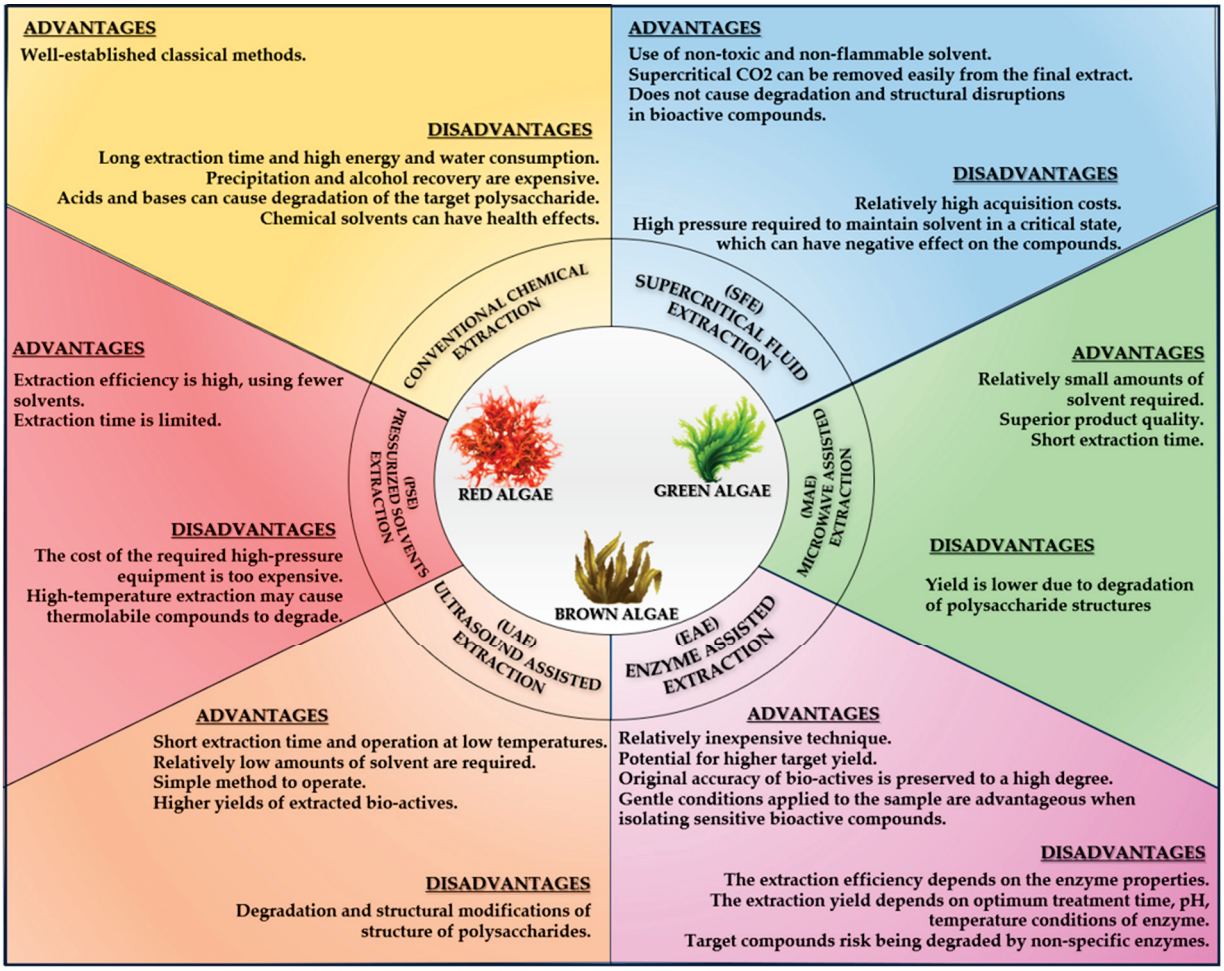

Figure 2. Different conventional and alternative extractive methods used to isolate biocompounds from seaweeds.

3.3.2. Proximate Nutritional Composition

The nutritional composition of algae is presented in the table below. Table 1 includes the following data: moisture and ash content, sulfate compound and total nitrogen content, and protein, lipid, carbohydrate and total dietary fiber content, which have been reported for algae that are representative of the three categories of algae: green, red, and brown. The green algae studied come from different marine habitats found in different seas and oceans. The green algae are 5 species of *Ulva* sp., 3 species of *Ulva* (formerly *Enteromorpha*), 2 species of *Cladophora vagabunda*, 1 species *Acrosiphonia orientalis*, and 3 species of *Caulerpa* sp. The Black Sea algae *Ulva lactuca*, *Ulva intestinalis* (formerly *Enteromorpha intestinalis*), and *Cladophora vagabunda* were reported by Sirbu et al. (2019) and Cadar et al. (2023) [31,49]. The Arabian Sea algae, *Ulva lactuca*, *Acrosiphonia orientalis*, and *Caulerpa scalpelliformis*, were reported by Choudhary et al. (2023) [53]. Algae from Atlantic water, *Ulva rigida* and *Caulerpa lentillifera*, were studied by Morais et al. (2020) [54]. The green algae from Indian waters, *Ulva lactuca* (formerly *Ulva fasciata*) and *Ulva flexuosa* (formerly *Enteromorpha flexuosa*), were studied by Ganesan et al. (2020) [55]. The green algae from the Gulf of Gökova of Aegean Sea, *Ulva intestinalis* (formerly *Enteromorpha intestinalis*), were investigated by Metin et al. (2018) [56]. All these results are systematized in Table 1. The red algae examined in this study come from various marine habitats. Cadar E. (2017) investigated marine algae from the Black Sea, specifically *Ceranium virgatum* (formerly *Ceramium rubrum*) (Rhodophyta) [57].

Table 1. Composition data on proximate nutritional composition from macroalgae (results are expressed in mean % ± standard deviation).

	Green algae											
	Ulva lactuca	*Ulva lactuca*	*Ulva rigida*	*Ulva lactuca* (as *Ulva fasciata*)	*Cladophora vagabunda*	*Cladophora vagabunda*	*Acrosiphonia orientalis*	*Caulerpa scalpelliformis*	*Caulerpa lentillifera*	*Ulva intestinalis* (as *Enteromorpha intestinalis*)	*Ulva flexuosa* (as *Enteromorpha flexuosa*)	*Ulva intestinalis* (as *Enteromorpha intestinalis*)
	Black Sea	Arabian Sea	Atlantic waters	Indian waters	Black Sea	Black Sea	Arabian Sea	Arabian Sea	Atlantic waters	Black Sea	Indian waters	Gulf Gökova Aegean Sea
Moisture (%)	10.85 ± 0.26	25.0 ± 1.0	-	-	5.71 ± 0.92	11.98 ± 0.84	19 ± 2.0	20.0 ± 1.0	-	11.98 ± 0.84	-	12.14 ± 1.11%
Ash (%)	23.62 ± 0.59	16.0 ± 2.0	28.6	27.0 ± 0.024	26.38 ± 0.31	24.63 ± 0.84	22 ± 2.0	15.0 ± 2.0	24–37	25.65 ± 0.98	32.2 ± 0.92	14.81 ± 0.23
Sulphates (%)	70.46 ± 1.87	-	-	-	67.92 ± 0.53	68.65 ± 1.78	-	-	-	67.68 ± 1.63	-	-
Nitrogen (%)	2.26 ± 0.48	66.0 ± 4.0	-	-	2.45 ± 0.02	2.39 ± 0.26	41 ± 3.0	51.0 ± 2.0	-	2.18 ± 0.39	-	-
Protein (%)	14.13 ± 0.85	6.0 ± 1.0	18–19	22.7 ± 0.22	15.43 ± 0.36	14.94 ± 0.92	7 ± 0.2	6.0 ± 1.0	10–13	13.63 ± 0.96	17.29 ± 1.24	13.42 ± 1.31
Lipid (%)	2.78 ± 0.69	1.0 ± 0.5	0.9–2.0	0.89 ± 0.12	3.85 ± 0.47	2.86 ± 0.75	3.0 ± 0.2	4.0 ± 0.5	0.86–1.11	1.72 ± 0.56	0.76 ± 0.24	1.31 ± 0.5
Carbohydrates (%)	58.36 ± 1.64	56.0 ± 2.0	43–56	32.0 ± 0.04	48.45 ± 0.5	62.37 ± 1.74	16 ± 2.0	23 ± 2.0	38–59	60.68 ± 1.36	30.1 ± 0.18	58.03 ± 2.31
Total dietary fiber (%)	60.56 ± 1.1	11.0 ± 0.9	38–41	-	61.56 ± 1.5	63.35 ± 1.24	27.0 ± 0.5	24.0 ± 2.2	33	59.66 ± 1.95	-	52.36 ± 3.26
References	[49]	[53]	[54]	[55]	[30]	[49]	[53]	[53]	[54]	[49]	[55]	[56]
	Red algae											
	Halymenia porphyri-formis	*Palmaria palmata*	*Porphyra umbilicalis*	*Acanthophora spicifera*	*Gracilaria edulis*	*Ceramium virgatum* (as *Ceramium rubrum*)	*Jania pedunculata* var. *adhaerens* (as *Jania adhaerens*)	*Gracilaria corticata*	*Scinaia carnosa*	*Gracilaria edulis*	*Gracilaria corticata*	*Laurencia obtusa*
	Arabian Sea	Atlantic waters	Atlantic waters	Indian waters	Indian waters	Black Sea	Sri Lanka coastal area	Sri Lanka coastal area	Arabian Sea	Southeast coast of India	Southeast coast of India	Red sea coast
Moisture (%)	19.0 ± 1.1	-	-	-	-	11.01 ± 0.13	92.96 ± 0.27	96.32 ± 0.02	21.0 ± 2.0	10.40 ± 0.69	8.40 ± 0.65	-
Ash (%)	17.0 ± 1.2	12–37	12	21.0 ± 0.08	22.8 ± 0.04	13.83 ± 1.68	05.01 ± 0.01	07.15 ± 0.01	46.0 ± 2.0	7.36 ± 0.39	8.10 ± 0.49	-
Sulphates (%)	-	-	-	-	-	75.16 ± 1.56	-	-	-	-	-	-
Nitrogen (%)	75. 0 ± 8.0	-	-	-	-	3.19 ± 0.41	-	-	45.0 ± 8.0	-	-	-
Protein (%)	3.0 ± 1.0	8–35	29–39	20.2 ± 0.12	18.04 ± 0.03	19.94 ± 2.56	29.47 ± 0.15	28.70 ± 0.46	2.0 ± 0.1	25.29 ± 0.67	22.84 ± 0.87	5.41 ± 0.11
Lipid (%)	1.0 ± 0.4	0.7–3	0.3	0.48 ± 0.04	0.72 ± 0.04	3.43 ± 0.25	1.52 ± 0.08	1.66 ± 0.18	3.0 ± 1.0	4.76 ± 0.73	7.07 ± 0.33	3.04 ± 0.12
Carbohydrate (%)	22 ± 1.0	46–56	43.0	26.2 ± 0.02	24.8 ± 0.12	51.90 ± 4.35	-	-	30.0 ± 1.0	4.71 ± 0.60	8.30 ± 0.49	20.17 ± 0.1
Total dietary fiber (%)	3.0 ± 0.2	29–46	29–35	-	-	-	56.81 ± 0.38	59.15 ± 0.76	5.0 ± 0.5	-	-	-
References	[53]	[54]	[54]	[55]	[55]	[57]	[58]	[58]	[53]	[59]	[59]	[60]
	Brown algae											
	Sargassum linearifolium	*Fucus vesiculosus*	*Laminaria digitata*	*Undaria pinnatifida*	*Saccharina latissima*	*Padina gymnospora*	*Gongolaria barbata* (as *Cystoseira barbata*)	*Sargassum ilicifolium*	*Sargassum polycystum*	*Sargassum oligocystum*	*Himanthalia elongata*	*Sargassum asperifolium*
	Arabian Sea	Atlantic waters	Atlantic waters	Atlantic warers	Atlantic waters	Indian waters	Black Sea	Sri Lanka coastal area	Sri Lanka coastal area	Indo-West Pacific area	North-eastern Atlantic coast	Red Sea at Hurghada Coast
Moisture (%)	14.0 ± 1.0	-	-	-	-	-	9.27 ± 0.42	95.92 ± 0.37	92.58 ± 0.32	-	-	88.08
Ash (%)	24 ± 2.0	14–30	38	26–40	34.78	23.2 ± 0.03	17.63 ± 1.73	13.15 ± 0.41	18.48 ± 0.21	21.91 ± 0.28	-	19.60
Sulphates (%)	-	-	-	-	-	-	-	-	-	-	-	-
Nitrogen (%)	56 ± 3.0	-	-	-	-	-	-	-	-	-	-	-
Protein (%)	5 ± 1.0	3–14	8.15	12–23	6–6.26	12.07 ± 0.78	14.13 ± 2.11	28.02 ± 0.68	16.15 ± 0.33	9.26 ± 0.16	5.4 ± 0.46	3.50
Lipid (%)	7 ± 0.5	1.9	1.9	1.05–45	0.5–1.1	1.4 ± 0.82	1.03 ± 0.54	4.45 ± 0.12	4.50 ± 0.21	3.51 ± 0.21	17.06 ± 1.50	0.17
Carbohydrate (%)	53.0 ± 3.0	46.8	48	45–51	52–61	28.0 ± 0.12	58.05 ± 0.72	-	-	52.06	26.3	39.25
Total dietary fiber (%)	12 ± 0.5	43–59	37	16–51	30	-	-	51.46 ± 0.53	54.49 ± 0.95	-	53.3 ± 3.5	-
References	[53]	[54]	[54]	[54]	[54]	[55]	[57]	[58]	[58]	[61]	[62]	[63]

Choudhary et al. (2023) studied *Scinaia carnosa* and *Halymenia porphyriformis* from the Arabian Sea [53]. Morais et al. (2020) analyzed *Palmaria palmata* and *Porphyra umbilicalis* from Atlantic waters [54]. Ganesan et al. (2020) researched *Acanthophora spicifera* and *Gracilaria edulis* from Indian waters [55]. Premarathna et al. (2022) reported on *Jania pedunculata* var. *adhaerens* (formerly *Jania adhaerens*) and *Gracilaria corticata* from the coastal waters of Sri Lanka [58]. Rosemary et al. (2019) provided data on *Gracilaria corticata* and *Gracilaria edulis* from the southeastern coast of India [59]. Additionally, Farghl et al. (2021) published findings on *Laurencia obtusa* from the Red Sea coast [60]. Similarly, the brown algae considered in this study are also presented in Table 1. Choudhary et al. (2023) examined *Iyengaria stellata* and *Sargassum linearifolium* from Arabian Sea waters [53]. Morais et al. (2020) analyzed several brown algae species from Atlantic waters, including *Fucus vesiculosus*, *Laminaria digitata*, *Undaria pinnatifida*, and *Saccharina latissima* [54]. Ganesan et al. (2020) studied the nutritional composition of *Padina gymnospora* from Indian Ocean waters [55]. Cadar E. (2017) provided data on the nutritional composition of the brown alga *Gongolaria barbata* (formerly *Cystoseira barbata*) from Black Sea waters [57]. Premarathna et al. (2022) reported the biochemical composition of the brown algae *Sargassum ilicifolium* and *Sargassum polycystum* from the coastal waters of Sri Lanka [58]. Praiboon et al. (2018) examined the biochemical composition of *Sargassum oligocystum* from the Indo-West Pacific region [61]. Ilyas et al. (2023) studied the proximate composition of the brown alga *Himanthalia elongata* from the North-eastern Atlantic Ocean [62]. Fouda et al. (2019) analyzed the chemical composition of *Sargassum asperifolium* from the Red Sea, specifically the Hurghada Coast [63]. Carbohydrates are present in all types of algae, varying in proportion and structure. In green algae, polysaccharides with ulvan structures are predominant, along with other structural types. The carbohydrate content ranges from 62.37% in *Cladophora vagabunda* from the Black Sea, as reported by Cadar et al. (2023), to 16% in *Acrosiphonia orientalis* from the Arabian Sea, as documented by Choudhary et al. (2023) [49,53]. In red algae, carbohydrate content varies from 56% in *Palmaria palmata* from Atlantic waters, reported by Morais et al. (2020) [54], to as low as 4.71% in *Gracilaria edulis* from the southeast coast of India, as noted by Rosemary et al. (2019) [59]. For brown algae, carbohydrate levels range from 58.05% in *Gongolaria barbata* from the Black Sea, reported by Cadar E. (2017), to 9% in *Iyengaria stellata* (Phaeophyceae) from the Arabian Sea, reported by Choudhary et al. (2023) [49,53]. Additionally, carbohydrates can exist in sulfated forms, as highlighted by Sirbu et al. (2020) and Cadar et al. (2023) [30,49]. Proteins are also found in all algae, though their content varies. In green algae, protein levels range from 6.0% in *Ulva lactuca* and *Caulerpa scalpelliformis* from the Arabian Sea, reported by Choudhary et al. (2023), to 22.7% in *Ulva lactuca* (as *Ulva fasciata*), as documented by Ganesan et al. (2020) [53,55]. The protein content in red algae varies significantly, ranging from 3.0% in *Halymenia porphyriformis* from the Arabian Sea, as reported by Choudhary et al. (2023), to 29–39% in *Porphyra umbilicalis* from Atlantic waters, as noted by Morais et al. (2020) [53,54]. In brown algae, protein levels range from 3–14% in *Fucus vesiculosus* from the Atlantic, reported by Morais, to 28.02% in *Sargassum ilicifolium* from Sri Lanka, as documented by Premerathna et al. (2022) [54,58]. Lipid content is found in all algae but varies widely. In green algae, lipid levels range from 4% in *Caulerpa scalpellifera* from the Arabian Sea, as reported by Choudhary et al. (2023), to 0.76% in *Ulva flexuosa* from Indian waters, as reported by Ganesan et al. (2020) [53,55]. In red algae, lipid content varies from 0.3% in *Porphyra umbilicalis* from Atlantic waters, reported by Morais et al. (2020), to 7.07% in *Gracilaria corticata* from the southeastern coast of India, as noted by Rosemary et al. (2019) [54,59]. Brown algae show the widest lipid variation, with levels ranging from 17.06% in *Himanthalia elongata* from Sri Lanka, as recorded by Ilyas et al. (2023), to just 0.17% in *Sargassum asperifolium* from the Red Sea,

reported by Fouda et al. (2019) [62,63]. Total dietary fiber is present in all algae, with green algae exhibiting the highest levels. *Caulerpa racemosa* from the coastal waters of Sri Lanka contains the most fiber, at 81.59%, as documented by Premarathna et al. (2022) [58]. Among red algae, the highest fiber content is 56.81% in *Jania pedunculata* var. *adhaerens* from Sri Lanka, also reported by Premarathna et al. (2022) [58]. For brown algae, the highest dietary fiber levels range from 43 to 59% in *Fucus vesiculosus* from the Atlantic, as studied by Morais et al. (2020) [54]. Additionally, recent studies by Ullah et al. (2024) and Xie et al. (2024) have provided valuable insights into the nutritional composition of brown algae [64,65].

3.4. Active Metabolites from Seaweeds

The composition of macroalgae is rich in important bioactive metabolites that are currently barely utilized for human health. The most widespread use of macroalgae has been as food. Recent studies emphasize a wide range of possibilities for the utilization of algae compositions that offer a rich range of secondary metabolites. Other researchers such as Xie et al. (2024), Choudhary et al. (2021) have also evaluated the existence and biological activities of metabolites in macroalgae [65,66].

3.4.1. Polysaccharides (MAPs)

Marine algae polysaccharides (MAPs) are vital nutritional components found in all algae, serving as an energy source for the algal body. Based on molecular size and complexity, they are categorized into monosaccharides, disaccharides, oligosaccharides, and polysaccharides. Xie et al. (2024) identified mannose, glucose, fructose, galactose, fucose, xylose, and arabinose as the most common monosaccharides [65]. Dobrinčić et al. (2020) explored extraction technologies, as well as the isolation and structural characterization of MAPs from marine macroalgae [67].

Additionally, Premarathna et al. (2024) investigated how different extraction methods influence the physicochemical properties and antioxidant activity of polysaccharides in red algae [68]. The extraction of polysaccharides from seaweed and their application as hydrogels were explored by Lin et al. (2022), who demonstrated that polysaccharide composition and structure vary based on factors such as species, harvesting season, collection sites, and water quality [69]. Additionally, the extraction and purification conditions significantly impact the properties of polysaccharides and the hydrogels derived from them [69]. Ummat et al. (2021) emphasized the importance of pre-treatment steps conducted before extraction [70]. Oh et al. (2020) proposed improvements to the extraction of bioactive compounds like polysaccharides by moving away from traditional water and organic solvent-based methods, instead advocating for enzyme-assisted extraction techniques, which offer lower energy consumption and enhanced metabolite quality [71]. Yao et al. (2020) highlighted the structural diversity of polysaccharides and their varying effects depending on the algal category, while Akter et al. (2024) detailed specific polysaccharide structures with biomedical applications, including antiviral potential [72,73]. Figure 3 illustrates the polysaccharide extraction process, including pre-treatment steps.

The key polysaccharide structures are depicted in Figure 4.

Carrageenans are polysaccharides found in red algae, alongside agar and agarose. Carrageenans are anionic, sulphated galactans, with their structure illustrated in Figure 4. According to Xie et al. (2024), the linear chains of carrageenans consist of repeating disaccharide units of 3, 6-anhydro-galactose and D-galactose, linked by alternating 4-α-D-galactose and 3-β-D-galactose. These chains are further modified by methyl, sulfate ester, or pyruvate substitutions, with sulfate ester groups making up 15–40% depending on the specific type of carrageenan [65]. Figure 4 shows the three main commercial forms: Kappa,

Lambda, and Iota. Kappa forms rigid, strong gels in the presence of potassium ions and is primarily derived from *Kappaphycus alvarezii*. Iota, which forms soft gels in the presence of calcium ions, comes mainly from *Eucheuma denticulatum*. Lambda, on the other hand, does not form gels, as shown by Udo et al. (2023) [74].

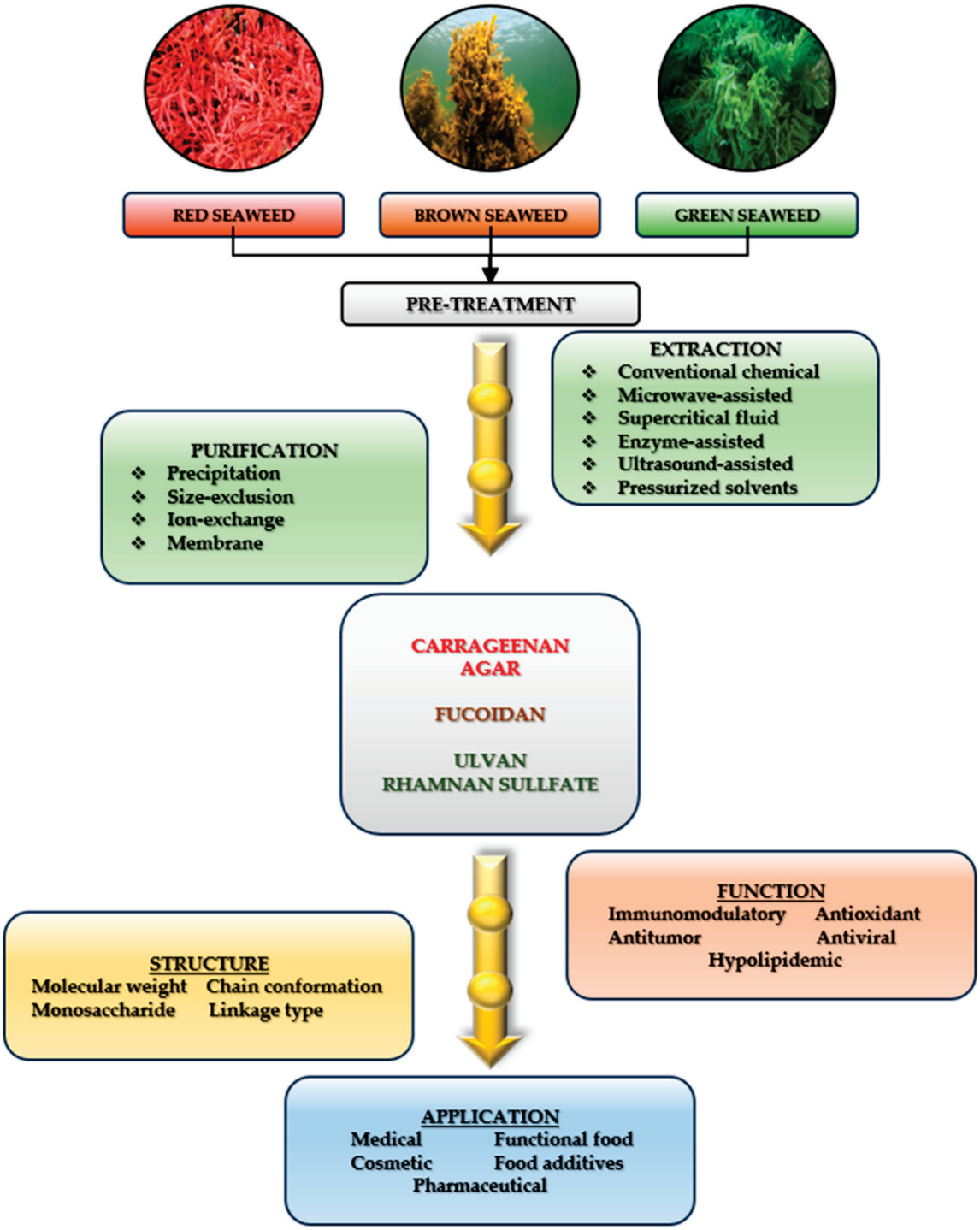

Figure 3. Scheme for the isolation, structural and functional analyses, and applications of polysaccharides.

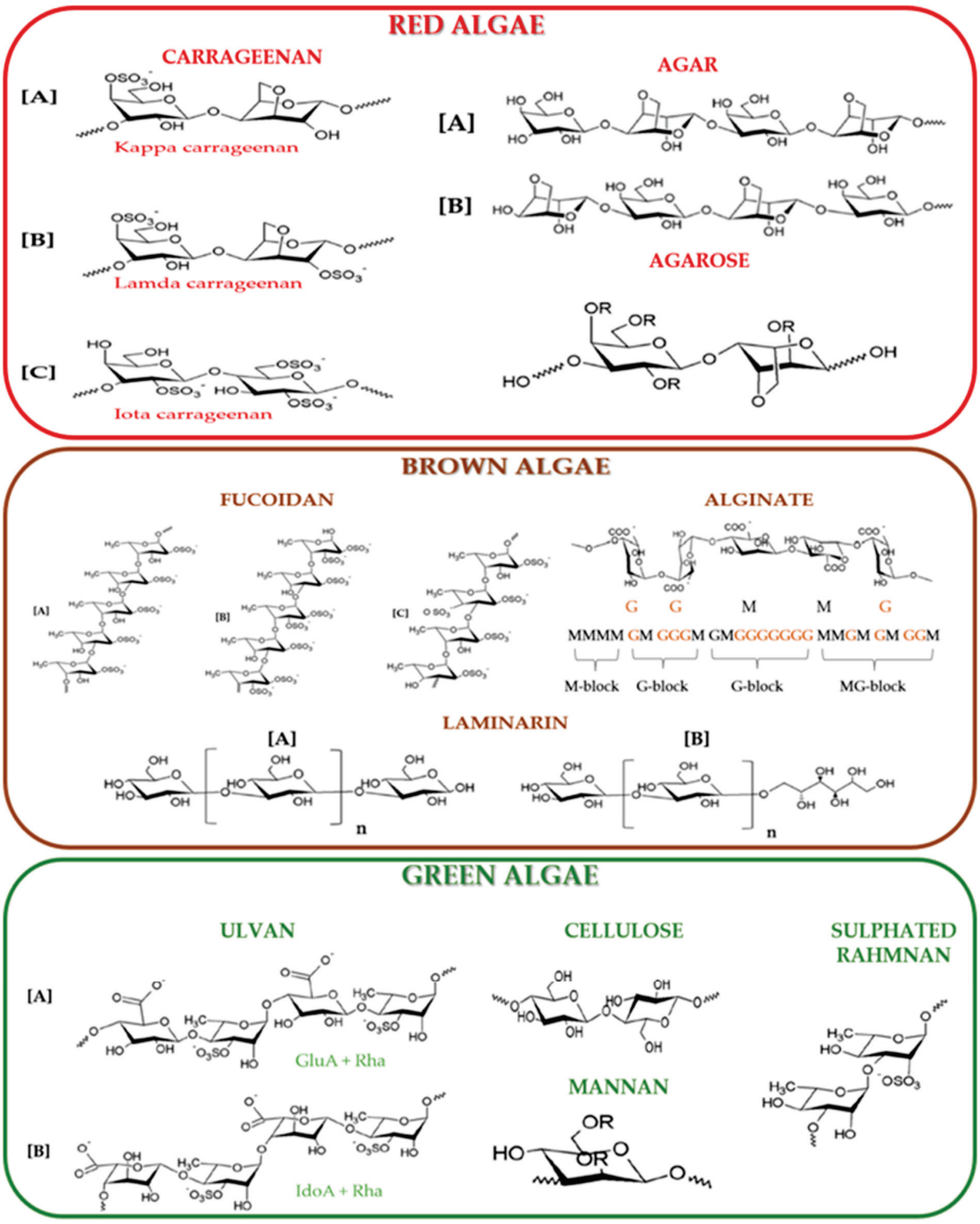

Figure 4. Chemical structure of polysaccharides from seaweed.

Agars are also widely used in various industries due to their excellent hydrocolloid properties. They are extracted from species like *Gelidium* spp., *Gracilaria* spp., and *Pterocladiella capillacea* [65]. Xie et al. (2024) explain that agars are hydrocolloids composed mainly of agarose and agaropectin [65].

As shown in Figure 4**,** agars are linear polysaccharides made up of alternating residues of α-(1→3)-D-galactopyranose and β-(1→4)-linked 3,6-anhydro-L-galactopyranose, with intermittent sulfate groups at the C-6 position. Like carrageenans, agars are sulphated galactans. Zhang et al. (2019) demonstrated that the anionic charges in agar polymers vary depending on the degree of sulfation [75]. Dragan et al. (2022) noted that further research is needed to understand the biosynthesis of c arrageenans [76].

Fucoidans are a key component of brown algae, along with other major MAPs such as alginates and laminarin. They belong to the group of sulfated polysaccharides, primarily composed of sulfated α-L-fucose residues, but also include glucose, xylose, mannose, galactose, uronic acids, and acetyl groups. Shao et al. (2022) demonstrated that fucoidans are a primary constituent of the cell walls in brown seaweeds, distinguishing them from terrestrial plants [77].

According to Xie et al. (2024), the fucoidan content in brown algae typically ranges from 10% to 20%, depending on factors like the species, season, reproductive cycles, environmental conditions, and tissue position. The highest concentration reported to date is 46.6% in *Laminaria digitata* [65]. Fucoidan structures mainly consist of two types of backbones: one made of α-(1→3)-L-fucose residues, and another alternating between (1→3)-linked and (1→4)-linked α-L-fucose residues [65]. Wang et al. (2020) explored the structure of fucoidans from *Sargassum siliquosum* [78], and Dragan et al. (2023) analyzed fucoidans from *Gongolaria barbata*, focusing on their potential health benefits for humans [79].

Laminarins are low molecular weight polysaccharides found specifically in brown algae. Their polymeric structure consists of a chain of (1→3)-linked β-D-glucopyranose units, with varying degrees of β-(1→6)-linkages between chains. Rajauria et al. (2021) studied laminarin rings in species such as *Saccharina* sp., *Laminaria* sp., and *Fucus* sp., identifying two primary types of polymer chains: G-chain and M-chain. These chains have a lower molecular weight compared to other seaweed polysaccharides and vary based on the degree of polymerization [80]. Li et al. (2021) explained that the distinction between the two chains lies in the presence of D-mannitol at the reducing end of the M-chain, whereas the G-chain lacks D-mannitol at this position [81].

Alginates are the predominant polysaccharides found in the intercellular matrix and cell walls of brown algae. Xie et al. (2024) reported that alginate content is highest in young algae during July, varying between 17% and 47% [65]. Shao et al. (2022) described alginates as linear anionic polymers composed of α-L-guluronic acid (G) and β-D-mannuronic acid (M) units, linked by (1→4) glycosidic bonds [77]. Tanna et al. (2019) also confirmed that these isomeric residues are connected by (1→4) glycosidic bonds [82]. Ramos et al. (2018) noted that the M/G ratio can be influenced by factors such as species, growth conditions, harvesting time, and extraction methods [83]. Pengyan et al. (2021) showed that the gel stiffness follows this order: gel formed from homo-polymeric G blocks > gel formed from homo-polymeric M blocks > gel formed from hetero-polymeric MG blocks [84]. Abkakhajouei et al. (2022) evaluated the structural characteristics of alginates from seaweed and highlighted their diverse applications [85].

Ulvans, the most abundant polysaccharides found in green algae, include ulvan, cellulose, mannan, and sulfated rhamnan. The structure of ulvan has been studied by Glasson et al. (2022), Li Q et al. (2020), and Sari-Chmayssem et al. (2019) [86–88]. Ulvan is a polyanionic heteropolysaccharide composed of uronic acids (iduronic acid and glucuronic acid), rhamnose 3-sulfate, and xylose. Tanna et al. (2019) demonstrated that ulvan has a complex, heterogeneous composition, featuring repeating disaccharide units, such as xylose, sulfated rhamnose, and uronic acids (iduronic or glucuronic acid) [82]. Xie et al. (2024) further clarified that sulfated rhamnose residues typically occupy the C-3 position or both C-1 and C-3 positions, while sulfated xylose residues may replace uronic acids [65]. Additional studies on the structures of green algae polysaccharides were conducted by Ciancia et al. (2020) and Gomaa et al. (2022) [89,90]. The polysaccharide content was presented for representative algae in Table 1 where the nutritional composition of macroalgae was demonstrated.

Researchers have also focused on optimizing the extraction of these valuable biocompounds. Carrageenans have been extracted from various red algae by Firdayanti et al. (2023), Martín-del-Campo et al. (2021), and Heriyanto et al. (2018) [91–93]. Firdayanti et al. (2023) reported the highest extraction yield using bead mill extraction, while the lowest yield was obtained by Heriyanto et al. (2018) using conventional extraction methods [91,93]. Agar extraction from red algae species has been explored by Lebbar et al. (2018), Martínez-Sanz et al. (2019), and Xiao et al. (2019) through various methods [94–96]. The highest yield was achieved using alkaline extraction by Xiao et al. (2019) from *Gracilariopsis lemaneiformis* (formerly *Gracilariopsis lemaneiformis*) (Rhodophyta) [96]. Table 2 presents different polysaccharide types alongside the optimal yields achieved through various extraction methods. Fucoidan extraction has been studied using alternative methods by Alboofetileh et al. (2018), Hmelkov et al. (2018), Alboofetileh et al. (2019), Liu et al. (2020), and Hanjabam et al. (2019) from different brown algae species [97–101]. The highest extraction efficiency was reported by Hanjabam et al. (2019), who employed the UAE method for isolating fucoidans from *Sargassum wightii*, a brown algae species [101]. Alginates have been extracted by Montes et al. (2021), Rashedy et al. (2021), and Trica et al. (2019) [102–104]. Finally, ulvan extraction from different *Ulva* species was conducted by Malvis Romero et al. (2023), Kidgell et al. (2019), Yuan et al. (2018), and Tabarsa et al. (2018) [105–108].

Table 2. Extraction methods and yields for different types of polysaccharides.

Polysaccharides	Species	Yield	Method	References
Carrageenans	*Kappaphycopsis cottonii* (formerly *Eucheuma cottonii*)—red algae	67.86%	Bead mill extraction	[91]
	Chondracantus canaliculatus—red algae	45.05%	UAE—Ultrasound-assisted extraction	[92]
	Euchema cottonii—red algae	30.20%	Conventional extraction method of semi-refined carrageenan	[93]
	Gelidium corneum (formerly *Gelidium sesquipedale*)—red algae	8.4%	Solubilization in hot water and alkali treatment	[94]
Agars	*Gelidium corneum* (formerly *Gelidium sesquipedale*)—red algae	10–12%	Sonication with hot water treatment	[95]
	Gracilariopsis lemaneiformis—red algae	12.32%	Alkaline extraction	[96]
	Gracilariopsis lemaneiformis—red algae	2.52%	EAE—Enzyme extraction	[96]
	Gracilariopsis lemaneiformis—red algae	5.33%	EA—Enzyme-assisted extraction	[96]
	Nizamuddinia zanardinii—brown algae	3.51%	UA—Ultrasound-assisted extraction	[97]
	Fucus distichus subsp. *evanescens* (formerly *Fucus evanescens*)—brown algae	4.44%	UAE—Ultrasound-assisted extraction	[98]
Fucoidans	*Nizamuddinia zanardinii*—brown algae	Alcalase, cellulase, flavourzyme, viscozyme, hot water 10–15%	EAE—Enzyme-assisted extraction	[99]
	Sargassum fusiforme—brown algae	11.24%	Conventional extraction with dilute hydrochloric acid	[100]
	Sargassum wightii—brown algae	14.61%	UAE—Ultrasound-assisted extraction	[101]
Alginates	*Ascophyllum nodosum*—brown algae	18.3–23.7%	UAE and Conventional method (HCl)	[102]
	Turbinaria triquetra—brown algae	22.2%	Conventional method (formaldehyde)	[103]
	Gongolaria barbata—brown algae	19%	Conventional method (HCl)	[104]
	Ulva fenestrata—green algae	9.03%	EAE–Enzyme assisted extraction	[105]
	Ulva fenestrata—green algae	8.65%	UAE–Ultrasound assisted extraction	[105]
Ulvans	*Ulva fenestrata*—green algae	17.92%	U-EAE—combined ultrasound with enzymatic extraction	[105]
	Ulva lactuca—green algae	36.4%	Conventional extraction (strong acid produces higher extraction yields)	[106]
	Ulva prolifera—green algae	36.38%	Microwave-assisted hydrothermal extraction	[107]
	Ulva intestinalis—green algae	12%	Conventional extraction (ethanol)	[108]

The highest extraction yield for ulvan was reported by Kidgell et al. (2019) by conventional extraction, followed by Yuan et al. (2018) by microwave-assisted hydrothermal

extraction, who extracted ulvan from various species of *Ulva* sp. and by different methods [106,107]. Table 2 presents different polysaccharide types alongside the optimal yields achieved through various extraction methods.

3.4.2. Terpenoids Content

Terpenic compounds, along with other secondary metabolites, are significant in marine macroalgae. These compounds include monoterpenes, sesquiterpenes, diterpenes, and triterpenes. Structurally, terpenes are a large and diverse group of compounds with the general formula $(C_5H_8)_n$, composed of isoprene units (2-methylbuta-1,3-diene). They are found not only in marine algae but also in the volatile oils of terrestrial plants, as noted by Cikoš et al. (2019) [109]. Polzin et al. (2018) focused on monoterpenes from red algae of the genus *Ochtodes*, particularly *Ochtodes secundiramea* [110]. Figure 5 displays the chemical structures of the diterpenes identified from several *Dictyota* species.

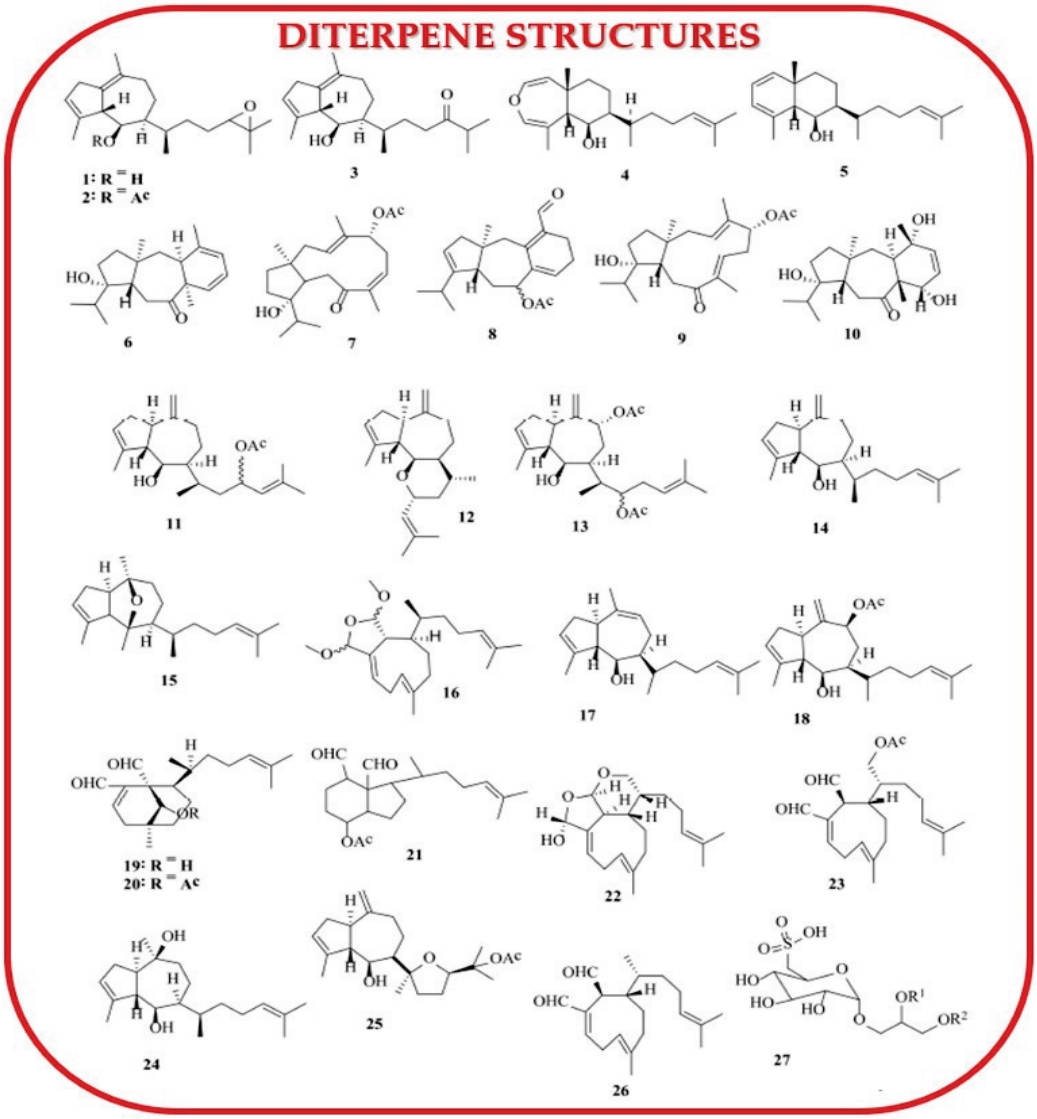

Figure 5. Structure of diterpenes from species of the genus *Dictyota*.

Diterpenes, another significant category, are a large and structurally diverse class of compounds found widely in marine macroalgae. Chen et al. (2018) highlighted the strong cytotoxic and antiviral properties of diterpenes [111]. They identified diterpenes

1–5 from *Dictyota acutiloba*, diterpenes 6–10 from *Dictyota bartayresiana*, diterpenes 11–16 from *Dictyota binghamiae*, diterpenes 17–21 from *Dictyota caribaea*, and diterpenes 22–26, along with sulfonoglycolipid 27, from *Dictyota ciliolata* (Phaeophyceae). Monoterpenes were extracted through conventional chemical methods by Cikoš et al. (2019), who also examined the influence of solvents on extraction and the interference of other compounds with monoterpenes during GC-MS analysis [109]. Cikoš et al. (2019) also extracted halogenated monoterpenes from *Plocamium cartilagineum* using supercritical fluid extraction [109]. Their work focused on red algae from the genera *Plocamium* and *Portieria*, which are rich in cyclic and acyclic halogenated monoterpenes, demonstrating their role as antitumor agents [109]. Polzin et al. (2018) also investigated the extraction of halogenated monoterpenes from *Ochtodes* species [110]. Furthermore, Chen et al. (2018) reported that, by the end of 2017, a total of 233 diterpenes had been isolated from *Dictyota* species, particularly from the brown alga *Dictyota dichotoma* [111].

Rajamani et al. (2018) conducted studies on the extraction and characterization of triterpenes isolated from the brown alga *Padina boergesenii* [112]. Using microwave-assisted extraction (MAE), Nie et al. (2021) identified three novel terpenoids from the brown seaweed *Sargassum fusiforme* [113]. Rushdi et al. (2022) reported a large-scale study over a longer period (1976–2022) on bioactive compounds isolated from brown seaweeds of the genus *Dictyota* and indicated that numerous compounds such as diterpenes and sesquiterpene exhibited various biological activities [114].

3.4.3. Seaweeds Lipids, Fatty Acids (AFs), and Sterols

Santos et al. (2019) reported the lipid profiles of three seaweed species from Brazilian marine waters using a modified Folch method, revealing that glycolipids were the most abundant lipid class in all species, making up 60–70% of the total lipids [115]. This was followed by phospholipids (10–25%) and neutral lipids (10–15%) [115]. Table 3 provides a detailed breakdown of fatty acid content by fatty acid structure categories for several representative macroalgae species from the three major classes: green, red, and brown. Peñalver et al. (2020) also highlighted the main lipid classes in macroalgae, including neutral lipids (fatty acids, triglycerides, and sterols), glycolipids, and phospholipids [116].

Foseid et al. (2020) reported lipid extraction studies using a modified Folch method, which involved extraction followed by GC-MS analysis of lipids from the red alga *Parmaria palmata* and two brown algae species, *Alaria esculenta* and *Saccharina latissima* [117]. Rocha et al. (2021) investigated the composition and concentration of lipids in macroalgae, finding significant variation in lipid content across species, which was influenced by season, temperature, geographical area, and environmental conditions [118]. El-Sheekh et al. (2021) demonstrated lipid extraction using the modified Folch method on algae harvested from the Abu Qiu Bay area in Egypt. They found that the highest lipid content occurred in the spring season for *Ulva fascinata* (14.66%) and *Ulva compressa* (9.94%) [119]. Jaworowska et al. (2023) highlighted that macroalgae are a rich source of biologically active lipids, particularly unsaturated fatty acids [120]. Kord et al. (2019) examined the fatty acid content of *Gongolaria sauvageauana* (formerly *Cystoseira sauvageauana*) (Phaeophyceae) and *Osmundea pinnatifida* (formerly *Laurencia pinnatifida*) (Rhodophyta), algae collected from the Algerian coast [121]. Their methods for determining SFA, MUFA, PUFA, and the ω-6/ω-3 ratio were later expanded upon by Rodriguez-Gonzalez et al. (2022), who conducted a more comprehensive study [121,122]. Rodriguez-Gonzalez et al. (2022) also explored several alternative extraction techniques for fatty acid analysis, including ultrasound-assisted extraction (UAE), enzyme-assisted extraction (EAE), pulsed electric fields-assisted extraction (PEF), pressurized liquid extraction (PLF), microwave-assisted extraction (MAE), and

supercritical CO_2 extraction (Sc-CO_2) [122]. The fatty acid content of algae has been widely studied. Susanto et al. (2019) and Pangestuti et al. (2021) also presented findings on the fatty acid content of green marine macroalgae [123,124]. Lopes et al. (2020) explored the role of lipids in aquaculture red macroalgae for various biotechnological applications [125], while Lopes et al. (2019) reported the lipid content and properties of the red alga *Palmaria palmata* [126]. Al-Adilah et al. (2021) provided additional nutritional information, including fatty acid content, for various brown macroalgae species [127]. According to Rocha et al. (2021) and Jaworowska et al. (2023), the percentage of saturated fatty acids (SFAs) ranged from 7.53% to 95.21%, monounsaturated fatty acids (MUFAs) ranged from 2.30% to 47.10%, and polyunsaturated fatty acids (PUFAs) ranged from 2.60% to 73.70% [118,120]. Among fatty acids, palmitic acid is the most prevalent, followed by oleic acid, based on their percentages in the total fatty acid profile, as reported by Jaworowska et al. (2023) [120]. Both Jaworowska et al. (2023) and Harwood et al. (2019) demonstrated that seaweeds are an important source of essential PUFAs, such as acids ALA, C18:3, and n-3 and acids LA, C18:2, and n-6, which mammals cannot synthesize [120,128]. According to Jaworowska et al. (2023), green algae have the lowest ω-6/ω-3 ratio, followed by brown algae, with red algae exhibiting the highest ratio [120]. It is important to note that significant amounts of docosahexaenoic acid (DHA) and eicosapentaenoic acid (EPA) are found in macroalgae, as humans have limited endogenous synthesis of these acids. Table 3 also highlights the omega-6/omega-3 ratio, which impacts human health by reducing the risk of cardiovascular, neurological, and inflammatory diseases. Of the two, EPA is the dominant (n-3) LC-PUFA and its concentration exceeds that of DHA, as shown in Table 3.

The percentage of EPA in total fatty acids decreases in the order of Rhodophyta, Heterokontophyta, and Chlorophyta, with the lowest EPA content in Chlorophyta. Similarly, DHA content follows the same decreasing order: Rhodophyta, Heterokontophyta, and Chlorophyta.

3.4.4. Proteins and Amino Acids

Seaweeds are a significant source of proteins, as well as key ingredients in food, nutraceuticals, and functional foods for both humans and animals. Pliego-Cortésa et al. (2020) reported that seaweeds contain valuable protein content, reaching up to 50% of their dry weight (d.w.), including peptides, enzymes, glycoproteins, lectins, amino acids with mycosporine structures, and phycobiliproteins found in red algae [129]. Similarly, Dhaouafi et al. (2024) highlighted that marine macroalgae serve as an important reservoir of biologically active compounds such as proteins, peptides, and amino acids, along with enzymes, carotenes, fatty acids, flavonoids, vitamins, minerals, and polysaccharides [130]. The protein content varies among different algae species, with studies by Pliego-Cortésa et al. (2020) and Fleuence et al. (2018) indicating that red algae have the highest protein content (20–47%), followed by green algae (9–26%) and brown algae (3–15%) [129,131]. Rawiwan et al. (2022) further emphasized that the high protein content (up to 47%) and essential amino acids (EAAs) in red seaweeds make them a valuable protein source [132]. Beyond their nutritional value, seaweed proteins also exhibit bioactive properties. Feng et al. (2021) investigated peptide proteins from the brown alga *Undaria pinnatifida*, which demonstrated antihypertensive activity [133]. However, Pliego-Cortésa et al. (2020) warned that seaweeds contain sources of non-protein nitrogen, such as nitrite, pigments, and nucleic acids, which may lead to an overestimation of the protein content calculated with the conversion factor of 6.25 [129]. To address this, their analysis of 44 studies covering 103 algae species led to the proposal of new seaweed nitrogen–protein conversion factors (SNPs): 5.38 for brown algae, 4.59 for red algae, and 5.13 for green algae [129]. Various protein types have been identified in seaweeds.

Table 3. Fatty acid content, reported for some representative seaweeds for each of the three classes: green, red, and brown macroalgae.

	Green Algae				Red Algae				Brown Algae				
Fatty Acids	*Cladophora albida*	*Ulva intestinalis*	*Caulerpa lentillifera*	*Ulva lactuca*	*Ceramium des-longchampsii* (as *Ceramium strictum*)	*Gracilaria gracilaris*	*Porphyra dioica*	*Palmaria palmata*	*Stephanocystis hakodatensis* (as *Cystoseira hakodatensis*)	*Dictyota dichotoma*	*Undaria pinnati-fida*	*Sargassum horneri*	*Padina boergesenii*
C16:0	33.04 ± 0.52	31.05 ± 11.10	33.69 ± 0.64	33.39 ± 12.87	24.00 ± 0.60	27.1 ± 1.2	25.71 ± 3.40	24.32 ± 1.11	18.49 ± 0.30	24.75 ± 0.32	11.51 ± 0.01	25.24 ± 1.91	49.20 ± 0.30
C18:0	1.28 ± 0.19	n.d.a	13.57 ± 0.91	2.21 ± 1.32	3.30 ± 0.20	4.6 ± 0.8	3.53 ± 1.93	12.45 ± 6.74	n.d.a	2.85 ± 0.08	0.64 ± 0.02	28.90 ± 2.33	2.30 ± 0.10
∑SFA	50.03 ± 0.56	42.80 ± 25.17	29.80 ± 1.65	54.95 ± 26.77	34.80	34.9 ± 0.9	34.32 ± 4.49	36.77 ± 6.95	n.d.a	35.98 ± 0.47	12.15	26.98 ± 0.00	58.00 ± 0.40
C16:1	13.90 ± 0.09	4.85 ± 4.31	n.d.a	3.31 ± 3.64	7.30 ± 0.30	2.8 ± 0.8	10.78 ± 11.90	2.03 ± 0.43	0.63 ± 0.08	15.49 ± 0.09	1.66 ± 0.06	n.d.a	3.20 ± 0.30
C18:1	12.51 ± 0.02	12.35 ± 4.03	n.d.a	8.88 ± 4.49	18.30 ± 0.20	9.7 ± 0.4	2.85 ± 0.63	2.82 ± 0.54	11.08 ± 0.24	8.49 ± 0.13	6.21 ± 0.11	n.d.a	16.80 ± 0.80
∑MUFA	27.73 ± 0.11	23.60 ± 1.69	9.08 ± 2.75	15.45 ± 7.71	30.30	12.5 ± 0.7	13.63 ± 9.94	4.85 ± 0.56	n.d.a	24.28 ± 0.13	10.35	14.24 ± 0.00	20.50 ± 0.80
C18:2(LA)	15.54 ± 0.22	7.10 ± 1.83	n.d.a	5.54 ± 3.57	2.00 ± 0.10	2 ± 0.4	1.67 ± 0.04	0.45 ± 0.19	6.95 ± 0.15	5.55 ± 0.02	3.87 ± 0.08	n.d.a	3.30 ± 0.10
C18:3 (ALA)	n.d.a	7.85 ± 9.26	n.d.a	5.64 ± 6.03	15.10 ± 0.30	2.7 ± 0.2	1.95 ± 0.07	n.d.a	6.87 ± 0.18	2.63 ± 0.20	19.84 ± 0.42	n.d.a	2.20 ± 0.1
∑PUFA	16.24 ± 0.24	25.95 ± 15.76	13.06 ± 0.32	17.62 ± 19.64	24.90	5.26 ± 1.4	13.78 ± 12.42	0.45 ± 0.19	n.d.a	19.74 ± 0.67	23.71	29.00 ± 0.00	6.40 ± 0.50
C20:4(ARA)	1.37 ± 0.07	n.d.a.	2.84 ± 0.53	2.50 ± 4.03	3.90 ± 0.10	35.4 ± 1.5	3.16 ± 0.19	0.92 ± 0.17	16.59 ± 0.11	11.46 ± 0.59	0.00	23.04 ± 0.52	2.0 ± 0.1
C20:5(EPA)	2.02 ± 0.05	0.55 ± 0.35	n.d.a	1.69 ± 1.12	n.d.a	5.5 ± 0.2	33.42 ± 18.27	51.68 ± 6.47	12.96 ± 0.18	6.57 ± 0.22	13.15 ± 0.02	n.d.a	0.3 ± 0.02
C22:6 (DHA)	0.86 ± 0.03	n.d.a	n.d.a	0.65 ± 0.63	n.d.a	n.d.a	n.d.a	n.d.a	n.d.a	n.d.a	8.55 ± 0.37	n.d.a	n.d.a
∑HUFA	4.25	0.55	2.84	4.84	3.90	40.9	36.58	52.6 ± 6.40	29.55	18.03	21.70	23.04	2.3
∑FA	98.25	92.9	54.78	92.86	93.90	93.56	98.31	3578	n.d.a	98.03	68.11	93.26	87.2
ω-6/ω-3	6.73	0.35 ± 0.21	0.79 ± 0.05	0.77 ± 0.48	n.d.a	2.47	1.22 ± 1.49	-	1.32	3.52	67.86	0.99 ± 0.30	1.4 ± 0.03
References	[120]	[120]	[123]	[120,124]	[120]	[125]	[125]	[126]	[120]	[120]	[118]	[123]	[127]

Results are expressed in mean % ± standard deviation. (LA)—linoleic acid; (ALA)—alpha linoleic acid; (ARA)—arachidonic acid; (DHA)—docosahexaenoic acid; (EPA)—eicosapentaenoic acid. (∑FA) content is the sum of fatty acid. This includes (∑SFA)—saturated fatty acids; (∑MUFA)—monounsaturated fatty acids; (∑PUFA)—polyunsaturated fatty acids. (∑HUFA)—highly unsaturated fatty acids. ω-6/ω-3 is the ratio of ω-6/ω-3.

Peptides, which are protein fragments consisting of 3 to 40 amino acids, are one such category. Marine algae also contain enzymes, including alkaline phosphatase, a zinc-containing metalloproteinase that catalyzes the hydrolysis of phosphate monoesters, as demonstrated by Pliego-Cortésa et al. (2020) in extracts from *Ulva australis* (formerly *Ulva pertusa*) (Chlorophyta) [129]. Ünlü et al. (2019) identified alternative oxidase proteins (AOXs) in *Caulerpa cylindracea*, which contribute to the alga's ability to invade new environments [134].

Glycoproteins (GPs). Another key group is glycoproteins (GPs), which consist of proteins covalently linked to oligosaccharide chains. Echave et al. (2022) classified these chains into two major types: those linked by O-glycosyl bonds and those linked by N-glycosyl bonds [135]. Lectins, a class of proteins that bind specifically to mono- and oligosaccharides, are particularly abundant in red algae. Echave et al. (2022) highlighted that marine lectins are predominantly mannose-specific and exhibit strong binding affinities [135]. Barre et al. (2019) noted that lectins play crucial roles in reproductive cell fusion, pathogen defense, and possess significant anti-cancer properties [136].

Arabinogalactan proteins (AGPs). Additionally, some proteins are associated with the algal cell wall, such as arabinogalactan proteins (AGPs), which are glycoproteins rich in hydroxyproline. While AGPs are well-studied in terrestrial plants, their role in marine algae remains less understood. According to Pliego-Cortésa et al. (2020), the carbohydrate portion of AGPs (90–95%) consists of arabinose, rhamnose, and glucuronic acid residues, while the protein backbone is composed of hydroxyproline/proline, alanine, and serine/threonine sequences [129]. Figure 6 illustrates the structures of key protein classes found in seaweeds, including phycobiliproteins, mycosporine-like amino acids, and significant bioactive peptides.

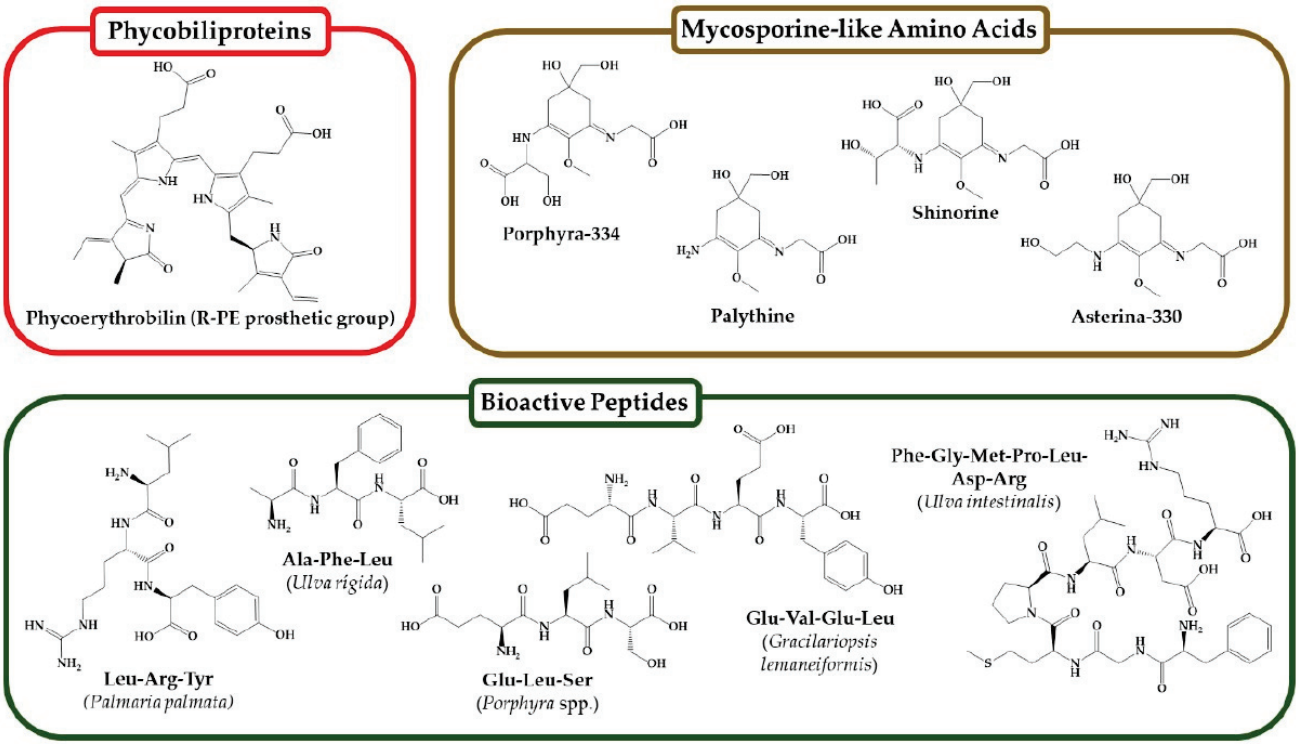

Figure 6. Structures for phycobiliproteins, mycrosporine-like amino acids, and bioactive peptides.

Phycobiliproteins (PBPs) are the main pigments that play a role in light capture, and are the only water-soluble pigments. Pliego-Cortésa et al. (2020) show that PBPs are made

up of four classes: phycoerythrin (PE), phycocyanin (PC), phycoerythrocyanin (PEC), and allophycocyanin (APC); Phycoerythrin (PE) is the main pigment and is divided into R-for hodophyta (R-PE) and B-for Bingiales (B-PE) [129].

Mycosporine-like Amino Acids (MAAs). These compounds are small in size (<400 Da), are secondary metabolites with strong absorption in UVR, and are stable under variable light conditions, temperature, and pH. Pliego-Cortésa et al. (2020) show that they have main functions in UVR protection and antioxidant activity, and facilitate the adaptation of algae to stressful environments [129].

Extraction of peptides from seaweed. The extraction of peptides from seaweed requires several pre-treatment steps to enhance efficiency. Echave et al. (2021) outlined common pre-treatment methods, including osmotic shock, mechanical grinding, alkaline treatment, freeze–thaw cycles, and ultrasonic sonication [135]. Protein extraction techniques include solid–liquid extraction (SLE), microwave-assisted extraction (MAE), pulsed electric field (PEF), ultrasound-assisted extraction (UAE), enzyme-assisted extraction (EAE), and high hydrostatic pressure extraction (HHPE). According to Echave et al. (2021), pre-treatment simplifies the extraction process and improves yield, while protein hydrolysis facilitates the production of bioactive peptide-rich protein hydrolysates (BAPs) [135]. Vásquez et al. (2019) explored enzyme-assisted protein extraction from *Macrocystis pyrifera* (Phaeophyceae) and *Chondracanthus chamissoi* (Rhodophyta) [137]. O'Connor et al. (2020) compared three physical extraction methods applied to four algae species: two red (*Palmaria palmata* and *Chondrus crispus*) and two brown (*Fucus vesiculosus* and *Alaria esculenta*). Their study highlighted the challenge of breaking the algal cell wall to release proteins efficiently [138]. They also found that combining heat and pressure (as in the autoclave method) resulted in the highest extraction yields for *Palmaria palmata*, while physical pre-treatment increased the essential amino acid (EAA) content of extracts compared to raw biomass [138].

Amino acid composition varies among seaweed species. Vieira et al. (2018) studied amino acids in the green alga *Ulva rigida* and several brown algae [139]. Further research on *Ulva rigida* was conducted by Sonchaeng et al. (2023) and Machado et al. (2020) [140,141]. For red algae, amino acid compositions were analyzed by O'Connor et al. (2020) for *Palmaria palmata* and *Chondrus crispus* and by Machado et al. (2020) for *Porphyra dioica* [138,141]. Ferreira et al. (2021) and Trigueros et al. (2021) investigated the amino acid profiles of *Gracilaria gracilis* and *Gelidium corneum* [142,143]. Regarding brown algae, Vieira et al. (2018) reported on *Fucus spiralis*, *Ascophyllum nodosum*, and *Undaria pinnatifida*, while Zheng et al. (2020) analyzed *Sargassum mcclurei* [139,144]. O'Connor et al. (2020) reported that *Chondrus crispus* has the highest protein content (35.2% d.w.), while Sonchaeng et al. (2023) found that *Ulva lactuca* has the lowest (5.67% d.w.) [138,140]. Ferreira et al. (2021) recorded the highest EAAs percentage in *Gracilaria gracilis* (45.6% d.w.) and Zheng et al. (2020) reported the lowest in *Sargassum mcclurei* (27.8% d.w. of protein content) [142,144]. Reynolds et al. (2022) emphasized the nutritional value of seaweed proteins for human diets [145]. Hydroxylysine (*Hyl*) has not been detected in marine algae, except in *Palmaria palmata*, where O'Connor et al. (2020) reported a concentration of 2.7% of total amino acids [138]. Hydroxyproline (*Hyp*) is mainly found in brown algae, as noted by Vieira et al. (2018) for *Fucus spiralis*, *Ascophyllum nodosum*, and *Undaria pinnatifida* [139]. Table 4 summarizes amino acid compositions across various algae.

Table 4. Amino acids content from different green, red, and brown seaweeds (% percentage of the total amino acids).

	Green Algae		Red Algae					Brown Algae			
Type of Algae	*Ulva rigida*	*Ulva rigida*	*Palmaria palmata*	*Chondrus crispus*	*Porphyra dioica*	*Gracilaria gracilis*	*Gelidium corneum*	*Fucus spiralis*	*Ascophylum nodosum*	*Undaria pinnati-fida*	*Sargassum mcclurei*
Proteins (% dw)	5.67	9.6	12.5	35.2	28.7	18.7	21	11.8	9.4	16.5	8.4
Essential amino acids (EAAs) (%)	-	40.8	37.7	40.9	39.8	45.6	44.1	38.7	39.2	37.2	27.8
Arginine (Arg)	0.7	6	6	6.5	2.3	1.4	-	1.5	1.7	2.7	3.8
Cysteine (Cys)	0.7	2.9	2.1	0.7	-	-	-	-	-	-	3.5
Glutamic acid (Glu)	1.4	-	15.5	12.1	3.1	12.5	1.6	7.2	7.2	7.6	29.7
Glycine (Gly)	1	6	5.8	5.2	1.8	1.3	0.8	-	-	0.2	4.2
Histidine (His)	0.2	-	4.6	2.1	0.6	0.1	0.3	1.6	1.1	1.4	1.3
Isoleucine (Ile)	0.2	4.4	3.6	4	-	0.9	0.9	1.9	1.6	2	3.7
Leucine (Leu)	0.7	7.8	5.9	6.9	2.2	1.2	1.6	-	2.3	3	6.2
Lysine (Lys)	0.5	4.7	5.6	5.3	2.2	1.3	1.2	3.7	3.3	2.8	4.1
Hydroxylysine (Hyl)	-	-	2.7	-	-	-	-	-	-	-	-
Methionine (Met)	0.2	1.3	-	3.3	0.5	0.3	0.1	0.2	0.4	0.7	1.3
Phenylalanine (Phe)	0.6	5.7	3.8	4.3	1.1	0.9	1	1.2	1.2	1.7	4
Proline (Pro)	0.6	4.4	4.4	5.6	0.9	0.9	1.5	-	-	-	3.9
Hydroxiproline (Hyp)	-	1	-	-	-	-	-	1.8	1.6	0.9	-
Threonine (Thr)	0.5	4.8	4.7	5.5	1.2	1	0.7	2.7	1.9	2.4	3.6
Valine (Val)	0.3	6.8	6.1	6.2	1.2	1	1.4	2.2	1.9	2.5	-
Alanine (Ala)	1	8.4	6.3	7.5	3	1.2	1.9	0.7	1.5	3.4	7.9
Aspartic acid (Asp)	2	12.5	10.2	12	3.3	2.1	2	5.2	4.1	4.3	8.2
Serine (Ser)	0.8	5.5	5	5.1	1.6	1.2	0.8	5.5	-	5.8	-
References	[140]	[141]	[138]	[138]	[141]	[142]	[143]	[139]	[139]	[139]	[144]

3.4.5. Pigments Content from Seaweeds

Marine algae produce pigments as secondary metabolites, which have significant bioactive properties and diverse applications in the food, pharmaceutical, and cosmetic industries. Extensive research has explored these pigments. Manzoor et al. (2024) demonstrated that marine algal pigments exhibit therapeutic benefits, including anti-cancer, antioxidant, anti-obesity, neuroprotective, anti-inflammatory, and anti-angiogenic activities [146]. Marine algal pigments are classified into three major groups: chlorophylls, carotenoids, and phycobiliproteins.

Chlorophylls are fat-soluble pigments essential for light harvesting, electron transport, and energy transmission in photosynthesis. Their chemical structure consists of a substituted porphyrin ring (acting as a chelating ligand) and a phytol carbon chain. The primary types of chlorophylls in seaweed are chlorophyll a, b, and c. Gomes et al. (2022) identified chlorophyll a ($C_{55}H_{72}MgN_4O_5$) as the most abundant pigment in seaweed, exhibiting antimicrobial potential and a blue-green color with a maximum absorption range of 660–665 nm [147]. Aryee et al. (2018) described chlorophyll b ($C_{55}H_{70}MgN_4O_6$) as the second most important, exclusive to green algae, and appearing green-yellow with an absorption range of 642–652 nm, relevant in food processing [148]. Chlorophyll c, found in brown algae, is a blue-green pigment with an absorption range of 447–452 nm and antimicrobial properties as shown by Gomes et al. (2022) [147]. It has three variants: chlorophyll c 1 ($C_{35}H_{30}MgN_4O_5$, absorption peak at 447 nm), chlorophyll c 2 ($C_{35}H_{28}MgN_4O_5$, absorption peak at 450 nm), and chlorophyll c 3, which is absent in marine algae [147].

Carotenoids, ranging in color from yellow to orange-red, have tetrapenoid structures that aid photosynthesis and are most abundant in brown algae as shown by Pérez-Gálvez et al., 2020 [149]. Manzoor et al. (2024) classified carotenoids into two groups based on molecular structure: xanthophylls (oxygen-containing) and hydrocarbons (carotene-based) [146]. According to Gomes et al. (2022), xanthophylls include fucoxanthin, astaxanthin, lutein, lorxanthin, violaxanthin, neoxanthin, and zeaxanthin, while carotenes lack oxygen atoms [147].

Phycobiliproteins (PBPs) are water-soluble, non-toxic proteins with high physiological stability. They are divided into three groups: phycoerythrins, allophycocyanins, and phycocyanins. Manzoor et al. (2024) found that PBPs constitute up to 60% of the soluble protein in cyanobacterial cells [146]. Cotas et al. (2020) reported that PBP absorption ranges from 450 to 570 nm, with B-phycoerythrin peaking at 499, 546, and 565 nm, C-phycoerythrin at 565 nm, and R-phycoerythrin at 498, 540, and 565 nm [150]. Ghosh et al. (2022) highlighted the importance of phycoerythrins as red-colored functional food ingredients [151]. Manivasagan et al. (2018) described phycocyanin as containing chromophore phycobilins, capturing blue light, and having an absorption range of 610–620 nm, with various therapeutic applications [152].

Regarding pigment extraction, Osório et al. (2020) investigated the separation of chlorophylls, fucoxanthin, and phycobiliproteins using conventional solvent-based extraction from commercial seaweeds, including brown algae (*Himanthalia elongata*, *Undaria pinnatifida*, *Laminaria ochroleuca*) and red algae (*Porphyra* spp.) [153]. The study found that extraction efficiency varied by solvent, with acetone yielding the highest chlorophyll extraction from brown algae, while methanol was most effective for red algae. Notably, *Porphyra* spp. contained significantly higher pigment levels than brown algae [153]. Manzoor et al. (2024) explored various green extraction methods for obtaining pigments from algae, including microwave-assisted extraction (MAE), pressurized liquid extraction (PLE), and supporting their supercritical fluid extraction (SFE) [146]. These techniques offer ecological

benefits such as lower operating temperatures, shorter extraction times, reduced use of chemical solvents, and automation that enhances compound recovery.

Figure 7 illustrates the structures of commonly found seaweed pigments.

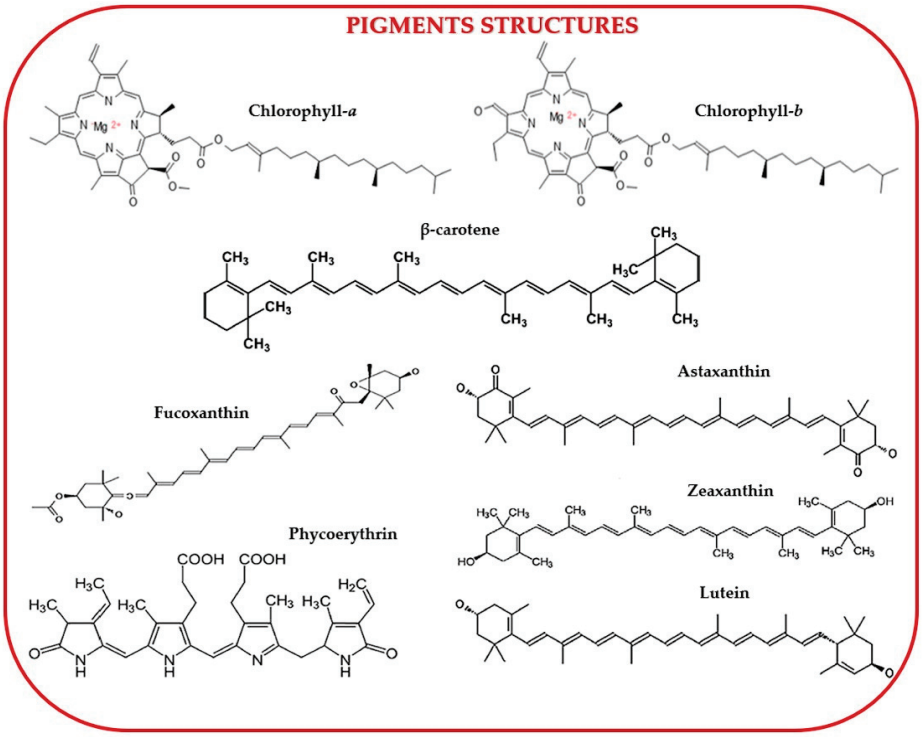

Figure 7. The structure of clorophyll-a, clorophyll-b, β-carotene, fucoxanthin, astaxantin, zeaxanthin, phycoerythtin, and lutein.

Fabrowska et al. (2018) and Martins et al. (2021) successfully extracted chlorophyll from green algae using the MAE method [154,155]. Similarly, Nie et al. (2021) reported the extraction of carotenoid pigments through ultrasound-assisted extraction (UAE) [156]. Carreira-Casais et al. (2021) conducted a comprehensive study on extracting bioactive compounds—including fucoxanthin, chlorophylls, β-carotene, polysaccharides, and phenolic compounds—from food-grade marine algae using UAE [157]. Brain-Isasi et al. (2022) also used UAE to obtain total phycobiliproteins from *Gracilaria chilensis* [158]. Additionally, Ktari et al. (2021) employed SFE to extract fucoxanthin from *Dictyopteris polypodioides* [159]. Another alternative approach, reported by Martinez et al. (2019), involved pulsed electric field (PEF) extraction of carotenoids from *Haematococcus pluvialis* [160]. Despite these advancements, alternative extraction methods remain under development and require further optimization. As Manzoor et al. (2024) highlighted, selecting an appropriate solvent is crucial for maximizing pigment extraction efficiency [146]. Several studies have highlighted the presence of pigments in green algae, emphasizing their role as secondary metabolites. Cadar et al. (2023) identified chlorophyll-α, chlorophyll-b, and total carotenoids in green algae from the Romanian Black Sea coast, specifically *Ulva lactuca*, *Ulva intestinalis*, and *Cladophora vagabunda*, supporting their antioxidant activity [49]. The total chlorophyll and total carotenoid content in algae have been widely studied by researchers such as Sirbu et al. (2020), Choudhary et al. (2023), and Ganesan et al. (2020) [30,53,55].

The identification and quantification of pigments were documented by the respective authors, with results summarized in Table 5, categorizing pigment content across green, red, and brown algae.

Table 5. Pigments content from diffent green, red, and brown marine macroalgae. Units of measurement are indicated in the first line of the table, at the top of each column.

Typ of Algae	Region	Total Clorophyll mg/g; mg/L *; µg/g **	Clorophyll-*a* mg/g; mg/L *; µg/g **	Clorophyll-*b* mg/g; µg/g **	Total Carotenoids mg/g; mg/L *; µg/g **	β-Carotene mg/g; g/100 g *; mg/100 g **; µg/g ***	Fucoxanthin mg/g; mg/100 g *; µg/g **	Astaxanthin mg/100 g	Zeaxanthin mg/100 g; µg/g *	Lutein mg/100 g; mg/g; *; µg/g**	References
Green algae											
Ulva lactuca (as *Ulva fasciata*)	Black Sea, Romanian coast	23.23 ± 0.67	19.16 ± 2.69	4.07 ± 0.36	9.97 ± 0.85	-	-	-	-	-	[30]
Ulva lactuca (as *Ulva fasciata*)	Black Sea, Romanian coast	35.37 ± 1.7	26.95 ± 1.5	8.42 ± 1.56	16.25 ± 1.3	-	-	-	-	-	[49]
Ulva lactuca (as *Ulva fasciata*)	Saurashtra Coast, India	14.00 ± 0.11 *	8.16 ± 2.69 *	4.97 ± 0.85	0.80 ± 0.02 *	-	-	-	-	-	[53]
Ulva fasciata	Indian waters	3.49 ± 0.62	2.09 ± 0.15	1.4 ± 0.46	0.60 ± 0.06	0.37 ± 0.02	-	-	-	-	[55]
Ulva fasciata	Coastal area of Philippines	6.82	2.18 ± 0.74	4.64 ± 0.6	-	0.72 ± 0.00	-	-	-	-	[161]
Ulva intestinalis	Black Sea, Romanian coast	20.97 ± 1.67	16.74 ± 1.65	4.25 ± 0.45	12.73 ± 1.32	-	-	-	-	-	[30]
Ulva intestinalis	Black Sea, Romanian coast	30.51 ± 1.82	23.56 ± 1.88	6.95 ± 1.6	15.98 ± 1.98	-	-	-	-	-	[49]
Ulva flexuosa	Indian waters	3.14 ± 0.09	1.90 ± 0.25	1.24 ± 0.06	0.49 ± 0.12	0.32 ± 0.04	-	-	-	-	[55]
Cladophora vagabunda	Black Sea, Romanian coast	43.67 ± 1.97	24.13 ± 2.57	19.54 ± 1.55	13.90 ± 0.42	-	-	-	-	-	[30]
Cladophora vagabunda	Black Sea, Romanian coast	41.64 ± 1.52	29.25 ± 1.56	12.39 ± 1.35	17.66 ± 1.56	-	-	-	-	-	[49]
Acrosiphonia orientalis	Saurashtra Coast, India	7.00 ± 0.05 *	-	-	11.00 ± 0.01 *	-	-	-	-	-	[53]
Caulerpa scalpelliformis	Saurashtra Coast, India	3.00 ± 0.05 *	-	-	8.00 ± 0.01 *	-	-	-	-	-	[53]
Caulerpa racemosa	Coastal area of Philippines	123.58	42.15 ± 0.21	81.42 ± 0.24	-	17.26 ± 1.88	-	-	-	-	[161]
Caulerpa racemosa	Indian waters	21.09 ± 0.60	10.14 ± 0.13	11.12 ± 0.57	11.45 ± 0.59	-	-	-	-	-	[162]
Caulerpa racemosa	Indonesian Coast	-	-	-	-	20.50 ± 0.10 *	1.40 ± 0.01 *	4.60 ± 0.10	4.70 ± 0.01	1.50 ± 0.50	[163]
Caulerpa lentillifera	Malaysian waters	7.29	3.32	3.97	63.47	10.7	-	-	21.30 *	21.13 **	[164]
Chlorococcum infusionum (as *Chlorococcum humicola*) (green microalga)	Thailand Coast	10.01 ± 0.13	5.90 ± 0.15	4.11 ± 0.03	2.01 ± 0.16	-	-	-	-	0.59 ± 0.12	[165]
Red algae											
Scinaia carnosa	Saurashtra Coast, India	1.50 ± 0.01 *	-	-	0.70 ± 0.01 *	-	-	-	-	-	[53]
Halymenia porphyriformis	Saurashtra Coast, India	7.00 ± 0.05 *	-	-	0.20 ± 0.01 *	-	-	-	-	-	[53]
Gracilaria corticata	Indian waters	-	-	-	-	4.13 ± 0.07 ***	6.06 ± 0.05 **	-	0.65 ± 0.04 *	0.26 ± 0.05 **	[166]
Gracilaria corticata	Southeast coast of India	-	8.96 ± 0.39 **	7.74 ± 0.33 **	12.82 ± 0.50 **	-	-	-	-	-	[59]
Eucheuma denticulatum	Malaysian waters	-	-	-	-	4.7 ± 0.1 **	4.0 ± 0.0 *	3.0 ± 0.0	21.3 ± 0.1	87.7 ± 0.1	[167]
Gracilaria edulis	Indian waters	0.79 ± 0.05	0.66 ± 0.26	0.13 ± 0.08	0.13 ± 0.02	0.11 ± 0.02	-	-	-	-	[55]
Gracilaria edulis	Southeast coast of India	-	17.14 ± 0.55 **	8.44 ± 0.63 **	2.99 ± 0.56 **	-	-	-	-	-	[59]
Acanthophora spicifera	Indian waters	1.41 ± 0.62	1.17 ± 0.18	0.24 ± 0.02	0.32 ± 0.12	0.24 ± 0.04	-	-	-	-	[55]
Kappaphycus striatus	Malaysian waters	4.52	3.41	1.1	57.02	7.59	-	-	4.4 *	38.6 **	[164]
Gracilaria tikvahiae	Malaysian waters	2.97	2.55	0.42	25.13	3.05	-	-	4.15 *	8.86 **	[164]
Brown algae											
Laminaria saccharina	Galician coastline from Spain	-	0.67	-	-	0.07	9.54	-	-	-	[16]
Iyengaria stellata	Saurashtra Coast, India	1.50 ± 0.02 *	-	-	0.7 ± 0.01*	-	-	-	-	-	[53]
Sargassum linearifolium	Saurashtra Coast, India	34.00 ± 0.27 *	-	-	3.0 ± 0.1 *	-	-	-	-	-	[53]
Undaria pinnatifida	Galician coastline from Spain	-	1.58	-	-	0.3	6.15	-	-	-	[168]
Padina gymnospora	Indian waters	2.13 ± 0.43	1.75 ± 0.42	0.38 ± 0.04	0.78 ± 0.08	0.48 ± 0.23					[55]
Himanthalia elongate	Atlantic North Coast	168.2 ± 15.0 **	67.6 ± 3.2 **	-	2.9 ± 0.3 **	-	2.79 ± 0.31 **	-	-	-	[153]
Laminaria ochroleuca	Atlantic North Coast	235.3 ± 15.4 **	183.5 ± 14.8 **	14.1 ± 0.5 **	27.0 ± 2.4 **	-	14.21 ± 0.31 **	-	-	-	[153]
Undaria pinnatifida	Atlantic North Coast	574.1 ± 33.2 **	321.3 ± 19.2 **	-	54.6 ± 1.3 **	-	26.81 ± 0.79 **	-	-	-	[153]
Padina pavonica	Malaysian water	7.51	3.4	-	100.89	9.14	-	-	10.87 *	7.21 **	[164]

Various species have been analyzed across different marine habitats and time periods to assess pigment composition. For instance, pigment values, including total chlorophyll, chlorophyll-a, chlorophyll-b, total carotenoids, and β-carotene, were reported for *Ulva lactuca* (formerly *Ulva fascinata*) from Indian waters and the coastal areas of the Philippines by Ganesan et al. (2020) and Magdugo et al. (2020) [55,161]. Similarly, pigment data for *Ulva intestinalis* from the Black Sea (Romanian coast) and Indian waters were documented by Sirbu et al. (2020) and Cadar et al. (2023) [30,49]. Additionally, *Ulva flexuosa* was studied by Ganesan et al. (2020) for the same pigment types [55]. Choudhary et al. (2023) reported pigment data, including total chlorophyll, chlorophyll-a, chlorophyll-b, total carotenoids, and β-carotene, for *Acrosiphonia orientalis* and *Caulerpa scalpelliformis* from the Saurashtra coast [53]. Magdugo et al. (2020) and Palaniyappan et al. (2023) examined *Caulerpa racemosa* from the coastal areas of the Philippines and Indian waters, respectively, documenting its pigment composition [161,162]. Kurniawan et al. (2023) identified additional pigments in *Caulerpa racemosa* from the Indonesian coast, including a high quantity of β-carotene (20.5 mg/g) alongside smaller amounts of fucoxanthin, astaxanthin, zeaxanthin, and lutein [163]. Other studies also reported pigment data from different algae species. Othman et al. (2018) analyzed *Caulerpa lentillifera* from Malaysian waters, and reported values for total chlorophyll, chlorophyll-a, chlorophyll-b, total carotenoids, β-carotene, zeaxanthin, and lutein [164]. Similarly, Babadi et al. (2020) reported total chlorophyll, chlorophyll-a, chlorophyll-b, total carotenoids, and lutein in *Chlorococcum infusionum* (formerly *Chlorococcum humicola*) (green microalga) from the Thai coast [165]. Among green algae, *Caulerpa racemosa* from the Philippines showed the highest total chlorophyll content (123.58 mg/g) according to Magdugo et al. (2020) [161]. The highest total carotenoid content (63.47 mg/g) was found in *Caulerpa lentillifera* (Chlorophyta), followed by *Kappaphycus striatum* (Rhodophyta) (57.02 mg/g) from Malaysian waters, as reported by Othman et al. (2018) [164].

Regarding red algae, Bhat et al. (2021) extracted carotenoids from *Gracilaria corticata*, while Balasubramaniam et al. (2020) identified β-carotene, fucoxanthin, astaxanthin, zeaxanthin, and lutein in eucheuma denticulatum from Malaysian waters [166,167]. The lowest total carotenoid content was reported in *Gracilaria edulis* (0.13 ± 0.02 mg/g) by Ganesan et al. (2020), while the highest was found in *Kappaphycus striatus* (57.02 mg/g) as shown by Othman et al. (2018) [55,164]. In brown algae, fucoxanthin is the dominant pigment alongside chlorophylls and β-carotene. The highest fucoxanthin content was found in *Saccharina latissima* (formerly *Laminaria saccharina*) (Phaeophyceae) (9.54 mg/g), followed by *Undaria pinnatifida* (6.15 mg/g) from the Galician coast of Spain, as reported by Lourenço-Lopes et al. (2022) [168]. Othman et al. (2018) studied *Padina pavonica* and found significant levels of total carotenoids (100.89 mg/g) along with zeaxanthin and lutein [164]. Osório et al. (2020) analyzed pigments in brown algae from the Atlantic North Coast, including *Himanthalia elongata*, *Laminaria ochroleuca*, and *Undaria pinnatifida*, though fucoxanthin levels varied between 2.79 μg/g and 26.8 μg/g [153]. Lastly, Negreanu-Pîrjol et al. (2020) examined chlorophyll pigment content in algae harvested from the Romanian coast of the Black Sea and correlated these findings with antioxidant activity [169].

3.4.6. Polyphenols from Seaweeds

Phenolic compounds are secondary metabolites essential for the defense and survival of marine organisms in highly competitive environments. According to Getachew et al. (2020), macroalgae rely on phenolic compounds in their metabolic pathways to protect against environmental stress and biological threats, including against UV radiation, herbivory, and oxidative damage [170]. Jacobsen et al. (2019) identified and characterized

various phenolic compounds in brown, green, and red seaweeds [171]. These marine phenolics exhibit diverse biological activities, such as anti-inflammatory effects, studied by Tenorio-Rodríguez et al. (2019), anti-cancer properties reported by Abdelhamid et al. (2019), and antioxidant and ACE inhibitory activities reported by Vijayan et al. (2018) [172–174].

Extraction of phenolic compounds. Traditionally, phenolic compounds have been extracted from marine sources using organic solvents, with solid–liquid extraction (SLE) being the most common method. The Soxhlet technique employs solvents such as methanol, acetone, ethanol, trichloromethane, ethyl acetate, and water-organic solvent mixtures in various ratios, as reported by Catarino et al. (2019) [175]. However, traditional methods face criticism due to their high solvent consumption, long extraction times, and high temperatures, which can lead to oxidation and hydrolysis of phenolic compounds as reported by Ojha et al. (2020) [176]. To address these limitations, alternative extraction technologies have been explored. Garcia-Vaquero et al. (2020) reviewed enzyme-assisted extraction (EAE), microwave-assisted extraction (MAE), ultrasound-assisted extraction (UAE), supercritical fluid extraction (SFE), and pressurized solvent extraction (PLE), which utilize novel solvents and milder conditions [177]. They also discussed less conventional methods like pulsed electric field (PEF)-assisted extraction and ohmic heating, which generate heat through electric currents, as well as combined extraction techniques [177]. Several studies have demonstrated the effectiveness of these methods. Habeebullah et al. (2020) used EAE to extract phenolic compounds from *Sargassum boveanum*, *Sargassum angustifolium*, and *Feldmannia irregularis* (Phaeophyceae), highlighting their antioxidant and antimicrobial properties [178]. Abdelhamid et al. (2019) used MAE on *Ericaria sedoides* (formerly *Cystoseira sedoides*) (Phaeophyceae), demonstrating anti-cancer effects, while Dang et al. (2018) applied MAE to *Sargassum vestitumsi*, and reported their antioxidant activity [173,179]. UAE was employed by Dang et al. (2018) to extract phenolics from *Hormosira banksia* (Phaeophyceae), showing antioxidant potential [179]. Týskiewicz et al. (2018) conducted an in-depth analysis of the SFE method for plant-derived phenolics, and Gallego et al. (2019) provided insights into subcritical and supercritical fluid extraction for bioactive compounds from plants, seaweeds, and microalgae [180,181]. Pangestuti et al. (2019) investigated subcritical water extraction for functional materials from the tropical red seaweed *Hypnea musciformis* (Rhodophyta) [182]. Another promising method is pressurized liquid extraction (PLE). Otero et al. (2019) demonstrated its effectiveness for extracting bioactive fatty acids and phenols from *Laminaria ochroleuca* [183]. These advancements in extraction technologies offer more sustainable and efficient approaches to harnessing the bioactive potential of marine phenolic compounds. Getachew et al. (2020) showed that the most frequently reported phenolic compounds are simple phenolic components such as gallic acid, epicatechin, epigallocatechin, and flavonoids such as myricetin, quercetin, and rutin, which are presented in [170]. Choudhary et al. (2023) reported TFC and TPC for representative algae from all three categories: green (*Ulva lactuca*, *Acrosiphonia orientalis*, and *Caulerpa scalpelliformis*), red (*Scinaia carnosa* and *Halymenia porphyriformis*), and brown (*Sargassum linearifolium* and *Iyengaria stellata*) from the Arabian Sea [53].

For green algae, TPC and TFC values have been documented by various studies. Sirbu et al. (2020) provided data for *Cladophora vagabunda*, while Cadar et al. (2023) examined *Ulva lactuca*, *Enteromorpha intestinalis*, and *Cladophora vagabunda* [30,49]. Gentscheva et al. (2022) reported TPC and TFC values for *Ulva intestinalis*, while Wekre et al. (2019) and Dimova et al. (2019) analyzed TPC and TFC content for *Ulva rigida* [184–186]. Haq et al. (2019) presented TPC and TFC content for *Chaetomorpha* sp. [187]. Additionally, Sanger et al. (2019) reported TPC values for *Halimeda macroloba* [188]. Notably, Cadar et al. (2023) found the highest TPC (416.6 $\pm$ 1.56 mg GAE/100 g d.w.) and TFC (15.6 $\pm$ 1.65 mg QE/100 g

d.w.) in *Ulva lactuca* harvested from the Black Sea, Romania [49]. The chemical structures of phenolic and flavonoid compounds are shown in Figure 8.

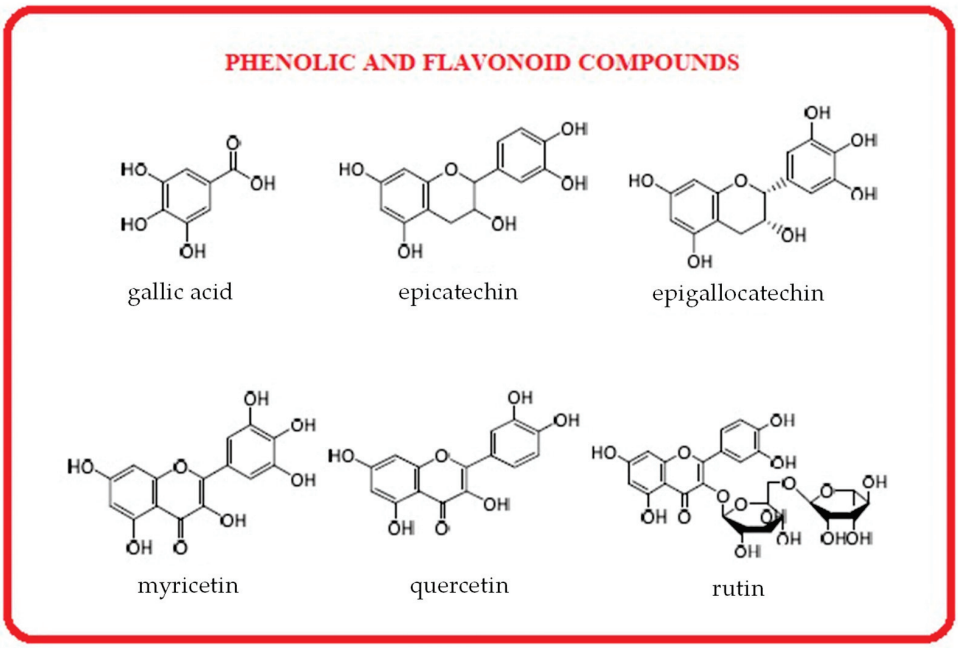

Figure 8. Chemical structures of some seaweed phenolic and flavonoid compounds.

For red algae, several studies have reported TPC and TFC values. Sasadara et al. (2021) examined *Gracilaria* sp. (Bulung sangu), while Sobuj et al. (2021) analyzed *Hypnea pannosa* [189,190]. El Shafay et al. (2021) raported TPC and TFC values for *Jania rubens* and *Ellisolandia elongata* (formerly *Corallina elongata*) (Rhodophyta) and Hmani et al. (2021) for *Gracilaria gracilis* and *Asparagopsis armata* [191,192]. Studies by Farghl et al. (2021) reported TFC and TPC values for red algae *Laurencia obtusa* and *Chondrus crispus* from the Red Sea Coast [60]. Other studies by Nursid et al. (2020) for Gracilaria verrucosa, Gunathilaka et al. (2019) for Gracilaria edulis and Siangu et al. (2019) for Eucheuma denticulatum have highlighted the content of TPC and TFC polyphenols [193–195].

The highest TPC (176.7 ± 6.9 mg GAE/g d.w.) and TFC (173.7 ± 6.8 mg QE/g d.w.) were recorded in *Jania rubens*, as demonstrated by El Shafay et al. (2021) [191]. For brown algae, the phenolic content (TPC) was reported by by Praiboon et al. (2018) for the brown algae *Sargassum oligocystum*, by Fouda et al. (2019) for the algae *Sargassum aspirofolium* and Cadar et al. (2019) for the brown algae *Cystoseira barbata*, [61,63,196]. Iylias et al. (2023) reported TPC and TFC values for *Himanthalia elongata*, [62]. Table 6 summarizes the TPC and TFC values for representative macroalgae across all three categories—green, red, and brown algae.

Gentscheva et al. (2022) reported TPC and TFC values for the algae *Ericaria crinita* [184]. Sobuj et al. (2021) identified TPC and TFC values in *Sargassum corrifolium*, and El Shafay et al. (2021) reported results for polyphenols analyzed in *Taoria atomaria* and *Padina pavonica* [190,191]. Additionally, Subbiah et al. (2023) reported TPC and TFC values for Phyllospora comosa and *Ecklonia radiata*, while Abdelhamid et al. (2018) studied polyphenols from *Cladostephus spongiosum* that support antioxidant, anti-inflammatory, and antinociceptive potential [197,198]. The highest TPC content was reported by Cadar et al. (2019) for *Cystoseira barbata* collected from the Black Sea coast [196]. Overall, all studies confirm the presence of phenolic compounds in marine algae.

Table 6. Phenols content from green, red, and brown seaweeds. Units of measurements are indicated in the first column of the table.

Green algae													
Algae	***Ulva lactuca***	***Ulva lactuca***	***Ulva intestinalis***	***Ulva intestinalis***	***Ulva intestinalis***	***Ulva rigida***	***Chaetomorpha linum***	***Chaetomorpha* sp.**	***Halimeda macroloba***	***Cladophora vagabunda***	***Cladophora vagabunda***	***Caulerpa scalpelliformis***	***Acrosiphonia orientalis***
Region	Black Sea Romania	Arabian Sea	Black Sea	Black Sea Bulgaria	Western coast of Norway	Black Sea Bulgaria	Black Sea Coast Bulgaria	Arabian Gulf	Indonesian waters	Black Sea Romania	Black Sea Romania	Arabian Sea	Arabian Sea
TFC mg CE /100 g d.w. * mg QE/g d.w. **	15.6 ± 1.65 *	56 ± 9 **	13.1 ± 1.68 *	-	-	-	-	189.14 ± 0.99 **	-	-	12.3 ± 1.78 *	25.0 ± 5.0 **	277 ± 3.0 **
TPC mg GAE/100 g d.w. * mg GAE/g d.w. ** µgGAE/g d.w. ***	416.6 ± 1.56 *	285.5 ± 0.6 **	412.5 ± 1.26 *	512.8 ± 23.5 *	11.3 ± 1.4 **	32.80 ± 2.16 ***	403.9 ± 16.4 *	21.92 ± 0.43 **	186.80 ± 15.54 ***	356.8 ± 0.3 *	409.8 ± 1.68 *	26.0 ± 1.0 *	107 ± 1.0 **
References	[49]	[53]	[49]	[184]	[185]	[186]	[184]	[187]	[188]	[30]	[49]	[53]	[53]
Red algae													
Algae	***Scinaia carnosa***	***Halymenia porphyri-formis***	***Laurencia obtusa***	***Gracilaria* sp.**	***Hypnea pannosa***	***Jania rubens***	***Ellisolandia elongata***	***Gracilaria gracilis***	***Asparagopsis armata***	***Chondrus crispus***	***Gracilaria verrucosa***	***Gracilaria edulis***	***Eucheuma denticulatum***
Region	Arabian Sea	Arabian Sea	Red Sea Coast	Bali Coast	Saint Martin Island, Bangladesh	Egyptian waters	Egyptian waters	North coast of Tunisia	North coast of Tunisia	Red Sea Coast	Kupang, East Nusa Tenggara	Northwestern coast of Sri Lanka	Kenyan South Coast
TF C mgQE/g d.w. * mgCE/ g d.w. ** µg/g ***	95.0 ± 1.5 *	18.0 ± 1.0 *	4.78 ± 0.05 **	45.933 ± 0.56 *	43.12 ± 0.98 *	173.7 ± 6.8 *	69.7 ± 2.5 *	-	464 ± 0.63 **	202.66 ± 3.05 ***	-	541.02 ± 51.84 ***	9.36 ± 0.12 *
TPC mg. GAE/g d.w. * µgGAE/g d.w. **	31.0 ± 1.0 *	10.0 ± 1.0 *	7.83 ± 0.14 *	36.273 ± 0.2 *	89.89 ± 1.13 *	176.7 ± 6.9 *	22.9 ± 3.8 *	19.29 ± 1.8 *	14.95 ± 0.5 *	12.38 ± 2.31 **	11.27 *	1007.81 ± 54.21 **	146.15 ± 1.11 *
References	[53]	[53]	[60]	[189]	[190]	[191]	[191]	[192]	[192]	[193]	[194]	[195]	[196]
Brown algae													
Algae	***Gongolaria barbata* (as *C. barbata*)**	***Iyengaria stellata***	***Sargassum linearifolium***	***Sargassum oligocystum***	***Himanthalia elongata***	***Sargassum asperifolium***	***Ericaria crinita***	***S. odonto-carpum* (as *S.coriifolium*)**	***Padina pavonica***	***Taoria atomaria***	***Phyllospora comosa***	***Ecklonia radiata***	***Cladostephus spongiosum***
Region	Black Sea	Arabian Sea	Arabian Sea	Indo-West Pacific Ocean area	North-eastern Atlantic Ocean	Red Sea at Hurghada Coast	Black Sea Coast Bulgaria	Saint Martin Island, Bangladesh	Egyptian waters	Egyptian waters	Australian Beach Coast	Australian Beach Coast	Mediterranean waters, Tunisia coast
TFC mg CE/g d.w. *	-	39 ± 4.0 *	200 ± 18.0 *	-	31.9 ± 2.65 *	-	-	58.29 ± 1.19 *	206.7 ± 4.7 *	374.1 ± 27.41 *	0.22 ± 0.01 *	0.03 ± 0.01 *	-
TPC mg. GAE/100 g d.w. * ppm **	358.6 ± 1.85 *	61 ± 1.0 *	61 ± 2.0 *	1.55 ± 0.11 *	52.7 ± 1.93 *	141.9 **	2662.4 ± 54.2 *	128.56 ± 0.59 *	152.5 ± 8.8 *	157.3 ± 5.9 *	3.01 ± 0.15 *	0.52 ± 0.05 *	10.91 *
References	[196]	[53]	[53]	[61]	[62]	[63]	[184]	[190]	[191]	[191]	[197]	[197]	[198]

3.4.7. Vitamins from Marine Macroalgae

Macroalgae are potential sources of vitamins. Bekah et al. (2023) highlighted that the global ocean provides abundant seaweeds rich in essential nutrients, particularly vitamins and minerals, which are crucial for human consumption in both water-soluble and fat-soluble forms [199]. Among the most prevalent water-soluble vitamins in seaweeds are vitamin C (ascorbic acid), B1 (thiamine), B2 (riboflavin), B3 (niacin), and B12 (cobalamin) as Lovander et al. (2018) reported [200]. Fat-soluble vitamins, such as A and E, have also been identified. Various extraction methods have been reported, such as: alcoholic and water extracts for green algae reported by Cadar et al. (2023) and soluble acid and enzymatic hydrolysis for brown algae reported by Ilyas et al. (2023) [49,62]. The determination of vitamins follows official AOAC/2019 regulations [201].

Figure 9 illustrates the structures of the most common vitamins found in marine macroalgae.

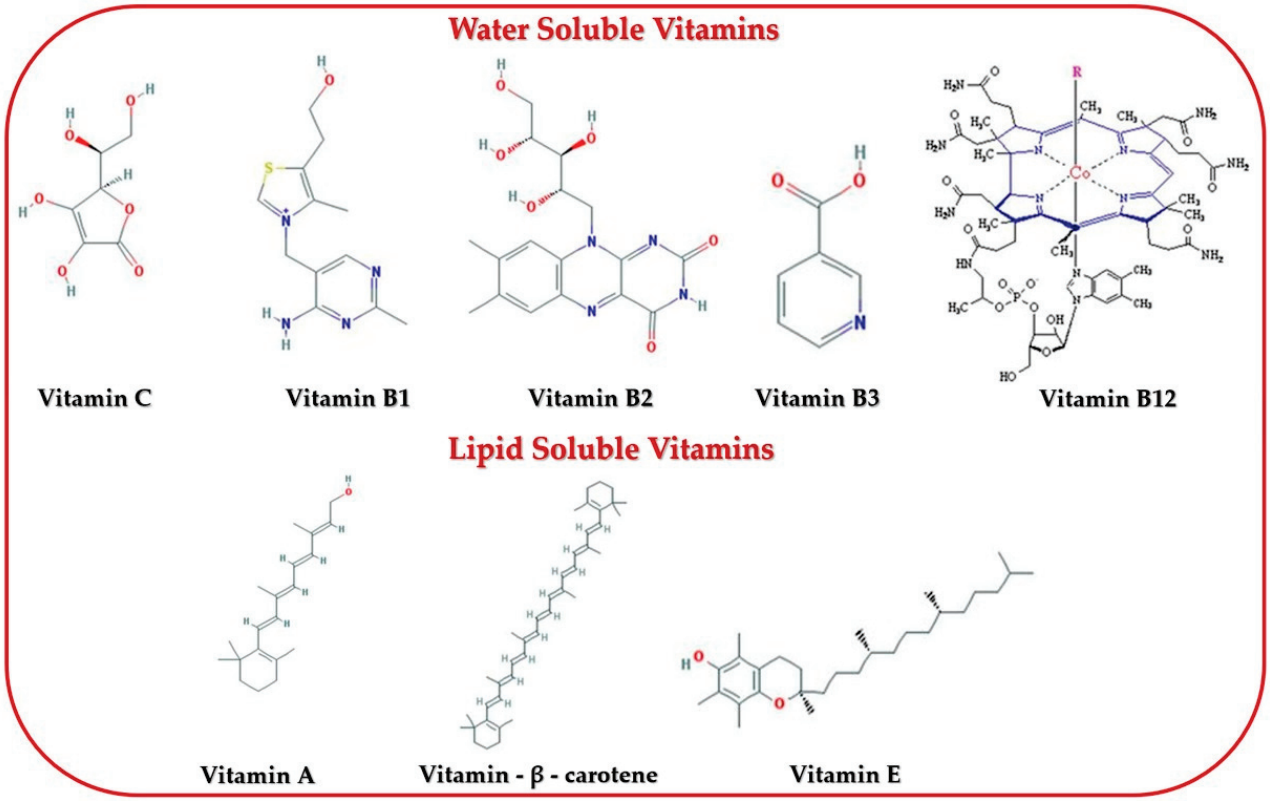

Figure 9. Chemical structure of the most common vitamins in seaweeds.

The following quantification techniques are highlighted as techniques for determining vitamins: UV-Vis spectrophotometry, HPLC, fluorimetry, chemiluminescence, capillary electrophoresis, and microbiology [49,62,201]. Table 7 presents values for the most representative vitamins identified in the composition of seaweeds. The analysis of the values reported for the vitamin content highlighted the existence of significant amounts of vitamin C, followed by vitamin E in almost all the seaweeds presented.

Additionally, Susanti et al. (2020) explored alternative methods, including ultrasonic-assisted extraction (UAE) of vitamin B12 (cobalamin) from the green alga *Ulva lactuca*, comparing it to traditional methods [202]. Chandra-Hioe et al. (2020) further contributed to improving UAE efficiency by implementing measures to protect cyanocobalamin from thermal degradation during extraction [203].

Bekah et al. (2023) showed the highest content of vitamin C for *Udotea argentea* harvested from the Mauritio coast as well as significant quantities for vitamins B1 and B3 [199]. High vitamin C percentages were also reported by Cadar et al. (2023) for the green alga *Cladophora vagabunda* (149.66 ± 0.58 mg/100 g. d.w.) and Metin et al. (2018) for the alga *Ulva intestinalis* (147 ± 2.00 mg/100 g. d.w.) [49,56]. Pereira et al. (2021) provided data on the fat-soluble and water-soluble vitamin content of the green alga *Ulva lactuca*, identifying vitamin B2 (0.533 mg/100 g d.w.) as the most abundant among the vitamins analyzed [204]. Several studies have also reported the vitamin composition in different algal species. Sirbu et al. (2020) and Cadar et al. (2023) analyzed the presence of vitamins A, C, E, B1, B2, and B3 in *Cladophora vagabunda*, while Morais et al. (2020) examined *Ulva rigida* for their vitamin content [30,49,54]. Ganesan et al. (2020) reported the existence of vitamins C, B2, and B3 in the composition of the green algae *Ulva lactuca* (as *Ulva fascinata)* and *Ulva flexuosa* harvested from Indian waters and vitamins A, C, E, B1, B2, and B3 were reported by Metin et al. (2018) for the algae *Ulva intestinalis* from Gulf of Gökova of Aegean Sea [55,56]. Morais et al. (2020) also documented the vitamin composition of the red algae *Palmaria palmata* and *Porphyra umbilicalis* in the Atlantic Ocean [54].

Further studies by Ganesan et al. (2020) identified vitamins C, B2, and B3 in *Gracilaria edulis* from Indian waters, while Cadar (2017) reported the vitamin content in *Ceramium virgatum* from the Black Sea [55,57]. Rosemary et al. (2019) provided data on vitamins A, C, E, B1, B2, and B3 in the red algae *Gracilaria eludis* and *Gracilaria corticata* [59]. Bekah et al. (2023) highlighted the presence of vitamins B1 and B12 in *Gracilaria corticata* from the Mauritius coast [199]. Pereira et al. (2021) also reported the vitamin content in *Chondrus crispus* from the Spanish coast [204]. Sultana et al. (2013) confirmed both fat-soluble and water-soluble vitamins in *Porphyra umbilicalis* [205]. Ryzhik et al. (2021) identified only vitamins B3 and B12 in *Palmaria palmata* from the Barents Sea [206].

Overall, red algae are rich sources of vitamins C and A. The vitamin content of brown algae has also been extensively studied. Morais et al. (2020) reported vitamins in several species from the Atlantic Ocean: *Fucus vesiculosus* (A, C, B1, B2), *Laminaria digitata* (C, E, B1, B2, B3), and *Undaria pinnatifida* (A, C, E, B1, B2, B3) [54]. Ganesan et al. (2020) identified vitamins C, B2, and B3 in *Padina gymnospora* [55]. Cadar (2017) reported vitamins C, E, B1, B2, and B3 in *Cystoseira barbata* from the Romanian Black Sea coast [57]. Ilyas et al. (2023) reported vitamins E, B1, and B2 in *Himanthalia elongata* from the North-Eastern Atlantic Ocean [62]. Bekah et al. (2023) analyzed seaweeds from the Mauritius coast, detecting vitamins B1, B2, and B3 in *Sargassum obovatum* and vitamins B1, B2, and B12 in *Padina boryana* [199]. Pereira et al. (2021) also found vitamins A, C, E, B1, and B2 in *Himanthalia elongata* from the Spanish coast [204]. Sultana et al. (2013) identified vitamins C, E, B1, B2, and B12 in *Ascophyllum nodosum* from the Irish coast [205]. In conclusion, brown seaweeds contain significant levels of vitamins C and E. Given their high vitamin content, seaweeds have potential applications as nutraceuticals and functional ingredients, contributing to their roles as antioxidants, antimicrobials, and growth factors. Furthermore, Dragomir et al. (2024) studied the impact of vitamins for pregnant women with implications on the health of the newborn for the prenatal phase and important consequences for the human body [207].

Table 7. Vitamin content from green, red, and brown seaweeds. Units of measurements are indicated in the first column of the table.

Green algae										
Seaweed species	*Cladophora vagabunda*	*Cladophora vagabunda*	*Ulva lactuca*	*Ulva lactuca*	*Ulva rigida*	*Ulva fasciata*	*Ulva intestinalis*	*Ulva flexuosa*	*Ulva intestinalis*	*Udotea argentea*
Region	Black Sea	Black Sea	Black Sea	Ireland coast	Atlantic waters	Indian waters	Black Sea	Indian waters	Gulf of Gökova of Aegean Sea	Mauritius coast
Vitamin Content										
Vitamin A; mg/100 g d.w.	0.151 ± 1.83	0.58 ± 0.03	0.57 ± 0.06	0.017	9581	-	0.49 ± 0.05	-	0.081 ± 1.54	-
Vitamin C; mg/100 g d.w.	89.665 ± 2.58	149.66 ± 0.58	146.63 ± 0.95	0.242	9.42	0.38 ± 0.04	136.16 ± 0.85	0.36 ± 0.02	147 ± 2.00	435
Vitamin E; mg/100 g d.w.	8.132 ± 1.03	8.54 ± 0.63	8.22 ± 0.11	0.024	19.70	-	9.93 ± 0.83	-	5.13 ± 1.03	-
Vitamin B1; mg/100 g d.w.	0.153 ± 0.02	4.16 ± 0.25	3.72 ± 0.25	-	0.47	-	3.95 ± 0.52	-	0.17 ± 0.1	48.3
Vitamin B2; mg/100 g d.w.	0.893 ± 0.16	0.89 ± 0.06	0.99 ± 0.07	0.533	0.199	0.32 ± 0.29	0.97 ± 0.02	0.26 ± 0.32	0.89 ± 0.02	-
Vitamin B3; mg/100 g d.w.; ppm *	2.495 ± 0.19	2.59 ± 0.32	2.97 ± 0.28	98 *	0.5	1.02 ± 0.41	1.84 ± 0.45	0.92 ± 0.48	2.42 ± 0.09	32.8
References	[30]	[49]	[49]	[204]	[54]	[55]	[49]	[55]	[56]	[199]
Red algae										
Seaweed species	*Palmaria palmata*	*Porphyra umbilicalis*	*Gracilaria edulis*	*Ceramium virgatum*	*Gracilaria cortica*	*Gracilaria edulis*	*Gracilaria corticata*	*Chondruscrispus*	*Porphyra umbilicalis*	*Palmaria palmata*
Region	Atlantic waters	Atlantic waters	Indian waters	Black sea	Southeast coast of India	Southeast coast of India	Mauritius coast	Spanish coast	Ireland coast	Barents Sea
Vitamin Content										
Vitamin A; mg/100 g d.w. *; mg/g **	1.59 *	3.65 *	-	-	2.67 ± 0.30 **	2.07 ± 0.06 **	-	0.1 *	3.65 *	-
Vitamin C; mg/100 g d.w. *; mg/g **; ppm ***	6.34–34.5 *	4.214 *	0.25 ± 0.06 *	50.0 ± 0.5 *	14.66 ± 0.23 **	13.41 ± 0.57 **	-	10 ***	12.885 *	-
Vitamin E; mg/100 g d.w.; mg/g **	2.2–13.9	-	-	250 ± 1.1	1.40 ± 0.10 **	1.49 ± 0.10 **	-	-	0.114	-
Vitamin B1; mg/100 g d.w.; mg/g **	0.073–1.56	0.144	-	4.2 ± 0.3	0.38 ± 0.02 **	0.36 ± 0.02 **	23.3	0.1	0.077	-
Vitamin B2; mg/100 g d.w.; mg/g **; µg/100 g ***	0.51–1.91	0.36	0.12 ± 0.15	6.6 ± 0.4	0.05 ± 0.01 **	1.54 ± 0.07 **	-	2.5	0.274	35.38 ± 2.22 ***
Vitamin B3; mg/100 g d.w.; mg/g **; µg/100 g ***	1.89	-	0.52 ± 0.28	15.0 ± 0.6	1.54 ± 0.39 **	1.10 ± 0.29 **	-	3.2	0.761	18.6 ± 1.10 ***
Vitamin B12; mg/100 g d.w.; ppm **; µg/100 g ***	-	-	-	-	-	-	26.9	0.6 **	0.769 ***	-
References	[54]	[54]	[55]	[57]	[59]	[59]	[199]	[204]	[205]	[206]
Brown algae										
Seaweed species	*Fucus vesiculosus*	*Laminaria digitata*	*Undariapinnatifida*	*Padina gymnospora*	*Gongolaria barbata*	*Himanthalia elongata*	*Sargassum obovatum*	*Padina boryana*	*Himanthalia elongata*	*Ascophyllum nodosum*
Region	Atlantic waters	Atlantic waters	Atlantic waters	Indian waters	Black sea	North-Eastern Atlantic Ocean	Mauritius coast	Mauritius coast	Spanish coast	Ireland coast
Vitamin Content										
Vitamin A; mg/100 g d.w.	0.30–7	-	0.04–0.22	-	-	-	-	-	0.079	-
Vitamin C; mg/100 g d.w.	14.124	35.5	5.29	0.29 ± 0.02	22.0 ± 1.2	-	-	-	28.56	0.654
Vitamin E; mg/100 g d.w.; µg/g d.w. *	-	3.43	1.4–2.5	-	120 ± 1.9	33.3 ± 4.2 *	-	-	5.8	0.029
Vitamin B1; mg/100 g d.w.; g/g d.w. **	0.02	1.250	0.17–0.30	-	2.3 ± 0.5	0.14 ± 0.02 **	56.8	8.87	0.020	0.216
Vitamin B2; mg/100 g d.w.; g/g d.w. **	0.035	0.138	0.23–1.4	0.08 ± 0.18	5.5 ± 0.8	1.14 ± 0.14 **	3.27	1.67	0.020	0.058-
Vitamin B3; mg/100 g d.w.	-	61.2	2.56	0.34 ± 0.16	22.0 ± 0.9	-	17.3	-	-	-
Vitamin B12; mg/100 g d.w.; µg/100 g d.w. ***	-	-	-	-	-	-	-	24.5	-	1.840 ***
References	[54]	[54]	[54]	[55]	[57]	[62]	[199]	[199]	[204]	[205]

3.4.8. Mineral Content of Seaweeds

Minerals are found in the composition of all seaweeds in different percentages. Soares, et al. (2020) showed that there are diverse criteria by which minerals are categorized according to their importance and quantity needed by plants as macronutrients: N, P, K (essential for plants in large amounts), secondary macronutrients: Ca, Mg, S (needed by plants in large doses), micronutrients: Fe, Mn, Zn, Cu, Ni, B, Mo, Cl (vital for plants in small quantities and usually toxic in high concentrations), beneficial minerals: Na, Si, Co, Al, V, Ni, Se, As, F, Br, I, Cd, Cr, Pb (essential for some plants), and potentially toxic elements: Cd, Cr, Pb, Hg, Ni, Se, As (mainly toxic to humans and animals) [208]. Choudhary et al. (2021) reported that seaweed can contain a high mineral content, sometimes comprising up to 40% of its biomass. This is due to seaweed's ability to absorb metal ions from salt water and store them as carbonate salts [66]. Several studies, including those by Choudhary et al. (2023), de Morais et al. (2020), and Ganesan et al. (2020), have highlighted that seaweed contains significant amounts of minerals such as Na, K, Ca, and Mg, while other minerals are present in trace amounts [53–55]. Both conventional and modern extraction methods have been used to analyze seaweed minerals. Soares et al. (2020) employed subcritical water extraction (SWE) for extracting minerals from the brown algae *Saccorhiza polyschides*, with mineral composition analyzed via inductively coupled plasma mass spectrometry (ICP-MS) [208]. Other researchers, including Amlani et al. (2022), Choudhary et al. (2023), and Adamassu et al. (2018), have reported the use of Atomic Absorption Spectroscopy (AAS) for mineral analysis [50,53,209]. Specifically for iodine content, Choudhary et al. (2023) identified ion chromatography (IC) as an analytical method, whereas Ganesan et al. (2020) used AAS [53,61]. Brown seaweeds have the highest iodine content, while red and green seaweeds contain lower levels. Choudhary et al. (2021) further noted that seaweeds contain higher iodine levels than terrestrial plants, making them a viable dietary alternative for meeting iodine requirements compared to plant- and animal-based foods [66]. In some seaweed species, iodine concentrations exceed the daily recommended intake of 150 mg/day [66].

Ganesan et al. (2020) also found that the Na:K ratio in seaweed varies by species, ranging from 0.59 to 0.82 [55]. The highest Na content in green algae was recorded by Cadar et al. (2023) in *Ulva intestinalis* (1230.56 ± 1.65 mg/100 g d.w.) [49]. For red algae, de Morais et al. (2017) reported the highest Na concentration in *Palmaria palmata* (1600–2500 mg/100 g d.w.) [54], while in brown algae, Choudhary et al. (2023) recorded the highest Na level in *Iyengaria stellata* (11,000 ± 250 mg/100 g d.w.) [53].

Potassium (K), an essential element for human health, was found in the highest concentration in green algae *Caulerpa scalpelliformis* (9300 ± 250 mg/100 g d.w.) and in brown algae *Iyengaria stellata* (117,000 ± 400 mg/100 g d.w.), as reported by Choudhary et al. (2023) [53]. The highest K content in red algae was reported by de Morais et al. (2020) in *Palmaria palmata* (7000–9000 mg/100 g d.w.) [54].

Calcium (Ca), a secondary macronutrient, was found in the highest concentration in green algae *Ulva lactuca* (1790.35 ± 2.55 mg/100 g d.w.), as identified by Cadar et al. (2023) [49]. The highest Ca content in red algae was recorded in *Laurencia obtusa* (845.35 ± 0.11 mg/100 g d.w.) by Farghl et al. (2021) [60], while in brown algae, Ilyas et al. (2023) reported the highest level in *Himanthalia elongata* (3469 ± 1526 mg/100 g d.w.) [62].

In Table 8 are presented values for the mineral content reported by different authors in the composition of marine seaweeds: green, red, and brown.

Table 8. Mineral content from green, red, and brown seaweed. Units of measurements are indicated in the first column of the table.

Green algae											
Algae	***Ulva lactuca***	***Ulva intestinalis***	***Cladophora vagabunda***	***Caulerpa scalpelliformis***	***Acrosiphonia orientalis***	***Ulva lactuca***	***Ulva rigida***	***Caulerpa lentillifera***	***Ulva lactuca***	***Ulva flexuosa***	***Ulva intestinalis***
Region	Black Sea	Black Sea	Black Sea	Arabian Sea	Arabian Sea	Arabian Sea	Atlantic waters	Atlantic waters	Indian waters	Indian waters	Gulf Gökova Aegean Sea
Minerals (Inorganic compounds)											
Na, mg/kg d.w.	825 ± 1.6	793.31 ± 1.20	853.15 ± 0.89	600 ± 110	1400 ± 125	2000 ± 100	1595	8917	20.12 ± 0.02	13.2 ± 0.8	-
K, mg/100 g d.w.	1120.54 ± 1.03	1230.56 ± 1.65	985.64 ± 2.03	9300 ± 250	4400 ± 120	3000 ± 220	1561	700–1142	27.2 ± 1.02	22.32 ± 1.08	1052.70
Ca, mg/100 g d.w.	1790.35 ± 2.55	1604.15 ± 2.96	1720.64 ± 2.87	44 ± 7.0	270 ± 30	62 ± 20	524	780–1874	740 ± 0.28	712 ± 0.04	15,977
Mg, mg/100 g d.w.	95.26 ± 1.05	90.87 ± 0.96	93.45 ± 0.91	800 ± 100	1400 ± 100	-	2094	630–1650	420 ± 0.02	436 ± 0.24	90.87 ± 0.96
Fe, mg/100 g d.w.	524.25 ± 0.64	490.36 ± 1.56	565.35 ± 1.05	0.5 ± 0.01	2.0 ± 0.01	0.40 ± 0.01	-	-	47 ± 0.04	40 ± 0.28	338.70
Zn, mg100 g d.w.; µg/100 g d.w. *	21.62 ± 0.65	24.74 ± 0.86	20.26 ± 0.85	2.0 ± 0.01	2.2 ± 0.01	4.00 ± 0.01	-	-	2.34 ± 0.48 *	1.518 ± 0.81 *	-
I (iodine content); mg/100 g); µg/100 g d.w. *	-	-	-	4.0 ± 1.0	15.0 ± 1.0	30 ± 11	-	-	38.89 ± 1.08 *	42.03 ± 1.02 *	-
References	[49]	[49]	[49]	[53]	[53]	[53]	[54]	[54]	[55]	[55]	[56]
Red algae											
Algae	***Scinaia carnosa***	***Halymenia porphyriformis***	***Palmaria palmata***	***Porphyra umbilicalis***	***Acanthophora spicifera***	***Gracilaria edulis***	***Jania pedunculata***	***Gracilaria corticata***	***Gracilaria edulis***	***Gracilaria corticata***	***Laurencia obtusa***
Region	Arabian Sea	Arabian Sea	Atlantic waters	Atlantic waters	Indian waters	Indian waters	Sri Lanka coastal area	Sri Lanka coastal area	Southeast coast of India	Southeast coast of India	Red sea coast
Minerals (Inorganic compounds)											
Na; mg/100 g d.w.	1400 ± 70	2700 ± 30	1600–2500	940	36.08 ± 1.08	32.03 ± 0.28	86.23	67.06	-	-	102.55 ± 0.03
K; mg/100 g d.w.	25.2 ± 2.2	5800 ± 50.0	7000–9000	2030	52.08 ± 0.22	52.12 ± 0.07	121.61	125.82	-	-	870.38 ± 0.13
Ca; mg/100 g d.w.	70.0 ± 10.0	85.0 ± 15.0	560–1200	330	430 ± 0.14	410 ± 0.08	181.64	176.05	-	-	845.35 ± 0.11
Mg; mg/100 g d.w.	4000 ± 80	2200 ± 80	170–610	370	480 ± 1.02	580 ± 0.98	60.02	58.54	8.956 ± 0.77	46.32 ± 8.87	101.2 ± 0.13
Fe; mg/100 g d.w.	-	1.0 ± 0.01	-	-	52 ± 0.24	72 ± 0.24	73.97	49.48	55.736 ± 0.57	107.24 ± 20.9	-
Zn; mg/100 g d.w.; µg/100 g d.w. *	2.2 ± 0.01	3.00 ± 0.01	-	-	4.08 ± 0.28 *	5.21 ± 0.24 *	70.94	8.61	4.273 ± 2.12	3.152 ± 0.69	4.6 ± 0.05
I (iodin content); mg/100 g; µg/100 g d.w. *	2.0 ± 0.2	2.0 ± 0.1	-	-	64.8 ± 0.12 *	72.2 ± 0.08	-	-	-	-	-
References	[53]	[53]	[54]	[54]	[55]	[55]	[58]	[58]	[59]	[59]	[60]
Brown algae											
Algae	***Iyengaria stellata***	***Sargassum linearifolium***	***Fucus vesiculosus***	***Laminaria digitata***	***Saccharina latissima***	***Padina gymnospora***	***Sargassum ilicifolium***	***Sargassum polycystem***	***Himanthalia elongata***	***Sargassum oligocystum***	***Sargassum asperifolium***
Region	Arabian Sea	Arabian Sea	Atlantic waters	Atlantic waters	Atlantic Waters	Indian waters	Sri Lanka coastal area	Sri Lanka coastal area	North-eastern Atlantic area	Indo-West Pacific area	Red Sea Coast
Minerals (Inorganic compounds)											
Na; mg/100 g d.w.	11,000 ± 250	7000 ± 130	2450–5469	3818	2620	36.36 ± 0.18	64.55	80.87	25.805 ± 7924	4.09 ± 0.13	-
K; mg/100 g d.w.	11,700 ± 400	6800 ± 190	2500–4322	11.5–79	4330	30.02 ± 0.17	127.47	127.66	57.480 ± 19.976	38.57 ± 8.57	12
Ca; mg/100 g d.w.	820 ± 35	300 ± 20	725–938	1005	810	820 ± 0.34	198.15	187.43	3469 ± 1526	30.95 ± 1.11	15.200
Mg; mg/100 g d.w.	1700 ± 110	900 ± 75	670–994	659	715	780 ± 0.08	84.73	86.38	3537 ± 1497	6.40 ± 0.13	5.778
Fe; mg/100 g d.w.	6.00 ± 0.12	0.30 ± 0.01	-	-	-	14.8 ± 0.32	48.50	128.46	17.8 ± 3.3	416.95 ± 4.24	0.802
Zn; mg/100 g d.w.; µg/100 g d.w. *;	2.60 ± 1.203	2.5 ± 1.1	-	-	-	4.19 ± 0.08 *	4.58	5.76	21.3 ± 13	21.84 ± 4.04	0.316
I (iodin content); mg100/g; µg/100 g d.w. *;	8.0 ± 1.0	41.0 ± 2.0	-	-	-	46.2 ± 1.03 *	-	-	-	3.79 ± 0.03	-
References	[53]	[53]	[54]	[54]	[54]	[55]	[58]	[58]	[61]	[60]	[63]

For magnesium (Mg), Choudhary et al. (2023) recorded the highest concentration in green algae *Acrosiphonia orientalis* (1400 ± 100 mg/100 g d.w.) and in red algae *Scinaia carnosa* (4000 ± 80 mg/100 g d.w.) [53]. In brown algae, Ilyas et al. (2023) reported the highest Mg content in *Himanthalia elongata* (3537 ± 1497 mg/100 g d.w.) [62]. Cadar et al. (2023) reported the highest iron (Fe) content in green algae, specifically in *Cladophora vagabunda* (565.35 ± 1.05 mg/100 g d.w.) [49]. For red algae, Rosemary identified the highest Fe content in *Gracilaria corticata* (107.24 ± 20.9 mg/100 g d.w.), while Praiboon et al. (2018) recorded the highest Fe level in brown algae, specifically *Sargassum oligocystum* (416.92 ± 4.24 mg/100 g d.w.) [59,61]. The Fe content in seaweeds varies significantly, ranging from the highest value of 565.35 ± 1.05 mg/100 g d.w. (Cadar et al., 2023) to as low as 0.3 ± 0.01 mg/100 g d.w., observed in the brown alga *Sargassum linearifolium* by Choudhary et al. (2023) [49,53]. Ganesan et al. (2020) emphasized that seaweed-derived iron could serve as a complementary and viable source to meet physiological iron requirements, particularly for pregnant women [55]. Regarding zinc (Zn), Ganesan et al. (2020) reported the highest Zn content in green algae, specifically *Ulva flexuosa* (1.518 ± 0.81 µg/100 g d.w.) [55]. In red algae, Premarathana et al. (2022) found the highest Zn content in *Jania adhaereus* (70.94 mg/100 g d.w.), while Praiboon et al. (2018) recorded the highest Zn levels in the brown alga *Sargassum oligocystum* (21.84 ± 4.04 mg/100 g d.w.) [58,61]. Zn content in seaweeds ranges from 1.518 ± 0.81 µg/100 g d.w. in *Ulva flexuosa* (Ganesan et al., 2020) to 70.94 mg/100 g d.w. in *Jania pedunculata* var. *adhaerens* (Premarathana et al., 2022) [55,58]. Choudhary et al. (2023) found that seaweeds contain higher levels of essential microelements such as sodium (Na), potassium (K), calcium (Ca), and magnesium (Mg) compared to terrestrial vegetables like spinach, potatoes, carrots, and tomatoes [53]. Additionally, Premarathana et al. (2022) and Lozano Muñoz et al. (2022) provided comprehensive reports on seaweed nutrition, highlighting the crucial role of minerals in hormone and enzyme synthesis, as well as the importance of trace elements in disease prevention and healing [58,210].

Heavy metals, including mercury (Hg), arsenic (As), cadmium (Cd), lead (Pb), and copper (Cu), have been detected in seaweed compositions. Ganesan et al. (2020) reported Hg levels of 0.031 ppm in *A. specifera* [55]. Arsenic has been detected in several seaweed species, but only in very low concentrations (expressed in ppm). Díaz et al. (2012) reported studies on the arsenic content in different species of seaweeds collected from the Chilean marine coast [211]. They showed that the levels of inorganic arsenic in the studied seaweeds ranged from 0.8% to 13% of the total arsenic concentrations, so the arsenic present in the studied seaweeds is in the form of organic arsenic; in addition, the inorganic arsenic concentrations are relatively low compared to the total arsenic found in seaweeds and do not represent a major health risk to consumers [211]. Pb and Cu have also been identified in various seaweeds. According to Ganesan et al. (2020), regulatory limits for heavy metals in edible seaweeds are established, with Pb restricted to < 0.5 mg/kg d.w., Hg to < 0.1 mg/kg d.w., and inorganic As to < 3 mg/kg d.w. [55]. Studies by Cadar et al. (2019), Ganesan et al. (2020), Lozano Muñoz et al. (2022), and Díaz et al. (2012) confirmed that while heavy metals are present in seaweeds, they remain within the toxicological safety limits established by food safety authorities [9,55,210,211].

4. The Relationship Between the Biological Activities of Biocompounds—Potential Health and Nutraceutical Application

In the context of harnessing the benefits of utilizing biocompounds from natural resources in the treatment of various diseases as compared to traditional chemically synthesized drugs, medical and nutraceutical applications of seaweeds based on the biological

actions of their biocompounds have been considerably increased. Biocompounds in seaweed compositions present important biological actions that have been studied by multiple researchers for different medical and nutraceutical applications, such as those presented by Ahmed N. et al. (2024), Xu et al. (2023), and Silva M. et al. (2024) [212–214].

Figure 10 systematizes the biomedical applications of marine algae biocompounds for treating various conditions.

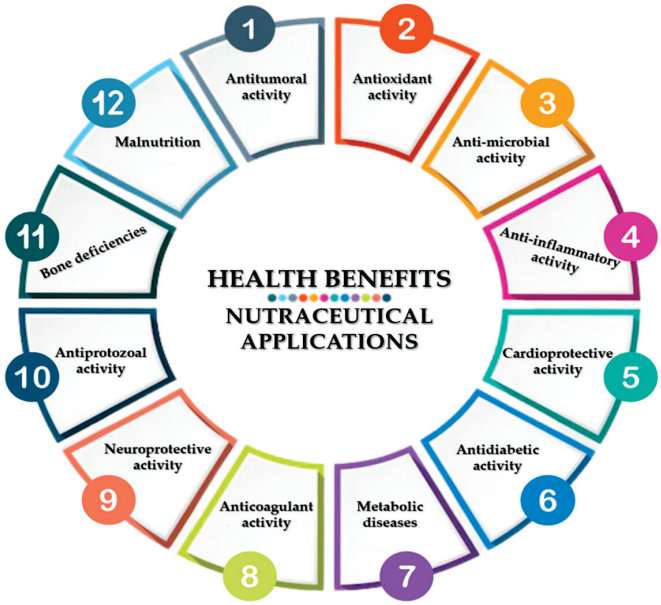

Figure 10. Diseases treated with nutraceuticals containing marine algae biocompounds with various biological activities.

4.1. Antitumoral Activity

Cancer is a major public health problem and the second leading cause of death worldwide after cardiovascular disease as shown by Ouyang et al. (2021) [16]. It is important for health that alternative treatments can be used for certain diseases such as cancer. Antitumor activity has been reported for various active metabolites from seaweed such as polysaccharides, terpenoids, pigments, and polyphenols, as argued by various studies.

Several studies have been reported in which polysaccharides exhibit multiple anticancer activities. Thus, the antitumor activity of fucoidans was reported by Mabate et al. (2023) in studies on three brown algae, *Fucus vesiculosus*, *Ecklonia radiata*, and *Sargassum elegans* [215]. Shiau et al. (2022), in the research carried out on *Fucus vesiculosus*—brown algae—showed that fucoidans have the activity of reducing colony formation, cancer cell formation, and cell adhesion [216]. Cao et al. (2022) indicate the antitumor activity of fucoidans in studies conducted on *Ulva conglobate*—green algae—by the induction of apoptosis and cell cycle reduction in HT-29 cells in the S and G2/M phase and accumulation in G1 phase cells [217]. Gao et al. (2021) demonstrated that fucoidans from *Sargassum pallidum* have antitumoral and immune-enhancing activities [218]. Bellan et al. (2020) showed that biocompounds with sulphated galactan structures from *Codium isthmocladum*—green algae—exhibited reduced cell invasion, colony-forming capacity, and reduced solid tumour growth and metastasis [219]. Examples of studies that have shown antitumoral activity of biocompounds from seaweed are presented in Table 9.

Zhao et al. (2020) discovered antitumoural activities of polysaccharides from *Ulva Lactuca*—green algae—manifested by decreasing dicarboxylic aldehyde methane dicar-

boxylic acid levels and inhibiting the activation of signaling pathways in human uveal melanoma cells [220]. Yao et al. (2020) reported that porphyrans from *Pyropia haitanensis* (formerly *Porphyra haitanensis*)—red algae—exhibited direct cytotoxic effects, inducing oxidative stress and apoptosis in cells and causing G0-G1 phase arrest of cells [72]. Cicinskas et al. (2020) demonstrated the antitumoral activities of carrageenans from *Chondrus armatus*—red algae—by reducing the cell viability of cancer cells, and Choi et al. (2019) reported that sulfated glucuronorhamnoxylan from *Capsosiphon fulvescens*—green algae—inhibits the growth of human colon cancer cells HT-29 [221,222]. Mendes Marques et al. (2019) studied sulfated galactans from *Udotea flabellum*—green algae—and showed that the anti-proliferative activity was dependent on their degree of sulfation, and Narayani et al. (2019) reported that polysaccharides from *Sargassum cinereum*—brown algae—produced a reduction in the cell viability of cancer cells [223,224].

Other classes of biocompounds have also shown anti-cancer activities. Bharathi et al. (2021) showed anti-cancer effects of SiO2–ZnO nanocomposites with diterpenes from *Dictyota bartayresiana*—brown algae—and developed a drug with antitumoral activity against a cell line of colon cancer [225]. From the class of pigments, fucoxanthin from *Undaria pinnatifida*—brown algae—reported by Wang et al. (2019), produced a decrease in the level of vascular endothelial growth factor (VEGF)-C, VEGF-3 receptor, nuclear factor kappa β, phospho-Akt, and phospho-PI3K in HLEC [226]. They showed that fucoxanthin decreases microlymphatic vascular density in a nude mouse model of MDA-MB-231 breast cancer [226].

Polyphenols also showed antitumoral activities. Thus, Mahendran et al. (2024) indicated that polyphenolic compounds from *Sargassum tenerrimum*—brown algae—by MTT assay show antitumor activity against HeLa cells [227]. In alternative treatments for drugs obtained by chemical synthesis, Cadar et al. (2023) showed that biocompounds from other natural resources can be successfully used in the treatment of cancer diseases [228].

4.2. Antioxidant Activity

Antioxidant activity is the most widely encountered biological activity of marine algae biocompounds. Table 9 systematizes examples of antioxidant and anticoagulant activities corresponding to the classes of biocompounds that constitute active metabolites in marine macroalgae. Antioxidant activity is manifested by the following classes of compounds in seaweed: polysaccharides, terpenoids, pigments, polyphenols, and vitamins. Antioxidant activity was exhibited by polysaccharides mostly for brown algae as reported by Alboofetileh et al. (2022) for the brown algae *Nizamuddinia zanardinii* and Wang et al. (2020 a) for the brown algae *Sargassum fusiforme* (formerly *Hizikia fusiforme*) [229,230]. Oh et al. (2020) demonstrated antioxidant activity exhibited by polysaccharides from *Undaria pinnatifida*—brown algae [71]. The antioxidant activity of polysaccharides was shown by Wang et al. (2020 b) from *Ecklonia maxima* and Jayawardena et al. (2020) from *Padina boryana*, respectively [231,232]. Le et al. (2019) reported the antioxidant activity of ulvan for the green alga *Ulva lactuca* (as *Ulva pertusa*) [233]. Wang et al. (2019) and Maneesh et al. (2018) reported the antioxidant activity of polysaccharides also from brown algae: *Sargassum fulvellum* and *Sargassum wightii*, respectively [234,235]. Yang et al. (2021) evidenced the protective actions of polysaccharide extracts from *Ulva lactuca*, which suppresses kidney damage and decreases oxidative stress in the kidneys [236]. The antioxidant activity due to terpenoids in the composition of algae was reported by Zhang et al. (2020) from the red algae *Laurencia tristicha* [237]. The antioxidant activity of fatty acids was evaluated from *Palmaria palmata*—red algae—by Lopes et al. (2019), and from *Grateloupia turuturu*—red algae—by Da Costa et al. (2021) [126,238]. The antioxidant activity due to proteins and

protein compounds in the composition of algae was reported by Echave et al. (2022) for representatives of brown, green, and red algae, by Zhang et al. (2019) in the red algae *Gracilariopsis lemaneiformis* [135,239], Torres et al. (2019) and Torres et al. (2018) in the red algae *Pyropia yezoensis* and other red algae from the phylum *Rodophyta—Porphyra* spp. [240,241]. The antioxidant actions of peptides from other marine resources such as those due to collagen from marine organisms were reported by Cadar et al. in 2023 and 2024 [242,243]. Pigments constitute a category of active biocompounds, secondary metabolites that have intense anti-oxidant activity. Thus, Cadar et al. (2023) reported the antioxidant activity of chlorophyll pigments and total carotenoids from the green algae *Ulva lactuca*, *Ulva intestinalis*, and *Cladophora vagabunda* [49]. Sudhakar et al. (2023) reported the antioxidant activity of the pigments from *Gracilaria corticate*—red algae [244]. Yalçın et al. (2021) indicate the antioxidant activity of chlorophyll pigments, carotenoids, and fucoxanthin, respectively, from the green algae *Caulerma racemosa*, *Hypnea musciformis*—red algae—and from *Cladostephus spongiosus*—brown algae [245]. Radman et al. (2021) reported the antioxidant activity of pigments from the green alga *Codium adhaeresn*, Ulagesan et al. (2021) from the red alga *Pyropia Yezoensis*, and Jerković et al. (2021) from the brown alga *Fucus virsoides* [246–248]. We thus find that pigments with important antioxidant activity were identified in representative algae from all green, red, and brown taxa. Negreanu-Pîrjol et al. (2020, 2021) studied the antioxidant activity of pigments from red and green algae from the Black Sea basin, *Ceramium virgatum*, and *Ulva lactuca* [169,249]. The antioxidant activity due to fucoxanthin from brown algae was reported by Karkhaneh et al. (2020) from the alga *Dictyota cervicornis* (formerly *Dictyota indica*) [250]. Ghaliaoui et al. (2020) showed the antioxidant activity of pigments from *Phyllariopsis brevipes* (formerly *Phyllaria reniformis*) (Phaeophyceae) [251]. Mohibbullah et al. (2018) showed the neuroprotective effects of fucoxanthin from *Undaria pinnatifida* in attenuating oxidative stress in hippocampal neurons [252]. Fu et al. (2024) explained through scientific arguments the relationship between the structure of polysaccharide biocompounds from macroalgae and biological actions in curing various diseases such as antioxidant, anti-inflammatory, anticoagulant, antiviral, immunomodulatory, and antitumoral activities [253]. Polyphenols constitute another valuable category of compounds that have antioxidant activity. For brown algae, Mahendran et al. (2024) reported the antioxidant activity of polyphenols from *Sargassum tenerrimum*, [227]. Generalić Mekinić et al. (2021) reported the antioxidant activity of polyphenols from *Dictyota dichotoma* and from *Padina pavonica*—brown algae—and Hassan et al. (2021) reported the antioxidant activity of polyphenols from *Padina boryana*—brown algae—and *Acanthophora spicifera*—red algae [254,255]. The antioxidant activity of phenolic compounds from *Gongolaria barbata*—brown algae—was revealed by Cadar et al. (2019) and from *Chondrus crispus* species—red algae—by Alkhalaf et al. (2021) [196,256]. The antioxidant activity of flavonoid compounds was reported by Ak et al. (2018) from *Gongolaria barbata*—brown algae—and *Gigartina acicularis*—red algae [257]. Neuroprotective actions due to polyphenolic compounds from macroalgae have also been presented by Alghazwi et al. (2020), Shrestha et al. (2020), and Yang et al. (2018) from various brown algae [258–260]. Vitamins from the composition of marine algae also have antioxidant activity. Thus, Le et al. (2024) studied the antioxidant activity of vitamins from *Odonthalia dentata*—red algae [261]. In particular, vitamin C shows antioxidant activity as reported by Subramoni 2023 for *Caulerpa chemnitzia*—green algae [262]. Methods for demonstrating antioxidant activity are ABTS, Frap, and CUPRAC assay. Antioxidant activity decreases intracellular ROS and lipid peroxidation, increases the body's immunity, protects against oxidative stress, and participates in metabolic regulatory mechanisms.

Table 9. Biological compounds of seaweeds with antitumoral and antioxidant activity.

Type of Seaweed	Bioactive Metabolites/ Compounds	Mechanism of Action	Biological Activity	References
Antitumoral activity				
Polysaccharides				
Fucus vesiculosus—brown algae	Fucoidan	Decreases colony formation, cancer cell formation, and cell adhesion.	Antitumoral activity	[215]
Ecklonia radiata—brown algae	Fucoidan	Decreases cancer cell formation and cell adhesion.	Antitumoral activity	[215]
Sargassum elegans—brown algae	Fucoidan	Decreases colony formation, cancer cell formation, and cell adhesion.	Antitumoral activity	[215]
Fucus vesiculosu—brown algae	Fucoidans	Decreases cancer cell sphere formation and cell adhesion.	Antitumoral activity	[216]
Ulva conglobata—green algae	Fucoidans	Induced apoptosis and decreased the cell cycle in HT-29 cells in S and G2/M phases and accumulation in cells in G1 phase. It has been proven that H_2O_2 has an antioxidant effect on HT-29 cells.	Antitumoral activity	[217]
Sargassum pallidum—brown algae	Fucoidans	Decreases colony formation, cancer cell sphere formation, and cell adhesion.	Antitumoral activity	[218]
Codium isthmocladum—green algae	Sulphated galactan	Reducing cell invasion, colony-forming capacity, and membrane glycoconjugates and reducing solid tumour growth and metastasis.	Antitumor activity	[219]
Ulva Lactuca—green algae	Polysaccharides	Decreased the level of methane dicarboxylic aldehyde and inhibited the activation of signaling pathways in human uveal melanoma cells	Antitumor activity	[220]
Pyopia haitanensis—red algae	Porphyrans	Direct cytotoxic effects, inducing the oxidative stress and apoptosis in cells, and causing the cell G0–G1 phase arrest.	Antitumoral activity	[73]
Chondrus armatus—red algae	Carrageenans	Decreases cell viability of cancerous cells.	Antitumoral activity	[221]
Capsosiphon fulvescens—green algae	Sulfated glucuronorhamnoxylan	Inhibits the growth of HT-29 human colon cancer cells.	Antitumor activity	[222]
Udotea flabellum—green algae	Sulfated galactans	The anti-proliferative activity was dependent on their degree of sulfation.	Antitumoral activity	[223]
Sargassum cinereum—brown algae	Polysaccharides	Decreases cell viability of cancerous cells.	Antitumoral activity	[224]
Terpenoides				
Dictyota bartayresiana—brown algae	SiO_2–ZnO nanocomposites with diterpenes from algae	Antitumor effect on HT29. Antimicrobian effect. Excellent antioxidant activity.	Antitumor potential	[225]
Pigments				
Undaria pinnatifida—brown algae	Fucoxanthin	Decreases levels of vascular endothelial growth factor (VEGF)-C, VEGF receptor-3, nuclear factor kappa β, phospho-Akt, and phospho-PI3K in HLEC. Decreases micro-lymphatic vascular density in an MDA-MB-231 nude mouse model of breast cancer.	Antitumoral activity on breast cancer.	[226]
Polyphenols				
Sargassum tenerrimum—brown algae	Polyphenol compounds	Polyphenols have anti-cancer activity against HeLa cells.	Antitumoral activity	[227]

Table 9. *Cont.*

Type of Seaweed	Bioactive Metabolites/ Compounds	Mechanism of Action	Biological Activity	References
Antioxidant activity				
Polysaccharides				
Nizamuddinia zanardinii—brown algae	Fucoidan	It decreases the intracellular production of ROS, having a protective effect	Antioxidant activity	[229]
Sargassum fusiforme (as *Hizikia fusiforme*)—brown algae	Fucoidan	It reduced apoptosis by eliminating intracellular ROS, by increasing intracellular SOD-1 and CAT expressed by up-regulation of Nrf2. Prevented cell death.	Antioxidant activity	[230]
Undaria pinnatifida—brown algae	Fucoidan	Decreases cell death, intracellular ROS, and lipid peroxidation	Antioxidant activity	[71]
Ecklonia maxima—brown algae	Sulfated polysaccharides	It decreases oxidative stress and cell death, improves inhibition of MMPs.	Antioxidant, activity	[231]
Padina boryana—brown algae	Sulfated polysaccharides	Decreases cell death, intracellular ROS, and lipid peroxidation	Antioxidant activity	[232]
Ulva australis (as *Ulva pertusa*)—green algae	Ulvan	Showed antioxidant activity by increasing antioxidant enzymes CAT, SOD, GPx	Antioxidant activity	[233]
Sargassum fulvellum—brown algae	Polysaccharides	Decreases cell death, decreases intracellular ROS and lipid peroxidation	Antioxidant activity	[234]
Sargassum wightii—brown algae	Sulfated polygalacto-pyranosyl-fucopyranan	The presence of sulphate groups in the composition of the isolated polysaccharide seems to play a major role in the scavenging potential of free radicals.	Antioxidant activity	[235]
Ulva lactuca—green algae	Polysaccharides	protective effect on renal lesions by decreasing atrophy and serum levels of creatinine and cystatin C. Decreases oxidative stress in the kidneys.	Kidney injury caused by oxidative stress	[236]
Terpenoides				
Laurencia tristicha—red algae	Laurane-type sesquiterpene	Different methods of evaluating antioxidant activity	Antioxidant activity	[237]
Fatty acids				
Grateloupia turuturu—red algae	EPA and PUFA	Free radical scavenging activity: DPPH and ABTS	Antioxidant activity	[238]
Palmaria palmata—red algae	EPA	Antioxidant assay by DPPH and ABTS	Antioxidant activity	[126]
Proteins				
Red, brown, and green seaweeds	Proteins, peptides, lectins	For antioxidant activity of amino acids: Test DPPH and ABTS assay	Antioxidant activity	[136]
Gracilariopsis lemaneiformis—red algae	Peptide sequence ELWKTF	Scavenging DPPH free radicals assay	Antioxidant activity	[239]
Pyropia yezoensis—red algae	Amino acid: Taurine	Different methods of evaluating antioxidant activity	Antioxidant activty	[240]
Rodophyta–Porfira spp.	Amino acids inred algae	Evaluate antioxidant capacity—DPPH, ferrous ion-chelating, ABTS, FRAP, β-carotene/linoleic acid, and ORAC	Antioxidant activity	[241]

Table 9. *Cont.*

Type of Seaweed	Bioactive Metabolites/ Compounds	Mechanism of Action	Biological Activity	References
		Pigments		
Ulva lactuca—green algae	Chlorophyll a and b; total carotenoids	Antioxidants activity by DPPH, FRAP, TEAC assay	Antioxidant activity	[49]
Ulva intestinalis—green algae	Chlorophyll a and b; total carotenoids	Antioxidants activity by DPPH, FRAP, TEAC assay	Antioxidant activity	[49]
Cladophora vagabunda—green algae	Chlorophyll a and b; total carotenoids	Antioxidants activity by DPPH, FRAP, TEAC assay	Antioxidant activity	[49]
Gracilaria corticata—red algae	R-phycoerythrin	Resulted activity by MTT assay, and the colon cancer cell lines SW620 and HCT-116 were inhibited by the compound in a concentration-dependent manner.	Antioxidant activity	[241]
Caulerma racemosa—green algae	Chlorophyll a and b, β-carotene	Showed antioxidant activity by CUPRAC and ABTS assays.	Antioxidant activity	[245]
Hypnea musciformis—red algae	Fucoxanthin, chlorophyll a and b, β-carotene	Showed antioxidant activity by CUPRAC and ABTS assays.	Antioxidant activity	[245]
Cladostephus spongiosus—brown algae	Fucoxanthin, pheophytin-α, chlorophyll a	Showed antioxidant activity by CUPRAC and ABTS assays.	Antioxidant activity	[245]
Codium adhaerens—green algae	Fucoxanthin, pheophytin-α	Showed antioxidant activity by FRAP, DPPH, and ABTS assays.	Antioxidant activity	[246]
Pyropia yezoensis—red algae	R-phycoerythrin	Antioxidant activity by ABTS and FRAP assays and had significant cytotoxicity against Hep G2 cells	Antioxidant activity Antitumoral activity	[247]
Fucus virsoides—brown algae	Fucoxanthin, pheophytin-α	Proapoptotic activity for human cervical adenocarcinoma HeLa cells.	Antioxidant activity	[248]
Ceramium virgatum—red algae	Carotenoids, xanthophyll and β-carotene	Showed antioxidant activity by TEAC assay	Antioxidant activity	[249]
Ulva lactuca—green algae	Chlorophyll a and b	Showed antioxidant activity by TEAC assay	Antioxidant activity	[169]
Dictyota cervicornis (formerly *Dictyota indica*)—brown algae	Fucoxanthin	Strong antioxidant activity by FRAP assay	Antioxidant activity	[250]
Phyllariopsis brevipes (formerly *Phyllaria reniformis*)—brown algae	Fucoxanthin, pheophytin-α,	Antioxidant activity by DPPH assay	Antioxidant activity	[251]
Undaria pinnatifida—brown algae	Fucoxanthin	Showed protection from neurite breakage	Neurodegenerative diseases	[252]

Table 9. *Cont.*

Type of Seaweed	Bioactive Metabolites/ Compounds	Mechanism of Action	Biological Activity	References
		Polyphenols		
Sargassum tenerrimum—brown algae	Polyphenol compound	Showed potential activity by TEAC, FRAP, H_2O_2, DPPH, and ABTS assays	Antioxidant activity	[227]
Dictyota dichotoma—brown algae	Protocatechuic, *p*-hydroxybenzoic, coumaric, and ferulic acid	Showed activity by FRAP, DPPH, ORAC assays	Antioxidant activity	[254]
Padina pavonica—brown algae	Protocatechuic, ferulic, *p*-hydroxy-benzoic acid	Showed activity by FRAP, DPPH, ORAC assays	Antioxidant activity	[254]
Padina boryana—brown algae	Polyphenolic compound	DPPH and FRAP assay	Antioxidant activity	[255]
Acanthophora spicifera—red algae	Polyphenolic compound: Velutin	DPPH and FRAP assay	Antioxidant activity	[255]
Gongolaria barbata—brown algae	Total phenolic content	DPPH radical scavenging activity and reducing power	Antioxidant activity	[256]
Gongolaria barbata—brown algae	Flavonoids	DPPH assay	Antioxidant activity	[257]
Gigartina acicularis—red algae	Flavonoids	DPPH assay	Antioxidant activity	[257]
Ecklonia radiata—brown algae	Phlorotannim	Inhibition of apoptosis induced by Aβ1–42	Neuroprotective activity	[258]
Ecklonia radiata—brown algae	Eckol-type phlorotannins	Showed neuroprotective activity against the neurotoxic amyloid β-protein (Aβ1–42) in a neuronal PC-12 cell line in vitro experiment.	Neuroprotective activity	[259]
Eklonia cava—brown algae	Phloroglucinol	Decreases the amyloid β-peptide burden and pro-inflammatory cytokines in the hippocampus.	Neurodogenerative disease	[260]
		Vitamins		
Odonthalia dentata—red algae	A, B1, B2, B3, B6, B9, C, and E	Increases the body's immunity. Protects against oxidative stress. Involved in metabolic regulation processes.	Antioxidant activity	[261]
Caulerpa chemnitzia—green algae	Vitamin C	Strengthening the immune system. Involvement in the cell regeneration process	Antioxidant activity	[262]

4.3. Antimicrobial Activity

Antimicrobial activity has been identified in the following classes of biocompounds from seaweeds as shown in Table 10: terpenoids, pigments, and polyphenols. Rushdi et al. (2022) showed that diterpenes such as dictyols from *Dictyota dichotoma*—brown algae—have antimicrobial activities on the murine macrophage cell line RAW 264.7 [114]. Sumayya et al. (2020) studied the antimicrobial activity against *Streptococcus mutans*, using purified terpenoid fractions from red algae: *Gracillaria dura*, *Hypnea musciformis*, and *Kappapycus alvarezii* algae [263]. For the evaluation of antimicrobial activity, Kuete et al. (2010) considered MIC (Minimum inhibitory concentration (MIC)) as the optimal evaluation parameter and set the antimicrobial activity parameters as follows: for extracts, the criteria were significant (MIC < 100 μg/mL), moderate (100 < MIC ≤ 625 μg/mL), or weak (MIC > 625 μg/mL) and for compounds, these stringent criteria were significant (MIC < 10 μg/mL), moderate (10 < MIC ≤ 100 μg/mL), and weak or negligible (MIC > 100 μg/mL) [264]. Sumayya et al. (2020) showed that the MIC values for terpenoid extracts purified from *Gracillaria dura*, *Hypnea musciformis*, and *Kappapycus alvarezii* against *S. mutans* were 65, 500, and 1. 500 μg/mL, respectively [263]. Also, Tamokou et al. (2017) established criteria for edible plant extracts or their parts and they were estimated to be highly active if MIC values < 100 μg/mL, significantly active if 100 ≤ MIC ≤ 512 μg/mL, moderately active if 512 ≤ MIC ≤ 2048 μg/mL, and not highly active if MIC > 2048 μg/mL [265]. The results of the MIC value study showed that purified terpenoid extracts from *Gracilaria dura* (65 μg/mL) had significant antimicrobial activity against *S. mutans*, (while weak against *E. faecalis*, *P. aeruginosa*, and *K. pneumoniae*), and *Hypnea musciformis* (MIC 500 μg/mL) showed moderate action against *S. mutans*, taking into consideration the criteria established by Kuete et al. (2010) and Tamokou et al. (2017) [263–265]. Ríos et al. (2005) have shown that the presence of antimicrobial activity is very interesting at concentrations below 100 μg/mL for extracts and 10 μg/mL for isolated compounds [266]. MIC 65 μg/mL for purified terpenoid extracts from *Gracillaria dura* also meets the criteria set by Rios et al. (2005), showing intense antimicrobial activity against *S. mutans* [263,266].

Anjali et al. (2019) studied the antimicrobial activities (by diffusion) against *E. coli*, *K. pneumonia*, and *S. typhi* due to sesquiterpenoids from *Ulva lactuca*—green algae [267]. Da Graça Pedrosa de Macena et al. (2023) studied the anti-Herpes simplex virus type 2 (HSV-2) activities of terpenoids from two brown algae, *Stypopodium zonale* and *Canistrocarpus cervicornis* [268]. Cirne-Santos et al. (2020) showed antiviral activity on *Zika* and *Chikungunya* viruses due to *Dolastane*-type diterpenoids from *Canistrocarpus cervicornis*—brown algae [269]. Pigments were studied by Oliyaei et al. (2021), who reported antimicrobial activity against *S. aureus* due to fucoxanthin from *Sargassum angustifolium* and *Cystoseira indica* brown algae [270]. Generalić Mekinić et al. (2021) reported the antimicrobial activities of phenolic compounds from the brown algae *Padina pavonica* (Dictyotaceae) against *B. subtilis*, *P. aeruginosa*, *S. aureus*, and *C. albicans* [254].

4.4. Anti-Inflammatory Activity

Biocompounds with anti-inflammatory properties include polysaccharides, fatty acids, and pigments; see Table 10. Fucoidans derived from brown algae have demonstrated anti-inflammatory activity, as reported by Liyanage et al. (2023) from *Sargassum autumnale*, Jayasinghe et al. (2023) from *Sargassum siliquastrum*, and Jayasinghe et al. (2022) from *Sargassum confusum* [271–273]. Other researchers have also reported anti-inflammatory activity due to seaweed biocompounds, such as Apostolova et al. (2022) from *Cystoseira crinita*, and Jayawardena et al. (2020) from *Sargassum swartzii* [274,275]. This activity is generally attributed to the inhibition of inflammatory mediators and pro-inflammatory cytokines.

The anti-inflammatory effects of sulfated polysaccharides have also been documented. Wang L et al. (2022) studied sulfated polysaccharides from *Codium fragile*, while Chen et al. (2021) focused on those from *Saccharina japonica* [276,277]. In addition, other studies were conducted by Je et al. (2021) on *Sargassum binderi*, Wang L et al. (2021) on *Sargassum fulvellum*, and Wang S. et al. (2020) on *Saccharina japonica* [278–280]. These compounds exert anti-inflammatory effects by reducing cell death while modulating nitric oxide (NO) and reactive oxygen species (ROS) generation. Fatty acids have also been shown to possess anti-inflammatory properties. Jaworovska et al. (2023) identified this activity in saturated fatty acids (SAs) and eicosapentaenoic acid (EPA) derived from *Fucus spiralis* and *Undaria pinnatifida* [120]. Similarly, Foseid et al. (2020) reported anti-inflammatory effects from *Palmaria palmata* (red algae), while Rocha et al. (2021) found evidence of these properties in *Undaria pinnatifida* (brown algae) and *Gracilaria gracilis* (red algae) [117,118]. Pereira et al. (2021) and Berneira et al. (2020) further highlighted the role of fatty acids from marine macroalgae, particularly SFA, MUFA, and PUFA, in modulating inflammation [281,282]. Finally, pigments such as fucoxanthin, pheophytin-α, chlorophyll-a, and β-carotene have demonstrated anti-inflammatory activity. Dai et al. (2021) investigated these pigments in *Sargassum fusiforme* (brown algae) and found that they inhibit prostaglandin E2 (PGE2), cyclooxygenase-2 (COX-2), and the production of interleukins (IL)-1β and IL-6 in HaCaT keratinocytes [283].

4.5. Cardioprotective and ACE Inhibitory Activity

Cardiovascular diseases significantly impact human health, driving interest in natural biocompounds with cardioprotective properties. In recent years, there has been growing attention on natural ACE inhibitory peptides derived from these biocompounds, as highlighted by Cadar et al. (2024) [243]. Table 10 presents various biocompounds from marine macroalgae that exhibit both cardioprotective and ACE inhibitory activity. Marine algae contain several classes of bioactive compounds, such as polysaccharides and fatty acids, known for their cardioprotective effects. Maneesh et al. (2018) demonstrated that sulfated poly-galactopyranosyl-fucopyranan compounds from *Sargassum wightii* (brown algae) possess antihypertensive activity [235]. Similarly, Cheng et al. (2020) reported that fucoidans from *Fucus vesiculosus* (brown algae) exhibit cardioprotective properties [284]. Fatty acids from seaweeds have also shown significant potential in cardiovascular health. Polyphenols from *Palmaria palmata* (red algae) and *Alaria esculenta* (brown algae) were identified by Foseid et al. (2020) as having potential activity against coronary heart disease [117]. Furthermore, Rocha et al. (2021) highlighted the cardioprotective properties of fatty acids from *Undaria pinnatifida* (brown algae) and *Gracilaria gracilis* (red algae) [118]. Pereira et al. (2021) and Berneira et al. (2020) explored the cardioprotective effects of fatty acids—including SFA, MUFA, and PUFA—derived from *Ulva lactuca* (green algae), *Ulva intestinalis* (green algae), particularly through COX-2 enzyme inhibition mechanisms [281,282]. ACE inhibitory activity has been demonstrated in proteins and pigments from marine algae. Kumagai et al. (2021) investigated ACE inhibitory properties in 42 peptide preparations from *Pyropia pseudolinearis*, selecting ARY, YLR, and LRM peptides for further study. Their results indicated that LRM had the lowest IC50 value (0.15 mol), compared to ARY (1.3 mol) and YLR (5.8 mol) [285]. Proteins from macroalgae also exhibit strong ACE inhibitory activity, as reported by Dhaouafi et al. (2024) for protein hydrolysates (MW 300–1800 Da) from *Gelidium spinosum* (red algae) [130].

Table 10. Biocompounds of marine algae with biological activity results in antimicrobial, anti-inflammatory diseases, cardioprotective, and ACE inhibitory activity.

Type of Seaweed	Bioactive Metabolites/Compounds	Mechanism of Action	Biological Activity	References
Antimicrobial activity				
Terpenoides				
Dictyota dichotoma—brown algae	Diterpenes as dictyols.	Have effects on cell viability in murine macrophage cell line RAW 264.7	Antimicrobial potential	[114]
Kappapycus alvarezii—red algae	Purified terpenoids fractions	Minimum inhibitory concentration (MIC) value was 1.5 mg/mL against *S. mutans*. Minimal bactericidal concentration (MBC) value was 3.0 mg/mL	Antimicrobial activity	[263]
Gracillaria dura—red algae	hexadecanoic acid methyl ester, n-hexadecenoic acid, 11-octadecanoic acid, and phytol	Minimum inhibitory concentration (MIC) value was 0.065 mg/mL against *S. mutans*. Minimal bactericidal concentration (MBC) value was 0.12 mg/mL	Antimicrobial activity	[263]
Ulva lactuca—green algae	Sesquiterpenoid as neophytadiene	Showed excellent inhibitory effects with the maximum activity (by diffusion) against *E. coli*, *K. pneumonia*, and *S. typhi*	Antimicrobial activity	[267]
Stypopodium zonale—brown algae	Atomaric acid and 4-acetoxydolastane, secundary metabolites,	Anti-HSV-2 activity with low cytotoxicity, inactivated 90% of the viral particle.	Anti-Herpes simplex virus	[268]
Canistrocarpus cervicornis—brown algae	Atomaric acid and 4-acetoxydolastane	Anti-HSV-2 activity with low cytotoxicity	Anti-Herpes simplex virus	[269]
Canistrocarpus cervicornis—brown algae	Dolastane-type diterpenoids	For *Chikungunya virus*, the compound was able to inhibit around 90% of the virus infectivity and for *Zika* virus, the effects were at approximately 64%	Anti-viral activity on *Zika* and *Chikungunya* viruses	[269]
Pigments				
Sargassum angustifolium—brown algae	Fucoxanthin	Showed antimicrobial activity against *S. aureus* by diffusion method	Antimicrobial activity	[270]
Gongolaria indica—brown algae	Fucoxanthin	Significant inhibition zone against *E. Coli* and *S. aureus*.	Antimicrobial activity	[270]
Polyphenols				
Padina pavonica—brown algae	Protocatechuic acid; *p-h*droxybenzoic acid; *p*-coumaric acid; *t*-ferulic acid; *o*-coumaric acid	Inhibition zone: *B. subtilis*: 12.7 ± 0.6 mm; *P. aeruginosa*: 15.7 ± 2.1 mm; *S. aureus*: 10.3 ± 1.5 mm and *C. albicans*: 10 ± 0.9 mm	Antimicrobial activity	[254]
Anti-inflammatory activity				
Polysaccharides				
Sargassum autumnale—brown algae	Fucoidan	Down-regulation of iNOS and COX2 and signaling pathways (NF-κB and MAPK).	Anti-inflammatory activity	[271]
Sargassum siliquastrum—brown algae	Fucoidan	Down-regulated the expression of inflammatory mediators (NO, PGE2, iNOS, COX-2), and pro-inflammatory cytokines via regulating MAPK and NF-κB.	Anti-inflammatory activity	[272]
Sargassum confusum—brown algae	Fucoidan	Reducing the expression of inflammatory mediators through regulation of NF-κB and MAPKs signaling pathways via activating Nrf2/HO-1 signaling.	Anti-inflammatory activity	[273]
Cystoseira crinita—brown algae	Fucoidan	Decreases IL-1 β production.	Anti-inflammatory activity	[274]
Sargassum swartzii—brown algae	Sulfated Polysaccharide (fucoidan)	Inhibition of inflammatory mediators and pro-inflammatory cytokines.	Anti-inflammatory activity	[275]
Codium fragile—green algae	Sulfated polysaccharides	Decreases cell death and the generation of NO and ROS.	Anti-inflammatory activity	[276]
Saccharina japonica—brown algae	Sulfated galactofucan	Decreases cell death and the generation of NO and ROS.	Anti-inflammatory activity	[277]
Sargassum binderi—brown algae	Sulfated polysaccharides	Decreases LPS-induced cell death and NO production.	Anti-inflammatory activity	[278]
Sargassum fulvellum—brown algae	Sulfated polysaccharides	Decreases cell death and the generation of NO and ROS.	Anti-inflammatory activity	[279]
Saccharina japonica—brown algae	Sulfated polysaccharides	Decreases cell death and the generation of NO and ROS.	Anti-inflammatory activity	[280]

Table 10. *Cont.*

Type of Seaweed	Bioactive Metabolites/Compounds	Mechanism of Action	Biological Activity	References
		Fatty acids		
Fucus spiralis—brown algae	EPA and octadecatetraenoic acid	Showed dose-dependent effect on murine macrophage RAW 264.7 cell line, SA: IC50 values of 160 µg on ear for edema, 314 µg on ear for erythema, 235 µg on ear for blood flow. EPA: IC50 values of 230 µg on ear for edema, 462 µg on ear for erythema, 236 µg on ear for blood flow.	Anti-inflammatory activity	[120]
Undaria pinnatifida—brown algae	SA, EPA		Anti-inflammatory activity	[120]
Palmaria palmata—red algae	Palmitic acid, Oleic acid, and EPA	Inhibition of the COX-2 enzyme	Anti-inflammatory activity	[117]
Gracilaria gracilis—red algae	SFA, MUFA, PUFA, HUFA, omega-3, omega-6	Inhibition of the COX-2 enzyme	Anti-inflammatory activity	[118]
Undaria pinnatifida—brown algae	SFA, MUFA, PUFA, HUFA, omega-3, omega-6	Inhibition of the COX-2 enzyme	Anti-inflammatory activity	[118]
Ulva lactuca—green algae	SFA, MUFA, PUFA, omega-3, omega-6	Inhibition of the COX-2 enzyme	Anti-inflammatory activity	[281]
Ulva intestinalis—green algae	SFA, MUFA, and PUFA	Inhibition of the COX-2 enzyme	Anti-inflammatory activity	[282]
		Pigments		
Sargassum fusiformis—brown algae	Fucoxanthin, pheophytin-α, chlorophyll-a, β-carotene	Inhibiting production of prostaglandin E2 (PGE2), cyclooxygenase-2, interleukin (IL)-1β, and IL-6 from exposed HaCaT keratinocytes	Anti-inflammatory activity	[283]
		Cardioprotective activity andACE inhibitory activity		
		Polysaccharides		
Sargassum wightii—brown algae	Sulfated polygalacto-pyranosyl-fucopyranan	The formation of hydrogen bonds with Zn^{2+} and other amino acid residues by the electronegative functionalities can lead to effective inhibition of ACE.	Antihipertensive activity	[235]
Fucus vesiculosus—brown algae	Fucoidan	Decreases lipid levels and the carotid atherosclerotic plaque formation.	Cardioprotective activity	[284]
		Fatty acids		
Alaria esculenta—brown algae	Palmitic acid, Oleic acid and EPA	Showed high content of linoleic acid which indicates potential activity on coronary heart disease	Coronary hearth diseases,	[117]
Palmaria palmata—red algae	Palmitic acid, Oleic acid and EPA	Inhibition of the COX-2 enzyme	Coronary hearth disease	[117]
Undaria pinnatifida—brown algae	SFA, MUFA, PUFA, HUFA, omega-3, omega-6	Inhibition of the COX-2 enzyme	Cardioprotective activity	[118]
Gracilaria gracilis—red algae	SFA, MUFA, PUFA, HUFA	Inhibition of the COX-2 enzyme	Cardioprotective activity	[118]
Ulva lactuca—green algae	SFA, MUFA, PUFA	Inhibition of the COX-2 enzyme	Cardioprotective activity	[281]
Ulva intestinalis—green algae	SFA, MUFA, and PUFA	Inhibition of the COX-2 enzyme	Cardioprotective activity	[282]
Curdiea racovitzae—red algae	SFA, MUFA, PUFA	Inhibition of the COX-2 enzyme	Cardioprotective activity	[282]

Table 10. *Cont.*

Type of Seaweed	Bioactive Metabolites/Compounds	Mechanism of Action	Biological Activity	References
		Proteins		
Sphaerococcus coronopifolius—red algae	Protein hydrolysates with MW 300–1800 Da	ACE inhibitory activity IC50 = 160.32 µM; ACE inhibitory activity IC50 = 656.15 µM;	ACE inhibitory activity	[130]
Gelidium spinosum—red algae	Protein hydrolysates with MW 300–1800 Da (Fractions F1–F10)	F4: ACE inhibitory activity IC50 = 149.35 µM; F6: ACE inhibitory activity IC50 = 656.15 µM;	ACE inhibitory activity	[130]
Palmaria palmata—red algae	Protein hydrolysates	Positive role in glucose transport, increasing glucose uptake	ACE inhibitory activity	[286]
Mazzaella japonica—red algae	Protein sequences	Significant IC50 values were found in sequence IY from the peptide chain	ACE inhibitory activity	[287]
Porphyra dioica—red algae	Peptides sequences	TYIA: ACE inhibitory activity and YLVA: DPP-IV inhibitory activity	ACE inhibitory activity	[288]
Undaria pinnatifida—brown algae	Peptide	ACE inhibitory activity with IC50 = 225.87 µM	Antihypertensive activity	[133]
Sargassum mcclurei—brown algae	Peptide sequence	activity on endothelin-1 suppressing capacity for ACE inhibitory activity	Antihypertensive activity	[144]
Ulva intestinalis—green algae	Peptide sequences	Sequences: FGMPLDR: ACE inhibitory and MELVLR: ACE inhibitory	Antihypertensive activity	[289]
		Pigments		
Sargassum wightii—brown algae	Fucoxanthin	Showed inhibition of ACE with half maximal inhibitory value	ACE inhibitory activity	[290]

A potent ACE inhibitory activity has also been reported by McLaughlin (2021) for protein hydrolysates from Palmaria palmata (red algae), Kumagai et al. (2020) for protein sequences from Mazzaella japonica (red algae), and Cermeño et al. (2019) for peptide sequences TYIA and YLVA from Porphyra dioica (red algae) [286–288]. The antihypertensive effects of peptides from macroalgae have also been noted in studies by Feng et al. (2021) on *Undaria pinnatifida* (brown algae), Zheng et al. (2020) on *Sargassum mcclurei* (brown algae), and Sun et al. (2019) on *Ulva intestinalis* (green algae) [133,144,289]. Additionally, pigments exhibit ACE inhibitory activity; for instance, Raji et al. (2020) demonstrated that fucoidans from *Sargassum wightii* (brown algae) possess this property [290].

4.6. Antidiabetic Activity

Table 11 presents bioactive compounds from marine algae with antidiabetic, anticoagulant, and metabolic disease properties, along with other health benefits. Ahmed et al. (2024) highlighted the antidiabetic potential of marine macroalgae, proposing two mechanisms for diabetes management: lowering blood glucose levels and reducing diabetic complications [212]. They identified several compounds with antidiabetic effects, including polysaccharides (fucoidans, alginates, and laminarins), carotenoids (fucoxanthin), phlorotannins, and sterols (fucosterols) found in marine algae [212]. Further studies support these findings. Lin et al. (2023) demonstrated the antidiabetic activity of fucoidan from *Sargassum pallidum* (brown algae) [291]. Thambi et al. (2022) reported that sulfated pyruvylated polysaccharide from *Gracilaria edulis* (formerly *Hydropuntia edulis*) (red algae) exhibits an anti-hyperglycemic effect [292]. Maneesh et al. (2018) found that sulfated polygalacto-pyranosyl-fucopyranan compounds from *Sargassum wightii* (brown algae) show significant antidiabetic potential for type 2 diabetes treatment [235].

4.7. Activities in the Treatment of Metabolic Diseases

Metabolic diseases are often challenging to detect and manage. Table 11 summarizes studies that explore the use of biocompounds from marine macroalgae—specifically fatty acids and minerals—as alternative treatments for these conditions. Research has highlighted the beneficial effects of fatty acids derived from marine algae. Rocha et al. (2021) reported that fatty acids from *Undaria pinnatifida*, a type of brown algae, exhibit positive effects [118]. Similarly, Berneira et al. (2020) demonstrated that fatty acids, including SFA, MUFA, and PUFA, extracted from *Ulva intestinalis* (green algae) and *Curdia racovitzae* (red algae) have beneficial impacts on metabolic diseases [282]. Minerals also play a crucial role in metabolic processes. Xavier et al. (2020) reviewed studies indicating that iron and zinc are essential for human metabolic activities [293]. Iron is particularly vital for physiological functions, as it is required for the production of hemoglobin and myoglobin, which facilitate oxygen transport throughout the body. Zinc contributes to metabolism, immune function, and cellular repair. According to Xavier et al. (2020), *Valoniopsis pachynema* (green algae) contains the highest levels of iron, while *Gelidium latifolium* (red algae) has the highest concentration of zinc [293].

4.8. Anticoagulant Activity

Polysaccharides from all types of macroalgae exhibit anticoagulant properties described in various studies, as shown in Table 11. Mendes Marques et al. (2019) reported anticoagulant activities for polysaccharide extracts from *Udotea flabellum*—green algae [223]. de Carvalho et al. (2020) reported anticoagulant activities of polysaccharide extracts from the green algae *Ulva lactuca* (formerly *Ulva fasciata*), Chagas et al. (2020) for polysaccharide extracts from *Gelidiella acerosa*—red algae—and Sun et al. (2018) for polysaccharide extracts

from *Sargassum fusiforme* [294–296]. The anticoagulant activity is supported by polysaccharide biocompounds (polycarboxyl ulvans, sulfated polysaccharides, sulfated galactan, and polysaccharides with low MW) [296].

4.9. Neuroprotective Activity and Alzheimer's Disease (AD)

The classes of biocompounds that have shown beneficial effects in neuroprotective conditions and in the treatment of Alzheimer's disease are pigments, polysaccharides, and fatty acids, as shown in Table 11. Cho et al. (2018) evidenced that carotenoid pigments from seaweed have multiple activities such as antioxidant, anti-inflammatory, and autophagy-modulating activities in the context of neurodegenerative diseases [297].

The mechanisms of treatment of Alzheimer's disease with seaweed extracts (poly/oligosaccharides) include the following: (I) anti-inflammatory and antioxidant activities; (II) scavenging of free radicals; (III) inhibition of ROS production and inhibition of nitric oxide (NO) and prostaglandin formation; (IV) decreased expression of mitochondria-mediated proteins and protein aggregation; (V) direct interaction with the aggregated peptide, preventing Aβ oligomerization and fibrillation; (VI) attenuation of Aβ-induced apoptosis through the JNK pathway; and (VII) impact on gut microbial processing and subsequent neuroinflammation. Bauer et al. (2021) highlighted the use of algal polysaccharides for the treatment of neurodegenerative diseases such as Alzheimer's disease [298]. Park et al. found that mice treated with fucoidan extracts from *Ecklonia cava*—brown algae—experienced beneficial effects in the treatment of Alzheimer's disease [299]. Bogie et al. (2019) showed that the use of fatty acid extracts from *Sargassum fusiforme* in the treatment of Alzheimer's disease led to beneficial effects [300].

4.10. Antiprotozoal Activity

The effects that were generated by the appearance of malaria, leishmanicide, and trypanocide have required multiple studies to detect natural biocompounds that are effective in antiprotozoal activities. In this sense, Hassan et al. (2021) studied phenolic compounds from *Padina boryana*—brown algae—and showed that they exhibit antiprotozoal activity against *Trypzanosoma cruzi*, and against *Leishmania donovani*, as shown in Table 11 [255].

4.11. Bone Deficiencies

This condition is quite widespread both in children and especially in the elderly. Xavier et al. (2020) show that in the treatment of bone deficiencies, Ca intake is important, as shown in Table 11 [293]. Calcium obtained from seaweed helps increase bone density regardless of age. The authors show that the disadvantage of calcium obtained conventionally through calcium supplements can also generate other gastrointestinal side effects, such as bloating, nausea, and constipation [293]. It has been indicated that algal calcium also possesses other essential minerals (magnesium, phosphorus, potassium, and zinc) and vitamins such as vitamin C, D [293]. Mohan et al. (2023) showed that seaweed has applications in the treatment of bone deficiencies through the content of minerals, vitamins, and proteins that they possess [301].

4.12. Malnutrition

Folic acid and vitamin B12 deficiency is common in children, along with iron deficiencies. Koseki et al. (2023) showed that vitamin B12 (Cyanocobolamin) and B9 (folic acid) deficiency disrupts the biosynthesis of methionine necessary for the accumulation of homocysteine, which is a risk factor for many diseases, as shown in Table 11. The authors demonstrated that these deficiencies can be remedied by supplementation with vitamin B9 and Vitamin B12 from marine macroalgae [302].

Table 11. Biocompounds of marine algae with biological activity results in antidiabetic activity, anticoagulant activity, metabolic diseases, and in other applications for health.

Type of Seaweed	Bioactive Metabolites/Compounds	Mechanism of Action	Biological Activity	References
Antidiabetic activity				
Polysaccharides				
Sargassum pallidum—brown algae	Fucoidan	Decreases lipid peroxidation. Reduces the activation of NF-κB signaling pathway.	Antidiabetic activity	[291]
Gracilaria edulis—red algae	Sulphated pyruvylated polysaccharide	Anti-hyperglycemic effect. Activities against type II transmembrane serine exopeptidase DPP-IV and carbolytic enzyme bundles.	Antidiabetic activity	[292]
Sargassum wightii—brown algae	Sulfated polysaccharide	Sulfated polygalacto-pyranosyl-fucopyranan could function as a potential pharmacophore lead against inflammation, type 2 diabetes.	Antidiabetic activity	[235]
Metabolic Deseases				
Fatty acids				
Undaria pinnatifida—brown algae	SFA, MUFA, PUFA, HUFA,	Inhibition of the COX-2 enzyme	Metabolic diseases	[118]
Ulva intestinalis—green algae	SFA, MUFA, and PUFA	Inhibition of the COX-2 enzyme	Metabolic diseases	[282]
Curdiea racovitzae—red algae	SFA, MUFA, PUFA	Inhibition of the COX-2 enzyme	Metabolic diseases	[282]
Minerals				
Valoniopsis pachynema—green algae	Iron	Iron is vital because it is used in the production of hemoglobin and myoglobin. The iron content was high in *V. pachynema.*	Metabolic activities	[293]
Gelidium spinosum (as *Gelidium latifolium*)—red algae	Zinc	Zinc is associated with metabolism and immune function. Zinc is involved in the repairing the body cells.	Metabolic activities	[293]
Anticoagulant Activity				
Polysaccharides				
Udotea flabellum—green algae	Sulfated galactan	Inhibited B16-F10 cell adhesion, migration, and proliferation.	Anticoagulant activity	[223]
Ulva lactuca (as *Ulva fasciata*)—green algae	Polycarboxyl ulvans	Anticoagulant activity by increasing the carboxyl groups.	Anticoagulant activity	[294]
Gelidiella acerosa—red algae	Sulfated polysaccharides	For anticoagulant, antiplatelet and antithrombotic activities, the mechanism of action is mainly due to the chemical structure of the isolated polysaccharide.	Anticoagulant, antiplatelet activity	[295]
Sargassum fusiforme—brown algae	Polysaccharides with low MW	These low MW polysaccharides possessed anticoagulant activity in the intrinsic, extrinsic, and common coagulation pathways.	Anticoagulant activity	[296]

Table 11. *Cont.*

Type of Seaweed	Bioactive Metabolites/Compounds	Mechanism of Action	Biological Activity	References
Neuroprotective Activity and Alzheimer's Disease (AD)				
Pigments				
Macroalgae	Carotenoids	The potent antioxidant properties of carotenoids may explain the neuroprotective effects of carotenoids by inhibiting neuroinflammation and activating autophagy.	Neuroprotective activity	[297]
Polysaccharides				
Macroalgae	Polysaccharides	Seaweed polysaccharides reduced lipid peroxidation and erythrocyte hemolysis.	Alzheimer's disease	[298]
Ecklonia cava—brown algae	Fucoidan	Polysaccharide extracts inhibit BACE-1 protease, resulting in decreased amyloid-beta.	Alzheimer's disease	[299]
Fatty acids				
Sargassum fusiforme	Fatty acids extract	Derived lipid extract to AD mice significantly improved short-term memory and reduced hippocampal Aβ plaque load by 81%	Alzheimer's disease	[300]
Antiprotozoal Activitaty				
Polyphenolic compound				
Padina boryana—brown algae	Ellagic acid	Activity against *Trypzanosoma cruzi* showed a value of IC50 = 9.2 ± 0.87 μg/mL and against *Leishmania donovani*, showed IC50 = 8.87 ± 2.3 μg/mL	Antiprotozoal activity	[255]
Bone Deficiencies				
Minerals				
Valoniopsis pachynema—green algae	Calcium	Calcium to improve bone density	Bone deficiencies	[293]
Ulva lactuca (as *Ulva fasciata*)—green algae	Ca, Mg, Na, K, and Fe	Supplementing the body with exogenous daily intake. Calcium to improve bone density	Bone deficiencies	[301]
Malnutrition				
Vitamins				
Saccharina japonica—brown algae	Vitamin B9, B12	Supplementing daily intake	Malnutrition	[302]

5. Nutraceutical Applications

Functional food or nutraceutical food are foods that provide not only nutritional value but can also help prevent health problems. Seaweed-based foods are considered nutraceutical products due to their positive effects on human health, for example, in anti-cancer diseases, in cardiovascular diseases for diabetes amelioration and as antioxidants, antimicrobials, and anti-inflammatory agents, as reported by Lomartire et al. (2021) [19].

5.1. Anti-Nutritional Compounds

Several studies have identified the presence of anti-nutritional compounds in seaweeds. Ahmed et al. (2024) reported that seaweeds contain anti-nutrients such as phytic acid, polyphenolic compounds (e.g., tannins), phlorotannins, lectins, and inhibitors of amylase and trypsin, which can impact the bioavailability and digestibility of nutrients like proteins and trace elements [212]. However, Choudhary et al. (2023) noted that these compounds were found in such small quantities that they are considered harmless. Their study also highlighted that while alkaloids can be toxic at high concentrations due to their interference with electrochemical transmissions in the nervous system, they are safe at low levels [53]. Additionally, Choudhary et al. (2023) detected only trace amounts of tannic acid and phytic acid in various seaweed samples, making their presence negligible, and found no detectable saponins, which can affect metabolism by inhibiting certain digestive enzymes [53].

Beyond anti-nutritional compounds, Xu et al. (2023) warned that nutrient losses in seaweed-derived products can occur due to processing and poor digestion in the human body [213]. Another concern, highlighted by Ownsworth et al. (2019), is seaweeds' tendency to accumulate metals, and other pollutants [303]. Studies have shown that the accumulation of inorganic arsenic increases the risk of cancer, nervous system disorders, and cardiovascular diseases [213,303]. Cadar et al. (2018, 2019) studied the content of potentially toxic heavy metals (Pb, Cd, Cu, and Zn) included *in Cystoseira barbata*, *Ceramium rubrum*, *Ulva lactuca*, *Ulva intestinalis*, and *Cladophora vagabunda*, harvested from the Black Sea, and showed the maintenance of low levels of pollution of contaminants of algal biomass in terms of heavy metal content [9,304].

Given these concerns, Ahmed et al. (2024), Xu et al. (2023), and Silva et al. (2024) emphasized the need to develop high-value seaweed-based foods while detecting and minimizing toxic substance concentrations to ensure they meet health standards [212–214].

5.2. Nutraceutical Applications of Marine Algae Products

Based on the medical benefits of biocompounds from marine macroalgae, these algae can be used as functional foods in various forms, such as staple foods or beverages. Mendes et al. (2022) highlight that algae-based foods have become increasingly important in Europe, as they serve as a natural source of micro- and macronutrients, along with trace elements, which enhance their nutritional and pharmacological value [305]. Peñalver et al. (2020) argue that algae are a natural resource of significant interest, as they contain compounds with diverse biological activities and can be used as functional ingredients in numerous technological applications to create functional foods [116]. For example, plant-based oils contain other bioactive compounds, such as oil-soluble vitamins, phytosterols, tocopherols, and pigments, but terrestrial crops typically lack essential ω-3 fatty acids, like EPA or DHA. Belkacemi et al. (2020) note that seaweed and phytoplankton are the primary producers of ω-3 polyunsaturated fatty acids (PUFAs), making them a promising source for nutraceutical applications [306]. Geranpour et al. (2020) reported studies on the spray-drying encapsulation of fatty acids and functional oils [307]. Mouritsen et al. (2019)

demonstrate that seaweed can be consumed as food or as an ingredient in prepared foods in various forms, including fresh, fermented, dried, or frozen, either whole or processed into flakes, granules, or powders [308]. Cornish et al. (2019) describe how, in Brittany, dulse and kombu are used to prepare the traditional "bread of the sea" (bara mor), while minced seaweed in butter (beurre des algues) is used to cook fish or spread on bread to accompany shellfish [309]. Granato et al. (2020) note that the current trend is to select new natural resources with added health benefits, specifically functional foods [310]. Tanna et al. (2018) emphasize the growing interest in secondary metabolites from marine macroalgae with antioxidant properties, particularly for nutraceutical applications [311]. El-Beltagi et al. (2022) provide a comprehensive review that characterizes active biocompounds as secondary metabolites, helping to understand the progress and limitations of seaweeds' bioactivity as nutraceuticals [312]. Cotas et al. (2020) mention that several macroalgae products possess exceptional nutraceutical, pharmacological, and biomedical properties, with key compounds including fatty acids, pigments, phenols, and polysaccharides [313]. Ganesan et al. (2019) demonstrate that seaweed bioactives, including polysaccharides, pigments, fatty acids, polyphenols, and peptides, exhibit various beneficial biological properties that could enhance functional foods and nutraceutical products [314]. Din et al. (2022) show that brown algae can be used as a functional food source of fucoxanthin [3]. André et al. (2021) indicate that brown algae can be used as a functional food to combat hypercholesterolemia [15]. Barot et al. (2019) suggest that the nutritional composition of seaweeds makes them a potential source of natural food [314]. Lastly, Shannon et al. (2019) discuss recent advancements in the use of seaweed for human health from an epidemiological standpoint and as a functional food ingredient [315].

6. Conclusions

The active biocompounds in seaweeds make them, as a natural resource, attract attention not only as food but also as sources for various naturally pharmacologically active products and nutraceuticals. We can state that the medical and nutraceutical benefits of seaweeds are supported by the biological activities documented on multiple studies related to antitumor, antioxidant, cardioprotective, antimicrobial, and anti-inflammatory effects, as well as their role in the management of metabolic diseases, malnutrition, and Alzheimer's disease. This review is important because it primarily utilizes a systematic and unitary approach to the information on the classification and description of macroalgal species, their nutritional composition, and various extraction methods. Each category of biocompounds from the three algal types is analyzed in terms of chemical structure, extraction techniques, and quantitative analysis. The characterization of algal biocompounds, as active secondary metabolites, was also complemented by their medical and nutraceutical applications, in alternative treatments for various ailments compared to classical medicine that uses drugs obtained by chemical synthesis.

A significant challenge, however, is the potential presence of harmful pollutants (e.g., heavy metals, high iodine content, or other toxic compounds), which need to be carefully considered in terms of risks to human health. The growing interest in bioactive substances with proven therapeutic potential has led to the need for modern, environmentally friendly extraction, purification, and analysis techniques. These advances are essential for the development of value-added functional products that promote human health.

Future directions for research on seaweed-derived bioactive compounds need to focus on the optimization of modern extraction techniques (such as enzyme-assisted and ultrasound-assisted methods) to improve the efficiency and yield of extractions. The discovery of novel compounds from unexplored seaweed species presents opportunities

for pharmaceutical and nutraceutical applications. More in-depth clinical studies are also needed to validate their health benefits, bioavailability, and safety.

Exploring the incorporation of algae as functional foods and supplements could enhance both their commercial viability and contribution to global food security. Advances in marine biotechnology, including genetic engineering, may boost the production of high-value compounds, while sustainable farming methods are crucial for meeting rising demand without harming marine biodiversity. Further research should investigate their potential in preventing chronic diseases such as cancer, cardiovascular disease, diabetes, and neurodegenerative disorders. Additionally, nanoformulation strategies could improve the stability and delivery of bioactive compounds, opening new avenues for targeted drug therapies.

With rising inflation in recent years, the commercial use of algae for health and nutrition shows promising growth. However, making seaweed more palatable remains a key challenge for consumer acceptance as a functional food. Meeting the demand for raw seaweed requires both cost-effective production and the exploration of previously overlooked natural sources.

Author Contributions: Conceptualization E.C., A.-M.-L.D., C.P., A.-M.P., A.P. and R.S.; methodology, E.C., A.-M.I., C.L.T., C.F.B.-A., A.P. and R.S.; writing—original draft preparation A.-M.-L.D., C.P., A.-M.P., R.S., A.P., E.C., A.-M.I., C.L.T., V.A., I.P., B.S.V. and C.F.B.-A.; writing—review and editing, R.S., A.-M.-L.D., C.P., A.-M.P., E.C., A.P., C.F.B.-A., V.A., I.P., B.S.V. and A.-M.I.; supervision, E.C., A.P., A.-M.I. and R.S. All authors have read and agreed to the published version of the manuscript.

Funding: This research received no external funding.

Conflicts of Interest: The authors declare no conflicts of interest.

Abbreviations

SFE	Supercritical Fluid Extraction	HPLC	High-performance liquid chromatography
SWE	Subcritical Water Extraction	CG-MS	Gas Chromatography coupled with mass spectrometry
SFE	Supercritical Fluid Extraction	GP	Glycoproteins
PSE	Pressurized Solvents Extraction	AGPs	Arabinogalactan proteins
MAE	Microwave-Assisted Extraction	PBPs	Phycobiliproteins
EAE	Enzyme-Assisted Extraction	TPC	Total phenolic content
UAE	Ultrasound-assisted extraction	TFC	Total flavonoid content
CSE	Conventional Solvent Extraction	DPPH	2,2-diphenyl-1-picrylhydrazyl
SLE	Solid–Liquid Extraction	ABTS	2,2′-azino-bis(3-ethylbenzothi-azoline-6-sulfonic acid
LLE	Liquid–Liquid Extraction	TEAC	Trolox equivalent antioxidant capacity
CSE	Conventional solvent extraction	FRAP	Ferric reducing ability of plasm
MAPs	Marine algae Polysaccharides	AAS	Atomic absorption spectroscopy
AF	Fatty acids	ICP-MS	Inductively coupled plasma mass spectrometry.
MUFAs	Monounsaturated fatty acids	SFAs	Saturated fatty acids
PUFAs	Polyunsaturated fatty acids	EPA	Eicosapentaenoic acid
DHA	Docosahexaenoic acid	ACE inhibitors	Angiotensin-converting enzyme (ACE) inhibitors

References

1. Leandro, A.; Pacheco, D.; Cotas, J.; Marques, J.C.; Pereira, L.; Gonçalves, A.M.M. Seaweed's Bioactive Candidate Compounds to Food Industry and Global Food Security. *Life* **2020**, *10*, 140. [CrossRef] [PubMed]
2. Lopez-Santamarina, A.; Miranda, J.M.; Del Carmen Mondragon, A.; Lamas, A.; Cardelle-Cobas, A.; Franco, C.M.; Cepeda, A. Potential use of marine seaweeds as prebiotics: A review. *Molecules* **2020**, *25*, 1004. [CrossRef] [PubMed]

3. Din, N.A.S.; Mohd Alayudin, A.S.; Sofian-Seng, N.S.; Rahman, H.A.; Mohd Razali, N.S.; Lim, S.J.; Wan Mustapha, W.A. Brown Algae as Functional Food Source of Fucoxanthin: A Review. *Foods* **2022**, *11*, 2235. [CrossRef]
4. Cadar, E.; Axinte, E.R.; Amzoiu, M.; Jurja, S.; Cherim, M. Preliminary study on the marine algae from the romanian Black Sea coast. *J. Sci. Arts* **2019**, *4*, 989–1000.
5. Ferrara, L. Seaweeds: A Food for Our Future. *J. Food Chem. Nanotechnol.* **2020**, *6*, 56–64. [CrossRef]
6. Ferdouse, F.; Holdt, S.L.; Smith, R.; Murúa, P.; Yang, Z. *The Global Satus of Seaweed Production, Trade and Utilization*; Pub. FAO Report Global Seaweed 2018; Food and Agriculture Organization of the United Nations: Rome, Italy, 2018; Volume 124, pp. 1–77. Available online: https://orbit.dtu.dk/en/publications/the-global-status-of-seaweed-production-trade-and-utilization (accessed on 24 February 2025).
7. Embling, R.; Neilson, L.; Randall, T.; Mellor, C.; Lee, D.M.; Wilkinson, L.L. Edible seaweeds as an alternative to animal-based proteins in the UK: Identifying product beliefs and consumer traits as drivers of consumer acceptability for macroalgae. *Food Qual. Prefer.* **2022**, *100*, 104613–104623. [CrossRef]
8. Cherry, P.; O'Hara, C.; Magee, P.J.; McSorley, E.M.; Allsopp, P.J. Risks and benefits of consuming edible seaweeds. *Nutr. Rev.* **2019**, *77*, 307–329. [CrossRef]
9. Cadar, E.; Sirbu, R.; Negreanu-Pirjol, B.S.; Ionescu, A.-M.; Negreanu-Pirjol, T. Heavy metals bioaccumulation capacity on marine algae biomass from romanian Black Sea coast. *Rev. Chim.* **2019**, *70*, 3065–3072. [CrossRef]
10. Cherim, M.; Sirbu, R.; Tomescu, A.; Popa, M.F.; Cadar, E. Comparative studies on the physico-chemical characteristics of biomaterials with collagen from calf and fish skins from Black Sea. *Mater. Plast.* **2019**, *56*, 179–185. [CrossRef]
11. Sirbu, R.; Mustafa, A.; Tomescu, A.; Stanciu, G.; Cadar, E. Rheological and microbiological study on biocomposites with marine chitosan polymers from Black Sea stone crabs used in medical therapy of tissue regeneration. *Mater. Plast.* **2019**, *56*, 148–155. [CrossRef]
12. Araújo, R.; Vázquez Calderón, F.; Sánchez López, J.; Azevedo, I.C.; Bruhn, A.; Fluch, S.; Garcia Tasende, M.; Ghaderiardakani, F.; Ilmjärv, T.; Laurans, M.; et al. An Emerging sector of the blue bioeconomy. *Front. Mar. Sci.* **2021**, *7*, 626389. [CrossRef]
13. Cai, J. *Global Status of Seaweed Production, Trade and Utilization*; Food and Agriculture Organisation of United Nations: Rome, Italy, 2021; pp. 1–18. Available online: https://www.competecaribbean.org/wp-content/uploads/2021/05/Global-status-of-seaweed-production-trade-and-utilization-Junning-Cai-FAO.pdf (accessed on 24 February 2025).
14. FAO. Fishery and Aquaculture Statistics. Global Production Statistics 1950–2019. In FAO Fisheries Division. FishStaJ—Software for Fishery and Aquaculture Statistical Time Series. 2021. Available online: https://www.fao.org/fishery/en/statistics/software/fishstatj/en (accessed on 1 September 2022).
15. André, R.; Pacheco, R.; Bourbon, M.; Serralheiro, M.L. Brown, Algae Potential as a Functional Food against Hypercholesterolemia: Review. *Foods* **2021**, *10*, 234. [CrossRef] [PubMed]
16. Ouyang, Y.; Qiu, Y.; Liu, Y.; Zhu, R.; Chen, Y.; El-Seedi, H.R.; Chen, X.; Chao Zhao, C. Cancer-fighting potentials of algal polysaccharides as nutraceuticals. *Food Res. Int.* **2021**, *147*, 110522. [CrossRef]
17. Moga, M.A.; Dima, L.; Balan, A.; Blidaru, A.; Dimienescu, O.G.; Podasca, C.; Toma, S. Are Bioactive Molecules from Seaweeds a Novel and Challenging Option for the Prevention of HPV Infection and Cervical Cancer Therapy?—A Review. *Int. J. Mol. Sci.* **2021**, *22*, 629. [CrossRef] [PubMed]
18. Saeed, M.; Arain, M.A.; Ali Fazlani, S.; Marghazani, I.B.; Umar, M.; Soomro, J.; Bhutto, Z.A.; Soomro, F.; Noreldin, A.E.; Alagawany, M. A comprehensive review on the health benefits and nutritional significance of fucoidan polysaccharide derived from brown seaweeds in human, animals and aquatic organisms. *Aquac. Nutr.* **2021**, *27*, 633–654. [CrossRef]
19. Lomartire, S.; Marques, J.C.; Gonçalves, A.M. An Overview to the Health Benefits of Seaweeds Consumption. *Mar. Drugs* **2021**, *19*, 341. [CrossRef] [PubMed]
20. FAO; WHO. *Report of the Expert Meeting on Food Safety for Seaweed—Current Status and Future Perspectives*; Food Safety and Quality Series No. 13; FAO: Rome, Italy, 2022; Available online: https://www.fao.org/fishery/en/publication/289063 (accessed on 24 February 2025).
21. Park, E.; Yu, H.; Lim, J.-H.; Choi, J.H.; Park, K.J.; Lee, J. Seaweed metabolomics: A review on its nutrients, bioactive compounds and changes in climate change. *Food Res. Int.* **2023**, *163*, 112221. [CrossRef]
22. Beaumont, M.; Tran, R.; Vera, G.; Niedrist, D.; Rousset, A.; Pierre, R.; Shastri, V.P.; Forget, A. Hydrogel-Forming Algae Polysaccharides: From Seaweed to Biomedical Applications. *Biomacromolecules* **2021**, *22*, 1027–1052. [CrossRef]
23. Caf, F.N.; Özdemira, N.S.; Yılmazb, O.; Durucanc, F.; Akd, I. Fatty acid and lipophilic vitamin composition of seaweeds from Antalya and Çanakkale (Turkey). *Grasas Aceites* **2019**, *70*, e312. [CrossRef]
24. Zhong, R.; Wan, X.; Wang, D.; Zhao, C.; Liu, D.; Gao, L.; Wang, M.; Wu, C.; Nabavid, S.M.; Daglia, M.; et al. Polysaccharides from Marine Enteromorpha: Structure and function. *Trends Foods Sci. Technol.* **2020**, *99*, 11–20. [CrossRef]
25. Pereira, L. Macroalgae. *Encyclopedia* **2021**, *1*, 177–188. [CrossRef]

26. Cadar, E.; Cherim, M. Studies on the physico-chemical characteristics of the marine algae ecosystem from the Romanian Black Sea. *J. Sci. Arts* **2018**, *3*, 717–726.
27. Gaspar, R.; Fonseca, R.; Pereira, L. *Illustrated Guide to the Macroalgae of Buarcos Bay, Figueira da Foz, Portugal*, 1st ed.; MARE UC, DCV, FCT: Coimbra, Portugal, 2020; pp. 3–129. [CrossRef]
28. Veluchamy, C.; Palaniswamy, R. A Review on Marine Algae and its Applications. *Asian J. Pharm. Clin. Res.* **2020**, *13*, 21–27. [CrossRef]
29. Kennedy, J. Marine Algae: The 3 Types of Seaweed. 2019. Available online: https://www.thoughtco.com/types-of-marinealgae-2291975 (accessed on 24 February 2025).
30. Sirbu, R.; Negreanu-Pirjol, T.; Mirea, M.; Negreanu-Pirjol, B.S. Bioactive Compounds from Three Green Algae Species along Romanian Black Sea Coast with Therapeutically Properties. *Eur. J. Nat. Sci. Med.* **2020**, *3*, 67–86. [CrossRef]
31. Sirbu, R.; Stanciu, G.; Tomescu, A.; Ionescu, A.M.; Cadar, E. Evaluation of Antioxidant and Antimicrobial Activity in Relation to Total Phenolic Content of Green Algae from Black Sea. *Rev. Chim.* **2019**, *70*, 1197–1203. [CrossRef]
32. Tanna, B.; Choudhary, B.; Mishra, A.; Chauhan, O.P.; Patel, M.K.; Shokralla, S.; El-Abedin, T.K.Z.; Elansary, H.O.; Mahmoud, E.A. Antioxidant, Scavenging, Reducing, and Anti-Proliferative Activities of Selected Tropical Brown Seaweeds Confirm the Nutraceutical Potential of *Spatoglossum asperum*. *Foods* **2021**, *10*, 2482. [CrossRef]
33. Hakim, M.M.; Patel, I.C. A review on phytoconstituents of marine brown algae. *Future J. Pharm. Sci.* **2020**, *6*, 129. [CrossRef]
34. Badar, S.N.; Mohammad, M.; Emdadi, Z.; Yaakob, Z. Algae and their growth requirements for bioenergy: A review. *Biofuels* **2021**, *12*, 307–325. [CrossRef]
35. Buschmann, A.H.; Camus, C. An introduction to farming and biomass utilisation of marine macroalgae. *Phycologia* **2019**, *58*, 443–445. [CrossRef]
36. Muñoz-Molina, N.; Parada, J.; Simirgiotis, M.; Montecinos-González, R. The Potential of Using Cochayuyo (*Durvillaea incurvata*) Extract Obtained by Ultrasound-Assisted Extraction to Fight against Aging-Related Diseases. *Foods* **2024**, *13*, 269. [CrossRef]
37. Pacheco, L.V.; Parada, J.; Pérez-Correa, J.R.; Mariotti-Celis, M.S.; Simirgiotis, M. Cochayuyo (*Durvillaea incurvata*) extracts: Their impact on starch breakdown and antioxidant activity in pasta during in vitro digestion. *Foods* **2023**, *12*, 3326. [CrossRef] [PubMed]
38. Kumar, B.R.; Mathimani, T.; Sudhakar, M.P.; Rajendran, K.; Nizami, A.-S.; Brindhadevi, K.; Pugazhendhi, A. A state of the art review on the cultivation of algae for energy and other valuable products: Application, challenges, and opportunities. *Renew. Sustain. Energy Rev.* **2021**, *138*, 110649. [CrossRef]
39. Suthar, P.; Gajaria, T.K.; Reddy, C.R.K. Production of quality seaweed biomass through nutrient optimization for the sustainable land-based cultivation. *Algal Res.* **2019**, *42*, 101583. [CrossRef]
40. Hwang, E.K.; Park, C.S. Seaweed cultivation and utilization of Korea. *Algae* **2020**, *35*, 107–121. [CrossRef]
41. Obando, J.M.C.; Cunha dos Santos, T.; Martins, R.C.C.; Teixeira, V.L.; Barbarino, E.; Cavalcanti, D.N. Current and promising applications of seaweed culture in laboratory conditions. *Aquaculture* **2022**, *560*, 738596. [CrossRef]
42. Regal, A.L.; Alves, V.; Gomes, R.; Matos, J.; Bandarra, N.M.; Afonso, C.; Cardoso, C. Drying process, storage conditions, and time alter the biochemical composition and bioactivity of the anti-greenhouse seaweed *Asparagopsis taxiformis*. *Eur. Food Res. Technol.* **2020**, *246*, 781–793. [CrossRef]
43. Olsson, J.; Toth, G.B.; Oerbekke, A.; Cvijetinovic, S.; Wahlstrom, N.; Harrysson, H.; Steinhagen, S.; Kinnby, A.; White, J.; Edlund, U. Cultivation conditions affect the monosaccharide composition in *Ulva fenestrata*. *J. Appl. Phycol.* **2020**, *32*, 3255–3263. [CrossRef]
44. Alvarez-Gomez, F.; Korbee, N.; Figueroa, F.L. Effects of UV Radiation on Photosynthesis, Antioxidant Capacity and the Accumulation of Bioactive Compounds in *Gracilariopsis longissima*, *Hydropuntia cornea* and *Halopithys incurva* (Rhodophyta). *J. Phycol.* **2019**, *55*, 1258–1273. [CrossRef]
45. Sobuj, M.K.A.; Islam, M.A.; Islam, M.S.; Islam, M.M.; Mahmud, Y.; Rafiquzzaman, S.M. Effect of solvents on bioactive compounds and antioxidant activity of *Padina tetrastromatica* and *Gracilaria tenuistipitata* seaweeds collected from Bangladesh. *Sci. Rep.* **2021**, *11*, 19082. [CrossRef]
46. Mansur, A.A.; Brown, M.T.; Billington, R.A. The cytotoxic activity of extracts of the brown alga *Cystoseira tamariscifolia* (Hudson) Papenfuss, against cancer cell lines changes seasonally. *J. Appl. Phycol.* **2020**, *32*, 2419–2429. [CrossRef]
47. Uribe, E.; Pardo-Orellana, C.M.; Vega-Gálvez, A.; Ah-Hen, K.S.; Pastén, A.; García, V.; Aubourg, S.P. Effect of drying methods on bioactive compounds, nutritional, antioxidant, and antidiabetic potential of brown alga *Durvillaea antarctica*. *Dry. Technol.* **2019**, *38*, 1915–1928. [CrossRef]
48. Getachew, A.T.; Holdt, S.L.; Meyer, A.S.; Jacobsen, C. Effect of Extraction Temperature on Pressurized Liquid Extraction of Bioactive Compounds from *Fucus vesiculosus*. *Mar. Drugs* **2022**, *20*, 263. [CrossRef] [PubMed]
49. Cadar, E.; Negreanu-Pirjol, T.; Sirbu, R.; Dragan, A.-M.L.; Negreanu-Pirjol, B.-S.; Axente, E.R.; Ionescu, A.-M. Biocompounds from Green Algae of Romanian Black Sea Coast as Potential Nutraceuticals. *Processes* **2023**, *11*, 1750. [CrossRef]

50. Amlani, M.; Yetgin, S. Seaweeds: Bioactive Components and Properties, Potential Risk Factors, Uses, Extraction and Purification Methods. *Mar. Sci. Technol. Bull.* **2022**, *11*, 9–31. [CrossRef]
51. Jönsson, M.; Allahgholi, L.; Sardari, R.R.R.; Hreggviðsson, G.O.; Nordberg Karlsson, E. Extraction and Modification of Macroalgal Polysaccharides for Current and Next-Generation Applications. *Molecules* **2020**, *25*, 930. [CrossRef]
52. Sirbu, R.; Stanciu, G.; Cadar, E.; Tomescu, A.; Cherim, M. Validation of a Quantitative Analysis Method for Collagen Extracted from *Grey mullet* Marine Fish. *Rev. Chim.* **2019**, *70*, 835–842. [CrossRef]
53. Choudhary, B.; Khandwal, D.; Gupta, N.K.; Patel, J.; Mishra, A. Nutrient composition, physicobiochemical analyses, oxidative stability and antinutritional assessment of abundant tropical seaweeds from the Arabian Sea. *Plants* **2023**, *12*, 2302. [CrossRef]
54. Morais, T.; Inácio, A.; Coutinho, T.; Ministro, M.; Cotas, J.; Pereira, L.; Bahcevandziev, K. Seaweed Potential in the Animal Feed: A Review. *J. Mar. Sci. Eng.* **2020**, *8*, 559. [CrossRef]
55. Ganesan, A.R.; Subramani, K.; Shanmugam, M.; Seedevi, P.; Park, S.; Alfarhan, A.H.; Rajagopal, R.; Balasubramanian, B. A comparison of nutritional value of underexploited edible seaweeds with recommended dietary allowances. *J. King Saud Univ.* **2020**, *32*, 1206–1211. [CrossRef]
56. Metin, C.; Baygar, T. Determination of nutritional composition of *Enteromorpha intestinalis* and investigation of its usage as food. *Ege J. Fish. Aq. Sci.* **2018**, *35*, 7–14. [CrossRef]
57. Cadar, E. Research and Development of Semi-Solid Pharmaceutical Systems Based on Marine Resources. Ph.D. Thesis, IOSUD Carol Davila UMF, Bucharest, Romania, 2017.
58. Premarathna, A.D.; Tuvikene, R.; Fernando, P.H.P. Comparative analysis of proximate compositions, mineral and functional chemical groups of 15 different seaweed species. *Sci. Rep.* **2022**, *12*, 19610. [CrossRef]
59. Rosemary, T.; Arulkumar, A.; Paramasivam, S.; Mondragon-Portocarrero, A.; Miranda, J.M. Biochemical, Micronutrient and Physicochemical Properties of the Dried Red Seaweeds *Gracilaria edulis* and *Gracilaria corticata*. *Molecules* **2019**, *24*, 2225. [CrossRef] [PubMed]
60. Farghl, A.A.M.; Al-Hasawi, Z.M.; El-Sheekh, M.M. Assessment of Antioxidant Capacity and Phytochemical Composition of Brown and Red Seaweeds Sampled off Red Sea Coast. *Appl. Sci.* **2021**, *11*, 11079. [CrossRef]
61. Praiboon, J.; Palakas, S.; Noiraksa, T. Seasonal variation in nutritional composition and anti-proliferative activity of brown seaweed, *Sargassum oligocystum*. *J. Appl. Phycol.* **2018**, *30*, 101–111. [CrossRef]
62. Ilyas, Z.; Ali Redha, A.; Wu, Y.S. Nutritional and Health Benefits of the Brown Seaweed *Himanthalia elongata*. *Plant Foods Hum. Nutr.* **2023**, *78*, 233–242. [CrossRef] [PubMed]
63. Fouda, W.A.; Ibrahim, W.; Ellamie, A.M.; Ramadan, G. Biochemical and mineral composition of six brown seaweeds collected from Red Sea at Hurghada Coast. *Indian J. Mar. Sci.* **2019**, *48*, 484–491.
64. Ullah, M.R.; Akhter, M.; Khan, A.B.S.; Yasmin, F.; Hasan, M.M.; Bosu, A.; Haque, M.A.; Islam, M.S.; Islam, M.A.; Mahmud, Y. Nutritional composition and phenolic contents of *Gracilariopsis longissima*, *Padina tetrastromatica* and *Ulva intestinalis* from the Bay of Bengal, Bangladesh coast. *Heliyon* **2024**, *10*, e31128. [CrossRef]
65. Xie, C.; Lee, Z.J.; Ye, S.; Barrow, C.J.; Dunshea, F.R.; Suleria, H.A.R. A Review on Seaweeds and Seaweed-Derived Polysaccharides: Nutrition, Chemistry, Bioactivities, and Applications. *Food Rev. Int.* **2024**, *40*, 1312–1347. [CrossRef]
66. Choudhary, B.; Chauhan, O.P.; Mishra, A. Edible seaweeds: A potential novel source of bioactive metabolites and nutraceuticals with human health benefits. *Front. Mar. Sci.* **2021**, *8*, 740054. [CrossRef]
67. Dobrinčić, A.; Balbino, S.; Zorić, Z.; Pedisić, S.; Bursać Kovačević, D.; Elez Garofulić, I.; Dragović-Uzelac, V. Advanced Technologies for the Extraction of Marine Brown Algal Polysaccharides. *Mar. Drugs* **2020**, *18*, 168. [CrossRef]
68. Premarathna, A.D.; Ahmed, T.A.E.; Kulshreshtha, G.; Humayun, S.; Darko, C.N.S.; Rjabovs, V.; Hammami, R.; Critchley, A.T.; Tuvikene, R.; Hincke, H.T. Polysaccharides from red seaweeds: Effect of extraction methods on physicochemical characteristics and antioxidant activities. *Food Hydrocoll.* **2024**, *147*, 109307. [CrossRef]
69. Lin, J.; Jiao, G.; Kermanshahi-pour, A. Algal Polysaccharides-Based Hydrogels: Extraction, Synthesis, Characterization, and Applications. *Mar. Drugs* **2022**, *20*, 306. [CrossRef]
70. Ummat, V.; Sivagnanam, S.P.; Rajauria, G.; O'Donnell, C.; Tiwari, B.K. Advances in pre-treatment techniques and green extraction technologies for bioactives from seaweeds. *Trends Food Sci. Technol.* **2021**, *110*, 90–106. [CrossRef]
71. Oh, J.Y.; Kim, E.A.; Kang, S.I.; Yang, H.W.; Ryu, B.; Wang, L.; Lee, J.S.; Jeon, Y.J. Protective Effects of Fucoidan Isolated from Celluclast-Assisted Extract of *Undaria pinnatifida* Sporophylls against AAPH-Induced Oxidative Stress In Vitro and In Vivo Zebrafish Model. *Molecules* **2020**, *25*, 2361. [CrossRef]
72. Yao, W.Z.; Veeraperumal, S.; Qiu, H.-M.; Chen, X.-Q.; Cheong, K.L. Anti-cancer effects of *Porphyra haitanensis* polysaccharides on human colon cancer cells via cell cycle arrest and apoptosis without causing adverse effects in vitro. *3 Biotech* **2020**, *10*, 386. [CrossRef]

73. Akter, A.; Khairul, M.; Sobuj, A.; Islam, S.; Chakroborty, K.; Tasnim, N.; Ayon, M.H.; Hossain, F.; Rafiquzzaman, S.M. Seaweed polysaccharides: Sources, structure and biomedical applications with special emphasis on antiviral potentials. *Future Foods* **2024**, *10*, 100440. [CrossRef]
74. Udo, T.; Gopinath Mummaleti, G.; Mohan, A.; Singh, R.K.; Kong, F. Current and emerging applications of carrageenan in the food industry. *Food Res. Int.* **2023**, *173*, 113369. [CrossRef]
75. Zhang, Y.; Duan, D.; Fu, X.; Gao, X.; Xu, J. Preparation and characterization of agar, agarose, and agaropectin from the red alga *Ahnfeltia plicata*. *J. Oceanol. Limnol.* **2019**, *37*, 815–824. [CrossRef]
76. Dragan, A.M.L.; Sirbu, R.; Cadar, E. Valuable Bioactive Compounds Extracted from *Ceramium rubrum* on the Romanian Seaside with Medical Interest. *Eur. J. Nat. Sci. Med.* **2022**, *5*, 64–74. [CrossRef]
77. Shao, Z.; Duan, D. The Cell Wall Polysaccharides Biosynthesis in Seaweeds: A Molecular Perspective. *Front. Plant Sci.* **2022**, *13*, 902823. [CrossRef]
78. Wang, S.H.; Huang, C.Y.; Chen, C.Y.; Chang, C.C.; Huang, C.Y.; Dong, C.D.; Chang, J.S. Structure and Biological Activity Analysis of Fucoidan Isolated from *Sargassum siliquosum*. *ACS Omega* **2020**, *5*, 32447–32455. [CrossRef]
79. Dragan, A.M.L.; Sirbu, R.; Cadar, E. Brown Seaweeds from Black Sea Coast as an Important Source of Bioactive Compouns of Interest for Human Health. *Eur. J. Nat. Sci. Med.* **2023**, *6*, 100–113. [CrossRef]
80. Rajauria, G.; Ravindran, R.; Garcia-Vaquero, M.; Rai, D.K.; Sweeney, T.; O'Doherty, J. Molecular Characteristics and Antioxidant Activity of Laminarin Extracted from the Seaweed Species *Laminaria hyperborea*, Using Hydrothermal-Assisted Extraction and a Multi-Step Purification Procedure. *Food Hydrocoll.* **2021**, *112*, 106332. [CrossRef]
81. Li, Y.; Zheng, Y.; Zhang, Y.; Yang, Y.; Wang, P.; Imre, B.; Wong, A.C.Y.; Hsieh, Y.S.Y.; Wang, D. Brown Algae Carbohydrates: Structures, Pharmaceutical Properties, and Research Challenges. *Mar. Drugs* **2021**, *19*, 620. [CrossRef]
82. Tanna, B.; Mishra, A. Nutraceutical Potential of Seaweed Polysaccharides: Structure, Bioactivity, Safety, and Toxicity. *Compr. Rev. Food Sci. Food Saf.* **2019**, *18*, 817–831. [CrossRef] [PubMed]
83. Ramos, P.E.; Silva, P.; Alario, M.M.; Pastrana, L.M.; Teixeira, J.A.; Cerqueira, M.A.; Vicente, A.A. Effect of Alginate Molecular Weight and M/G Ratio in Beads Properties Foreseeing the Protection of Probiotics. *Food Hydrocoll.* **2018**, *77*, 8–16. [CrossRef]
84. Pengyan, Z.; Chang, L.; Zhanru, S.; Fuli, L.; Jianting, Y.; Delin, D. Genome-Wide Transcriptome Profiling and Characterization of Mannuronan C5-Epimerases in *Saccharina Japonica*. *Algal Res.* **2021**, *60*, 102491. [CrossRef]
85. Abka-khajouei, R.; Tounsi, L.; Shahabi, N.; Patel, A.K.; Abdelkafi, S.; Michaud, P. Structures, Properties and Applications of Alginates. *Mar. Drugs* **2022**, *20*, 364. [CrossRef]
86. Glasson, C.R.K.; Luiten, C.A.; Carnachan, S.M.; Daines, A.M.; Kidgell, J.T.; Hinkley, S.F.R.; Praeger, C.; Martinez, M.A.; Sargison, L.; Magnusson, M. Structural Characterization of Ulvans Extracted from Blade *Ulva ohnoi* and Filamentous (*Ulva tepida* and *Ulva prolifera*) Species of Cultivated *Ulva*. *Int. J. Biol. Macromol.* **2022**, *194*, 571–579. [CrossRef]
87. Li, Q.; Hu, F.; Zhu, B.; Ni, F.; Yao, Z. Insights into *Ulvan lyase*: Review of source, biochemical characteristics, structure and catalytic mechanism. *Crit. Rev. Biotechnol.* **2020**, *40*, 432–441. [CrossRef]
88. Sari-Chmayssem, N.; Taha, S.; Mawlawi, H.; Guegan, J.P.; Jeftić, J.; Benvegnu, T. Extracted Ulvans from green seaweeds *Ulva linza* of Lebanese origin and amphiphilic derivatives: Evaluation of their physico-chemical and rheological properties. *J. Appl. Phycol.* **2019**, *31*, 1931–1946. [CrossRef]
89. Ciancia, M.; Ferna'ndez, P.V.; Leliaert, F. Diversity of Sulfated Polysaccharides From Cell Walls of Coenocytic Green Algae and Their Structural Relationships in View of Green Algal Evolution. *Front. Plant Sci.* **2020**, *11*, 554585. [CrossRef]
90. Gomaa, M.; Al-Badaani, A.A.; Hifney, A.F.; Adam, M.S. Utilization of Cellulose and Ulvan from the Green Seaweed *Ulva lactuca* in the Development of Composite Edible Films with Natural Antioxidant Properties. *J. Appl. Phycol.* **2022**, *34*, 2615–2626. [CrossRef]
91. Firdayanti, L.; Yanti, R.; Rahayu, E.S.; Hidayat, C. Carrageenan extraction from red seaweed (*Kappaphycopsis cottonii*) using the bead mill method. *Algal Res.* **2023**, *69*, 102906. [CrossRef]
92. Martín-del-Campo, A.; Fermín-Jiménez, J.A.; Fernández-Escamilla, V.V. Improved extraction of carrageenan from red seaweed (*Chondracantus canaliculatus*) using ultrasound-assisted methods and evaluation of the yield, physicochemical properties and functional groups. *Food Sci. Biotechnol.* **2021**, *30*, 901–910. [CrossRef] [PubMed]
93. Heriyanto, H.; Kustiningsih, I.; Sari, D.K. The effect of temperature and time of extraction on the quality of Semi Refined Carrageenan (SRC). *MATEC Web Conf.* **2018**, *154*, 01034. [CrossRef]
94. Lebbar, S.; Fanuel, M.; Le Gall, S.; Falourd, X.; Ropartz, D.; Bressollier, P.; Gloaguen, V.; Faugeron-Girard, C. Agar Extraction By-Products from *Gelidium sesquipedale* as a Source of Glycerol-Galactosides. *Molecules* **2018**, *23*, 3364. [CrossRef]
95. Martínez-Sanz, M.; Gómez-Mascaraque, L.G.; Ballester, A.R.; Martínez-Abad, A.; Brodkorb, A.; López-Rubio, A. Production of unpurified agar-based extracts from red seaweed *Gelidium sesquipedale* by means of simplified extraction protocols. *Algal Res.* **2019**, *38*, 101420. [CrossRef]

96. Xiao, Q.; Weng, H.; Ni, H.; Hong, Q.; Lin, K.; Xiao, A. Physicochemical and gel properties of agar extracted by enzyme and enzyme-assisted methods. *Food Hydrocoll.* **2019**, *87*, 530–540. [CrossRef]
97. Alboofetileh, M.; Rezaei, M.; Tabarsa, M.; You, S. Ultrasound-assisted extraction of sulfated polysaccharide from *Nizamuddinia zanardinii*: Process optimization, structural characterization, and biological properties. *J. Food Process. Eng.* **2018**, *42*, e12979. [CrossRef]
98. Hmelkov, A.B.; Zvyagintseva, T.N.; Shevchenko, N.M.; Rasin, A.B.; Ermakova, S.P. Ultrasound-assisted extraction of polysaccharides from brown alga *Fucus evanescens*. Structure and biological activity of the new fucoidan fractions. *J. Appl. Phycol.* **2018**, *30*, 2039–2046. [CrossRef]
99. Alboofetileh, M.; Rezaei, M.; Tabarsa, M. Enzyme-assisted extraction of *Nizamuddinia zanardinii* for the recovery of sulfated polysaccharides with anticancer and immune-enhancing activities. *J. Appl. Phycol.* **2019**, *31*, 1391–1402. [CrossRef]
100. Liu, J.; Wu, S.Y.; Chen, L.; Li, Q.J.; Shen, Y.Z.; Jin, L.; Zhang, X.; Chen, P.C.; Wu, M.J.; Choi, J.; et al. Different extraction methods bring about distinct physicochemical properties and antioxidant activities of *Sargassum fusiforme* fucoidans. *Int. J. Biol. Macromol.* **2020**, *155*, 1385–1392. [CrossRef] [PubMed]
101. Hanjabam, M.D.; Kumar, A.; Tejpal, C.S.; Krishnamoorthy, E.; Kishore, P.; Kumar, K.A. Isolation of crude fucoidan from *Sargassum wightii* using conventional and ultra-sonication extraction methods. *Bioact. Carbohydr. Diet. Fibre* **2019**, *20*, 100200. [CrossRef]
102. Montes, L.; Gisbert, M.; Hinojosa, I.; Sineiro, J.; Moreira, R. Impact of drying on the sodium alginate obtained after polyphenols ultrasound-assisted extraction from *Ascophyllum nodosum* seaweeds. *Carbohydr. Polym.* **2021**, *272*, 118455. [CrossRef]
103. Rashedy, S.H.; Abd El Hafez, M.S.M.; Dar, M.A.; Cotas, J.; Pereira, L. Evaluation and Characterization of Alginate Extracted from Brown Seaweed Collected in the Red Sea. *Appl. Sci.* **2021**, *11*, 6290. [CrossRef]
104. Trica, B.; Delattre, C.; Gros, F.; Ursu, A.V.; Dobre, T.; Djelveh, G.; Michaud, P.; Oancea, F. Extraction and Characterization of Alginate from an Edible Brown Seaweed (*Cystoseira barbata*) Harvested in the Romanian Black Sea. *Mar. Drugs* **2019**, *17*, 405. [CrossRef]
105. Malvis Romero, A.; Picado Morales, J.J.; Klose, L.; Liese, A. Enzyme-Assisted Extraction of Ulvan from the Green Macroalgae *Ulva fenestrata*. *Molecules* **2023**, *28*, 6781. [CrossRef]
106. Kidgell, J.T.; Magnusson, M.; de Nys, R.; Glasson, C.R.K. Ulvan: A systematic review of extraction, composition and function. *Algal Res.* **2019**, *39*, 101422. [CrossRef]
107. Yuan, Y.; Xu, X.; Jing, C.; Zou, P.; Zhang, C.; Li, Y. Microwave assisted hydrothermal extraction of polysaccharides from *Ulva prolifera*: Functional properties and bioactivities. *Carbohydr. Polym.* **2018**, *181*, 902–910. [CrossRef]
108. Tabarsa, M.; You, S.; Dabaghian, E.H.; Surayot, U. Water-soluble polysaccharides from *Ulva intestinalis*: Molecular properties, structural elucidation and immunomodulatory activities. *J. Food Drug Anal.* **2018**, *26*, 599–608. [CrossRef] [PubMed]
109. Cikoš, A.M.; Jurin, M.; Čož-Rakovac, R.; Jokić, S.; Jerković, I. Update on Monoterpenes from Red Macroalgae: Isolation, Analysis, and Bioactivity. *Mar. Drugs* **2019**, *17*, 537. [CrossRef]
110. Polzin, J.; Rorrer, G.L. Selective production of the acyclic monoterpene β-myrcene by microplantlet suspension cultures of the macrophytic marine red alga *Ochtodes secundiramea* under nutrient perfusion cultivation with bromide-free medium. *Algal Res.* **2018**, *36*, 159–166. [CrossRef]
111. Chen, J.; Li, H.; Zhao, Z.; Xia, X.; Li, B.; Zhang, J.; Yan, X. Diterpenes from the marine algae of the genus *Dictyota*. *Mar. Drugs* **2018**, *16*, 159. [CrossRef]
112. Rajamani, K.; Balasubramanian, T.; Thirugnanasambandan, S.S. Bioassay-guided isolation of triterpene from brown alga *Padina boergesenii* possess anti-inflammatory and anti-angiogenic potential with kinetic inhibition of β-carotene linoleate system. *LWT* **2018**, *93*, 549–555. [CrossRef]
113. Nie, J.; Chen, D.; Ye, J.; Lu, Y.; Dai, Z. Preparative separation of three terpenoids from edible brown algae *Sargassum fusiforme* by high-speed countercurrent chromatography combined with preparative high-performance liquid chromatography. *Algal Res.* **2021**, *59*, 102449. [CrossRef]
114. Rushdi, M.I.; Abdel-Rahman, I.A.M.; Attia, E.Z.; Saber, H.; Saber, A.A.; Bringmann, G.; Abdelmohsen, U.R. The Biodiversity of the Genus *Dictyota*: Phytochemical and Pharmacological Natural Products Prospectives. *Molecules* **2022**, *27*, 672. [CrossRef]
115. Santos, J.P.; Guihéneuf, F.; Fleming, G.; Chow, F.; Stengel, D.B. Temporal stability in lipid classes and fatty acid profiles of three seaweed species from the north-eastern coast of Brazil. *Algal Res.* **2019**, *41*, 101572. [CrossRef]
116. Peñalver, R.; Lorenzo, J.M.; Ros, G.; Amarowicz, R.; Pateiro, M.; Nieto, G. Seaweeds as a functional ingredient for a healthy diet. *Mar. Drugs* **2020**, *18*, 301. [CrossRef]
117. Foseid, L.; Natvik, I.; Devle, H.; Ekeberg, D. Identification of fatty acids in fractionated lipid extracts from *Palmaria palmata*, *Alaria esculenta* and *Saccharina latissimi* by off-line SPE GC-MS. *J. Appl. Phycol.* **2020**, *32*, 4251–4262. [CrossRef]
118. Rocha, C.P.; Pacheco, D.; Cotas, J.; Marques, J.C.; Pereira, L.; Gonçalves, A.M.M. Seaweeds as Valuable Sources of Essential Fatty Acids for Human Nutrition. *Int. J. Environ. Res. Public Health* **2021**, *18*, 4968. [CrossRef] [PubMed]

119. El-Sheekh, M.M.; Bases, E.A.; El-Shenody, R.A.; El Shafay, S.M. Lipid extraction from some seaweeds and evaluation of its biodiesel production. *Biocatal. Agric. Biotechnol.* **2021**, *35*, 102087. [CrossRef]
120. Jaworowska, A.; Murtaza, A. Seaweed derived Lipids sre a potential Anti-Inflammatory agent: A Review. *Int. J. Environ. Res. Public Health* **2023**, *20*, 730. [CrossRef]
121. Kord, A.; Cherif, Y.F.; Amiali, M.; Mustapha, M.A.; Benfares, R.; Soumia, B.; Belfadel, O. Fatty acids composition of *Cystoseira sauvageauana* and *Laurencia pinnatifida* collected from the algerian coast. *Acta Period. Technol.* **2019**, *50*, 113–122. [CrossRef]
122. Rodríguez-González, I.; Diaz-Reinos, B.; Domínguez, H. Intensification Strategies for the Extraction of Polyunsaturated Fatty Acids and Other Lipophilic Fractions from Seaweeds. *Food Bioprocess Technol.* **2022**, *15*, 978–997. [CrossRef]
123. Susanto, E.; Fahmi, A.S.; Hosokawa, M.; Miyashita, K. Variation in lipid components from 15 species of tropical and temperate seaweeds. *Mar. Drugs* **2019**, *17*, 630. [CrossRef]
124. Pangestuti, R.; Haq, M.; Rahmadi, P.; Chun, B.S. Nutritional value and biofunctionalities of two edible green seaweeds (*Ulva lactuca* and *Caulerpa racemosa*) from Indonesia by subcritical water hydrolysis. *Mar. Drugs* **2021**, *19*, 578. [CrossRef]
125. Lopes, D.; Melo, T.; Rey, F.; Meneses, J.; Monteiro, F.L.; Helguero, L.A.; Abreu, M.H.; Lillebø, A.I.; Calado, R.; Domingues, M.R. Valuing bioactive lipids from green, red and brown macroalgae from aquaculture, to foster functionality and biotechnological applications. *Molecules* **2020**, *25*, 3883. [CrossRef] [PubMed]
126. Lopes, D.; Melo, T.; Meneses, J.; Abreu, M.H.; Pereira, R.; Domingues, P.; Lillebø, A.I.; Calado, R.; Domingues, M.R. A New Look for the Red Macroalga *Palmaria palmata*: A Seafood with Polar Lipids Rich in EPA and with Antioxidant Properties. *Mar. Drugs* **2019**, *17*, 533. [CrossRef]
127. Al-Adilah, H.; Al-Sharrah, T.K.; Al-Bader, D.; Ebel, R.; Küpper, F.C.; Kumari, P. Assessment of Arabian Gulf seaweeds from Kuwait as sources of nutritionally important polyunsaturated fatty acids (PUFAs). *Foods* **2021**, *10*, 2442. [CrossRef]
128. Harwood, J.L. Algae: Critical sources of very long-chain polyunsaturated fatty acids. *Biomolecules* **2019**, *9*, 708. [CrossRef]
129. Pliego-Cortés, H.; Wijesekara, I.; Lang, M.; Bourgougnon, N.; Bedoux, G. Current knowledge and challenges in extraction, characterization and bioactivity of seaweed protein and seaweed-derived proteins, Chapter Nine. In *Advances in Botanical Research*; Bourgougnon, N., Ed.; Elsevier: Amsterdam, The Netherland, 2020; Volume 95, pp. 289–326. [CrossRef]
130. Dhaouafi, J.; Romdhania, M.; Deracinoisa, B.; Flahauta, C.; Nedjara, N.; Baltic, R. Fractionation and identification of bioactive peptides from red macroalgae protein hydrolysates: In silico analysis and in vitro bioactivities. *Biocat. Agric. Biotechnol.* **2024**, *58*, 103211. [CrossRef]
131. Fleurence, J.; Morançais, M.; Dumay, J. Seaweed proteins. In *Proteins in Food Processing*; Yada, Y.R., Ed.; Elsevier: Amsterdam The Netherlands, 2018; Volume 2, pp. 245–262. [CrossRef]
132. Rawiwan, P.; Peng, Y.; Paramayuda, Y.G.P.B.; Quek, S.Y. Red seaweed: A promising alternative protein source for global food sustainability. *Trends Food Sci. Technol.* **2022**, *123*, 37–56. [CrossRef]
133. Feng, X.; Liao, D.; Sun, L.; Wu, S.; Lan, P.; Wang, Z.; Li, C.; Zhou, Q.; Lu, Y.; Lan, X. Affinity Purification of Angiotensin Converting Enzyme Inhibitory Peptides from Wakame (*Undaria pinnatifida*) Using Immobilized ACE on Magnetic Metal Organic Frameworks. *Mar. Drugs* **2021**, *19*, 177. [CrossRef] [PubMed]
134. Ünlü, E.S.; Ünüvar, Ö.C.; Aydın, M. Identification of alternative oxidase encoding genes in *Caulerpa cylindracea* by de novo RNA-Seq assembly analysis. *Mar. Genom.* **2019**, *46*, 41–48. [CrossRef]
135. Echave, J.; Otero, P.; Garcia-Oliveira, P.; Munekata, P.E.S.; Pateiro, M.; Lorenzo, J.M.; Simal-Gandara, J.; Prieto, M.A. Seaweed-Derived Proteins and Peptides: Promising Marine Bioactives. *Antioxidant* **2022**, *11*, 176. [CrossRef]
136. Barre, A.; Simplicien, M.; Benoist, H.; Van Damme, E.J.M.; Rougé, P. Mannose-Specific Lectins from Marine Algae: Diverse Structural Scaffolds Associated to Common Virucidal and Anti-Cancer Properties. *Mar. Drugs* **2019**, *17*, 440. [CrossRef]
137. Vásquez, V.; Martínez, R.; Bernal, C. Enzyme-assisted extraction of proteins from the seaweeds *Macrocystis pyrifera* and *Chondracanthus chamissoi*: Characterization of the extracts and their bioactive potential. *J. Appl. Phycol.* **2019**, *31*, 1999–2010. [CrossRef]
138. O'Connor, J.; Meaney, S.; Williams, G.A.; Hayes, M. Extraction of protein from four different seaweeds using three different physical pre-treatment strategies. *Molecules* **2020**, *25*, 2005. [CrossRef]
139. Vieira, E.F.; Soares, C.; Machado, S.; Correia, M.; Ramalhosa, M.J.; Oliva-teles, M.T.; Paula Carvalho, A.; Domingues, V.F.; Antunes, F.; Oliveira, T.A.C. Seaweeds from the Portuguese coast as a source of proteinaceous material: Total and free amino acid composition profile. *Food Chem.* **2018**, *269*, 264–275. [CrossRef]
140. Sonchaeng, U.; Wongphan, P.; Pan-utai, W.; Paopun, Y.; Kansandee, W.; Satmalee, P.; Tamtin, M.; Kosawatpat, P.; Harnkarnsujarit, N. Preparation and Characterization of Novel Green Seaweed Films from *Ulva rigida*. *Polymers* **2023**, *15*, 3342. [CrossRef]
141. Machado, M.; Machado, S.; Pimentel, F.B.; Freitas, V.; Alves, R.C.; Oliveira, M.B.P.P. Amino acid profile and protein quality assessment of macroalgae produced in an integrated multi-trophic aquaculture system. *Foods* **2020**, *9*, 1382. [CrossRef] [PubMed]

142. Ferreira, M.; Teixeira, C.; Abreu, H.; Silva, J.; Costas, B.; Kiron, V.; Valente, L.M.P. Nutritional value, antimicrobial and antioxidant activities of micro- and macroalgae, single or blended, unravel their potential use for aquafeeds. *J. Appl. Phycol.* **2021**, *33*, 3507–3518. [CrossRef]
143. Trigueros, E.; Sanz, M.T.; Alonso-Riaño, P.; Beltrán, S.; Ramos, C.; Melgosa, R. Recovery of the protein fraction with high antioxidant activity from red seaweed industrial solid residue after agar extraction by subcritical water treatment. *J. Appl. Phycol.* **2021**, *33*, 1181–1194. [CrossRef]
144. Zheng, Y.; Zhang, Y.; San, S. Efficacy of a novel ACE-inhibitory peptide from *Sargassum maclurei* in hypertension and reduction of intracellular endothelin-1. *Nutrients* **2020**, *12*, 653. [CrossRef]
145. Reynolds, D.; Caminiti, J.; Edmundson, S.; Gao, S.; Wick, M.; Huesemann, M. Seaweed proteins are nutritionally valuable components in the human diet. *Am. J. Clin. Nutr.* **2022**, *116*, 855–861. [CrossRef] [PubMed]
146. Manzoor, M.F.; Afraz, M.A.; Yılmaz, B.B.; Adil, M.; Arshad, N.; Goksen, G.; Ali, M.; Zeng, X.-A. Recent progress in natural seaweed pigments: Green extraction, health-promoting activities, techno-functional properties and role in intelligent food packaging. *J. Agric. Food Res.* **2024**, *15*, 100991. [CrossRef]
147. Gomes, L.; Monteiro, P.; Cotas, J.; Gonçalves, A.M.; Fernandes, C.; Gonçalves, T.; Pereira, L. Seaweeds' pigments and phenolic compounds with antimicrobial potential. *Biomol. Concepts* **2022**, *13*, 89–102. [CrossRef]
148. Aryee, A.N.; Agyei, D.; Akanbi, T.O. Recovery and utilization of seaweed pigments in food processing. *Curr. Opin. Food Sci.* **2018**, *19*, 113–119. [CrossRef]
149. Pérez-Gálvez, A.; Viera, I.; Roca, M. Carotenoids and Chlorophylls as Antioxidants. *Antioxidants* **2020**, *9*, 505. [CrossRef]
150. Cotas, J.; Leandro, A.; Pacheco, D.; Gonçalves, A.M.M.; Pereira, L.A. Comprehensive Review of the Nutraceutical and Therapeutic Applications of Red Seaweeds (*Rhodophyta*). *Life* **2020**, *10*, 19. [CrossRef]
151. Ghosh, S.; Sarkar, T.; Pati, S.; Kari, Z.A.; Edinur, H.A.; Chakraborty, R. Novel Bioactive Compounds From Marine Sources as a Tool for Functional Food Development. *Front. Mar. Sci.* **2022**, *9*, 832957. [CrossRef]
152. Manivasagan, P.; Bharathiraja, S.; Santha Moorthy, M.; Mondal, S.; Seo, H.; Dae Lee, K.; Oh, J. Marine natural pigments as potential sources for therapeutic applications. *Crit. Rev. Biotechnol.* **2018**, *38*, 745–761. [CrossRef]
153. Osório, C.; Machado, S.; Peixoto, J.; Bessada, S.; Pimentel, F.B.; Alves, R.C.; Oliveira, M.B.P.P. Pigments Content (Chlorophylls, Fucoxanthin and Phycobiliproteins) of Different Commercial Dried Algae. *Separations* **2020**, *7*, 33. [CrossRef]
154. Fabrowska, J.; Messyasz, B.; Szyling, J.; Walkwik, J.; Łęska, B. Isolation of chlorophylls and carotenoids from freshwater algae using different extraction methods. *Phycol. Res.* **2018**, *66*, 52–57. [CrossRef]
155. Martins, M.; Oliveira, R.; Coutinho, J.A.; Faustino, M.A.F.; Neves, M.G.P.; Pinto, D.C.; Ventura, S.P. Recovery of pigments from *Ulva rigida*. *Sep. Purif. Technol.* **2021**, *255*, 117723. [CrossRef]
156. Nie, J.; Chen, D.; Ye, J.; Lu, Y.; Dai, Z. Optimization and kinetic modeling of ultrasonic-assisted extraction of fucoxanthin from edible brown algae *Sargassum fusiforme* using green solvents. *Ultrason. Sonochem.* **2021**, *77*, 105671. [CrossRef]
157. Carreira-Casais, A.; Otero, P.; Garcia-Perez, P.; Garcia-Oliveira, P.; Pereira, A.G.; Carpena, M.; Soria-Lopez, A.; Simal-Gandara, J.; Prieto, M.A. Benefits and Drawbacks of Ultrasound-Assisted Extraction for the Recovery of Bioactive Compounds from Marine Algae. *Int. J. Environ. Res. Public Health* **2021**, *18*, 9153. [CrossRef]
158. Brain-Isasi, S.; Correa, S.; Amado-Hinojosa, J.; Buschmann, A.H.; Camus, C.; Lienqueo, M.E. Combined extraction methodology for simultaneous recovery of phycobiliproteins and agar from the red alga *Gracilaria chilensis*. CJ Bird, McLachlan & EC Oliveira. *Algal Res.* **2022**, *67*, 102821. [CrossRef]
159. Ktari, L.; Mdallel, C.; Aoun, B.; Chebil Ajjabi, L.; Sadok, S. Fucoxanthin and Phenolic Contents of Six Dictyotales From the Tunisian Coasts With an Emphasis for a Green Extraction Using a Supercritical CO_2 Method. *Front. Mar. Sci.* **2021**, *8*, 647159. [CrossRef]
160. Martínez, J.M.; Gojkovic, Z.; Ferro, L.; Maza, M.; Álvarez, I.; Raso, J.; Funk, C. Use of pulsed electric field permeabilization to extract astaxanthin from the Nordic microalga *Haematococcus pluvialis*. *Bioresour. Technol.* **2019**, *289*, 121694. [CrossRef] [PubMed]
161. Magdugo, R.P.; Terme, N.; Lang, M.; Pliego-Cortés, H.; Marty, C.; Hurtado, A.Q.; Bedoux, G.; Bourgougnon, N. An Analysis of the Nutritional and Health Values of *Caulerpa racemosa* (Forsskål) and *Ulva fasciata* (Delile)—Two Chlorophyta Collected from the Philippines. *Molecules* **2020**, *25*, 2901. [CrossRef]
162. Palaniyappan, S.; Sridhar, A.; Kari, Z.A.; Téllez-Isaías, G.; Ramasamy, T. Evaluation of Phytochemical Screening, Pigment Content, In Vitro Antioxidant, Antibacterial Potential and GC-MS Metabolite Profiling of Green Seaweed *Caulerpa racemosa*. *Mar. Drugs* **2023**, *21*, 278. [CrossRef] [PubMed]
163. Kurniawan, R.; Nurkolis, F.; Taslim, N.A.; Subali, D.; Surya, R.; Gunawan, W.B.; Alisaputra, D.; Mayulu, N.; Salindeho, N.; Kim, B. Carotenoids Composition of Green Algae *Caulerpa racemosa* and Their Antidiabetic, Anti-Obesity, Antioxidant, and Anti-Inflammatory Properties. *Molecules* **2023**, *28*, 3267. [CrossRef] [PubMed]

164. Othman, R.; Amin, N.A.; Sani, M.S.A.; Fadzillah, N.A.; Jamaludin, M.A. Carotenoid and Chlorophyll Profiles in Five Species of Malaysian Seaweed as Potential Halal Active Pharmaceutical Ingredient (API). *Int. J. Adv. Sci. Eng. Inf. Techol.* **2018**, *8*, 1610–1616.
165. Babadi, F.E.; Boonnoun, P.; Nootong, K.; Powtongsook, S.; Goto, M.; Shotipruk, A. Identification of carotenoids and chlorophylls from green algae *Chlorococcum humicola* and extractionby liquefied dimethyl ether. *Food Bioprod. Process.* **2020**, *123*, 296–303. [CrossRef]
166. Bhat, I.; Haripriya, G.; Jogi, N.; Mamatha, B.S. Carotenoid composition of locally found seaweeds of Dakshina Kannada district in India. *Algal Res.* **2021**, *53*, 102154. [CrossRef]
167. Balasubramaniam, V.; Chelyn, L.J.; Vimala, S.; Mohd Fairulnizal, M.N.; Brownlee, I.A.; Amin, I. Carotenoid composition and antioxidant potential of *Eucheuma denticulatum*, *Sargassum polycystum* and *Caulerpa lentillifera*. *Heliyon* **2020**, *6*, e04654. [CrossRef]
168. Lourenço-Lopes, C.; Fraga-Corral, M.; Garcia-Perez, P.; Carreira-Casais, A.; Silva, A.; Simal-Gandara, J.; Prieto, M.A. A HPLC -DAD method for identifying and estimating the content of fucoxanthin, β-carotene and chlorophyll a in brown algal extracts. *Food Chem. Adv.* **2022**, *1*, 100095. [CrossRef]
169. Negreanu-Pîrjol, T.; Sîrbu, R.; Mirea, M.; Negreanu-Pîrjol, B.S. Antioxidant Activity Correlated with Chlorophyll Pigments and Magnesium Content of some Green Seaweeds. *Eur. J. Nat. Sci. Med.* **2020**, *3*, 87–96. [CrossRef]
170. Getachew, A.T.; Jacobsen, C.; Holdt, S.L. Emerging Technologies for the Extraction of Marine Phenolics: Opportunities and Challenges. *Mar. Drugs* **2020**, *18*, 389. [CrossRef] [PubMed]
171. Jacobsen, C.; Sørensen, A.D.M.; Holdt, S.L.; Akoh, C.C.; Hermund, D.B. Source, extraction, characterization, and applications of novel antioxidants from seaweed. *Annu. Rev. Food Sci. Technol.* **2019**, *10*, 541–568. [CrossRef] [PubMed]
172. Tenorio-Rodríguez, P.A.; Esquivel-Solis, H.; Murillo-Álvarez, J.I.; Ascencio, F.; Campa-Córdova, Á.I.; Angulo, C. Biosprospecting potential of kelp (Laminariales, Phaeophyceae) from Baja California Peninsula: Phenolic content, antioxidant properties, anti-inflammatory, and cell viability. *J. Appl. Phycol.* **2019**, *31*, 3115–3129. [CrossRef]
173. Abdelhamid, A.; Lajili, S.; Elkaibi, M.A.; Ben Salem, Y.; Abdelhamid, A.; Muller, C.D.; Majdoub, H.; Kraiem, J.; Bouraoui, A. Optimized extraction, preliminary characterization and evaluation of the in vitro anticancer activity of phlorotannin-rich fraction from the Brown Seaweed, *Cystoseira sedoides*. *J. Aquat. Food Prod. Technol.* **2019**, *28*, 892–909. [CrossRef]
174. Vijayan, R.; Chitra, L.; Penislusshiyan, S.; Palvannan, T. Exploring bioactive fraction of *Sargassum wightii*: In vitro elucidation of angiotensin-I-converting enzyme inhibition and antioxidant potential. *Int. J. Food Prop.* **2018**, *21*, 674–684. [CrossRef]
175. Catarino, M.; Silva, A.; Mateus, N.; Cardoso, S. Optimization of phlorotannins extraction from *Fucus vesiculosus* and evaluation of their potential to prevent metabolic disorders. *Mar. Drug* **2019**, *17*, 162. [CrossRef]
176. Ojha, K.S.; Aznar, R.; O'Donnell, C.; Tiwari, B.K. Ultrasound technology for the extraction of biologically active molecules from plant, animal and marine sources. *(TrAC) Trends Anal. Chem.* **2020**, *122*, 115663. [CrossRef]
177. Garcia-Vaquero, M.; Ummat, V.; Tiwari, B.; Rajauria, G. Exploring ultrasound, microwave and ultrasound–microwave assisted extraction technologies to increase the extraction of bioactive compounds and antioxidants from brown macroalgae. *Mar. Drugs* **2020**, *18*, 172. [CrossRef]
178. Habeebullah, S.F.K.; Alagarsamy, S.; Sattari, Z.; Al-Haddad, S.; Fakhraldeen, S.; Al-Ghunaim, A.; Al-Yamani, F. Enzyme-Assisted extraction of bioactive compounds from brown seaweeds and characterization. *J. Appl. Phycol.* **2020**, *32*, 615–629. [CrossRef]
179. Dang, T.T.; Bowyer, M.C.; Van Altena, I.A.; Scarlett, C.J. Optimum conditions of microwave-assisted extraction for phenolic compounds and antioxidant capacity of the brown alga *Sargassum vestitum*. *Sep. Sci. Technol.* **2018**, *53*, 1711–1723. [CrossRef]
180. Týskiewicz, K.; Konkol, M.; Rój, E. The application of supercritical fluid extraction in phenolic compounds isolation from natural plant materials. *Molecules* **2018**, *23*, 2625. [CrossRef] [PubMed]
181. Gallego, R.; Bueno, M.; Herrero, M. Sub- and supercritical fluid extraction of bioactive compounds from plants, food-by-products, seaweeds and microalgae—An update. *(TrAC) Trends Anal. Chem.* **2019**, *116*, 198–213. [CrossRef]
182. Pangestuti, R.; Getachew, A.T.; Siahaan, E.A.; Chun, B.S. Characterization of functional materials derived from tropical red seaweed *Hypnea musciformis* produced by subcritical water extraction systems. *J. Appl. Phycol.* **2019**, *31*, 2517–2528. [CrossRef]
183. Otero, P.; López-Martínez, M.I.; García-Risco, M.R. Application of pressurized liquid extraction (PLE) to obtain bioactive fatty acids and phenols from *Laminaria ochroleuca* collected in Galicia (NW Spain). *J. Pharm. Biomed. Anal.* **2019**, *164*, 86–92. [CrossRef]
184. Gentscheva, G.; Milkova-Tomova, I.; Pehlivanov, I.; Gugleva, V.; Nikolova, K.; Petkova, N.; Andonova, V.; Buhalova, D.; Pisanova, E. Chemical Characterization of Selected Algae and Cyanobacteria from Bulgaria as Sources of Compounds with Antioxidant Activity. *Appl. Sci.* **2022**, *12*, 9935. [CrossRef]
185. Wekre, M.E.; Kåsin, K.; Underhaug, J.; Holmelid, B.; Jordheim, M. Quantification of Polyphenols in Seaweeds: A Case Study of *Ulva intestinalis*. *Antioxidants* **2019**, *8*, 612. [CrossRef] [PubMed]
186. Dimova, D.; Dobreva, D.; Panayotova, V.; Makedonski, L. DPPH Antiradical Activity and Total Phenolic Content of Methanol and Ethanol Extracts from Macroalgae (*Ulva rigida*) and Microalgae (*Chlorella*). *Scr. Sci. Pharm.* **2019**, *6*, 37–41. [CrossRef]

187. Haq, S.H.; Al-Ruwaished, G.; Al-Mutlaq, M.A.; Naji, S.A.; Al-Mogren, M.; Al-Rashed, S.; Ain, Q.T.; Al-Amro, A.A.; Al-Mussallam, A. Antioxidant, Anticancer Activity and Phytochemical Analysis of Green Algae, *Chaetomorpha* Collected from the Arabian Gulf. *Sci. Rep.* **2019**, *9*, 18906. [CrossRef]
188. Sanger, G.; Rarung, L.K.; Kaseger, B.E.; Assa, J.R.; Agustin, A.T. Phenolic content and antioxidant activities of five seaweeds from North Sulawesi, Indonesia. *AACL Bioflux* **2019**, *12*, 2041–2050.
189. Sasadara, M.M.V.; Wirawan, I.G.P. Effect of extraction solvent on total phenolic content, total flavonoid content, and antioxidant activity of *Bulung sangu* (*Gracilaria* sp.) Seaweed. *IOP Conf. Ser. Earth Environ. Sci.* **2021**, *712*, 012005. [CrossRef]
190. Sobuj, M.K.A.; Islam, A.; Haque, A.; Islam, M.; Alam, J.; Rafquzzaman, S.M. Evaluation of bioactive chemical composition, phenolic, and antioxidant profling of diferent crude extracts of *Sargassum coriifolium* and *Hypnea pannosa* seaweeds. *J. Food Measurem. Charact.* **2021**, *15*, 1653–1665. [CrossRef]
191. El Shafay, S.; El-Sheekh, M.; Bases, E.; El-Shenody, R. Antioxidant, antidiabetic, anti-inflammatory and anticancer potential of some seaweed extracts. *Food Sci. Technol.* **2022**, *42*, e20521. [CrossRef]
192. Hmani, I.; Ktari, L.; Ismail, A.; M'dallel, C.; El Bour, M. Assessment of the antioxidant and antibacterial properties of red algae (Rhodophyta) from the north coast of Tunisia. *Euro-Mediterr. J. Environ. Integr.* **2021**, *6*, 13. [CrossRef]
193. Nursid, N.; Khatulistiani, T.S.; Noviendri, D.; Hapsari, F.; Hardiyati, T. Total phenolic content, antioxidant activity and tyrosinase inhibitor from marine red algae extract collected from Kupang, East Nusa Tenggara. *IOP Conf. Ser. Earth Environ. Sci.* **2020**, *493*, 012013. [CrossRef]
194. Gunathilaka, T.L.; Samarakoon, K.W.; Ranasinghe, P.; Peiris, L.D.C. In-Vitro Antioxidant, Hypoglycemic Activity, and Identification of Bioactive Compounds in Phenol-Rich Extract from the Marine Red Algae *Gracilaria edulis* (Gmelin) Silva. *Molecules* **2019**, *24*, 3708. [CrossRef] [PubMed]
195. Siangu, B.N.; Sauda, S.; John, M.K.; Njue, W.M. Antioxidant activity, total phenolic and flavonoid content of selected Kenyan medicinal plants, sea algae and medicinal wild mushrooms. *Afr. J. Pure Appl. Chem.* **2019**, *13*, 43–48. [CrossRef]
196. Cadar, E.; Sirbu, R.; Ibram, A.; Ionescu, A.M. Evaluation of Total Phenolic Content in Relation to Antioxidant Activity of Brown Algae *Cystoseira barbata* from Black Sea. *Rev. Chim.* **2019**, *70*, 2684–2689. [CrossRef]
197. Subbiah, V.; Duan, X.; Agar, O.T.; Dunshea, F.R.; Barrow, C.J.; Suleria, H.A.R. Comparative study on the effect of different drying techniques on phenolic compounds in Australian beach-cast brown seaweeds. *Algal Res.* **2023**, *72*, 103140. [CrossRef]
198. Abdelhamid, A.; Jouini, M.; Amor, H.B.H.; Mzoughi, Z.; Dridi, M.; Said, R.B.; Bouraoui, A. Pytochemical analysis and evaluation of the antioxidant, anti-inflammatory, and antinociceptive potential of phlorotannin-rich fractions from three Mediterranean brown seaweeds. *Mar. Biotechnol.* **2018**, *20*, 60–74. [CrossRef]
199. Bekah, D.; Thakoor, A.D.; Ramanjooloo, A.; Phul, I.C.; Botte, S.; Roy, P.; Oogarah, P.; Curpen, S.; Goonoo, N.; Bolton, J.; et al. Vitamins, minerals and heavy metals profiling of seaweeds from Mauritius and Rodrigues for food security. *J. Food Comp. Anal.* **2023**, *115*, 104909. [CrossRef]
200. Lovander, M.D.; Lyon, J.D.; Parr, D.L.; Wang, J.; Parke, B.; Leddy, J. Critical Review—Electrochemical Properties of 13 Vitamins: A, Critical Review and Assessment. *J. Electrochem. Soc.* **2018**, *165*, 18–49. [CrossRef]
201. AOAC. *Official Methods of Analysis of AOAC International*, 19th ed.; AOAC International: Washington, DC, USA, 2019.
202. Susanti, D.; Ruslan, F.S.; Shukor, M.I.; Nor, N.M.; Aminudin, N.I.; Taher, M.; Khotib, J. Optimisation of Vitamin B12 Extraction from Green Edible Seaweed (*Ulva lactuca*) by Applying the Central Composite Design. *Molecules* **2022**, *27*, 4459. [CrossRef] [PubMed]
203. Chandra-Hioe, M.V.; Xu, H.; Arcot, J. The Efficiency of Ultrasonic-Assisted Extraction of Cyanocobalamin Is Greater than Heat Extraction. *Heliyon* **2020**, *6*, e03059. [CrossRef]
204. Pereira, L.; Valado, A. The Seaweed Diet in Prevention and Treatment of the Neurodegenerative Diseases. *Mar. Drugs* **2021**, *19*, 128. [CrossRef] [PubMed]
205. Sultana, F.; Wahab, A.; Nahiduzzaman, M.; Mohiuddin, M.; Iqbal, M.Z.; Shakil, A.; Mamun, A.A.; Khan, S.R.; Wong, L.; Asaduzzaman, M. Seaweed farming for food and nutritional security, climate change mitigation and adaptation, and women empowerment: A review. *Aquac. Fish.* **2023**, *8*, 463–480. [CrossRef]
206. Ryzhik, I.V.; Klindukh, M.P.; Dobychina, E.O. The B-group vitamins in the red alga *Palmaria palmata* (Barents Sea): Composition, seasonal changes and influence of abiotic factors. *Algal Res.* **2021**, *59*, 102473. [CrossRef]
207. Dragomir, R.E.; Toader, D.O.; Gheoca Mutu, D.E.; Dogaru, I.A.; Răducu, L.; Tomescu, L.C.; Moleriu, L.C.; Bordianu, A.; Petre, I.; Stănculescu, R. Consequences of Maternal Vitamin D Deficiency on Newborn Health. *Life* **2024**, *14*, 714. [CrossRef]
208. Soares, C.; Švarc-Gajić, J.; Oliva-Teles, M.T.; Pinto, E.; Nastić, N.; Savić, S.; Almeida, A.; Delerue-Matos, C. Mineral Composition of Subcritical Water Extracts of Saccorhiza Polyschides, a Brown Seaweed Used as Fertilizer in the North of Portugal. *J. Mar. Sci. Eng.* **2020**, *8*, 244. [CrossRef]

209. Admassu, H.; Abera, T.; Abraha, B.; Yang, R.; Zhao, W. Proximate, mineral and amino acid composition of dried laver (*Porphyra* spp.) seaweed. *J. Artif. Intell. Res.* **2018**, *6*, 149–154.
210. Lozano Muñoz, I.; Díaz, N.F. Minerals in edible seaweed: Health benefits and food safety issues. *Crit. Rev. Food Sci. Nutr.* **2022**, *62*, 1592–1607. [CrossRef]
211. Díaz, O.; Tapia, Y.; Muñoz, O.; Montoro, R.; Velez, D.; Almela, C. Total and inorganic arsenic concentrations in different species of economically important algae harvested from coastal zones of Chile. *Food Chem. Toxicol.* **2012**, *50*, 744–749. [CrossRef]
212. Ahmed, N.; Sheikh, M.A.; Ubaid, M.; Chauhan, P.; Kumar, K.; Choudhary, S. Comprehensive exploration of marine algae diversity, bioactive compounds, health benefits, regulatory issues, and food and drug applications. *Meas. Food* **2024**, *14*, 100163. [CrossRef]
213. Xu, J.; Liao, W.; Liu, Y.; Guo, Y.; Jiang, S.; Zhao, C. An overview on the nutritional and bioactive components of green seaweeds. *Food Prod. Process. Nutr.* **2023**, *5*, 18. [CrossRef]
214. Silva, M.; Avni, D.; Varela, J.; Barreira, L. The Ocean's Pharmacy: Health Discoveries in Marine Algae. *Molecules* **2024**, *29*, 1900. [CrossRef] [PubMed]
215. Mabate, B.; Daub, C.D.; Pletschke, B.I.; Edkins, A.L. Comparative Analyses of Fucoidans from South African Brown Seaweeds That Inhibit Adhesion, Migration, and Long-Term Survival of Colorectal Cancer Cells. *Mar. Drugs* **2023**, *21*, 203. [CrossRef]
216. Shiau, J.P.; Chuang, Y.T.; Yang, K.H.; Chang, F.R.; Sheu, J.H.; Hou, M.F.; Jeng, J.H.; Tang, J.Y.; Chang, H.W. Brown Algae-Derived Fucoidan Exerts Oxidative Stress-Dependent Antiproliferation on Oral Cancer Cells. *Antioxidants* **2022**, *11*, 841. [CrossRef]
217. Cao, S.; Yang, Y.; Liu, S.; Shao, Z.; Chu, X.; Mao, W. Immunomodulatory Activity In Vitro and In Vivo of a Sulfated Polysaccharide with Novel Structure from the Green Alga *Ulva conglobata* Kjellman. *Mar. Drugs* **2022**, *20*, 447. [CrossRef]
218. Gao, Y.; Li, Y.; Niu, Y.; Ju, H.; Chen, R.; Li, B.; Song, X.; Song, L. Chemical Characterization, Antitumor, and Immune-Enhancing Activities of Polysaccharide from *Sargassum pallidum*. *Molecules* **2021**, *26*, 7559. [CrossRef]
219. Bellan, D.L.; Biscaia, S.M.P.; Rossi, G.R.; Cristal, A.M.; Gonçalves, J.P.; Oliveira, C.C.; Simas, F.F.; Sabry, D.A.; Rocha, H.A.O.; Franco, C.R.C.; et al. Green does not always mean go: A sulfated galactan from *Codium isthmocladum* green seaweed reduces melanoma metastasis through direct regulation of malignancy features. *Carbohydr. Polym.* **2020**, *250*, 116869. [CrossRef]
220. Zhao, C.; Lin, G.; Wu, D.; Liu, D.; You, L.; Hogger, P.; Simal-Gandara, J.; Wang, M.; da Costa, J.G.M.; Marunaka, Y.; et al. The algal polysaccharide ulvan suppresses growth of hepatoma cells. *Food Front.* **2020**, *1*, 83–101. [CrossRef]
221. Cicinskas, E.; Begun, M.A.; Tiasto, V.A.; Belousov, A.S.; Vikhareva, V.V.; Mikhailova, V.A.; Kalitnik, A.A. In vitro antitumor and immunotropic activity of carrageenans from red algae *Chondrus armatus* and their low-molecular weight degradation products. *J. Biomed. Mater. Res.* **2020**, *108*, 254–266. [CrossRef]
222. Choi, J.W.; Lee, J.; Kim, S.C.; You, S.; Lee, C.W.; Shin, J.; Park, Y.I. Glucuronorhamnoxylan from *Capsosiphon fulvescens* inhibits the growth of HT29 human colon cancer cells in vitro and in vivo via induction of apoptotic cell death. *Int. J. Biol. Macromol.* **2019**, *124*, 1060–1068. [CrossRef] [PubMed]
223. Mendes Marques, M.L.; Presa, F.B.; Viana, R.L.S.; Costa, M.S.S.P.; Amorim, M.O.R.; Bellan, D.L.; Alves, M.G.C.F.; Costa, L.S.; Trindade, E.S.; Rocha, H.A.O. Anti-Thrombin, Anti-Adhesive, Anti-Migratory, and Anti-Proliferative Activities of Sulfated Galactans from the Tropical Green Seaweed, *Udotea flabellum*. *Mar. Drugs* **2019**, *17*, 5. [CrossRef]
224. Narayani, S.S.; Saravanan, S.; Ravindran, J.; Ramasamy, M.S.; Chitra, J. In vitro anticancer activity of fucoidan extracted from *Sargassum cinereum* against Caco-2 cells. *Int. J. Biol. Macromol.* **2019**, *138*, 618–628. [CrossRef] [PubMed]
225. Bharathi, D.S.; Raja, A.B.; Deshpande, M.N.; Chakrapani, I.S.; Priyadarsini, A.I.; Anbazhagan, M.; Sampath, V. New record of *Dictyota bartayresiana*, a marine brown algal species revealed from rich seaweed diversity area of south India. *J. Coast. Life Med.* **2023**, *11*, 825–830.
226. Wang, J.J.; Ma, Y.; Yang, J.; Jin, L.; Gao, Z.; Xue, L.; Hou, L.; Sui, L.; Liu, J.; Zou, X. Fucoxanthin inhibits tumour-related lymphangiogenesis and growth of breast cancer. *J. Cell. Mol. Med.* **2019**, *23*, 2219–2229. [CrossRef]
227. Mahendran, S.; Sankaralingam, S.; Sethupathi, S.M. Evaluation of antioxidant and cytotoxicity activities of polyphenol extracted from brown seaweed *Sargassum tenerrimum* biomass. *Biomass Conv. Bioref.* **2024**, *14*, 2063–2069. [CrossRef]
228. Cadar, E.; Negreanu-Pirjol, T.; Pascale, C.; Sirbu, R.; Prasacu, I.; Negreanu-Pirjol, B.-S.; Tomescu, C.L.; Ionescu, A.-M. Natural Bio-Compounds from *Ganoderma lucidum* and Their Beneficial Biological Actions for Anticancer Application: A Review. *Antioxidants* **2023**, *12*, 1907. [CrossRef]
229. Alboofetileh, M.; Rezaei, M.; Hamzeh, A.; Tabarsa, M.; Cravotto, G. Cellular antioxidant and emulsifying activities of fucoidan extracted from *Nizamuddinia zanardinii* using different green extraction methods. *J. Food Process. Preserv.* **2022**, *46*, e17238. [CrossRef]
230. Wang, L.; Jayawardena, T.U.; Yang, H.W.; Lee, H.G.; Kang, M.C.; Sanjeewa, K.K. Isolation, Characterization, and Antioxidant Activity Evaluation of a Fucoidan from an Enzymatic Digest of the Edible Seaweed, *Hizikia fusiforme*. *Antioxidants* **2020**, *9*, 363. [CrossRef]

231. Wang, L.; Jayawardena, T.U.; Yang, H.W.; Lee, H.G.; Jeon, Y.J. The Potential of Sulfated Polysaccharides Isolated from the Brown Seaweed *Ecklonia maxima* in Cosmetics: Antioxidant, Anti-melanogenesis, and Photoprotective Activities. *Antioxidants* **2020**, *9*, 724. [CrossRef] [PubMed]
232. Jayawardena, T.U.; Wang, L.; Sanjeewa, K.K.A.; Kang, S.I.; Lee, J.S.; Jeon, Y.J. Antioxidant Potential of Sulfated Polysaccharides from *Padina boryana;* Protective Effect against Oxidative Stress in In Vitro and In Vivo Zebrafish Model. *Mar. Drugs* **2020**, *18*, 212. [CrossRef] [PubMed]
233. Le, B.; Golokhvast, K.S.; Yang, S.H.; Sun, S. Optimization of Microwave-Assisted Extraction of Polysaccharides from *Ulva pertusa* and Evaluation of Their Antioxidant Activity. *Antioxidants* **2019**, *8*, 129. [CrossRef]
234. Wang, L.; Oh, J.Y.; Hwang, J.; Ko, J.Y.; Jeon, Y.J.; Ryu, B. In Vitro and In Vivo Antioxidant Activities of Polysaccharides Isolated from Celluclast-Assisted Extract of an Edible Brown Seaweed, *Sargassum fulvellum*. *Antioxidants* **2019**, *8*, 493. [CrossRef]
235. Maneesh, A.; Chakraborty, K. Pharmacological potential of sulphated polygalacto-pyranosyl-fucopyranan from the brown seaweed *Sargassum wightii*. *J. Appl. Phycol.* **2018**, *30*, 1971–1988. [CrossRef]
236. Yang, Q.; Jiang, Y.; Fu, S.; Shen, Z.; Zong, W.; Xia, Z.; Zhan, Z.; Jiang, X. Protective Effects of *Ulva lactuca* Polysaccharide Extract on Oxidative Stress and Kidney Injury Induced by D-Galactose in Mice. *Mar. Drugs* **2021**, *19*, 539. [CrossRef]
237. Zhang, J.; Shi, L.Y.; Ding, L.P.; Liang, H.; Tu, P.F.; Zhang, Q.Y. Antioxidant terpenoids from the red alga *Laurencia tristicha*. *Nat. Prod. Res.* **2020**, *35*, 5048–5054. [CrossRef]
238. Da Costa, E.; Melo, T.; Reis, M.; Domingues, P.; Calado, R.; Abreu, M.H.; Domingues, M.R. Polar Lipids Composition, Antioxidant and Anti-Inflammatory Activities of the Atlantic Red Seaweed *Grateloupia turuturu*. *Mar. Drugs* **2021**, *19*, 414. [CrossRef]
239. Zhang, X.; Cao, D.; Sun, X. Preparation and identification of antioxidant peptides from protein hydrolysate of marine alga *Gracilariopsis lemaneiformis*. *J. Appl. Phycol.* **2019**, *31*, 2585–2596. [CrossRef]
240. Torres, M.D.; Flórez-Fernández, N.; Domínguez, H. Integral Utilization of Red Seaweed for Bioactive Production. *Mar. Drugs* **2019**, *17*, 314. [CrossRef]
241. Torres, P.; Santos, J.P.; Chow, F.; Pena Ferreira, M.J.; dos Santos, D.Y.A.C. Comparative analysis of in vitro antioxidant capacities of mycosporine-like amino acids (MAAs). *Algal Res.* **2018**, *34*, 57–67. [CrossRef]
242. Cadar, E.; Pesterau, A.-M.; Sirbu, R.; Negreanu-Pirjol, B.S.; Tomescu, C.L. Jellyfishes—Significant Marine Resources with Potential in the Wound-Healing Process: A Review. *Mar. Drugs* **2023**, *21*, 201. [CrossRef] [PubMed]
243. Cadar, E.; Pesterau, A.-M.; Prasacu, I.; Ionescu, A.-M.; Pascale, C.; Dragan, A.-M.L.; Sirbu, R.; Tomescu, C.L. Marine Antioxidants from Marine Collagen and Collagen Peptides with Nutraceuticals Applications: A Review. *Antioxidants* **2024**, *13*, 919. [CrossRef] [PubMed]
244. Sudhakar, M.P.; Dharani, G.; Paramasivam, A. Evaluation of antimicrobial, antioxidant and cytotoxicity potential of R-phycoerythrin extracted from *Gracilaria corticata* seaweed. *Curr. Res. Green Sustain. Chem.* **2023**, *6*, 100352. [CrossRef]
245. Yalçın, S.; Karakaş, Ö.; Okudan, E.Ş.; Başkan, K.S.; Çekiç, S.D.; Apak, R. HPLC detection and antioxidant capacity determination of brown, red and green algal pigments in seaweed extracts. *J. Chromatogr. Sci.* **2021**, *59*, 325–337. [CrossRef]
246. Radman, S.; Cikoš, A.M.; Flanjak, I.; Babić, S.; Čižmek, L.; Šubarić, D.; Čož-Rakovac, R.; Jokić, S.; Jerković, I. Less Polar Compounds and Targeted Antioxidant Potential (In Vitro and In Vivo) of *Codium adhaerens* C. Agardh 1822. *Pharmaceuticals* **2021**, *14*, 944. [CrossRef]
247. Ulagesan, S.; Nam, T.-J.; Choi, Y.-H. Extraction and Purification of R-Phycoerythrin Alpha Subunit from the Marine Red Algae *Pyropia yezoensis* and Its Biological Activities. *Molecules* **2021**, *26*, 6479. [CrossRef]
248. Jerković, I.; Cikoš, A.-M.; Babić, S.; Čižmek, L.; Bojanić, K.; Aladić, K.; Ul'yanovskii, N.V.; Kosyakov, D.S.; Lebedev, A.T.; Čož-Rakovac, R.; et al. Bioprospecting of Less-Polar Constituents from Endemic Brown Macroalga *Fucus virsoides* J. Agardh from the Adriatic Sea and Targeted Antioxidant Effects In Vitro and In Vivo (Zebrafish Model). *Mar. Drugs* **2021**, *19*, 235. [CrossRef]
249. Negreanu-Pîrjol, T.; Negreanu-Pîrjol, B.S.; Popoviciu, D.R.; Roncea, F.N. Preliminary Data Regarding Pharmaceutical Forms Type Gels Based on Marine Algae Extracts with Antioxidant Activity. *Eur. J. Nat. Sci. Med.* **2021**, *4*, 55–65. [CrossRef]
250. Karkhaneh, Y.M.; Seyed, H.M.; Mashinchian, M.A.; Ghassempour, A.R. Seasonal variation of fucoxanthin content in four species of brown seaweeds from Qeshm Island, persian gulf and evaluation of their antibacterial and antioxidant activities. *Iran. J. Fish. Sci.* **2020**, *19*, 2394–2408. [CrossRef]
251. Ghaliaoui, N.; Mokrane, H.; Hazzit, M.; Hadjadj, M.; Otmani, F.S.; Touati, S.; Seridi, H. Impact of freezing and drying preprocessing on pigments extraction from the brown seaweed *Phyllaria reniformis* collected in algerian coast. *Carphatian J. Food Sci. Technol.* **2020**, *12*, 81–94. [CrossRef]
252. Mohibbullah, M.; Haque, M.N.; Khan, M.N.A.; Park, I.; Moon, I.; Hong, Y.K. Neuroprotective effects of fucoxanthin and its derivative fucoxanthinol from the phaeophyte *Undaria pinnatifida* attenuate oxidative stress in hippocampal neurons. *J. Appl. Phycol.* **2018**, *30*, 3243–3252. [CrossRef]

253. Fu, Y.; Jiao, H.; Sun, J.; Okoye, C.O.; Zhang, H.; Li, Y.; Lu, X.; Wang, Q.; Liu, J. Structure-activity relationships of bioactive polysaccharides extracted from macroalgae towards biomedical application: A review. *Carbohydr. Polym.* **2024**, *324*, 121533. [CrossRef] [PubMed]
254. Generalić Mekinić, I.; Šimat, V.; Botić, V.; Crnjac, A.; Smoljo, M.; Soldo, B.; Ljubenkov, I.; Čagalj, M.; Skroza, D. Bioactive Phenolic Metabolites from Adriatic Brown Algae *Dictyota dichotoma* and *Padina pavonica* (*Dictyotaceae*). *Foods* **2021**, *10*, 1187. [CrossRef]
255. Hassan, S.; Hamed, S.; Almuhayawi, M.; Hozzin, W.; Selim, S.; AbdElgawad, H. Bioactivity of Ellagic Acid and Velutin: Two Phenolic Compounds Isolated from Marine Algae. *Egypt. J. Bot.* **2021**, *61*, 219–231. [CrossRef]
256. Alkhalaf, M.I. Chemical composition, antioxidant, anti-inflammatory and cytotoxic effects of *Chondrus crispus* species of red algae collected from the Red Sea along the shores of Jeddah city. *J. King Saud Univ.–Sci.* **2021**, *33*, 101210. [CrossRef]
257. Ak, I.; Turker, G. Antioxidant Activity of Five Seaweed Extracts. *New Know. J. Sci.* **2018**, *7*, 149–155.
258. Alghazwi, M.; Charoensiddhi, S.; Smid, S.; Zhang, W. Impact of Ecklonia radiata Extracts on the Neuroprotective Activities against Amyloid Beta (Aβ1-42) Toxicity and Aggregation. *J. Funct. Foods* **2020**, *68*, 103893. [CrossRef]
259. Shrestha, S.; Zhang, W.; Begbie, A.J.; Pukala, T.L.; Smid, S.D. *Ecklonia radiata* Extract Containing Eckol Protects Neuronal Cells against Aß1-42evoked Toxicity and Reduces Aggregate Density. *Food Funct.* **2020**, *11*, 6509–6516. [CrossRef]
260. Yang, E.J.; Mahmood, U.; Kim, H.; Choi, M.; Choi, Y.; Lee, J.P.; Cho, J.Y.; Hyun, J.W.; Kim, Y.S.; Chang, M.J.; et al. Phloroglucinol Ameliorates Cognitive Impairments by Reducing the Amyloid β Peptide Burden and Pro-Inflammatory Cytokines in the Hippocampus of 5XFAD Mice. *Free Radic. Biol. Med.* **2018**, *126*, 221–234. [CrossRef]
261. Le, A.T.; Prabhu, N.S.; Almoallim, H.; Awad Alahmadi, T. Assessment of nutraceutical value, physicochemical, and anti-inflammatory profile of *Odonthalia floccose* and *Odonthalia dentata*. *Environ. Res.* **2024**, *259*, 119487. [CrossRef]
262. Subramoni, M.; Kumar, S.; Abraham, J. Nutritional content of selected macroalgae of the south-west coast of India. *Egypt. J. Phycol.* **2023**, *24*, 161–193. [CrossRef]
263. Sumayya, S.S.; Lubaina, A.S.; Murugan, K. Bactericidal Potentiality of Purified Terpenoid Extracts from the Selected Sea Weeds and its Mode of Action. *J. Trop. Life Sci.* **2020**, *10*, 197–205. [CrossRef]
264. Kuete, V.; Efferth, T. Cameroonian medicinal plants: Pharmacology and derived natural products. *Front. Pharmacol.* **2010**, *1*, 123. [CrossRef]
265. Tamokou, J.D.D.; Mbaveng, A.T.; Kuete, V. Chapter 8—Antimicrobial Activities of African Medicinal Spices and Vegetables. In *Medicinal Spices and Vegetables from Africa*; Kuete, V., Ed.; Academic Press: Cambridge, MA, USA, 2017; pp. 207–237. [CrossRef]
266. Ríos, J.L.; Recio, M.C. Perspective paper Medicinal plants and antimicrobial activity. *J. Ethnopharmacol.* **2005**, *100*, 80–84. [CrossRef]
267. Anjali, K.P.; Sangeetha, B.M.; Devi, G.; Raghunathan, R.; Dutta, S. Bioprospecting of seaweeds (*Ulva lactuca* and *Stoechospermum marginatum*): The compound characterization and functional applications in medicine-a comparative study. *J. Phytochem. Photobiol.* **2019**, *200*, 111622. [CrossRef]
268. da Graça Pedrosa de Macena, L.; dos Santos Corrêa Amorim, L.; Francisco Corrêa de Souza e Souza, K.; Dantas Pereira, L.; Cirne dos Santos, C.C.; de Souza Barros, C.; Nunes de Palmer Paixão, I.C. Antiviral activity of terpenes isolated from marine brown seaweeds against herpes simplex virus type 2. *Nat. Prod. Res.* **2023**, *39*, 712–717. [CrossRef]
269. Cirne-Santos, C.C.; de Souza Barros, C.; de Oliveira, M.C. In vitro Studies on The Inhibition of Replication of Zika and Chikungunya Viruses by Dolastane Isolated from Seaweed *Canistrocarpus cervicornis*. *Sci. Rep.* **2020**, *10*, 8263. [CrossRef]
270. Oliyaei, N.; Moosavi-Nasab, M. Ultrasound-assisted extraction of fucoxanthin from *Sargassum angustifolium* and *Cystoseira indica* brown algae. *J. Food Process. Preserv.* **2021**, *45*, e15929. [CrossRef]
271. Liyanage, N.M.; Lee, H.G.; Nagahawatta, D.P.; Jayawardhana, H.; Song, K.M.; Choi, Y.S.; Jeon, Y.J.; Kang, M.C. Fucoidan from *Sargassum autumnale* Inhibits Potential Inflammatory Responses via NF-kappaB and MAPK Pathway Suppression in Lipopolysaccharide-Induced RAW264.7 Macrophages. *Mar. Drugs* **2023**, *21*, 374. [CrossRef]
272. Jayasinghe, A.M.K.; Kirindage, K.; Fernando, I.P.S.; Kim, K.N.; Oh, J.Y.; Ahn, G. The Anti-Inflammatory Effect of Low MolecularWeight Fucoidan from *Sargassum siliquastrum* in Lipopolysaccharide-Stimulated RAW 264.7 Macrophages via Inhibiting NFkappaB/MAPK Signaling Pathways. *Mar. Drugs* **2023**, *21*, 347. [CrossRef]
273. Jayasinghe, A.M.K.; Kirindage, K.; Fernando, I.P.S.; Han, E.J.; Oh, G.W.; Jung, W.K.; Ahn, G. Fucoidan Isolated from *Sargassum confusum* Suppresses Inflammatory Responses and Oxidative Stress in TNF-alpha/IFN-gamma-Stimulated HaCaT Keratinocytes by Activating Nrf2/HO-1 Signaling Pathway. *Mar. Drugs* **2022**, *20*, 117. [CrossRef]
274. Apostolova, E.; Lukova, P.; Baldzhieva, A.; Delattre, C.; Molinie, R.; Petit, E.; Elboutachfaiti, R.; Nikolova, M.; Iliev, I.; Murdjeva, M.; et al. Structural Characterization and In Vivo Anti-Inflammatory Activity of Fucoidan from *Cystoseira crinita* (Desf.) Borry. *Mar. Drugs* **2022**, *20*, 714. [CrossRef]
275. Jayawardena, T.U.; Sanjeewa, K.K.A.; Nagahawatta, D.P.; Lee, H.G.; Lu, Y.A.; Vaas, A.; Abeytunga, D.T.U.; Nanayakkara, C.M.; Lee, D.S.; Jeon, Y.J. Anti-Inflammatory Effects of Sulfated Polysaccharide from *Sargassum swartzii* in Macrophages via BlockingTLR/NF-Kappab Signal Transduction. *Mar. Drugs* **2020**, *18*, 601. [CrossRef]

276. Wang, L.; Je, J.G.; Huang, C.; Oh, J.Y.; Fu, X.; Wang, K.; Ahn, G.; Xu, J.; Gao, X.; Jeon, Y.J. Anti-Inflammatory Effect of Sulfated Polysaccharides Isolated from *Codium fragile* In Vitro in RAW 264.7 Macrophages and In Vivo in Zebrafish. *Mar. Drugs* **2022**, *20*, 391. [CrossRef]
277. Chen, X.; Ni, L.; Fu, X.; Wang, L.; Duan, D.; Huang, L.; Xu, J.; Gao, X. Molecular Mechanism of Anti-Inflammatory Activities of a Novel Sulfated Galactofucan from *Saccharina japonica*. *Mar. Drugs* **2021**, *19*, 430. [CrossRef]
278. Je, J.G.; Lee, H.G.; Fernando, K.H.N.; Jeon, Y.J.; Ryu, B. Purification and Structural Characterization of Sulfated Polysaccharides Derived from Brown Algae, *Sargassum binderi*: Inhibitory Mechanism of iNOS and COX-2 Pathway Interaction. *Antioxidants* **2021**, *10*, 822. [CrossRef]
279. Wang, L.; Yang, H.W.; Ahn, G.; Fu, X.; Xu, J.; Gao, X.; Jeon, Y.J. In Vitro and In Vivo Anti-Inflammatory Effects of SulfatedPolysaccharides Isolated from the Edible Brown Seaweed, *Sargassum fulvellum*. *Mar. Drugs* **2021**, *19*, 277. [CrossRef]
280. Wang, S.; Ni, L.; Fu, X.; Duan, D.; Xu, J.; Gao, X. A Sulfated Polysaccharide from *Saccharina japonica* Suppresses LPS-Induced Inflammation Both in a Macrophage Cell Model via Blocking MAPK/NF-kappaB Signal Pathways In Vitro and a Zebrafish Model of Embryos and Larvae In Vivo. *Mar. Drugs* **2020**, *18*, 593. [CrossRef]
281. Pereira, T.; Horta, A.; Barroso, S.; Mendes, S.; Gil, M.M. Study of the Seasonal Variations of the Fatty Acid Profiles of Selected Macroalgae. *Molecules* **2021**, *26*, 5807. [CrossRef]
282. Berneira, L.; da Silva, C.; Poletti, T. Evaluation of the volatile composition and fatty acid profile of seven Antarctic macroalgae. *J. Appl. Phycol.* **2020**, *32*, 3319–3329. [CrossRef]
283. Dai, Y.L.; Jiang, Y.F.; Lu, Y.A.; Yu, J.B.; Kang, M.C.; Jeon, Y.J. Fucoxanthin-rich fraction from *Sargassum fusiformis* alleviates particulate matter-induced inflammation in vitro and in vivo. *Toxicol. Rep.* **2021**, *6*, 349–358. [CrossRef]
284. Cheng, Y.; Pan, X.; Wang, J.; Li, X.; Yang, S.; Yin, R.; Ma, A.; Zhu, X. Fucoidan Inhibits NLRP3 Inflammasome Activation by Enhancing p62/SQSTM1-Dependent Selective Autophagy to Alleviate Atherosclerosis. *Oxid. Med. Cell. Longev.* **2020**, *2020*, 3186306. [CrossRef]
285. Kumagai, Y.; Toji, K.; Katsukura, S.; Morikawa, R.; Uji, T.; Yasui, H.; Shimizu, T.; Kishimura, H. Characterization of ACE Inhibitory Peptides Prepared from *Pyropia pseudolinearis* Protein. *Mar. Drugs* **2021**, *19*, 200. [CrossRef]
286. McLaughlin, C.M.; Harnedy-Rothwell, P.A.; Lafferty, R.A. Macroalgal protein hydrolysates from *Palmaria palmata* influence the 'incretin effect' in vitro via DPP-4 inhibition and upregulation of insulin, GLP-1 and GIP secretion. *Eur. J. Nutr.* **2021**, *60*, 4439–4452. [CrossRef]
287. Kumagai, Y.; Kitade, Y.; Kobayashi, M. Identification of ACE inhibitory peptides from red alga *Mazzaella japonica*. *Eur. Food Res. Technol.* **2020**, *246*, 2225–2231. [CrossRef]
288. Cermeño, M.; Stack, J.; Tobin, P.R.; O'Keeffe, M.B.; Harnedy, P.A.; Stengel, D.B.; FitzGerald, R.J. Peptide Identification from a *Porphyra Dioica* Protein Hydrolysate with Antioxidant, Angiotensin Converting Enzyme and Dipeptidyl Peptidase IV Inhibitory Activities. *Food Funct.* **2019**, *10*, 3421–3429. [CrossRef]
289. Sun, S.; Xu, X.; Sun, X.; Zhang, X.; Chen, X.; Xu, N. Preparation and Identification of ACE Inhibitory Peptides from the Marine Macroalga Ulva intestinalis. *Mar. Drugs* **2019**, *17*, 179. [CrossRef]
290. Raji, V.; Loganathan, C.; Sadhasivam, G.; Kandasamy, S.; Poomani, K.; Thayumanavan, P. Purification of fucoxanthin from *Sargassum wightii* greville and understanding the inhibition of angiotensin 1-converting enzyme: An in vitro and in silico studies. *Int. J. Biol. Macromol.* **2020**, *148*, 696–703. [CrossRef]
291. Lin, Z.; Wang, F.; Yan, Y.; Jin, J.; Quan, Z.; Tong, H.; Du, J. Fucoidan derived from *Sargassum pallidum* alleviates metabolism disorders associated with improvement of cardiac injury and oxidative stress in diabetic mice. *Phytother. Res.* **2023**, *37*, 4210–4223. [CrossRef]
292. Thambi, A.; Chakraborty, K. A novel anti-hyperglycemic sulfated pyruvylated polysaccharide from marine macroalga *Hydropuntia edulis*. *Nat. Prod. Res.* **2023**, *37*, 2987–2999. [CrossRef]
293. Xavier, J.; Jose, J. Study of mineral and nutritional composition of some seaweeds found along the coast of Gulf of Mannar, India. *Plant Sci. Today* **2020**, *7*, 631–637. [CrossRef]
294. de Carvalho, M.M.; Noseda, M.D.; Juliana, C.C.; Dallagnol, J.C.C.; Ferreira, L.G.; Ducatti, D.R.B.; Gonçalves, A.G.; de Freitas, R.A.; Duarte, M.E.R. Conformational analysis of ulvans from *Ulva fasciata* and their anticoagulant polycarboxylic derivatives. *Int. J. Bio. Macromol.* **2020**, *162*, 599–608. [CrossRef]
295. Chagas, S.F.D.; Lima, G.C.; dos Santos, V.I.N.; Costa, L.E.C.; de Sousa, W.M. Sulfated polysaccharide from the red algae *Gelidiella acerosa*: Anticoagulant, antiplatelet and antithrombotic effects. *Int. J. Biol. Macromol.* **2020**, *159*, 415–421. [CrossRef]
296. Sun, Y.; Chen, X.; Liu, S.; Yu, H.; Li, R.; Wang, X. Preparation of low molecular weight *Sargassum fusiforme* polysaccharide and its anticoagulant activity. *J. Oceanol. Limnol.* **2018**, *36*, 882–891. [CrossRef]
297. Cho, K.S.; Shin, M.; Kim, S.; Lee, S.B. Recent advances in studies on the therapeutic potential of dietary carotenoids in neurodegenerative diseases. *Oxid. Med. Cell. Longev.* **2018**, *2018*, 4120458. [CrossRef]

298. Bauer, S.; Jin, W.; Zhang, F.; Linhardt, R.J. The application of seaweed polysaccharides and their derived products with potential for the treatment of Alzheimer's disease. *Mar. Drugs* **2021**, *19*, 89. [CrossRef]
299. Park, S.K.; Kang, J.Y.; Kim, J.M.; Yoo, S.K.; Han, H.J.; Chung, D.H.; Kim, D.O.; Kim, G.H.; Heo, H.J. Fucoidan-rich substances from Ecklonia cava improve trimethyltin-induced cognitive dysfunction via down-regulation of amyloid_production/Tau Hyperphosphorylation. *Mar. Drugs* **2019**, *17*, 591. [CrossRef]
300. Bogie, J.; Hoeks, C.; Schepers, M.; Tiane, A.; Cuypers, A.; Leijten, F.; Chintapakorn, Y.; Suttiyut, T.; Pornpakakul, S.; Struik, D.; et al. Dietary Sargassum fusiforme improves memory and reduces amyloid plaque load in an Alzheimer's disease mouse model. *Sci. Rep.* **2019**, *9*, 4908. [CrossRef]
301. Mohan, E.H.; Madhusudan, S.; Baskaran, R. The sea lettuce *Ulva sensu* lato: Future food with health-promoting bioactivities. *Algal Res.* **2023**, *71*, 103069. [CrossRef]
302. Koseki, K.; Yoshimura, R.; Ido, K.; Katsuura, K.; Bito, T.; Watanabe, F. Determination of Vitamin B12 and Folate Compounds in Commercially Available Edible Seaweed Products. *Front. Biosci.* **2023**, *15*, 10. [CrossRef]
303. Ownsworth, E.; Selby, D.; Ottley, C.J.; Unsworth, E.; Raab, A.; Feldmann, J.; Bücker, P. Tracing the natural and anthropogenic influence on the trace elemental chemistry of estuarine macroseaweeds and the implications for human consumption. *Sci. Total Environ.* **2019**, *685*, 259–272. [CrossRef]
304. Cadar, E.; Mustafa, A.; Tomescu, A.; Cherim, M. Studies Regarding Polluting Agents in Black Sea Algae. *J. Sci. Arts* **2018**, *42*, 255–264.
305. Mendes, M.C.; Navalho, S.; Ferreira, A.; Paulino, C.; Figueiredo, D.; Silva, D.; Speranza, L.G. Algae as food in Europe: An overview of species diversity and their application. *Foods* **2022**, *11*, 1871. [CrossRef]
306. Belkacemi, L.; Belalia, M.; Djendara, A.; Bouhadda, Y. Antioxidant and antibacterial activities and dentification of bioactive compounds of various extracts of *Caulerpa racemosa* from Algerian coast. *Asian Pac. J. Trop. Biomed.* **2020**, *10*, 87–94. [CrossRef]
307. Geranpour, M.; Seid, E.A.; Jafari, M. Recent advances in the spray drying encapsulation of essential fatty acids and functional oils. *Trends Food Sci. Technol.* **2020**, *102*, 71–90. [CrossRef]
308. Mouritsen, O.G.; Rhatigan, P.; Pérez-Lloréns, J.L. The rise of seaweed gastronomy: Phycogastronomy. *Bot. Mar.* **2019**, *62*, 195–209. [CrossRef]
309. Cornish, L. Those curious and delicious seaweeds: A fascinating voyage from biology to gastronomy. *Phycologia* **2019**, *58*, 578–579. [CrossRef]
310. Granato, D.; Barba, F.J.; Kovačević, D.B.; Lorenzo, J.M.; Cruz, A.G.; Putnik, P. Functional Foods: Product Development, Technological Trends, Efficacy Testing, and Safety. *Annu. Rev. Food Sci. Technol.* **2020**, *11*, 93–118. [CrossRef]
311. Tanna, B.; Choudhary, B.; Mishra, A. Metabolite profiling, antioxidant, scavenging and anti-proliferative activities of selected tropical green seaweeds reveal the nutraceutical potential of *Caulerpa* spp. *Algal Res.* **2018**, *36*, 96–105. [CrossRef]
312. El-Beltagi, H.S.; Mohamed, A.A.; Mohamed, H.I.; Ramadan, K.M.A.; Barqawi, A.A.; Mansour, A.T. Phytochemical and Potential Properties of Seaweeds and Their Recent Applications: A Review. *Mar. Drugs* **2022**, *20*, 342. [CrossRef]
313. Ganesan, A.R.; Tiwari, U.; Rajauria, G. Seaweed nutraceuticals and their therapeutic role in disease prevention. *Food Sci. Hum. Wellness* **2019**, *8*, 252–263. [CrossRef]
314. Barot, M.; Nirmal Kumar, J.I.; Kumar, R.N. An Evaluation of the Nutritional Composition of Seaweeds as Potential Source of Food and Feed. *Natl. Acad. Sci. Lett.* **2019**, *42*, 459–464. [CrossRef]
315. Shannon, E.; Abu-Ghannam, N. Seaweeds as nutraceuticals for health and nutrition. *Phycologia* **2019**, *58*, 563–577. [CrossRef]

marine drugs

MDPI

Review

Anticancer Properties of Macroalgae: A Comprehensive Review

Sara Frazzini * and Luciana Rossi

Department of Veterinary Medicine and Animal Sciences—DIVAS, University of Milan, via dell'Università 6, 26900 Lodi, Italy; luciana.rossi@unimi.it
* Correspondence: sara.frazzini@unimi.it

Abstract: In recent years, the exploration of bioactive molecules derived from natural sources has gained interest in several application fields. Among these, macroalgae have garnered significant attention due to their functional properties, which make them interesting in therapeutic applications, including cancer treatment. Cancer constitutes a significant global health burden, and the side effects of existing treatment modalities underscore the necessity for the exploration of novel therapeutic models that, in line with the goal of reducing drug treatments, take advantage of natural compounds. This review explores the anticancer properties of macroalgae, focusing on their bioactive compounds and mechanisms of action. The key findings suggest that macroalgae possess a rich array of bioactive compounds, including polysaccharides (e.g., fucoidans and alginates), polyphenols (e.g., phlorotannins), and terpenoids, which exhibit diverse anticancer activities, such as the inhibition of cell proliferation, angiogenesis, induction of apoptosis, and modulation of the immune system. This review provides an overview of the current understanding of macroalgae's anticancer potential, highlighting the most promising compounds and their mechanisms of action. While preclinical studies have shown promising results, further research is necessary to translate these findings into effective clinical applications.

Keywords: macroalgae; seaweed; cancer; anticancer; anticarcinogenic; bioactive compounds; fucoidans; phlorotannins; terpenoids; immunotherapy

1. Introduction

Algae, the most primitive group of plants, are simple photosynthetic organisms that have been thriving on Earth for an astonishing 3.5 billion years [1]. This longevity is a testament to their resilience and adaptability. Over the course of their existence, these remarkable organisms have evolved, giving rise to two distinct types: macroalgae, also known as seaweed, and microalgae [2,3]. These diverse forms of algae play a crucial role as primary producers, kickstarting the aquatic food chain and providing sustenance for a wide array of organisms, including fish, crustaceans, and gastropods [4].

Algae, an incredibly diverse group of organisms, encompass a wide range of simple, typically autotrophic life forms [5]. Just like plants, algae are capable of photosynthesis, harnessing the power of sunlight to convert carbon dioxide and water into energy-rich nutrients [6,7]. Algae hold immense ecological significance in the marine biome, playing a pivotal role in the survival and well-being of countless organisms. They perform a vital function in global oxygen production and are responsible for generating approximately 70% of the Earth's oxygen [8]. This staggering contribution underscores the urgent need to preserve and protect these organisms. In recent years, there has been a growing interest in the use of algae in various industrial and research fields. The reason for this keen

fascination lies in the findings of marine biologists who have successfully identified an array of over 10,000 algae-produced bioactive compounds [9–11]. These biochemical compounds are recognized for their functional properties, which are capable of producing various biological effects, such as antioxidant or antimicrobial activity [12]. Given the diverse effects that these bioactive compounds exhibit, algae play a significant role in functional nutrition, offering a diverse array of health benefits that are increasingly recognized in dietary practices. Marine algae, such as brown and blue-green algae, have been identified as potential sources of anticancer agents [13,14]. Research has shown that compounds isolated from marine algae can effectively target gastrointestinal cancers, such as stomach and colon cancer, which are among the most prevalent forms of cancer globally [15,16]. The bioactive compounds derived from algae have been reported to not only prevent cancer development but also enhance the efficacy of conventional treatments. For instance, these compounds can modulate cancer cell metabolism and influence the tumor microenvironment, thereby reducing tumorigenesis and preventing metastasis [17,18]. Furthermore, the antioxidant and anti-inflammatory properties of algal components contribute to their protective effects against cancer [16]. As research continues to uncover the diverse mechanisms through which these bioactive compounds operate, the integration of algae into functional foods and nutraceuticals is becoming increasingly relevant for cancer prevention and treatment strategies [15,17]. Thus, algae represent a promising avenue for enhancing health outcomes in cancer care.

Cancer represents the second leading cause of death worldwide since, according to the latest global cancer burden data released by the World Health Organization (WHO)'s International Agency for Research on Cancer (IARC), 20 million new cancer cases were diagnosed worldwide in 2020, with mortality equal to 9 million of people worldwide [19].

Research has been focused on the development of new therapeutic strategies to extend life expectancy and reduce cancer mortality. Although surgical resection, radiotherapy, and chemotherapy remain the conventional treatment strategies, they often lead to drug resistance and unpleasant side effects [20,21]. In recent years, new anticancer therapies have emerged, and in this context, natural products, such as algae, have gained attention [22]. Thereby, the hypothesis that bioactive compounds in algae may have an antitumor function has direct parallels with the contemporary era of chemotherapy, which seeks to exclusively target and eliminate cancer cells while minimizing damage to healthy cells.

2. Macroalgae: A Comprehensive Overview

Algae are a notable group of non-flowering organisms that resemble plants, and they share the presence of chlorophyll and the ability to carry out photosynthesis. Unlike plants, they do not have typical stems, leaves, and roots, nor do they possess vascular tissue. Algae can be made by single cells or colonies or can be multicellular organisms [23]. They can be found abundantly in oceans, ponds, and lakes and have various practical uses, including providing food for both humans and animals and producing natural plant chemicals, pharmaceuticals, cosmetics, and industrial products [24,25]. Algae also have a vital role in the environment as they help purify it by removing excessive nutrients and CO_2 [26,27]. Due to their vast array of morphological, anatomical, and reproductive characteristics, as well as the various types of photosynthetic pigments and cell wall composition, algae become difficult to classify. The main basis for classification lies in their photosynthetic pigments and major cell products. This leads to the subdivision of the plant kingdom into numerous phyla, where algae are grouped either independently or alongside other less complex plants. Within these phyla, ten distinct categories can be identified, with some comprising only one algae class and others consisting of multiple

classes. In the first instance, algae are differentiated between macro- and microalgae [28–30]. Macroalgae, also known as seaweeds, are generally found in the ocean, representing an important biological resource as well as an alternative food source [31], given their high protein, dietary fiber, vitamin, and mineral content [32,33]. Nowadays, macroalgae are taxonomically classified based on the nature of their pigments. Following this classification, weeds are divided into red (Rhodophyta), brown (Phaeophyta), and green (Chlorophyta) (Figure 1) [34]. Red macroalgae belong mainly to the maritime environment, constituting a unique group distinguished by their eukaryotic cells devoid of flagella and centrioles. Their chloroplasts lack external endoplasmic reticulum and contain unstacked thylakoids known as stroma. Additionally, they utilize phycobiliproteins as accessory pigments, imparting their characteristic red hue. Their red pigment allows them to photosynthesize at deeper depths than other algae. Similarly, another element that distinguishes this category of algae from others is that red algae are able to store carbohydrates as Floridean starch outside the chloroplasts [35–37]. Brown macroalgae, exclusively multicellular organisms, are the second largest group of macroscopic algae, with around 2000 identified species worldwide, mainly located in the colder waters of the Northern Hemisphere [38]. Brown algae produce a large amount of carotenoid, among which is fucoxanthin, the pigment responsible for their distinctive greenish-brown color [39,40]. Green algae exhibit great diversity of form and function. Like red algae, they can be unicellular, multicellular, colonial, or coenocytic. They have membrane-bound chloroplasts and nuclei. Most green algae are aquatic and found commonly in freshwater (mainly charophytes) and marine habitats (mostly chlorophytes); some are terrestrial, growing on soil, trees, or rocks (mostly trebouxiophytes) [41–43].

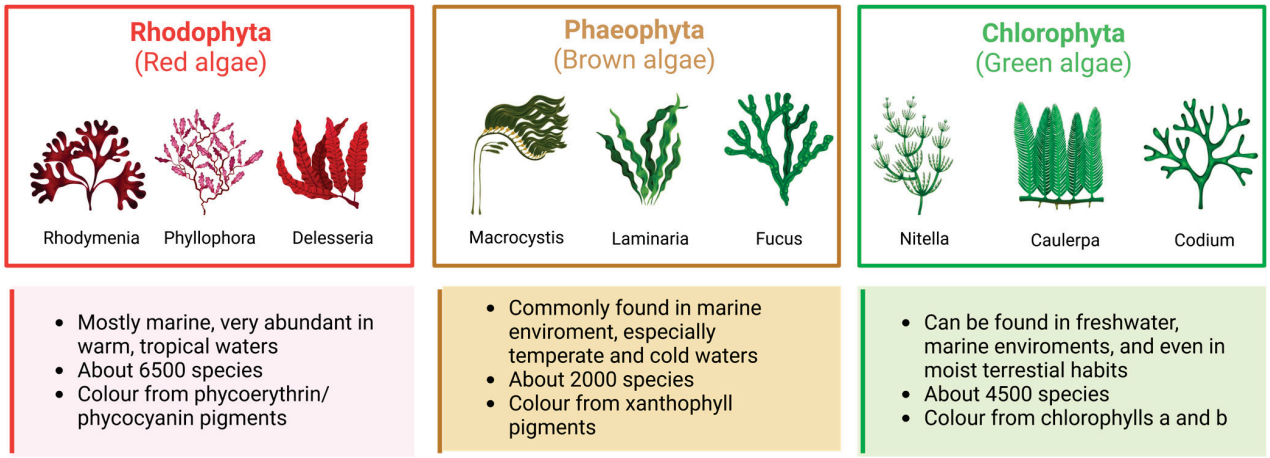

Figure 1. Classification of macroalgae and their main characteristics: Rhodophyta (red algae); Phaeophyta (brown algae); and Chlorophyta (green algae).

3. Macroalgae's Bioactive Compounds with Anticancer and Anticarcinogenic Potential

Nowadays, there is an increasing interest in algae. This is because, in addition to their nutritional qualities, they are a rich source of many biologically active compounds and one of the richest sources of natural bioactive substances, such as polysaccharides, proteins, lipids, polyphenols, carotenoids, pigments, vitamins, sterols, and enzymes [44,45]. All these compounds confer to the algae different functional properties, such as antioxidant, antibacterial, antiviral, and antifungal [46–48]. Among all the possible potentiality of algae in the last year, scientific research has delved deeper into the realm of algae, developing a growing awareness regarding their potential health benefits, particularly in terms of cancer prevention and tumor regression [49]. In fact, it was recently demonstrated that the

bioactive compounds of seaweeds could exhibit cytotoxic effects on cancer cells, inhibiting tumor growth through apoptosis induction and interference with kinases and cell cycle pathways, safeguarding cells from DNA damage, reducing chronic inflammation, and contributing to the prevention and regression of tumors [50–54]. According to their different categories, algae species are characterized by different bioactive compounds (Figure 2; Table 1).

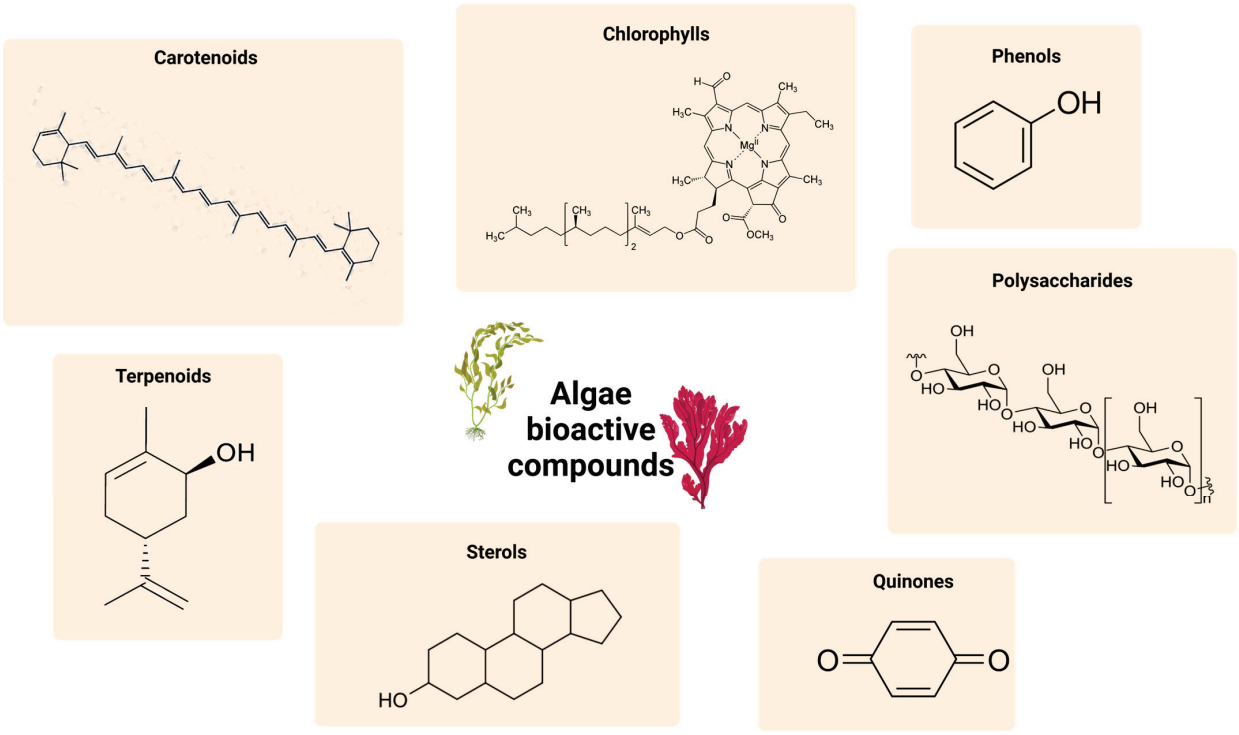

Figure 2. Representation of the molecular structure of the main compound classes of algae-derived bioactive compounds.

Table 1. Main classes of bioactive compounds and relative chemical compounds in algae species.

Compound Class	Example Compounds	Algae Species	Reference
Carotenoids	Alloxantin	*Cryptomonas ovata* (Cryptophyceae) *Cryptomonas erosa* (Cryptophyceae) *Rhodomonas salina* (Cryptophyceae)	[55–58]
	Crocoxanthin	*Karenia brevis* (Dinoflagellata)	
	Fucoxanthin	*Undaria pinnatifida* (Phaeophyceae) *Phaeodactylum tricornutum* (Bacillariophycae)	
	Fucoxanthinol	*Undaria pinnatifida* (Phaeophyceae) *Saccharina japonica* (formerly *Laminaria japonica*) (Phaeophyceae) *Sargassum* spp. (Phaeophyceae)	
	Siphonaxanthin	*Codium fragile* (Chlorophyta) *Caulerpa lentillifera* (Chlorophyta) *Umbraulva japonica* (Chlorophyta)	
	Xanthophylls	*Undaria pinnatifida* (Phaeophyceae) *Laminaria japonica* (formerly *Laminaria japonica*) (Phaeophyceae) *Sargassum* spp. (Phaeophyceae)	
Chlorophylls	Chlorophyll a and b	*Ulva lactuca* (Chlorophyta) *Codium fragile* (Chlorophyta) *Caulerpa lentillifera* (Chlorophyta)	[59–61]

Table 1. *Cont.*

Compound Class	Example Compounds	Algae Species	Reference
Phenols	2-Bromophenol Phloroglucinol Phlorotannins	*Rhodomela larix* (formerly *Rhodomela larix*) (Rhodophyta) *Ecklonia cava* (Phaeophyceae) *Sargassum* spp. (Phaeophyceae) *Himanthalia elongata* (Phaeophyceae) *Halopteris scoparia* (formerly *Stypocaulon scoparium*) (Phaeophyceae) *Ascophyllum nodosum* (Phaeophyceae) *Ecklonia cava* subsp. stolonifera (formerly *Ecklonia stolonifera*) (Phaeophyceae) *Fucus vesiculosus* (Phaeophyceae) *Macrocystis pyrifera* (Phaeophyceae)	[62,63]
Polysaccharides	Alginate Carrageenan Fucoidan Laminarin	*Laminaria digitata* (Phaeophyceae) *Laminaria hyperborea* (Phaeophyceae) *Macrocystis pyrifera* (Phaeophyceae) *Ascophyllum nodosum* (Phaeophyceae) *Kappaphycus alvarezii* (Rhodophyta) *Eucheuma denticulatum* (Rhodophyta) *Fucus vesiculosus* (Phaeophyceae) *Laminaria* spp. (Phaeophyceae) *Saccharina latissima* (Phaeophyceae) *Laminaria* spp. (Phaeophyceae)	[64–67]
Quinones	Hydroquinone Quinone	*Sargassum polycystum* (Phaeophyceae) *Sargassum* spp. (Phaeophyceae)	[68,69]
Sterols	Fucosterol Phytosterol	*Pelvetia canaliculata* (Phaeophyceae) *Fucus vesiculosus* (Phaeophyceae) *Codium tomentosum* (Chlorophyta) *Saccharina latissima* (Phaeophyceae) *Gracilaria* spp. (Rhodophyta)	[70,71]
Terpenoids	Diterpenoid Monoterpene Triterpenoid	*Dictyota* spp. (Phaeophyceae) *Bifurcaria bifurcata* (Phaeophyceae) *Portieria hornemannii* (Rhodophyta) *Gracilaria salicornia* (Rhodophyta) *Padina boergesenii* (Phaeophyceae)	[72–76]

Green algae, due to their diversity, offer different anticancer bioactive compounds, which possess potent antioxidant properties and exhibit significant antitumor activities [77]. Their ability to inhibit tumor growth, reduce DNA damage, and block the formation of mutagenic agents makes them promising candidates for the development of novel anticancer therapies and preventive strategies. Additionally, the antioxidant properties of these bioactive compounds play a crucial role in protecting cells from oxidative damage, which is a major contributor to the development of cancer. By neutralizing harmful free radicals, the green pigments found in algae can help reduce the risk of DNA mutations and subsequent tumor formation [78–80]. Going into detail about the different bioactive compounds characterizing green algae, chlorophylls, such as chlorophyll a and b, are magnesium-rich pigments that have been found to possess antitumor, antigenotoxic, and antimitotic properties. These compounds have shown promising results in reducing liver tumors induced by aflatoxin B1 and other chemical carcinogens in experimental animal models. They have also demonstrated the ability to decrease DNA damage and inhibit the formation of carcinogen-derived DNA adducts, which are mutagenic agents. As well as chlorophylls, their derivatives, such as tetraprenyltol and siphonaxanthin, disclose anticancer activity [59–61,81]. In particular, siphonaxanthin has shown remarkable cytotoxicity

against human colon cancer cell lines, demonstrating its potential as a powerful weapon against this disease [82]. Xanthophylls, including lutein and zeaxanthin, are another group of green pigments that exhibit chemopreventive effects against oral and liver cancer [83]. Dietary intake of these compounds has been associated with a decreased incidence of tumors and preneoplastic lesions, particularly in the liver. Finally, β-carotene was discovered to be capable of converting into retinol and stimulating the induction of retinol-binding protein in the body, which, in turn, plays a vital role in the prevention and mitigation of cancer [21]. In the realm of red algae, until now, only a few species have been studied for their natural products and biological activities. To date, bioactive compounds with undetected anticancer properties belong mainly to the classes of polysaccharides, secondary metabolites, and halogenated compounds [84]. Specifically, sulfated polysaccharides, such as carrageenans and agarans, have been identified as potent anticancer agents. Their effectiveness lies in their immunomodulatory effects, which have been shown to inhibit cancer cell growth and metastasis. These polysaccharides act as warriors, fighting against cancer's destructive tendencies and offering hope for improved patient outcomes [85]. Guaiane sesquiterpenoids are a type of secondary metabolite produced by plants, which have been found to possess anticancer properties. This compound exists in the form of sesquiterpenoid alcohol and has shown promising results in both in vitro and in vivo tests on leukemia L1210 cells where it functions as an expellant by inducing apoptosis in the early stages of polynucleosome formation [86,87]. Moreover, red algae are a valuable source of halogenated compounds, including bromide, bromoform, and bromophenols, which are recognized as potential anticancer agents. Unfortunately, due to their limited availability and negative side effects, further exploration of these compounds is necessary to better clarify their role in cancer therapy [88–91]. Turning our attention to brown algae, renowned for their rich bioactive content, they have also exhibited promising anticancer activity [92,93]. Among the bioactive substances found in brown algae, fucoxanthin, a xanthophyll, has garnered significant attention. Information gathered from various research studies suggests that fucoxanthin can hinder the development of various forms of tumors and impede their spread to other parts of the body [94–96].

4. Mechanisms of Action

The anticancer effect of algae-derived compounds occurs through multiple mechanisms of action (Figure 3).

One strategy is to induce apoptosis. Algal compounds, such as phlorotannins from brown algae and fucoxanthin, are shown to upregulate apoptosis-associated proteins [22,97], including caspase activation, which are crucial enzymes in the apoptosis process, and modulate mitochondrial pathways and death receptor signaling, leading to the effective elimination of cancer cells [98,99]. Additionally, seaweed-derived polyphenols and other bioactive compounds interfere with cell cycle progression, arresting cancer cell growth at various stages and preventing proliferation [51]. For instance, compounds from *Chlorella* sp. have been found to inhibit the AKT/mTOR survival signaling pathway, which is essential for cell growth and survival, thereby inducing apoptosis in cancer cells [100]. Among bioactive algal compounds with apoptotic activity, Eo et al. highlight that Phlorofucofuroeckol A is able to induce apoptosis by interfering with the pathway of AFT3, a major regulator of metabolic homeostasis that can influence cancer cell proliferation [101]. On the other hand, Zhangfan et al. disclosed that fucosterol extract could target the Raf/MEK/ERK signaling pathway, which, given its involvement in the proliferation and tumorigenesis of several cancer types, is to be considered an essential therapeutic target [102,103]. Moreover, marine-derived compounds, such as polysaccharides, pep-

tides, and terpenoids, exhibit cytotoxic effects on cancer cells by disrupting key signaling networks, like the PI3K/AKT, ROS, and p53 pathways, which are involved in cell survival, oxidative stress response, and DNA repair mechanisms [104]. The anti-angiogenic and anti-metastatic properties of these compounds further contribute to their anticancer efficacy by inhibiting the formation of new blood vessels and the spread of cancer cells to other parts of the body [105]. The possible molecular mechanisms are attributed to inhibiting the signal transduction by the angiogenic factor VEGF (Vascular Endothelial Growth Factor) and migration of cancer cells. Additionally, these algae-derived compounds possess the ability to modulate different signaling pathways that regulate cell survival, proliferation, and metastasis. These bioactive components exert their effects by interacting with specific targets involved in tumor progression, such as growth factor receptors, cell adhesion molecules, and transcription factors [106,107]. Additionally, studies have revealed that algae-derived compounds, including polyphenols, carotenoids, lipids, and polysaccharides, can modulate the tumor microenvironment, influencing critical factors such as inflammation, immune response, and angiogenesis. By targeting these components, they contribute to creating an unfavorable environment for tumor growth and progression. Furthermore, these compounds possess antioxidant properties, effectively neutralizing harmful free radicals and reducing oxidative stress, which is known to promote tumor development. Furthermore, the inclusion of these alga-derived bioactive compounds in cancer treatment approaches has displayed promising therapeutic outcomes. They have been shown to enhance the effectiveness of traditional chemotherapy drugs, reducing their toxic side effects while increasing their anticancer activity. Moreover, compounds like fucoidan, phlorotannins, laminarin, carrageenan, and ulvans have demonstrated the potential to sensitize cancer cells to radiation therapy, improving its efficacy in eradicating tumor cells and preventing recurrence [108–110]. The diverse chemical structures of these marine bioactive compounds allow them to target multiple pathways simultaneously, making them effective against various cancer types and potentially overcoming drug resistance [111,112]. Furthermore, the presence of specific bioactive compounds, like gallic acid and lutein, in algal extracts has been confirmed to reduce cancer cell viability significantly, highlighting their potential as therapeutic agents [100]. Overall, the multifaceted mechanisms of action of algae and algae-derived compounds, including apoptosis induction, cell cycle arrest, and modulation of critical signaling pathways, underscore their promising role in cancer therapy and warrant further clinical studies to validate their efficacy and safety.

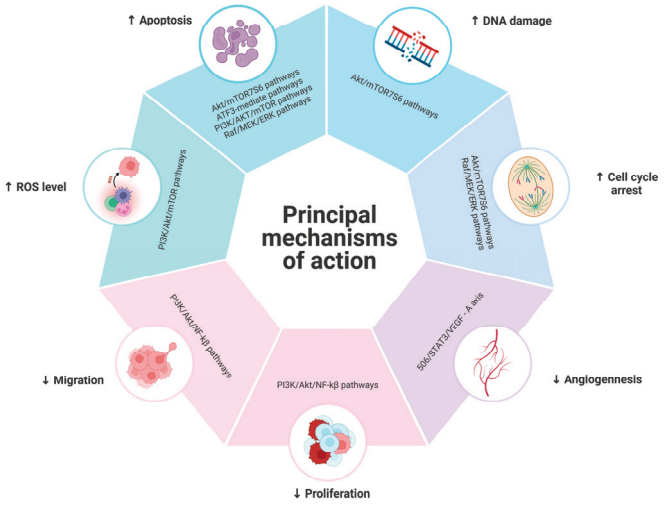

Figure 3. Representation of the main mechanisms of action regulating the antitumor effect of algae-derived bioactive compounds.

5. In Vitro Studies

In vitro studies have extensively assessed the anticancer activity of various algae, revealing promising results across different species of macroalgae (Table 2). Marine algae extracts have been tested for their potential inhibitory or toxic effects on different cell lines. This testing is important in screening the therapeutic and toxic effects of new algal compounds. Growth inhibition is often used as a measure of the extract's potential anticancer activity. To determine this, cell count, protein synthesis, MTT reduction, and cell cycle monitoring are employed. Marine macroalgae, such as *Gelidiella acerosa* (Rhodophyta), have shown significant antiproliferative activity against A549 lung cancer cells, with ethyl acetate extracts inducing apoptosis through the activation of caspase 3 and altering the Bax:Bcl2 ratio [113]. Furthermore, the butanolic extracts of *Gracillaria corticata* (Rhodophyta) have demonstrated greater anticancer activity against HeLa, K-562, and MDA-MB cell lines compared to other solvent extracts [114]. Green algae, such as *Caulerpa lentillifera* (Chlorophyta), have also exhibited wide-ranging anticancer effects on colorectal, hepatoma, breast cancer cell lines, and leukemia, attributed to their sulfated polysaccharides [115]. Additionally, the methanolic extracts of *Caulerpa taxifolia*, *Ulothrix flacca*, and *Ulva fasciata* (formerly *Ulva fasciata*) (Chlorophyta) have shown ROS-dependent mitochondrial damage-induced cytotoxicity in neuroblastoma cells [116]. Antarctic seaweeds, like *Pyropia endiviifolia* (Rhodophyta), have displayed selective antitumor activity against glioma and lung cancer cells, with extracts reducing cell viability significantly without affecting non-transformed cells [117]. Additionally, it was shown that lipoxygenase products can induce p53-independent apoptosis in tumor cells. These findings, which have sparked a growing interest in using marine algal compounds for cancer treatment, are a testament to the promising results of the in vitro testing of algal extracts and isolated compounds on various cancer cell lines.

In vitro studies remain a crucial step in the preclinical evaluation of macroalgae-derived compounds for cancer treatment, serving as an indispensable first step in identifying bioactive compounds, elucidating their mechanisms of action, and assessing cytotoxicity against cancer cells. Therefore, understanding the mechanisms behind their anticancer effects paves the way for future research, potentially leading to the development of effective and safe chemotherapeutic agents derived from algae [118–120].

Table 2. In vitro studies reporting the anticancer potential of brown, red, and green macroalgae.

Algal Species (Compounds)	Cell Line	Effects	Reference
Brown Macroalgae			
Gongolaria usneoides (formerly *Cystoseira usneoides*) (Phaeophyceae) (meroterpenoids isolate)	HT-29	↓ in ERK/JNK/AKT signaling pathways	[121]
Dictyota ciliolata (Phaeophyceae) (Aqueous and methanol extract)	HCT116; HepG2	Cytotoxic effect ↑ Activity of caspase 3 and 9 in HepG2	[122]
Dictyota cervicornis (formerly *Dictyota Indica*) (Phaeophyceae) (fucoxanthin)	MDA-MB-231	Fucoxanthin extract has anticancer activity without toxic effects to the normal cells	[123]
Ecklonia cava (Phaeophyceae) (Dieckol, commercial Sigma-Aldrich, St. Louis, MO, USA)	PANC-1	Induction of apoptosis and inhibition of the progression of PANC-1 cell lines	[124]
Ecklonia cava (Phaeophyceae) (Fucosterol, commercial Sigma-Aldrich, St. Louis, MO, USA)	HCC827; A549; SK-LU-1; A427	Growth inhibition Induction of apoptosis and cell cycle arrest	[103]
Fucus vesiculosus (Phaeophyceae) (acetonic extract)	PANC-1; PancTu1; Panc89; Colo357	↓ Cell viability ↑ Apoptotic effects	[125]

Table 2. *Cont.*

Algal Species (Compounds)	Cell Line	Effects	Reference
Fucus vesiculosus (Phaeophyceae) (Fucoidan, commercial Sigma-Aldrich, St. Louis, MO, USA)	A549; CL1-5	Induction of apoptosis cell death	[126]
Padina pavonica (Phaeophyceae) (methanol extract)	HepG2	↓ Number and viability of cells	[127]
Sargassum incisifolium (formerly *Sargassum heterophyllum*) (Phaeophyceae) (tetraprenylquinone, and sargaquinoic acid)	MCF-7; MDA-MB-231	Apoptosis induction via caspase-3, -6, -8, -9, and -13 ↓ in Bcl-2 gene Arrest of G1 phase in MDA-MB-231 cells	[128]
Sargassum ilicifolium (Phaeophyceae) (alcoholic extract)	MCF-7; MDA-MB-231; HeLa; HepG2; HT-29	All the extracts were antiproliferative against all the cancer cell lines, dose-dependently, with the *G. corticata* methanol extract showing the greatest inhibition activity against the MCF-7 cell line	[129]
Sargassum sp. (Phaeophyceae) (Ethanol fraction)	MCF-7	Ethanol fraction induced cell shrinkage, cell membrane blebbing, and formation of apoptotic bodies	[130]
Sargassum wightii (Phaeophyceae) (Methanol extract)	HT-29	Inhibition of the proliferation	[131]
Undaria piannatifida (Phaeophyceae) (fucoxanthin, commercial Wuhan Heli)	MDA-MB-231	↓ in growth and cell proliferation	[132]
	Green Macroalgae		
Botryidiopsidaceae sp. (Chlorophyta) (ethanol extract)	HeLa; HCT116	↑ Expression of pro-apoptotic gene (p53) ↓ Expression of anti-apoptotic gene (Bcl-2)	[133]
Caulerpa lentillifera (Chlorophyta) (sulfated polysaccharide)	HCT-8; HL-60; K-562; KG-1a; MCF-7; MDA-MB-231	Cytotoxic effect	[115]
Caulerpa racemosa (Chlorophyta) (methanol extract)	HL-60	↓ Cancer cell growth Apoptotic body formation	[134]
Caulerpa racemosa (Chlorophyta) (chloroform extract)	KAIMRC1	Chloroform fraction and crude polyphenolic extract exhibited moderate cytotoxic activity	[135]
Cladophoropsis sp. (Chlorophyta) (ethanol extract)	MDA-MB-231; MCF-7; T-47D	Growth inhibition due to an estrogen receptor/progesterone receptor-independent mechanism	[136]
Ulva lactuca (formerly *Ulva fasciata*) (Chlorophyta) (alcoholic extract)	MCF-7; MDA-MB-231; HeLa; HepG2; HT-29	All the extracts were antiproliferative against all the cancer cell lines, dose-dependently, with the *G. corticata* methanol extract showing the greatest inhibition activity against the MCF-7 cell line	[129]
Ulva lactuca (formerly *Ulva fasciata*) (Chlorophyta) (Chloroform extracts)	HepG2; MCF-7; HeLa; PC-3	Strong activity against PC3 and HePG2 cell lines	[137]
Ulva lactuca (Chlorophyta) (phycocyanin, methanolic extract)	HepG2; MCF-7	Antiproliferative and pro-apoptotic activities	[138]
Ulva lactuca (Chlorophyta) (Chloroform extracts)	HepG2; MCF-7; HeLa; PC-3	Strong activity against MCF-7 and Hela cell lines	[137]
Asparagopsis armata (Rhodophyta) (dichloromethane and methanol extracts)	Caco-2	↓ Cell viability ↓ Cell proliferation	[139]
Gracilaria corticata (Rhodophyta) (methanol extract)	MDA-MB 231	Cytotoxic effect	[140]
Gracilaria corticata (Rhodophyta) (acqueous extract)	Jurkat; molt-4	Cytotoxic effect of water crude extract	[141]
Gracillaria corticata (Rhodophyta) (alcoholic extract)	MCF-7; MDA-MB-231; HeLa; HepG2; HT-29	All the extracts were antiproliferative against all the cancer cell lines, dose-dependently, with the *G. corticata* methanol extract showing the greatest inhibition activity against the MCF-7 cell line	[129]

Table 2. *Cont.*

Algal Species (Compounds)	Cell Line	Effects	Reference
	Red Macroalgae		
Gracilaria foliifera (Rhodophyta) (ethanol extract)	MDA-MB-231; MCF-7; T-47D	Growth inhibition due to an estrogen receptor/progesterone receptor-independent mechanism	[136]
Gracilariopsis lemaneiformis (Rhodophyta) (polysaccharides, water extraction)	A549; MKN28; B16	Inhibition of cell proliferation Induction of apoptosis	[142]
Iridaea cordata (Rhodophyta) (ethyl acetate extract)	A-431	High cytotoxic activity	[143]
Jania rubens (Rhodophyta) (methanol extract)	HepG2	↓ Number and viability of cells	[127]
Laurencia obtuse (Rhodophyta) (Hex:AcOEt fraction)	AGS	Hex:AcOEt fraction of *L. obtusa* was the most cytotoxic against AGS cells	[144]
Pyropia endiviifolia (Rhodophyta) (hexan, ethanol and chloroform extract)	U87-MG; HTB-14; A549; CCL-185	Antiproliferative effect of hexane and ethanol extract ↓ Glioma cell with hexane and ethanol extract ↓ Lung adenocarcinoma cell viability with chloroform extract	[117]
Plocamium cartilagineum (Rhodophyta) (methan extract)	Caco-2	↓ Cell viability ↓ Cell proliferation	[139]
Plocamium corallorhiza (Rhodophyta) (polyhalogenated monoterpene)	MCF-7; MDA-MB-231	Apoptosis induction via caspase-3, -6, -8, -9, and -13 ↓ in Bcl-2 gene Arrest of G1 phase in MDA-MB-231 cells	[128]
Plocamium cornutum (Rhodophyta) (polyhalogenated monoterpene)	MCF-7; MDA-MB-231	Apoptosis induction via caspase-3, -6, -8, -9, and -13 ↓ in Bcl-2 gene Arrest of G1 phase in MDA-MB-231 cells	[128]
Sphaerococcus cornopifolius (Rhodophyta) (dichloromethane and methanol extracts)	Caco-2	↓ Cell viability ↓ Cell proliferation	[139]

A427: human lung carcinoma; A-431: human epidermoid carcinoma; A549: human lung adenocarcinoma; AGS: human gastric adenocarcinoma; B16: mouse melanoma skin tissue; Caco-2: human colorectal cancer; CCL-185: human lung adenocarcinoma; CL1-5: human lung cancer; Colo357: human pancreas adenocarcinoma; HCC827: human lung adenocarcinoma; HCT116: human colon cancer; HCT-8: human colorectal cancer; HeLa: human cervical cancer; HepG2: human hepatocellular carcinoma; HL-60: human promyelocytic leukemia; HT-29: human colon carcinoma; HTB-14: human glioma; Jurkat: human leukemia; K-562: human leukemia; KAIMRC1: human breast cancer; KG-1a: human leukemia; MCF-7: human breast cancer; MDA-MB-231: human breast cancer; MKN28: stomach adenocarcinoma; molt-4: human leukemia; PANC-1: human pancreatic carcinoma; Panc89: pancreatic cancer; PancTu1: human pancreatic carcinoma; PC-3: human prostate cancer; SK-LU-1: human lung adenocarcinoma; T-47D: human breast cancer; U87-MG: human glioma.

6. In Vivo Studies

Given the promising and numerous results obtained in vitro, research focused on the evaluation of the anticancer capacity of algae was also carried out in different in vivo models, of which the murine model is a major representative (Table 3). Currently, in vivo studies reporting the use of pure phytochemicals derived from macroalgae are small due to the variability in the biomass used as a starting point [145]. In a study conducted by Jin et al., rats were injected with the carcinogen diethylnitrosamine (DEN), and the experimental group received fucoxanthin from brown macroalgae in their diet. At the end of the experiment, the incidence of tumors was significantly lower in the group receiving fucoxanthin. During the autopsy, it was further noted that the rats taking fucoxanthin had fewer tumorous characteristics. As a result, the scientists hypothesized that fucoxanthin might have a blocking effect against DEN during both the tumor initiation phase and the promotion phase [146]. In another study, rats were induced with colorectal cancer using a carcinogen and were then given alginates from *Laminaria hyperborea* (Phaeophyceae) as part of their diet. The results demonstrate a significant reduction in the incidence of cancer nodules in the rat intestines, and the reduction in size of these nodules was dose-dependent. Additionally, when the same approach was used on adenoma in the

rats' intestinal tract, the growth of the adenoma was found to be inhibited [147]. Another study conducted by Hwang et al. disclosed that brown algae polyphenols, administered both orally and topically, significantly reduced UVB-induced skin tumor multiplicity and volume in SKH-1 mice, likely by inhibiting oxidative stress and inflammation [148]. Lastly, eckol, a phlorotannin from brown algae, exhibited potent antitumor effects in sarcoma 180 xenograft-bearing mice by promoting apoptosis, inhibiting cell proliferation, and enhancing immune responses, including increased T lymphocyte activity and dendritic cell infiltration [149]. Concurrent with studies that have seen the administration of extracts of bioactive molecules, several studies report the use of whole algae within the diet. In rats, it was observed that supplementation of the brown algae *Dictyota dichotoma* (Phaeophyceae) in the diet was well-tolerated at high doses, indicating its potential for safe anticancer applications [150]. Different studies were also conducted in mice models. In this context, the administration of extracts from the brown alga *Padina pavonica* (Phaeophyceae) and the red alga *Jania rubens* discloses the ability to reduce the tumor cell number in vivo and enhance the immune responses in mice challenged with Ehrlich ascites carcinoma cells [127]. The administration of seaweed makes it possible to evaluate the synergistic effect of the algal phytocomplexes, which could lead to a greater antitumor effect, as the bioactive compounds working synergistically are able to reduce the cytotoxic effects that the administration of a single concentrated compound could cause not only toward cancer cells but also toward healthy ones [151]. In addition to this aspect, the administration of algal biomass in its entirety meets the recommendations of the guidelines in the field of precision and functional nutrition as a key element in cancer treatment [152,153].

Collectively, these studies underscore the diverse and potent anticancer properties of various algae. They not only validate the potential of algae as therapeutic agents but also highlight their role as dietary supplements in cancer prevention and treatment. This dual role of algae in combating cancer is a significant finding of our research.

Table 3. In vivo studies reporting the anticancer potential of brown, red, and green macroalgae.

Algae Species	Animal Model	Experimental Group	Effect	Reference
Brown algae polyphenols	Female SKH-1 hairless mice (7–8 weeks of age)	Oral treatment groups: (i) control; (ii) UVB control; (iii) UVB + brown algae polyphenols. Topical treatment groups: (i) solvent vehicle control; brown algae polyphenol control; UVB + solvent vehicle control; UVB + brown algae polyphenols.	Dietary feeding: - ↓ Tumor multiplicity (45% and 56%); - ↓ Tumor volume (54% and 65%). Topical administration (3 and 6 mg): - ↓ Tumor multiplicity (60% and 46%); - ↓ Tumor volume (66% and 57%). Inhibition of cyclooxygenase-2 activity and cell proliferation.	[148]
Ericaria selaginoides (formerly *Cystoseira tamariscifolia*) (Phaeophyceae)	Swiss albinos mice (6–8 weeks of age)	Lot 1 (1250 mg/kg); Lot 2 (1041.66 mg/kg); Lot 3 (868.05 mg/kg); Lot 4 (723.27 mg/kg); Lot 5 (602.81 mg/kg); Lot 6 (502.34 mg/kg); Lot 7 (0 mg/kg).	Toxic effect of the alga on the mice with LD_{50} of 738.61 ± 34 µg of alga/g of body weight.	[154]
Chlorella vulgaris (Chlorophyta)	Female Balb/c mice and nude mice	(1) Control; (2) Laser; (3) RT; (4) Laser + RT; (5) Algae@SiO_2; (6) Algae@SiO_2 + laser; (7) Algae@SiO_2 + RT; (8) Algae@SiO_2 + laser + RT.	- Algae@SiO_2 ↑ oxygen production capability that alleviates the tumor hypoxia; - With X-ray irradiation, proliferation and mitigation of 4T1 cells were suppressed; - Inhibition of tumor development with laser and RT treatment for the Algae@SiO_2-mediated combination therapy; - RT and PDT combination therapy inhibit the pulmonary metastasis of the 4T1 breast tumor.	[155]

Table 3. *Cont.*

Algae Species	Animal Model	Experimental Group	Effect	Reference
Eckol derived from marine brown algae	Male Kunming mice	(1) Control; (2) Eckol low dose (0.25 mg kg^{-1}); (3) Eckol middle dose (0.5 mg kg^{-1}); (4) Eckol high dose (1.0 mg kg^{-1}).	- ↑ TUNEL-positive apoptotic cells; - ↑ Caspase-3 and Caspase-9 expression; - ↓ Bcl-2, Bax, EGFR, and p-EGFR expression stimulation of mononuclear phagocytic system. ↑ CD4+/CD8+ T lymphocyte ratio; - ↑ Cytotoxic T lymphocyte responses.	[149]
Pandina pavonica (Phaeophyceae) Jania rubens (Rhodophyta)	Female Swiss albino mice CD1 (6–8 weeks old)	(1) Naïve EAC control (i.p. saline solution after EAC transplantations); (2) Positive EAC control (10 μg Cisplatin®/mouse i.p. after EAC transplantations); (3) *P. pavonica* extract (2.5 μg/mouse i.p. after EAC transplantations); (4) *P. pavonica* extract (1.3 μg/mouse i.p. after EAC transplantations); (5) *J. rubens* extract (2.3 μg/mouse i.p. after EAC transplantations); (6) *J. rubens* extract (1.2 μg/mouse i.p. after EAC transplantations); (7) *P. pavonica* extract (2.5, μg/mouse i.p. before EAC transplantations); (8) *J. rubens* extracts (2.3 μg/mouse i.p. before EAC transplantations).	- ↓ Number and viability of EAC tumor cells; - ↑ EAC apoptosis.	[127]
Dimethylsulfoniopropionate (DMSP) of green algae	Male ICR/Jcl mice (4 weeks old)	(1) Control; (2) EAC control; (3) DMSP (5 mM) + EAC; (4) DMSP (10 mM) + EAC; (5) DMPS (20 mM) + EAC.	- 10 and 20 mM DMSP solutions prolonged the lives span of mice; - 10 mM DMSP solution activated delayed-type hypersensitivity.	[156]

7. Potential Applications in Cancer Treatment

To date, the most effective method of treating cancer is the use of toxic chemicals that preferentially kill cancer cells. Unfortunately, these chemical drugs lack selectivity and affect normal cells, causing a number of side effects, including damage to the immune system and organs, such as the liver and kidneys. This often leads to reducing the dosage of the therapy so that the side effects are tolerable [157,158]. In recent years, there has been a growing interest in the study of using algae in cancer treatment. This is largely due to the observations that many types of algae have substantially different effects when tested on normal cells compared to cancerous cells. This selectiveness for cancer cells is the desired characteristic of an anticancer agent. Therefore, the hypothesis currently being tested identifies algae as a potential adjuvant in therapies to support either the synthetic or natural anticancer drugs that are currently being used. This may improve their effectiveness by acting as a sensitizer, or it may allow a lower dosage of the drug to be used [159,160].

In the context of combination therapy, it is now possible to utilize antioxidants and anticancer agents derived from algae to enhance the effectiveness of standard chemotherapeutic agents. By combining an anticancer agent with an antioxidant, it is potentially possible to decrease the toxic side effects of chemotherapy on healthy cells [161,162]. There are various types of combination therapy available to fight different forms of cancer. For instance, research has demonstrated that the administration of vitamin E and vitamin C can aid the anticancer activity of certain cytotoxic agents. This is because these vitamins can reduce the amount of cytotoxic destruction caused by free radicals on normal cells [163–166]. Moreover, the use of PUFA derived from algae has the potential to enhance the cytotoxic effects of chemotherapeutic agents on hormone-dependent cancers. Recent research has, in fact, demonstrated that combining PUFA with tamoxifen can effectively induce apoptosis in cancer cells. This may be attributed to the ability of PUFA to increase the expression of estrogen receptors, which has been associated with a higher susceptibility of hormone-dependent cancers to tamoxifen [167,168]. Additionally, PUFAs are known to be highly effective in inhibiting the synthesis of cyclooxygenase enzymes and PGE2, both of which have been implicated in tumor progression [169–171].

The success of drug delivery depends on the carrier system used. The carrier must ensure that the therapeutic agent remains undisturbed until it reaches its target site, and once released, it should not be metabolized or excreted prematurely [172–174]. Therefore, researchers have shown interest in utilizing macrophages to deliver anticancer drugs to tumors. In fact, macrophages have the ability to migrate and penetrate solid tumors, as well as express certain receptors absent or present in low concentrations on non-malignant cells. One such example is suicide gene therapy for metastatic melanoma and other metastatic cancers, employing genetically modified human CD14+ peripheral blood macrophages. These macrophages carry the tumor migration inhibitory factor (TMIG) gene under a heat-inducible promoter and are encapsulated in alginate microcapsules containing low-cost synthetic cis aconitate-based fluorinated anti-metabolites with antitumor properties. By systemically delivering these TMIG gene macrophages to metastatic tumor sites through heat induction, the macrophages revert their phenotype from migratory to non-migratory, effectively trapping them at the tumor site and maximizing the antitumor effect [62,175]. The field of gene therapy presents an opportunity for macro- and microalgae to be utilized in targeted drug delivery.

8. Side Effects

Exploring macroalgae as potential antitumor agents has gained significant attention due to their diverse bioactivities and the unique compounds they produce. However, like

any therapeutic intervention, these natural compounds are not without their risks. The side effects and potential toxicities of macroalgae-derived treatments are influenced by the specific bioactive compounds present, their mechanisms of action, and the administered dosage. As reported in the preceding paragraphs, some macroalgae-derived compounds can exert a cytotoxic effect against cancer cells, but, at the same time, they might demonstrate the same effect against cells of healthy tissues. This is, for example, the case found by Alves and colleagues, where extracts from *Asparagopsis armata* and *Sphaerococcus coronopifolius* demonstrated potent cytotoxic activity against colorectal cancer cells but without precise targeting, so these effects could extend to normal cells, leading to unintended toxicity [139]. In addition, some macroalgae-derived metabolites, particularly brominated compounds found in red algae, exhibit broad-spectrum activity that does not always differentiate between cancerous and healthy cells, thus necessitating the need for appropriate targeting [176]. Additional to the direct toxicity that can be caused by algae compounds, it is known that the pro-apoptotic properties of algal extracts are often mediated by the induction of oxidative stress, which facilitates the destruction of malignant cells. However, this same mechanism can adversely impact normal cells, leading to neurotoxicity and broader cytotoxic effects. Research on MCF-7 breast cancer cells suggests that oxidative stress induced by certain algal compounds can be a double-edged sword, requiring careful modulation to minimize collateral damage [177]. Moreover, the use of algae in the treatment of cancer can lead to modulation of the immune system. In this context, certain algae-derived compounds have immunomodulatory properties that can either enhance or suppress immune system activity. While some polysaccharides stimulate immune responses to target tumors, others may inadvertently trigger excessive inflammation or immune suppression, leading to unintended consequences such as autoimmune reactions or increased susceptibility to infections [178]. The identification of the aforementioned adverse effects is primarily attributable to the fact that the exact correlation between the chemical structure of macroalgae-derived compounds and their biological activity is not yet fully understood [176]. This lack of knowledge makes it difficult to predict, control, and mitigate the potential toxicities associated with these natural products. Furthermore, although numerous in vitro and in vivo studies highlight the promising antitumor properties of macroalgae, clinical studies remain scarce, showing significant variations in both antitumor efficacy and toxicity among different species and even among individuals of the same species [119].

The side effects reported to date may be further reduced in the coming years, as a deeper understanding of the molecular mechanisms underlying the antitumor effects of macroalgae—including their ability to promote apoptosis and inhibit angiogenesis—can aid in designing more selective treatments. At the same time, certain macroalgae-derived compounds, such as phlorotannins, possess antioxidant properties that can counteract oxidative stress-induced damage. This contributes to mitigating the side effects associated with oxidative toxicity, providing protection to non-cancerous cells [22]. By refining these mechanisms, researchers could develop therapies that minimize harm to healthy cells while maximizing antitumor efficacy [97,119].

9. Challenges and Future Directions

Algal compounds have shown potential in combating cancer, but further research is needed before clinical trials can be conducted. Prior to clinical trials, a preclinical pathway must be followed to evaluate the effectiveness of algal compounds for cancer treatment. This pathway will include (i) standardizing algal extracts chemically and biologically;

(ii) conducting toxicity studies using normal cells and animal models; and (iii) investigating the mechanisms of action of the algal compounds [160,179–181].

As mentioned above, the compounds with anticancer activity derived from macroalgae comprise intricate mixtures primarily consisting of polysaccharides, proteins, lipids, pigments, vitamins, and minerals. Therefore, it is necessary to find for each compound the best extraction method since the efficacy of the extraction process, as well as the chosen solvent, heavily influences the quantity and quality of the algal extracts, which ultimately impacts their biological functions. To ensure reliable findings in forthcoming research, it is imperative to establish a standardized technique for extracting algal compounds [182–186]. Although various methods exist for this purpose, there is no universally accepted approach. Nevertheless, the National Cancer Institute (NCI) method has been widely employed for standardizing extracts. This bioassay involves diluting the extract to determine its IC50 value, which indicates its ability to inhibit cancer cell growth. If the extract exhibits anticancer activity by preventing cell proliferation, an IC_{50} value of less than 20 μg/mL is obtained. Even if this approach is not official, the information obtained from this assay is valuable as it allows for comparisons of an extract's potency over time and across different research groups [187]. Once the extraction is complete, the identification and isolation of particular compounds will allow further evaluation of these pure compounds' use in vitro and in vivo cancer models. Despite the benefits, there are drawbacks to consider, including the need for substantial amounts of extract, the lack of correlation to in vivo activity, and the associated cost [188].

Moreover, another crucial point that has to be investigated before proceeding with clinical trials is formulation development. This could involve simply administering extracts in the form of capsules or taking more complex steps to develop the extracts into functional foods or nutraceuticals. Preliminary investigations are conducted to evaluate the physical and chemical characteristics of medication and the viability of creating a specific drug form. When it comes to natural substances, there is limited knowledge regarding the primary elements found in extracts. Nevertheless, in certain cases where the active ingredient has been isolated, additional spectroscopic examinations can be conducted to determine the compound's structure [189–192]. Subsequently, the design of the formulation and the optimization of the product can be carried out, which can vary in complexity based on the nature of the extract and the intended form of administration.

10. Conclusions

This review provides an overview of the anticancer properties of extracts derived from macroalgae. Research in recent years has highlighted the potential of several algae-derived compounds, such as pigments, polyphenols, polysaccharides, proteins, and peptides, to inhibit cancer cell growth and proliferation, induce apoptosis (programmed cell death), modulate the immune system, and reduce side effects associated with traditional therapies. Algae represent a renewable and sustainable source of bioactive compounds with high potential for the development of new anticancer therapies. Their multifunctional nature and low toxicity make them ideal candidates for combination with traditional chemotherapeutic drugs, enhancing their efficacy and reducing their side effects. However, it is important to note that research in this field is still in its early stages, and further clinical trials are needed to confirm the efficacy and safety of algae in cancer therapy. Nevertheless, their prospects are promising, and algae represent real hope for the development of new, more effective, and less invasive cancer therapies.

Author Contributions: Conceptualization: S.F. and L.R.; methodology, S.F.; investigation, S.F.; resources, L.R.; data curation, S.F.; writing—original draft preparation, S.F.; writing—review and editing, S.F. and L.R.; visualization, S.F. and L.R.; supervision, L.R. All authors have read and agreed to the published version of the manuscript.

Funding: This research received no external funding.

Conflicts of Interest: The authors declare no conflicts of interest.

References

1. Chapman, R.L. Algae: The World's Most Important "Plants"—An Introduction. *Mitig. Adapt. Strateg. Glob. Chang.* **2013**, *18*, 5–12. [CrossRef]
2. Mapelli-Brahm, P.; Gómez-Villegas, P.; Gonda, M.L.; León-Vaz, A.; León, R.; Mildenberger, J.; Rebours, C.; Saravia, V.; Vero, S.; Vila, E.; et al. Microalgae, Seaweeds and Aquatic Bacteria, Archaea, and Yeasts: Sources of Carotenoids with Potential Antioxidant and Anti-Inflammatory Health-Promoting Actions in the Sustainability Era. *Mar. Drugs* **2023**, *21*, 340. [CrossRef]
3. Frazzini, S.; Scaglia, E.; Dell'Anno, M.; Reggi, S.; Panseri, S.; Giromini, C.; Lanzoni, D.; Sgoifo Rossi, C.A.; Rossi, L. Antioxidant and Antimicrobial Activity of Algal and Cyanobacterial Extracts: An In Vitro Study. *Antioxidants* **2022**, *11*, 992. [CrossRef]
4. Stevenson, R.J.; Smol, J.P. Use of Algae in Environmental Assessments. In *Freshwater Algae of North America*; Elsevier: Amsterdam, The Netherlands, 2003; pp. 775–804.
5. Gaurav, K.; Neeti, K.; Singh, R. Microalgae-Based Biodiesel Production and Its Challenges and Future Opportunities: A Review. *Green. Technol. Sustain.* **2024**, *2*, 100060. [CrossRef]
6. Enamala, M.K.; Dixit, R.; Tangellapally, A.; Singh, M.; Dinakarrao, S.M.P.; Chavali, M.; Pamanji, S.R.; Ashokkumar, V.; Kadier, A.; Chandrasekhar, K. Photosynthetic Microorganisms (Algae) Mediated Bioelectricity Generation in Microbial Fuel Cell: Concise Review. *Environ. Technol. Innov.* **2020**, *19*, 100959. [CrossRef]
7. Shlosberg, Y.; Schuster, G.; Adir, N. Harnessing Photosynthesis to Produce Electricity Using Cyanobacteria, Green Algae, Seaweeds and Plants. *Front. Plant Sci.* **2022**, *13*, 955843. [CrossRef] [PubMed]
8. Shlosberg, Y.; Meirovich, M.M.; Yehezkeli, O.; Schuster, G.; Adir, N. Production of Photocurrent and Hydrogen Gas from Intact Plant Leaves. *Biosens. Bioelectron.* **2022**, *215*, 114558. [CrossRef]
9. Bošnjaković, M.; Sinaga, N. The Perspective of Large-Scale Production of Algae Biodiesel. *Appl. Sci.* **2020**, *10*, 8181. [CrossRef]
10. Trubetskaya, A.; Lê, H.Q.; Leppiniemi, J.; Koso, T.; Välisalmi, T.; Linder, M.B.; Pisano, I.; Dou, J.; Leahy, J.J.; Kontturi, E. Microwave Hydrolysis, as a Sustainable Approach in the Processing of Seaweed for Protein and Nanocellulose Management. *Algal Res.* **2024**, *78*, 103406. [CrossRef]
11. Lisha, V.S.; Kothale, R.S.; Sidharth, S.; Kandasubramanian, B. A Critical Review on Employing Algae as a Feed for Polycarbohydrate Synthesis. *Carbohydr. Polym. Technol. Appl.* **2022**, *4*, 100242. [CrossRef]
12. Babich, O.; Sukhikh, S.; Larina, V.; Kalashnikova, O.; Kashirskikh, E.; Prosekov, A.; Noskova, S.; Ivanova, S.; Fendri, I.; Smaoui, S.; et al. Algae: Study of Edible and Biologically Active Fractions, Their Properties and Applications. *Plants* **2022**, *11*, 780. [CrossRef] [PubMed]
13. Drețcanu, G.; Știrbu, I.; Leoplold, N.; Cruceriu, D.; Danciu, C.; Stănilă, A.; Fărcaș, A.; Borda, I.M.; Iuhas, C.; Diaconeasa, Z. Chemical Structure, Sources and Role of Bioactive Flavonoids in Cancer Prevention: A Review. *Plants* **2022**, *11*, 1117. [CrossRef] [PubMed]
14. Bouyahya, A.; Bakrim, S.; Chamkhi, I.; Taha, D.; El Omari, N.; El Mneyiy, N.; El Hachlafi, N.; El-Shazly, M.; Khalid, A.; Abdalla, A.N.; et al. Bioactive Substances of Cyanobacteria and Microalgae: Sources, Metabolism, and Anticancer Mechanism Insights. *Biomed. Pharmacother.* **2024**, *170*, 115989. [CrossRef]
15. Kim, S.-K.; Karagozlu, M.Z. Marine algae: Natural product source for gastrointestinal cancer treatment. *Adv. Food Nutr. Res.* **2011**, *64*, 225–233.
16. Domínguez, H. *Functional Ingredients from Algae for Foods and Nutraceuticals*; Woodhead Publishing Limited: Sawston, UK, 2013; ISBN 978-0-85709-512-1.
17. Pistollato, F.; Giampieri, F.; Battino, M. The Use of Plant-Derived Bioactive Compounds to Target Cancer Stem Cells and Modulate Tumor Microenvironment. *Food Chem. Toxicol.* **2015**, *75*, 58–70. [CrossRef]
18. Kris-Etherton, P.M.; Hecker, K.D.; Bonanome, A.; Coval, S.M.; Binkoski, A.E.; Hilpert, K.F.; Griel, A.E.; Etherton, T.D. Bioactive Compounds in Foods: Their Role in the Prevention of Cardiovascular Disease and Cancer. *Am. J. Med.* **2002**, *113*, 71–88. [CrossRef] [PubMed]
19. Ferlay, J.; Colombet, M.; Soerjomataram, I.; Parkin, D.M.; Piñeros, M.; Znaor, A.; Bray, F. Cancer Statistics for the Year 2020: An Overview. *Int. J. Cancer* **2021**, *149*, 778–789. [CrossRef]

20. van den Boogaard, W.M.C.; Komninos, D.S.J.; Vermeij, W.P. Chemotherapy Side-Effects: Not All DNA Damage Is Equal. *Cancers* **2022**, *14*, 627. [CrossRef] [PubMed]
21. Anand, R.; Mohan, L.; Bharadvaja, N. Disease Prevention and Treatment Using β-Carotene: The Ultimate Provitamin A. *Rev. Bras. Farmacogn.* **2022**, *32*, 491–501. [CrossRef] [PubMed]
22. Pradhan, B.; Ki, J.S. Antioxidant and chemotherapeutic efficacies of seaweed-derived phlorotannins in cancer treatment: A review regarding novel anticancer drugs. *Phytother. Res. PTR* **2023**, *37*, 2067–2091. [CrossRef]
23. Figueroa-Martinez, F.; Nedelcu, A.M.; Smith, D.R.; Reyes-Prieto, A. When the Lights Go out: The Evolutionary Fate of Free-living Colorless Green Algae. *New Phytol.* **2015**, *206*, 972–982. [CrossRef] [PubMed]
24. Abdur Razzak, S.; Bahar, K.; Islam, K.M.O.; Haniffa, A.K.; Faruque, M.O.; Hossain, S.M.Z.; Hossain, M.M. Microalgae Cultivation in Photobioreactors: Sustainable Solutions for a Greener Future. *Green. Chem. Eng.* **2024**, *5*, 418–439. [CrossRef]
25. Carlsson, A.S.; Bowles, D.J. *Micro- and Macro-Algae: Utility for Industrial Applications*; Bowles, D., Ed.; Epobio; CPL Press: Chippenham, UK, 2007.
26. Ammar, E.E.; Aioub, A.A.A.; Elesawy, A.E.; Karkour, A.M.; Mouhamed, M.S.; Amer, A.A.; EL-Shershaby, N.A. Algae as Bio-Fertilizers: Between Current Situation and Future Prospective. *Saudi J. Biol. Sci.* **2022**, *29*, 3083–3096. [CrossRef] [PubMed]
27. Bai, A.; Popp, J.; Pető, K.; Szőke, I.; Harangi-Rákos, M.; Gabnai, Z. The Significance of Forests and Algae in CO_2 Balance: A Hungarian Case Study. *Sustainability* **2017**, *9*, 857. [CrossRef]
28. Beetul, K.; Gopeechund, A.; Kaullysing, D.; Mattan-Moorgawa, S.; Puchooa, D.; Bhagooli, R. Challenges and Opportunities in the Present Era of Marine Algal Applications. In *Algae—Organisms for Imminent Biotechnology*; IntechOpen Limited: London, UK, 2016.
29. Baweja, P.; Sahoo, D. Classification of Algae. In *The Algae World*; Springer: Dordrecht, The Netherlands, 2015; pp. 31–55.
30. Ulvskov, P.; Paiva, D.S.; Domozych, D.; Harholt, J. Classification, Naming and Evolutionary History of Glycosyltransferases from Sequenced Green and Red Algal Genomes. *PLoS ONE* **2013**, *8*, e76511. [CrossRef]
31. Lozano Muñoz, I.; Díaz, N.F. Minerals in Edible Seaweed: Health Benefits and Food Safety Issues. *Crit. Rev. Food Sci. Nutr.* **2022**, *62*, 1592–1607. [CrossRef]
32. Chan, P.T.; Matanjun, P. Chemical Composition and Physicochemical Properties of Tropical Red Seaweed, *Gracilaria changii*. *Food Chem.* **2017**, *221*, 302–310. [CrossRef] [PubMed]
33. Rodrigues, D.; Freitas, A.C.; Pereira, L.; Rocha-Santos, T.A.P.; Vasconcelos, M.W.; Roriz, M.; Rodríguez-Alcalá, L.M.; Gomes, A.M.P.; Duarte, A.C. Chemical Composition of Red, Brown and Green Macroalgae from Buarcos Bay in Central West Coast of Portugal. *Food Chem.* **2015**, *183*, 197–207. [CrossRef]
34. Bleakley, S.; Hayes, M. Algal Proteins: Extraction, Application, and Challenges Concerning Production. *Foods* **2017**, *6*, 33. [CrossRef] [PubMed]
35. Borg, M.; Krueger-Hadfield, S.A.; Destombe, C.; Collén, J.; Lipinska, A.; Coelho, S.M. Red Macroalgae in the Genomic Era. *New Phytol.* **2023**, *240*, 471–488. [CrossRef]
36. Aziz, E.; Batool, R.; Khan, M.U.; Rauf, A.; Akhtar, W.; Heydari, M.; Rehman, S.; Shahzad, T.; Malik, A.; Mosavat, S.H.; et al. An Overview on Red Algae Bioactive Compounds and Their Pharmaceutical Applications. *J. Complement. Integr. Med.* **2021**, *17*. [CrossRef]
37. Torres, M.D.; Flórez-Fernández, N.; Domínguez, H. Integral Utilization of Red Seaweed for Bioactive Production. *Mar. Drugs* **2019**, *17*, 314. [CrossRef] [PubMed]
38. Ruiz Martínez, E.; Schroeder, D.C.; Thuestad, G.; Hoell, I.A. Brown Algae (Phaeophyceae) Stressors and Illnesses: A Review for a Sustainable Aquaculture under Climate Change. *Front. Aquac.* **2024**, *3*, 1390415. [CrossRef]
39. Kergosien, N.; Stiger-Pouvreau, V.; Connan, S.; Hennequart, F.; Brébion, J. Mini-Review: Brown Macroalgae as a Promising Raw Material to Produce Biostimulants for the Agriculture Sector. *Front. Agron.* **2023**, *5*, 1109989. [CrossRef]
40. Reboleira, J.; Freitas, R.; Pinteus, S.; Silva, J.; Alves, C.; Pedrosa, R.; Bernardino, S. Brown Seaweeds. In *Nonvitamin and Nonmineral Nutritional Supplements*; Elsevier: Amsterdam, The Netherlands, 2019; pp. 171–176.
41. Xu, J.; Liao, W.; Liu, Y.; Guo, Y.; Jiang, S.; Zhao, C. An Overview on the Nutritional and Bioactive Components of Green Seaweeds. *Food Prod. Process. Nutr.* **2023**, *5*, 18. [CrossRef]
42. Moreira, A.; Cruz, S.; Marques, R.; Cartaxana, P. The Underexplored Potential of Green Macroalgae in Aquaculture. *Rev. Aquac.* **2022**, *14*, 5–26. [CrossRef]
43. Surget, G.; Roberto, V.P.; Le Lann, K.; Mira, S.; Guérard, F.; Laizé, V.; Poupart, N.; Cancela, M.L.; Stiger-Pouvreau, V. Marine Green Macroalgae: A Source of Natural Compounds with Mineralogenic and Antioxidant Activities. *J. Appl. Phycol.* **2017**, *29*, 575–584. [CrossRef]
44. Kumar, C.S.; Ganesan, P.; Suresh, P.V.; Bhaskar, N. Seaweeds as a Source of Nutritionally Beneficial Compounds—A Review. *J. Food Sci. Technol.* **2008**, *45*, 1–13.

45. Garcia-Vaquero, M.; Rajauria, G.; O'Doherty, J.V.; Sweeney, T. Polysaccharides from Macroalgae: Recent Advances, Innovative Technologies and Challenges in Extraction and Purification. *Food Res. Int.* **2017**, *99*, 1011–1020. [CrossRef]
46. Gupta, S.; Abu-Ghannam, N. Recent Developments in the Application of Seaweeds or Seaweed Extracts as a Means for Enhancing the Safety and Quality Attributes of Foods. *Innov. Food Sci. Emerg. Technol.* **2011**, *12*, 600–609. [CrossRef]
47. Frazzini, S.; Torresani, M.C.; Hejna, M.; Di Dio, M.; Rossi, L. *Ascophillum nodosum* and *Lithothamnium calcareum* and Their Prebiotic Potential on *Lactobacillus strains*. *J. Funct. Foods* **2024**, *118*, 106257. [CrossRef]
48. Rossi, L.; Canala, B.; Fifi, A.P.; Frazzini, S. In Vitro Evaluation of Functional Properties of Extracts of Fucus Vesiculosus Obtained with Different Conventional Solvents. *Algal Res.* **2024**, *84*, 103787. [CrossRef]
49. Sharma, R.; Mondal, A.S.; Trivedi, N. Anticancer Potential of Algae-Derived Metabolites: Recent Updates and Breakthroughs. *Future J. Pharm. Sci.* **2023**, *9*, 44. [CrossRef]
50. Klapp, V.; Álvarez-Abril, B.; Leuzzi, G.; Kroemer, G.; Ciccia, A.; Galluzzi, L. The DNA Damage Response and Inflammation in Cancer. *Cancer Discov.* **2023**, *13*, 1521–1545. [CrossRef]
51. Lee, H.; Selvaraj, B.; Lee, J.W. Anticancer Effects of Seaweed-Derived Bioactive Compounds. *Appl. Sci.* **2021**, *11*, 11261. [CrossRef]
52. Kidane, D.; Chae, W.J.; Czochor, J.; Eckert, K.A.; Glazer, P.M.; Bothwell, A.L.M.; Sweasy, J.B. Interplay between DNA Repair and Inflammation, and the Link to Cancer. *Crit. Rev. Biochem. Mol. Biol.* **2014**, *49*, 116–139. [CrossRef] [PubMed]
53. Quail, D.F.; Joyce, J.A. Microenvironmental Regulation of Tumor Progression and Metastasis. *Nat. Med.* **2013**, *19*, 1423–1437. [CrossRef]
54. Grivennikov, S.I.; Greten, F.R.; Karin, M. Immunity, Inflammation, and Cancer. *Cell* **2010**, *140*, 883–899. [CrossRef]
55. Galasso, C.; Corinaldesi, C.; Sansone, C. Carotenoids from Marine Organisms: Biological Functions and Industrial Applications. *Antioxidants* **2017**, *6*, 96. [CrossRef] [PubMed]
56. Bjørnland, T.; Haxo, F.T.; Liaaen-Jensen, S. Carotenoids of the Florida Red Tide Dinoflagellate *Karenia brevis*. *Biochem. Syst. Ecol.* **2003**, *31*, 1147–1162. [CrossRef]
57. Lourenço-Lopes, C.; Fraga-Corral, M.; Jimenez-Lopez, C.; Carpena, M.; Pereira, A.G.; Garcia-Oliveira, P.; Prieto, M.A.; Simal-Gandara, J. Biological Action Mechanisms of Fucoxanthin Extracted from Algae for Application in Food and Cosmetic Industries. *Trends Food Sci. Technol.* **2021**, *117*, 163–181. [CrossRef]
58. Pereira, A.G.; Otero, P.; Echave, J.; Carreira-Casais, A.; Chamorro, F.; Collazo, N.; Jaboui, A.; Lourenço-Lopes, C.; Simal-Gandara, J.; Prieto, M.A. Xanthophylls from the Sea: Algae as Source of Bioactive Carotenoids. *Mar. Drugs* **2021**, *19*, 188. [CrossRef] [PubMed]
59. McQuistan, T.J.; Simonich, M.T.; Pratt, M.M.; Pereira, C.B.; Hendricks, J.D.; Dashwood, R.H.; Williams, D.E.; Bailey, G.S. Cancer Chemoprevention by Dietary Chlorophylls: A 12,000-Animal Dose–Dose Matrix Biomarker and Tumor Study. *Food Chem. Toxicol.* **2012**, *50*, 341–352. [CrossRef] [PubMed]
60. Simonich, M.T.; Egner, P.A.; Roebuck, B.D.; Orner, G.A.; Jubert, C.; Pereira, C.; Groopman, J.D.; Kensler, T.W.; Dashwood, R.H.; Williams, D.E.; et al. Natural Chlorophyll Inhibits Aflatoxin B_1-Induced Multi-Organ Carcinogenesis in the Rat. *Carcinogenesis* **2007**, *28*, 1294–1302. [CrossRef] [PubMed]
61. Martins, T.; Barros, A.N.; Rosa, E.; Antunes, L. Enhancing Health Benefits through Chlorophylls and Chlorophyll-Rich Agro-Food: A Comprehensive Review. *Molecules* **2023**, *28*, 5344. [CrossRef] [PubMed]
62. Li, M.; Jiang, P.; Wei, S.; Wang, J.; Li, C. The Role of Macrophages-Mediated Communications among Cell Compositions of Tumor Microenvironment in Cancer Progression. *Front. Immunol.* **2023**, *14*, 1113312. [CrossRef] [PubMed]
63. Leyton, A.; Pezoa-Conte, R.; Barriga, A.; Buschmann, A.H.; Mäki-Arvela, P.; Mikkola, J.-P.; Lienqueo, M.E. Identification and Efficient Extraction Method of Phlorotannins from the Brown Seaweed *Macrocystis pyrifera* Using an Orthogonal Experimental Design. *Algal Res.* **2016**, *16*, 201–208. [CrossRef]
64. Mostolizadeh, S. Alginate, Polymer Purified from Seaweed. In *Alginate—Applications and Future Perspectives*; IntechOpen: London, UK, 2024.
65. Firdayanti, L.; Yanti, R.; Rahayu, E.S.; Hidayat, C. Carrageenan Extraction from Red Seaweed (*Kappaphycopsis cottonii*) Using the Bead Mill Method. *Algal Res.* **2023**, *69*, 102906. [CrossRef]
66. Sterner, M.; Gröndahl, F. Extraction of Laminarin from *Saccharina latissima* Seaweed Using Cross-Flow Filtration. *J. Appl. Phycol.* **2021**, *33*, 1825–1844. [CrossRef]
67. Rajauria, G.; Ravindran, R.; Garcia-Vaquero, M.; Rai, D.K.; Sweeney, T.; O'Doherty, J. Molecular Characteristics and Antioxidant Activity of Laminarin Extracted from the Seaweed Species *Laminaria hyperborea*, Using Hydrothermal-Assisted Extraction and a Multi-Step Purification Procedure. *Food Hydrocoll.* **2021**, *112*, 106332. [CrossRef]
68. Widyaswari, S.G.; Metusalach, M.; Kasmiati, K.; Amir, N. Bioactive Compounds and DPPH Antioxidant Activity of Underutilized Macroalgae (*Sargassum* spp.) from Coastal Water of Makassar, Indonesia. *Biodiversitas* **2024**, *25*, 176–182. [CrossRef]

69. Máximo, P.; Ferreira, L.M.; Branco, P.; Lima, P.; Lourenço, A. Secondary Metabolites and Biological Activity of Invasive Macroalgae of Southern Europe. *Mar. Drugs* **2018**, *16*, 265. [CrossRef]
70. Resende, J.; Sosa, F.H.B.; Coutinho, J.A.P.; Rocha, J.; Silvestre, A.J.D.; Santos, S.A.O. Sustainable Phytosterol Extraction from *Codium tomentosum* Using Eutectic Solvents. *ACS Sustain. Chem. Eng.* **2024**, *12*, 9037–9044. [CrossRef]
71. Sohn, S.-I.; Rathinapriya, P.; Balaji, S.; Jaya Balan, D.; Swetha, T.K.; Durgadevi, R.; Alagulakshmi, S.; Singaraj, P.; Pandian, S. Phytosterols in Seaweeds: An Overview on Biosynthesis to Biomedical Applications. *Int. J. Mol. Sci.* **2021**, *22*, 12691. [CrossRef] [PubMed]
72. Obando, J.M.C.; dos Santos, T.C.; Bernardes, M.; Nascimento, N.; Villaça, R.C.; Teixeira, V.L.; Barbarino, E.; Cavalcanti, D.N. Chemical Variation and Analysis of Diterpenes from Seaweed *Dictyota menstrualis* under Controlled Conditions. *Algal Res.* **2022**, *62*, 102637. [CrossRef]
73. Pais, A.C.S.; Pinto, C.A.; Ramos, P.A.B.; Pinto, R.J.B.; Rosa, D.; Duarte, M.F.; Abreu, M.H.; Rocha, S.M.; Saraiva, J.A.; Silvestre, A.J.D.; et al. High Pressure Extraction of Bioactive Diterpenes from the Macroalgae *Bifurcaria bifurcata*: An Efficient and Environmentally Friendly Approach. *RSC Adv.* **2019**, *9*, 39893–39903. [CrossRef]
74. Wright, A.D.; König, G.M.; Sticher, O.; de Nys, R. Five New Monoterpenes from the Marine Red Alga *Portieria hornemannii*. *Tetrahedron* **1991**, *47*, 5717–5724. [CrossRef]
75. Rajamani, K.; Balasubramanian, T.; Thirugnanasambandan, S.S. Bioassay-Guided Isolation of Triterpene from Brown Alga *Padina boergesenii* Possess Anti-Inflammatory and Anti-Angiogenic Potential with Kinetic Inhibition of β-Carotene Linoleate System. *LWT* **2018**, *93*, 549–555. [CrossRef]
76. Antony, T.; Chakraborty, K. Anti-Inflammatory Polyether Triterpenoids from the Marine Macroalga *Gracilaria salicornia*: Newly Described Natural Leads Attenuate pro-Inflammatory 5-Lipoxygenase and Cyclooxygenase-2. *Algal Res.* **2020**, *47*, 101791. [CrossRef]
77. Haq, S.H.; Al-Ruwaished, G.; Al-Mutlaq, M.A.; Naji, S.A.; Al-Mogren, M.; Al-Rashed, S.; Ain, Q.T.; Al-Amro, A.A.; Al-Mussallam, A. Antioxidant, Anticancer Activity and Phytochemical Analysis of Green Algae, *Chaetomorpha* Collected from the Arabian Gulf. *Sci. Rep.* **2019**, *9*, 18906. [CrossRef]
78. Michalak, I.; Tiwari, R.; Dhawan, M.; Alagawany, M.; Farag, M.R.; Sharun, K.; Emran, T.B.; Dhama, K. Antioxidant Effects of Seaweeds and Their Active Compounds on Animal Health and Production—A Review. *Vet. Q.* **2022**, *42*, 48–67. [CrossRef] [PubMed]
79. Vignaud, J.; Loiseau, C.; Hérault, J.; Mayer, C.; Côme, M.; Martin, I.; Ulmann, L. Microalgae Produce Antioxidant Molecules with Potential Preventive Effects on Mitochondrial Functions and Skeletal Muscular Oxidative Stress. *Antioxidants* **2023**, *12*, 1050. [CrossRef] [PubMed]
80. Saleh, E.A.M.; Al-dolaimy, F.; Qasim almajidi, Y.; Baymakov, S.; Kader M, M.A.; Ullah, M.I.; Abbas, A.h.R.; Khlewee, I.H.; Bisht, Y.S.; Alsaalamy, A.H. Oxidative Stress Affects the Beginning of the Growth of Cancer Cells through a Variety of Routes. *Pathol. Res. Pract.* **2023**, *249*, 154664. [CrossRef] [PubMed]
81. Rasouli, H.; Nayeri, F.D.; Khodarahmi, R. May Phytophenolics Alleviate Aflatoxins-Induced Health Challenges? A Holistic Insight on Current Landscape and Future Prospects. *Front. Nutr.* **2022**, *9*, 981984. [CrossRef]
82. Sugawara, T.; Ganesan, P.; Li, Z.; Manabe, Y.; Hirata, T. Siphonaxanthin, a Green Algal Carotenoid, as a Novel Functional Compound. *Mar. Drugs* **2014**, *12*, 3660–3668. [CrossRef]
83. Pereira, L.; Morrison, L.; Shukla, P.S.; Critchley, A.T. A Concise Review of the Brown Macroalga *Ascophyllum nodosum* (Linnaeus) Le Jolis. *J. Appl. Phycol.* **2020**, *32*, 3561–3584. [CrossRef]
84. Bhuyan, P.P.; Nayak, R.; Patra, S.; Abdulabbas, H.S.; Jena, M.; Pradhan, B. Seaweed-Derived Sulfated Polysaccharides; The New Age Chemopreventives: A Comprehensive Review. *Cancers* **2023**, *15*, 715. [CrossRef]
85. Pradhan, B.; Bhuyan, P.; Ki, J.-S. Immunomodulatory, Antioxidant, Anticancer, and Pharmacokinetic Activity of Ulvan, a Seaweed-Derived Sulfated Polysaccharide: An Updated Comprehensive Review. *Mar. Drugs* **2023**, *21*, 300. [CrossRef]
86. Estévez-Sarmiento, F.; Saavedra, E.; Ruiz-Estévez, M.; León, F.; Quintana, J.; Brouard, I.; Estévez, F. Chlorinated Guaiane-Type Sesquiterpene Lactones as Cytotoxic Agents against Human Tumor Cells. *Int. J. Mol. Sci.* **2020**, *21*, 9767. [CrossRef] [PubMed]
87. Dhyani, P.; Sati, P.; Sharma, E.; Attri, D.C.; Bahukhandi, A.; Tynybekov, B.; Szopa, A.; Sharifi-Rad, J.; Calina, D.; Suleria, H.A.R.; et al. Sesquiterpenoid Lactones as Potential Anti-Cancer Agents: An Update on Molecular Mechanisms and Recent Studies. *Cancer Cell Int.* **2022**, *22*, 305. [CrossRef] [PubMed]
88. Md Akhir, F.N.; Mohd Nazaruddin, F.H.; Othman, N.; Hara, H.; Ahmad, I. Role of Algae in Cancer. In *Handbook of Research on Algae as a Sustainable Solution for Food, Energy, and the Environment*; IGI Global Scientific Publishing: Hershey, PA, USA, 2022; pp. 562–584.

89. Alves, C.; Silva, J.; Pintéus, S.; Guedes, R.A.; Guedes, R.C.; Alvariño, R.; Freitas, R.; Goettert, M.I.; Gaspar, H.; Alfonso, A.; et al. Bromoditerpenes from the Red Seaweed *Sphaerococcus coronopifolius* as Potential Cytotoxic Agents and Proteasome Inhibitors and Related Mechanisms of Action. *Mar. Drugs* **2022**, *20*, 652. [CrossRef]
90. Liu, M.; Hansen, P.E.; Lin, X. Bromophenols in Marine Algae and Their Bioactivities. *Mar. Drugs* **2011**, *9*, 1273–1292. [CrossRef] [PubMed]
91. Cabrita, M.T.; Vale, C.; Rauter, A.P. Halogenated Compounds from Marine Algae. *Mar. Drugs* **2010**, *8*, 2301–2317. [CrossRef] [PubMed]
92. Remya, R.R.; Samrot, A.V.; Kumar, S.S.; Mohanavel, V.; Karthick, A.; Chinnaiyan, V.K.; Umapathy, D.; Muhibbullah, M. Bioactive Potential of Brown Algae. *Adsorpt. Sci. Technol.* **2022**, *2022*, 9104835. [CrossRef]
93. Catarino, M.D.; Amarante, S.J.; Mateus, N.; Silva, A.M.S.; Cardoso, S.M. Brown Algae Phlorotannins: A Marine Alternative to Break the Oxidative Stress, Inflammation and Cancer Network. *Foods* **2021**, *10*, 1478. [CrossRef] [PubMed]
94. Younas, U.; Tehseen, S.; Khan, F.; Niaz, K. Brown Algae (Fucoxanthin) Against Cancer. In *Nutraceuticals and Cancer Signaling*; Springer: Cham, Switzerland, 2021; pp. 99–127.
95. Ahmed, S.A.; Mendonca, P.; Elhag, R.; Soliman, K.F.A. Anticancer Effects of Fucoxanthin through Cell Cycle Arrest, Apoptosis Induction, Angiogenesis Inhibition, and Autophagy Modulation. *Int. J. Mol. Sci.* **2022**, *23*, 16091. [CrossRef] [PubMed]
96. Din, N.A.S.; Mohd Alayudin, 'A.S.; Sofian-Seng, N.-S.; Rahman, H.A.; Mohd Razali, N.S.; Lim, S.J.; Wan Mustapha, W.A. Brown Algae as Functional Food Source of Fucoxanthin: A Review. *Foods* **2022**, *11*, 2235. [CrossRef]
97. Agena, R.; de Jesús Cortés-Sánchez, A.; Hernández-Sánchez, H.; Jaramillo-Flores, M.E. Pro-Apoptotic Activity of Bioactive Compounds from Seaweeds: Promising Sources for Developing Novel Anticancer Drugs. *Mar. Drugs* **2023**, *21*, 182. [CrossRef] [PubMed]
98. Shahid, A.; Khurshid, M.; Aslam, B.; Muzammil, S.; Mehwish, H.M.; Rajoka, M.S.R.; Hayat, H.F.; Sarfraz, M.H.; Razzaq, M.K.; Nisar, M.A.; et al. Cyanobacteria Derived Compounds: Emerging Drugs for Cancer Management. *J. Basic Microbiol.* **2022**, *62*, 1125–1142. [CrossRef] [PubMed]
99. Tripathi, R.; Shalini, R.; Singh, R.K. Prophyletic Origin of Algae as Potential Repository of Anticancer Compounds. In *Evolutionary Diversity as a Source for Anticancer Molecules*; Elsevier: Amsterdam, The Netherlands, 2021; pp. 155–189.
100. Sawasdee, N.; Jantakee, K.; Wathikthinnakon, M.; Panwong, S.; Pekkoh, J.; Duangjan, K.; Yenchitsomanus, P.; Panya, A. *Microalga Chlorella* sp. Extract Induced Apoptotic Cell Death of Cholangiocarcinoma via AKT/MTOR Signaling Pathway. *Biomed. Pharmacother.* **2023**, *160*, 114306. [CrossRef]
101. Eo, H.; Kwon, T.-H.; Park, G.; Song, H.; Lee, S.-J.; Park, N.-H.; Jeong, J. In Vitro Anticancer Activity of Phlorofucofuroeckol A via Upregulation of Activating Transcription Factor 3 against Human Colorectal Cancer Cells. *Mar. Drugs* **2016**, *14*, 69. [CrossRef] [PubMed]
102. Asati, V.; Mahapatra, D.K.; Bharti, S.K. PI3K/Akt/MTOR and Ras/Raf/MEK/ERK Signaling Pathways Inhibitors as Anticancer Agents: Structural and Pharmacological Perspectives. *Eur. J. Med. Chem.* **2016**, *109*, 314–341. [CrossRef]
103. Mao, Z.; Shen, X.; Dong, P.; Liu, G.; Pan, S.; Sun, X.; Hu, H.; Pan, L.; Huang, J. Fucosterol Exerts Antiproliferative Effects on Human Lung Cancer Cells by Inducing Apoptosis, Cell Cycle Arrest and Targeting of Raf/MEK/ERK Signalling Pathway. *Phytomedicine* **2019**, *61*, 152809. [CrossRef] [PubMed]
104. Manoharan, S.; Perumal, E. Potential Role of Marine Bioactive Compounds in Cancer Signaling Pathways: A Review. *Eur. J. Pharmacol.* **2022**, *936*, 175330. [CrossRef]
105. Zuo, W.; Kwok, H.F. Development of Marine-Derived Compounds for Cancer Therapy. *Mar. Drugs* **2021**, *19*, 342. [CrossRef]
106. Sajadimajd, S.; Momtaz, S.; Haratipour, P.; El-Senduny, F.F.; Panah, A.I.; Navabi, J.; Soheilikhah, Z.; Farzaei, M.H.; Rahimi, R. Molecular Mechanisms Underlying Cancer Preventive and Therapeutic Potential of Algal Polysaccharides. *Curr. Pharm. Des.* **2019**, *25*, 1210–1235. [CrossRef] [PubMed]
107. Bhardwaj, N.; Goel, B.; Tripathi, N.; Sahu, B.; Jain, S.K. A Comprehensive Review on Chemistry and Pharmacology of Marine Bioactives as Antimetastatic Agents. *Eur. J. Med. Chem. Rep.* **2022**, *4*, 100023. [CrossRef]
108. Srinivasan, S.; Arockiasamy, P.; Gideon, D.A.; Sekaran, S.; Arumugasamy, H.; Devanga Ragupathi, N.K. Immunomodulatory Algal Metabolites for Alleviating Inflammation and Cancer. In *Handbook of Oxidative Stress in Cancer: Therapeutic Aspects*; Springer Nature: Singapore, 2022; pp. 443–463.
109. Teoh, M.-L.; Choo, W.-T.; Anuwar, S.; Wong, C.-Y.; Convey, P. Microalgae-Based Products and Their Immunomodulatory Activities. In *Handbook of Food and Feed from Microalgae*; Elsevier: Amsterdam, The Netherlands, 2023; pp. 279–290.
110. Jabeen, Y.; Yousaf, N.; Sarjadi, M.S.; Gansau, J.A.; Goh, L.P.W. Bioactive Compounds Derived from Marine Source: A Potential Immunotherapy Treatment. *J. Biomol. Struct. Dyn.* **2024**, *42*, 5657–5668. [CrossRef] [PubMed]
111. Chaudhry, G.-S.; Md Akim, A.; Sung, Y.Y.; Sifzizul, T.M.T. Cancer and Apoptosis: The Apoptotic Activity of Plant and Marine Natural Products and Their Potential as Targeted Cancer Therapeutics. *Front. Pharmacol.* **2022**, *13*, 842376. [CrossRef]

112. Khan, A.W.; Farooq, M.; Haseeb, M.; Choi, S. Role of Plant-Derived Active Constituents in Cancer Treatment and Their Mechanisms of Action. *Cells* **2022**, *11*, 1326. [CrossRef] [PubMed]
113. Fazeela Mahaboob Begum, S.M.; Hemalatha, S. Phytoconstituents from *Gelidiella acerosa* Induce Apoptosis by Regulating Bax, Bcl2 Expression in A549 Cells. *Biocatal. Agric. Biotechnol.* **2020**, *29*, 101757. [CrossRef]
114. Shaik, I.; Shameem, A.; Sasi Bhushana Rao, P. Anti-Cancer Activity of Selected Seaweeds Against HeLa, K-562 and MDA-MB Cell Lines. In *Biotechnology and Bioforensics*; Springer: Singapore, 2015; pp. 35–42.
115. Nurkolis, F.; Kurniawan, R.; Kurniatanty, I.; Park, M.N.; Moon, M.; Fatimah, S.; Gunawan, W.B.; Surya, R.; Taslim, N.A.; Song, H.; et al. New Insight on In Vitro Biological Activities of Sulfated Polysaccharides from Ulvophyte Green Algae. *Molecules* **2023**, *28*, 4531. [CrossRef] [PubMed]
116. Boominathan, M. Cytotoxic Effect of Methanol Extracts of Seaweeds. *Int. J. Pharm. Bio Sci.* **2016**, *7*, 98–105.
117. de Souza, P.O.; Silva, F.A.; Frozza, C.O.d.S.; Frassini, R.; Roesch-Ely, M.; dos Santos, M.A.Z.; Freitag, R.A.; Colepicolo, P.; Pereira, C.M.P.; Braganhol, E. Bioprospecting of New Antarctic Seaweed Selective Antitumor Molecules: Chemical Characterization and in Vitro Analysis. *Phytomed. Plus* **2022**, *2*, 100246. [CrossRef]
118. Alves, C.; Pinteus, S.; Horta, A.; Pedrosa, R. High Cytotoxicity and Anti-Proliferative Activity of Algae Extracts on an in Vitro Model of Human Hepatocellular Carcinoma. *Springerplus* **2016**, *5*, 1339. [CrossRef] [PubMed]
119. Gopeechund, A.; Bhagooli, R.; Neergheen, V.S.; Bolton, J.J.; Bahorun, T. Anticancer Activities of Marine Macroalgae: Status and Future Perspectives. In *Biodiversity and Biomedicine*; Elsevier: Amsterdam, The Netherlands, 2020; pp. 257–275.
120. Saxena, A.; Raj, A.; Tiwari, A. Exploring the Anti-Cancer Potential of Microalgae. In *Progress in Microalgae Research—A Path for Shaping Sustainable Futures*; IntechOpen: London, UK, 2022.
121. Zbakh, H.; Zubía, E.; De Los Reyes, C.; Calderón-Montaño, J.M.; Motilva, V. Anticancer Activities of Meroterpenoids Isolated from the Brown Alga *Cystoseira usneoides* against the Human Colon Cancer Cells HT-29. *Foods* **2020**, *9*, 300. [CrossRef] [PubMed]
122. Maddah, M.R.; Huwait, E.A.; Al-balawi, A.A.; Moselhy, S.S.; ALghamdi, M.A.; Zeyadi, M.A.; Al-Malki, A.L.; Kumosani, T.A. In Vitro Study Anti-Proliferative Potential of Algae Extract against Cancer Cell Line. *J. Pharm. Res. Int.* **2019**, *26*, 1–10. [CrossRef]
123. Karkhane Yousefi, M.; Seyed Hashtroudi, M.; Mashinchian Moradi, A.; Ghasempour, A.R. In Vitro Investigating of Anticancer Activity of Focuxanthin from Marine Brown Seaweed Species. *Glob. J. Environ. Sci. Manag.* **2018**, *8*, 566–577.
124. Xu, J.W.; Yan, Y.; Wang, L.; Wu, D.; Ye, N.K.; Chen, S.H.; Li, F. Marine Bioactive Compound Dieckol Induces Apoptosis and Inhibits the Growth of Human Pancreatic Cancer Cells PANC-1. *J. Biochem. Mol. Toxicol.* **2021**, *35*, e22648. [CrossRef] [PubMed]
125. Geisen, U.; Zenthoefer, M.; Peipp, M.; Kerber, J.; Plenge, J.; Managò, A.; Fuhrmann, M.; Geyer, R.; Hennig, S.; Adam, D.; et al. Molecular Mechanisms by Which a Fucus Vesiculosus Extract Mediates Cell Cycle Inhibition and Cell Death in Pancreatic Cancer Cells. *Mar. Drugs* **2015**, *13*, 4470–4491. [CrossRef]
126. Hsu, H.-Y.; Lin, T.-Y.; Lu, M.-K.; Leng, P.-J.; Tsao, S.-M.; Wu, Y.-C. Fucoidan Induces Toll-like Receptor 4-Regulated Reactive Oxygen Species and Promotes Endoplasmic Reticulum Stress-Mediated Apoptosis in Lung Cancer. *Sci. Rep.* **2017**, *7*, 44990. [CrossRef] [PubMed]
127. El-Sheekh, M.M.; Nassef, M.; Bases, E.; El Shafay, S.; El-shenody, R. Antitumor Immunity and Therapeutic Properties of Marine Seaweeds-Derived Extracts in the Treatment of Cancer. *Cancer Cell Int.* **2022**, *22*, 267. [CrossRef] [PubMed]
128. de la Mare, J.-A.; Lawson, J.C.; Chiwakata, M.T.; Beukes, D.R.; Edkins, A.L.; Blatch, G.L. Quinones and Halogenated Monoterpenes of Algal Origin Show Anti-Proliferative Effects against Breast Cancer Cells in Vitro. *Investig. New Drugs* **2012**, *30*, 2187–2200. [CrossRef] [PubMed]
129. Namvar, F.; Baharara, J.; Mahdi, A.A. Antioxidant and Anticancer Activities of Selected Persian Gulf Algae. *Indian. J. Clin. Biochem.* **2014**, *29*, 13–20. [CrossRef] [PubMed]
130. Mary, J.S.; Vinotha, P.; Pradeep, A.M. Screening for in Vitro Cytotoxic Activity of Seaweed, *Sargassum* sp. Against Hep-2 and MCF-7 Cancer Cell Lines. *Asian Pac. J. Cancer Prev.* **2012**, *13*, 6073–6076. [CrossRef] [PubMed]
131. Neelakandan, Y. In Vitro Anti-Tumor, Anti-Inflammatory, Antioxidant and Antibacterial Activities of Marine Brown Alga *Sargassum* Wightii Collected from Gulf of Mannar. *Glob. J. Pharmacol.* **2014**, *8*, 566–577.
132. Wang, J.; Ma, Y.; Yang, J.; Jin, L.; Gao, Z.; Xue, L.; Hou, L.; Sui, L.; Liu, J.; Zou, X. Fucoxanthin Inhibits Tumour-related Lymphangiogenesis and Growth of Breast Cancer. *J. Cell. Mol. Med.* **2019**, *23*, 2219–2229. [CrossRef]
133. Suh, S.-S.; Kim, S.-M.; Kim, J.E.; Hong, J.-M.; Lee, S.G.; Youn, U.J.; Han, S.J.; Kim, I.-C.; Kim, S. Anticancer Activities of Ethanol Extract from the Antarctic Freshwater Microalga, *Botryidiopsidaceae* sp. *BMC Complement. Altern. Med.* **2017**, *17*, 509. [CrossRef]
134. Lakmal, H.C.; Samarakoon, K.W.; Lee, W.; Lee, J.-H.; Abeytunga, D.; Lee, H.-S.; Jeon, Y.-J. Anticancer and Antioxidant Effects of Selected Sri Lankan Marine Algae. *J. Natl. Sci. Found.* **2014**, *42*, 315. [CrossRef]
135. Dissanayake, I.H.; Bandaranayake, U.; Keerthirathna, L.R.; Manawadu, C.; Silva, R.M.; Mohamed, B.; Ali, R.; Peiris, D.C. Integration of in Vitro and In-Silico Analysis of Caulerpa Racemosa against Antioxidant, Antidiabetic, and Anticancer Activities. *Sci. Rep.* **2022**, *12*, 20848. [CrossRef]

136. Moein, M.; Nazemosadat, Z.; Erfani, N. Cytotoxic Activity of Ten Algae from the Persian Gulf and Oman Sea on Human Breast Cancer Cell Lines; MDA-MB-231, MCF-7, and T-47D. *Pharmacogn. Res.* **2015**, *7*, 133. [CrossRef] [PubMed]
137. Abotaleb, S.; Gheda, S.; Alam, N.; ELMehalawy, A.; Saeed, A. In Vitro Assessment of Antimicrobial, Antioxidant and Anticancer Activities of Some Marine Macroalgae. *Egypt. J. Bot.* **2019**, *12*, 81–96. [CrossRef]
138. Al-Malki, A.L. In Vitro Cytotoxicity and Pro-Apoptotic Activity of Phycocyanin Nanoparticles from *Ulva lactuca* (Chlorophyta) Algae. *Saudi J. Biol. Sci.* **2020**, *27*, 894–898. [CrossRef]
139. Alves, C.; Pinteus, S.; Rodrigues, A.; Horta, A.; Pedrosa, R. Algae from Portuguese Coast Presented High Cytotoxicity and Antiproliferative Effects on an In Vitro Model of Human Colorectal Cancer. *Pharmacogn. Res.* **2018**, *10*, 24–30. [CrossRef]
140. Jayasree, P.; Thiruchelvi, R.; Balashanmugam, P. Evaluation of antibacterial, antioxidant, and anticancer potentials from marine red algae *Gracilaria corticata*. *Asian J. Pharm. Clin. Res.* **2018**, *11*, 347. [CrossRef]
141. Zandi, K.; Tajbakhsh, S.; Nabipour, I.; Rastian, Z.; Yousefi, F.; Sharafian, S.; Sartavi, K. In Vitro Antitumor Activity of Gracilaria Corticata (a Red Alga) against Jurkat and Molt-4 Human Cancer Cell Lines. *Afr. J. Biotechnol.* **2010**, *9*, 6787–6790.
142. Kang, Y.; Wang, Z.-J.; Xie, D.; Sun, X.; Yang, W.; Zhao, X.; Xu, N. Characterization and Potential Antitumor Activity of Polysaccharide from *Gracilariopsis lemaneiformis*. *Mar. Drugs* **2017**, *15*, 100. [CrossRef]
143. Martins, R.M.; Nedel, F.; Guimarães, V.B.S.; da Silva, A.F.; Colepicolo, P.; de Pereira, C.M.P.; Lund, R.G. Macroalgae Extracts From Antarctica Have Antimicrobial and Anticancer Potential. *Front. Microbiol.* **2018**, *9*, 412. [CrossRef]
144. Monteiro, J.R.B.; Rodrigues, R.P.; Mazzuco, A.C.; de Cassia Ribeiro Gonçalves, R.; Bernardino, A.F.; Kuster, R.M.; Kitagawa, R.R. In Vitro and In Silico Evaluation of Red Algae *Laurencia obtusa* Anticancer Activity. *Mar. Drugs* **2023**, *21*, 318. [CrossRef]
145. Wahlen, B.D.; Roni, M.S.; Cafferty, K.G.; Wendt, L.M.; Westover, T.L.; Stevens, D.M.; Newby, D.T. Managing Variability in Algal Biomass Production through Drying and Stabilization of Feedstock Blends. *Algal Res.* **2017**, *24*, 9–18. [CrossRef]
146. Jin, X.; Zhao, T.; Shi, D.; Ye, M.B.; Yi, Q. Protective Role of Fucoxanthin in Diethylnitrosamine-induced Hepatocarcinogenesis in Experimental Adult Rats. *Drug Dev. Res.* **2019**, *80*, 209–217. [CrossRef]
147. Teas, J.; Harbison, M.L.; Gelman, R.S. Dietary Seaweed (Laminaria) and Mammary Carcinogenesis in Rats. *Cancer Res.* **1984**, *44*, 2758–2761. [PubMed]
148. Hwang, H.; Chen, T.; Nines, R.G.; Shin, H.; Stoner, G.D. Photochemoprevention of UVB-induced Skin Carcinogenesis in SKH-1 Mice by Brown Algae Polyphenols. *Int. J. Cancer* **2006**, *119*, 2742–2749. [CrossRef] [PubMed]
149. Zhang, M.; Guo, J.; Hu, X.; Zhao, S.; Li, S.; Wang, J. An in Vivo Anti-Tumor Effect of Eckol from Marine Brown Algae by Improving the Immune Response. *Food Funct.* **2019**, *10*, 4361–4371. [CrossRef]
150. El-Shaibany, A.; AL-Habori, M.; Al-Maqtari, T.; Al-Mahbashi, H. The Yemeni Brown Algae *Dictyota dichotoma* Exhibit *High In Vitro* Anticancer Activity Independent of Its Antioxidant Capability. *Biomed. Res. Int.* **2020**, *2020*, 2425693. [CrossRef]
151. Vujović, T.; Paradžik, T.; Babić Brčić, S.; Piva, R. Unlocking the Therapeutic Potential of Algae-Derived Compounds in Hematological Malignancies. *Cancers* **2025**, *17*, 318. [CrossRef] [PubMed]
152. Arends, J.; Bachmann, P.; Baracos, V.; Barthelemy, N.; Bertz, H.; Bozzetti, F.; Fearon, K.; Hütterer, E.; Isenring, E.; Kaasa, S.; et al. ESPEN Guidelines on Nutrition in Cancer Patients. *Clin. Nutr.* **2017**, *36*, 11–48. [CrossRef]
153. Martínez-Garay, C.; Djouder, N. Dietary Interventions and Precision Nutrition in Cancer Therapy. *Trends Mol. Med.* **2023**, *29*, 489–511. [CrossRef] [PubMed]
154. Zineb, S. Toxic And Anti-Cancerogenic Effect Of Brown Seaweed Cystoseira Tamariscifolia. *Int. J. Sci. Technol. Res.* **2016**, *5*, 282–285.
155. Li, W.; Zhong, D.; Hua, S.; Du, Z.; Zhou, M. Biomineralized Biohybrid Algae for Tumor Hypoxia Modulation and Cascade Radio-Photodynamic Therapy. *ACS Appl. Mater. Interfaces* **2020**, *12*, 44541–44553. [CrossRef]
156. Nakajima, K.; Yokoyama, A.; Nakajima, Y. Anticancer Effects of a Tertiary Sulfonium Compound, Dimethylsulfoniopropionate, in Green Sea Algae on Ehrlich Ascites Carcinoma-Bearing Mice. *J. Nutr. Sci. Vitaminol. (Tokyo)* **2009**, *55*, 434–438. [CrossRef]
157. Kahn, A.M.; Blenman, K.R.M.; Sonis, S.T.; Lustberg, M.B. Strategies to Mitigate the Toxicity of Cancer Therapeutics. *Adv. Cancer Res.* **2022**, *155*, 215–244.
158. Feng, Y. Cancer Chemotherapy: Time for New Solution. *Chemotherapy* **2014**, *3*, 2. [CrossRef]
159. Dmytryk, A.; Tuhy, Ł.; Chojnacka, K. Algae as Source of Pharmaceuticals. In *Prospects and Challenges in Algal Biotechnology*; Springer: Singapore, 2017; pp. 295–310.
160. Ferdous, U.T.; Yusof, Z.N.B. Medicinal Prospects of Antioxidants From Algal Sources in Cancer Therapy. *Front. Pharmacol.* **2021**, *12*, 593116. [CrossRef]
161. Yanagawa, H.; Koyama, Y.; Kobayashi, Y.; Kobayashi, H.; Shimada, S. The Development of a Novel Antioxidant-Based Antiemetic Drug to Improve Quality of Life during Anticancer Therapy. *Biochem. Biophys. Rep.* **2022**, *32*, 101363. [CrossRef]
162. Arya, B.; Krishnaveni, K.; Sambathkumar, R. Review on Antioxidant Supplements Use in Cancer Chemotherapy. *Res. J. Pharmacol. Pharmacodyn.* **2020**, *12*, 21. [CrossRef]

163. Barnhart, A.; Anthony, A.; Conaway, K.; Sibbitt, B.; Delaney, E.; Haluschak, J.; Kathula, S.; Chen, A. Safety and Efficacy of Vitamin C, Vitamin E, and Selenium Supplementation in the Oncology Setting: A Systematic Review. *J. Oncol. Pharm. Pract.* **2024**, *30*, 678–696. [CrossRef]
164. Abiri, B.; Vafa, M. Vitamin C and Cancer: The Role of Vitamin C in Disease Progression and Quality of Life in Cancer Patients. *Nutr. Cancer* **2021**, *73*, 1282–1292. [CrossRef] [PubMed]
165. Sánchez-Machado, D.I.; López-Cervantes, J.; Servín de la Mora-López, D.; Quintero-Guerrero, A.A. Vitamins (C, D and E) Against Cancer. In *Nutraceuticals and Cancer Signaling*; Springer: Cham, Switzerland, 2021; pp. 531–543.
166. Butt, G.; Farooqi, A.A.; Adylova, A.; Attar, R.; Yilmaz, S.; Konysbayevna, K.K.; Sabitaliyevich, U.Y.; Gasparri, M.L.; Xu, B. Vitamin C as an Anticancer Agent: Regulation of Signaling Pathways. *Curr. Top. Med. Chem.* **2020**, *20*, 1868–1875. [CrossRef]
167. Abd-Alhaseeb, M.M.; Massoud, S.M.; Elsayed, F.; Omran, G.A.; Salahuddin, A. Evening Primrose Oil Enhances Tamoxifen's Anticancer Activity against Breast Cancer Cells by Inducing Apoptosis, Inhibiting Angiogenesis, and Arresting the Cell Cycle. *Molecules* **2022**, *27*, 2391. [CrossRef] [PubMed]
168. Fatemizadeh, M.; Tafvizi, F.; Shamsi, F.; Amiri, S.; Farajzadeh, A.; Akbarzadeh, I. Apoptosis Induction, Cell Cycle Arrest and Anti-Cancer Potential of Tamoxifen-Curcumin Loaded Niosomes Against MCF-7 Cancer Cells. *Iran. J. Pathol.* **2022**, *17*, 183–190. [CrossRef]
169. Zhang, C.; Yu, H.; Ni, X.; Shen, S.; Das, U.N. Growth Inhibitory Effect of Polyunsaturated Fatty Acids (PUFAs) on Colon Cancer Cells via Their Growth Inhibitory Metabolites and Fatty Acid Composition Changes. *PLoS ONE* **2015**, *10*, e0123256. [CrossRef]
170. Jongthawin, J.; Chusorn, P.; Techasen, A.; Loilome, W.; Boonmars, T.; Thanan, R.; Puapairoj, A.; Khuntikeo, N.; Tassaneeyakul, W.; Yongvanit, P.; et al. PGE2 Signaling and Its Biosynthesis-Related Enzymes in Cholangiocarcinoma Progression. *Tumor Biol.* **2014**, *35*, 8051–8064. [CrossRef]
171. Das, U.N. PUFAs and Their Metabolites in Carcinogenesis. In *Molecular Biochemical Aspects of Cancer*; Springer: New York, NY, USA, 2020; pp. 159–179.
172. Jesús Villarreal-Gómez, L.; Lizeth Pérez-González, G. Novel Drug Carries: Properties and Applications. In *Drug Carriers*; IntechOpen: London, UK, 2022.
173. Ezegbe, C.; Umeh, O.; Ofoefule, S. Drug Carriers. *J. Curr. Biomed. Res.* **2022**, *2*, 77–105. [CrossRef]
174. Bandopadhyay, S.; Manchanda, S.; Chandra, A.; Ali, J.; Deb, P.K. Overview of Different Carrier Systems for Advanced Drug Delivery. In *Drug Delivery Systems*; Elsevier: Amsterdam, The Netherlands, 2020; pp. 179–233.
175. Arora, L.; Kalia, M.; Pal, D. Role of Macrophages in Cancer Progression and Targeted Immunotherapies. *Adv. Protein Chem. Struct. Biol.* **2022**, *135*, 281–311.
176. Liao, W.; Chen, Y.; Shan, S.; Chen, Z.; Wen, Y.; Chen, W.; Zhao, C. Marine Algae-derived Characterized Bioactive Compounds as Therapy for Cancer: A Review on Their Classification, Mechanism of Action, and Future Perspectives. *Phytother. Res.* **2024**, *38*, 4053–4080. [CrossRef]
177. Kurt, O.; Özdal-Kurt, F.; Tuğlu, M.; Akçora, C. The Cytotoxic, Neurotoxic, Apoptotic and Antiproliferative Activities of Extracts of Some Marine Algae on the MCF-7 Cell Line. *Biotech. Histochem.* **2014**, *89*, 568–576. [CrossRef] [PubMed]
178. Murphy, E.J.; Fehrenbach, G.W.; Abidin, I.Z.; Buckley, C.; Montgomery, T.; Pogue, R.; Murray, P.; Major, I.; Rezoagli, E. Polysaccharides—Naturally Occurring Immune Modulators. *Polymers* **2023**, *15*, 2373. [CrossRef]
179. Varshney, K.; Mishra, K. Preclinical Research to Clinical Practice: A Review of Phytochemicals in Cancer Treatment. *Int. J. Innov. Res. Eng. Manag.* **2022**, 147–151. [CrossRef]
180. Choudhari, A.S.; Mandave, P.C.; Deshpande, M.; Ranjekar, P.; Prakash, O. Phytochemicals in Cancer Treatment: From Preclinical Studies to Clinical Practice. *Front. Pharmacol.* **2020**, *10*, 1614. [CrossRef]
181. Abrams, D.I.; Velasco, G.; Twelves, C.; Ganju, R.K.; Bar-Sela, G. Cancer Treatment: Preclinical & Clinical. *JNCI Monogr.* **2021**, *2021*, 107–113. [CrossRef]
182. Quitério, E.; Grosso, C.; Ferraz, R.; Delerue-Matos, C.; Soares, C. A Critical Comparison of the Advanced Extraction Techniques Applied to Obtain Health-Promoting Compounds from Seaweeds. *Mar. Drugs* **2022**, *20*, 677. [CrossRef]
183. Monteiro, M.; Santos, R.A.; Iglesias, P.; Couto, A.; Serra, C.R.; Gouvinhas, I.; Barros, A.; Oliva-Teles, A.; Enes, P.; Díaz-Rosales, P. Effect of Extraction Method and Solvent System on the Phenolic Content and Antioxidant Activity of Selected Macro- and Microalgae Extracts. *J. Appl. Phycol.* **2020**, *32*, 349–362. [CrossRef]
184. Cikoš, A.-M.; Jokić, S.; Šubarić, D.; Jerković, I. Overview on the Application of Modern Methods for the Extraction of Bioactive Compounds from Marine Macroalgae. *Mar. Drugs* **2018**, *16*, 348. [CrossRef]
185. Garcia-Vaquero, M.; Rajauria, G.; Tiwari, B. Conventional Extraction Techniques: Solvent Extraction. In *Sustainable Seaweed Technologies*; Elsevier: Amsterdam, The Netherlands, 2020; pp. 171–189.
186. Sosa-Hernández, J.E.; Escobedo-Avellaneda, Z.; Iqbal, H.M.N.; Welti-Chanes, J. State-of-the-Art Extraction Methodologies for Bioactive Compounds from Algal Biome to Meet Bio-Economy Challenges and Opportunities. *Molecules* **2018**, *23*, 2953. [CrossRef]

187. Evans, J.R.; Akee, R.K.; Chanana, S.; McConachie, G.D.; Thornburg, C.C.; Grkovic, T.; O'Keefe, B.R. National Cancer Institute (NCI) Program for Natural Product Discovery: Exploring NCI-60 Screening Data of Natural Product Samples with Artificial Neural Networks. *ACS Omega* **2023**, *8*, 9250–9256. [CrossRef]
188. Miyata, Y.; Matsuo, T.; Ohba, K.; Mitsunari, K.; Mukae, Y.; Otsubo, A.; Harada, J.; Matsuda, T.; Kondo, T.; Sakai, H. Present Status, Limitations and Future Directions of Treatment Strategies Using Fucoidan-Based Therapies in Bladder Cancer. *Cancers* **2020**, *12*, 3776. [CrossRef]
189. Shahgholian, N. Encapsulation and Delivery of Nutraceuticals and Bioactive Compounds by Nanoliposomes and Tocosomes as Promising Nanocarriers. In *Handbook of Nutraceuticals and Natural Products*; Wiley: Hoboken, NJ, USA, 2022; pp. 403–439.
190. Almoselhy, R.I.M. Formulation and Evaluation of Novel Nutraceuticals Rich in Protein, Vitamins, Minerals, Natural Flavors, and Steviol Glycosides for Improving Quality of Life. *Food Sci. Appl. Biotechnol.* **2023**, *6*, 357–371. [CrossRef]
191. Puri, V.; Nagpal, M.; Singh, I.; Singh, M.; Dhingra, G.A.; Huanbutta, K.; Dheer, D.; Sharma, A.; Sangnim, T. A Comprehensive Review on Nutraceuticals: Therapy Support and Formulation Challenges. *Nutrients* **2022**, *14*, 4637. [CrossRef]
192. Chaturvedi, K.; Shah, H.; Gajera, B. Challenges in Oral Delivery of Nutraceuticals: From Formulation Scale-Up to Clinical Assessment. In *Nutraceutical Delivery Systems*; Apple Academic Press: New York, NY, USA, 2022; pp. 241–278.

MDPI AG
Grosspeteranlage 5
4052 Basel
Switzerland
Tel.: +41 61 683 77 34

Marine Drugs Editorial Office
E-mail: marinedrugs@mdpi.com
www.mdpi.com/journal/marinedrugs

Academic Open
Access Publishing

mdpi.com

ISBN 978-3-7258-4944-4